

ANNUAL REPORTS ON NMR SPECTROSCOPY

Edited by

G. A. WEBB

Department of Chemical Physics, University of Surrey, Guildford, Surrey, England

VOLUME 7

1977



ACADEMIC PRESS

London · New York · San Francisco

A Subsidiary of Harcourt Brace Jovanovich, Publishers

ACADEMIC PRESS INC. (LONDON) LTD.
24-28 Oval Road,
London, NW1 7DX

U.S. Edition Published by

ACADEMIC PRESS INC.
111 Fifth Avenue
New York, New York 10003

Copyright © 1977 by ACADEMIC PRESS INC. (LONDON) LTD.

All Rights Reserved

No part of this book may be reproduced in any form by photostat, microfilm, or
any other means, without written permission from the publishers

Library of Congress Catalog Card Number: 68-17678
ISBN: 0-12-505307-X

Printed in Great Britain at The Spottiswoode Ballantyne Press by
William Clowes & Sons Limited, London, Colchester and Beccles

LIST OF CONTRIBUTORS

- R. FIELDS, *Department of Chemistry, University of Manchester, Institute of Science and Technology, Manchester M60 1QD., England*
- L. STEFANIAK, *Institute of Organic Chemistry, Polish Academy of Sciences, Warsaw, Poland*
- RODERICK E. WASYLISHEN, *Department of Chemistry, University of Winnipeg, Manitoba, Canada R3B 2E9*
- G. A. WEBB, *Department of Chemical Physics, University of Surrey, Guildford, Surrey, GU2 5XH, England*
- M. WITANOWSKI, *Institute of Organic Chemistry, Polish Academy of Sciences, Warsaw, Poland*

ACKNOWLEDGMENTS

For permission to reproduce, in whole or in part, certain figures and diagrams we are grateful to the following publishers:

Pergamon Press Ltd.

Detailed acknowledgements are given in the legends to the figures.

PREFACE

Due to the pressure of his numerous other commitments Eric Mooney has decided to stand down as Editor of this series and I have been asked to take his place. A very considerable debt of gratitude is owed to Eric for initiating *Annual Reports on NMR Spectroscopy* and for editing it so successfully during the past ten years.

As the volume of literature relating to NMR expands annually it is essential, for people applying this technique to various problems, to have access to authoritative reviews on selected NMR topics. It is the aim of *Annual Reports* to provide such reviews particularly in those areas which are of widespread current interest. Thus the general review on NMR which has been featured in this series will be removed and a continuing emphasis given to the NMR of nuclei other than protons.

In concurrence with the title every effort will be made to produce volumes annually. The reviews should thus be timely even though each volume may have a smaller number of contributors than has sometimes been the case in the past.

Volume 7 contains two reviews which update previous chapters by the same authors in Volume 5B. Dr. Fields has devoted his ^{19}F NMR review to fluoroalkyl and fluoroaryl derivatives of transition metals, while Dr. Witanowski and his co-authors have covered all of the literature, pertaining to nitrogen NMR, which appeared between 1972 and 1976. A valuable contribution of spin-spin coupling interactions between carbon and first row nuclei has been provided by Dr. Wasylishen.

Finally, I wish to express my appreciation of the efforts made by these authors in the careful preparation of their manuscripts and for their forbearance during the preparation of this volume.

G. A. WEBB

*University of Surrey,
Guildford, Surrey,
England*

Fluorine-19 NMR Spectroscopy of Fluoroalkyl and Fluoroaryl Derivatives of Transition Metals

R. FIELDS

Department of Chemistry, University of Manchester Institute of Science and Technology, Manchester M60 1QD, England

I. Introduction	1
II. Fluoroalkyl Derivatives	2
A. Groups IIIb-Vb, including the lanthanides and actinides	2
B. Chromium, molybdenum, and tungsten	3
C. Manganese and rhenium	11
D. Iron, ruthenium, and osmium	17
E. Cobalt, rhodium, and iridium	45
F. Nickel, palladium, and platinum	69
G. Copper, silver, and gold	100
III. Fluoroaromatic and Fluoroheteroaromatic Derivatives	102
Acknowledgement	111
References	111

I. INTRODUCTION

This chapter is concerned with the ^{19}F NMR spectra of transition metal derivatives containing fluoroalkyl or fluoroaryl (including heteroaryl) groups; it includes compounds where the organofluorine group is bonded to the metal via some other atom (e.g., N, P, O, S) as well as those in which the fluorine-carrying carbon is directly bonded to the metal. Compounds in which fluorine is attached only to elements other than carbon are not considered.

The review covers the period January 1972 to December 1975 inclusive, and is intended to extend the sections on transition metal complexes in the earlier reviews in Vols. 1–6. (1) Like them, it is intended to gather together as much as possible of the scattered information, including, where possible, that deposited as “Supplementary Material” with the British Library, on chemical shifts and coupling constants of this important group of compounds.

As in previous years, all chemical shifts are given relative to CFCl_3 ($\delta_{\text{CFCl}_3} = 0$) with negative values when the resonance is to lower frequency (i.e. to higher field) than the reference. The following shift values have been used where necessary to bring reported shifts to the CFCl_3 scale:

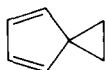
PhCF_3	-63.9(0)
$\text{CFCl}_2\text{CFCl}_2$	-67.3(0)
$\text{CF}_3\text{CO}_2\text{Me}$	-74.2(0)
$\text{CF}_3\text{CO}_2\text{H}$	-78.5(0)
C_6F_6	-162.9(0)

So far as possible, the same order has been used for the fluoroalkyl derivatives in each group of transition metals: σ -bonded alkyl, alkenyl, and alkynyl derivatives, π -bonded derivatives, and then derivatives bonded via N, P, O, or S in that order. In some cases, notably olefin complexes, there is ambiguity about the bonding and this should be borne in mind when searching for particular compounds. Fluoroaryl and heteroaryl derivatives form a more homogeneous group of compounds, and their parameters are considered together across the transition series.

II. FLUOROALKYL DERIVATIVES

A. Groups IIIb-Vb, including the lanthanides and actinides

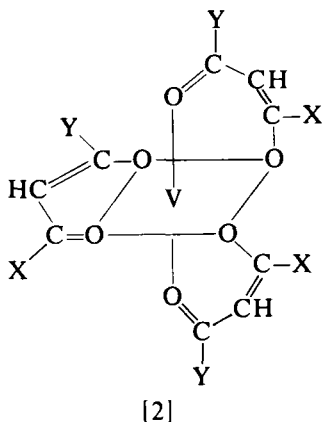
The main interest in fluorocarbon-containing derivatives of these groups lies in the use of lanthanide derivatives as shift reagents. Thus the preparation of $\text{Eu}(\text{FHD})_3$ [$\text{FHD} = \text{C}_2\text{F}_5\text{C}(\text{O}):\text{CHC}(\text{O}^\ominus)\text{C}_2\text{F}_5$] and of the ligand HFHD are described in the patent literature, (2) and $\text{Eu}(\text{TFN})_3$ [$\text{TFN} = n\text{-C}_3\text{F}_7\text{C}(\text{O})\text{CH}:\text{C}(\text{O}^\ominus)\text{C}_3\text{F}_7\text{-}n$] is reported to be a more effective shift reagent than $\text{Eu}(\text{FOD})_3$ for weakly basic substrates such as sulphides; (3) the resonances of cyclopentadiene and of the spiro-compound [1] are also appreciably shifted by this reagent.



[1]

The complex formed by extraction of uranium(IV) from an acidic aqueous solution by benzoyltrifluoroacetone in carbon tetrachloride is also reported to be a useful shift reagent, the shifts induced being to lower frequency. (4) Adducts with complexes formed from uranium(IV) and other fluorinated diketones are also mentioned, but no details of shifts are given.

The inability of normal shift reagents to complex with olefinic double bonds has been overcome by the use of a mixture of silver heptafluorobutyrate and europium or praseodymium heptafluorooctanedionate, the silver interacting with the olefin and the lanthanide with the carboxylate group. (5) The shifts observed are, however, rather small, as expected in view of the distance of the lanthanide from the hydrogens.



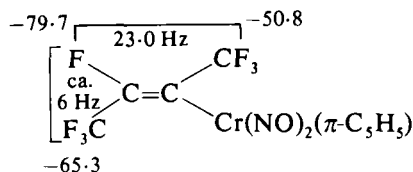
Sixteen structures of the type [2] ($X, Y = \text{CH}_3$ or CF_3) are possible, and the thirty-two possible CF_3 resonances, as well as the same number of CH_3 signals, and 35 of the 36 CH signals have been identified in the spectra of solutions formed by mixing $\text{V}(\text{acac})_3$, $\text{V}(\text{tfacac})_3$ or $\text{V}(\text{hfacac})_3$ with the appropriate free ligand. The results agree well with isotropic shifts calculated on the basis of a model which is discussed in detail in the paper. (6) Chemical shifts for the resonances of a similar system [2] ($X, Y = \text{Ph}, \text{CF}_3$) are also reported.

Complexes are readily formed in solution between lanthanide ions and 2-acetamidohexafluoropropan-2-ol (HAcfp), but in an organic solvent the original complexes decompose to give products tentatively formulated as $\text{M}_2(\text{Acfp})_4(\text{OH})_2 \cdot \text{CH}_3\text{CONH}_2$. (7) The lanthanum complex is the only one of the ten studied ($M = \text{La}, \text{Pr}, \text{Nd}, \text{Sm}, \text{Eu}, \text{Tb}, \text{Dy}, \text{Ho}, \text{Er}, \text{Yb}$) to be diamagnetic, and shows two peaks at $\delta -81.4$ and -82.1 (compared with -82.5 for the free ligand HAcfp). Cerium(III) under similar conditions gives only the neutral eight-coordinate $\text{Ce}(\text{Acfp})_4$, with a singlet at $\delta -80.7$.

B. Chromium, molybdenum, and tungsten

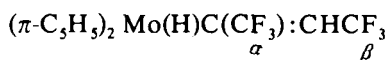
Perfluoro(1-methylpropenyl)silver reacts readily with cyclopentadienyldinitrosylchromium chloride in dichloromethane, to give the

corresponding propenyl derivative [3] with the ^{19}F parameters shown. (8) No coupling between the CF_3 groups was observable, indicating retention of the original *trans* configuration of the silver compound.

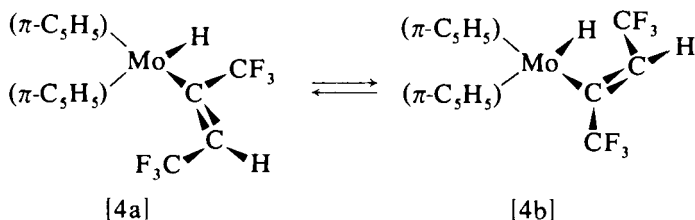


[3]

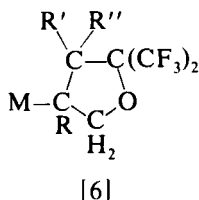
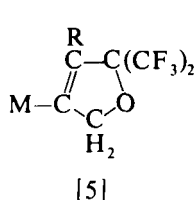
The complex formed by the reaction of dicyclopentadienyldihydromolybdenum with hexafluorobut-2-yne showed, in toluene at room temperature, a pair of equally intense doublets of quartets [δ -58.3 and -59.6, $J(\text{CF}_3\text{-H})$ 9 Hz, $J(\text{CF}_3\text{-CF}_3)$ 2 Hz] for the $\beta\text{-CF}_3$ groups in [4]



[4]

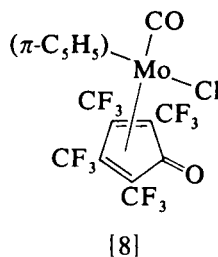
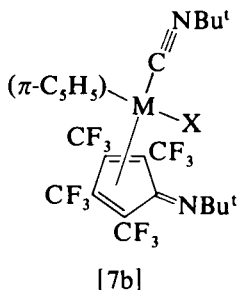
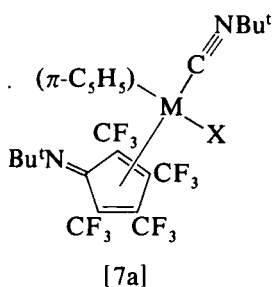


and two equally intense quintets [δ -59.0, -63.9, $J(\text{CF}_3\text{-H}) = J(\text{CF}_3\text{-CF}_3) = 2$ Hz] for the $\alpha\text{-CF}_3$ groups. (9) At -77°C (in THF, immediately after preparation at -78°C) the low-field doublet of quartets and quintet were four times as intense as the high-field pair of signals, but the relative areas changed slowly at room temperature, and equilibration was complete at 54°C in 2 hours. The coupling constants preclude any geometrical isomerization about the double bond, and the appearance of doubled signals is attributed to the presence of two conformers [4a, b], interconversion being slow on the NMR time scale.



A series of complexes containing the dihydrofuranato- or tetrahydrofuranato ring, [5] and [6] respectively, has been prepared by the reaction of the molybdenum or tungsten 2-alkynyl- or 2-alkenyl-complexes with hexafluoroacetone. (10) The CF_3 groups of [5] [$\text{M} = (\pi\text{-C}_5\text{H}_5)\text{Mo}(\text{CO})_3$, $\text{R} = \text{Ph}$] appear as a singlet ($\delta -73.6$), but for [6] [$\text{M} = (\pi\text{-C}_5\text{H}_5)\text{Mo}(\text{CO})_3$, $\text{R} = \text{R}' = \text{H}$, $\text{R}'' = \text{Ph}$, and $\text{M} = (\pi\text{-C}_5\text{H}_5)\text{W}(\text{CO})_3$, $\text{R} = \text{R}' = \text{H}$, $\text{R}'' = \text{Me}$] they appear as pairs of quartets ($\delta -74.4$, -70.4 , J 9.4 Hz, and $\delta -76.2$, -72.2 , J 8.8 Hz respectively), as expected for geminal CF_3 groups adjacent to an unsymmetrically substituted ring carbon.

The dimeric acetylene complex $[(\pi\text{-C}_5\text{H}_5)\text{Mo}(\text{CF}_3\text{C}_2\text{CF}_3)\text{Cl}]_2$ shows a single ^{19}F absorption ($\delta -50.12$), as do the 16-electron bisalkyne complexes $(\pi\text{-C}_5\text{H}_5)\text{Mo}(\text{CF}_3\text{C}_2\text{CF}_3)_2\text{X}$ ($\text{X} = \text{Cl}$, Br , I , $\delta -56.85$ to -56.68) at 307 K, but at 193 K the latter show two signals ($\delta -56.0$ to -55.74 and -57.61 to -57.70). (10a) Discussion of the spectra is reserved for a later paper.



The ^{19}F (and ^1H) spectra of [7a] ($\text{M} = \text{Mo}$, $\text{X} = \text{CF}_3$; $\text{M} = \text{W}$, $\text{X} = \text{Cl}$) are stated to be temperature dependent, consistent with the presence of isomeric species such as [7b], and similar changes are reported for [8], but no details are given. (11)

The reaction of a series of trifluoromethylphosphorus derivatives with tetracarbonylnorbornadiene-molybdenum or -chromium allows the preparation of the corresponding complexes [9] which give well resolved

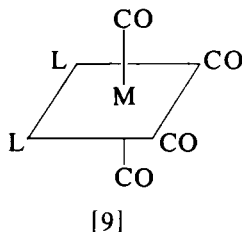


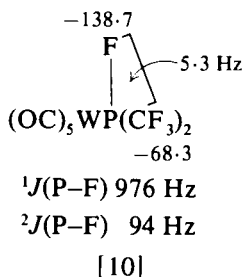
TABLE I

Some ^{19}F NMR parameters^a for *cis*- $\text{L}_2\text{M}(\text{CO})_4$ [9] (12)

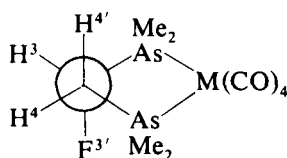
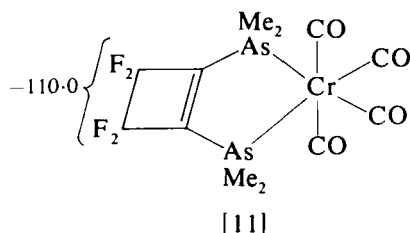
M	L	$^2J(\text{P-P}')$	$^2J(\text{P-F})$	$\Delta^2J(\text{P-F})^b$	$^4J(\text{P-F}')$	δ_{F}	$\Delta\delta_{\text{F}}^c$
Mo	$(\text{CF}_3)_2\text{PCl}$	37.5 ± 0.5	88.4	+3.3	0.7	-65.0	-3.6
Mo	$(\text{CF}_3)_2\text{PBr}$	36.5 ± 0.5	83.4	+2.8	0.5	-63.05	-3.55
Mo	$(\text{CF}_3)_2\text{PI}$	34.4 ± 0.4	74.9	+1.7	0.6	-60.1	-4.7
Mo	$(\text{CF}_3)_2\text{PH}^d$	23 ± 2	73.6	+5.0	0.4	-53.9	-6.4
Mo	CF_3PCl_2	45.4 ± 0.3	97.6	+17.7	0.8	-75.0	-2.9
Mo	CF_3PBr_2	45.8 ± 0.3	87.9	+18.3	0.9	-72.5	-4.7
Mo	CF_3PH_2^e	<i>f</i>	59.7^k	(+11.2)		-51.1	-8.7
Cr	CF_3PH_2^h	<i>f</i>	57.6^k	(+9.1)		-51.0	-8.6
Mo	$(\text{CF}_3)_2\text{PNCS}$	<i>i</i>	91.4^j			-65.7	-3.8
Mo	$(\text{CF}_3)_2\text{PNMe}_2$	<i>i</i>	72.5^j			-59.6	+0.4

^a Chemical shifts in ppm, coupling constants in Hz.^b $^2J(\text{P-F})$ observed - $^2J(\text{P-F})$ ligand.^c δ_{F} observed - δ_{F} ligand.^d $^3J(\text{F-H}) = 7.1$ Hz.^e $^3J(\text{F-H}) = 9.0$ Hz.^f Not resolved.^g $^2J(\text{P-F}) + ^4J(\text{P-F}')$.^h $^3J(\text{F-H}) = 8.8$ Hz.ⁱ Not observed.^j Observed doublet splitting.

^{19}F spectra, the X parts of $[\text{X}_n\text{A}]_2$ systems, in which $J(\text{A-A}') (= ^2J(\text{P-P}'))$ can usually be obtained by inspection. (12) Some of the parameters obtained are given in Table I. The P-F coupling constants have the same sign in all the compounds studied, presumably positive. It is suggested that the simple doublets observed for [9] $[\text{L} = (\text{CF}_3)_2\text{PNMe}_2]$ and $[\text{L} = (\text{CF}_3)_2\text{PNCS}]$ result from chemical exchange between the complexes and small amounts of free ligand in solution, since such exchange is known to relax AX coupling in $\text{AA}'\text{X}$ systems, the resulting spectrum appearing as a doublet when A and A' are strongly coupled. (13) In all the complexes where it could be observed, $^4J(\text{F-F})$ was small, and in most of the $(\text{CF}_3)_2\text{PX}$ complexes $^2J(\text{P-F})$ was within 5 Hz of the value for the free ligand. This coupling constant changed much more markedly for the CF_3PX_2 complexes (9–18.3 Hz). The thermal reaction between $\text{W}(\text{CO})_6$ and $(\text{CF}_3)_2\text{P.P}(\text{CF}_3)_2$ gave mainly [10] with the



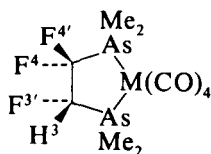
parameters shown, (14) which are similar to those of other complexes of $(\text{CF}_3)_2\text{PF}$. (15)



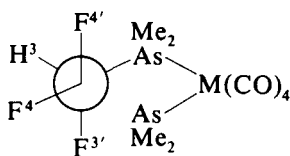
[12]

	12: a, M = Cr	b, M = Mo
$\delta\text{F}^{3'}$	-193.17	-193.47
$J(3-3')$	49.6	49.1 Hz
$J(3'-4)$	15.7	14.0 Hz
$J(3'-4')$	48.3	49.2 Hz

NMR parameters for a wide range of fluorocarbon-containing chelate complexes of di-tertiary arsines and phosphines have been reported. (16-22) The parameters for some are shown in [11] to [19]. Selective $^{19}\text{F}-\{^{19}\text{F}\}$ double resonance studies of the chromium complex [13a] show that $J(\text{F}^4-\text{F}^{3'})$ and $J(\text{F}^{4'}-\text{F}^{3'})$ have the same relative signs, and $J(\text{F}^4-\text{F}^{4'})$ and $J(\text{F}^{4'}-\text{F}^{3'})$ have opposite signs, whence the vicinal F-F couplings are negative. (17) The vicinal H-F couplings in [13a] show that the complex has a strong preference for the conformation in which the two fluorines are in axial positions [14a], and the single fluorine in the monofluoroethane-complex is similarly found to prefer the axial

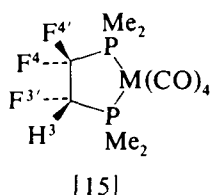


[13]



[14]

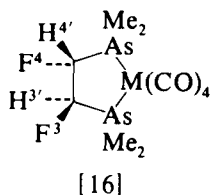
	a, M = Cr	b, M = Mo	c, M = W
$\delta\text{F}^{3'}$	-219.67	-219.29	-219.31
δF^4	-120.06	-119.69	-119.90
$\delta\text{F}^{4'}$	-129.51	-128.42	-130.51
$J(3-3')$	49.1	48.9	48.7
$J(3-4)$	5.3	4.7	4.5
$J(3-4')$	14.8	16.1	15.1
$J(3'-4)$	-23.8	-23.2	-23.6
$J(3'-4')$	-15.9	-16.3	-16.4
$J(4-4')$	267.9	268.4	269.9



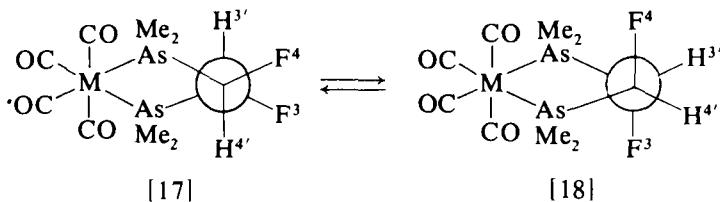
	a, M = Cr	b, M = Mo
$\delta F^{3'}$	-219.49	-219.39
δF^4	-122.40	-122.06
$\delta F^{4'}$	-127.99	-127.50
$J(3-3')$	48.4	48.0
$J(3-4)$	6.0	5.2
$J(3-4')$	18.5	19.7
$J(3'-4)$	-17.6	-16.8
$J(3'-4')$	-15.5	-15.4
$J(4-4')$	269.5	269.8

position [12]. In the solid state, complex [13a] has been shown to have the "equatorial H" structure in accord with the NMR results. (18)

Similar systematic studies of the spectra of the molybdenum and tungsten complexes [13b, c], and of the molybdenum complex [12b] (the tungsten analogue of [12] could not be prepared, the ligand acting in this case only in a non-chelating monodentate fashion) show a similar preference for conformations in which fluorine is axial, and ^{19}F parameters for solutions in CHCl_3 are shown with the structures. (19) Parameters obtained for solutions in other solvents are also given in the paper. The diphosphine derivatives [15a] and [15b], with the parameters shown (the coupling constants between the two different phosphorus atoms and each of the fluorines are also tabulated in ref. 19), were also prepared, and appear to have a similar conformational preference. The complexes [16a] and [16b] of the racemic 1,2-bis(dimethylarsino)-1,2-difluoroethane, however, show a slight preference for the conformation

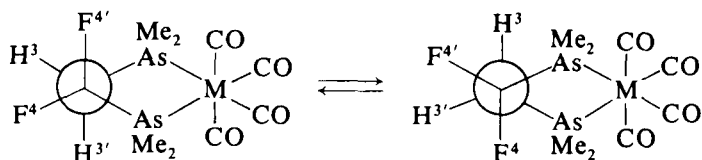


	a, M = Mo	b, M = Cr
δF	-211.96	-212.10
$J(3-3') = J(4-4')$	50.1	49.9
$J(3-4)$	-26.3	-27.9
$J(3-4') = J(3'-4)$	10.4	11.1
$J(3'-4')$	7.4	7.1



[17], in which the fluorine atoms are equatorial rather than [18], with axial fluorines, as shown by the vicinal H-H and H-F coupling constants, and in [19] the vicinal coupling constants are completely

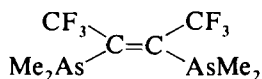
averaged, presumably by rapid (NMR time scale) interconversion of the conformers shown, and only the sum (72, 73, 72 Hz for M = Cr, Mo, W respectively) could be obtained. Variation in the solvents used caused only small and inconclusive changes in the spectra. (19)



δ_F (in C_6H_6) -105.8 for M = Cr (not reported for M = Mo, W)

[19]

Variable temperature studies of [12], [13a], [17] and [19, M = Cr] show little change in coupling constants with temperature, except for [17a], for which the conformer with axial hydrogens has the lower energy. (20) Five-membered ring chelate complexes incorporating a



[20]

double bond have also been prepared from the appropriate metal hexacarbonyl and the ligand [20]. (21) The 1 : 1 complexes $L-LM(CO)_4$ (M = Cr, Mo, W) all show singlet CF_3 absorptions ($\delta -50.2$ to -50.6)

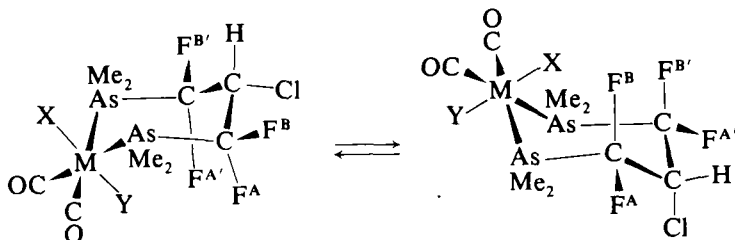
TABLE II

Some ^{19}F NMR parameters for complexes of [20] (21)

Compound ^a	δ_F	$J(F-F)$ Hz
<i>fac</i> -(L-L) ^B (L-L) ^{MC} Cr(CO) ₃	-52.0s, -53.6q, -54.6q	12.0
<i>fac</i> -(L-L) ^B (L-L) ^{MT} Cr(CO) ₃	-51.6s, -50.4q, -52.0q	2.2
<i>cis</i> -(L-L) ₂ ^B Cr(CO) ₂	-50.6s	
<i>trans</i> -(L-L) ₂ ^B Cr(CO) ₂	-49.8s	
<i>fac</i> -(L-L) ^B (L-L) ^{MC} Mo(CO) ₃	-50.8s, -52.9q, -53.0q	11.3
<i>fac</i> -(L-L) ^B (L-L) ^{MT} Mo(CO) ₃	-50.2s, -49.2q, -50.3q	2.3
<i>cis</i> -(L-L) ₂ ^B Mo(CO) ₂	-50.6s	
<i>trans</i> -(L-L) ₂ ^B Mo(CO) ₂	-49.6s	
<i>fac</i> -(L-L) ^B (L-L) ^{MC} W(CO) ₃	-50.8s, -52.7q, -53.0q	13.5
<i>fac</i> -(L-L) ^B (L-L) ^{MT} W(CO) ₃	-50.8br s, -49.6q	2.2
<i>cis</i> -(L-L) ₂ ^B W(CO) ₂	-50.2s	

^a (L-L)^B, bidentate ligand [20]; (L-L)^{MC}, monodentate ligand, *cis* CF_3 groups; (L-L)^{MT}, monodentate ligand, *trans* CF_3 groups.

and also a single As-CH₃ signal, indicating that the chelate ring is either planar in solution, or is in rapid conformational equilibrium between envelope forms. Further reaction of the 1:1 complexes with the ligand gives rise to further substitution products in which the ligand may be bidentate, displacing two carbonyl groups, or may be monodentate and, when co-ordinated in this way, may undergo geometric isomerization photochemically, as shown by the change in $J(\text{CF}_3-\text{CF}_3)$. The parameters reported are summarized in Table II. The complexes *cis*-(L-L)₂M(CO)₂ (M = Cr, Mo, W) each show four signals for the As(CH₃)₂ groups, as expected, but only a single CF₃ signal, and it is presumed that the CF₃ groups are insensitive to the different environments about each arsenic atom.



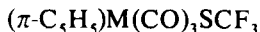
[21a] M = Cr, X = Y = CO

[21b] M = Mo, X = Y = CO

[21c] M = Mn, X = CO, Y = I or X = I, Y = CO

	δ_A	δ_B	$J(\text{A-B})$	$J(\text{A-B}')$	$J(\text{A-A}')$	$J(\text{B-B}')$	$J(\text{F-H})$
[21a]	-91.58	-97.27	+275.2	+2.0	+9.3	+47.2	5.6, 15.2
[21b]	-90.29	-97.34	+276.9	+2.0	+8.3	+49.1	6.0, 15.8

The NMR spectra of the six-membered chelate ring complexes [21] have been analysed with the aid of proton decoupling and weak F-F decoupling to give the complete energy level diagram. The parameters derived are shown. (22) The vicinal H-F couplings are sufficiently different to exclude conformers with the chlorine locked in an axial position, and to make it unlikely that they are very predominant in solution; there are too many uncertainties about the assignments of the fluorines (from the AA'BB' analysis, which does not allow unique assignment of $J(\text{A-A}')$ and $J(\text{B-B}')$) and about the effects of conformation and substitution on $J(\text{F-F}_{vic})$ to clarify the conformational problem further, but an X-ray diffraction study of [21a] shows that the chlorine is equatorial in the crystal. (23)



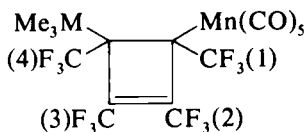
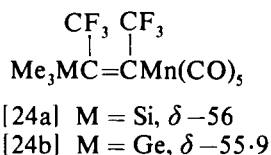
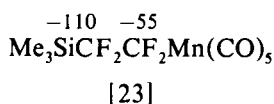
[22a] M = Mo, δ -26.2

[22b] M = W, δ -27.0

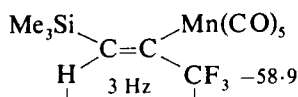
The photochemical reaction between bis(trifluoromethyl)disulphide and $(\pi\text{-C}_5\text{H}_5)\text{Mo}(\text{CO})_3\text{I}$ or $[(\pi\text{-C}_5\text{H}_5)\text{Mo}(\text{CO})_3]_2$ gives the trifluoromethylthio-derivative [22a] with the ^{19}F shift shown, and a similar reaction with $[(\pi\text{-C}_5\text{H}_5)\text{W}(\text{CO})_3]_2$ gives the analogous tungsten compound [22b]. (24) Decarbonylation of [22a] readily gives the dimer $[(\pi\text{-C}_5\text{H}_5)\text{Mo}(\text{CO})_2(\text{SCF}_3)]_2$, which, in view of its single ^{19}F signal ($\delta -40.6$) is assigned the *syn*-form, although the authors point out that this could also be consistent with flexing of the molecule. The analogous tungsten compound could not be isolated, but both molybdenum and tungsten compounds $[\text{M}(\text{CO})_4(\text{SCF}_3)]_2$ ($\text{M} = \text{Mo}$, $\delta -40.5$; $\text{M} = \text{W}$, $\delta -43.1$) were obtained from the reaction between $\text{M}(\text{CO})_6$ and bis(trifluoromethyl)disulphide. (25)

C. Manganese and rhenium

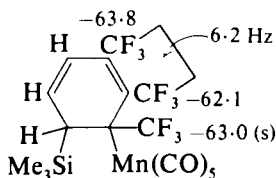
The reactions of $\text{Me}_3\text{MMn}(\text{CO})_5$ ($\text{M} = \text{Si}, \text{Ge}$) with fluoro-olefins and fluoroacetylenes give a range of σ -bonded alkyl- and alkenyl-manganese complexes for which the parameters shown in [23] to [27] are reported. (26) The chemical shifts for [23] are similar to those reported previously (27) for the germanium and tin analogues, but the compounds [24a and



		$\delta\text{CF}_3(1)$	$\delta\text{CF}_3(2)$	$\delta\text{CF}_3(3)$	$\delta\text{CF}_3(4)$
[25a]	$\text{M} = \text{Si}$	-52.8	-54.9	-50.8	-54.9
[25b]	$\text{M} = \text{Ge}$	-53.9	-55.0	-51.1	-56.0
[25c]	$\text{M} = \text{Sn}$	-53.8	-56.9	-51.0	-60.7

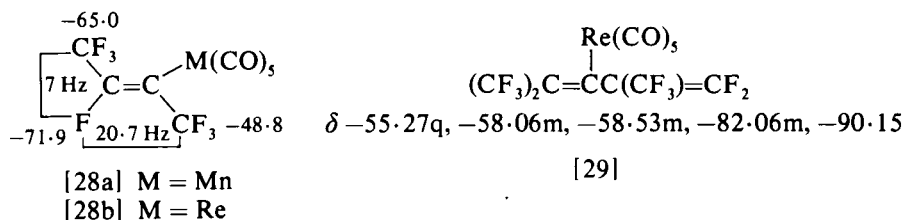


[26]

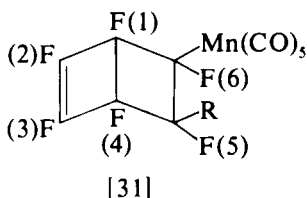
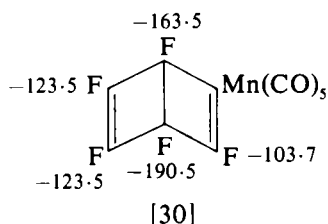


[27]

b] show only a single absorption, presumably because of accidental equivalence. The corresponding tin compound shows the expected two peaks at δ -49.7 and -50.9. (28) In the series [25a-c] the singlets at δ -53 to -54 show coupling to ^{31}P when one carbonyl group is displaced from manganese by triphenyl phosphite, and are therefore assigned to $\text{CF}_3(1)$, and the peaks at highest field are assigned to $\text{CF}_3(4)$ since they show the largest changes in the series. The remaining peaks both show quartet splitting (J 19 Hz) and are assigned to the vinylic CF_3 groups. The structure of [26] was deduced from the chemical shift of the CF_3 group and its coupling to hydrogen, along with the IR data. The reaction of perfluoro-(1-methylpropenyl)silver with bromopentacarbonyl-manganese or -rhenium gives [28a], with the parameters shown, and



[28b] (δ -48.4, -63.3, -80.5, $J(\text{CF}_3-\text{F}_{gem}) \sim 6$, $J(\text{CF}_3-\text{F}_{cis})$ 19.7 Hz), respectively. (8) Rhenium carbonyl anion reacts with perfluoro-(tetramethylallene) to give [29] for which the chemical shifts (only) were reported. (29)

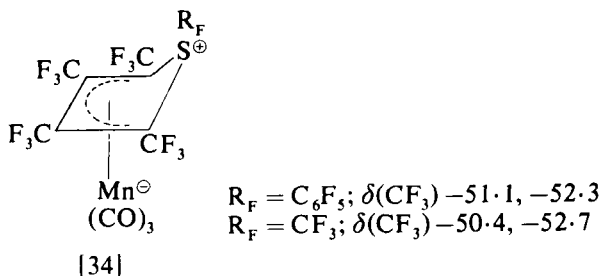
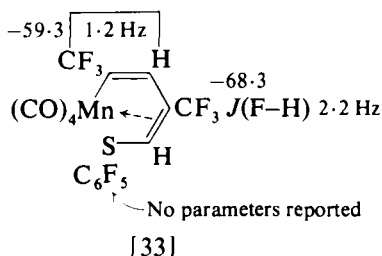
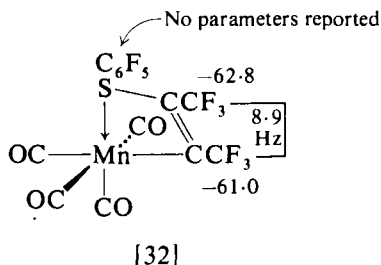


	R	F(1)	F(2)	F(3)	F(4)	F(5)	F(6)
[31a]	H	-159.5	-121.0 ^a	-123.5 ^a	-181.5	-193.5 ^b	-117.1
[31b]	Me	-159.5 ^a	-118.9	-123.9	-188.5	-152.7 ^a	-115.3
[31c]	Ph	-160.1 ^a	-119.3	-125.4	-181.6	-162.1 ^a	-106.1

^a Assignments may be reversed within the pair. ^b Doublet, $J(\text{F}-\text{H})$ 50 Hz.

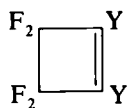
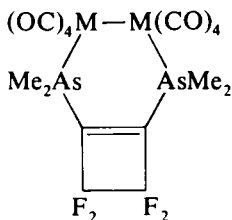
The reaction of perfluorobicyclo[2,2,0]hexa-2,5-diene [(perfluoro)-Dewar-benzene] with $[\text{Mn}(\text{CO})_5]^\ominus$ gives [30], (30) the parameters shown being similar to those reported (31) for the rhenium analogue. The addition-compounds [31a-c] were formed in photochemical reactions of $\text{RMn}(\text{CO})_5$ with the Dewar-benzene. The assignment of the band at highest frequency ($\delta -117.1$) in the spectrum of [31a] to F(6), is in accord with the results for [31b and c], and differs from a previous assignment. (31) The deshielding of the bridgehead fluorines in [31b and c] is taken as evidence that the metal and group R are both on the same side of the molecule as the bridgehead fluorines.

The pentafluorophenylthiolate complex $\{\text{Mn}(\text{CO})_4\text{SC}_6\text{F}_5\}_2$ reacts readily with perfluorobut-2-yne to give the adduct [32], with the



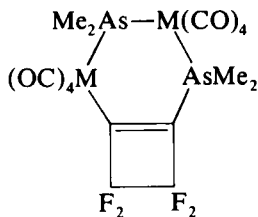
parameters shown. (32) 3,3,3-Trifluoropropyne also reacts readily with the thiolate complex to give [33]. At higher temperatures, $\{\text{Mn}(\text{CO})_4\text{SC}_6\text{F}_5\}_2$ gives [34, $\text{R} = \text{C}_6\text{F}_5$], the structure of which, with the five-membered ring in an envelope conformation with the sulphur displaced away from the metal, has been confirmed crystallographically. (33) The trifluoromethylthiolate $\{\text{Mn}(\text{CO})_4\text{SCF}_3\}_2$ fails to react with perfluorobut-2-yne below 75°C , but above this temperature, [34, $\text{R} = \text{CF}_3$] is formed. The zwitterionic character of this complex is suggested by the chemical shift observed for the $\text{S}-\text{CF}_3$ group ($\delta -68.2$) compared with the normal $\text{S}-\text{CF}_3$ range of $\delta -30$ to -50 .

Parameters reported for the dihydrofuranato- and tetrahydrofuranato-complexes of $\text{Mn}(\text{CO})_5$, [5, $\text{M} = \text{Mn}(\text{CO})_5$, $\text{R} = \text{Me}$,

[35a] Y = AsMe₂[35b] Y = PPh₂

[36a] M = Mn; -107.0

[36b] M = Re; -106.8

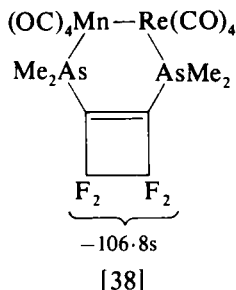


[37a] M = Mn; -103.0, -106.8, complex

[37b] M = Re; -130.5, -134.5, complex

Ph], (δ -75.5s) and [6, M = Mn(CO)₅, R = Ph], (δ -74.7, -71.4, quartets, J 9 Hz), are similar to those of the molybdenum, tungsten, and iron analogues. (10)

The reaction between Mn₂(CO)₁₀ and [35a] ("f₄fars") under UV irradiation in acetone gives the symmetrical product [36a], (16) which, when refluxed in xylene, gives [37a], both structures having been determined crystallographically. (34) A by-product, f₄farsMn(CO)₃Cl (δ -110.3) was also formed. Parameters for the rhenium analogues, [36b] and [37b], and for some similar compounds are given with formulae [36] to [43]. (16, 35, 36) The complex patterns observed for



f₄fosMn₂(CO)₈
Complex patterns,
-106.5, -110.1

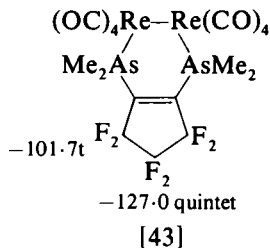
[41]

f₄farsMn(CO)₃I
-110.5s
[39]

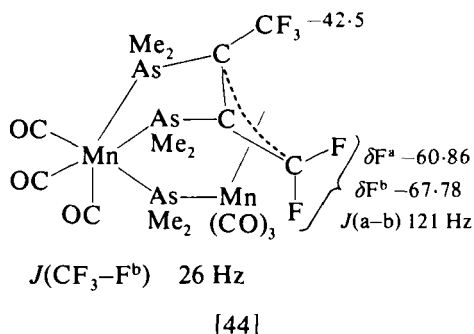
f₄farsRe₂(CO)₈I
-104.8s

[42]

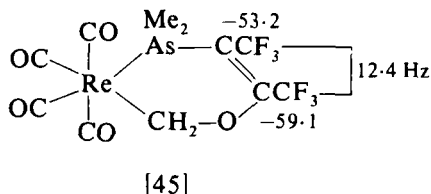
f₄fosRe₂(CO)₈
-107.8s
[40]



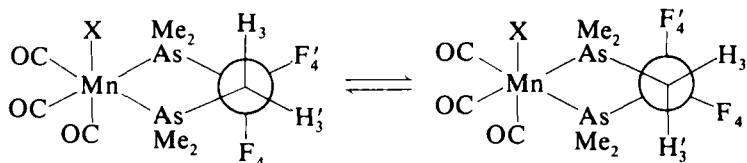
[41], the product of the reaction between [35b] ("f₄fos") and $\text{Mn}_2(\text{CO})_{10}$, contrast with the singlet for the product from $\text{Re}_2(\text{CO})_{10}$. The latter, [40], is thought to be symmetrical, like [36], but the structure of [41] is not yet known. The thermal reaction of $\text{Mn}_2(\text{CO})_{10}$ with *cis*- $\text{CF}_3\text{C}(\text{AsMe}_2):\text{C}(\text{CF}_3)\text{AsMe}_2$ gave a product with a completely different structure, shown crystallographically to be [44], with the parameters



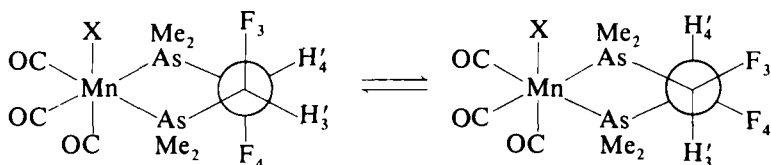
shown. (37) Photochemical reaction of the ligand with $\text{Re}_2(\text{CO})_{10}$ leads to incorporation of a CH_2O group into the product, for which structure [45] is preferred, since the other structure which would fit most of the spectroscopic parameters would contain the grouping $\text{Re}-\text{O}-\text{CH}_2-\text{C}(\text{CF}_3)_2$, and would be expected to show CH_2-CF_3 coupling. (37a) The high frequency quartet in [45] shows further fine structure due to coupling the adjacent AsMe_2 group.



The preparation of a series of five-membered chelate complexes [46a-c], [47a-c], and [48a-c], analogous to the chromium, molybdenum, and tungsten compounds [12-19] and the analysis of their NMR spectra in a range of solvents and at a range of temperatures has been reported. (38) Complete analysis was possible, with the assistance of $^{19}\text{F}\{^1\text{H}\}$ noise decoupled spectra, and the parameters given with the formulae result from iterative analyses. The two conformers of [46a-c] are expected to have very similar vicinal coupling constants, and the relative populations could not therefore be established. The coupling constants in [46a-c] showed the biggest changes with change of solvent of all the chelate

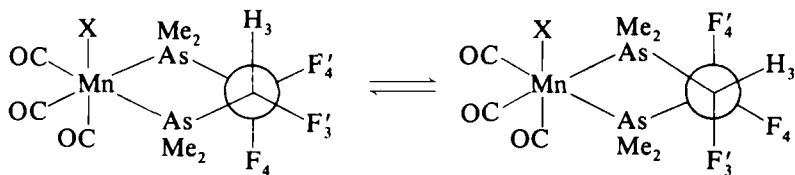


		δF_4	$\delta F_4'$	$J(3-4)$	$J(3-4')$	$J(3'-4)$	$J(3'-4')$	$J(4-4')$
[46a]	X = Cl	-92.06	-107.06	44.9	6.7	12.7	7.0	248.5
[46b]	X = Br	-91.79	-106.62	42.0	7.0	14.9	7.2	248.4
[46c]	X = I	-92.93	-103.59	40.5	7.7	14.5	8.2	245.1



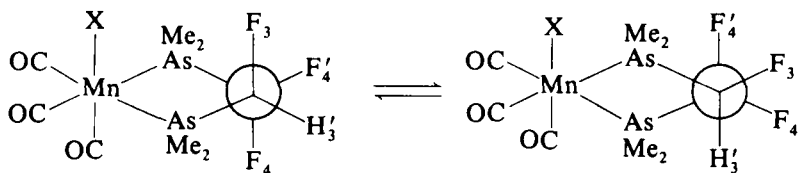
		δF_3^a	δF_4^a	$J(3-3')$	$J(3-4')$	$J(3'-4)$	$J(3'-4')$	$J(4-4')$
[47a]	X = Cl	-214.42	-219.62	52.8	17.4	16.9	-14.2	52.0
[47b]	X = Br	-214.02	-218.66	52.7	17.4	17.1	-15.3	51.9
[47c]	X = I	-213.73	-217.29	52.6	17.9	17.1	-15.6	51.7

^a Arbitrary assignment



		$\delta F_3'$	δF_4	$\delta F_4'$	$J(3-3')$
[48a]	X = Cl	-235.51	-114.55	-121.23	48.5
[48b]	X = Br	-234.27	-114.42	-120.92	48.5
[48c]	X = I	-232.54	-114.59	-120.60	48.3

		$J(3-4)$	$J(3-4')$	$J(3'-4)$	$J(3'-4')$	$J(4-4')$
[48a]	X = Cl	26.4	7.2	-10.9	-12.8	250.4
[48b]	X = Br	26.2	7.3	-10.6	-13.2	251.4
[48c]	X = I	25.2	7.5	-10.9	-13.5	251.0



[48']

complexes studied, but no firm conclusions could be drawn from this. The vicinal H-F couplings for [47a-c] show that the fluorine atoms are gauche both to hydrogens and to each other in the preferred conformation, and for [48a-c] suggest an "equatorial" hydrogen in the preferred conformation, as for the group VI derivatives, (19), possibly with a somewhat smaller "equatorial preference" in [48]. The authors point out, however, that the influence of other changes (e.g. in metal) on the coupling constants are still unknown. No choice is possible on the basis of the present evidence between structure [48] (axial H *syn* to X) and [48'] (axial H *anti* to X), but it is pointed out that the two isomers would be unlikely to have identical shifts and coupling constants, since in [47] the two equatorial fluorines have shifts differing by some 5 ppm.

The six-membered chelate complex [21c] corresponding to the group VI complexes [21a, b] has also been prepared, but only the H-F couplings (4.0, 21.2 Hz) are reported. It is suggested that the higher value for J (H-F *trans*) in this complex may indicate a greater proportion of the conformer with axial hydrogen. (22)

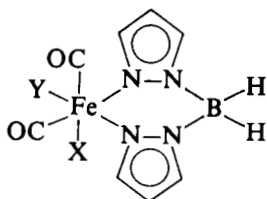
The preparation of pentacarbonyl(trifluoroacetato)manganese has been reinvestigated, and the ^{19}F NMR spectrum is now found to consist of a singlet ($\delta -76.2$) in the range reported for other trifluoroacetate derivatives. (39) Thus the explanation advanced by earlier workers (40) for their failure to obtain ^{19}F NMR spectra for the compounds $\text{Mn}(\text{CO})_5(\text{O}_2\text{CR}_\text{F})$ ($\text{R}_\text{F} = \text{CF}_3$, C_2F_5 , $n\text{-C}_3\text{F}_7$) (that the signals were broadened by coupling to ^{55}Mn , $I = 5/2$) must be discounted.

Photolysis of CF_3SSCF_3 in an open system in the presence of $\text{Mn}_2(\text{CO})_{10}$ gives the known bridged complex $[\text{Mn}(\text{CO})_4(\text{SCF}_3)]_2$, (24, 41) but in a sealed tube, the unstable monomeric complex $\text{Mn}(\text{CO})_5\text{SCF}_3$ ($\delta -25.3$) may be identified spectroscopically. (25)

D. Iron, ruthenium, and osmium

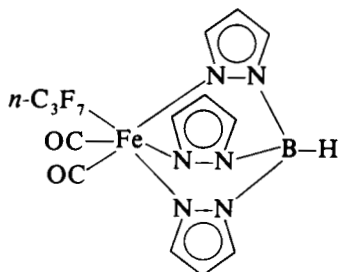
Heptafluoro-*n*-propyliron tetracarbonyl iodide reacts with potassium bis- and tris-pyrazolylborate to give complexes [49] and [50], with the parameters shown. The product [49] was shown by its ^1H NMR spectrum to contain about 30% of the facial isomer [49a], but ^{19}F parameters for this isomer are not reported. (42) The shift to higher frequency of the CF_2 group adjacent to the metal in these complexes is rather less than that in [51]; the parameters for complexes [53, $\text{R}_\text{F} = \text{C}_2\text{F}_5$, $i\text{-C}_3\text{F}_7$] are similar to those shown for [51] and [52]. (8)

The ^{19}F NMR spectrum of $(\pi\text{-C}_5\text{H}_5)\text{Fe}(\text{CO})(\text{PPh}_3)\text{CF}_3$ consists of a doublet [$J(\text{P-F}) 2.9$ Hz] ($\delta +13.5$) which broadens and coalesces as the temperature is reduced. (43) The α -fluorines of the corresponding C_2F_5



[49a] X = CO, Y = $n\text{-C}_3\text{F}_7$

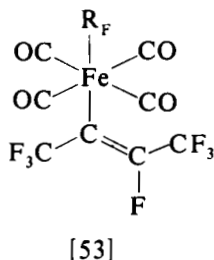
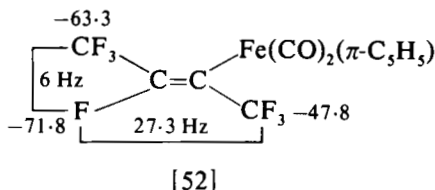
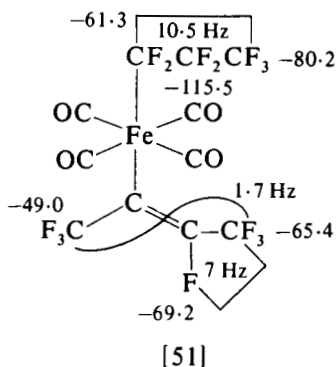
[49b] X = $n\text{-C}_3\text{F}_7$, Y = CO



[50]

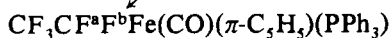
	δCF_3	$\delta\text{CF}_2(\beta)$	$\delta\text{CF}_2(\alpha)$	$J(\text{CF}_3\text{-CF}_2(\alpha))$
[49a]	-80.4	-117	-87.3	14
[50]	-80.3	-117.5	-87.8	14

compound [54] are diastereotopic, due to the chiral iron atom but, as expected for a predominance of conformer [54'], the ^{19}F parameters do not change greatly with temperature. (44) The analogous complexes [55] containing perfluoroisopropyl groups show the expected diastereotopic CF_3 groups, and selective decoupling of these resonances allows observation of the vicinal P-F coupling, the value of which for [55a] ($\text{L} = \text{PPh}_3$) is essentially invariant over the range 200–300 K, again



suggesting a predominance of a single conformation, expected to be that shown. On this basis the larger coupling in [54] might also be assigned

-81.7 -63.3 -59.9

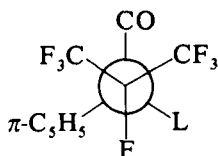
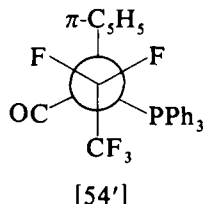


$J(\text{P-F}^{\text{a}})$ 43.6 Hz

$J(\text{P-F}^{\text{b}})$ 1.4 Hz

$J(\text{CF}_3\text{-CF}_2)$ 2.1 Hz

[54]



[55a] L = PPh₃

δCF_3 -66.3, -66.9; $J(\text{CF}_3\text{-CF}_3)$ 9 Hz

δCF -173.2; $J(\text{F-CF}_3)$ 11 Hz, $J(\text{P-F})$ 37.9 Hz

[55b] L = PMePh₂

δCF_3 -66.1, -67.4; $J(\text{CF}_3\text{-CF}_3)$ 10 Hz

δCF -175.6; $J(\text{F-CF}_3)$ 10 Hz, $J(\text{P-F})$ 26.4 Hz

(at room temperature)

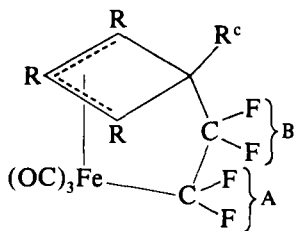
to the gauche coupling and the smaller one to $^3J(\text{P-F}_{\text{trans}})$, but substituent effects may also be important. This coupling changes, however, in [55b] (L = PMePh₂) from 30.0 Hz at 350 K to 18.3 Hz at 210 K (in toluene and methylene chloride respectively, but solvent effects were shown to be small), suggesting that the decrease in ligand size (PMePh₂ < PPh₃) allows the population of other rotamers to a significant extent. The parameters for the compounds $\text{Fe}(\text{CO})_3\text{-LCF}(\text{CF}_3)_2$ [56a, L = PPh₃; b, L = PMePh₂; c, L = PMe₂Ph] are



	δCF_3	$J(\text{P-CF}_3)$	δCF	$J(\text{P-CF})$	$J(\text{CF}_3\text{-CF}_3)$
[56a] L = PPh ₃	-66.5	1.9	-155.8	10	10.5
[56b] L = PMePh ₂	-67.0	2.0	-156.8	11	10.4
[56c] L = PMe ₂ Ph	-67.1	1.9	-157.1	11	10.4

shown with the formulae. Although the phosphines have quite different steric requirements, $^3J(\text{P-F})$ is essentially the same in all three compounds and molecular models support the rationalization that this is due in all three compounds to essentially unhindered rotation about the Fe-C bond.

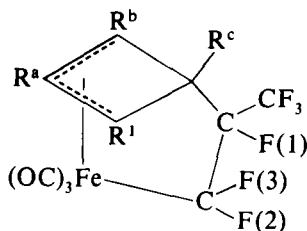
The photochemical reactions of tricarbonylcyclobutadieneiron compounds with tetrafluoroethylene and hexafluoropropene give rise to 1:1 addition compounds [57] to [59], the structures of which were determined spectroscopically. (45) ^{19}F parameters are given with the



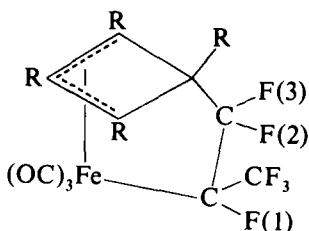
[57a] $R = H$ $\delta CF_2^A -118.0$, $\delta CF_2^B -66.1$, $J(CF_2^B-H^c)$ 5 Hz

[57b] $R = Me$ $\delta -70.8$, -120.8

structures. The CF_2 groups of [57b] both showed triplet splitting ($J(F-F)$ 3.0 Hz), but this was not observable in [57a]. The band at $\delta -66.1$ showed H-F coupling (5 Hz), and was thus assigned to the CF_2-CH group (CF_2^B), leaving the band at -118.0 for the CF_2-Fe group (CF_2^A). Such a low frequency absorption for a CF_2 group adjacent to a low-valent transition metal is certainly unusual (although the authors point out that shifts of $\delta -112$ have been observed for MCF_2CF_2 in metallacyclopentanes (46)), but the H-F coupling in the low-field band appears to preclude the alternative assignment.



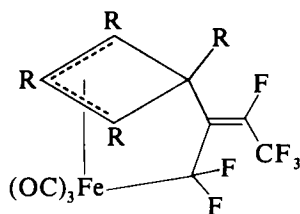
[58]



[59]

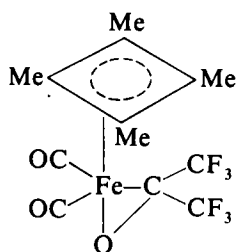
	δCF_3	$\delta F(1)$	$\delta F(2)$	$\delta F(3)$	$J(CF_3-F1)$
a; $R = H$	-69.3	-143.5	-111.8	-120.2	11.0
b; $R = Me$	-69.3	-155.0	-107.5	-123.0	11.0
	$J(CF_3-F2)$	$J(CF_3-F3)$	$J(1-2)$	$J(1-3)$	$J(2-3)$
a; $R = H$	3.0	16.0	—	9.0	244
b; $R = Me$	3.0	17.0	11.0	8.0	240

Both structures [58] and [59] could fit the spectroscopic properties of the adducts with hexafluoropropene, the authors tentatively favouring [58]. A long-range coupling in [58a] between H^a and F1 (3 Hz) is noteworthy, as is the absence of detectable coupling between H^c and fluorine (cf. [57a]). The ^{19}F NMR spectra of the reaction products from the tricarbonylcyclobutadieneiron compounds and hexafluorobutadiene clearly establish that rearrangement of the perfluorodiene has taken

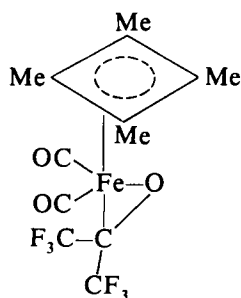


	δCF_3	δCF	δCF_2	$J(\text{CF}_3-\text{CF}_2)$	$J(\text{CF}_3-\text{CF})$	$J(\text{CF}_2-\text{CF})$
[60a] R = H	-68.1	-94.8	-95.8	15.0	11.0	5.0
[60b] R = Me	-68.2	-94.8	-96.8	16.0	11.0	8.0

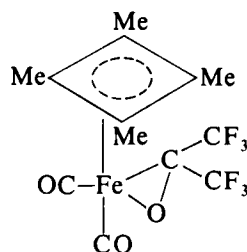
place to give [60]. Hexafluoroacetone reacts with tricarbonyl-(tetramethylcyclobutadiene)iron to give a product shown by its NMR spectra to be a 3:2 mixture of compounds, the minor one of which has chemically equivalent CF_3 groups (sharp singlet, δ -80.0) as required by either [61] or [62], and the major isomer shows a broad signal (δ



[61]

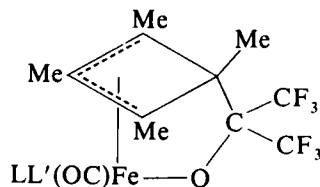


[62]



[63]

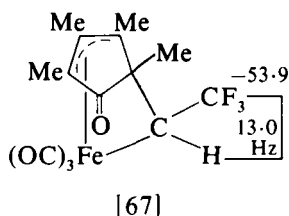
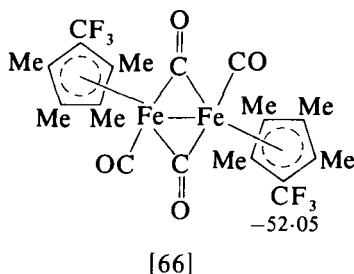
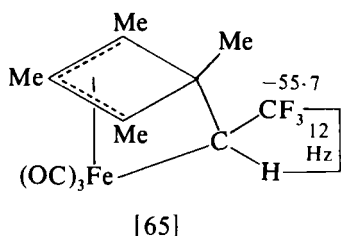
-82.8), in accord with [63]. These complexes react with phosphines or phosphites to give products [64] (δCF_3 -70.4 to -72.4) analogous to [57], [58], and [59], the absence of P-F coupling suggesting that the structures are as shown, rather than having the $\text{FeC}(\text{CF}_3)_2\text{O}$ grouping.



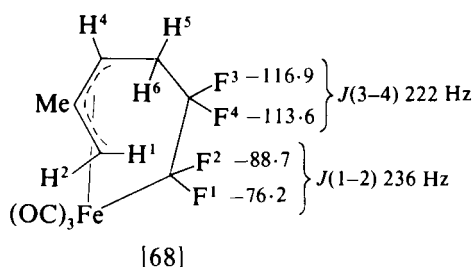
[64]

The reaction of trifluoroethylene with tricarbonyltetramethylcyclobutadieneiron resulted in the unusual insertion product [65], with

^{19}F NMR parameters shown, as well as the product analogous to [57]. (47) When heated, [65] gave a mixture of [66] and [67].

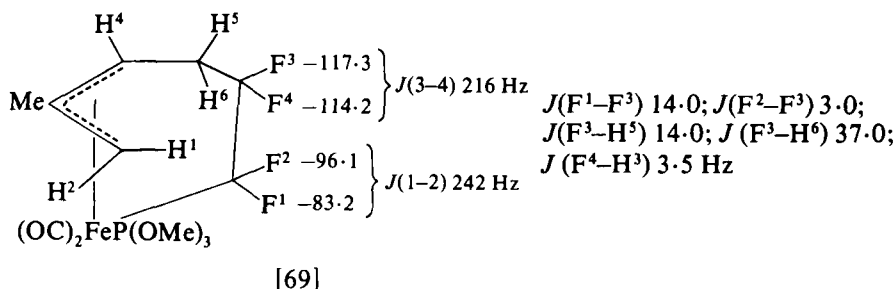


Formally similar products, involving formation of a π -allyl-metal system and insertion of fluoro-olefin between the metal and the terminal carbon of the original diene, are obtained from tricarbonyl(diene)iron compounds and fluoro-olefins. (48) Heteronuclear decoupling was necessary for assignment of some of the coupling constants; some of the decoupling experiments are illustrated in the paper. The parameters obtained for diene = isoprene and fluoro-olefin = C_2F_4 are given with structure [68]; those for diene = butadiene, *trans*-penta-1,3-diene, and

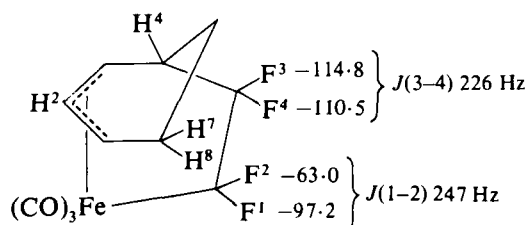


$J(\text{F}^1-\text{H}^5)$ 7.0; $J(\text{F}^1-\text{F}^3)$ 14.0;
 $J(\text{F}^1-\text{F}^4)$ 7.0;
 $J(\text{F}^2-\text{H}^3)$ 3.5; $J(\text{F}^2-\text{H}^1)$ 3.0;
 $J(\text{F}^2-\text{F}^3) = J(\text{F}^2-\text{F}^4) = 3.0$;
 $J(\text{F}^3-\text{H}^5)$ 14.0; $J(\text{F}^3-\text{H}^6)$ 36.0;
 $J(\text{F}^4-\text{H}^3)$ 3.5 Hz.

2,3-dimethylbuta-1,3-diene and fluoro-olefin = C_2F_4 are very similar. The assignment of the high frequency resonances to F1 and F2 is supported by the changes in the shifts and couplings observed when one carbon monoxide is replaced by trimethyl phosphite, to give [69], and the coupling between H^1 and F^2 is apparently a through-space coupling.

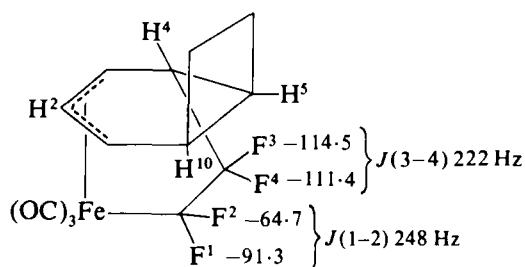


Cyclohexa-1,3-diene- and bicyclo[4,2,0]octa-1,3-diene-tricarbonyl-iron give similar π -allyl systems [70] and [71] in which the CF_2 groups again appear as AB systems with large geminal couplings. The assignments given with [70] are taken from the results section of ref. 48, where the assignments are made on the basis of the observed 7.5 Hz



$$J(\text{F}^2\text{--H}^8) 7.5; J(\text{F}^3\text{--H}^4) 15.0; J(\text{F}^4\text{--H}^2) 4.0 \text{ Hz}$$

[70]

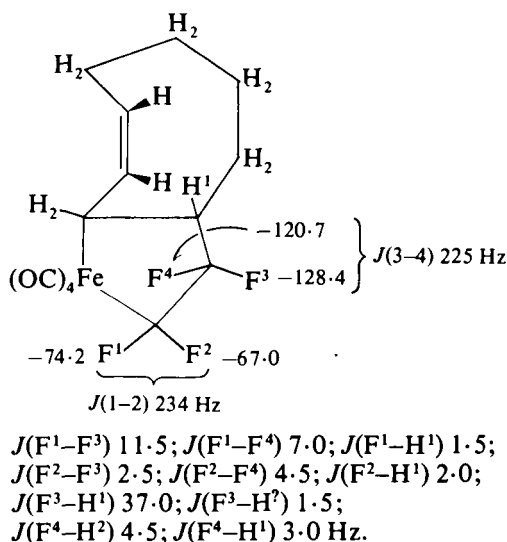


$$\begin{aligned} J(\text{F}^2\text{--F}^3) 13.0; J(\text{F}^2\text{--F}^4) = J(\text{F}^2\text{--H}^{10}) 7.5 \text{ Hz} \\ J(\text{F}^1\text{--F}^3) 8.5; J(\text{F}^1\text{--F}^4) 3.0; J(\text{F}^4\text{--H}^4) 3.0; \\ J(\text{F}^4\text{--H}^2) 3.5; J(\text{F}^3\text{--H}^4) 8.5 \text{ Hz} \end{aligned}$$

[71]

coupling of the band at -63.0 to H^8 by a through-space mechanism, and the authors comment that this represents a reversal of the chemical shifts of F^1 and F^2 compared with [68] and [69].* The parameters for [71] are stated in the Results section to be similar to those of [70], and the figures given with the structure are taken from the Experimental section.

With tricarbonyl(cyclo-octa-1,3-diene)iron, C_2F_4 gives a compound similar to [70] as major product, together with [72] in which the C_2F_4

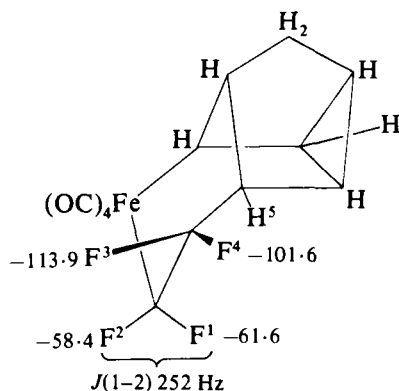


[72]

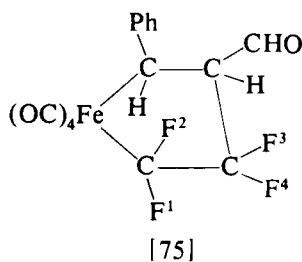
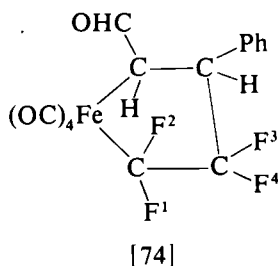
group forms part of a ferracyclopentane ring. The major product has several methylene hydrogens close to the $-CF_2-CH_2-$ chain, and shows more complex multiplet structure for each of the fluorines [F^1 , $\delta -89.8$, F^2 , $\delta -56.6$, $J(F^1-F^2)$ 258 Hz, F^3 , $\delta -107.8$, F^4 , $\delta -103.8$, $J(F^3-F^4)$ 222 Hz] than is found in the other compounds, presumably arising from extensive through-space H-F coupling.

With tricarbonyl(norbornadiene)iron the C_2F_4 group is incorporated into a six-membered ring, suggested to be in the chair form as shown [73]. Ferracyclopentanes [74] and [75] are obtained from the reaction of C_2F_4 with tetra- or tri-carbonyl(*trans*-cinnamaldehyde)iron; although the 1H spectrum shows resonances due to both isomers, the ^{19}F spectrum

* In the Experimental section of ref. 48, however, the band at -63.0 is assigned to F^1 and that at -97.2 to F^2 , and some of the couplings also differ from those given in the Results section. Where there is conflict, the parameters and assignments in the Results section are the correct ones (M. Green, personal communication).



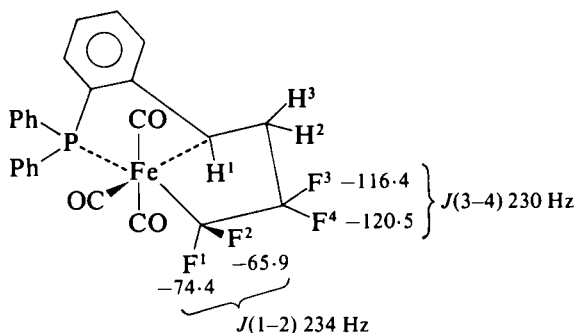
[73]


 $\delta F^1 - 71.8; \delta F^2 - 67.0; \delta F^3 - 125.8; \delta F^4 - 118.2$
 $J(F^1-F^2) \text{ 231}; J(F^3-F^4) \text{ 229}; J(F^1-F^3) \text{ 12.5*}; J(F^1-F^4) \text{ 8.5 Hz*}.$
* From F^1 resonance only

of the mixture shows only four bands, three of which, however, are rather complex, presumably due to overlapping resonances of the two isomers.

With tricarbonyl(*o*-styryldiphenylphosphine)iron, a similar compound, best formulated as [76] in view of the coupling of phosphorus to the α -CF₂ group, is obtained.

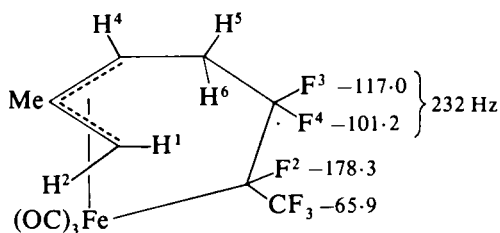
The structure of the complex formed from tricarbonyl(isoprene)iron and hexafluoropropene has been established crystallographically as [77], allowing the assignment of the parameters shown with the structure, and similar assignments for the products from the butadiene- and 2,3-dimethylbutadiene-tricarbonyliron complexes then follow. (49) With tricarbonyl(cyclohexa-1,3-diene)iron, hexafluoropropene gave [78], in



$$J(\text{F}^1-\text{F}^4) = J(\text{F}^1-\text{H}^3) 5.5; J(\text{P}-\text{F}^1) 17.5; J(\text{P}-\text{F}^2) 18.0;$$

$$J(\text{F}^1-\text{F}^3) = J(\text{F}^3-\text{H}^3) 11.0; J(\text{F}^3-\text{H}^2) 33.0 \text{ Hz.}$$

[76]



$$J(\text{CF}_3-\text{F}^2) = J(\text{CF}_3-\text{F}^3) = J(\text{CF}_3-\text{F}^4) 10.5;$$

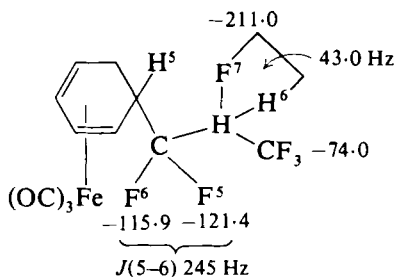
$$J(\text{F}^2-\text{F}^3) 10.5; J(\text{F}^2-\text{H}^1) 8.0;$$

$$J(\text{F}^3-\text{H}^5) 14.5; J(\text{F}^3-\text{H}^6) 39.0;$$

$$J(\text{F}^4-\text{H}^6) 10.6 \text{ Hz.}$$

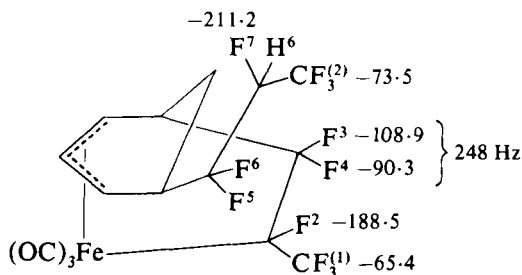
[77]

which the $\text{CF}_3\text{CHFCF}_2$ grouping was readily recognized in the ^{19}F spectrum, [79], which contains both $\text{CF}_3\text{CHFCF}_2$ and the π -allyl group linked to iron via the C_3F_6 group, and [80], with both $\text{CF}_3\text{CHFCF}_2$ and the ferracyclopentane system. The structure of [80] has also been determined crystallographically. The reaction between tricarbonyl(2-ethylcyclohexa-1,3-diene)iron and C_3F_6 gave a single product with spectroscopic properties very similar to those of [79], and the reaction with tricarbonyl(cyclohexa-1,3-diene)ruthenium gave the π -allyl complex [81] analogous to [77], with very similar ^{19}F shifts and coupling constants; the long-range coupling between H^2 and F^4 is again noteworthy.



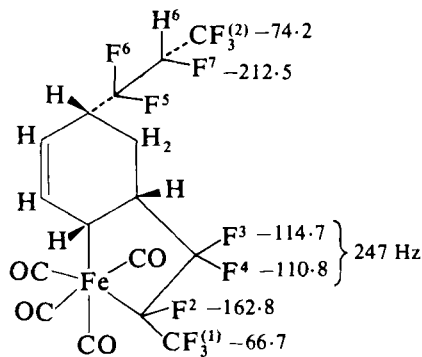
$J(CF_3-F^5)$ 6.0;
 $J(CF_3-F^6) = J(CF_3-F^7) = J(CF_3-H^6)$ 11.0 Hz.

[78]



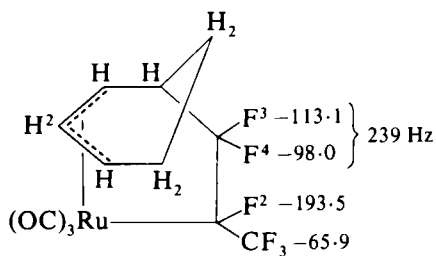
$\delta(F^5, F^6)$ -112.8
 $J(CF_3^{(1)}-F^3)$ 17.0; $J(CF_3^{(1)}-F^2) = J(CF_3^{(1)}-F^4)$ 9.0;
 $J(CF_3^{(2)}-F^6) = J(CF_3^{(2)}-F^7) = J(CF_3^{(2)}-H^6)$ 11.0;
 $J(CF_3^{(2)}-F^5)$ 6.0; $J(F^4-H^2)$ 5.0;
 $J(F^7-H^6)$ 43.0 Hz

[79]



$\delta(F^5, F^6)$ -117.4

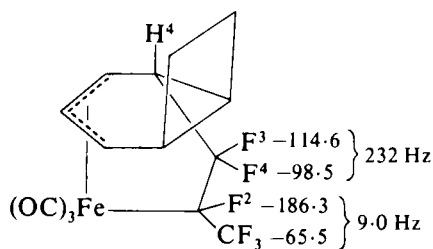
[80]



$$J(\text{CF}_3-\text{F}^3) 17.0; J(\text{CF}_3-\text{F}^2) = J(\text{CF}_3-\text{F}^4) 9.5;$$

$$J(\text{F}^4-\text{H}^2) 4.5 \text{ Hz}$$

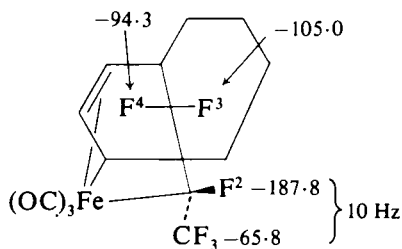
[81]



$$J(\text{F}^2-\text{F}^3) 15.0; J(\text{F}^3-\text{H}^4) 15.0$$

$$J(\text{F}^3-\text{CF}_3) 15.0; J(\text{F}^4-\text{CF}_3) 9.0 \text{ Hz.}$$

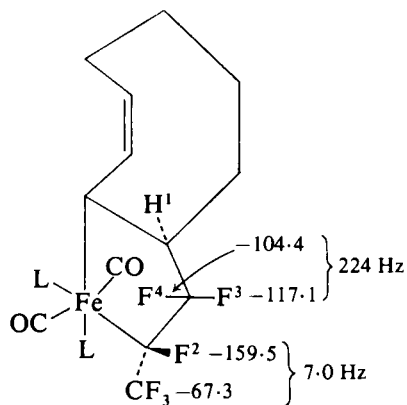
[82]



$$J(\text{F}^3-\text{F}^4) 234; J(\text{CF}_3-\text{F}^3) 15.0;$$

$$J(\text{CF}_3-\text{F}^2) = J(\text{CF}_3-\text{F}^4) 10.0 \text{ Hz.}$$

[83]

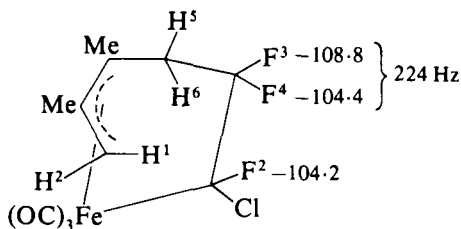


$$J(\text{F}^2-\text{F}^4) 18.0; J(\text{F}^3-\text{H}^1) 41.0 \text{ Hz}$$

[84a] L = P(OMe)₃; Parameters given

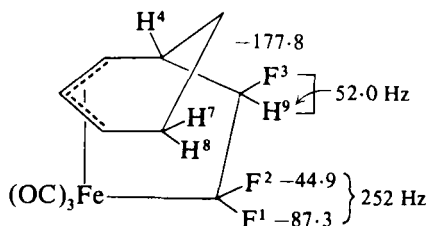
[84b] L = CO

Hexafluoropropene reacted with tricarbonyl(bicyclo[4,2,0]octa,2,4-diene)iron and with the cyclo-octa-1,3-diene complex to give the single products [82] and [83] respectively. When [83] was refluxed with trimethyl phosphite, [84a] was formed, with the parameters shown. Refluxing [83] in hexane alone gave [84b] with reportedly similar parameters. The reaction of tricarbonyl(2,3-dimethylbutadiene)iron with chlorotrifluoroethylene gave [85], analogous to [77], but the orientation of the CF_2CFX chain was reversed when trifluoroethylene gave [86] and [87]. The configuration is indicated by the large coupling of F3 to



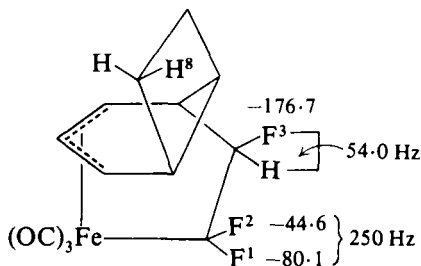
$J(\text{F}^2-\text{F}^3)$ 11.0; $J(\text{F}^2-\text{F}^4)$ 20.0; $J(\text{F}^2-\text{H}^1)$ 5.0;
 $J(\text{F}^2-\text{H}^6)$ 4.0; $J(\text{F}^3-\text{H}^5)$ 15.0; $J(\text{F}^3-\text{H}^6)$ 35.0;
 $J(\text{F}^4-\text{H}^5)$ 1.0; $J(\text{F}^4-\text{H}^6)$ 4.0 Hz.

[85]



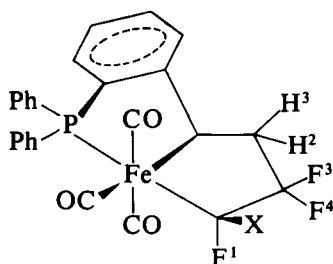
$J(\text{F}^1-\text{F}^3)$ 15.0; $J(\text{F}^2-\text{F}^3)$ 17.0; $J(\text{F}^2-\text{H}^8)$ 7.5;
 $J(\text{F}^3-\text{H}^4)$ 16.0 Hz.

[86]



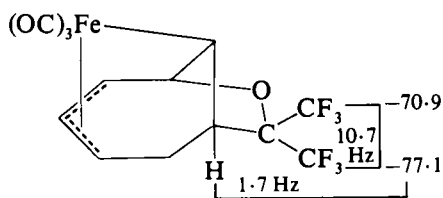
[87]

H4 and the through-space coupling of F2 to H8 in [86], and by the broadening of the CF_2 group resonances, but not of the CFH resonance, when [87] is treated with trimethyl phosphite.

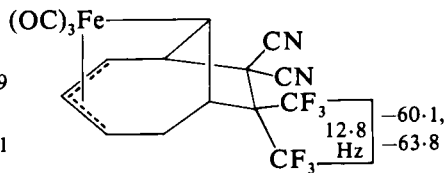


	X	δF^1	δF^3	δF^4	$J(F^3-F^4)$	$J(F^3-H^2)$	$J(F^3-H^3)$
[88a]	CF_3	-162.3	-119.1	-108.3	236	36.0	7.5
[88b]	H	-55.2	-115.3	-94.2	219	35.0	13.0
[88c]	Cl	-79.7	-106.2	-115.9	225	35.0	12.5

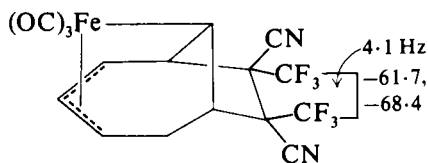
Irradiation of tricarbonyl(*o*-styryldiphenylphosphine)iron with the fluoro-olefins $\text{CF}_2:\text{CFX}$ ($\text{X} = \text{CF}_3, \text{Cl}, \text{H}$) gave the complexes [88] (cf.



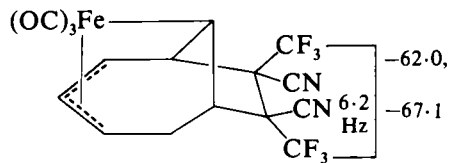
[89]



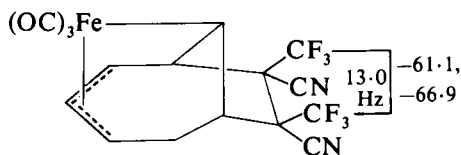
[90]



[91]



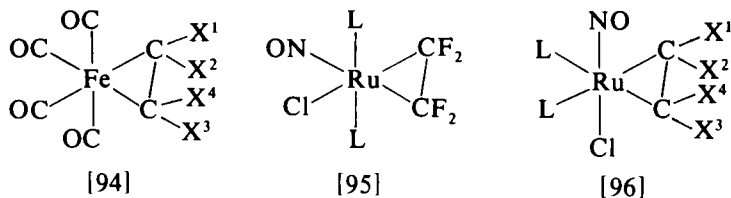
[92]



[93]

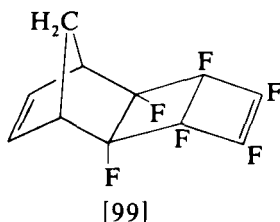
	δF^1	δF^3	δF^4	δF^5	δF^6
[97]	-176.1	-108.3	-187.5	-124.5	-123.7
[98a]	-177.1	-103.3	-187.1	-180.3	-179.5
[98b]	-179.5	-106.3	-189.5	-186.1	-185.5

TABLE III

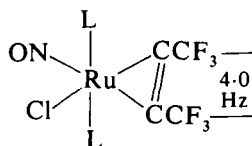
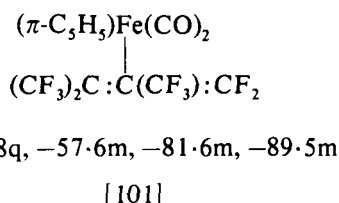
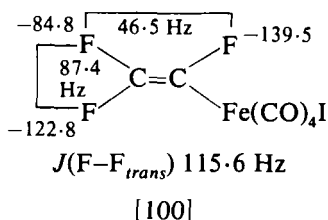
Some ^{19}F NMR parameters of olefin complexes [94]–[96]

Compound	Olefin $\text{CX}^1\text{X}^2:\text{CX}^3\text{X}^4$	$\delta\text{X}(1)$	$\delta\text{X}(2)$	$\delta\text{X}(3)$	$\delta\text{X}(4)$	$J(\text{X}^1-\text{X}^2)$	Notes	Ref.
94	$\text{CFF}:\text{CFH}$	-92.5	-101.5	-205.5	—	138		51
94	$\text{CFF}:\text{CHCl}$	-81.9	-88.1	—	—	113		51
94	$\text{CFF}:\text{CHBr}$	-84.9	-89.1	—	—	109		51
94	$\text{CFF}:\text{CBrBr}$	-77.9	-77.9	—	—	—		51
94	$\text{CFH}:\text{CHH}$	-159.5	—	—	—	68		51
94	$\text{C}(\text{CF}_3)_2:\text{C}(\text{CF}_3)_2$	-50.5	-50.5	-50.5	-50.5	—		51
94	$\text{CF}(\text{CF}_3):\text{CF}(\text{CF}_3)$	-175.5	-68.9	-175.5	-68.9	—		51
94	$\text{CF}(\text{CF}_3):\text{C}(\text{CF}_3)\text{F}$	-167.5	-68.4	-68.4	-167.5	—		51
94	$\text{CH}(\text{CF}_3):\text{CHCF}_3$	—	-60.5	—	-60.5	—		51
94	$\text{CHF}:\text{CFCF}_3$	—	-192.5	-179.5	-71.8	61.7		51
94	$\text{C}(\text{CF}_3)\text{H}:\text{CHH}$	-59.3	—	—	—	2.6		51
95 ^a	$\text{CFF}:\text{CFF}$	-112.9	-112.9	-122.9	-122.9	—	Poorly resolved	52
95 ^b	$\text{CFF}:\text{CFF}$	-113.6	-113.6	-115.1	-115.1	—	Assignment may be reversed	52
96	$\text{CFF}:\text{CClF}$	-99.5	-104.8	—	-111.7	132.0		52
96	$\text{CFF}:\text{C}(\text{CF}_3)\text{F}$	-96.8	-99.8	-66.8	-146.0	142.0		52

^a L = PMePh₂. ^b L = PMe₂Ph.

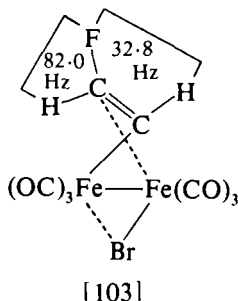


Parameters for tetracarbonyliodo(trifluorovinyl)iron [100], (51) for the product of the reaction of perfluoro(tetramethylallene) with $\text{Na}[\text{Fe}(\text{CO})_2(\pi\text{-C}_5\text{H}_5)]$ [101], (29) and for some ruthenium complexes of



- [102a] $\text{L} = \text{PMePh}_2$; -49.8 , $J(\text{P}-\text{F})$ 2.0 Hz
 -52.7 , $J(\text{P}-\text{F})$ 3.3 Hz
 [102b] $\text{L} = \text{PMe}_2\text{Ph}$; -50.9 ; $J(\text{P}-\text{F})$ 1.7 Hz
 -54.0 , $J(\text{P}-\text{F})$ 2.8 Hz

hexafluorobut-2-yne [102] (52) are given with the structures. The stereochemistry of the ruthenium complexes follows from the observation of triplet splittings from phosphorus in the non-equivalent CF_3 resonances. Irradiation of the olefin complex $(\text{CHFCHBr})\text{Fe}(\text{CO})_4$ resulted in a complex reaction sequence giving [103], with the coupling constants shown. (54)

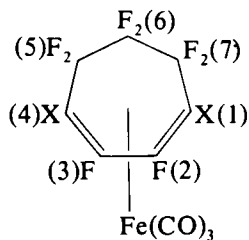


The dihydrofuranato complexes [5, $M = (\pi\text{-C}_5\text{H}_5)\text{Fe}(\text{CO})_2$, $R = \text{Me}$, Ph] show singlet ^{19}F resonances ($\delta -74.1$, -73.6 respectively), but for $M = (\pi\text{-C}_5\text{H}_5)\text{Fe}(\text{CO})\text{PPh}_3$ the iron is chiral and the two CF_3 groups are thus non-equivalent ($\delta -74.0$, -72.9 , J 9.0 Hz). (10) The tetrahydrofuranato-compounds [6, $M = (\pi\text{-C}_5\text{H}_5)\text{Fe}(\text{CO})_2$, R^1 , R^2 , R^3 variously H, Me, Ph] give pairs of quartets ($\delta -71.1$ to -81.0 , J 8.5–10.3 Hz).

The preparation of some (polyfluorocyclohepta-1,3-diene)iron tricarbonyl complexes [104] is reported, and parameters are given in Table IV. (55) The appearance of the geminal fluorines at C5 and C7 as an AB quartet when the adjacent carbon (C4 or C1) carries a fluorine, but as a singlet when the vinylic neighbour is hydrogen is noteworthy. Since a crystallographic study shows that the ring is puckered across the line C1–C4, (56) this must be due to accidental equivalence.

TABLE IV

Some ^{19}F NMR parameters for (polyfluorocycloheptadiene)iron tricarbonyl compounds [104] (55)

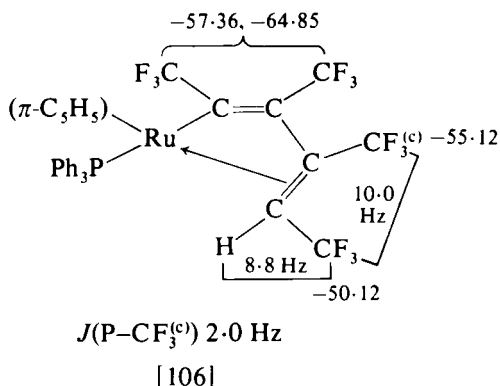
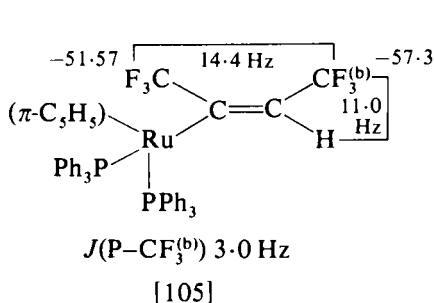


[104]

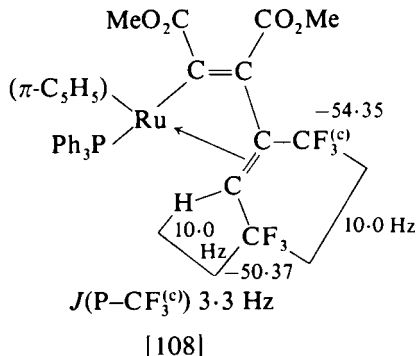
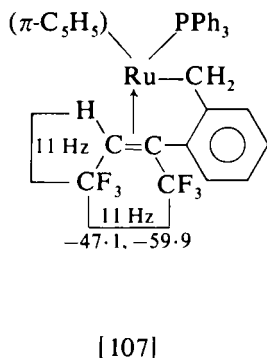
		Chemical Shifts (δ)						
X(1)	X(4)	X(1)	F(2)	F(3)	X(4)	CF ₂ (5)	CF ₂ (6)	CF ₂ (7)
F	F	-179.6	-171.7	-171.7	-179.6	-104.9 ^a -116.4 ^a	-144.4 ^b -144.4 ^b	-104.9 ^a -116.4 ^a
H	F	—	-148.6	-168.9	-177.2	-104.7 ^c -115.9 ^c	-114.5 ^d -141.5 ^d	-93.5 -93.0
H	H	—	-148.1	-148.1	—	-93.0	-113.9 ^d -140.1 ^d	-93.0

^a $J(\text{A}-\text{B})$ 263 Hz. ^b $J(\text{A}-\text{B})$ 281 Hz. ^c $J(\text{A}-\text{B})$ 259 Hz. ^d $J(\text{A}-\text{B})$ 276 Hz.

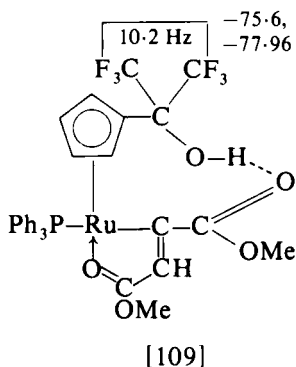
The reaction of the ruthenium hydride $\text{RuH}(\text{PPh}_3)_2(\pi\text{-C}_5\text{H}_5)$ with $(\text{CF}_3)_2\text{C}:\text{C}(\text{CN})_2$ gives the 1:1 adduct $(\pi\text{-C}_5\text{H}_5)(\text{Ph}_3\text{P})_2\text{RuC}(\text{CN})_2\cdot\text{CH}(\text{CF}_3)_2$ ($\delta\text{CF}_3 - 68.31$, $J(\text{F}-\text{H})$ 8.2 Hz), and with hexafluorobut-2-yne both the 1:1-adduct [105], the stereochemistry shown following from the $\text{CF}_3\text{--CF}_3$ coupling, and a double-insertion



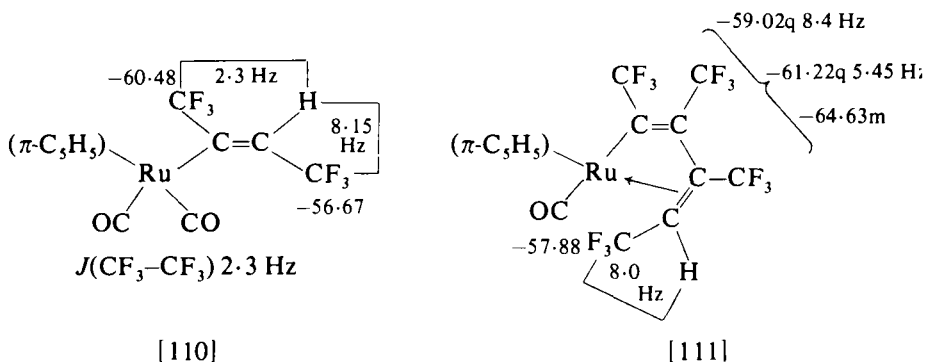
product [106], the four signals for which were assigned by decoupling experiments. (51) Similar products [107], (58) in which hexafluorobut-2-yne is thought to have inserted into an *ortho* C-H bond of the benzyl group as shown, and [108] (57) are also reported, but hexafluoroacetone



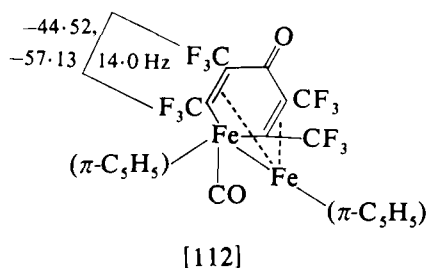
attacked the $\pi\text{-C}_5\text{H}_5$ ring of $\text{Ru}(\text{PPh}_3)(\pi\text{-C}_5\text{H}_5)(\text{MeO}_2\text{CC}:\text{CHCOMe})$ to give [109], in which the high frequency CF_3 group is also coupled to



hydrogen ($J(\text{F}-\text{H})$ 1.5 Hz). The structure of [109] has been confirmed crystallographically. (59) Insertion of perfluorobut-2-yne into a $\text{Ru}-\text{H}$ bond to give *trans* CF_3 groups, as shown by the low values of $J(\text{CF}_3-\text{CF}_3)$ in [110] and [111] shows that the course of the insertion reaction

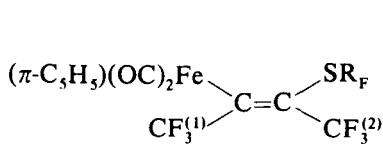


depends on the other ligands attached to the metal. (60) Although [110] can also be obtained from the reaction of hexafluorobut-2-yne with $[\text{Ru}(\text{CO})(\pi\text{-C}_5\text{H}_5)_2]$, with $[\text{Fe}(\text{CO})(\pi\text{-C}_5\text{H}_5)_2]$, a quite different compound, shown crystallographically to be [112], results.

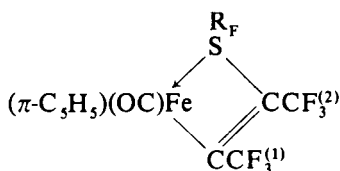


The reaction of $[(\pi\text{-C}_5\text{H}_5)(\text{OC})_2\text{Fe}(\text{SR}_f)]$ ($\text{R}_f = \text{CF}_3$ or C_6F_5) gives [113], with the parameters shown, the geometry of the olefinic group following from the high CF_3-CF_3 coupling. (32) These compounds are decarbonylated photochemically to give the cyclic compounds [114] in which the coupling between the CF_3 groups, necessarily *cis*, is much reduced (cf. also compound [32]).

The parameters for a number of cyclopentadienyliron and related compounds containing fluoroalkyl groups attached to the ring(s) are given with structures [115] to [118]. (32, 60-62) (see also [66] and [109]) The CF_2 resonance in [115] surprisingly appears as a triplet, presumably because of equal coupling to two different hydrogens, but

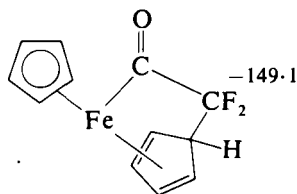


[113]

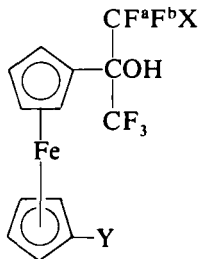


[114]

	$\delta\text{CF}_3^{(1)}$	$\delta\text{CF}_3^{(2)}$	$J(\text{CF}_3-\text{CF}_3)$
[113a] $\text{R}_\text{F} = \text{CF}_3$ (−42.7)	−52.0	−56.6	15.8
[113b] $\text{R}_\text{F} = \text{C}_6\text{F}_5^a$	−49.3	−53.8	16.0
[114a] $\text{R}_\text{F} = \text{CF}_3$ (−47.9)	−59.9	−62.6	8.5
[114b] $\text{R}_\text{F} = \text{C}_6\text{F}_5^a$	−60.1	−62.9	7.9

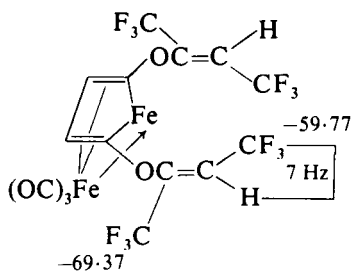
^aNo parameters reported for C_6F_5 group


[115]

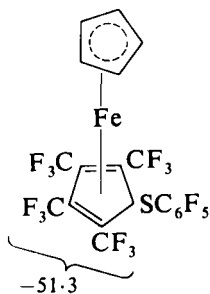

 [116a] $\text{X} = \text{F}, \text{Y} = \text{H}; \delta -75.00$ brs

 [116b] $\text{X} = \text{Y} = \text{H}; \delta\text{CF}_3 -74.94, \delta\text{F}^a -126.25,$
 $\delta\text{F}^b -130.45, J(\text{F}^a-\text{F}^b) 292,$
 $J(\text{F}^a-\text{H}) 55, J(\text{F}^b-\text{H}) 54, J(\text{F}^a-\text{CF}_3) 10,$
 $J(\text{F}^b-\text{CF}_3) 8$ Hz.

 [116c] $\text{X} = \text{F}, \text{Y} = \text{COMe}; \delta\text{CF}_3 -75.21$ s

 [116d] $\text{X} = \text{F}, \text{Y} = \text{COPh}; \delta\text{CF}_3 -74.81$ s


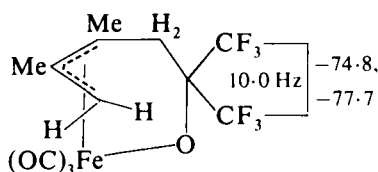
[117]



[118]

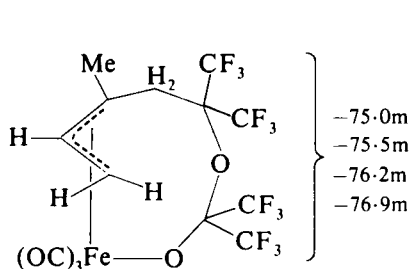
the structure is firmly established crystallographically. (60) The CF_3 groups in [117] show no quartet splittings, and so are clearly *trans*. The comment in the paper (62) that "values for $J(\text{CF}_{3\text{gem}}-\text{H})$ are generally $< 2 \text{ Hz}$ ", is clearly a slip of the pen ($\text{CF}_{3\text{gem}}$ for $\text{CF}_{3\text{vic}}$; see, e.g. Table V, p. 122 Vol. 5A, and compounds in this review) and the assignments shown are made on the usual basis.

The reaction of hexafluoroacetone with tricarbonyl(2,3-dimethylbutadiene)iron slowly gives [119], the chemical shift of the CF_3 groups

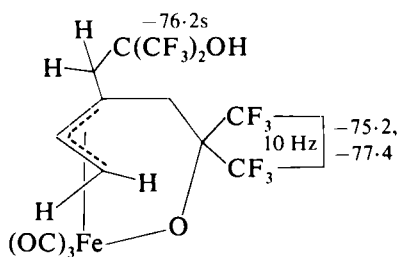


[119]

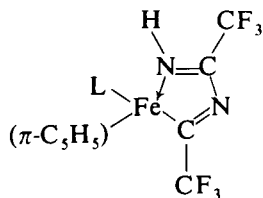
favouring the formulation shown, rather than the possible isomer containing the $\text{FeC}(\text{CF}_3)_2\text{O}$ grouping. (63) The corresponding (isoprene)iron compound however, rapidly gives a 2:1 insertion product, for which structure [120] is favoured, partly on the basis of its thermal rearrangement to [121].



[120]



[121]

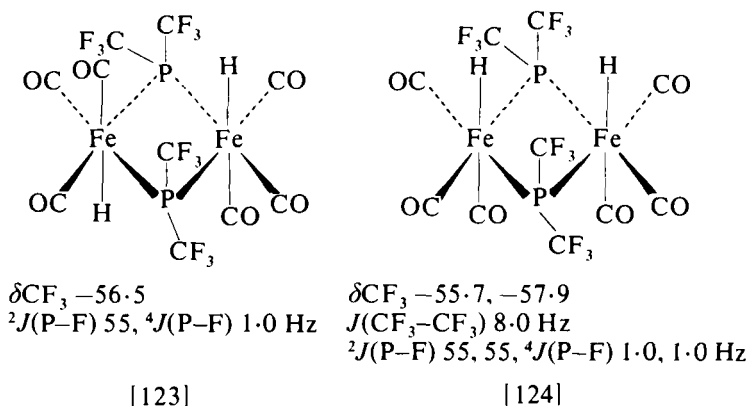


[122a] $\text{L} = \text{CO}$

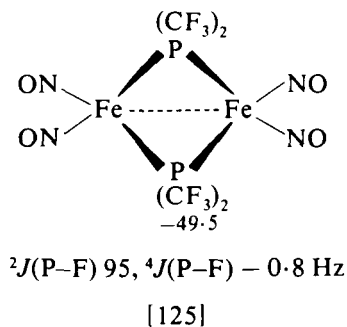
[122b] $\text{L} = \text{PMe}_2\text{Ph}$

δCF_3 -63.90s, -68.35s

The reaction between $[\text{FeMe}(\text{CO})_2(\pi\text{-C}_5\text{H}_5)]$ and CF_3CN has been reinvestigated, (64) and an X-ray structure determination shows that the initial product, which had identical spectroscopic properties to those originally reported, (65) has the structure [122a, $\text{L} = \text{CO}$] rather than the original formulation as $[\text{Fe}(\text{CO})\{\text{C}(\text{CF}_3):\text{NH}\}(\text{CF}_3\text{CN})(\pi\text{-C}_5\text{H}_5)]$. Chemical shifts for the derivative [122b, $\text{L} = \text{PMe}_2\text{Ph}$] are given with the structure.



The NMR parameters for a series of iron complexes containing $\text{P}(\text{CF}_3)_2$ and $\text{P}(\text{CF}_3)$ groups are shown with formulae [123] to [130] and in Tables V and VI, (66–70) and for some fluorophosphine complexes containing $\text{C}(\text{CF}_3)_2$ groups in [131]–[133]. (71). The assignment of *trans* and *cis* geometries to [123] and [124] respectively is based on the ^1H and ^{19}F NMR spectra, [123] giving a ^{19}F spectrum analysed as an $[\text{AX}_6]_2$ system, as does the nitrosyl compound [125]. (66) Oxidation of



the terminal phosphido group in $(\pi\text{-C}_5\text{H}_5)\text{Fe}(\text{CO})_2\text{P}(\text{CF}_3)_2$ leads to shifts of the CF_3 resonance to lower frequency, as expected for a $\text{P}(\text{V})$ compound, and an increase in $J(\text{P}-\text{CF}_3)$ (see Table V). (67) Prolonged

TABLE V

Some NMR parameters for $(\text{CF}_3)_2\text{P}$ compounds

Compound	δ_F	$^2J(\text{P}-\text{F})$	Ref.
$(\text{CO})_4\text{Fe}\{\text{PH}(\text{CF}_3)_2\}^a$	-57.2	79	66
$(\pi\text{-C}_5\text{H}_5)\text{Fe}(\text{CO})_2\{\text{P}(\text{CF}_3)_2\}$	-45.5	54.3	67
$(\pi\text{-C}_5\text{H}_5)\text{Fe}(\text{CO})_2\{\text{P}(\text{O})(\text{CF}_3)_2\}$	-70.5	71.8	67
$(\pi\text{-C}_5\text{H}_5)\text{Fe}(\text{CO})_2\{\text{P}(\text{S})(\text{CF}_3)_2\}$	-67.0	71.0	67
$(\pi\text{-C}_5\text{H}_5)\text{Fe}(\text{CO})_2\{\text{P}(\text{Se})(\text{CF}_3)_2\}$	-65.4	67.0	67
$[(\pi\text{-C}_5\text{H}_5)\text{Fe}(\text{CO})\{\text{P}(\text{CF}_3)_2\}]_2$	-52.4	ca. 50	67
$(\pi\text{-C}_5\text{H}_5)\text{Fe}(\text{CO})_2\{\text{SP}(\text{CF}_3)_2\}$	-59.5	71.0	67
$(\pi\text{-C}_5\text{H}_5)\text{Fe}(\text{CO})_2\{\text{SeP}(\text{CF}_3)_2\}$	-56.6	66.0	67
$(\pi\text{-C}_5\text{H}_5)\text{Fe}(\text{CO})_2\{\text{SP}(\text{S})(\text{CF}_3)_2\}$	-71.2	92.0	67
$[(\pi\text{-C}_5\text{H}_5)\text{Fe}(\text{CO})_2\{\text{P}(\text{CF}_3)_2\text{Cl}\}]\text{Cl}_3$	-62.4	96	68
$[(\pi\text{-C}_5\text{H}_5)\text{Fe}(\text{CO})_2\{\text{P}(\text{CF}_3)_2\text{Br}\}]\text{Br}_3$	-61.5	92	68
$[(\pi\text{-C}_5\text{H}_5)\text{Fe}(\text{CO})_2\{\text{P}(\text{CF}_3)_2\text{I}\}]\text{I}_3$	-58.4	78	68
$[(\pi\text{-C}_5\text{H}_5)\text{Fe}(\text{CO})_2\{\text{P}(\text{CF}_3)_2\text{H}\}]^\oplus$	-52.6	79	68
$[(\pi\text{-C}_5\text{H}_5)\text{Fe}(\text{CO})_2\{\text{P}(\text{CF}_3)_2\text{OH}\}]^\oplus$	-67.3	85	68
$[(\pi\text{-C}_5\text{H}_5)\text{Fe}(\text{CO})_2\{\text{P}(\text{CF}_3)_2\text{SH}\}]^\oplus$	-61.4	86	68
$[(\pi\text{-C}_5\text{H}_5)\text{Fe}(\text{CO})_2\{\text{P}(\text{CF}_3)_2\text{SeH}\}]^\oplus$	-59.3	71	68

^a $J(\text{F}-\text{H})$ 6.9 Hz.

UV irradiation of $(\pi\text{-C}_5\text{H}_5)\text{Fe}(\text{CO})_2\text{P}(\text{O})(\text{CF}_3)_2$ gives, *inter alia*, a "trimer" formulated as $(\text{C}_5\text{H}_5)_2\text{Fe}_3(\text{CO})_2[\text{OP}(\text{CF}_3)_2]_4$, which shows three broad signals (δ -69.4, -34.2, -11.0, with intensities 1:2:2). The shifts of the two high frequency bands are temperature dependent in a manner suggesting that they are attached to a paramagnetic centre (the solid has a magnetic moment of *ca.* 4.6 B.M.), but no structure has been advanced for the compound.

The spectrum of $[(\pi\text{-C}_5\text{H}_5)\text{Fe}(\text{CO})_2\{\text{P}(\text{CF}_3)_2\text{H}\}]^\oplus[\text{SnCl}_3]^\ominus$ [Table V] is a broad doublet at 293 K, but is fully resolved at 253 K. (68) The ^{19}F

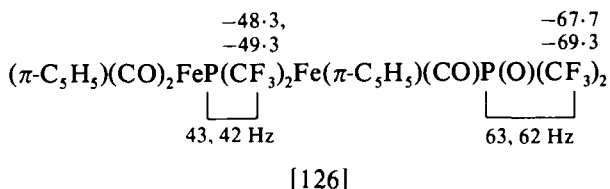
TABLE VI

NMR parameters for some iron complexes of $(\text{CF}_3)_2\text{PEP}(\text{CF}_3)_2$

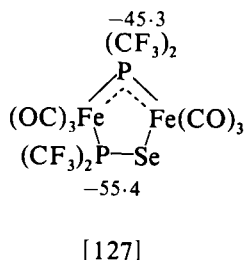
Compound	$\delta\text{F}(1)^a$	$^2J(\text{P}-\text{F})$	$\delta\text{F}(2)^a$	$^2J(\text{P}-\text{F})$	$^4J(\text{P}-\text{F}(2))$
$\text{Fe}(\text{CO})(\text{NO})_2\{(\text{CF}_3)_2\text{POP}(\text{CF}_3)_2\}$	-63.8	94	-67.0	104.5	—
$\text{Fe}(\text{CO})(\text{NO})_2\{(\text{CF}_3)_2\text{PSP}(\text{CF}_3)_2\}$	-54.8	81	-61.4	81	5
$\text{Fe}(\text{CO})(\text{NO})_2\{(\text{CF}_3)_2\text{PSeP}(\text{CF}_3)_2\}$	-52.7	75	-59.9	81	4
$\text{Fe}(\text{CO})_4\{(\text{CF}_3)_2\text{POP}(\text{CF}_3)_2\}$	-63.5	92	-68.1	97	3
$\text{Fe}(\text{CO})_4\{(\text{CF}_3)_2\text{PSP}(\text{CF}_3)_2\}$	-54.4	81	-62.6	81	5

^a F(1) is the CF_3 groups attached to the unco-ordinated phosphorus, F(2) those attached to the co-ordinated phosphorus.

NMR spectra of the complexes of $(\text{CP}_3)_2\text{PEP}(\text{CF}_3)_2$ ($\text{E} = \text{O}, \text{S}, \text{Se}$) (see Table VI for the parameters) show clearly the inequivalence of the two $\text{P}(\text{CF}_3)_2$ groups, one set having shifts close to those of the free ligands, and the other at lower frequency, as expected for the co-ordinated ligands. (69) The reaction of $(\text{CF}_3)_2\text{POP}(\text{CF}_3)_2$ with $[(\pi\text{-C}_5\text{H}_5)\text{Fe}(\text{CO})_2]_2$ gives a product [126] which, at 233 K, gives well-resolved spectra

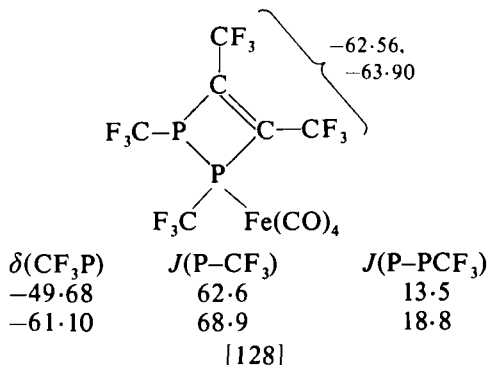


showing two chemically distinct $\text{P}(\text{CF}_3)_2$ groups, in each of which the CF_3 groups are inequivalent. The chemical shifts suggest that the $\text{P}(\text{CF}_3)_2$ group is the bridge, the temperature dependence of the spectrum arising from hindered rotation about the bridging phosphorus. The selenium compound [127], however, appears to be cyclic, as shown,

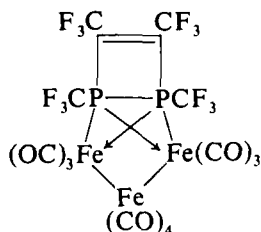


with a metal-metal bond which can invert through the ring to bring about the observed equivalence within the pairs of CF_3 groups.

The ^{19}F NMR spectrum of [128] shows two different CF_3P and two

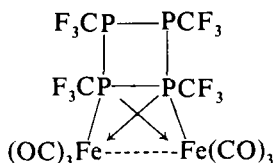


different CF_3C environments, as required for co-ordination of only one of the CF_3P groups, but the CF_3P region of [129] shows an $\text{X}_3\text{AA}'\text{X}'_3$ pattern and only a single CF_3C resonance, while both CF_3P resonances in [130] are deceptively simple. (70)

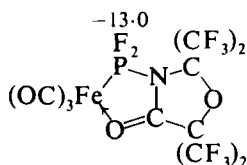


$\delta(\text{CF}_3\text{P}) -56.4$; $\delta(\text{CF}_3\text{C}) -61.6$ $\delta\text{CF}_3 -43.9$ "deceptively simple triplet"
 -45.70 "deceptively simple triplet"

[129]

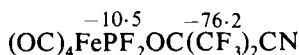


[130]



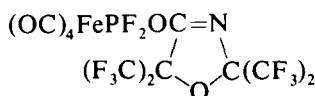
$\delta\text{CF}_3 -72.0\text{s}, -76.5\text{s}$
 $^1J(\text{P-F}) 1264 \text{ Hz}$

[131]



$^1J(\text{P-F}) 1178 \text{ Hz}$

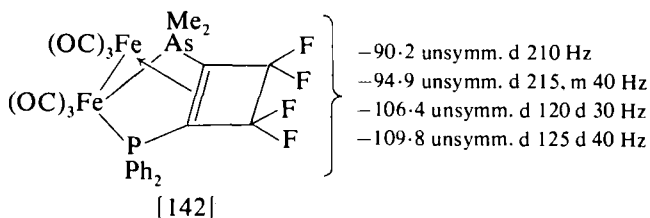
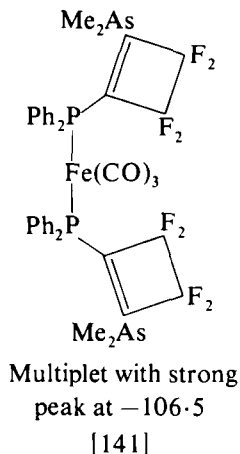
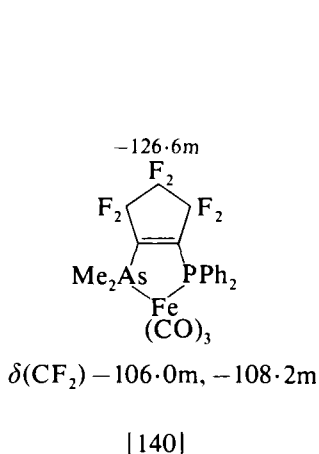
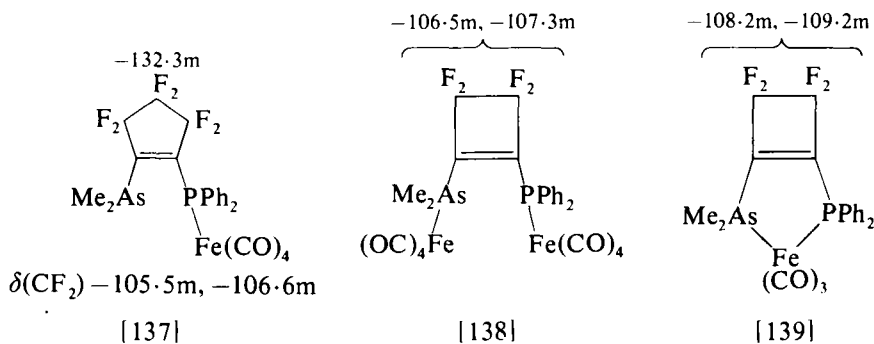
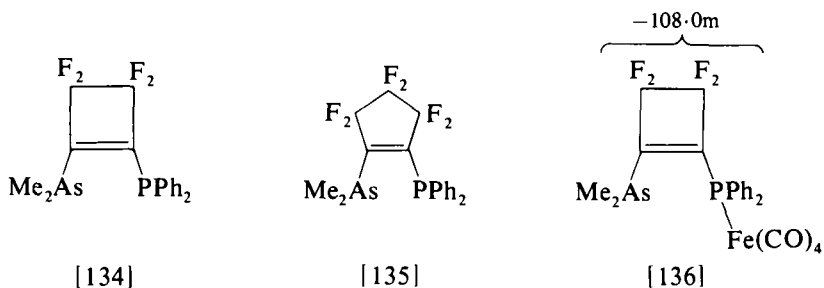
[132]

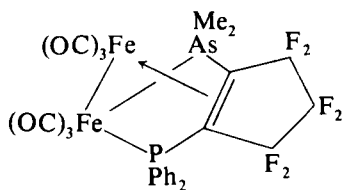


$\delta\text{CF}_3 -75.4$
 $^1J(\text{P-F}) 1189 \text{ Hz}$

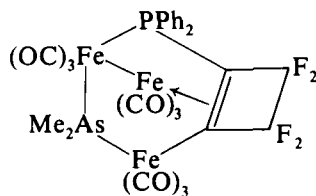
[133]

^{19}F Chemical shifts for a series of carbonyliron derivatives of the new ligands [134] and [135] have been reported, and are shown with the structures deduced in [136] to [146]. (72) The spectra all show multiplet structures for the bands, and analysis was not possible. Some of the structures have been confirmed crystallographically (e.g. [136] (73), [144] (74), [145] (75)), and others are analogous to structures which have been confirmed. The *meso* and *dl* isomers of $\text{cis-PhMeAsC}(\text{CF}_3):\text{C}(\text{CF}_3)\text{AsMePh}$ both form $\text{L-LFe}(\text{CO})_3$ [147 and

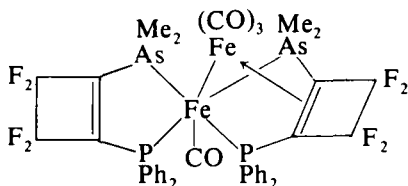




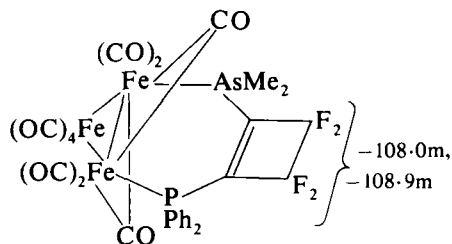
Multiplets at -72.4 , -83.3 , -95.9 ,
 -100.4 , -109.5 , -122.3
 [143]



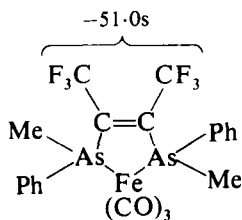
Complex mult., -91.5 , -94.7 ,
 -99.0 , -101.6
 [144]



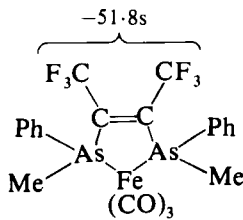
Complex mult., strong peaks at
 -108.0 , -110.0
 [145]



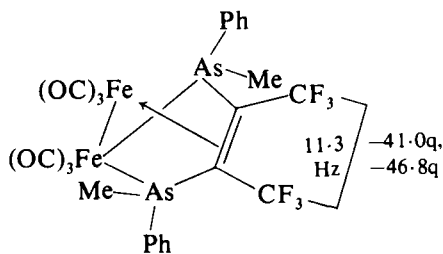
[146]



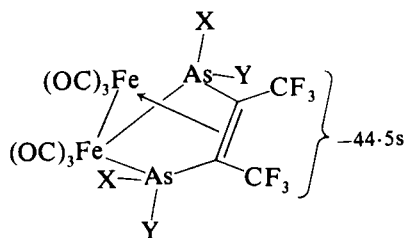
[147]



[148]



[149]



X = Ph, Y = Me or X = Me, Y = Ph
 [150]

148] and $L-LFe_2(CO)_6$ complexes with iron carbonyls; (76) the spectra of the $L-LFe_2(CO)_6$ complexes [149 and 150] allow distinction between the *meso* and *dl* ligands, since two different CF_3 resonances would be expected only for the complex with the *dl* ligand, shown as [149].

Bis(trifluoroacetato) complexes of ruthenium and osmium $[M-(PPh_3)_2(CO)(CF_3CO_2)_2]$ show exchange between bidentate and unidentate trifluoroacetate linkage which is sufficiently slow at room temperature for the two CF_3 groups to be resolved; (77) *fac*-stereochemistry is indicated by the reactivity of the compounds.

Several compounds containing SCF_3 groups attached to iron have been reported, and parameters are given in Table VII.

TABLE VII

Some ^{19}F Chemical shifts for CF_3S derivatives of iron

Compound	$\delta(CF_3)$	Ref.
<i>anti</i> - $[Fe(CO)_3(SCF_3)]_2$	-22.7, -34.3	24
<i>syn</i> - $[Fe_2(CO)_6(SCF_3)]_2S$	-32.4	24
<i>anti</i> - $[Fe(CO)_2(PPh_3)(SCF_3)]_2$	-21.9, -31.9	24
<i>syn</i> - $[Fe(CO)_2(PPh_3)(SCF_3)]_2$	-28.9	24
$[(\pi-C_5H_5)Fe(CO)(SCF_3)]_2 A$	-37.4 ^a	25
$[(\pi-C_5H_5)Fe(CO)(SCF_3)]_2 B$	-34.0	25
<i>anti</i> - $Fe_2(CO)_5(PPh_3)(SCF_3)_2$	-26.3, -36.3	25
<i>syn</i> - $Fe_2(CO)_5(PPh_3)(SCF_3)_2$	-32.9	25
$[Fe(NO)_2(SCF_3)]_2$	-23.0	25

^a Thought to be the all-*trans* structure.

The structures of the two isomers of $[(\pi-C_5H_5)Fe(CO)(SCF_3)]_2$ could not be determined, but A had spectroscopic properties consistent with an all *trans* structure. Each isomer showed only one CF_3 singlet, consistent either with equivalent CF_3 groups or with fluxional behaviour leading to equivalence.

E. Cobalt, rhodium, iridium

Parameters reported for a range of fluoroalkyl groups σ -bonded to metal are collected in Table VIII. (42, 78–81) The triplet splitting in the CF_3 resonance of $(\pi-Me_5C_5)Rh(PF_3)CF_3I$ (79) presumably arises from equal coupling to the phosphorus and rhodium, but these couplings do not appear to be observable in the more complex spectra of the compounds containing larger fluoroalkyl groups. All four compounds show a widely spaced doublet [$^1J(P-F)$ 1379–1392 Hz], further split [$^2J(Rh-F)$ 20–25 Hz] by coupling to rhodium, at δ -21.7 to -24.7 for

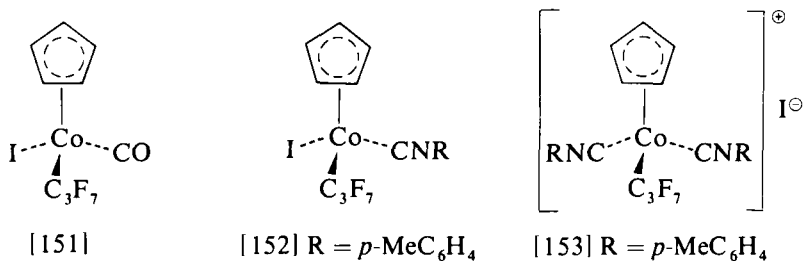
TABLE VIII

Some ^{19}F NMR parameters for fluoroalkyl-cobalt and -rhodium compounds

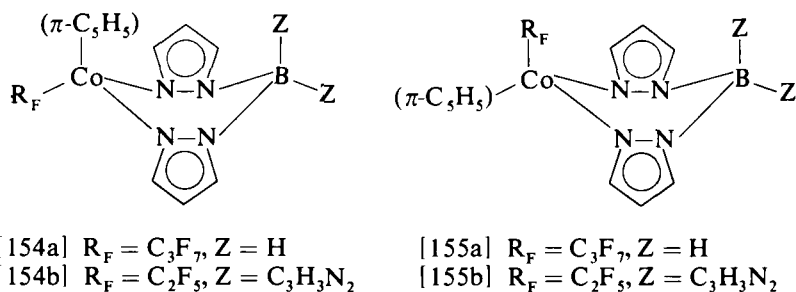
Compound	δCF^a	δCF^b	δCF^c	Ref.
$(\pi\text{-Me}_5\text{C}_5)\text{Co}(\text{CO})\{\text{CF}(\text{CF}_3)_2\}\text{I}$	n.r. ^a	-66.1 (d ~ 10)	—	78
$(\pi\text{-Me}_5\text{C}_5)\text{Rh}(\text{PF}_3)(\text{CF}_3)\text{I}$	-1.6 (t, 10)	—	—	79
$(\pi\text{-Me}_5\text{C}_5)\text{Rh}(\text{PF}_3)(\text{C}_2\text{F}_5)\text{I}$	-68.8 ^b	-82.2	—	79
$(\pi\text{-Me}_5\text{C}_5)\text{Rh}(\text{PF}_3)(n\text{-C}_3\text{F}_7)\text{I}$	ca. -60	-114.8 (d, ~ 94)	-79.3 (t, 12)	79
$(\pi\text{-Me}_5\text{C}_5)\text{Rh}(\text{PF}_3)(\text{C}_2\text{F}_{15})\text{I}$	ca. -59	-111 (d, ~ 120)	c	79
$(\pi\text{-C}_5\text{H}_5)\text{Co}(\text{CO})(n\text{-C}_3\text{F}_7)\text{I}$ [151]	-56.5 (q) ^d	-113.2 (m) ^d	-88.6 (t) ^d	80
$(\pi\text{-C}_5\text{H}_5)\text{Co}(\text{CNC}_6\text{H}_4\text{Me-}p)(\text{C}_3\text{F}_7)\text{I}$ [152]	-61.0 (q)	-113.5	-88.5 (t)	80
$[(\pi\text{-C}_5\text{H}_5)\text{Co}(\text{CNC}_6\text{H}_4\text{Me-}p)(\text{C}_3\text{F}_7)]^\oplus\text{I}^\ominus$ [153]	-58.16 (q, 8)	-114.42	-88.42 (t, 8)	80
$(\pi\text{-C}_5\text{H}_5)\text{Co}(\text{CF}_3)\text{Pz}_2\text{BH}_2^e$	-11.9 (s)	—	—	42
$(\pi\text{-C}_5\text{H}_5)\text{Co}(\text{C}_2\text{F}_5)\text{Pz}_2\text{BH}_2^e$	-80	-82	—	42
$(\pi\text{-C}_5\text{H}_5)\text{Co}(n\text{-C}_3\text{F}_7)\text{Pz}_2\text{BH}_2^e$ A	-79.4	-115.8 (t, 7)	-80.9 (t, 11.5)	42
$(\pi\text{-C}_5\text{H}_5)\text{Co}(n\text{-C}_3\text{F}_7)\text{Pz}_2\text{BH}_2^e$ B	-78.4	-117.6	-82.0 (t, 11)	42
$(\pi\text{-C}_5\text{H}_5)\text{Co}[\text{CF}(\text{CF}_3)_2]\text{Pz}_2\text{BH}_2^e$	-175.9	-67.8 (d, 7.6)	—	42
$(\pi\text{-C}_5\text{H}_5)\text{Co}(\text{CF}_3)\text{Pz}_3\text{BH}^e$	-10.8	—	—	42
$(\pi\text{-C}_5\text{H}_5)\text{Co}(\text{C}_2\text{F}_5)\text{Pz}_3\text{BH}^e$ A	-75.0	-82.5	—	42
$(\pi\text{-C}_5\text{H}_5)\text{Co}(\text{C}_2\text{F}_5)\text{Pz}_3\text{BH}^e$ B	-75.4	-82.2	—	42
$(\pi\text{-C}_5\text{H}_5)\text{Co}(n\text{-C}_3\text{F}_7)\text{Pz}_3\text{BH}^e$	n.r. ^a	-119.8	n.r. ^a	42
$(\pi\text{-C}_5\text{H}_5)\text{Co}(\text{C}_2\text{F}_5)\text{Pz}_4\text{B}^e$	-80.6	-80.5	—	42
$(\pi\text{-C}_5\text{H}_5)\text{Co}(n\text{-C}_3\text{F}_7)\text{Pz}_4\text{B}^e$	-78	-117.5 (t, 5)	-80.4 (t, 13)	42
$(\pi\text{-C}_5\text{H}_5)\text{Co}(\text{C}_2\text{F}_5)\text{Pz}_2\text{H}^e$	-81	-85	—	42
$(\pi\text{-C}_5\text{H}_5)\text{Co}(n\text{-C}_3\text{F}_7)\text{Pz}_2\text{H}^e$	-82	-117	-80.1 (t, 13)	42
$(\pi\text{-C}_5\text{H}_5)\text{Co}[\text{CF}(\text{CF}_3)_2]\text{Pz}_2\text{H}^e$	-171	-67.9 (d, 8.4)	—	42
$\text{C}_3\text{F}_7\text{CoSalen} \cdot \text{H}_2\text{O}^f$	-91.0 (br)	-121.0	-78.4 (t)	81
$\text{C}_3\text{F}_7\text{CoSalphen} \cdot \text{H}_2\text{O}^g$ [158, R=H]	-94.7 (br)	-121.9	-78.5 (t)	81
$\text{C}_3\text{F}_7\text{CoSalphenC}_3\text{F}_7 \cdot \text{H}_2\text{O}^{g,h}$ [158, R = C ₃ F ₇]	-94.7 (br)	-122.0	-78.7 (t)	81
$(\text{OC})_4\text{CoCF}(\text{CF}_3)_2$	-150.5 (sept, 10)	-70.2 (d, 10)	—	82
$(\text{OC})_4\text{CoCF}_2\text{CF}_2\text{CF}_2\text{Co}(\text{CO})_4$	-43.8 (s) ⁱ	-97.7 (s) ⁱ	—	82

^a Not reported. ^b $J(\text{A}-\text{B})$ 253 Hz, $\delta(\text{AB})$ 11.6. ^c γ and δ CF₂ ca. -122; ϵCF_2 -122.9; ζCF_2 -126.4; CF₃ -81.3 (t, 10). ^d ABMNX₃ system. ^e Pz = pyrazolyl. ^f Salen = (CH₂N:CHC₆H₄O[⊖]-o)₂. ^g See [158]. ^h C₃F₇ in ligand; -109.0 (t), -124.9, -82.6 (t). ⁱ J ($\alpha\beta$) < 1.5 Hz.

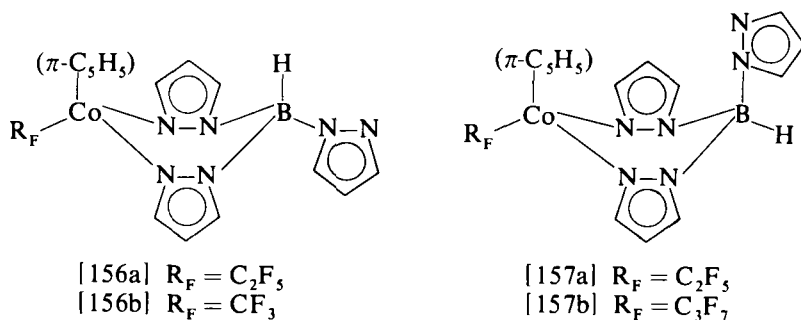
the PF_3 group. The spectra of [151] and [152] are complex because of the chiral metal, both α - and β - CF_2 groups showing geminal inequivalence, but the increased symmetry of [153] gives rise to a simpler



spectrum. (80) The isolation of two isomeric complexes of formula $(\pi\text{-C}_5\text{H}_5)\text{CoR}_\text{F}\text{Pz}_2\text{BZ}_2$ ($\text{R}_\text{F} = \text{C}_3\text{F}_7$, $\text{Z} = \text{H}$ and $\text{R}_\text{F} = \text{C}_2\text{F}_5$, $\text{Z} = \text{pyrazolyl}^*$) suggests the puckered structures [154] and [155] shown. (42) The proton

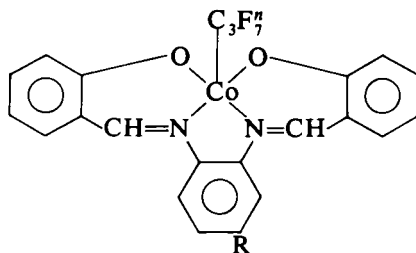


NMR spectra of the two isomers of $(\pi\text{-C}_5\text{H}_5)\text{CoR}_\text{F}\text{Pz}_3\text{BH}$ suggest, however, that both have axial cyclopentadienyl groups as in [156a] and [157a]. The CF_3 compound isolated is allocated structure [156b], but the C_3F_7 compound appears to be [157b].



* Parameters for only one isomer of the latter are given in the paper.

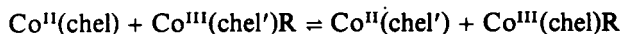
The reaction of alkylcobalt complexes ($\text{RCoSalphen} \cdot \text{H}_2\text{O}$, $\text{R} = \text{Me}$, Et) with $\text{C}_3\text{F}_7\text{I}$ gives the complex [158, $\text{R} = \text{H}$], parameters for which



[158a] $\text{R} = \text{H}$

[158b] $\text{R} = n\text{-C}_3\text{F}_7$

are shown in Table VIII, (81) and the same complex is formed from $[\text{Co}^{\text{I}}\text{Salphen}]^{-1}$, together with smaller amounts of a second complex identified spectroscopically as [158b, $\text{R} = n\text{-C}_3\text{F}_7$]. ^{19}F Integrations were used to follow the equilibria:



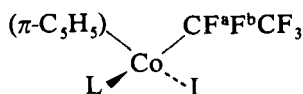
where (chel) and (chel') are chelating ligands, but the only ^{19}F parameters quoted were for the CF_3CH_2 group in $\text{Co}^{\text{III}}(\text{Tfacen})\text{CH}_2\text{CF}_3$ [$\delta -55.6\text{t}$, $J(\text{F}-\text{H}) 16\text{ Hz}$] and in $\text{Co}^{\text{III}}(\text{Acacen})\text{CH}_2\text{CF}_3$ ($\delta -56.3\text{t}$, 16 Hz). (81b)

^{19}F NMR parameters for a series of cyclopentadienylcobalt complexes containing C_2F_5 and $\text{CF}(\text{CF}_3)_2$ groups are shown in Table IX and with structures [159 and 160]. (83)

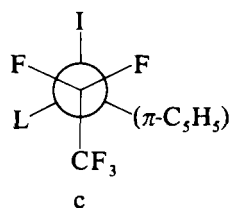
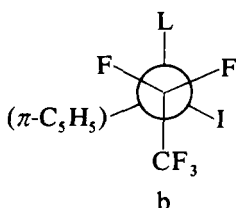
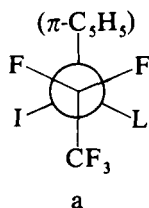
TABLE IX

Temperature dependence of the ^{19}F NMR parameters for cyclopentadienylperfluoroethylcobalt complexes [159]

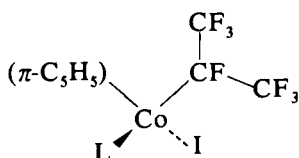
	L = PPh_3		L = PMePh_2		L = PMe_2Ph	
	200 K	296 K	200 K	296 K	200 K	300 K
δ_{A}	-66.51	-64.58	-66.54	-65.51	-68.10	-66.94
δ_{B}	-59.95	-58.21	-63.02	-61.52	-65.80	-63.62
δ_{CF_3}		-77.52		-78.35		-78.63
$^2J(\text{F}_{\text{a}}-\text{F}_{\text{b}})$	246.8	247.0	250.8	250.6	250.5	250.4
$^3J(\text{P}-\text{F}_{\text{a}})$	17.75	20.06	8.35	14.73	16.54	17.93
$^3J(\text{P}-\text{F}_{\text{b}})$	11.25	12.39	17.65	16.53	14.46	14.32



[159]



[159']



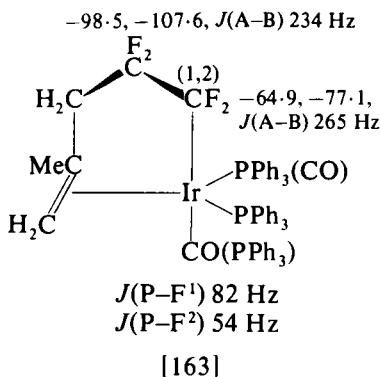
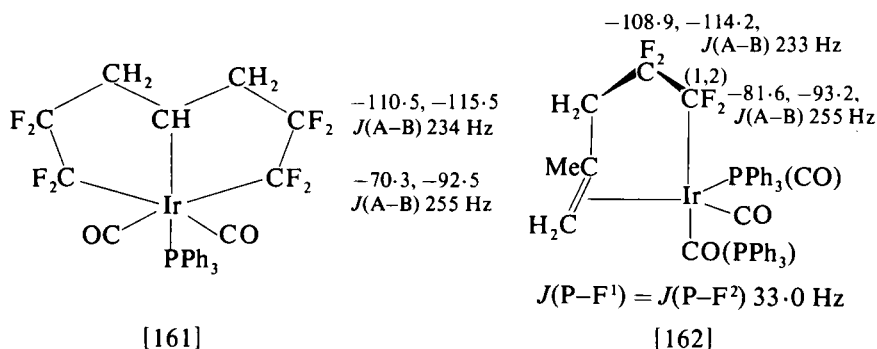
[160]

L	$\delta(\text{CF})$	$^3J(\text{P-F})$	$\delta(\text{CF}_3)(J(\text{P-F}), J(\text{CF-CF}_3))$	
CO	-156.9	—	-66.1 (—, 10)	-68.4 (—, 10)
P(OEt) ₃	-176.8	ca. 14	-64.1 (< 1, 8)	-67.7 (3.5, 10.5)
P(OPh) ₃	-172.3	ca. 11	-63.8 (< 1, 7.5)	-67.7 (3.5, 11)
PPh ₃	-173.6	ca. 10	-62.9 (< 1, 6.5)	-66.6 (5, 14.5)
PMePh ₂	-174.7	n.d.	-63.8 (< 1, 7.5)	-66.9 (5.5, 11)
PMe ₂ Ph	-176.9	n.d.	-63.6 (< 1, 8)	-66.6 (5.5, 11)

The chiral cobalt atoms cause the α -fluorines of the C_2F_5 groups and the CF_3 groups of the $\text{CF}(\text{CF}_3)_2$ groups to be diastereotopic. Coupling between the phosphorus of the ligand and the two α -fluorines of the C_2F_5 complexes [159] is different and the temperature dependence of the three-bond P-F coupling constants (values for only the extreme temperatures reported are given in Table IX) suggest that changes in rotamer population may be occurring, at least with $\text{L} = \text{PPh}_2\text{Me}$, although temperature dependence of the coupling constants themselves could not be discounted. The difference between the couplings was small, and their temperature dependence was also small, for $\text{L} = \text{PMe}_2\text{Ph}$, the least sterically demanding ligand used, suggesting that the rotamer population [159'a-c] may be essentially the same over the temperature range studied. Unfortunately, temperature dependence could not be studied for the perfluoroisopropyl complexes [160], but the

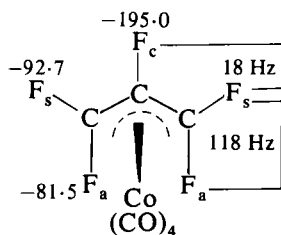
differences in the phosphorus coupling to the two CF_3 groups of each complex may indicate stereochemical dependence of these couplings. The $\text{CF}_3\text{--CF}_3$ coupling was 10–11 Hz in all the compounds of this series.

The symmetrical structure [161] is suggested for the product formed by heating the IrCF_2CF_2 compound [196, $\text{L} = \text{PPh}_3$] (see p. 60) with tetrafluoroethylene, (84) the values shown being typical of σ -bonded



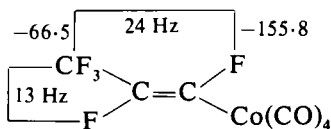
perfluoroalkyl groups. Compounds [162] and [163], containing only σ -bonded $\text{CF}_2\text{--CF}_2\text{R}$ groups were also obtained by displacement of co-ordinated C_2F_4 from complex [196, allyl group = 2-MeC₃H₄, $\text{L} = \text{PPh}_3$] by either CO or PPh_3 .

Parameters for the π -perfluoroallylcobalt complex [164], formed by the reaction of perfluoroallyl iodide with $\text{Zn}[\text{Co}(\text{CO})_4]_2$ are given with the structure. (85) The prop-1-enyl complex [165], identified as *trans* about the double bond by the large value of $J(\text{F--F})$, was also formed, and an octet at $\delta -41.6$, with coupling constants similar to those of



$$J(\text{F}_a\text{--F}_c) 74 \text{ Hz}$$

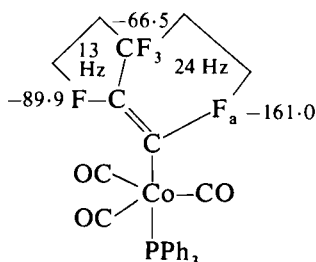
[164]



$$J(\text{F--F}_{trans}) 147 \text{ Hz}$$

[165]

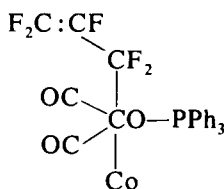
$\text{CF}_2\text{:CF.CF}_2\text{I}$,* is thought to be due to $\text{CF}_2\text{:CF.CF}_2\text{.Co(CO)}_4$ formed as an intermediate, but this compound could not be isolated. The resonance due to F_s in [164] is broadened, but the reason for this is not apparent from the first order analysis performed. The reaction of [164] with triphenylphosphine gave the prop-1-enyl complex [166], in which the large P–CF coupling was used to assign the stereochemistry, together with a second compound for which the vibrational spectrum suggested structure [167]. Unfortunately this compound decomposed rapidly above 10°C , and below this temperature was too insoluble for useful ^{19}F NMR measurements.



$$J(\text{F--F}_{trans}) 146 \text{ Hz}$$

$$J(\text{P--F}_a) 30 \text{ Hz}$$

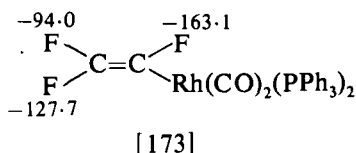
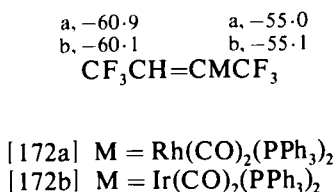
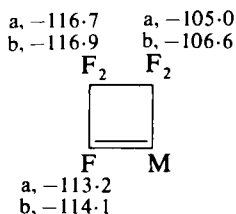
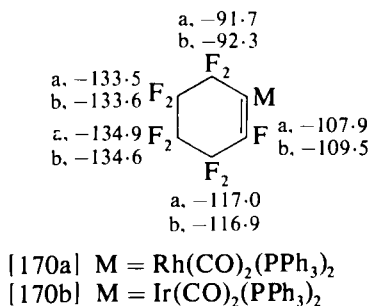
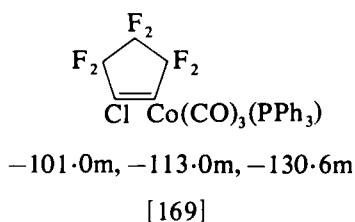
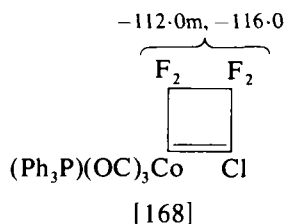
[166]



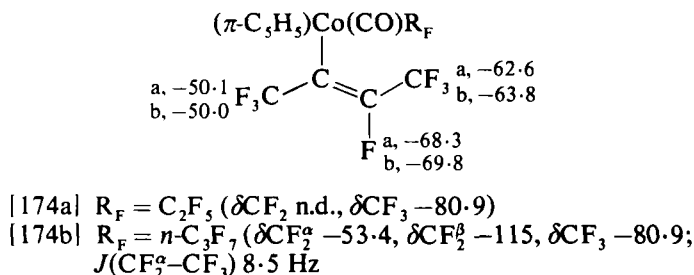
[167]

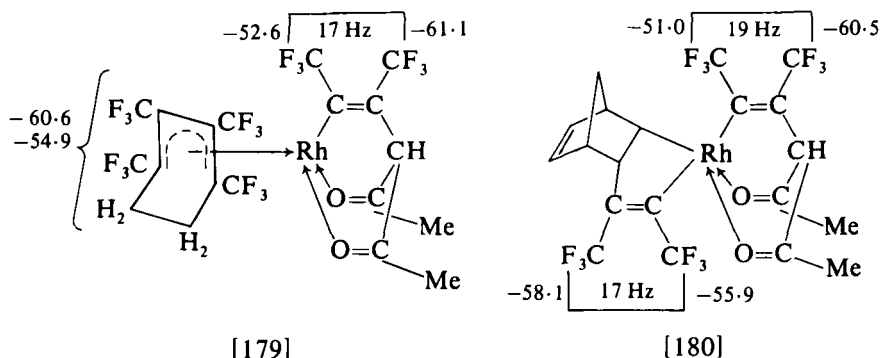
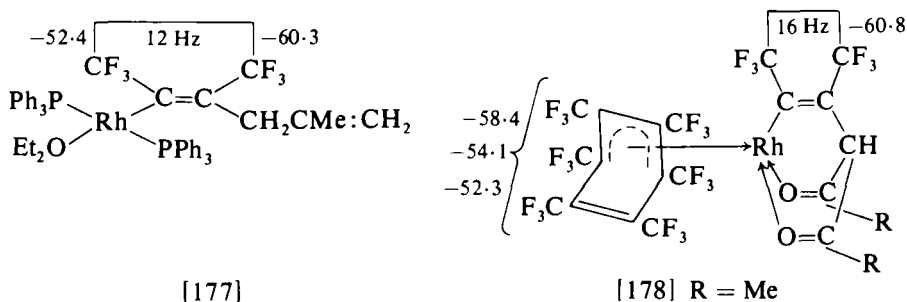
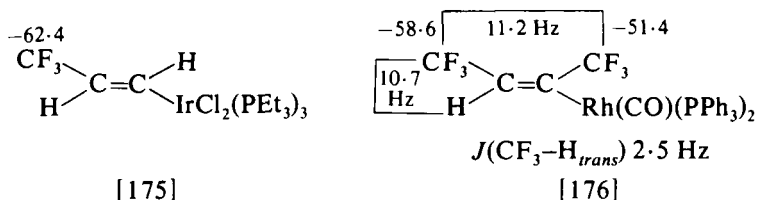
Other alkenyl complexes have been formed by displacement of fluoride or chloride ion from fluoro-olefins by metal carbonyl anions, by reactions of the perfluoroalkenylsilver derivative with metal halide compounds, and by insertion of an alkyne into a metal–X bond, and parameters are given with structures [168] to [187]. (8, 86–91) As

* $\delta(\text{CF}_2\text{I})$ in $\text{CF}_2\text{:CF.CF}_2\text{I}$ is reported (85) to be -49.7 , not -63.6 as previously reported (K. C. Ramey and W. S. Brey, *J. Chem. Phys.* 1964, **40**, 2349). The new value fits the trend shown by the chloro ($\delta -62.0$) and bromo ($\delta -55.1$) compounds.

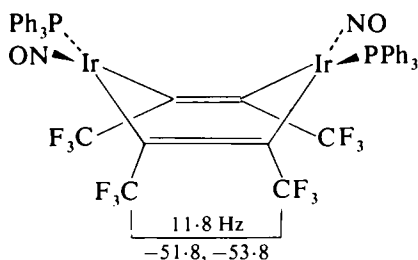


shown, the change from rhodium to iridium in [170], [171], and [172] makes little difference to the ^{19}F shifts. (87) Unfortunately, the low solubility of these compounds, and of [173], makes it impossible to extract any coupling constants, and the stereochemistry of [172] remains unknown. The lone fluorines of [174a] and [174b] show field-dependent doublet splitting, suggesting that two isomers are present in each case, but no further investigation has been reported. (8) The H-H



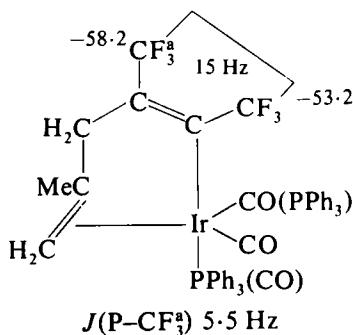


coupling shows that [175] has the *trans* configuration, (88) and the $\text{CF}_3\text{-CF}_3$ couplings in [176]–[180] all fall in the range for *cis* trifluoromethyl groups as indicated. (89) Parameters for [178, R = CMe₃] are very similar to those shown for the compound with R = Me. (89c) The orientation of the norbornene ring system in [180] could not be determined from the information available; the assignments of the CF_3 resonances were made by analogy with those of [178] and [179]. The structure of the dimetallic complex [181] was also confirmed by X-ray diffraction. (90)

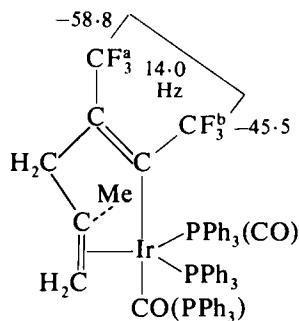


[181]

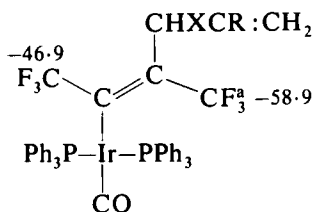
Insertion of perfluorobut-2-yne between the metal and one end of the allyl system in $\text{Ir}(\pi\text{-allyl})(\text{CO})(\text{PPh}_3)_2$ gives products of both *cis*- and *trans*-insertion [182] to [186], (91) the products with the *trans*- $\text{C}(\text{CF}_3):\text{C}(\text{CF}_3)-$ system showing only weak coupling (3.5–4.5 Hz)



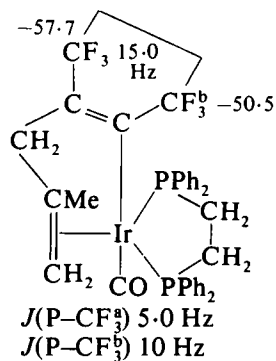
[182]



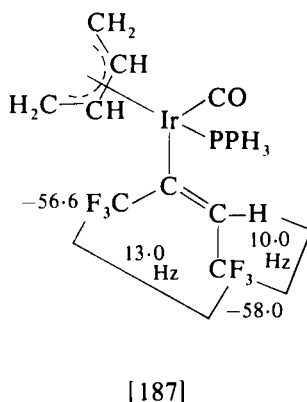
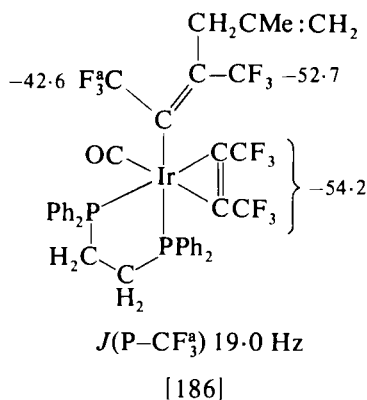
[183]



[184] X = H, R = Me

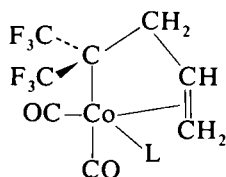


[185]

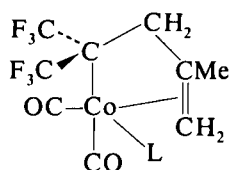


between the trifluoromethyl groups. Parameters for the allyl and 1-methylallyl products [184, $\text{R} = \text{X} = \text{H}$; $\text{R} = \text{H}$, $\text{X} = \text{Me}$] are very similar to those shown for [184, $\text{X} = \text{H}$, $\text{R} = \text{Me}$]. The spectra of [183] are temperature dependent, the structure shown being assigned to the isomer preferred at -30°C . At room temperature, the fine structure of the ^{19}F spectrum is lost. The two CF_3 absorptions of the $\text{IrC}(\text{CF}_3):\text{C}(\text{CF}_3)$ group in [186] were not resolved at 94.1 MHz . [187] is formed from $(\pi\text{-1-methylallyl})\text{Ir}(\text{CO})(\text{PPh}_3)_2$ and the butyne at room temperature. (91) Three alkynylrhodium complexes $\text{RhCl}(\text{CO})\text{-L}_2(\text{C}:\text{CCF}_3)$ [$\text{L} = \text{AsMe}_3$, $\text{AsMe}_2(p\text{-MeOC}_6\text{H}_4)$, SbPh_3] formed by the reaction of $\text{RhCl}(\text{CO})\text{L}_2$ with 3,3,3-trifluoropropyne, each showed a singlet in the range -46.9 to -47.3 , (92) but other signals, presumably due to impurities, were also present.

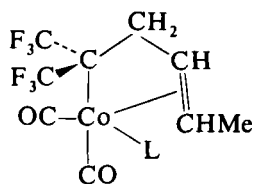
The spectra of compounds [188] to [191], formed by the reaction of bis(trifluoromethyl)diazomethane with the tricarbonyl(π -allyl)cobalt compounds, and the reaction of the products with triphenyl-phosphine or -arsine, each consist of two multiplets in the range $\delta -65$ to -70 , in accord with the distinctly different CF_3 environments. (93) In [189] to



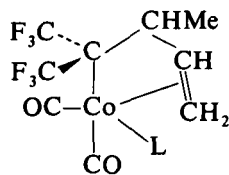
- [188a] $\text{L} = \text{CO}$
 [188b] $\text{L} = \text{PPh}_3$
 [188c] $\text{L} = \text{AsPh}_3$



- [189a] $\text{L} = \text{CO}$
 [189b] $\text{L} = \text{PPh}_3$
 [189c] $\text{L} = \text{AsPh}_3$

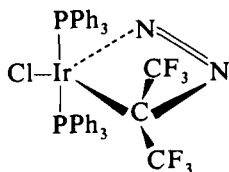


- [190a] L = CO
 [190b] L = PPh₃
 [190c] L = AsPh₃

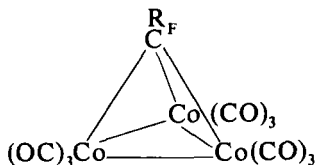


[191]

[191], the CF₃–CF₃ coupling is resolved (10 Hz), and coupling of one or both CF₃ groups to a single hydrogen of the hydrocarbon chain (e.g. 7 Hz for the low-frequency CF₃ in [189a and c] is also observed in [189] and [190]. The absence of this coupling from the spectrum of the minor isomer formed in the reaction of the 1-methylallyl complex, and its presence in that of the major isomer and of its derivatives (7.0 and 8.5, 7.0 and 6.5, 7 and 10 Hz in the high-frequency and low-frequency bands of [190a–c respectively]) provide evidence for the insertion of the (CF₃)₂C fragment between Co and CHMe groups in the minor and Co and CH₂ in the major isomers respectively. The reaction between chlorodinitrogenbis(triphenylphosphine)iridium and the diazoalkane gave [192], the ¹⁹F spectrum of which, a triplet (δ –57.2, |J(P–CF₃) + J(P'–CF₃)| 5.7 Hz) remained unchanged down to –90°C. (94)



[192]



- [193] R_F = CHF₂ –85.9 (d, 59 Hz)
 R_F = C₂F₅ –80.0 (t, 3.5 Hz), –80.5 (q, 3.5 Hz)
 R_F = CF₂CF₂Co(CO)₄ –46.5 (t, 21 Hz), –77.0 (t, 21 Hz)
 R_F = CF₂{CCO₃(CO)₉} –103.5s
 R_F = CF₂CF₂CO₂H –80.5 br, –110.5 br

TABLE X

¹⁹F NMR parameters for some fluoroacyliridium compounds (95)

Compound	Chemical Shift
$\text{IrCl}_2(\text{CO} \cdot \text{CF}_3)(\text{CO})(\text{PMePh}_2)_2^a$	-79.7 (s)
$\text{IrCl}_2(\text{COCF}_3)(\text{PPh}_3)_2$	-70.2 (s)
$\text{IrCl}_2(\text{CO} \cdot \text{CHF}_2)(\text{CO})(\text{PMePh}_2)_2^a$	-122.6 (d 56.2)
$\text{IrCl}_2(\text{COCHF}_2)(\text{PPh}_3)_2$	-116.5 (d 56.0)
$\text{IrCl}_2(\text{COCH}_2\text{F})(\text{CO})(\text{PMePh}_2)_2^a$	-207.2 (t 50.0)
$\text{IrCl}_2(\text{COCH}_2\text{F})(\text{PPh}_3)_2$	-191.6 (t 49.0)

^a Phosphine ligands are *trans* by ¹H NMR.

The preparation of a series of fluoroalkyl derivatives of the $\text{Co}_3(\text{CO})_9\text{C}$ cluster has been reported, and parameters are given with structure [193]. (82) The bright red product formed in low yield in the reaction of $(\text{CF}_3)_2\text{CFCo}(\text{CO})_4$ with $\text{NaCo}(\text{CO})_4$ is thought from its ¹⁹F NMR spectrum (sharp singlet, δ -43.5) and other properties to be $(\text{CO})_3\text{Co}(\text{CO})[\text{C}(\text{CF}_3)_2]\text{Co}(\text{CO})_3$.

Parameters for some fluoroacyliridium complexes are listed in Table X. (95) The spectrum of $\text{CF}_2\text{HCOCo}(\text{CO})_3\text{P}(\text{OPh})_3$ is described as a "doublet, ²*J*(F-H) 57 Hz, 6.71 ppm from $\text{CF}_3\text{CO}_2\text{Me}$." (96) A shift of 67.1 ppm from $\text{CF}_3\text{CO}_2\text{Me}$ would give δ = -141.4, which would be more in accord with the iridium complexes.

Parameters for a range of fluoro-olefin complexes of rhodium and iridium are given in Tables XI (97) and XII. The vinyl fluoride complex

TABLE XI

¹⁹F data for some tetrafluoroethylene complexes of iridium (97)

Compound	Chemical shift and comments
$[\text{IrCl}(\text{C}_8\text{H}_{14})(\text{C}_2\text{F}_4)]_n^a$	-113.6; -130.3, broadened AB
$\text{IrCl}(\text{PPh}_3)(\text{C}_2\text{F}_4)$	-101.2, apparent triplet
$\text{IrCl}(\text{AsPh}_3)(\text{C}_2\text{F}_4)$	-99.0, singlet
$[\text{Ir}(\text{NH}_3)_3(\text{C}_2\text{H}_4)(\text{C}_2\text{F}_4)]\text{Cl}$	-131.6; -134.0, broadened AB
$[\text{Ir}(\text{NH}_3)_3(\text{C}_8\text{H}_{14})(\text{C}_2\text{F}_4)]\text{Cl}^a$	-129.7 broad AB; -137.6 complex
$\text{Ir}(\text{acac})(\text{C}_2\text{H}_4)(\text{C}_2\text{F}_4)^b$	-123.0
$\text{Ir}(\text{acac})(\text{C}_8\text{H}_{14})(\text{C}_2\text{F}_4)^{a,b}$	-121.0, -129.1, AA'BB'
$\text{Ir}(\text{acac})(\text{COD})(\text{C}_2\text{F}_4)^{b,c}$	-121.6, -129.2, -130.4, -135.5, all complex
$\text{Ir}(\text{acac})(\text{CO})(\text{C}_2\text{F}_4)^b$	-112.9, -131.0, AA'BB'
$\text{Ir}(\text{acac})(\text{C}_8\text{H}_{14})(\text{C}_2\text{F}_4)\text{py}^{a,b}$	-127.8; -134.2, broadened AB
$\text{Ir}(\text{acac})(\text{C}_2\text{H}_4)(\text{C}_2\text{F}_4)(\text{NH}_3)^b$	-129.1; -131.8, broadened AB
$\text{Ir}(\text{acac})(\text{C}_8\text{H}_{14})(\text{C}_2\text{F}_4)(\text{NH}_3)^{a,b}$	-127.2; -136.7, broadened AB

^a C_8H_{14} = cyclo-octene. ^b acac = acetylacetonate. ^c COD = cyclo-octa-1,5-diene.

TABLE XII

Some ^{19}F NMR parameters for fluoro-olefin complexes(a) Chemical shifts (δ)

Compound	L	Other groups	$\delta\text{F}(1)$	$\delta\text{F}(2)$	$\delta\text{F}(3)$	$\delta\text{F}(4)$ (X)	Ref.
[194a]			-189.6				98
[194b]			-153.7				98
[195]	C_2H_4	F	-98.7	-98.7	-98.7	-98.7	99
[195]	PPh_3	F	-104.9	-113.7	-113.7	-104.9	99
[195]	AsPh_3	F	-100.9	-114.9	-114.9	-100.9	99
[195]	SbPh_3	F	-91.4	-115.1	-115.1	-91.4	99
[195]	C_2H_4	CF_3	-100.1	-86.9	-207.1	-66.88	99
[195]	PPh_3	CF_3	-96.1	-82.4	-177.2	-65.69	99
[195]	AsPh_3	CF_3	-97.5	-77.8	-171.1	-66.14	99
[195]	SbPh_3	CF_3	-98.7	-68.98	-159.4	-66.28	99
[195]	C_2H_4	Cl	-103.8	-98.5	-124.4	—	99
[195]	PPh_3	Cl	-101.6	-92.32	-108.0	—	99
[195]	AsPh_3	Cl	-103.3	-87.3	-103.3	—	99
[195]	SbPh_3	Cl	-105.6	-82.1	-95.0	—	99
[195]	C_2H_4	Br	-101.7	-97.1	-125.1	—	99
[195]	PPh_3	Br	-103.8	-90.6	-98.9	—	99
[195]	AsPh_3	Br	-100.8	-85.7	-100.3	—	99
[195]	SbPh_3	Br	-101.1	-77.0	-90.5	—	99
[196]	PPh_3	C_3H_5	-138.1	-110.0	-112.8	-115.2	84
[196]	PPh_3	1-MeC $_3\text{H}_4$	-138.9	-109.3	-111.1	-115.2	84
[196]	PPh_3	2-MeC $_3\text{H}_4$	-140.0	-112.1	-113.3	-115.1	84
[196]	AsPh_3	2-MeC $_3\text{H}_4$	-137.3	-109.4	-110.0	-113.2	84
[196]	PBu_2Me	2-MeC $_3\text{H}_4$	-139.0	-116.0	-107.8	-117.0	84
[197]			-103.2	-128.1	-135.5	-121.1	84
[198]	PPh_3^a		-138.1	-115.2	-101.9	-126.7	84
[198]	AsPh_3^b		-135.6	-111.3	-100.0	-125.1	84
[199] ^c			-133.4	-105.1	-103.1	-126.9	84
[200] ^c			-129.9	-114.3	-106.9	-123.1	84
$\text{Ir}(\text{NO})(\text{PPh}_3)_2(\text{C}_2\text{F}_4)$			-117.4	-117.4	-117.4	-117.4	89
$\text{IrF}(\text{CO})(\text{PPh}_3)_2(\text{C}_2\text{F}_4)$			-119.75	-119.75	-138.5	-138.5	100

^a $\delta\text{F}^5\text{—F}^8$ -74.7, -90.8, -98.7, -108.4 respectively.^b $\delta\text{F}^5\text{—F}^8$ -70.3, -92.0, -99.8, -108.9 respectively.^c See structures for $\delta\text{F}^5\text{—F}^8$.

(b) Coupling constants (in Hz)

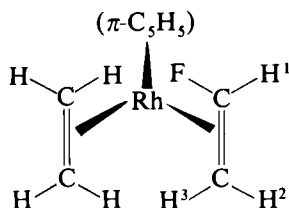
Compound	L	Other groups	$J(1-2)$	$J(1-3)$	$J(2-3)$	$J(2-4)$	$J(3-4)$	Ref.
[195]	C_2H_4	$\text{CF}_3(4)^a$	77.5	62.6	12.5	7.1	9.7	99
[195]	PPh_3	$\text{CF}_3(4)^a$	94.6	64.4	—	—	—	99
[195]	AsPh_3	$\text{CF}_3(4)^{a,b}$	89.8	59.9	25.6	8.6	14.1	99

TABLE XII—cont.

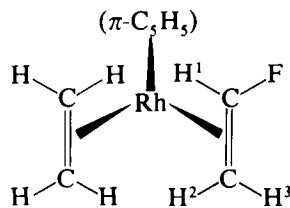
Compound	L	Other groups	$J(1-2)$	$J(1-3)$	$J(2-3)$	$J(2-4)$	$J(3-4)$	Ref.
[195]	SbPh ₃	CF ₃ (4) ^{a,b}	92.7	61.2	30.6	9.7	—	99
[195]	C ₂ H ₄	Cl ^b	77.0	62.5	8.5	—	—	99
[195]	PPh ₃	Cl ^{b,c}	87.5	59.9	17.1	—	—	99
[195]	SbPh ₃	Cl ^b	85.9	63.7	22.0	—	—	99
[195]	C ₂ H ₄	Br ^b	75.3	64.9	9.2	—	—	99
[195]	PPh ₃	Br ^{b,c}	87.0	63.6	19.9	—	—	99
[195]	SbPh ₃	Br ^b	89.7	64.2	24.0	—	—	99
[196]	PPh ₃	C ₃ H ₅ ^{b,d,e}	153	33	2	30	169	84
[196]	PPh ₃	1-MeC ₃ H ₄ ^{d,e}	157	35	0	33	169	84
[196]	PPh ₃	2-MeC ₃ H ₄ ^{d,e}	154	31	6	29	170	84
[196]	AsPh ₃	2-MeC ₃ H ₄ ^e	149	56	3	31	171	84
[196]	PBu ₂ ⁱ Me	2-MeC ₃ H ₄ ^{d,e}	158	34 ^a	4 ^c	32	170	84
[197]		^{d,e,f}	168	31	0	31	186	84
[198]	PPh ₃ ^{d,s}		156	39	2	39	168	84
[198]	AsPh ₃ ^{d,h}		150	38	3	39	168	84
[199] ⁱ			151	38		36	166	84
[200] ^j			151	38		38	167	84

^a $J(1-4)$ [$J(F^1-CF_3)$] 12.8–14.9 Hz in this group. ^b Couplings to Rh also given for these compounds. (99) ^c Second order effects noted. Couplings to phosphorus also given in the paper. These two compounds appear in Table 2 of ref. 99 by a misprint as Rh(dpm)(AsPh₃)(CF₂CFCl) and Rh(dpm)(AsPh₃)(CF₂CFBr) respectively (R. D. W. Kemmitt, personal communication). ^d $J(1-4) < 5$ Hz. ^e $J(P_1-F_1)$ 39–46, $J(P_1-F_2)$ 46–52, $J(P_1-F_3)$ 7–11, $J(P_1-F_4)$ 8–13. ^f $J(P_2-F_1)$ 39, $J(P_2-F_2)$ 5.0, $J(P_2-F_3)$ 4.0, $J(P_2-F_4)$ 3.1. ^g $J(5-6)$ 265, $J(7-8)$ 243, $J(1-6)$ 53, $J(4-6)$ 51, $J(P-1)$ 37, $J(P-2)$ 33, $J(P-3)$ 12, $J(P-4)$ 5, $J(P-5)$ 67. ^h $J(5-6)$ 263, $J(7-8)$ 243, $J(1-6)$ 56, $J(4-6)$ 51. ⁱ $J(P-1)$ 39, $J(P-2)$ 36, $J(P-3)$ 12, $J(P-5)$ 61. ^j $J(P-1)$ 41, $J(P-2)$ 37, $J(P-5)$ 105.

[194] exists as two distinct geometric isomers [194a and b], in which the fluorine is either “inside” or “outside” with respect to the C₂H₄ ligand, (98) and a similar situation is formally possible with the complexes [195]

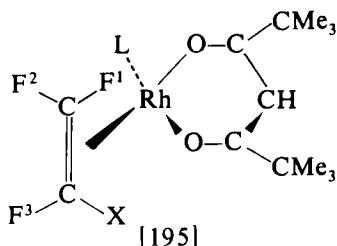


[194a] "F inside"



[194b] "F outside"

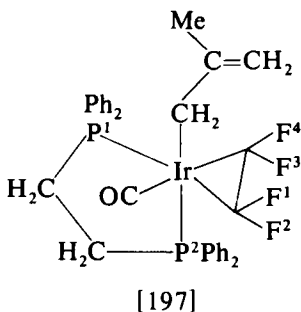
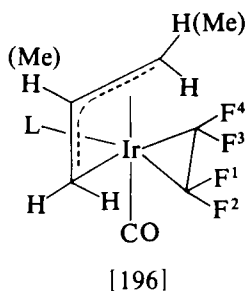
	[194a]	[194b]
$J(F-H^1)$	73.8	71.0
$J(F-H^2)$	24.2	22.0
$J(F-H^3)$	20.8	20.5
$J(Rh-F)$	12.5	6.2



from unsymmetrical olefins $\text{CF}_2:\text{CFX}$ ($\text{X} = \text{Cl}, \text{Br}, \text{CF}_3$); the preparative method used results in the formation of the isomer with X outside, (99) the “inside” fluorines showing larger couplings to the rhodium. (98) The $^{19}\text{F}\{^1\text{H}\}$ spectrum of the bis(vinyl fluoride) complex $(\pi\text{-C}_5\text{H}_5)\text{Rh}(\text{CH}_2:\text{CHF})_2$ shows the presence of all six possible stereoisomers, signals in the region -150.9 to -153.9 being associated with “outside” and -179.9 to -187.9 with “inside” fluorines. The spectrum flattens to the baseline at 120°C giving a value of 71 kJ mol^{-1} for the energy barrier to rotation. The maximum free energy difference between the rotamers appears, from the intensity ratio of the signals, to be *ca.* 3.5 kJ mol^{-1} .

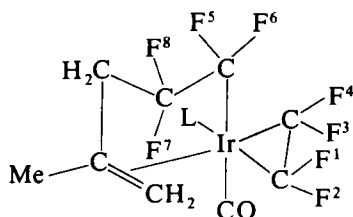
Although the geminal coupling constants $[J(\text{F}_1\text{--}\text{F}_2)]$ in [195] are larger than $J(\text{F}_1\text{--}\text{F}_3)$ or $J(\text{F}_2\text{--}\text{F}_3)$, the changes compared with the free olefins are less marked than has been observed previously in iron and nickel complexes, or in the iridium complexes also noted in Table XII, and it is suggested that this indicates a smaller amount of back-bonding from rhodium. (99) Although the complexes [195, $\text{X} = \text{Cl}, \text{Br}, \text{CF}_3$] are shown clearly to be rigid structures on the NMR time scale, the tetrafluoroethylene complex [195, $\text{L} = \text{C}_2\text{H}_4$, $\text{X} = \text{F}$] shows only a single resonance with rhodium coupling, which might suggest rotation about the $\text{C}_2\text{F}_4\text{--Rh}$ bond. The spectrum unexpectedly remains constant from 25°C to -90°C , however, more in keeping with a rigid structure, and further investigation of this complex is stated to be in progress. (99)

The iridium complexes [196], formed by the reaction of tetrafluoroethylene with the appropriate π -allyliridium complex, each show four



bands which may be analysed as a pair of AB quartets. The signal due to F1 is considerably shifted compared with the other three fluorines, perhaps by proximity to the π -allyl group. As usual in such olefin complexes, the geminal coupling constants are large compared with all the rest. In the complex [197], similar couplings are observed, and again one fluorine is markedly different to the other three, but in this case appears to high frequency, and is assigned position 1 as shown, since this appears to be the only site which would be unaffected by the phenyl groups.

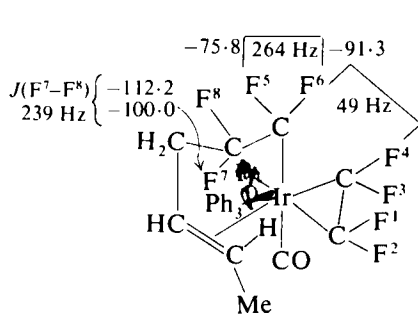
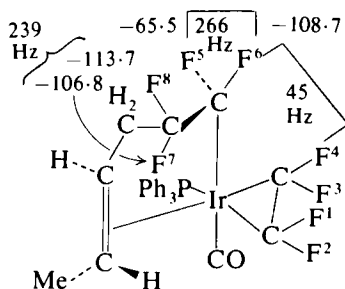
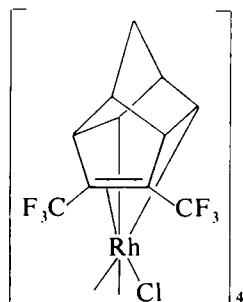
Further reaction of complexes [196, L = PPh₃, AsPh₃, Allyl group = 2-methylallyl] with C₂F₄ gave compounds for which structures [198] are



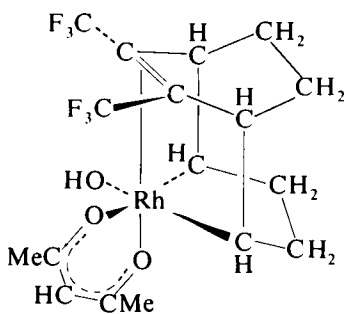
[198] L = PPh₃, AsPh₃

proposed on the basis of spectroscopic evidence. (84) Thus the signals ascribed to the IrCF_2CF_2 group remained essentially unchanged, as two AB quartets, (see Table XII) but in each case two more AB quartets, with $J(\text{A-B})$ *ca.* 265 Hz and *ca.* 240 Hz appeared, the former at high frequency (δ -65 to -75 and -90 to -107), suggesting an α -CF₂ group in a fluoroalkyl group σ -bonded to iridium. Strong coupling between F6 and F1 and between F6 and F4 (e.g., 53 and 51 Hz respectively in [198, L = PPh₃]) may be due to 'through space' interaction, since molecular models suggest a separation of only *ca.* 1.9 Å. The strong coupling between phosphorus and F5 (e.g., 67 Hz in [198, L = PPh₃]) is also suggested to be due to the close approach of these nuclei in the stereochemical arrangement shown. The double bond originating from the π -allyl group is thought to lie in the same plane as the IrCF_2CF_2 ring, but when the 1-methylallyl complex [196] reacts further with C₂F₄, the product has temperature-dependent NMR spectra suggesting the presence of interconverting isomers, one, as above, with the complexed double bond in the plane of the IrCF_2CF_2 ring [199] and the second with it lying perpendicularly to the IrCF_2CF_2 [200]. Support for this assignment comes from the through-space coupling of F1 to F6 (41 Hz).

The ¹⁹F spectrum of [201], the structure of which is confirmed by X-

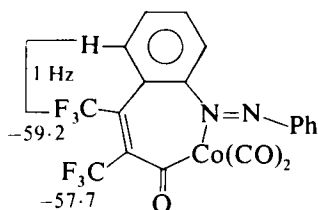
[199] $J(\text{F}^1-\text{F}^6)$ 57 Hz[200] $J(\text{F}^1-\text{F}^6)$ 41 Hz

[201]

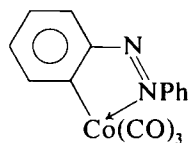


[202]

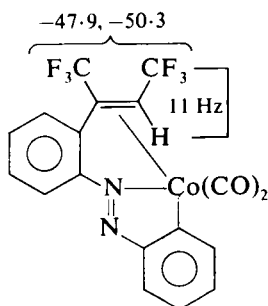
ray crystallography, shows a single band at 35°C (δ -59.1); this separates at -50°C into two broad absorptions of equal intensity (δ -58.6 and -60.3), but the reason for the change is not known. (101) Compound [202] also shows a sharp singlet (δ -60.22) at room temperature, but although the ^1H spectrum shows substantial changes at lower temperatures, only broadening of the ^{19}F signal was observable down to -90°C. (102) The absence of measurable coupling between the CF_3 groups in the spectrum of [203], formed by the reaction of the azobenzene cobalt carbonyl complex [204] with perfluorobut-2-yne, is ascribed to the distortion of the olefinic system shown crystal-



[203]



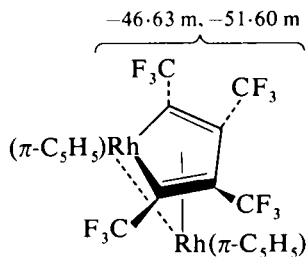
[204]



[205]

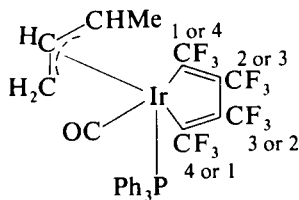
lographically. (103) Thermolysis of [203] gives [205], the ¹⁹F pattern of which is stated to show the *cis*-stereochemistry about the double bond, but no value for the F–F coupling is given in the paper.

Five- and six-coordinate rhodium and iridium complexes containing MC(CF₃):C(CF₃).C(CF₃):C(CF₃) rings have been prepared including one example where such a ring is co-ordinated to a second metal atom [206]. (104) The rhodium complexes all show complex bands in the



[206]

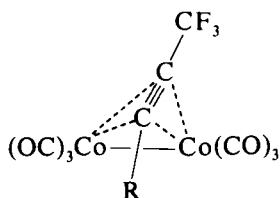
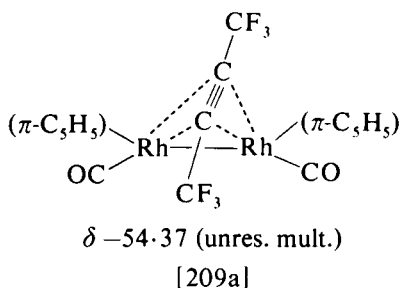
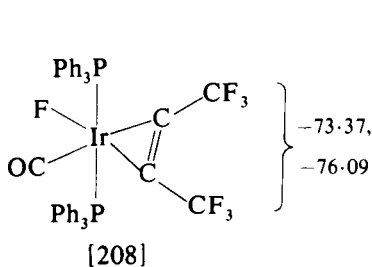
range δ -48.7 to -58.9, (chemical shifts for over 30 examples are given in refs. 92 and 105) but the spectra were too complex for analysis. Temperature-dependent changes in the high-frequency signals due to the α -CF₃ groups for some of the compounds are illustrated in ref. 105. In contrast, the CF₃–CF₃ coupling can be resolved in all four bands of



[207]

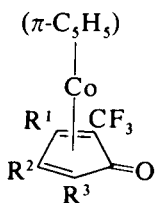
[207]. (91) Quartets at -49.1 and -51.5 for the $\alpha\text{-CF}_3$ groups were coupled to septets at -56.4 and -57.5 respectively [$J(\text{CF}_3^1\text{-CF}_3^2) = J(\text{CF}_3^2\text{-CF}_3^3) = 15$ Hz; $J(\text{CF}_3^3\text{-CF}_3^4) = 16$ Hz]. Four metallacyclic diketones $\text{L}_2\text{ClRhC(O)C(CF}_3\text{):C(CF}_3\text{)CO, } n\text{C}_6\text{H}_6$ ($\text{L} = \text{AsPh}_3, \text{As(C}_6\text{H}_{11}\text{)}_3, \text{As}(p\text{-Tol})_3, \text{As}(p\text{-FC}_6\text{H}_4\text{)}_3$) each show a singlet at *ca.* $\delta -60.7$. (92)

The reactions of fluoroalkyl acetylenes with complexes of cobalt, rhodium, and iridium give a wide range of compounds, some of which have been indicated above. Other examples for which ^{19}F NMR

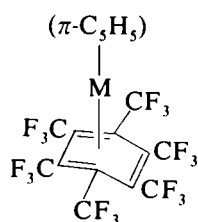


$\text{R} = \text{H}, -52.45\text{s}$
 $\text{R} = \text{Me}_3\text{Si}, -52.41\text{s}$
 $\text{R} = \text{C(CF}_3\text{)(C}_2\text{F}_5\text{)}_2 -53.8 (3), -62.1 (3),$
 $-77.2 (6), -103.7 (4)$

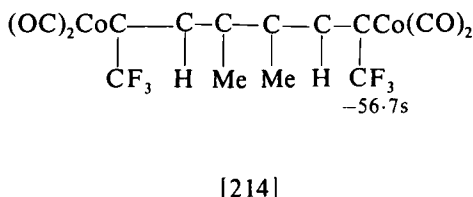
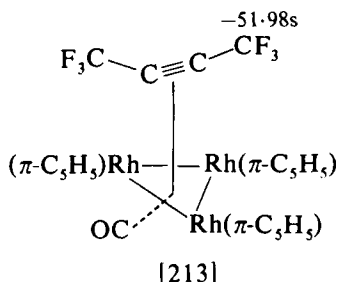
$[\text{IrCl}(\text{cod})(\text{CF}_3\text{C}_2\text{CF}_3)]_2$
 $\delta -52.36\text{s}, -57.45\text{s}$
 [210]



$\text{R}^1 = \text{R}^2 = \text{R}^3 = \text{CF}_3 -52.04\text{m}, -55.71\text{m}$
 $\text{R}^1 = \text{R}^3 = \text{H}, \text{R}^2 = \text{CF}_3 -58.68\text{s}, -58.94\text{s}$
 $\text{R}^1 = \text{R}^2 = \text{H}, \text{R}^3 = \text{CF}_3 -58.41$

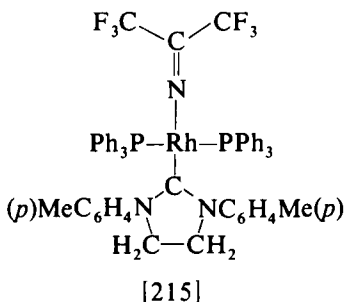


$\text{M} = \text{Co} -49.72, -51.52, -56.54$
 $\text{M} = \text{Rh} -49.24, -52.15, -56.45$



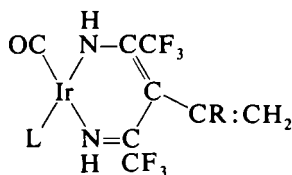
parameters have been reported are shown in structures [208] to [214]. (100, 104, 106–111) A crystal structure determination shows the two different environments of the CF_3 groups in the centrosymmetric dimer [210]. (108) Parameters for the rhodium analogue of compound [211, $\text{R}^1 = \text{R}^2 = \text{R}^3 = \text{CF}_3$] (δ -52.55 , -55.98) (109) are very similar to those for the cobalt compound, and the similarity is maintained with the tetrahapto(hexakistrifluoromethylbenzene) complexes [212]. (104, 109) The singlet in the ^{19}F spectrum of the compound assigned structure [213] presumably indicates free rotation of the “triply bridging” alkyne. (104) Compound [214] has the “flyover” structure (cf. Vol. 5A, p. 272), the positions of the groups being assigned by comparison with other examples for which X-ray crystal structure determinations have been carried out. (111) The product of the reaction of perfluorobut-2-yne with $[\text{Co}(\text{CO})_3(\text{SC}_6\text{F}_5)]_2$ has also been shown crystallographically to have a $-\{\text{C}(\text{CF}_3)\}_4\text{S}-$ “flyover” (δ -50.7 , -54.3 , -58.0 , -65.2) linking the two $\text{Co}(\text{CO})_2$ groups. (32)

Several rhodium and iridium complexes containing the $\text{M}-\text{N}:\text{C}(\text{CF}_3)_2$ group have shifts in the range δ -68.5 to -70.0 . (112–114) The well-resolved triplet observed at 25°C for [215] ($J(\text{P}-\text{CF}_3)$ 2.0 Hz)



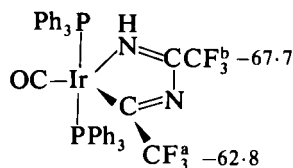
indicates that the CF_3 groups are equivalent at this temperature, but at lower temperature the signal broadens. Individual *syn* and *anti* CF_3 groups are not frozen out at -80°C , however, and the precise process leading to the broadening (slowing down of planar inversion at nitrogen,

or a decrease in rate of rotation about the Rh-N bond) has not been determined. (113) Parameters for other compounds containing M-N:C(CF₃) groups and M-N(CF₃) groups are shown with formulae [216] to [219]. The structure of [216] was confirmed crystal-



L = PPh₃, R = Me δ -63.9s, -69.3s

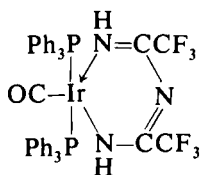
[216]



$J(\text{P}-\text{CF}_3^a)$ 14.0 Hz

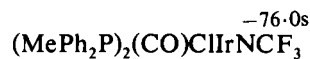
$J(\text{P}-\text{CF}_3^b)$ 8.5 Hz

[217]



-73.2s, -74.4s

[218]



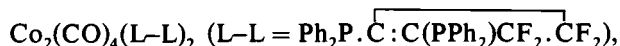
-76.0s

[219]

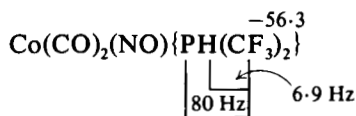
lographically, (64) and similar ¹⁹F parameters were obtained for the analogous compounds [216, R = Me, L = Ph₃As] and [216, R = H, L = Ph₃P]. Structure [218], however, was assigned only somewhat tentatively. Compound [219] is formulated as the nitrene complex, but the stereochemistry about the metal is not known. (115)

Complexes of cobalt containing PCF₃ groups have been prepared independently by two groups, (116, 117) and parameters reported are shown with structures [220]* to [224]. The P-CF₃ coupling constant is increased in each case compared with that in the free ligand, as expected. Compound [222] appears from the spectra to be a mixture of isomers *a* and *b*; the separation of the second order doublet for the major isomer is 88 Hz. The spectrum of [223] is also second order, with a major doublet separation of 68 Hz. Compound [224] shows inequivalent CF₃ groups attached to phosphorus, and a bent Co-Co bond is invoked to account for this. (117)

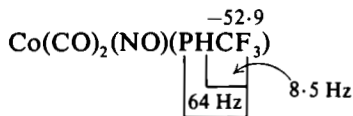
Two new isomeric complexes



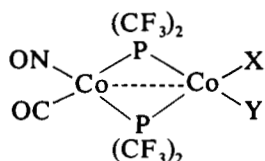
* Parameters for this compound reported in ref. 117 are very similar: δ -53.4, $J(\text{P}-\text{F})$ 78 Hz, $J(\text{P}-\text{H})$ 6.8 Hz.



[220]

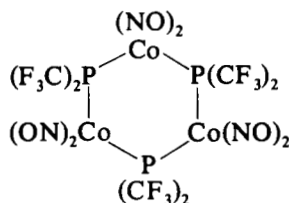


[221]

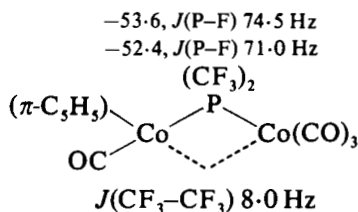


[222a] X = NO, Y = CO

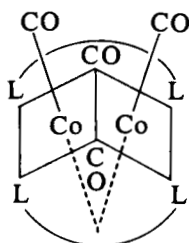
[222b] X = CO, Y = NO



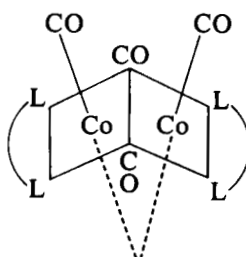
[223]



[224]

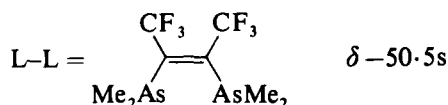
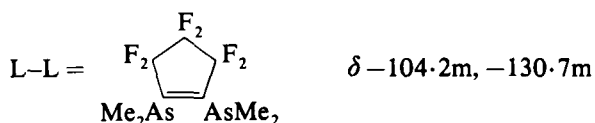
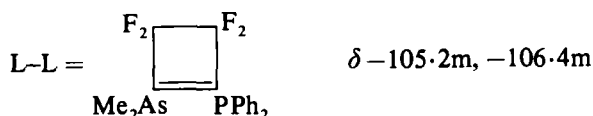
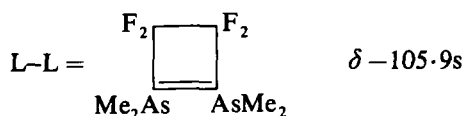


[225]



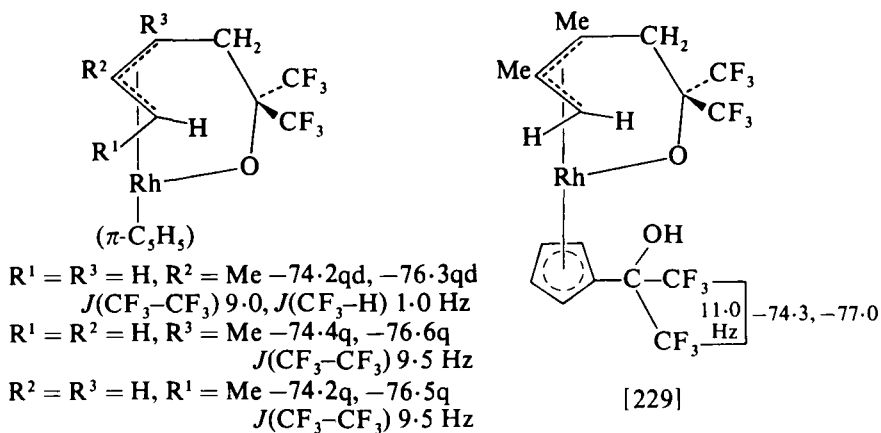
[226]

with structures in which L-L is either bridging [225] or chelating [226] have been prepared; their ^{19}F parameters are almost identical, (δ -108.0 , -107.8) in each case indicating a symmetrical structure. (118) Such bidentate ligands also displace CO from the alkyne-dicobalthexacarbonyls, to give complexes for which the ^{19}F spectra are very similar to those of the free ligands. Some examples are given with formula [227]. (119) The complex $[\text{Co}(\text{CO})_3(\text{L}-\text{L}')_2]$ of the unsymmetrical ligand $\text{Me}_2\text{AsC}:\text{C}(\text{NMe}_2)\text{CF}_2\cdot\text{CF}_2$, only the arsenic atom of which is co-ordinated to the metal, shows two equally intense singlets at δ -108.0 , -108.4 . (118)



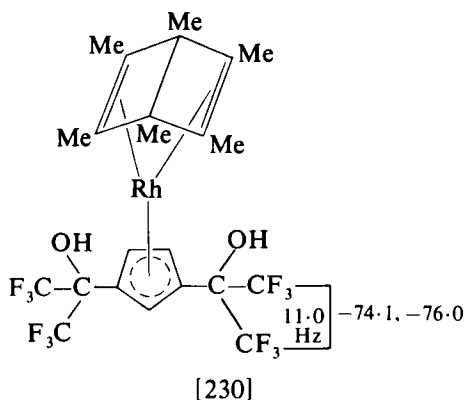
[227]

Like the (diene)ironcarbonyl compounds (see p. 38), cyclopentadienyl(diene)rhodium reacts with hexafluoroacetone to give products in which the $(CF_3)_2C-O$ group links the metal and one end of the original diene [228], the absence of $Rh-F$ coupling suggesting the direction of insertion shown. (63) Attack on the cyclopentadienyl group



[228]

[229]



also gives [229] and [230], the $\text{CF}_3\text{--CF}_3$ coupling being taken to be due to restricted rotation about the ring $\text{--C}(\text{CF}_3)_2$ bond as suggested by molecular models.

^{19}F Spectra of complexes formed by the reaction of cobalt trifluoroacetate with alkylpyridines show the presence of *cis* and *trans* isomers of $\text{CoL}_4(\text{O}_2\text{CCF}_3)_2$ at low temperatures; the two distinct bands broaden and disappear into the baseline at $40\text{--}60^\circ\text{C}$, and reappear at higher temperatures as single time-averaged bands. Shifts reported range from $\delta +10$ to $+110$, as expected for such magnetically anisotropic species. (120)

The chemical shifts for $[(\pi\text{-C}_5\text{H}_5)\text{Co}(\text{SCF}_3)]_2$ ($\delta -33.1$) (121) and *trans*- $\text{Ir}(\text{SCF}_3)(\text{CO})(\text{PPh}_3)_2$ ($\delta -25.4$) have been reported. (122) The triplet coupling to phosphorus (J 1.0 Hz) establishes the stereochemistry of the latter compound.

F. Nickel, palladium, and platinum

The pseudotrigonal nickel complexes $(\pi\text{-C}_5\text{H}_5)\text{NiR}_\text{F}\text{PPh}_3$ [$\text{R}_\text{F} = \text{CF}_3$, $\delta -3.1$, $J(\text{P--F})$ 14 Hz; $\text{R}_\text{F} = \text{C}_2\text{F}_5$, δCF_2 $\delta \text{CF}_2 -80.2$, $J(\text{P--F})$ 38.0, $J(\text{CF}_3\text{--CF}_2)$ 2.0 Hz, $\delta \text{CF}_3 -87.0$; $\text{R}_\text{F} = (\text{CF}_3)_2\text{CF}$, $\delta \text{CF} -188.0$, $J(\text{P--F})$ 85.5 Hz, $\delta \text{CF}_3 -67.7$, $J(\text{CF}_3\text{--CF})$ 11 Hz] show little or no change in chemical shifts or P--F couplings over the temperature range 293 to 173 or 183 K, (44) in contrast to some of the analogous iron (44) and cobalt (83) complexes studied (see pp. 19 and 49), which may indicate free rotation about the M--C-- over the whole temperature range.

Trifluoromethylplatinum(II) complexes, both cationic ($[\text{Pt}(\text{CF}_3)(\text{PMe}_2\text{Ph})_2\text{L}]^+\text{X}^-$) and non-electrolytes $[\text{Pt}(\text{CF}_3)(\text{PMe}_2\text{Ph})_2\text{Y}]$ (where L is a neutral ligand, X^- is PF_6^- or BF_4^- , and Y is an anion), have been prepared from $\text{PtCF}_3(\text{PMe}_2\text{Ph})_2\text{I}$. (123) All the resulting complexes

TABLE XIII

Some ^{19}F NMR parameters for $\text{CF}_3\text{—Pt(II)}$ complexes^a

Compound	δ	$J(\text{Pt—CF}_3)$	Ref.
$[\text{PtCF}_3\text{Q}_2(\text{acetone})]\text{PF}_6$	−11.20	858	123
$[\text{PtCF}_3\text{Q}_2(\text{NCCH:CH}_2)]\text{PF}_6$	−15.22	780	123
$[\text{PtCF}_3\text{Q}_2(p\text{—NCC}_6\text{H}_4\text{OMe})]\text{PF}_6$	−14.71	778	123
$[\text{PtCF}_3\text{Q}_2\{\text{NH:C(OMe)(C}_6\text{F}_5)\}]\text{PF}_6$	−13.68	724	123
$\{[\text{PtCF}_3\text{Q}_2]\}_2\{(p\text{—NH:COMe})_2\text{C}_6\text{F}_4\}\}\text{PF}_6$	−13.19	721	123
$[\text{PtCF}_3\text{Q}_2\text{Py}]\text{PF}_6$	−13.81	702	123
$[\text{PtCF}_3\text{Q}_2(\text{CO})]\text{PF}_6$	−22.28	656	123
$[\text{PtCF}_3\text{Q}_2(\text{CNEt})]\text{PF}_6^b$	−20.24	620	123
$[\text{PtCF}_3\text{Q}_2(p\text{—CNC}_6\text{H}_4\text{OMe})]\text{PF}_6^b$	−20.18	620	123
$[\text{PtCF}_3\text{Q}_2\text{AsPh}_3]\text{BF}_4$	−14.36	662	123
$[\text{PtCF}_3\text{Q}_2\text{PPh}_3]\text{BF}_4$	−15.40	566	123
$[\text{PtCF}_3\text{Q}_3]\text{PF}_6$	−15.75	550	123
$[\text{PtCF}_3\text{Q}_2\text{SbPh}_3]\text{BF}_4$	−14.64	708	123
$[\text{PtCF}_3\text{Q}_2\{\text{CH}_2\text{CH}_2\text{OCCH}_2\}]\text{PF}_6$	−19.97	482	123
$[\text{PtCF}_3\text{Q}_3\{\text{CMe(OMe)}\}]\text{PF}_6$	−19.85	468	123
$\text{PtCF}_3(\text{ONO}_2)\text{Q}_2$	−11.20	795	123
$\text{PtCF}_3\text{Q}_2\text{I}$	−11.95	754	123
$\text{PtCF}_3\text{Q}_2\text{Br}$	−10.79	763	123
$\text{PtCF}_3\text{Q}_2\text{Cl}$	−10.52	757	123
$\text{PtCF}_3\text{Q}_2(\text{NCO})$	−11.81	714	123
$\text{PtCF}_3\text{Q}_2(\text{NCS})$	−13.00	721	123
$\text{PtCF}_3\text{Q}_2(\text{N}_3)$	−11.60	710	123
$\text{PtCF}_3\text{Q}_2(\text{NO}_2)$	−15.04	644	123
$\text{PtCF}_3\text{Q}_2(\text{CN})$	−17.6	565	123
$\text{Pt}(\text{CF}_3)_2(\text{NC}_5\text{H}_4\text{Me})_2$	−24.80	793	124
$\text{Pt}(\text{CF}_3)_2(\text{SbPh}_3)_2$	−11.09	791	124
$\text{Pt}(\text{CF}_3)_2(\text{Me}_2\text{NCH}_2\text{CH}_2\text{NMe}_2)$	−24.60	752	124
$\text{Pt}(\text{CF}_3)_2(\pi\text{—1,5COD})$	−29.73	736	124
$\text{Pt}(\text{CF}_3)_2\text{Bipy}$	−23.90	741	124
$\text{Pt}(\text{CF}_3)_2(\text{AsPh}_3)_2$	−29.01	731	124
$\text{Pt}(\text{CF}_3)_2(\text{CNEt})_2$	−24.20	719	124
$\text{Pt}(\text{CF}_3)_2(\text{AsMe}_3)_2$	−19.61	713	124
$\text{Pt}(\text{CF}_3)_2\text{Q}_2^c$	−21.60	627	124

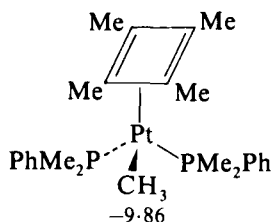
^a Q = PMe_2Ph throughout this Table.^b The phosphine ligands exchange at room temperature. Parameters are from spectra obtained at low temperature.^c $^3J(\text{P—F})$ 7.2 Hz.

have the two phosphine ligands *trans*, as shown by their ^1H methyl triplets, and ^{19}F shifts and couplings to ^{195}Pt are given in Table XIII. The CF_3 groups also show triplet splitting from the two equivalent *cis*-phosphorus nuclei (16–20 Hz), and larger (56–57 Hz) coupling when a phosphorus ligand is also *trans* to the CF_3 group. With few exceptions ($\text{L} = \text{SbPh}_3$ and, to a smaller extent, CO) $J(\text{Pt—CF}_3)$

shows a linear correlation with $J(\text{Pt}-\text{CH}_3)$, both for non-electrolytes, and for cations, each group having a slightly different slope, and there is also a general tendency for high values of the coupling constant to be associated with (numerically) low values of δ . The causes of these correlations, and their implications, are discussed in detail in the paper.

Bis(trifluoromethyl)platinum(II) compounds containing a wide range of other ligands have been prepared from $(\text{CF}_3)_2\text{Pt}(1,5\text{COD})$, (124) and the chemical shifts and $^{19}\text{F}-^{195}\text{Pt}$ coupling constants reported are also given in Table XIII. The magnitude of $J(^{195}\text{Pt}-^{19}\text{F})$ can be used to rank the ligands according to their *trans*-influence, a high *trans*-influence corresponding to a low value of the coupling constant.

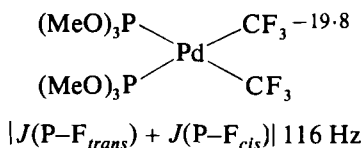
Parameters for some $\text{CF}_3\text{Pt}(\text{IV})$ complexes are given in Table XIV. It is pointed out that the spectrum of the tetramethylcyclobutadiene complex [231] shows $J(\text{Pt}-\text{PCH}_3)$ and $J(\text{Pt}-\text{F})$ similar to those of



$J(\text{Pt}-\text{F})$ 496 Hz

[231]

complexes of $\text{Pt}(\text{IV})$ rather than of $\text{Pt}(\text{II})$, (125) the absence of coupling from phosphorus to fluorine being ascribed to the pseudo-tetrahedral structure necessitated by the cyclobutadiene ligand. The structure of the complex has been confirmed crystallographically (126). A single bis-(trifluoromethyl)palladium complex [232] has also been reported. (127)

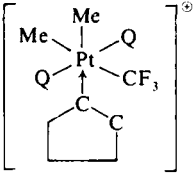
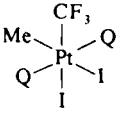
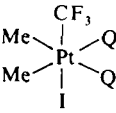
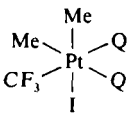
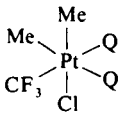


[232]

Protonation of tetrafluoroethylene platinum complexes $\text{L}_2\text{Pt}(\text{C}_2\text{F}_4)$ with trifluoroacetic acid gives tetrafluoroethyl complexes $\text{L}_2\text{Pt}(\text{CF}_2\text{CF}_2\text{H})(\text{OCOCF}_3)$. (128) The NMR spectra showed the illustrated *trans* stereochemistry for complexes [233] and [234], but the ^1H spectrum of [235] confirmed that it was the *cis*-isomer; the main signal

TABLE XIV

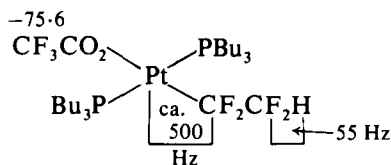
Some ^{19}F NMR parameters for $\text{CF}_3\text{—Pt(IV) complexes}^a$

Compound	δ	$J(\text{Pt—CF}_3)$	Other couplings	Ref.
	PF_6^- -18.94	249	$J(\text{P—F}) 7.2 \text{ Hz}$	125
	-17.0	505		123
	-19.3	517		123
	-22.62	419		123
	-29.45	411		123
$\text{Pt}(\text{CF}_3)_2(\text{PMe}_2\text{Ph})_2\text{I}_2$	-10.41 (t)	289	$^3J(\text{P—F}) 8.4 \text{ Hz}$	124
$\text{Pt}(\text{CF}_3)_2(\text{CNEt})_2\text{I}_2$	-11.61	452		124
$\text{Pt}(\text{CF}_3)_2\text{BipyI}_2$	-10.21	441		124

^a Q = PMe_2Ph throughout this Table.

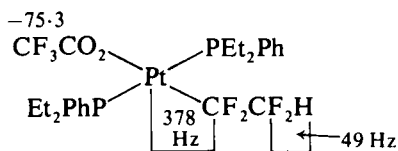
for the $\alpha\text{—CF}_2$ of this compound was obscured by the CF_3 -group, and the parameters given were taken from the platinum satellites. Chemical shifts for $(\text{Ph}_3\text{As})_2\text{Pt}(\text{CF}_2\text{CF}_2\text{H})(\text{OCOCF}_3)$ were similar to those for [233]–[236], but no platinum satellites were observable.

The reaction of bis(trifluoromethyl)diazomethane with (stilbene)bis-(triphenylphosphine)platinum unexpectedly gave the platinum fluorides [237] and [238], with the parameters shown, as minor products, (94) the



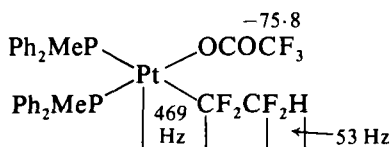
$J(\text{P}-\text{CF}_2^\alpha)$ 25 Hz (triplet)
 $J(\text{Pt}-\text{CF}_2^\beta)$ 102 Hz

[233]



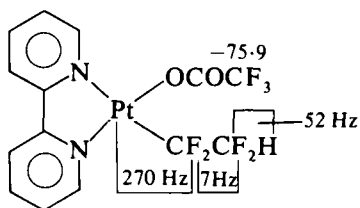
$J(\text{P}-\text{CF}_2^\alpha)$ 23 Hz (triplet)
 $J(\text{Pt}-\text{CF}_2^\beta)$ 98 Hz
 $J(\text{CF}_2^\alpha-\text{H}) = J(\text{CF}_2^\alpha-\text{CF}_2^\beta)$ 5.7 Hz

[234]

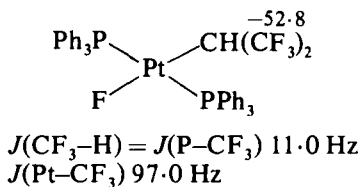


$J(\text{P}-\text{CF}_2^\alpha)$ 33 Hz (doublet)
 $J(\text{Pt}-\text{CF}_2^\beta)$ 99 Hz

[235]

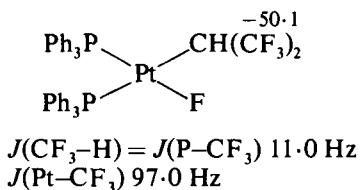


[236]



$J(\text{CF}_3-\text{H}) = J(\text{P}-\text{CF}_3)$ 11.0 Hz
 $J(\text{Pt}-\text{CF}_3)$ 97.0 Hz

[237]

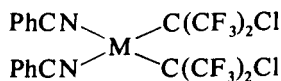


$J(\text{CF}_3-\text{H}) = J(\text{P}-\text{CF}_3)$ 11.0 Hz
 $J(\text{Pt}-\text{CF}_3)$ 97.0 Hz

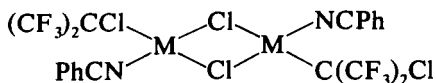
[238]

structure of [237] being confirmed crystallographically. (129) As frequently happens, the signal due to $\text{Pt}-\text{F}$, which would be coupled to several other nuclei, was unobservable. With bis(benzonitrile)-palladium or -platinum dichloride, insertion of $(\text{CF}_3)_2\text{C}$ into the $\text{M}-\text{Cl}$ bond gave [239] and [240], (94) and a similar insertion to give [241] has also been reported. (130)

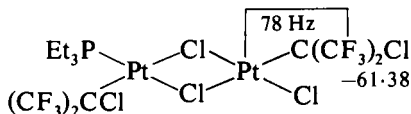
The preparation has been reported of several three-, four-, five-, and six-membered ring systems in which the metal is bonded to a CF_n or $\text{C}(\text{CF}_3)$ group, and parameters are given with structures [242] to [264]. The single hydrogen in [242] could not be located, but the geminal $\text{F}-\text{F}$ coupling constant is typical of the metallacyclopropane structure. (94) No platinum satellites were reported for the geminal fluorines, however, and a strong $\text{P}-\text{F}$ coupling (30.0 Hz) was distinguishable in only the

M = Pd δ -62.3sM = Pt δ -63.1, $J(\text{Pt}-\text{CF}_3)$ 53.0 Hz

[239]

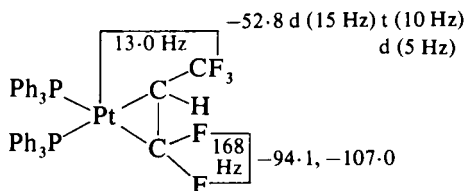
M = Pd δ -62.9s

[240]

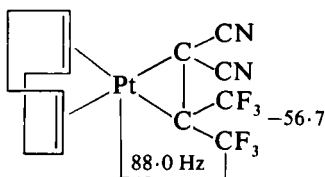


[241]

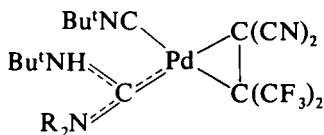
band at δ -107.0. The platinum-fluorine coupling for the CF_3 group is also considerably smaller than that found in [243]. (131) The carbene complexes [244] show only the expected singlets. (132)



[242]

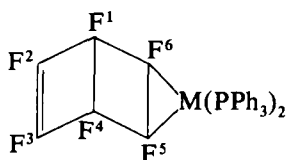


[243]

R = Me δ -55.3R = Et δ -55.4

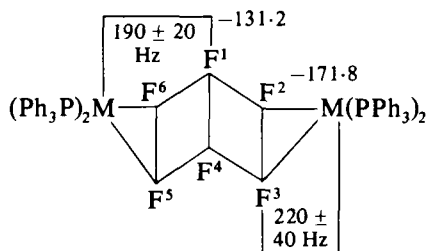
[244]

Hexafluorobicyclo[2,2,0]hexa-2,5-diene readily gives [245a and b] with $\text{Pd}(\text{PPh}_3)_4$ and $\text{Pt}(\text{PPh}_3)_4$ respectively. (30) The bands at δ -171.5 in [245a] and at δ -176.4 in [245b] are broader and more complex than those at δ -165.0 and -165.7, presumably because of phosphorus-fluorine coupling, and are thus assigned to F(5) and F(6). This reverses the assignment originally suggested for [245b]. (30b, 31) Both the band at -176.4 and that at -165.7 in [245b] show platinum satellites [$J(\text{Pt}-\text{F})$ 180 ± 5 Hz and 185 ± 5 Hz respectively], suggesting through-space



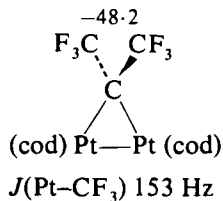
	$\delta(F^1F^4)$	$\delta(F^2F^3)$	$\delta(F^5F^6)$
[245a] M = Pd	-165.0	-126.9	-171.5
[245b] M = Pt	-165.7	-126.0	-176.4

coupling to $F(1)$ and $F(4)$ in the *exo* structure shown. Further reaction of [245a and b] with $Pd(Ph_3)_4$ or $Pt(Ph_3)_4$ respectively gives [246a and b], but [246a] is too insoluble for NMR measurements. The presence of

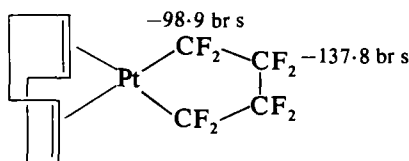


[246a] M = Pd	Too insoluble
[246b] M = Pt	Parameters given

only two bands in the spectrum of [246b], both showing Pt-F coupling, and the high-frequency shift of $F(1)$ and $F(4)$ suggests the *exo-exo* structure shown with $F(1)$ and $F(4)$ close to two metal atoms. The band due to $F(1)$ and $F(4)$ shows coupling to both the platinum atoms, though the outer bands are reported to be only just detectable. The novel diplatinacyclopentane [247], formed in the reaction of hexafluoropropene with $Pt(COD)_2$, also shows a 1:8:18:8:1 multiplet ($\delta -48.2$), consistent with coupling of the CF_3 groups to two equivalent ^{195}Pt nuclei [$J(Pt-CF_3)$ 153 Hz], and irradiation at the ^{195}Pt resonance frequency reduced the multiplet to a singlet. (133)

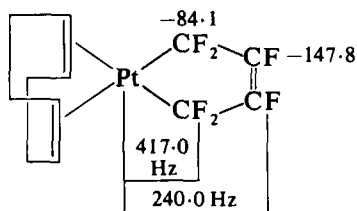


[247]



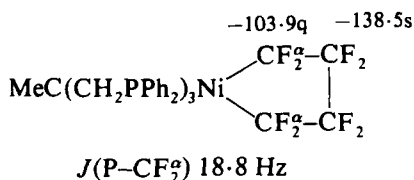
[248]

The ^{19}F spectrum of [248] consists only of broad singlets, the high-frequency signal being strongly coupled to platinum. In [249], each band

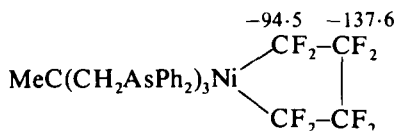


[249]

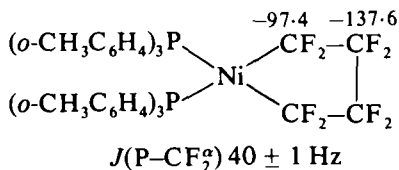
appears as a strong singlet in the centre of four pairs of doublets. Coalescence of the N lines of the expected $X_2AA'X'_2$ system would give the strong central lines, indicating that $|J_{AX} + J_{AX'}|$ is zero, and it is suggested that the very weak splitting observed in many octafluorometallacyclopentanes may arise because of couplings of similar magnitude but opposite sign. (131) In accord with this, the signals for [250], apart from quartet splitting of the α - CF_2 groups, which establishes that all three phosphorus atoms are co-ordinating to the metal, appear as singlets, and for [251] appear simply as two 3 Hz triplets; (134) [252] shows only triplet-splitting of the α - CF_2 by



[250]

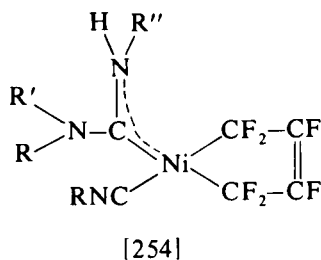
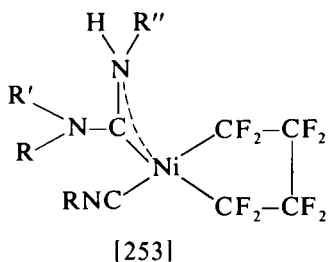


[251]

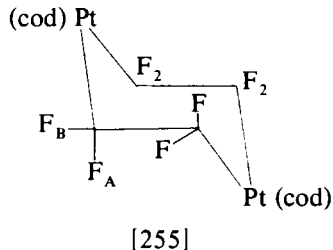


[252]

phosphorus. (135) The carbene complexes [253] show two different α -CF₂ resonances, [δ -104 to -111] as expected since one is *cis* to the isonitrile and the other *cis* to the carbene ligand, but the β -CF₂ absorptions (δ -136 to -141) are not resolved. (132) Again there are no large F-F couplings observable. No large couplings are seen in the corresponding hexafluoronickelacyclopentene complexes [254], but the two β -fluorines are readily resolved, as are the α -CF₂ groups (α -CF₂ -90.8 to -91.3 and -92.7 to -96.1, β -CF -148.6 to -148.8 and -149.6 to -150.1).

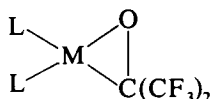


Tetrafluoroethylene reacts with Pt(COD)₂ to give the di-platinacyclohexane [255], which at 90°C shows a singlet (δ -86.2) with



two pairs of platinum satellites [²J(Pt-F) 388, ³J(Pt-F) 98 Hz]. (133) At lower temperatures the spectrum broadens and at -60°C gives an AB pattern (δ_A -81.6, δ_B -93.4; *J*(A-B) 225, *J*(Pt-A) 390, *J*(Pt'-A) 80, *J*(Pt-B) 350, *J*(Pt'-B) 133 Hz), consistent with F_A and F_B being axial and equatorial fluorines in a puckered (presumably chair) conformation which undergoes rapid inversion at room temperature.

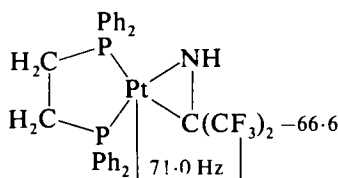
Chemical shifts in the palladium (127) and platinum (131) mono-(hexafluoroacetone) complexes [256] are almost independent of the metal or of the other ligands, and very similar values are reported for the hexafluoroisopropylideneimine complex [257]. (131) The difference between the coupling of the CF₃ groups to phosphorus ligands in the *cis* and *trans* positions, however, is notably larger for the platinum complexes than for those of palladium.



M	L or L ₂	δCF_3	$J(\text{P}_{\text{cis}}-\text{CF}_3)$	$J(\text{P}_{\text{trans}}-\text{CF}_3)$
Pt	(Ph ₂ PCH ₂) ₂	-66.2 ^a	2.0	12.0
Pt	P(OPh) ₃	-66.5 ^b	3.0	17.0
Pd	P(OPh) ₃	-66.1 ^c	13.0	13.0
Pd	PMePh ₂	-66.3	7.0	11.0
Pd	(Ph ₂ PCH ₂) ₂	-66.3	7.5	13.5

^a $J(\text{Pt}-\text{CF}_3)$ 71.0 Hz. ^b $J(\text{Pt}-\text{CF}_3)$ 60.0 Hz. ^c At -80°C.

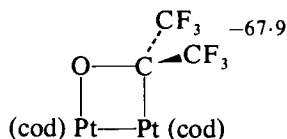
[256]



$J(\text{P}_{\text{cis}}-\text{CF}_3)$ 1.0 Hz
 $J(\text{P}_{\text{trans}}-\text{CF}_3)$ 11.0 Hz

[257]

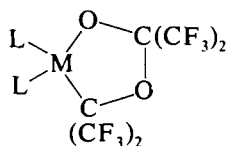
The four-membered ring compound [258], obtained by treatment of $\text{Pt}(\text{COD})_2$ with hexafluoroacetone, has been characterized by single



[258]

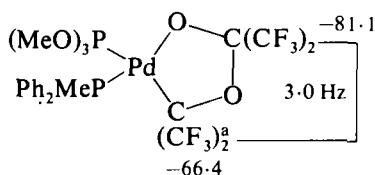
crystal X-ray diffraction. (134) The ^{19}F spectrum consists of a singlet (δ -67.9) with two pairs of satellite peaks [$^3J(\text{Pt}-\text{CF}_3)$ 115.9, $^4J(\text{Pt}-\text{CF}_3)$ 11.5 Hz], and four further peaks, showing second order effects, attributed to molecules containing two ^{195}Pt atoms with rather similar chemical shifts. A $^{19}\text{F}\{^{195}\text{Pt}\}$ INDOR investigation gives the separation as 634 ppm (21.4 MHz) with $^1J(\text{Pt}-\text{Pt})$ 5355 Hz, the first one-bond platinum-platinum coupling constant to be measured.

Chemical shifts of one $\text{C}(\text{CF}_3)_2$ group in each of the five-membered ring complexes [259], [260] and [261], and $\text{Pt}-\text{CF}_3$ coupling constants in the platinum compounds, are very similar to those in [256], and are



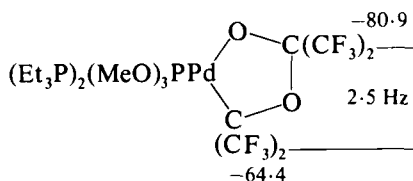
M	L or L ₂	$\delta(\text{CF}_3^\alpha)$	$J(\text{Pt}-\text{F})$	$\delta(\text{CF}_3^\beta)$
Pt	PPh ₂ Me	-64.9	76	-80.6
Pt	(Ph ₂ PCH ₂) ₂	-66.6	72	-80.7
Pt	P(OMe) ₃	-66.0	79.0	-82.5
Pt	1,5-cod	-67.1	68.5	-80.4
Pd	P(OMe) ₃	-65.7	—	-81.4
Pd	PPh ₂ Me	-64.1	—	-80.4
Pd	P(OMe) ₂ Ph	-64.8	—	-80.9
Pd	AsMe ₂ (CH ₂ Ph)	-65.5	—	-80.4
Pd	(Ph ₂ PCH ₂) ₂	-66.3	—	-81.1

[259]



$$J(\text{P}_{\text{cis}}-\text{CF}_3^\alpha) = J(\text{P}_{\text{trans}}-\text{CF}_3^\alpha) = 6.0 \text{ Hz}$$

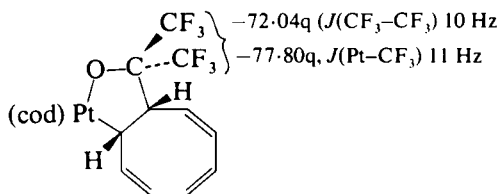
[260]



[261]

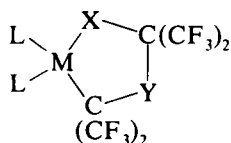
thus ascribed to the $\text{C}(\text{CF}_3)_2$ groups bonded to the metal. (127, 131) Weak coupling (*ca.* 3 Hz) between the two sets of $\text{C}(\text{CF}_3)_2$ groups could be observed in many of the compounds, and coupling of the $\alpha\text{-C}(\text{CF}_3)_2$ group to the *cis*- and *trans*-phosphorus ligands could also be observed. Parameters listed for nine carbene complexes of the type [259, M = Ni, Pd, Pt, L = CNR, $\text{C}(\text{NR}'\text{R}'')(\text{NHR}''')$] and for their bis(isonitrile) complex precursors [259, M = Pd, Pt, L = CNR] are very similar to those given with structure [259]. (132) A X-ray crystal structure determination shows that the $\text{C}(\text{CF}_3)_2$ group is *cis* to the isonitrile ligand in the carbene complex $(\text{Bu}^t\text{NC})[\text{Bu}^t\text{NH}(\text{Et}_2\text{N})\text{C}]\text{PdC}(\text{CF}_3)_2\text{OC}(\text{CF}_3)_2\text{O}$. (136)

Compound [261] differs from the rest in being pentaco-ordinate, and it is suggested that the oxygen will occupy an apical position. (127) Compound [262], in which the Pt-F couplings are small, suggesting the Pt-O- $\text{C}(\text{CF}_3)_2$ linkage, is obtained, like [258], from the reaction of $\text{Pt}(\text{COD})_2$ with hexafluoroacetone. (133)



[262]

Parameters for the "mixed" heterocyclic compounds [263] do not allow a distinction between the two possible structures with $X = O$, $Y = NH$ or $X = NH$, $Y = O$, but an X-ray crystallographic study of the

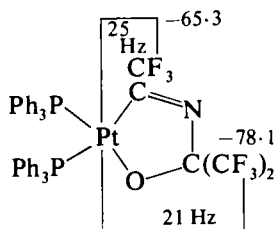


$X = O$, $Y = NH$ or $X = NH$, $Y = O$

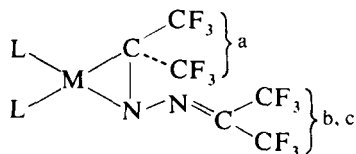
M	L or L_2	δCF_3^a	$J(Pt-F)$	δCF_3^b
Pt	PPh_2Me	-63.9	88	-80.9
Pd	$(Ph_2PCH_2)_2$	-65.3	—	-81.7
$X = Y = NH$				
Pt	PPh_2Me	-66.1	80	-81.65

[263]

corresponding nickel complex with $L = Bu^iNC$ corresponds to the former arrangement. (137) Complex [264], formed in the reaction of $(Ph_3P)_2Pt(CF_3CN)$ (see [306], p. 95 for ^{19}F parameters), with hexafluoroacetone, shows a triplet (5 Hz) suggesting that $J(P_{cis}-CF_3) = J(P_{trans}-CF_3)$ for the single CF_3 group. (138) The spectrum was unchanged at -90° , suggesting that this was not a time-averaging effect. The CF_3 groups in [265] are magnetically equivalent in solution, although an X-ray study shows the ring nitrogen to be sp^3 hybridized in



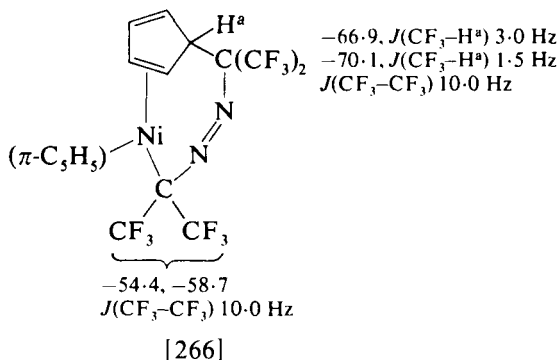
[264]



[265]

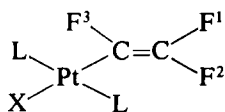
	M	L	δCF_3^a	δCF_3^b	δCF_3^c
[265a]	Pt	PPh_3	-59.5d	-63.5m	-65.8m
[265b]	Pt	PEt_3	-58.8d	-61.8m	-65.8m
[265c]	Pd	Bu^tNC	-62.5s	-62.5q	-66.8q
[265d]	Pd	$\text{c-C}_6\text{H}_{11}\text{NC}$	-62.3s	-62.4q	-66.7q
[265e]	Ni	Bu^tNC	-62.0s	-62.6q	-63.7q
[265f]	Ni	PMePh_2	-59.9d	-60.9m	-63.4m
[265g]	Ni	1,5 cod	-57.0s	-60.0q	-63.8q

the solid state. (94, 139) There must therefore be rapid inversion in solution, even at -95°C , at which temperature the NMR spectrum of [265a] was unchanged. (Essentially identical parameters for [265a] have been reported independently. (130)) Coupling of these CF_3 groups to platinum (79.0 Hz for [265a], 81.0 Hz for [265b]) is similar to that in [257], as is $J(\text{P}_{\text{trans}}-\text{CF}_3)$ (10 Hz in [265a, b, f]). The other two CF_3 groups are magnetically inequivalent and coupled ($J(\text{CF}_3-\text{CF}_3)$ 6.0 Hz in each case), and in [265a, b, and f] are also coupled differently to phosphorus ($J(\text{P}-\text{CF}_3^b)$ 2–2.5 Hz, $J(\text{P}-\text{CF}_3^c)$ 6.0 Hz). In [266] the



[266]

“free” $:\text{C}(\text{CF}_3)_2$ has become attached to the cyclopentadiene ring. (93) The appearance of two pairs of inequivalent CF_3 groups shows that there is no symmetry plane through the nickel atom and the two C_5 rings, in accord with a structure such as that shown, in which the nickel is bonded to only one double bond of the “attacked” cyclopentadiene.



[267a] $L = PPh_3$, $X = I$ [267b] $L = PPh_3$, $X = SCN$
 also $L = PPh_3$, $X = NO_2$, NO_3
 $L = PMePh_2$, $X = SCN$, NO_2

	δF^1	δF^2	δF^3
a	-100.6	-129.2	-147.5
b	-100.4	-128.7	-148.2

coupling constants									
	F^1-F^2	F^1-F^3	F^2-F^3	$P-F^1$	$P-F^2$	$P-F^3$	$Pt-F^1$	$Pt-F^2$	$Pt-F^3$
a	102	31	104	6	3.5	1.5	65	58	480
b	97	30	105	6	4	2	66	50	430

Rearrangement of the olefin complexes $L_2PtCF_2.CFBr$ and anion exchange gives a series of trifluorovinylplatinum complexes [267]. Parameters for two examples are given with the structure; apart from the platinum-fluorine couplings, which were not observable even with CAT accumulation, the parameters for the other members of the series were very similar to those shown. (140) Parameters for the complexes

$(Ph_2MeP)_2PtCFCI.CFCl$ (phosphine ligands *cis*, fluorines *cis* or *trans*) and for their rearrangement products $(Ph_2MeP)_2Pt(X)CF:CFCI$ (phosphine ligands *trans*, fluorines *cis* or *trans* about the double bond, $X = Cl$ or OAc) are similar to those for the bis(triphenylphosphine) complexes reported previously; (141, 142) parameters for

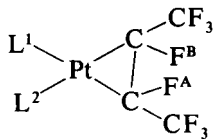
$(PEt_3)_2PtCF_2CF_2$ [$X_2AA'X'_2$ system centred at $\delta -127.5$, with platinum satellites, $J(Pt-F)$ 280 Hz] are also similar to those of the bis-(triphenylphosphine) complex. (143) The CF_3 group in the olefin complex formed by displacement of ethylene from ethylenebistri[(+)-bornan-2-yl]phosphitenickel with 2,2,2-trifluoroethyl acrylate showed only a complex triplet, but in the presence of $Eu(dpm)_3$, two triplets [both $J(F-H)$ 8.2 Hz], with intensities 1:1.44 could be seen with a separation of 0.17 ppm, indicating that the optically active bornanyl group had induced asymmetric formation of the complex. (144)

The reaction of an excess of a mixture of *cis*- and *trans*-perfluorobut-2-ene (*cis:trans* = 1:4) with *trans*-stilbenebis(triphenylphosphine)-platinum gave a single isomer of the perfluorobut-2-ene complex

$(Ph_3P)_2PtCF(CF_3).CFCF_3$, and a similar reaction with $Pt(AsPh_3)_4$ gave $(Ph_3As)_2PtCF(CF_3).CFCF_3$, which, on treatment with Ph_3P , gave the same $(Ph_3P)_2PtCF(CF_3)CFCF_3$. (145) Complexes with PPh_2Me or $Ph_2PCH_2CH_2PPh_2$ ligands were also prepared by ligand exchange and had similar spectroscopic properties (see Table XV; the diphos complex

TABLE XV

Some ^{19}F NMR parameters for compounds [268]

 [268]								
	L^1	L^2	δCF_3	$J(\text{Pt}-\text{CF}_3)$	δCF	$J(\text{Pt}-\text{CF})$	$J(\text{P}-\text{CF}_3)$	$ J(\text{P}-\text{CF}) + J(\text{P}'-\text{CF}) $
a	PPh_3	PPh_3	-68.2	78.1	-201	68.0	9.0	52.4
b	AsPh_3	AsPh_3	-68.3	92.2	-194.1	95.0	—	—
c	PMePh_2	PMePh_2	-68.0	80.0	-200.9	66.2	9.8	54.8
d	PPh_3	AsPh_3	n.r. ^a	n.r. ^a	-198.5 (F^{A}) -196.1 (F^{B})			
e	$\text{Ph}_2\text{PCH}_2\text{CH}_2\text{PPh}_2$ ^b							

^a n.r. = not reported. ^b Too insoluble for NMR measurements.

was insufficiently soluble for NMR measurements) so that all the complexes were known to have the same stereochemistry within the $\text{PtCF}(\text{CF}_3)\text{CF}(\text{CF}_3)$ group. A direct measure of $J(\text{CF}-\text{CF})$, needed to establish this stereochemistry, was obtained from the product of the reaction of $(\text{Ph}_3\text{As})_2\text{PtCF}(\text{CF}_3)\text{CFCF}_3$ with one equivalent of Ph_3P . In the major product [268d], the two CF groups are no longer equivalent (CF^{A} *trans* to P, CF^{B} *trans* to As) and the coupling between them (60 Hz) establishes that the fluorines are *trans* as shown. The CF region of the spectrum, both normal and with ^{31}P decoupling, is shown in the paper.

An X-ray crystal structure of compound [268a] has been reported independently, (146) and the ^{19}F shifts and splittings given in this paper agree well with those in Table XV. The triplet spacing in the CF signal, however, was incorrectly attributed to accidental equivalence of the *cis*- and *trans*-P-CF couplings, rather than to deceptive simplicity in the AA'XX' system.*

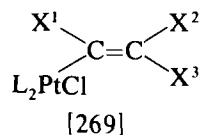
Rearrangement of the butene complexes [268a, c, e] and of the complexes $\text{L}_2\text{PtCF}_2\text{CFCF}_3$ ($\text{L} = \text{PPh}_3$, PMePh_2 , $\text{L}_2 = \text{diphos}$) in the presence of stannic chloride gave the vinyl complexes [269], parameters for which are given in Table XVI. The low values for the platinum coupling constants showed that the chlorine in [269a and b] must be attached to the α -carbon (cf. the large couplings to the signal at -99.0 in [269c]). The stereochemistry about the double bonds in [269c-f] follows from the coupling constants; $J(\text{F}^{\alpha}-\text{F}^{\beta})$ in [269c] is too low for *trans* fluorines, and $J(\text{CF}_3-\text{CF}_3)$ in [269d-f] is typical of CF_3 groups *trans* about a double bond. (146)

A study of platinum-fluorine coupling constants in compounds of the type *trans*- $\text{Pt}(\text{PEt}_3)_2(\text{X})\text{CF}^3:\text{CF}^1\text{F}^2$ (where F^1 is *trans* to the metal) shows that while $J(\text{Pt}-\text{F}^3)$ correlates linearly with other measures of the *trans*-influence of X, $J(\text{Pt}-\text{F}^1)$ and $J(\text{Pt}-\text{F}^2)$ do not, and reasons for this, including a through-space contribution which depends on the orientation of the C-F bond with respect to the co-ordination plane of the platinum, are discussed. (148)

Rearrangement of the hexafluorobuta-1,3-dieneplatinum complexes [270, $\text{L} = \text{PPh}_3$, AsPh_3 , PMePh_2] gives the corresponding complexes

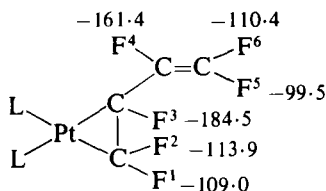
* This paper also comments, in the course of a discussion on the bonding in the complex, on the large change in the environment of the CF fluorines "the chemical shift of the resonances being 136.5 ppm further upfield in the complex than in the free olefin". (147) The actual change is 38.6 ppm, the signal in the spectrum of the free olefin attributed in the 1968 paper (147) to the CF group being that of the CF_3 groups of the less-abundant *cis*-isomer, unfortunately present in an approximately 1:3 ratio.

TABLE XVI

Some ^{19}F NMR parameters for compounds [269]

L	X^1	δX^1	X^2	δX^2	X^3	δX^3	Coupling constants (J in Hz)					
							(1-2)	(1-3)	(2-3)	(Pt-1)	(Pt-2)	(Pt-3)
a $\text{PPh}_3^{a,b}$	Cl	—	CF_3	-66.2	F	-115.7	—	—	14.0	—	28.1	136.8
b $\text{PPh}_2\text{Me}^{a,c}$	Cl	—	CF_3	-65.8	F	-116.3	—	—	13.6	—	25.0	134.0
c diphos d	F	-99.0	F	-153.2	CF_3	-66.4	38.2	9.1	16.0	352.3	—	—
d $\text{PPh}_3^{d,e}$	CF_3	-50.7	F	-102.3	CF_3	-66.9	18.4	1.5	11.2	124.0	278	19.0
e $\text{PPh}_2\text{Me}^{d,f}$	CF_3	-49.6	F	-102.2	CF_3	-66.9	15.0	2.0	12.1	87.0	200	17.8
f diphos d,g	CF_3	-50.4	F	-100.1	CF_3	-68.0	18.0	2.1	12.2	80.1	208	18.1

a Phosphines are *trans*. $^b J(\text{P}-\text{CF}_3)$ 3.4, $J(\text{P}-\text{CF})$ 5.3 Hz. $^c J(\text{P}-\text{CF}_3)$ 3.0, $J(\text{P}-\text{CF})$ 5.3 Hz. d Phosphines *cis*. $^e J(\text{P}-\text{X}^1)$ 2.0 Hz. $^f J(\text{P}-\text{X}^1)$ 6.4 Hz. $^g J(\text{P}-\text{X}^1)$ 6.2 Hz.

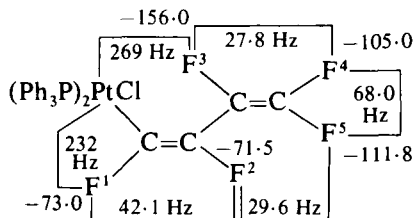


$J(1-2)$ 176.2; $J(1-3)$ 1.5;
 $J(2-3)$ 56.3; $J(2-4)$ 14.9;
 $J(3-4)$ 16.2; $J(3-5)$ 2.1; $J(3-6)$ 19.8;
 $J(4-5)$ 112.6; $J(4-6)$ 27.8;
 $J(5-6)$ 62.4 Hz.

[270a] L = PPh_3 Parameters given

[270b] L = AsPh_3

[270c] L = PMePh_2



$J(1-3)$ 1.9; $J(1-4)$ 7.0; $J(1-5)$ 8.0;
 $J(2-3)$ 23.2; $J(2-4)$ 13.9;
 $J(3-5)$ 108.2 Hz

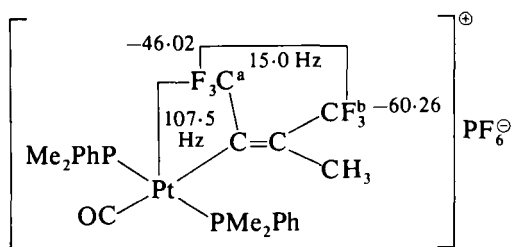
[271a] L = PPh_3 Parameters given

[271b] L = AsPh_3

[271c] L = PMePh_2

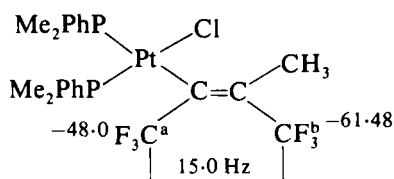
[271], (149) in which the stereochemistry of the diene system is defined by the ^{19}F parameters. The compound assigned structure [270a], for which the parameters are given with the structure, was completely characterized, but has different physical and chemical properties to the compound reported previously to be obtained, (150) and the authors were unable to obtain material corresponding to the 1968 report. Complex [270, L = AsPh_3] has similar NMR parameters to those given for [270a], and parameters for analogues of [271a] with PMePh_2 and AsPh_3 ligands are also given in the paper.

Reactions of perfluorobut-2-yne and of 3,3,3-trifluoropropyne with appropriate platinum and palladium complexes give the vinyl-metal complexes [272] to [276]. (125, 131, 151) The CF_3 groups in [272], [273] and [274] are *cis*, as shown by the CF_3 - CF_3 coupling. (125, 151) Parameters for three examples of structure [275] are given with the formula, and those for other complexes of this type ($\text{X} = \text{NCS}$, NO_2 , CN) and of the corresponding ionic compounds *trans*- $[\text{Pt}(\text{PMe}_2\text{Ph})_2(\text{L})\{\text{C}(\text{CF}_3):\text{CHOMe}\}]\text{PF}_6$ (L = EtNC , AsPh_3 , SbPh_3 , CO , Me_2CO , $\text{MeC}:\text{CMe}$, PMe_2Ph , $:\text{CCH}_2\text{CH}_2\text{CH}_2\text{O}$) are tabulated in ref. 153. The CF_3 groups absorb in the range -46.9 to -51.3 , with no observable coupling to phosphorus. The $\text{Pt}-\text{CF}_3$ couplings range from 78 Hz for the carbene complex to 143 Hz for the acetone complex, and correlate



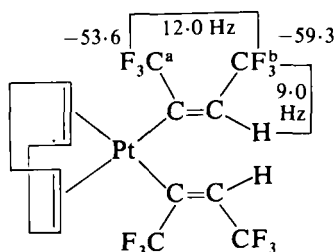
$J(\text{CF}_3^a\text{--CH}_3)$ 2.0 Hz
 $J(\text{Pt--CF}_3^b)$ ca. 6 Hz
 $J(\text{P--CF}_3^b)$ 3.0 Hz

[272]



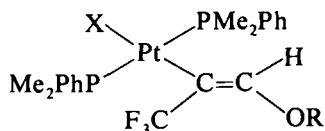
$J(\text{Pt--CF}_3^a)$ 98.5 Hz
 $J(\text{Pt--CF}_3^b)$ 5 Hz
 $J(\text{P--CF}_3^a)$ 9.1 Hz
 $J(\text{P--CF}_3^b)$ 2.0 Hz
 $J(\text{CF}_3^a\text{--CH}_3)$ 2.2 Hz

[273]



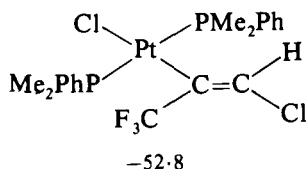
$J(\text{Pt--CF}_3^a)$ 111.0 Hz
 $J(\text{Pt--CF}_3^b)$ 12.0 Hz

[274]



X	R	δCF_3	$J(\text{Pt--CF}_3)$
Cl	Me	-49.8	128.2
I	Me	-51.3	125.8
Cl	Et	-49.7	128.4

[275]

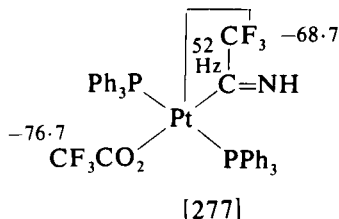


$J(\text{Pt--CF}_3)$ 121.5 Hz

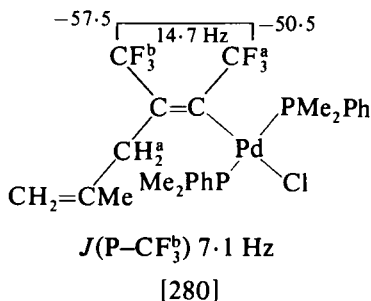
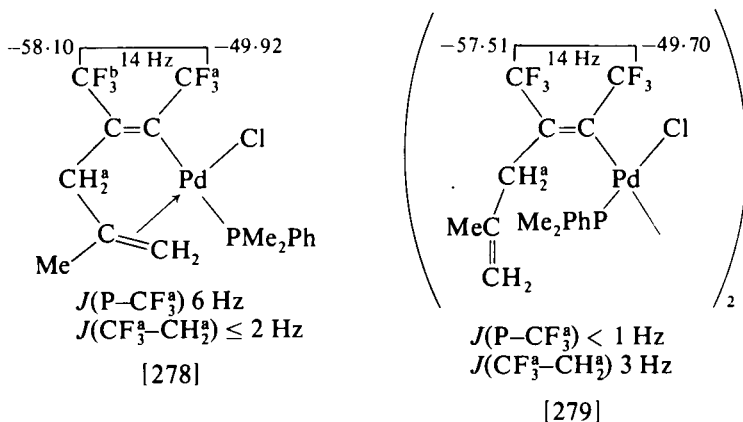
[276]

well with the coupling of platinum to the vinylic hydrogen, and also, apart from the value for $\text{L} = \text{SbPh}_3$, with $J(\text{Pt--CF}_3)$ in the corresponding methyl complexes. The coupling of the unique phosphorus *trans* to the $\text{C}(\text{CF}_3)\text{:CHOMe}$ group in the tris-phosphine complex (J 9.4 Hz) contrasts with the zero coupling of the two

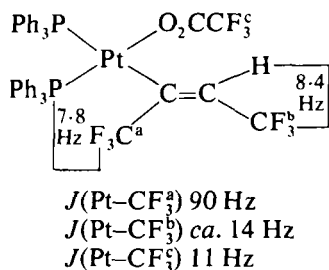
phosphorus atoms *cis* to the vinyl group, as expected. The lack of phosphorus coupling to the CF_3 group in [277] is also taken as an indication of the *trans* disposition of the phosphine ligands. (138)



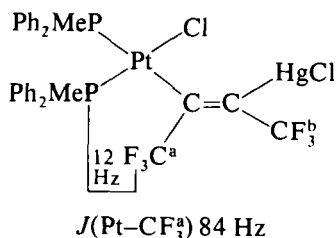
Compounds [278] and [279] are rapidly interconverted at room temperature, but separate signals for the two species (illustrated in the



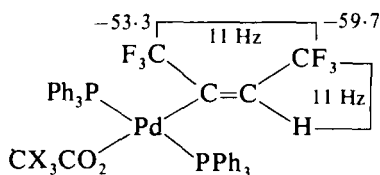
paper) can be seen at -50°C . (154) Compound [280], formed from [278/9] by the addition of one mole of the phosphine, maintains the stereochemistry of [279]; a triplet splitting in the signal due to CF_3^a (2.6 Hz) may be assigned to coupling either to CH_2^a or to the two phosphorus atoms. Vinylic complexes such as [281] to [284] are also formed by



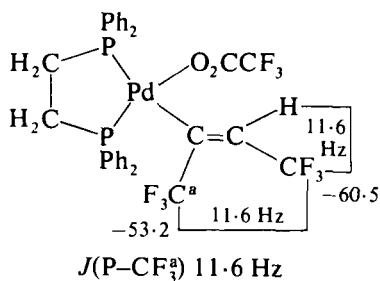
[281]



[282]

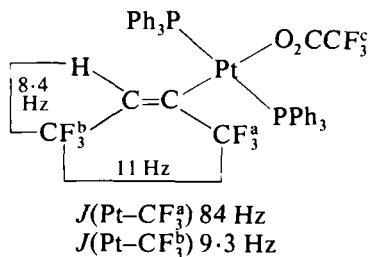


[283]



[284]

electrophilic addition to the appropriate perfluorobut-2-yne-platinum (155) or -palladium (156) complex. Parameters for other complexes of this type $\text{L}_2\text{Pt}(\text{X})[\text{C}(\text{CF}_3):\text{CHCF}_3]$ ($\text{X} = \text{OCCF}_3, \text{OSO}_3\text{H}, \text{Cl}$; $\text{L} = \text{PPh}_3, \text{AsPh}_3, \text{PMePh}_2, \text{PEt}_2\text{Ph}$; $\text{L}_2 = \text{Ph}_2\text{PCH}_2\text{CH}_2\text{PPh}_2$) are very similar to those given here for [281] and [282], and are tabulated in ref. 155.* In all cases the CF_3-CF_3 coupling (10–12 Hz) indicates the *cis*-butenyl structure. The *cis*-complex [281] is isomerized in $(\text{CD}_3)_2\text{CO}$ to give the *trans*-complex [285]. The mercury-containing complex [282],

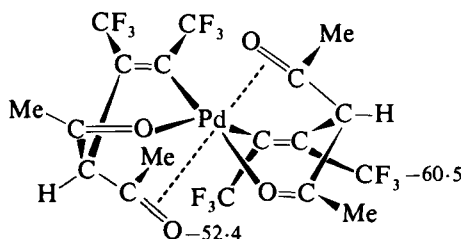


[285]

*The values in column 11 of Table 2, ref. 155 are for $J(\text{Pt}-\text{O}_2\text{CCF}_3)$, not $J(\text{F}-\text{H})$ as printed at the head of the column (R. D. W. Kemmitt, personal communication).

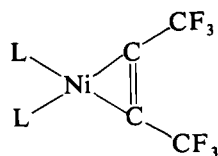
and its bromo-mercury analogue, show coupling from ^{199}Hg to CF_3^b of 270–290 Hz.

The complex formed by the reaction of perfluorobut-2-yne with $\text{Pd}(\text{acac})_2$ has been identified crystallographically as [286], (157) confirming the *cis* disposition of the CF_3 groups deduced from the coupling. Parameters for the perfluorobutyne-nickel and -platinum complexes [287] (158, 159) and [288], (144) and for the metalacyclopentadiene complex [289] (132) are given with the structures.



$J(\text{CF}_3\text{--CF}_3)$ 16 Hz

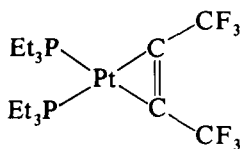
[286]



[287a] $\text{L} = \text{Me}_2\text{PhAs}$ $\delta -53.2\text{s}$

[287b] $\text{L} = \text{CO}$ $\delta -55.3\text{s}$

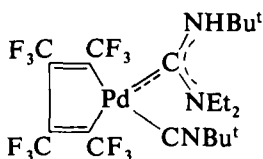
[287c] $\text{L}_2 = (\text{Ph}_2\text{PCH}_2)_2$ $\delta -53.5\text{t}$
 $J(\text{P--CF}_3)$ 4.4 Hz



$J(\text{P--CF}_3)$ 11 Hz

$J(\text{Pt--CF}_3)$ 65.5 Hz

[288]

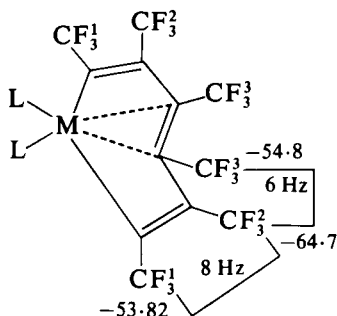


$\alpha\text{CF}_3 \left\{ \begin{array}{l} \delta -53.2\text{q}, J(\text{CF}_3\text{--CF}_3) 14.7 \text{ Hz} \\ -55.8\text{m} \end{array} \right.$

βCF_3 $\delta -57.0\text{m}$

[289]

Further reaction of [287a] with perfluorobut-2-yne gives [290a] for which the ^{19}F parameters are given. (159) The analogous complex [290b], which has been characterized by X-ray crystallography, (160) has very similar ^{19}F parameters, and additionally shows $J(\text{P--CF}_3^1)$ 11 Hz. Parameters for the isostructural platinum complex [290c], and for the similar complex [291], in which only one phosphine ligand is attached to the platinum, are also given with the structures. In contrast to the formation of these *cis,trans,cis*-metallacycloheptatriene com-



[290a] M = Ni, L = AsMe₂Ph; parameters given

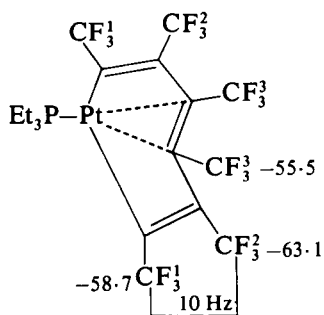
[290b] M = Ni, L = P(OMe)₃

[290c] M = Pt, L₂ = (Ph₂PCH₂)₂

δCF_3^1 -55.0, $J(\text{Pt}-\text{CF}_3^1)$ 39 Hz;

δCF_3^2 -65.2; δCF_3^3 -56.5,

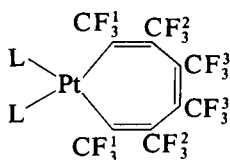
$J(\text{Pt}-\text{CF}_3^3)$ 53 Hz, $J(\text{P}-\text{CF}_3^3)$ 10 Hz



$J(\text{Pt}-\text{CF}_3^1)$ 61 Hz

$J(\text{Pt}-\text{CF}_3^3)$ 65 Hz

[291]



[292a] L = Bu^tNC

[292b] L = PMe₃ δCF_3 -52.6, -57.1, -57.2

plexes, treatment of hexakis(trifluoromethyl)benzene with *triangulo*-[Pt₃(Bu^tNC)₆] gives the *cis,cis,cis*-metallacycloheptatriene [292a], the ¹⁹F NMR spectrum of which, as of the analogous complex [292b], is temperature invariant. (161) The quartet (12.0 Hz) at δ -55.6 in the spectrum of [292a] shows platinum satellites [$J(\text{Pt}-\text{CF}_3)$ 120.0 Hz], and is presumably due to CF₃¹; the 12 Hz quartet at δ -56.5 can be attributed to CF₃², leaving the quartet at δ -58.7 (J 2.4 Hz) for CF₃³, with the weak coupling presumably not resolved in one of the other bands. The structure of [292a] has been confirmed by single crystal X-ray diffraction.

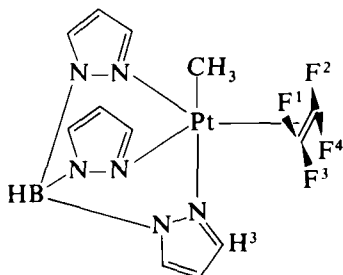
Alkyne complexes of platinum have also been prepared from 3,3,3-trifluoropropyne, and parameters for compounds [293] to [295] are given in Table XVII. (151) Parameters for the silylacetylene complex *trans*-Pt(PEt₃)₂(Cl)(SiH₂C \equiv CCF₃), δ -51.3 for the terminal CF₃ group, with ⁵ $J(\text{Pt}-\text{F})$ +23.7 Hz and ⁵ $J(\text{F}-\text{H})$ 2.2 Hz, were obtained by heteronuclear double resonance. (162)

TABLE XVII

Some ^{19}F NMR parameters for $\text{Pt}-\text{C}\equiv\text{CCF}_3$ complexes (151)

<div style="display: flex; justify-content: space-around; align-items: center;"> <div style="text-align: center;"> $\text{CF}_3\text{C}\equiv\text{C}-\text{Pt}(\text{L})_2-\text{C}\equiv\text{CCF}_3$ [293] </div> <div style="text-align: center;"> $\text{X}-\text{Pt}(\text{L})_2-\text{C}\equiv\text{CCF}_3$ [294] </div> <div style="text-align: center;"> $\text{L}-\text{Pt}(\text{Me})(\text{L})-\text{C}\equiv\text{CCF}_3$ [295] </div> </div>					
Compound	L	X	δCF_3	$J(\text{Pt}-\text{CF}_3)$	$J(\text{P}-\text{CF}_3)$
[293]	PMe_2Ph	—	-47.3	25.0	3.4
[293]	AsMe_3	—	-46.8	25.0	—
[293]	AsMe_2Ph	—	-47.2	24.6	—
[294]	PMe_2Ph	Cl	-46.9	34.1	3.5
[294]	PMe_2Ph	Me	-45.6	25.8	3.3
[295]	PMe_2Ph	—	-45.0	27.5	5.6 (<i>trans</i>) 2.8 (<i>cis</i>)

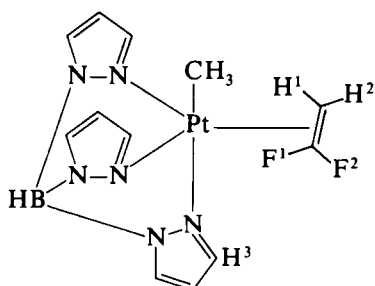
The five-co-ordinate tetrafluoroethyleneplatinum complex [296] shows a complex AA'BB' spectrum with platinum satellites, the AA' part showing quartet coupling to the $\text{Pt}-\text{CH}_3$ group, and the BB' part



$\delta(\text{F}^1\text{F}^2) - 132$; $\delta(\text{F}^3\text{F}^4) - 121$
 $J(\text{F}^{1,2}-\text{CH}_3) 2.0 \text{ Hz}$, $J(\text{Pt}-\text{F}^{1,2}) 325 \text{ Hz}$,
 $J(\text{F}^{3,4}-\text{H}^3) 2.0 \text{ Hz}$, $J(\text{Pt}-\text{F}^{3,4}) 185 \text{ Hz}$

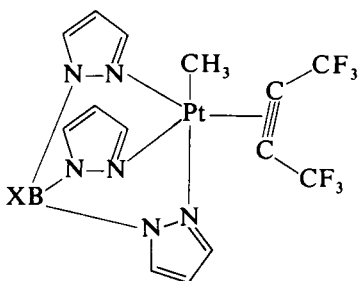
[296]

showing doublet splitting by H^3 of the axial pyrazolyl group. (163) The analogous 1,1-difluoroethylene complex [297] shows similar couplings for the two magnetically inequivalent fluorines to methyl and pyrazolyl hydrogens and these couplings are attributed to a through-space mechanism. Similar five-co-ordinate complexes of hexafluorobut-2-yne [298] and of 3,3,3-trifluoropropyne [299] have also been reported. (164) The trigonal-bipyramidal geometry about the metal is confirmed crystallographically for [298a]. (165) The planar trigonal geometry of



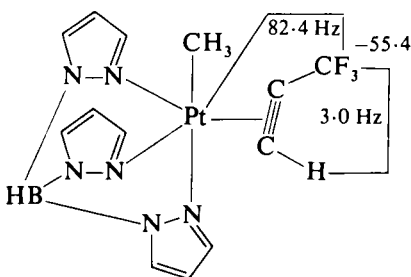
$\delta(\text{F}^1 - 106; \delta\text{F}^2 - 95$
 $J(\text{F}^1 - \text{CH}_3) 2.0 \text{ Hz}, J(\text{Pt} - \text{F}^1) 280 \text{ Hz},$
 $J(\text{F}^2 - \text{H}^3) 2.5 \text{ Hz}, J(\text{Pt} - \text{F}^2) 160 \text{ Hz}$

[297]



[298a] $\text{X} = \text{C}_3\text{H}_3\text{N}_2; \delta\text{CF}_3 - 56.70, J(\text{Pt} - \text{CF}_3) 66.6 \text{ Hz}$

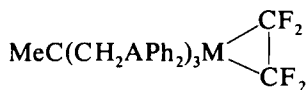
[298b] $\text{X} = \text{H}; \delta\text{CF}_3 - 67.40, J(\text{Pt} - \text{CF}_3) 65.0 \text{ Hz}$



[299]

$\text{Pt}(\text{C}_2\text{F}_4)(\text{C}_2\text{H}_4)_2$ [$\delta - 123.6, J(\text{Pt} - \text{F}) 248 \text{ Hz}$] has also been confirmed crystallographically. (166) Another series of five-co-ordinate complexes, containing tripodal ligands $\text{MeC}(\text{CH}_2\text{APh}_2)_3$ ($\text{A} = \text{P}, \text{As}$), is exemplified

in structures [300] to [302]. (134) The quartet splitting in the ^{19}F spectra of [300a and c] establishes the apparent equivalence of the three

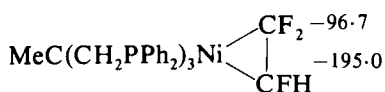


[300a] M = Ni, A = P; $\delta -111.4\text{q}$, $J(\text{P}-\text{F}) 46.4 \text{ Hz}$.

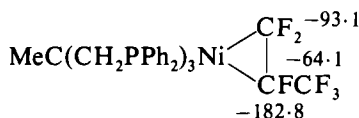
[300b] M = Ni, A = As; $\delta -107.5\text{s}$.

[300c] M = Pt, A = P; $\delta -127.0\text{q}$

$J(\text{P}-\text{F}) 27.0$, $J(\text{Pt}-\text{F}) 293.0 \text{ Hz}$.



[301]

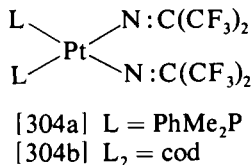
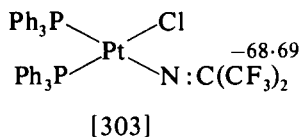


[302]

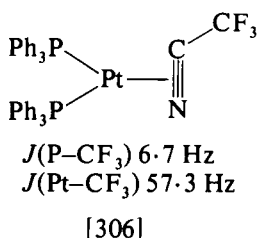
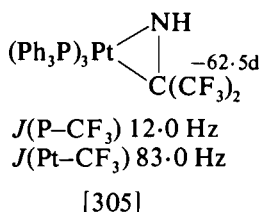
phosphorus atoms, indicating that all three are involved in co-ordination to the metal. In contrast to the four-co-ordinate C_2F_4 complexes such as $(\text{Ph}_3\text{P})_2\text{PtCF}_2\text{CF}_2$, in which there is a rather high barrier to rotation about the olefin-metal bond system, as indicated by temperature-invariant NMR spectra, both the ^1H and ^{19}F spectra of [300a, b and c] were broadened at -100°C . The simplicity of the ^{19}F spectrum of [300c] also contrasts with the $\text{X}_2\text{AA}'\text{X}'_2$ system shown by the rigid $\text{CF}_2\text{CF}_2\text{Pt}(\text{PPh}_3)_2$. Only the chemical shifts of the multiplets of [301] and [302] are reported ([301] is unstable in solution in the absence of an excess of $\text{CF}_2:\text{CFH}$), but the CF_2 group of [302] is stated to be an AB pattern similar to those observed for $\text{L}_2\text{NiCF}_2\text{CFCF}_3$ complexes.

The perfluorobut-2-yne-nickel complex [287b] decomposes at room temperature to a $\text{Ni}_4(\text{CO})_4(\text{CF}_3\text{C}_2\text{CF}_3)_3$ species ($\delta(\text{CF}_3) -53.6(\text{s})$ and $-56.9(\text{s})$) in which the nickel atoms are arranged in a trigonal pyramid, with the $\text{CF}_3\text{C}_2\text{CF}_3$ units co-ordinated onto the three faces of the pyramid. (158) Further reaction of this complex with cyclo-octatetraene gives $(\text{Ni}_3(\text{CO})_3(\text{C}_8\text{H}_8)(\text{CF}_3\text{C}_2\text{CF}_3))$ [$\delta(\text{CF}_3) -55.9(\text{s})$], with nickel atoms arranged in a triangle between a planar C_8H_8 group and the $\text{CF}_3\text{C}_2\text{CF}_3$ group. Chemical shifts for the bridging acetylene in $\{(\pi\text{-C}_5\text{H}_5)\text{Ni}\}_2\{\text{CF}_3\text{C}_2(\text{CF}_3)(\text{C}_2\text{F}_5)_2\}$ [$-50.3(3)$, $-59.7(3)$, $-75.2(6)$, $-105.0(4)$] have also been reported. (107)

The $\text{Pt}-\text{N}:\text{C}(\text{CF}_3)_2$ complexes [303, 304] show ^{19}F singlets at *ca.* $\delta -69$, (112, 131) consistent with a linear $\text{Pt}-\text{N}-\text{C}$ grouping, but *trans*- $\text{PtH}[\text{N}:\text{C}(\text{CF}_3)_2]_2(\text{PPh}_3)_2$ shows a complex multiplet. The " π -complex"



[305] in contrast shows coupling to phosphorus and platinum satellites. Complex [306], formed by the reaction of CF₃CN with *trans*-



stilbenebis(triphenylphosphine)platinum has been shown crystallographically to be almost planar. (138) The doublet P-CF₃ splitting is presumed to be due to the *trans* phosphorus. The CF₃ group resonance in 5-trifluoromethyltetrazolepalladium complexes L₂Pd(tet)₂ has been used as a probe to study *cis-trans* and linkage (N¹- vs N²-bound) isomerism in the complexes at a range of temperatures. (167)

The phosphorus-CF₃ coupling constants are increased in the complexes [307] to [309] compared with the free ligands, as expected, in

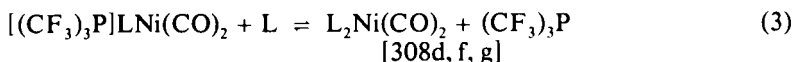
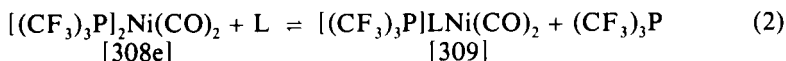
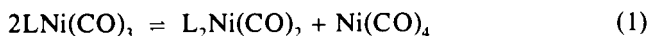
LNi(CO) ₃				
	L	δ	$J(\text{P}-\text{CF}_3)$	$J(\text{CF}_3-\text{H})$
[307a]	CF ₃ PH ₂	-52.8	63	9.0
[307b]	(CF ₃) ₂ PH	-56.2	77	7.3
[307c]	(CF ₃) ₂ PMe	-64.1	80.8	—
[307d]	(CF ₃) ₂ PEt	-61.9	73.6	—
[307e]	(CF ₃) ₃ P	-57.4	89.0	—
[307f]	2-(CF ₃) ₂ PB ₃ H ₈	-57.0	73	—

L ₂ Ni(CO) ₂				
	L	δ	$J(\text{P}-\text{CF}_3)$	$J(\text{CF}_3-\text{H})$
[308a]	CF ₃ PH ₂	-53.6	60	8.8
[308b]	(CF ₃) ₂ PH	-57.5	75	7.1
[308c]	(CF ₃) ₂ PMe	-64.0	82.4	—
[308d]	(CF ₃) ₂ PEt	-61.6	74.5	—
[308e]	(CF ₃) ₃ P	-56.6	90.6	—
[308f]	(CF ₃) ₂ PBu ⁱ	-60.6	75.9	—
[308g]	CF ₃ PEt ₂	-63.8	59.8	—



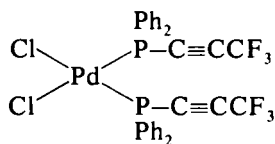
	L	$\delta\text{CF}_3^{\text{L}}$	$J(\text{P}-\text{CF}_3^{\text{L}})$	$\delta\text{CF}_3^{\text{a}}$	$J(\text{P}-\text{CF}_3^{\text{a}})$
[309a]	$(\text{CF}_3)_2\text{PMe}$	-63.1	80.0	-57.3	89.3
[309b]	$(\text{CF}_3)_2\text{PEt}$	-60.3	75.1	-57.2	85.8
[309c]	$(\text{CF}_3)_2\text{PBu}^{\text{I}}$	-60.4	75.4	-57.0	85.8
[309d]	CF_3PEt_2	-63.4	64.0	-58.0	91.4

accord with the observations on the cobalt complexes, *e.g.* [220, 221]. (116, 168, 169) The parameters reported are given with the structures. The spectra of the tertiary phosphine complexes [307e, 308c-g, and 309] were used to study equilibria (1)–(3).

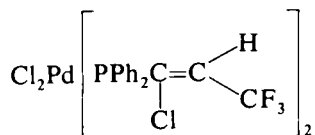


The spectrum of [307f] showed the presence of 10% of the known 1- $(\text{CF}_3)_2\text{PB}_5\text{H}_8\text{Ni}(\text{CO})_3$, (170) formed by isomerization of the phosphine ligand *in situ*. (169) The trigonal complex $(\text{PPh}_2\text{CF}_3)_3\text{Pt}$ shows only a broad hump ($\delta -61.61$) at 33°C , (171) which first of all starts to show fine structure as the temperature is reduced, but which rebroadens below -50°C . These observations suggest that phosphine exchange is rapid at $+30^\circ\text{C}$, and is slowed down on reduction of the temperature, but below -50°C a further process, perhaps a rotation, is being frozen out. The spectra in the presence of free CF_3PPh_2 were also examined over a range of concentrations and temperatures. At room temperature the mixtures gave a doublet [$J(\text{P}-\text{CF}_3)$ 73 Hz] with a chemical shift the weighted average of the phosphine and $\text{Pt}(\text{PPh}_2\text{CF}_3)_3$, but below *ca.* -60°C the spectra, which are illustrated in the original paper, also show signals due to $\text{Pt}(\text{PPh}_2\text{CF}_3)_4$ and another, as yet unidentified, species.

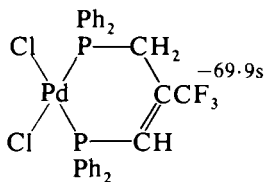
The reaction of HCl with the phosphine complex [310] gives as product a mixture of the *cis*- and *trans*-palladium complexes [311] in



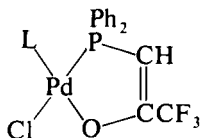
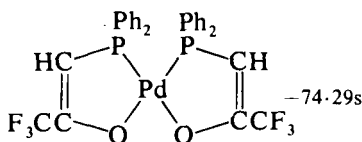
[310]

[311a] ligands *cis*, $\delta -67.3\text{m}$ [311b] ligands *trans*, $\delta -77.3$

which the CF_3 group and chlorine were shown to be *cis* by X-ray crystallography. (172) Parameters for some other complexes also derived from [310] are given with structures [312] to [314]. Rather

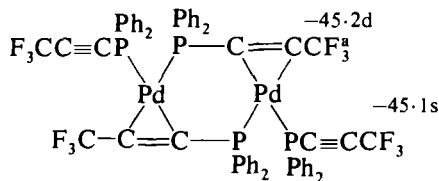


[312]

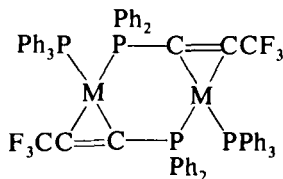
[313a] L = PPh_2OH ; $\delta -75.83\text{s}$ [313b] L = PPh_2OEt ; $\delta -73.46\text{s}$ 

[314]

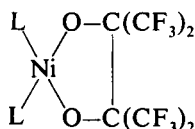
surprisingly, neither the $\text{P}-\text{CF}_3$ nor the $\text{H}-\text{CF}_3$ couplings were resolved. The ^{19}F spectrum of [313, R = Et] shows two singlets ($\delta -75.34$, -75.83) with intensity ratios 1:3, which are attributed to isomers with the phosphorus ligands *trans* and *cis*(major) around the metal. Complex [315], its platinum analogue (for which NMR parameters are simply stated to be similar), and the complexes [316] are the first examples of phosphinoacetylene π -complexes of $\text{Pd}(\text{O})$ and $\text{Pt}(\text{O})$; (173) the structure of [316a] has been confirmed crystallographically. The multiplets reported for [316a and b] (b showing ^{195}Pt satellites) are apparently the X parts of deceptively simple $\text{X}_3\text{AA}'\text{X}_3'$ systems.

 $J(\text{P}-\text{CF}_3) 5.7 \text{ Hz}$

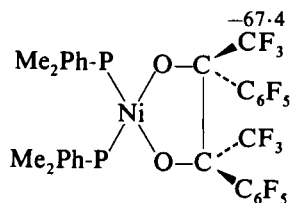
[315]

[316a] M = Pd; $\delta -45.4\text{m}$ [316b] M = Pt; $\delta -49.9\text{m}$

Complexes of perfluoropinacol with nickel [317] show a single peak in the range δ -70.6 to -71.3 , (174) with the exception of [317, $L_2 = \text{Me}_2\text{AsCH}_2\text{CHBu}^t\text{CH}_2\text{AsMe}_2$], for which the singlet is at δ -73.0 . (175)



[317] $L = \text{Et}_3\text{P}, \text{Me}_2\text{PPh}, \text{MePPh}_2, \text{Ph}_3\text{P},$
 $(\text{EtO})_3\text{P}$
 $L_2 = \text{diphos}, \text{bipy}, \text{TMED}, \text{TEED}$



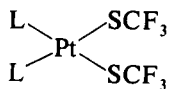
ortho-F $-132.6, -133.4$
meta-F $-164.2, -166.9$
para-F -157.4

[318]

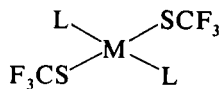
The analogous bis(triethylphosphine)palladium complex also shows a singlet at δ -71.0 . (127) The nickel complex [318] of (+)-perfluoro(2,3-diphenylbutane-2,3-diol), like the free diol (both *meso* and *DL* isomers) shows five inequivalent aromatic fluorines, due to hindered rotation of the C_6F_5 ring. Since the inequivalence persists in the complexes, the hindrance cannot be due to hydrogen bonding. (174)

The nickel trifluoroacetates $\text{NiL}_4(\text{OCOCF}_3)_2$ ($L = \beta$ -, γ -picoline, β -, γ -ethylpyridine) undergo slow *cis-trans* isomerization at room temperature (in contrast to the cobalt complexes, see p. 69), the major isomer in each case absorbing in the range δ -25 to -34 , and the minor, sometimes not detectable, in the range δ $+10$ to $+20$. (176)

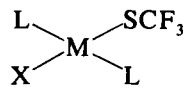
^{19}F parameters for a wide range of palladium and platinum complexes containing the SCF_3 group are reported in refs. 122, 177–179. The chemical shifts lie in the range -19.7 to -27.5 for both mononuclear [319]–[321] and dinuclear [322] complexes. The nickel complex *trans*-



[319]

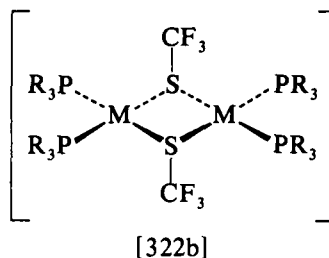
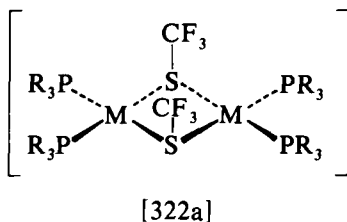


[320] $M = \text{Pd}, \text{Pt}$
 $L = \text{PPh}_3$



[321] $M = \text{Pd}, \text{Pt}$
 $X = \text{Cl}, \text{H}$

$\text{Ni}(\text{SCF}_3)_2(\text{PPh}_3)_2$ has δ -43.3 , (122) but the dinuclear $[(\pi\text{-C}_5\text{H}_5)\text{Ni}(\text{SCF}_3)]_2$, taken to be the *syn* isomer, has δ -27.7 (24) Coupling to *cis*-phosphorus is small ($1\text{--}3.5$ Hz), but in the range $5\text{--}11.5$ Hz for $J(\text{CF}_3\text{--P trans})$. The presence of the geometrical isomers [322a and b] was shown by the appearance of two sets of signals, with different intensities, in several cases. The dinuclear platinum complexes

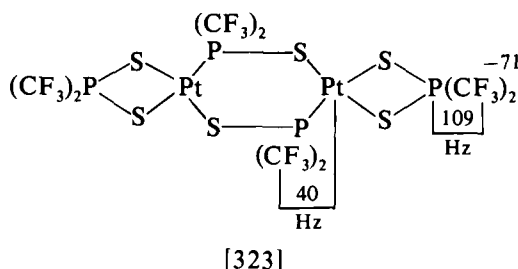


showed 1:8:18:8:1 quintets due to the presence of 2, 1, or no ^{195}Pt nuclei in the complex. For a wide range of platinum complexes, $J(\text{Pt}-\text{F})$ for the SCF_3 group is shown to correlate linearly with other measures of the *trans* influence of anionic and neutral ligands [e.g. $^2J(\text{Pt}-\text{H})$, $^2J(\text{Pt}-\text{F})$], and the inverse correlation between *cis*- and *trans*-influences of anionic ligands (4) is derived.

$$^3J(\text{Pt}-\text{F}_{\text{cis}}) = -0.25[^3J(\text{Pt}-\text{F}_{\text{trans}})] + 92 \quad (4)$$

(where $J(\text{Pt}-\text{F}_{\text{cis}})$ is the platinum-fluorine coupling in the complex with the anion *cis* to the CF_3 group and $J(\text{Pt}-\text{F}_{\text{trans}})$ is the corresponding coupling in the isomer with the anion *trans* to the CF_3 group). (177)

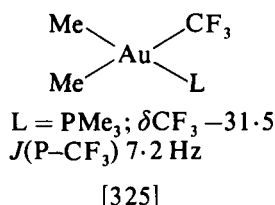
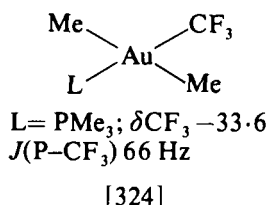
Nickel and palladium dithiophosphinates $\text{M}[\text{S}_2\text{P}(\text{CF}_3)_2]_2$ ($\text{M} = \text{Ni}$, $\delta\text{CF}_3 - 59.6$, $J(\text{P}-\text{CF}_3)$ 109 Hz, $\text{M} = \text{Pd}$, $\delta\text{CF}_3 - 71.5$, $J(\text{P}-\text{CF}_3)$ 108 Hz) are formed when dithiophosphinic acid is refluxed with metallic nickel or palladium dichloride respectively but the corresponding reaction between the acid and platinum dichloride gives a "sulphur-deficient" complex for which the ^{19}F signals, illustrated in the paper, are assigned as shown with formula [323]. (180) The band at $\delta - 71$ is a



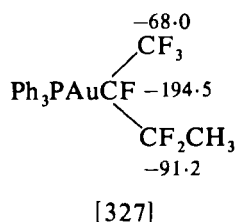
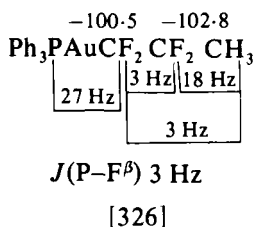
simple doublet, $J(\text{P}-\text{CF}_3)$ 109 Hz, and is assigned to the normal bidentate ligand units in view of its similarity to the signals for the nickel and palladium complexes, but the other band, centred at $\delta - 59$ is more complex and the authors suggest that it is the X part of an $\text{X}_6\text{AA}'\text{X}_6$ system, with platinum satellites.

G. Copper, silver, and gold

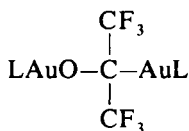
The reaction of MeAuL ($\text{L} = \text{PMe}_3$ or PMe_2Ph) with trifluoriodomethane gives a mixture of *cis*- and *trans*- isomers [324] and [325], the proportions depending on the solvent used and on L . (181) As usual, coupling of the CF_3 group to the *trans*-phosphine (in [324]) is considerably greater than to the *cis*-phosphine (in [325]).



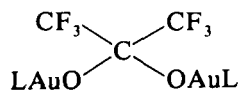
Parameters for some products of insertion into the $\text{Me}-\text{Au}$ bond of MeAuL ($\text{L} = \text{PPh}_3$, PMePh_2) are given with structures [326] and [327].



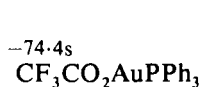
(182) The small difference between the chemical shifts for α - and β - CF_2 groups in [326] and in the corresponding complex containing PMePh_2 (for which parameters are very similar) is noteworthy; fortunately, the couplings to the methyl group establish which signal corresponds to the β - CF_2 group. In the corresponding complexes formed from hexafluoropropene, although it was clear from the spectra that only one isomer had been formed in each case, the couplings in the ^{19}F spectra could not be resolved, but the methyl ^1H signal was a 20 Hz triplet, establishing the structures. The pairs of complexes from hexafluoroacetone [328] and its hydrate [329] absorb at *ca.* $\delta -81$ and *ca.* δ



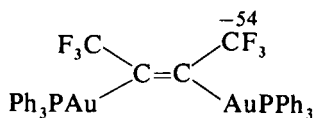
[328] $\text{L} = \text{PPh}_3, \text{PMePh}_2$



[329] $\text{L} = \text{PPh}_3, \text{PMePh}_2$



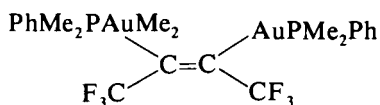
[330]



[331]

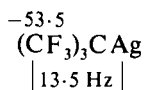
—83 respectively, and the trifluoroacetate [330] has also been prepared. The spectrum of the complex [331] obtained from hexafluorobutyne shows a poorly resolved $X_3AA'X'_3$ spectrum and only the phosphorus-phosphorus coupling (*ca.* 50 Hz) could be obtained.

The product of the reaction of $\text{MeAuPMe}_2\text{Ph}$ with perfluorobut-2-yne shows an unsymmetrical multiplet at δ —52.4, indicating that the two CF_3 environments are different. It was originally (183) thought to have a bridging acetylene structure, but subsequent work has shown the structure to be [332] (184) in which the two gold atoms are in different oxidation states.

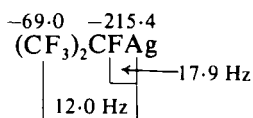


[332]

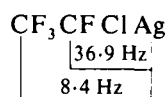
The reaction of silver salts with perfluoro-olefins in the presence of fluoride ion gives rise to perfluoroalkyl derivatives of silver [333] to [336]. (185) Silver fluoride also reacts with perfluorobut-2-yne to give [337], useful as a synthetic intermediate. (8) Coupling to silver can be observed in the spectra of [333], [334] (satellites from both ^{107}Ag , given with the structure, and ^{109}Ag were reported only for this compound),



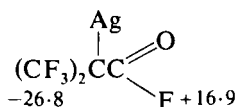
[333]



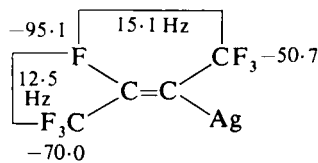
[334]



[335]



[336]

 $J(\text{CF}_3-\text{CF}_3) 1.7 \text{ Hz}$

[337]

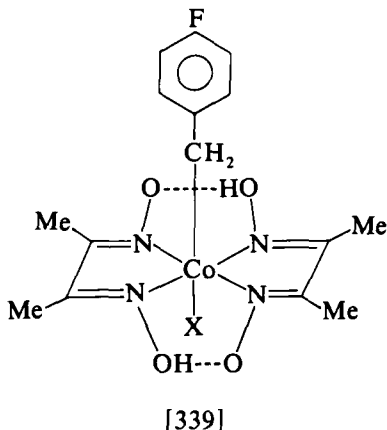
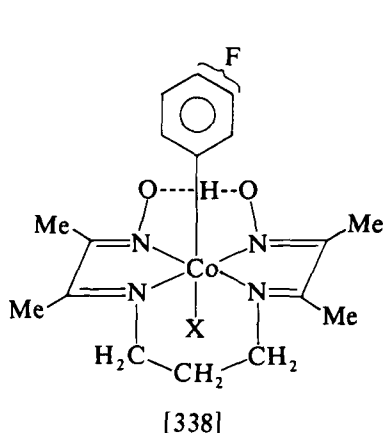
and [335] at room temperature in dimethyl-formamide, coalescence occurring at 60°C in this solvent for [333]. In 1,2-dimethoxyethane other signals, which appear to be solvent- and temperature-dependent, also showing coupling to silver, are observed in addition, and are thought to be due to the presence of complexes of the perfluoroalkyl-silver with different numbers of solvent molecules. The spectrum of perfluorocyclobutylsilver is reported to be complicated both by couplings to silver and also by an equilibrium between the silver compound and perfluorocyclobutene and AgF. No coupling to silver is observed at +34°C in the spectrum of [336], suggesting that this is undergoing metal exchange (i.e. is a more ionic compound). The spectrum is broadened at -110°C, but even at this temperature no coupling to silver could be resolved.

The reaction of [333] with sulphur gave $(\text{CF}_3)_3\text{CSAg}$ ($\delta -67.8$, s), in which no coupling to silver could be detected.

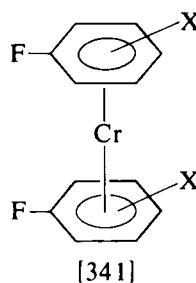
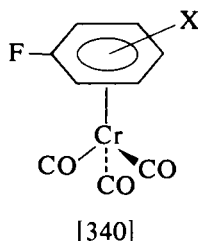
III. FLUOROAROMATIC AND FLUOROHETEROAROMATIC DERIVATIVES

Although a considerable volume of work on fluoroaromatic derivatives of transition metals has been reported in the period under review (see, e.g. ref. 186), comparatively few reports contain any mention of ^{19}F NMR parameters.

Chemical shifts for the single fluorine in *meta*- and *para*-fluorophenyl- and *para*-fluorobenzyl derivatives of cobalt complexes, e.g. [338] and [339] have been used to estimate the electron donor properties of the metal(ligands) group, and to study the effects of change of X and of the ligands. (187, 188) Cobalt(III) in [338] appears to be a strong donor,



and although somewhat poorer as a σ -donor than $-\text{Pt}(\text{PEt}_3)_2\text{X}$, stronger as a π -donor. (189) Similar studies of (fluorobenzene)chromium tricarbonyls [340] and of bis(fluoroarene)chromium complexes [341]



are also reported. (190, 191) The electron-withdrawing effect of the π bonded chromium in $(\text{C}_6\text{H}_4\text{FX})_2\text{Cr}$ is related to that of the corresponding fluorine in $\text{C}_6\text{F}_5\text{X}$ by the equations: (191)

$$\Delta_o^{\text{F}}(\text{complex}) = 0.76[\Delta_o^{\text{F}}(\text{C}_6\text{F}_5\text{X})] + 55.7$$

$$\Delta_m^{\text{F}}(\text{complex}) = 1.94[\Delta_m^{\text{F}}(\text{C}_6\text{F}_5\text{X})] - 154.6$$

$$\Delta_p^{\text{F}}(\text{complex}) = 1.18[\Delta_p^{\text{F}}(\text{C}_6\text{F}_5\text{X})] - 22.2$$

CF_3 group signals are shifted to higher frequency (by some 5–7 ppm) on complex formation compared with that of benzotrifluoride. Transmission of resonance effects in the chromium tricarbonyls [340] is very similar to that in the free arenes, but the shifts in the complexed *meta*-fluoroarenes are all very similar [δ –135.3 to –136.7 for substituents ranging from CF_3 to NH_2], suggesting that transmission by inductive effects have been markedly reduced. (190) The ^{19}F NMR spectrum of $(\text{C}_6\text{F}_6)\text{Cr}(\text{PF}_3)_3$ shows a shift to low frequency (to δ –184.2s) for the complexed C_6F_6 group; the PF_3 groups appear as a doublet [+6.1, $^1J(\text{P}-\text{F})$ 1315 Hz]. (192)

Chemical shifts for $\text{C}_6\text{F}_5\text{M}$ and $\text{C}_6\text{F}_4\text{X}_{5-n}\text{M}$ derivatives (where M is a transition metal group directly attached to the fluoroaryl ring) are summarized in Table XVIII and with structures [342] to [351]. (193–200) Compounds with heteroaromatic rings directly attached to the metal are included here.

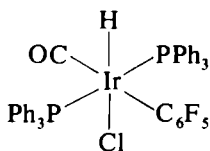
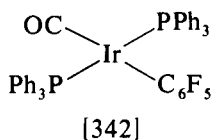
Oxidative additions to [342] give complexes in which all five fluorines of the C_6F_5 group are inequivalent, presumably because of restriction of rotation about the $\text{Ir}-\text{C}$ bond by the flanking PPh_3 groups (see also p. 98). The analogous complexes with the smaller PMePh_2 ligands instead of PPh_3 show only the usual three bands for the C_6F_5 group. The spectra of [343] are illustrated in ref. 193; the coupling constants for [343] are

TABLE XVIII

Some ^{19}F Chemical shifts for $(\text{C}_6\text{F}_n\text{Y}_{3-n})\text{M}$ derivatives

Complex	δF2	δF3	δF4	δF5	δF6	Ref.
$\text{Ir}(\text{C}_6\text{F}_5)(\text{CO})(\text{PPh}_3)_2$	-114.8	-165.1	-165.1	-165.1	-114.8	193
$\text{Rh}(\text{C}_6\text{F}_5)(\text{CO})(\text{PPh}_3)_2$	-107.5	-164.0	-164.0	-164.0	-107.5	193
$\text{Rh}(\text{C}_6\text{F}_5)(\text{C}_6\text{H}_{12})(\text{PPh}_3)$	-114.1	-164.4	-164.4	-164.4	-114.1	193
$\text{Fe}(\text{C}_6\text{F}_5)_2(\text{CO})_4$	-109.8	-162.0	-157.5	-162.0	-109.8	193
$\text{Pt}(\text{CF}:\text{CF}_2)(\text{C}_6\text{F}_5)(\text{PPh}_3)_2^a$	-117.3	-164.5	-164.5	-164.5	-117.3	193
$\text{IrHCl}(\text{C}_6\text{F}_5)(\text{CO})(\text{PPh}_3)_2$	-100.1	-164.5	-163.2	-166.0	-112.2	193
$\text{IrHBr}(\text{C}_6\text{F}_5)(\text{CO})(\text{PPh}_3)_2$	-99.5	-164.4	-163.1	-165.5	-108.8	193
$\text{IrCl}_2(\text{C}_6\text{F}_5)(\text{CO})(\text{PPh}_3)_2^b$	-103.3	-163.5	-162.0	-164.5	-108.6	193
$\text{IrCl}_2(\text{C}_6\text{F}_5)(\text{CO})(\text{PPh}_3)_2^b$	-100.1	-164.8	-163.1	-165.9	-112.1	193
$\text{IrBr}_2(\text{C}_6\text{F}_5)(\text{CO})(\text{PPh}_3)_2$	-101.8	-163.2	-161.4	-164.1	-104.0	193
$\text{IrI}_2(\text{C}_6\text{F}_5)(\text{CO})(\text{PPh}_3)_2$	-95.8	-162.9	-161.1	-164.3	-100.1	193
$\text{IrH}_2(\text{C}_6\text{F}_5)(\text{CO})(\text{PPh}_3)_2^c$	-100.5	-165.0	-166.0	-165.0	-100.5	193
	-102.3	-165.0	-166.0	-165.0	-102.3	193
$\text{IrH}(\text{SiCl}_3)(\text{C}_6\text{F}_5)(\text{PPh}_3)_2$	-100.1	-159.8	-162.0	-163.0	-102.9	193
$\text{Ir}(\text{C}_6\text{F}_5)(\text{C}_4\text{F}_6)(\text{CO})(\text{PPh}_3)_2^d$	-94.9	-162.3 or -163.9	-162.3 or -163.9	-162.3 or -163.9	-101.6	193
$\text{Ir}(\text{C}_6\text{F}_5)(\text{CO})(\text{PMePh}_2)_2$	-110.0	-166.0	-162.0	-166.0	-110.0	193
$\text{IrI}_2(\text{C}_6\text{F}_5)(\text{CO})(\text{PMePh}_2)_2$	-96.3	-165.2	-161.5	-165.2	-96.3	193
$\text{Co}(\text{C}_6\text{F}_4\text{CN})(\text{CO})_2(\text{PPh}_3)_2$	-104.8	-137.1	—	-137.1	-104.8	197
$\text{Ir}(\text{C}_6\text{F}_4\text{CN})(\text{CO})_2(\text{PPh}_3)_2$	-104.8	-137.1	—	-137.1	-104.8	197
$\text{Ir}(\text{C}_6\text{F}_4\text{CN})(\text{CO})_2(\text{PPh}_3)_2$	-112.8	-139.3	—	-139.3	-112.8	197
$\text{Ir}(\text{C}_6\text{F}_4\text{CO}_2\text{Et})(\text{CO})_2(\text{PPh}_3)_2$	-115.4	-144.6	—	-144.6	-115.4	197
$\text{Ir}[\text{C}_6\text{F}_3(\text{CN})_2](\text{CO})_2(\text{PPh}_3)_2$	-76.9	—	—	-137.1	-96.5	197
$\text{Mo}(\pi\text{-C}_5\text{H}_5)(\text{CO})_2(\text{PPh}_3)_2[\text{C}_6\text{F}_3(\text{CN})_2]^\dagger$		-59.8	—	-76.6	-135.2	198

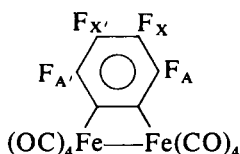
^a $\text{CF}:\text{CF}_2$ group, δ -95.8, -124.9, and -152.0. ^b One isomer is from $\text{Ir}(\text{C}_6\text{F}_5)(\text{CO})(\text{PPh}_3)_2 + \text{Cl}_2$, the other from $\text{Ir}(\text{C}_6\text{F}_5)(\text{CO})(\text{PPh}_3)_2 + \text{C}_3\text{F}_7\text{COCl}$, but the footnotes in ref. 193 are scrambled. ^c Two isomers, stereochemistry not determined. ^d $\text{CF}_3\text{C}_2\text{CF}_3$ group, -51.1 qd ($J(\text{CF}_3-\text{CF}_3)$ 5.5, $J(\text{CF}_3-\text{F2})$ 26.0 Hz), -51.8 q.



$J(2-3)$ 26.0; $J(2-5)$ 9.0;
 $J(3-4)$ 20.0; $J(3-5)$ 3.5;
 $J(3-6)$ 7.0; $J(4-5)$ 20.0;
 $J(5-6)$ 28.5; $J(2-H)$ 6 Hz

[343]

$(\pi-C_5H_5)UC_6F_5$
 δ -152.6 (2), -163.0 (2), -179.4 (1)
 [344]

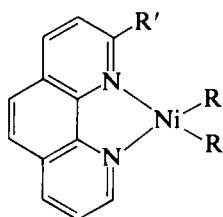


δF -131.72, -156.76 (-159.94)

$J(A-X) \pm 23.65$; $J(A-X') \mp 0.85$

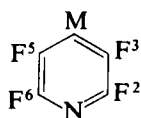
$|J(A-A')|$ 16.85 or 16.35; $|J(X-X')|$ 16.35 or 16.85 Hz

[345]



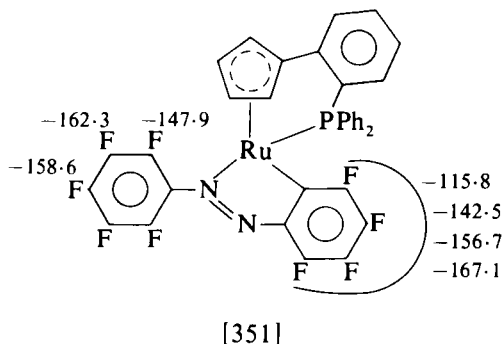
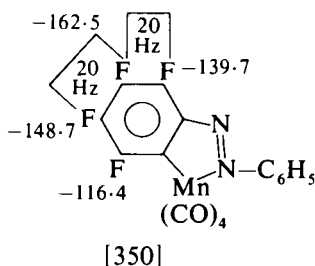
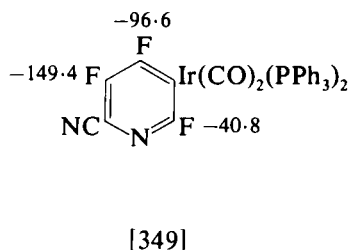
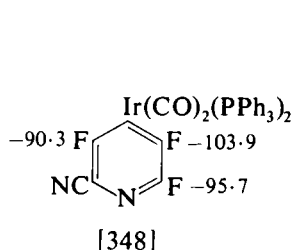
[346a] $R =$ $R' =$

[346b] $R =$ $R' = H$



[347]

M	$\delta F^2, F^6$	$\delta F^3, F^5$	Ref.
Co(CO) ₂ (PPh ₃) ₂	-98.3	-113.3	197
Ir(CO) ₂ (PPh ₃) ₂	-101.1	-120.0	197
Mo(π -C ₅ H ₅)(CO) ₂ (PPh ₃)	-100.0	-103.9	198

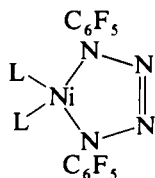


given with the structure, and similar values for the HBr, Cl₂, Br₂, and I₂ adducts are given in ref. 193(a).

The signals in the spectrum of the highly air-sensitive [344] were not assigned, but both of the two-fluorine signals are well to low frequency of the usual range for fluorines *ortho* to metal. The ¹H signals of the corresponding σ -bonded alkyl derivatives (π -C₃H₅)UR are also shifted considerably to lower frequency [R = (CH₃)₂CH, δ CH₃ -19.3, δ CH -190 from internal benzene]. (194) The authors suggest that the large value of $J(A-A')$ in the spectrum of [345]* and its similarity to $J(X-X')$ may be peculiar to transition-metal derivatives. (195) Parameters for *o*-phenanthroline-nickel complexes [346, R = C₆F₄OEt-*p* and R' = R or H] and also for the corresponding 2,2'-bipyridyl complexes [R' = H] are almost identical to those given with structure [346]. (196)

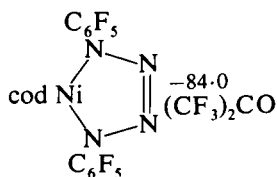
Parameters reported for other fluoroaryl compounds in which the transition metal is not directly attached to the aromatic ring are given with structures [352] to [372]. (115, 121, 201-203, 205-207) The structure of the hexafluoroacetone adduct [353], for which four signals in the aromatic region are reported, is not known. (115) The WF₅O

* The shifts for this compound are reported as -2637.9 Hz and -520.0 Hz from external C₆F₆ at 84.6 MHz in the experimental section of the paper, but the latter shift is given as -250.0 Hz in the discussion section.

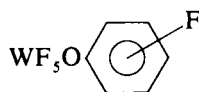


L or L ₂	$\delta F^2, F^6$	$\delta F^3, F^5$	δF^4	$J(2-3)$	$J(3-4)$	$J(2-5)$	$J(3-6)$
cod	-147.5m	-156.9m	-163.0m				
PMe ₂ Ph	-146.0	-162.0	-165.2	24.0	22.0	7.0	7.0
P(OMe) ₃	-148.0	-161.0	-166.1	17.0	21.0	5.0	5.0

[352]

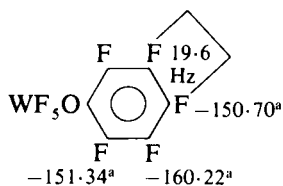
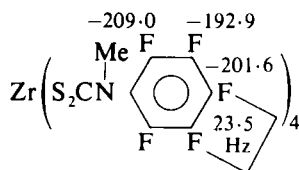
 δ -152.0, -161.2, -162.2, -165.0

[353]



	δC_6H_4F	δF_{ax}	δF_{eq}	$J(F_{ax}-F_{eq})$
F_{ortho}	-126.5	+119.87	+132.01	64.73
F_{meta}	-108.02	+120.54	+129.12	64.56
F_{para}	-106.11	+116.19	+127.67	64.58

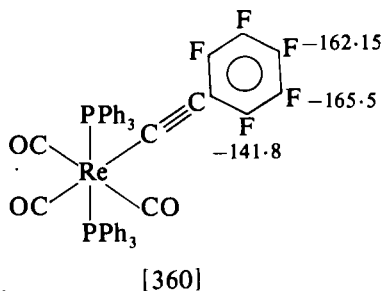
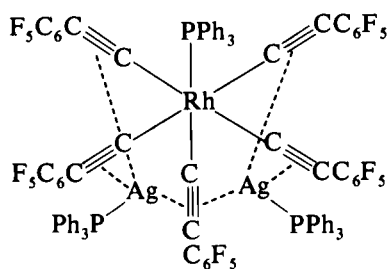
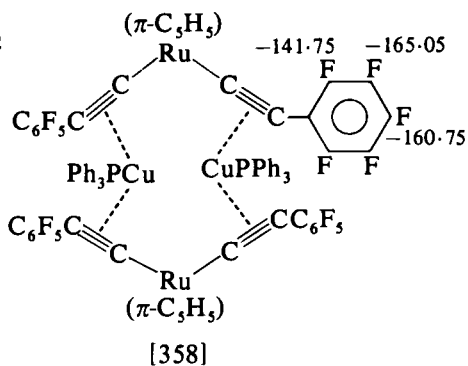
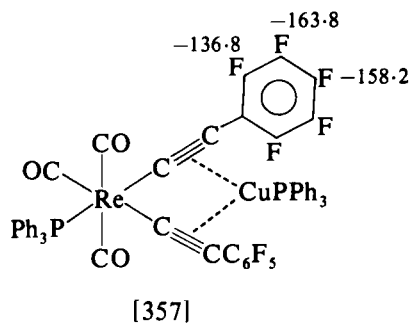
[354]

 $\delta F_{eq} + 145.04, \delta F_{ax} + 141.49$ $J(2-4) 1.25 \text{ Hz}$  $J(2-4) 1.9 \text{ Hz}$

[356]

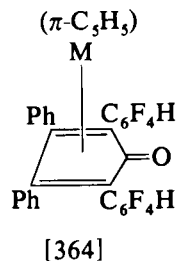
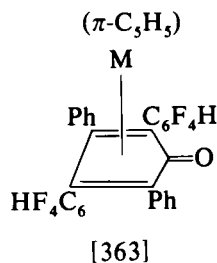
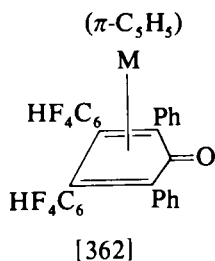
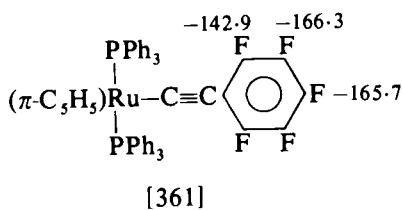
^a These values are stated to be measured from C₆F₆ and converted on the basis that C₆F₆ absorbs 163.0 ppm to high field of CFCl₃. (201)

[355]

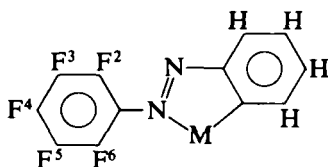


$\delta -137 (2), -160 (1), -164.5 (2)$ Total int. 4
 $\delta -134.5 (2), -159 (1), -163.5 (2)$ Total int. 1

[359]



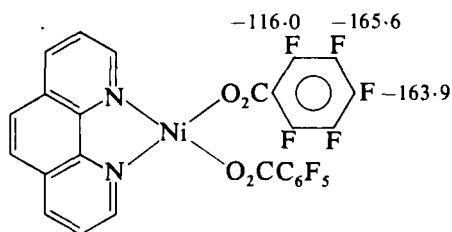
- a $M = \text{Co}$ δ -134.8 (2) -140.5 (1) -141.5 (1) -158.0 (4)
 $M = \text{Rh}$ δ -130.3 (2) -138.8 (1) -140.0 (1) -154.3 (2) -156.3 (2)
- b $M = \text{Co}$ δ -137.6 (2) -140.7 (2) -153.4 (4)
 $M = \text{Rh}$ δ -134.4 (2) -139.9 (2) -155.0 (4)
- c $M = \text{Co}$ δ -131.1 (2) -139.9 (2) -159.4 (4)
 $M = \text{Rh}$ δ -131.4 (2) -137.9 (2) -153.1 (4)



M	$\delta \text{F}^2, \text{F}^6$	$\delta \text{F}^3, \text{F}^5$	δF^4
$\text{Mn}(\text{CO})_4^a$	-150.4	-161.07	-155.0
$\text{Re}(\text{CO})_4^b$	-150.39	-161.33	-154.73
$\text{Pd}(\pi\text{-C}_5\text{H}_5)$	-148.4	-160.9	-155.0

^a $J(3-4)$ 21; $J(2-4)$ 0 Hz. ^b $J(3-4)$ 21.0, $J(2-4)$ 3.2 Hz.

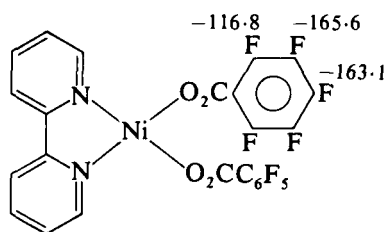
[365]



[366]

$[(\pi\text{-C}_5\text{H}_5)\text{Co}(\text{SC}_6\text{F}_5)]_2$
 δ -163.6, -158.0, -129.6

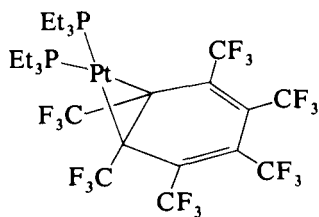
[368]



[367]

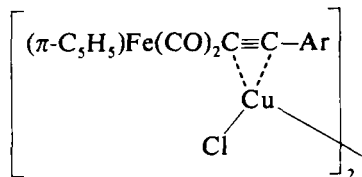
$(\pi\text{-C}_5\text{H}_5)\text{Co}(\text{CO})(\text{SC}_6\text{F}_5)$
 δ -162.2 (2) -157.0 (1) -128.2 (2)

[369]



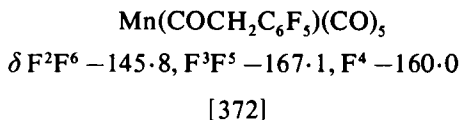
δ -51.2, $J(\text{P}-\text{CF}_3)$ 3.0 Hz
 $J(\text{Pt}-\text{CF}_3)$ 27.5 Hz

[370]



$\text{Ar} = \text{C}_6\text{H}_4\text{F}-p$ δ -114.3, $J(\text{F}-\text{H})$ 5.4, 8.4 Hz
 $\text{Ar} = \text{C}_6\text{F}_5$ $\delta \text{F}^{2,6}$ 138.3, $\text{F}^{3,5}$ 164.3, F^4 159

[371]



group shows strong electron withdrawal by an inductive effect when attached to a $\text{C}_6\text{H}_4\text{F}$ ring [354], and electron withdrawal by the WF_5 , evidently overcomes the usual resonance release by oxygen, since the derived value of σ_{R}^0 is $+0.065$. (201) Attachment to a C_6F_5 ring, however. [355], leads to a considerable reduction in the inductive withdrawal, and the σ_{R}^0 value of >-0.1 shows that in this situation the group is a resonance donor. Similar chemical shifts were reported for [355] by other authors, (202) who also obtained products of the type $\text{WF}_n(\text{C}_6\text{F}_5)_{6-n}$, but the complicated nature of the mixture did not allow assignment of the individual C_6F_5 groups. The eight-co-ordinate complex [356] was prepared in order to investigate the possibility of stereoisomerism in this type of compound. (203) No stereoisomers were detected, however; the broadening of the ^{19}F spectrum (observable below 0°C , severe below -60°C) was ascribed, like that in the ^1H spectra of all the $\text{M}(\text{S}_2\text{CNR}_2)_4$ complexes investigated previously, to the *quasi*-spherical symmetry of these molecules and a low rate of molecular tumbling at low temperatures.

Contact shifts for ^{19}F (and ^1H , ^{13}C , and ^{14}N) have been measured for the complexes $\text{Ni}(\text{acac})_2(\text{An})_2$ (*acac* = acetylacetonate, *An* = *ortho*-, *meta*-, and *para*-fluoroaniline, 2,4,6-trifluoroaniline, and pentafluoroaniline). (204) The hyperfine coupling constants derived from these measurements are in good agreement with those obtained by ESR, confirming that the unpaired spin density on the aromatic ring is delocalized in a manner similar to that of aromatic π -electron radicals.

The ^{19}F NMR spectra of [357] and [358] each show the presence of a single type of C_6F_5 group, (205) with the parameters shown, but for [359], two types, with intensity ratio 4:1 are observed. (206) The reaction between $(\pi\text{-C}_5\text{H}_5)\text{M}(\text{CO})_2$ ($\text{M} = \text{Co}, \text{Rh}$) and phenyl(2,3,4,5-tetrafluorophenyl)acetylene gives three isomers of formula $(\pi\text{-C}_5\text{H}_5)\text{M}[\text{C}_4(\text{C}_6\text{F}_4\text{H})_2\text{Ph}_2\text{CO}]$, presumed to be the positional isomers [362] to [364], but distinction between them has not yet been achieved. (207)

The platinum complex formed in the reaction between $\text{C}_6(\text{CF}_3)_6$ and tris(triethylphosphine)platinum shows only a single band at 30°C [$\delta -51.2$, $J(\text{P-CF}_3)$ 3.0, $J(\text{Pt-CF}_3)$ 27.5 Hz], which must result from fluxional behaviour in solution, since X-ray crystallography shows the structure of the solid to be as in [370], with alternate long and short bonds in the non-planar C_6 ring. (159, 160) At -90°C the spectrum

shows two unresolved multiplets ($\delta -47.7, -52.5$) in the ratio 1:2. The analogous nickel complexes $[Ni\{C_6(CF_3)_6\}L_2]$ also show only a singlet ^{19}F signal.

Acknowledgement

I am grateful to Dr. J. M. Birchall for considerable assistance with the literature search for the section on fluoroaromatic compounds.

REFERENCES

1. E. F. Mooney and P. H. Winson, "Ann. Review of NMR Spectroscopy", 1968, **1**, 243; K. Jones and E. F. Mooney, "Ann. Reports on NMR Spectroscopy", 1970, **3**, 261; 1971, **4**, 391; R. Fields, *ibid.*, 1972, **5A**, 99; L. Cavalli, *ibid.*, 1976, **6B**, 43.
2. C. A. Burgett, U.S.P. 3,867,418 (*Chem. Abs.*, 1975, **83**, 18844).
3. T. C. Morrill, R. A. Clark, D. Bilobran and D. S. Youngs, *Tetrahedron Lett.*, 1975, 397.
4. G. Folcher, J. Paris, P. Plurien, P. Rigny and E. Soulié, *J.C.S. Chem. Comm.*, 1974, 3.
5. D. F. Evans, J. N. Tucker and G. C. de Villardi, *J.C.S. Chem. Comm.*, 1975, 205.
6. D. R. Eaton and K. L. Chua, *Canad. J. Chem.*, 1973, **51**, 2260.
7. C. MacDonald and C. J. Willis, *Canad. J. Chem.*, 1973, **51**, 732.
8. R. B. King and W. C. Zipperer, *Inorg. Chem.*, 1972, **11**, 2119.
9. A. Nakamura and S. Otsuka, *J. Amer. Chem. Soc.*, 1972, **94**, 1886.
10. D. W. Lichtenberg and A. Wojcicki, *Inorg. Chem.*, 1975, **14**, 1295.
- 10a. J. L. Davidson and D. W. A. Sharp, *J.S.C. Dalton*, 1975, 2531.
11. J. L. Davidson, M. Green, J. A. K. Howard, S. A. Mann, J. Z. Nyathi, F. G. A. Stone and P. Woodward, *J.C.S. Chem. Comm.*, 1975, 803.
12. J. F. Nixon and J. R. Swain, *J.C.S. Dalton*, 1972, 1038.
13. J. P. Fackler, J. A. Fetchin, J. Mayhew, W. C. Seidel, T. J. Swift and M. Weeks, *J. Amer. Chem. Soc.*, 1969, **91**, 1941.
14. R. C. Dobbie, *Inorg. Nuclear Chem. Letters*, 1973, **9**, 191.
15. R. C. Dobbie, *J. Chem. Soc. (A)*, 1971, 230.
16. J. P. Crow, W. R. Cullen and F. L. Hou, *Inorg. Chem.*, 1972, **11**, 2125.
17. W. R. Cullen, L. D. Hall and J. E. H. Ward, *J. Amer. Chem. Soc.*, 1972, **94**, 5702.
18. I. W. Nowell, S. Rettig and J. Trotter, *J.C.S. Dalton*, 1972, 2381.
19. W. R. Cullen, L. D. Hall and J. E. H. Ward, *J. Amer. Chem. Soc.*, 1974, **96**, 3422.
20. W. R. Cullen, L. D. Hall and J. E. H. Ward, *Canad. J. Chem.*, 1975, **53**, 1038.
21. W. R. Cullen and L. Mihichuk, *Canad. J. Chem.*, 1975, **53**, 3401.
22. W. R. Cullen, L. D. Hall, H. K. Spendjian and J. E. H. Ward, *J. Fluorine Chem.*, 1973/4, **3**, 341.
23. I. W. Nowell and J. Trotter, *J.C.S. Dalton*, 1972, 2378.
24. J. L. Davidson and D. W. A. Sharp, *J.C.S. Dalton*, 1972, 107.
25. J. L. Davidson and D. W. A. Sharp, *J.C.S. Dalton*, 1973, 1957.
26. H. C. Clark and T. L. Hauw, *J. Organometallic Chem.*, 1972, **42**, 429.
27. H. C. Clark, J. D. Cotton and J. H. Tsai, *Inorg. Chem.*, 1966, **5**, 1582; H. C. Clark and J. H. Tsai, *ibid.*, 1407.
28. R. E. J. Bichler, M. R. Booth and H. C. Clark, *J. Organometallic Chem.*, 1970, **24**, 145.
29. A. N. Nesmeyanov, N. E. Kolobova, G. K. Znobina, K. N. Anisimov, I. B. Zlotina and M. D. Bargamova, *Izv. Akad. Nauk. SSSR, Ser. Khim.*, 1973, 2168 (*Chem. Abs.*, 1974, **80**, 15039).
30. (a) B. L. Booth, R. N. Haszeldine and N. I. Tucker, *J.C.S. Dalton*, 1975, 1439; (b) Preliminary communication, *J. Organometallic Chem.*, 1968, **11**, P5.

31. D. J. Cook, M. Green, N. Mayne and F. G. A. Stone, *J. Chem. Soc. (A)*, 1968, 1771.
32. M. J. Barrow, J. L. Davidson, W. Harrison, D. W. A. Sharp, G. A. Sim and F. B. Wilson, *J.C.S. Chem. Comm.*, 1973, 583.
33. M. J. Barrow, A. A. Freer, W. Harrison, G. A. Sim, D. W. Taylor and F. B. Wilson, *J.C.S. Dalton*, 1975, 197.
34. L. Y. Y. Chan and F. W. B. Einstein, *J.C.S. Dalton*, 1973, 111; F. W. B. Einstein and A. C. MacGregor, *J.C.S. Dalton*, 1974, 783.
35. W. R. Cullen and F. L. Hou, *Inorg. Chem.*, 1975, **14**, 3121.
36. W. R. Cullen and F. L. Hou, *Canad. J. Chem.*, 1975, **53**, 1735.
37. (a) W. R. Cullen, L. Mihichuk, F. W. B. Einstein and J. S. Field, *J. Organometallic Chem.*, 1974, **73**, C53; (b) F. W. B. Einstein and J. S. Field, *J.C.S. Dalton*, 1975, 172.
38. W. R. Cullen, L. D. Hall and J. E. H. Ward, *J. Amer. Chem. Soc.*, 1974, **96**, 3431.
39. C. D. Garner and B. Hughes, *J.C.S. Dalton*, 1974, 735.
40. R. B. King and R. N. Kapoor, *J. Organometallic Chem.*, 1968, **15**, 457.
41. J. Grobe and F. Kober, *Z. Nat.*, 1969, **24b**, 1346.
42. R. B. King and A. Bond, *J. Amer. Chem. Soc.*, 1974, **96**, 1334.
43. J. Thomson, W. Keeney, M. C. Baird and W. F. Reynolds, *J. Organometallic Chem.*, 1972, **40**, 205.
44. K. Stanley, R. A. Zelonka, J. Thomson, P. Fiess and M. C. Baird, *Canad. J. Chem.*, 1974, **52**, 1781.
45. A. Bond and M. Green, *J.C.S. Dalton*, 1972, 763.
46. C. S. Cundy, M. Green and F. G. A. Stone, *J. Chem. Soc. (A)*, 1970, 1647.
47. A. Bond, M. Green and S. H. Taylor, *J.C.S. Chem. Comm.*, 1973, 112.
48. A. Bond, B. Lewis and M. Green, *J.C.S. Dalton*, 1975, 1109.
49. M. Green, B. Lewis, J. J. Daly and F. Sanz, *J.C.S. Dalton*, 1975, 1118.
50. M. Green, S. Heathcock and D. C. Wood, *J.C.S. Dalton*, 1973, 1564.
51. R. Fields, G. L. Godwin and R. N. Haszeldine, *J.C.S. Dalton*, 1975, 1867.
52. J. Clemens, M. Green and F. G. A. Stone, *J.C.S. Dalton*, 1973, 375.
53. B. L. Booth, R. N. Haszeldine and N. I. Tucker, *J.C.S. Dalton*, 1975, 1446.
54. F. W. Grevels and E. K. von Gustorf, *Annalen*, 1975, 547.
55. P. Dodman and J. C. Tatlow, *J. Organometallic Chem.*, 1974, **67**, 87.
56. P. Dodman and T. A. Hamor, *J.C.S. Dalton*, 1974, 1010.
57. T. Blackmore, M. I. Bruce and F. G. A. Stone, *J.C.S. Dalton*, 1974, 106.
58. M. I. Bruce, R. C. F. Gardner and F. G. A. Stone, *J. Organometallic Chem.*, 1972, **40**, C39.
59. T. Blackmore, M. I. Bruce, F. G. A. Stone, R. E. Davis and N. V. Raghavan, *J. Organometallic Chem.*, 1973, **49**, C35.
60. J. L. Davidson, M. Green, F. G. A. Stone and A. J. Welch, *J.C.S. Chem. Comm.*, 1975, 286.
61. M. I. Bruce, F. G. A. Stone and B. J. Thomson, *J. Organometallic Chem.*, 1974, **77**, 77.
62. M. I. Bruce and T. A. Kuc, *Austral. J. Chem.*, 1974, **27**, 2487.
63. M. Green and B. Lewis, *J.C.S. Dalton*, 1975, 1137; preliminary communication, *J.C.S. Chem. Comm.*, 1973, 114.
64. M. Bottrill, R. Goddard, M. Green, R. P. Hughes, M. K. Lloyd, S. H. Taylor and P. Woodward, *J.C.S. Dalton*, 1975, 1150; preliminary communication, M. Green, S. H. Taylor, J. J. Daly and F. Sanz, *J.C.S. Chem. Comm.*, 1974, 361.
65. R. B. King and K. H. Pannell, *J. Amer. Chem. Soc.*, 1968, **90**, 3984.
66. R. C. Dobbie, M. J. Hopkinson and D. Whittaker, *J.C.S. Dalton*, 1972, 1020.
67. R. C. Dobbie and P. R. Mason, *J.C.S. Dalton*, 1973, 1124.
68. R. C. Dobbie and P. R. Mason, *J.C.S. Dalton*, 1974, 2439.
69. R. C. Dobbie and M. J. Hopkinson, *J.C.S. Dalton*, 1974, 1290.

70. A. H. Cowley and K. E. Hill, *Inorg. Chem.*, 1973, **12**, 1446.
71. D. P. Bauer, W. M. Douglas and J. K. Ruff, *J. Organometallic Chem.*, 1973, **57**, C19.
72. L. S. Chia, W. R. Cullen and D. A. Harbourn, *Canad. J. Chem.*, 1972, **50**, 2182.
73. F. W. B. Einstein and R. D. G. Jones, *J.C.S. Dalton*, 1972, 442.
74. F. W. B. Einstein and R. D. G. Jones, *J.C.S. Dalton*, 1972, 2563.
75. F. W. B. Einstein and R. D. G. Jones, *Inorg. Chem.*, 1973, **12**, 255.
76. W. R. Cullen and L. Mihichuk, *Canad. J. Chem.*, 1973, **51**, 936.
77. A. Dobson, S. D. Robinson and M. F. Uttley, *J.C.S. Dalton*, 1975, 370.
78. R. B. King, A. Efraty and W. M. Douglas, *J. Organometallic Chem.*, 1973, **56**, 345.
79. R. B. King and A. Efraty, *J. Organometallic Chem.*, 1972, **36**, 371.
80. H. Brunner and W. Rambold, *J. Organometallic Chem.*, 1973, **60**, 351.
81. (a) A. M. Van Den Bergen and B. O. West, *J. Organometallic Chem.*, 1975, **92**, 55; (b) A. M. Van Den Bergen and B. O. West, *J. Organometallic Chem.*, 1974, **64**, 1251.
82. B. L. Booth, R. N. Haszeldine and T. Inglis, *J.C.S. Dalton*, 1975, 1449.
83. R. J. Burns, P. B. Bulkowski, S. C. V. Stevens and M. C. Baird, *J.C.S. Dalton*, 1974, 415.
84. M. Green and S. H. Taylor, *J.C.S. Dalton*, 1975, 1128.
85. K. Stanley and D. W. McBride, *Canad. J. Chem.*, 1975, **53**, 2537.
86. W. R. Cullen and A. J. T. Jull, *Canad. J. Chem.*, 1973, **51**, 1521.
87. B. L. Booth, R. N. Haszeldine and I. Perkins, *J.C.S. Dalton*, 1975, 1847.
88. H. C. Clark and R. K. Mittal, *Canad. J. Chem.*, 1973, **51**, 1511.
89. (a) B. L. Booth and A. D. Lloyd, *J. Organometallic Chem.*, 1972, **35**, 195; (b) D. A. Clement, J. F. Nixon and J. S. Poland, *ibid.*, 1974, **76**, 117; (c) D. M. Barlex, A. C. Jarvis, R. D. W. Kemmitt and B. Y. Kimura, *J.C.S. Dalton*, 1972, 2549.
90. J. Clemens, M. Green, Ming-Cheng Kuo, C. J. Fritchier, J. T. Mague and F. G. A. Stone, *J.C.S. Chem. Comm.*, 1972, 53.
91. M. Green and S. H. Taylor, *J.C.S. Dalton*, 1975, 1142.
92. J. T. Mague, M. O. Nutt and E. H. Gause, *J.C.S. Dalton*, 1973, 2578.
93. J. Clemens, M. Green and F. G. A. Stone, *J.C.S. Dalton*, 1974, 93.
94. J. Clemens, M. Green and F. G. A. Stone, *J.C.S. Dalton*, 1973, 1620.
95. D. M. Blake, A. Winkelman and Yen Lung Chung, *Inorg. Chem.*, 1975, 1326.
96. E. Lindner and M. Zipper, *Chem. Ber.*, 1974, 1444.
97. H. L. M. Van Gaal and A. Van der Ent, *Inorg. Chim. Acta*, 1973, **7**, 653.
98. R. Cramer and G. S. Reddy, *Inorg. Chem.*, 1973, **12**, 346.
99. A. C. Jarvis and R. D. W. Kemmitt, *J. Organometallic Chem.*, 1974, **81**, 415.
100. C. T. Mortimer, J. L. McNaughton, J. Burgess, M. J. Hacker, R. D. W. Kemmitt, M. I. Bruce, G. Shaw and F. G. A. Stone, *J. Organometallic Chem.*, 1973, **47**, 439.
101. J. A. Evans, R. D. W. Kemmitt, B. Y. Kimura and D. R. Russell, *J.C.S. Chem. Comm.*, 1972, 509.
102. A. C. Jarvis, R. D. W. Kemmitt, B. Y. Kimura, D. R. Russell and P. A. Tucker, *J.C.S. Chem. Comm.*, 1974, 797.
103. M. I. Bruce, B. L. Goodall and F. G. A. Stone, *J.C.S. Dalton*, 1975, 1657.
104. R. S. Dickson and H. P. Kirsch, *Austral. J. Chem.*, 1972, **25**, 2535.
105. J. T. Mague, *J.C.S. Dalton*, 1975, 900.
106. R. S. Dickson and H. P. Kirsch, *Austral. J. Chem.*, 1972, **25**, 1815.
107. J. L. Davidson and D. W. A. Sharp, *J. Organometallic Chem.*, 1974, **80**, C39.
108. D. A. Clarke, R. D. W. Kemmitt, D. R. Russell and P. A. Tucker, *J. Organometallic Chem.*, 1975, **93**, C37.
109. R. S. Dickson and H. P. Kirsch, *Austral. J. Chem.*, 1974, **27**, 61.
110. R. S. Dickson and H. P. Kirsch, *Austral. J. Chem.*, 1973, **26**, 1911.
111. R. S. Dickson, P. J. Fraser and B. M. Gatehouse, *J.C.S. Dalton*, 1972, 2278; R. S. Dickson and P. J. Fraser, *Austral. J. Chem.*, 1972, **25**, 1179.

112. B. Cetinkaya, M. F. Lappert and J. McMeeking, *J.C.S. Dalton*, 1973, 1975.
113. M. J. Doyle, M. F. Lappert, G. M. McLaughlin and J. McMeeking, *J.C.S. Dalton*, 1974, 1494.
114. B. Cetinkaya, P. Dixneuf and M. F. Lappert, *J.C.S. Dalton*, 1974, 1827.
115. J. Ashley-Smith, M. Green and F. G. A. Stone, *J.C.S. Dalton*, 1972, 1805.
116. I. H. Sabherwal and A. B. Burg, *Inorg. Chem.*, 1973, **12**, 697.
117. R. C. Dobbie and D. Whittaker, *J.C.S. Dalton*, 1973, 2427.
118. L. S. Chia and W. R. Cullen, *Inorg. Chem.*, 1975, **14**, 482.
119. L. S. Chia, W. R. Cullen, M. Franklin and A. R. Manning, *Inorg. Chem.*, 1975, **14**, 2521.
120. P. Anstey and K. G. Orrell, *J.C.S. Dalton*, 1974, 870.
121. J. L. Davidson and D. W. A. Sharp, *J.C.S. Dalton*, 1975, 813.
122. K. R. Dixon, K. C. Moss and M. A. R. Smith, *J.C.S. Dalton*, 1973, 1528.
123. T. G. Appleton, M. H. Chisholm, H. C. Clark and L. E. Manzer, *Inorg. Chem.*, 1972, **11**, 1786.
124. H. C. Clark and L. E. Manzer, *J. Organometallic Chem.*, 1972, **38**, C41; 1973, **59**, 411.
125. M. H. Chisholm and H. C. Clark, *J. Amer. Chem. Soc.*, 1972, **94**, 1532.
126. D. B. Crump and N. C. Payne, *Inorg. Chem.*, 1973, **12**, 1663.
127. H. D. Empsall, M. Green and F. G. A. Stone, *J.C.S. Dalton*, 1972, 96.
128. R. D. W. Kemmitt, B. Y. Kimura, G. W. Littlecott and R. D. Moore, *J. Organometallic Chem.*, 1972, **44**, 403.
129. J. Howard and P. Woodward, *J.C.S. Dalton*, 1973, 1840.
130. D. J. Cardin, B. Cetinkaya, E. Cetinkaya and M. F. Lappert, *J.C.S. Dalton*, 1973, 514.
131. J. Browning, H. D. Empsall, M. Green and F. G. A. Stone, *J.C.S. Dalton*, 1973, 381.
132. C. H. Davies, C. H. Game, M. Green and F. G. A. Stone, *J.C.S. Dalton*, 1974, 357.
133. M. Green, J. A. K. Howard, A. Laguna, M. Murray, J. L. Spencer and F. G. A. Stone, *J.C.S. Chem. Comm.*, 1975, 451.
134. P. K. Maples, M. Green and F. G. A. Stone, *J.C.S. Dalton*, 1973, 388.
135. C. A. Tolman and W. C. Seidel, *J. Amer. Chem. Soc.*, 1974, **96**, 2774.
136. A. Modinos and P. Woodward, *J.C.S. Dalton*, 1974, 2065.
137. R. Countryman and B. R. Penfold, *Chem. Comm.*, 1971, 1598.
138. W. J. Bland, R. D. W. Kemmitt and R. D. Moore, *J.C.S. Dalton*, 1973, 1292.
139. J. Clemens, R. E. Davis, M. Green, J. D. Oliver and F. G. A. Stone, *Chem. Comm.*, 1971, 1095.
140. V. A. Mukhedkar, B. J. Kavathekar and A. J. Mukhedkar, *J. Inorg. Nuclear Chem.*, 1975, **37**, 483.
141. M. Green and G. J. Parker, *J.C.S. Dalton*, 1973, 2099.
142. J. Ashley-Smith, M. Green and D. C. Wood, *J. Chem. Soc. (A)*, 1970, 1847.
143. W. Cherwinski, B. F. G. Johnson and J. Lewis, *J.C.S. Dalton*, 1974, 1405.
144. S. Otsuka, K. Tani, I. Kato and O. Teranaka, *J.C.S. Dalton*, 1974, 2216.
145. P. K. Maples, M. Green and F. G. A. Stone, *J.C.S. Dalton*, 1973, 2069.
146. J. M. Baraban and J. A. McGinnety, *J. Amer. Chem. Soc.*, 1975, **97**, 4232.
147. D. M. Roundhill and G. Wilkinson, *J. Chem. Soc. (A)*, 1968, 506.
148. G. A. Rivett, *Diss. Abs.*, 1975, **36B**, 2214.
149. P. K. Maples, M. Green and F. G. A. Stone, *J.C.S. Dalton*, 1974, 1194.
150. M. Green, R. B. L. Osborn, A. J. Rest and F. G. A. Stone, *J. Chem. Soc. (A)*, 1968, 2525.
151. T. G. Appleton, H. C. Clark and R. J. Puddephatt, *Inorg. Chem.*, 1972, **11**, 2074.
152. M. H. Chisholm, H. C. Clark and L. E. Manzer, *Inorg. Chem.*, 1972, **11**, 1269.
153. T. G. Appleton, M. H. Chisholm, H. C. Clark and L. E. Manzer, *Canad. J. Chem.*, 1973, **51**, 2243.
154. T. G. Appleton, H. C. Clark, R. C. Poller and R. J. Puddephatt, *J. Organometallic Chem.*, 1972, **39**, C13.

155. R. D. W. Kemmitt, B. Y. Kimura and G. W. Littlecott, *J.C.S. Dalton*, 1973, 636.
156. J. Burgess, R. D. W. Kemmitt and G. W. Littlecott, *J. Organometallic Chem.*, 1973, **56**, 405.
157. A. C. Jarvis, R. D. W. Kemmitt, B. Y. Kimura, D. R. Russell and P. A. Tucker, *J. Organometallic Chem.*, 1974, **66**, C53.
158. J. L. Davidson, M. Green, F. G. A. Stone and A. J. Welch, *J. Amer. Chem. Soc.*, 1975, **97**, 7490.
159. J. Browning, M. Green, J. L. Spencer and F. G. A. Stone, *J.C.S. Dalton*, 1974, 97.
160. J. Browning, M. Green, B. R. Penfold, J. L. Spencer and F. G. A. Stone, *J.C.S. Chem. Comm.*, 1973, 31.
161. J. Browning, M. Green, A. Laguna, L. E. Smart, J. L. Spencer and F. G. A. Stone, *J.C.S. Chem. Comm.*, 1975, 723.
162. D. W. W. Anderson, E. A. V. Ebsworth and D. W. H. Rankin, *J.C.S. Dalton*, 1973, 2370; D. W. W. Anderson, E. A. V. Ebsworth, J. K. MacDougall and D. W. H. Rankin, *J. Inorg. Nuclear Chem.*, 1973, **35**, 2259.
163. H. C. Clark and L. E. Manzer, *J.C.S. Chem. Comm.*, 1973, 870; *Inorg. Chem.*, 1974, **13**, 1996.
164. H. C. Clark and L. E. Manzer, *Inorg. Chem.*, 1974, **13**, 1291.
165. B. W. Davies and N. C. Payne, *Inorg. Chem.*, 1974, **13**, 1843.
166. M. Green, J. A. K. Howard, J. L. Spencer and F. G. A. Stone, *J.C.S. Chem. Comm.*, 1975, 449.
167. D. A. Redfield, J. H. Nelson, R. A. Henry, D. W. Moore and H. B. Jonassen, *J. Amer. Chem. Soc.*, 1974, **96**, 6298.
168. Dae-Ki Kang and A. B. Burg, *Inorg. Chem.*, 1972, **11**, 902.
169. A. B. Burg, *Inorg. Chem.*, 1973, **12**, 3017.
170. A. B. Burg and I. B. Mishra, *J. Organometallic Chem.*, 1970, **24**, C33.
171. T. G. Attig, M. A. A. Beg and H. C. Clark, *Inorg. Chem.*, 1975, **14**, 2986.
172. A. J. Carty, S. E. Jacobson, R. T. Simpson and N. J. Taylor, *J. Amer. Chem. Soc.*, 1975, **97**, 7254; N. J. Taylor, S. E. Jacobson and A. J. Carty, *Inorg. Chem.*, 1975, **14**, 2648.
173. S. Jacobson, A. J. Carty, M. Mathew and G. J. Palenik, *J. Amer. Chem. Soc.*, 1974, **96**, 4330.
174. W. S. Cripps and C. J. Willis, *Canad. J. Chem.*, 1975, **53**, 817.
175. W. R. Cullen, L. D. Hall, J. T. Price and G. Spendjian, *Canad. J. Chem.*, 1975, **53**, 366.
176. P. Anstey and K. G. Orrell, *J.C.S. Dalton*, 1974, 1711.
177. K. R. Dixon, K. C. Moss and M. A. R. Smith, *Inorg. Nuclear Chem. Letters*, 1974, **10**, 373.
178. K. R. Dixon, K. C. Moss and M. A. R. Smith, *J.C.S. Dalton*, 1974, 971.
179. K. R. Dixon, K. C. Moss and M. A. R. Smith, *J.C.S. Dalton*, 1975, 990.
180. R. G. Cavell, W. Byers, E. D. Day and P. M. Watkins, *Inorg. Chem.*, 1972, **11**, 1598.
181. A. Johnson and R. J. Puddephatt, *Inorg. Nuclear Chem. Letters*, 1973, **9**, 1175.
182. C. M. Mitchell and F. G. A. Stone, *J.C.S. Dalton*, 1972, 102.
183. A. Johnson, R. J. Puddephatt and J. L. Quirk, *J.C.S. Chem. Comm.*, 1972, 938.
184. J. A. J. Jarvis, A. Johnson and R. J. Puddephatt, *J.C.S. Chem. Comm.*, 1973, 373.
185. B. L. D'yatkin, B. I. Martynov, L. G. Martynova, N. G. Kizim, S. R. Sterlin, Z. A. Stumbrevichute and L. A. Fedorov, *J. Organometallic Chem.*, 1973, **57**, 423.
186. M. G. Barlow, *Fluorocarbons and Related Compounds*, 1974, **2**, 420; J. M. Birchall, 1976, **3**, 424.
187. H. A. O. Hill, K. G. Morallee, F. Cernivez and G. Pellizer, *J. Amer. Chem. Soc.*, 1972, **94**, 277.
188. D. Dodd, M. D. Johnson and C. W. Fong, *J.C.S. Dalton*, 1974, 58.
189. G. W. Parshall, *J. Amer. Chem. Soc.*, 1964, **86**, 5387; 1966, **88**, 704.

190. J. L. Fletcher and M. J. McGlinchey, *Canad. J. Chem.*, 1975, **53**, 1525.
191. M. J. McGlinchey and Teong-Seng Tan, *Canad. J. Chem.*, 1974, **52**, 2439.
192. R. Middleton, J. R. Hull, S. R. Simpson, C. H. Tomlinson and P. L. Timms, *J.C.S. Dalton*, 1973, 120.
- 193a. R. L. Bennett, M. I. Bruce and R. C. F. Gardner, *J.C.S. Dalton*, 1973, 2653; (b) preliminary communication, *J. Fluorine Chem.*, 1972/3, **2**, 447.
194. T. J. Marks and A. M. Seyam, *J. Amer. Chem. Soc.*, 1972, **94**, 6545.
195. M. J. Bennett, W. A. G. Graham, R. P. Stewart and R. M. Tuggle, *Inorg. Chem.*, 1973, **12**, 2944.
196. P. G. Cookson and G. B. Deacon, *Austral. J. Chem.*, 1972, **25**, 2095.
197. B. L. Booth, R. N. Haszeldine and I. Perkins, *J.C.S. Dalton*, 1975, 1843.
198. M. I. Bruce, B. L. Goodall, D. N. Sharrock and F. G. A. Stone, *J. Organometallic Chem.*, 1972, **39**, 139.
199. M. I. Bruce, B. L. Goodall, G. L. Sheppard and F. G. A. Stone, *J.C.S. Dalton*, 1975, 591.
200. M. I. Bruce, R. C. F. Gardner, B. L. Goodall, F. G. A. Stone, R. J. Doedens and J. A. Moreland, *J.C.S. Chem. Comm.*, 1974, 185.
201. F. E. Brinckman, R. B. Johannesen and L. B. Handy, *J. Fluorine Chem.*, 1971/2, **1**, 493.
202. A. Majid, D. W. A. Sharp, J. M. Winfield and I. Hanley, *J.C.S. Dalton*, 1973, 1876.
203. E. L. Muetterties, *Inorg. Chem.*, 1974, **13**, 1011.
204. C. Chachaty, A. Forchioni and J. Virlet, *Canad. J. Chem.*, 1975, **53**, 648.
205. O. M. Abu Saleh and M. I. Bruce, *J.C.S. Dalton*, 1975, 2311.
206. O. M. Abu Saleh, M. I. Bruce, M. R. Churchill and B. G. DeBoer, *J.C.S. Chem. Comm.*, 1974, 688.
207. R. S. Dickson and L. J. Michel, *Austral. J. Chem.*, 1975, **28**, 1943.
208. R. L. Bennett, M. I. Bruce and F. G. A. Stone, *J. Organometallic Chem.*, 1975, **94**, 65.
209. O. M. Abu Saleh and M. I. Bruce, *J.C.S. Dalton*, 1974, 2302.

Nitrogen NMR Spectroscopy

M. WITANOWSKI AND L. STEFANIAK

*Institute of Organic Chemistry,
Polish Academy of Sciences, Warsaw, Poland*

AND

G. A. WEBB

*Department of Chemical Physics,
University of Surrey, Guildford, Surrey, England*

I. Introduction	118
II. Theory of nitrogen screening constants	118
A. <i>Ab initio</i> calculations	119
B. Semi-empirical calculations	122
III. Calibration of spectra	136
IV. Experimental techniques	144
A. Pulsed Fourier transform method	144
B. Differential saturation technique	148
V. Correlation of relative nitrogen screening constants with molecular structure	149
A. Amines	150
B. Aminosilanes and aminoboranes	156
C. Ammonium ions	164
D. Amino acids, peptides and related structures	164
E. Hydrazines	171
F. Amides, ureas, guanidines and related structures	171
G. Cyano, cyanato groups and related structures	175
H. Azides	176
I. Azoles and their derivatives	178
J. Sydnones, sydnonimines and related structures	187
K. Azines and their derivatives	190
L. Oximes and nitrones	200
M. Nitro compounds and nitrates	202
N. Nitroso compounds	206
O. Azo and diazo compounds	206
P. Miscellaneous structures	211
Q. Studies on paramagnetic molecules	213
R. Studies on diamagnetic metal complexes	214
VI. Correlation of nitrogen spin-spin coupling constants with molecular structure	215
A. $^1J(^{15}\text{N-H})$	216
B. $^2J(^{15}\text{N-H})$	219

C. $^3J(^{15}\text{N-H})$	224
D. $^4J(^{15}\text{N-H})$	226
E. $^{15}\text{N-}^{13}\text{C}$ couplings	226
F. $^{15}\text{N-}^{15}\text{N}$ couplings	232
G. Other couplings	232
VII. Relaxation phenomena	233
A. ^{14}N relaxation	233
B. ^{15}N relaxation	237
References	239

I. INTRODUCTION

During the past four years a considerable body of published work has appeared relating to nitrogen NMR. Significant developments have occurred in all the areas of investigation on which we reported previously. (1a, 2a) These developments are due to improvements in experimental techniques and instrumentation as well as to an increased awareness of the utility of both ^{14}N and ^{15}N nuclei in NMR spectroscopy.

In many ways the information available from NMR studies on these two isotopes is complementary. Although ^{14}N is by far the more common, in natural abundance, it has an electric quadrupole moment while the less abundant ^{15}N nucleus does not. Thus the ^{14}N nucleus has been more frequently used in chemical shift studies on natural abundance samples as well as in quadrupolar relaxation investigations. The larger magnetogyric ratio of the ^{15}N nucleus, together with its sharper lines, renders it more suitable for studies involving spin-spin coupling constants in addition to those on the less efficient nuclear relaxation processes.

It is our aim in this report to bring up to date those we presented four (1a) and six (2a) years ago, to which extensive reference is made. For comparison purposes some mention of earlier work is made where appropriate.

II. THEORY OF NITROGEN SCREENING CONSTANTS

It is not reasonable to expect of any theoretical treatment of nuclear screening constants that it exactly reproduces experimental values. Theoretical estimates are usually based upon an isolated molecule as a model. In contrast to this many experimental values are reported for liquid samples in which solvent effects may be present. Additionally the experimental results may be in considerable error, this being especially true for broad resonances. However, even if solvent effects and experimental errors are eliminated the observed relative screening

constant may depend upon the relative populations of rotational and vibrational levels of the molecule. In this case the screening may differ by several ppm from that calculated for the equilibrium molecular geometry. (3)

It is well known that the early treatment of nuclear screening, presented by Ramsey, (4–6) suffers from a number of drawbacks. (3, 7–10). These include the occurrence of diamagnetic, σ^d , and paramagnetic, σ^p , terms which become almost equal and opposite in sign for medium sized molecules, leaving the resultant screening as the relatively small difference between them.

Another difficulty arises from the necessity of summing over all the excited states of the molecule, including the continuum. In general little is known about such states for most molecules. In addition, Ramsey's formulation produces screening data which depend upon the choice of origin, i.e. are gauge dependent, unless a complete basis set of atomic orbitals is included in the molecular orbital description. This is rarely possible, even for diatomic molecules, without the use of large amounts of computer time.

A. *Ab initio* calculations

Various forms of Hartree–Fock perturbation theory have been applied to the calculation of nitrogen screening constants within the framework of Ramsey's treatment. These avoid the difficulties associated with the infinite summation over excited states by restricting the summation to states described by the molecular orbitals used in the calculation. (11–14)

The value of σ^d for the nitrogen atoms in pyridine and pyrazine have been obtained by means of Gaussian lobe SCF functions, but no suitable experimental data are available for comparison purposes. (15)

The nitrogen atom in ammonia has been considered in several *ab initio* calculations of nuclear screening (Table I). Where STO-5G refers to a minimal basis set of 5 Gaussians used for each Slater type orbital, LEMAO-5G is a similar minimal basis where the orbitals are found by minimizing the energies of the isolated atoms. SAMO is a minimal basis set found from Slater's rules, (24) BLMO differs from SAMO in that the exponents used are optimized for ammonia. In the slightly extended 4-31G set the valence shell of nitrogen is described by inner and outer parts which are represented by 3 and 1 Gaussians respectively, and the extended DZMO set uses double zeta functions for the nitrogen orbitals.

The theoretical results presented in Table I approach more closely to the experimental data, obtained from spin-rotation results, as the size of the basis set increases. The best agreement is afforded by the

TABLE I

Some calculated values of the nitrogen screening, in ppm, in NH_3

σ^d	σ^p	σ^{total}	Basis set used	Reference
353.6	-177.4	176.2	STO-5G	11 ^a
356.0	-173.0	183.0	SAMO	14 ^b
354.0	-162.0	192.0	BLMO	11 ^b
354.1	-157.3	196.8	LEMAO-5G	11 ^a
353.7	-109.5	244.2	4-31G	11 ^a
355.0	-101.0	254.0	DZMO	14 ^b
350.63	-78.29	272.34	32 STO	13 ^b
350.58	-78.23	272.35	32 STO	13 ^c
360.1	-89.7	270.4	Spin-rotation data	16, 17

^a Origin taken at centre of mass.^b Origin taken at the nitrogen atom.^c Origin taken at 0.0133 a.u. from nitrogen along the C_3 axis towards the protons to give the best gauge result.

calculations of Arrighini *et al.* (13) who used a basis set comprising 32 Slater type orbitals for ammonia. The small gauge dependence of these results reflects on the fact that they were obtained by means of a large basis set.

In general a carefully optimized set of Slater orbitals, approximately three times as large as the minimal set, is necessary to give results within a few percent of the experimental data. This tends to restrict *ab initio* calculations to small molecules. However, even if exact eigenfunctions were used to calculate σ within Ramsey's treatment, a change of gauge would still produce changes in the values of σ^d and σ^p . Consequently comparison of σ^d and σ^p data evaluated at different origins must be made with considerable care.

In NMR spectroscopy the main interest is in relative screening constants i.e. *chemical shifts*, both for different nuclei in the same molecule and for nuclei in different polyatomic molecules, rather than in absolute screening constants. A theoretical approach which gives gauge dependent results leads to difficulties when relative screenings for various nuclei are to be compared.

Chemical problems are usually related to larger molecules than ammonia for which only limited basis sets are practical such that σ becomes gauge dependent when obtained within the framework of Ramsey's method. Consequently this method is not very attractive as a means of calculating chemical shifts for most chemically interesting molecules.

The shortcomings of Ramsey's approach can be obviated by taking a linear combination of gauge dependent atomic orbitals to represent the

requisite molecular orbitals, as discussed by Pople (18), which give gauge independent results. In this method σ may be expressed as the sum of local, nonlocal and interatomic contributions. (18–21)

$$\sigma = \sigma_{\text{loc}}^{\text{d}} + \sigma_{\text{nonloc}}^{\text{d}} + \sigma_{\text{inter}}^{\text{d}} + \sigma_{\text{loc}}^{\text{p}} + \sigma_{\text{nonloc}}^{\text{p}} + \sigma_{\text{inter}}^{\text{p}} \quad (1)$$

The various diamagnetic and paramagnetic terms in equation (1) are not directly comparable to those terms bearing these names in Ramsey's theory.

The local terms $\sigma_{\text{loc}}^{\text{d}}$ and $\sigma_{\text{loc}}^{\text{p}}$ arise from electronic currents localized on the atom containing the nucleus of interest. Similarly $\sigma_{\text{nonloc}}^{\text{d}}$ and $\sigma_{\text{nonloc}}^{\text{p}}$ are contributions from currents on neighbouring atoms. (21) Finally, $\sigma_{\text{inter}}^{\text{d}}$ and $\sigma_{\text{inter}}^{\text{p}}$ are due to any non-localized currents between atoms in the molecule, e.g. ring currents, these usually produce a very small screening contribution, a few ppm at most. This is a negligible amount compared with the range of about 900 ppm exhibited by nitrogen chemical shifts.

Within the gauge dependent molecular orbital framework various levels of approach to the terms in equation (1) are possible. These differ in the choice of basis functions and the method of evaluating or approximating the necessary integrals. As is the case with Ramsey's method, limited basis set *ab initio* calculations have been performed on some small molecules. Ditchfield (21) has reported gauge dependent molecular orbital *ab initio* results for the nitrogen atoms in NH_3 and HCN. He employed the STO-5G, LEMAO-5G and 4-31G basis sets and obtained values of σ for the nitrogen in NH_3 as 309.3, 310.2 and 267.8 ppm respectively (cf. Table I). Similarly for HCN the calculated values are 42.8, -50.3 and -40.6 ppm compared with the experimental value of -37.0 ppm. (16) It is clear that the extended 4-31G basis set gives better agreement with experimental data than do the two minimum basis sets of functions. Thus, as in Ramsey's method, the best *ab initio* results are obtained with extended basis sets; however, the gauge dependence problem has been removed.

Since the number of integrals to be evaluated increases rapidly with molecular size, semi-empirical calculations are more practical at present for larger molecules. The most widely used semi-empirical approach is based upon Pople's theory (22, 23) of molecular diamagnetism within the independent electron framework. All explicit two electron terms become zero in this method. Thus the necessity of evaluating many integrals is avoided and the remainder can be approximated by the methods implicit in all valence electron molecular orbital calculations. (24)

B. Semi-empirical calculations

The resulting gauge independent expressions for the local diamagnetic and paramagnetic contributions to the screening of nucleus A , where α and β are labels for the cartesian components x, y and z , are given by:

$$(\sigma_A^d)_{\alpha\beta} = \frac{\mu_0}{4\pi} \frac{e^2}{2m} \sum_{\mu} P_{\mu\mu} \langle \mu | r^{-3} (r^2 \delta_{\alpha\beta} - r_{\alpha} r_{\beta}) | \mu \rangle \quad (2)$$

and

$$\begin{aligned} (\sigma_A^p)_{\alpha\beta} = & -\frac{\mu_0}{4\pi} \frac{2e^2 \hbar^2}{m^2} \sum_j^{\text{occ}} \sum_k^{\text{unocc}} (E_k - E_j)^{-1} \sum_{\mu < \nu}^A \sum_B \sum_{\lambda < \sigma}^B \\ & (C_{\mu j} C_{\nu k} - C_{\nu j} C_{\mu k}) (C_{\lambda j} C_{\sigma k} - C_{\sigma j} C_{\lambda k}) \\ & \times \langle \mu | r^{-3} L_{\alpha} | \nu \rangle \langle \lambda | L_{\beta} | \sigma \rangle \end{aligned} \quad (3)$$

In equation (2) $\delta_{\alpha\beta}$ is the Kronecker delta, which is unity if $\alpha = \beta$ otherwise it is zero, r refers to the separation between nucleus A and its surrounding electrons and P is an element of the charge density-bond order matrix defined by:

$$P_{\mu\lambda} = 2 \sum_j^{\text{occ}} C_{j\mu} C_{j\lambda} \quad (4)$$

where the C 's are the unperturbed LCAO coefficients of the atomic orbitals $\mu, \nu, \lambda, \sigma$ in the occupied and unoccupied molecular orbitals j and k , with energies E_j and E_k , respectively.

In equation (3) $\sum_{\mu < \nu}^A$ is a summation over all orbitals on the atom containing nucleus A such that $\mu \neq \nu$ and the sum \sum_B is over all nuclei in the molecule including A . The matrix elements involving the angular momentum operator, L , are one centre in character and are given in units of \hbar/i .

Experimental data taken on solids and liquid crystals can provide information on the diagonal components of the screening tensor and its anisotropy, $\Delta\sigma$. For linear and symmetric top molecules

$$\Delta\sigma = \sigma_{\parallel} - \sigma_{\perp} \quad (5)$$

where σ_{\parallel} refers to the screening along the major molecular axis and σ_{\perp} is that in the direction perpendicular to it. The average value of σ is then given by

$$\sigma = \frac{1}{3}(\sigma_{\parallel} + 2\sigma_{\perp}) \quad (6)$$

For less symmetrical molecules $\Delta\sigma$ may be defined as:

$$\Delta\sigma = \sigma_{\alpha\alpha} - \frac{1}{2}(\sigma_{\beta\beta} + \sigma_{\gamma\gamma}) \quad (7)$$

where the σ_{ii} 's are the three diagonal tensor components taken in accordance with the convention $\sigma_{\alpha\alpha} \geq \sigma_{\beta\beta} \geq \sigma_{\gamma\gamma}$ in this case the average value is obtained from:

$$\sigma = \frac{1}{3}(\sigma_{\alpha\alpha} + \sigma_{\beta\beta} + \sigma_{\gamma\gamma}) \quad (8)$$

The calculation of σ and $\Delta\sigma$ can provide a more demanding examination of a theoretical model than estimating chemical shifts since in the latter case a cancellation of errors, arising during the calculation of σ for two different nuclei, may occur. Some calculated and experimental values of σ and $\Delta\sigma$ are compared in Table VI.

In high resolution NMR experiments in relatively non-viscous liquids the observed chemical shifts relate to differences between values of the scalar σ , for different nuclei, as defined by equations (6) and (8).

By considering only the nitrogen 2s and 2p atomic orbitals the expressions, for nucleus A, of the rotationally averaged local terms in equations (2) and (3) become:

$$\sigma_A^d = \frac{\mu_0}{4\pi} \frac{e^2}{3m} \sum_{\mu} \rho_{\mu\mu} \langle \mu | r_{\mu A}^{-1} | \mu \rangle \quad (9)$$

and

$$\begin{aligned} \sigma_A^p = & -\frac{\mu_0}{4\pi} \frac{2\hbar^2 e^2}{3m^2} \langle r^{-3} \rangle_{2p} \sum_j^{\text{occ}} \sum_k^{\text{unocc}} (E_k - E_j)^{-1} \\ & (C_{j,X_A} C_{k,Y_A} - C_{j,Y_A} C_{k,X_A}) \sum_B (C_{j,X_B} C_{k,Y_B} - C_{j,Y_B} C_{k,X_B}) \\ & + (C_{j,Y_A} C_{k,Z_A} - C_{j,Z_A} C_{k,Y_A}) \sum_B (C_{j,Y_B} C_{k,Z_B} - C_{j,Z_B} C_{k,Y_B}) \\ & + (C_{j,Z_A} C_{k,X_A} - C_{j,X_A} C_{k,Z_A}) \sum_B (C_{j,Z_B} C_{k,X_B} - C_{j,X_B} C_{k,Z_B}) \quad (10) \end{aligned}$$

where C_{j,X_A} is the LCAO coefficient of the P_x orbital on atom A in molecular orbital j , etc., $r_{\mu A}$ represents the separation of the electrons in orbital μ from nucleus A and $\langle r^{-3} \rangle_{2p}$ is then mean inverse cube radius for the 2p orbitals on atom A. This is usually evaluated by means of the relationship,

$$\langle r^{-3} \rangle_{2p} = \frac{1}{3} \left(\frac{Z_{2p}}{2a_0} \right)^3 \quad (11)$$

where Z_{2p} is the effective nuclear charge for the $2p$ atomic orbital and a_0 is the Bohr radius. The value of Z_{2p} may be obtained from Slater's rules (25) or by Burns' method. (26)

The matrix element in equation (9) is similarly obtained from

$$\langle \mu | r_{\mu A}^{-1} | \mu \rangle = \frac{Z_{\mu}}{n^2 a_0} \quad (12)$$

where n is the principal quantum number of the atomic orbital μ .

The non-local contributions in equation (1) may be evaluated by assuming that the induced moment in the electrons on atom B can be replaced by a point dipole. (22, 27) The effect of this dipole on the screening of nucleus A is found to be negligible for first row atoms, although it can be significant for protons. (8, 28)

Thus, equations (9) and (10) are used to obtain nuclear screening data within semi-empirical applications of Pople's theory. In this theory σ^d for nitrogen, although often numerically larger than σ^p , is approximately constant for series of molecules and ions. (29, 38, 39) The nitrogen chemical shifts occurring in these series arise from changes in σ^p . The data reported in Table II were obtained from INDO molecular orbital calculations. (29) They show that σ^d is constant to within about 3% and that the non-local contribution is negligible when either Slater's or Burns' rules are employed.

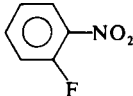
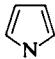
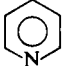

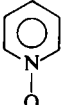
It is noteworthy that among the species included in Table II are some methylamines and their protonated forms and that σ^d does not vary significantly between them. This is in contrast to the conclusions reached following valence bond calculations within Ramsey's approach. (30) It has been claimed that the protonation shifts are primary due to changes in the diamagnetic component of the screening constant while shifts within each series of methylamines are due to changes in the paramagnetic term. (30) Apart from any shortcomings inherent in the valence bond method, this claim underlines the difficulties associated with a comparison of results obtained from gauge dependent calculations on the one hand and gauge independent ones, as presented in Table II, on the other.

Reports of significant changes in the local diamagnetic term have been made, (31, 32) for nitrogen nuclei based upon equation (13) which is adapted from Flygare's work. (16)

$$\sigma_A^d = \sigma_A^d(\text{free atom}) + \frac{\mu_0 e^2}{4\pi 3m} \sum_{B \neq A} \frac{Z_B}{r_{AB}} \quad (13)$$

where r_{AB} is the separation between the nucleus of interest, A , and its neighbour, B , which has a charge Z_B . It has been suggested that σ_A^d is a

TABLE II
Some calculated values of σ^d for nitrogen in ppm

Molecule	Pople's method with Slater's rules		Pople's method with Burns' rules		Flygare's method	
	σ_{loc}^d	σ_{nonloc}^d	σ_{loc}^d	σ_{nonloc}^d	σ_{loc}^d	σ_{nonloc}^d
NH ₃	326.69	0.00	315.85	0.00	326.77	25.43
CH ₃ NH ₂	326.45	-0.01	315.74	-0.01	326.57	53.98
CH ₃ CH ₂ NH ₂	326.52	-0.01	315.79	-0.01	326.63	54.27
(CH ₃) ₂ NH	326.25	-0.01	315.70	-0.01	326.41	83.42
(CH ₃) ₃ N	326.08	-0.02	315.63	-0.02	326.28	111.55
NH ₄ ⁺	324.42	0.00	314.50	0.00	325.02	27.22
CH ₃ NH ₃ ⁺	323.76	-0.09	314.10	-0.09	324.35	59.76
(CH ₃) ₂ NH ₂ ⁺	323.39	-0.01	313.88	-0.06	323.98	90.78
(CH ₃) ₃ NH ⁺	323.17	-0.13	313.77	-0.13	323.75	121.22
(CH ₃) ₄ N ⁺	322.81	-0.17	313.64	-0.17	323.39	157.63
(NH ₂) ₂ CO	326.76	-0.01	316.31	0.01	326.82	54.39
(CH ₃) ₂ NCON(CH ₃) ₂	326.74	0.00	316.47	0.00	326.80	112.82
(CH ₃) ₂ N ¹ -C=N ² CH ₃	326.46	-0.01	316.25	-0.01	326.58	111.41
 OCH ₃ N ²	327.37	0.00	316.19	0.00	327.31	73.81
CH ₃ NO ₂	318.41	-0.38	309.77	0.38	319.27	164.86
CH ₃ CH ₂ CH ₂ CH ₂ NO ₂	318.46	-0.40	309.80	-0.40	319.31	165.05
	318.35	-0.42	309.74	-0.42	319.21	167.41
CH ₃ CN	326.15	-0.02	315.04	-0.02	326.34	47.49
CH ₃ NC	323.89	0.26	314.09	0.26	324.49	87.35
CN ⁻	327.99	0.31	316.37	0.31	327.83	53.87
NO ₂ ⁺	315.37	-0.51	307.24	-0.51	316.68	128.87
NO ₂ ⁺	323.16	-0.34	312.89	-0.34	323.74	130.15
NO ₃ ⁺	316.36	-0.52	308.11	-0.52	317.50	194.58
	324.62	-0.17	314.80	-0.17	325.17	91.34
 H						
	326.20	-0.05	315.43	-0.05	326.38	79.24
	323.99	-0.03	314.26	-0.03	324.59	86.25
 H						
	321.62	-0.45	312.33	-0.45	322.23	139.09

“local” term when the summation in equation (13) is restricted to those atoms directly bonded to atom A . (31, 32) The actual charge density on atom A may be included in the calculation by means of equation (14).

$$\sigma_A^d (\text{atom in molecule}) = \sigma_A^d (\text{free atom}) \pm \Delta p_A \Delta \sigma_A^d \quad (14)$$

where Δp_A is the difference between the atomic number and the gross atomic population, which for the data given in Table II has been obtained from INDO calculations, $\Delta \sigma_A^d$ is the difference between the value of σ_A^d for a free atom and the corresponding positive or negative ion as appropriate. (33)

To account for the actual electronic populations of the bonded atoms the INDO gross atomic populations, P_B , rather than Z_B are used. Hence equation (13) becomes,

$$\sigma_A^d = \sigma_A^d (\text{free atom}) \pm \Delta p_A \Delta \sigma_A^d + \frac{\mu_0}{4\pi} \frac{e^2}{3m} \sum_{\substack{\text{Bonded} \\ B \text{ only}}} \frac{P_B}{r_{AB}} \quad (15)$$

The final two columns of data in Table II were calculated from equation (15).

It is clear from Table II that the large apparent changes in σ_N^d are due to the “non-local” final term in equation (15), while the first two “local” terms remain reasonably constant for the molecules reported. Changes in the final term predict a considerable increase in σ_A^d as the number of bonded atoms and electrons in the molecule increases. For example it implies an increase in the nitrogen screening constant by about 29 ppm as each H in NH_3 is replaced by CH_3 , whereas the experimentally obtained screening decreases by about 6 ppm.

Consequently values of σ_A^d obtained by the restricted summation of equation (15) are not those of a “local” term as defined in Pople’s gauge—dependent molecular orbital theory, (18, 19) but are comparable to those found for σ^d in Ramsey’s procedure. Thus values of σ_A^d calculated by the methods of Pople and Flygare are not comparable due to the significant and variable “non-local” contribution appearing in the latter. Attempts (32, 34–37) to discuss the variation in nitrogen screening for a series of molecules by obtaining σ_N^d from Flygare’s approach and σ_N^p from Pople’s method appear to be meaningless.

Equation (10) is not often used in calculations of the paramagnetic contribution to the screening within Pople’s theory. However, INDO calculations in conjunction with equation (10) have recently been reported for some ureas and related molecules, (38), some small nitrogen containing molecules and ions (39) and some five- and six-membered ring heterocycles. (40) In these calculations the excitation energies, $E_k - E_j$, are taken to be those of excited singlet states since these are

mixed with the ground state by an external magnetic field. Consequently

$$E_k - E_j = \varepsilon_k - \varepsilon_j - J_{jk} + 2K_{jk} \quad (16)$$

where ε_k and ε_j are eigenvalues of the unperturbed molecule, J_{jk} and K_{jk} are respectively the Coulomb and exchange integrals, defined by:

$$J_{jk} = \langle j, k | r_{12}^{-1} | j, k \rangle \quad (17)$$

and

$$K_{jk} = \langle j, k | r_{12}^{-1} | k, j \rangle \quad (18)$$

The results obtained for urea and some of its analogues are presented in Table III. (38) Comparison of the experimental and calculated nitrogen screening data is shown in Fig. 1 where the least squares line corresponds to a standard deviation of 7.05 ppm with a correlation coefficient of 0.9368. This probably reflects the relative insensitivity of the INDO eigenfunctions to changes in the nitrogen environment.

TABLE III

Comparison of theoretical and experimental nitrogen screenings for urea and some of its analogues in ppm (38)

Compound	Nitrogen nucleus	$\sigma^{\text{exp } a}$	σ^d	σ^p	σ^{total}	$\sigma^{\text{total}} - \sigma^{\text{exp}}$
$\text{NH}_2\text{-}\overset{\text{O}}{\underset{\parallel}{\text{C}}}\text{-NH}_2$	$-\text{NH}_2$	+302.8	327.7	-205.1	122.6	-180.2
$\text{CH}_3\text{NH-}\overset{\text{O}}{\underset{\parallel}{\text{C}}}\text{-NH}_2$	$-\text{NH}_2$		327.6	-198.8	128.8	
	$-\text{NHCH}_3$	+310.7	327.3	-194.6	132.7	-178.0
$\text{CH}_3\text{NH-}\overset{\text{O}}{\underset{\parallel}{\text{C}}}\text{-NHCH}_3$	$-\text{NHCH}_3$	+297.4	327.3	-190.8	136.5	-160.9
$(\text{CH}_3)_3\text{N-}\overset{\text{O}}{\underset{\parallel}{\text{C}}}\text{-N(CH}_3)_2$	$-\text{N(CH}_3)_2$	+320.0	326.7	-184.5	142.2	-177.8
$(\text{CH}_3)_2\text{N-}\overset{\text{OCH}_3}{\underset{\parallel}{\text{C}}}\text{=NH}$	$-\text{N(CH}_3)_2$	+320.0	326.5	-191.1	-35.4	-184.6
	$=\text{NH}$	+238.0	327.7	-250.6	77.1	-160.9
$(\text{CH}_3)_2\text{N-}\overset{\text{NH}}{\underset{\parallel}{\text{C}}}\text{-N(CH}_3)_2$	$-\text{N(CH}_3)_2$	+333.4	327.0	-187.0	140.0	-193.4
	$=\text{NH}$	+207.8	327.4	-229.9	97.5	-110.3
$(\text{CH}_3)_2\text{N-}\overset{\text{NH}}{\underset{\parallel}{\text{C}}}\text{-N(CH}_3)_2$	$-\text{N(CH}_3)_2$	+334.0	326.7	-188.5	138.2	-195.8
	$=\text{NCH}_3$	+187.0	328.5	-266.8	61.7	-125.3

^a These data refer to nitrogen screening expressed with respect to neat CH_3NO_2 on the screening constant scale, see Section III.

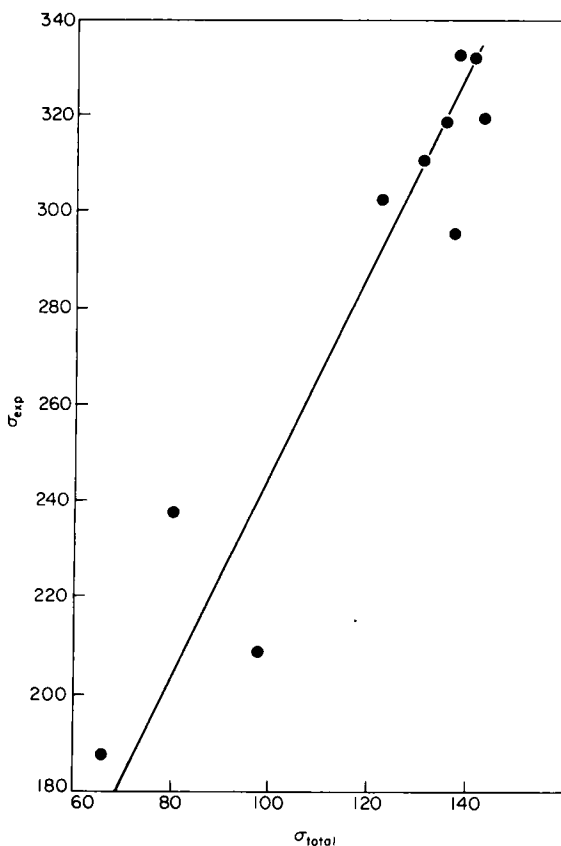


FIG. 1. Plot of experimental nitrogen screening constants, with respect to CH_3NO_2 , of urea and some of its analogues against calculated values of the nitrogen screening constant in these molecules. (38)

Theoretical and molecular beam investigations suggest that the absolute screening of N_2 is about -100 ppm. (41, 42) The difference between the screening in liquid N_2 and CH_3NO_2 is anticipated to be about -70 ppm, (43, 44), hence on the absolute scale CH_3NO_2 should appear at about -170 ppm. This value may be in error by up to ± 30 ppm since CH_3NO_2 has not been measured accurately relative to gaseous N_2 (Section III).

The differences between the total calculated value of σ for the urea analogues and their nitrogen chemical shifts, with respect to CH_3NO_2 , are presented in the final column of Table III. The mean of these differences is about -160 ppm which corresponds to the absolute value of σ for CH_3NO_2 , in reasonable agreement with expectation. (38)

Analysis of the various contributions to σ^p for urea and its analogues reveals that the major one arises from the lowest energy $n \rightarrow \pi^*$ transition. The lower energy of this transition for the isoamide-type, as opposed to the amide-type, of nitrogen atoms results in their relative deshielding.

The energy of this transition is found to be very sensitive to changes occurring in other parts of the molecule. (40) Thus as $-\text{OCH}_3$ is replaced by $-\text{N}(\text{CH}_3)_2$ the decrease in electronegativity of the substituent results in a lower $n \rightarrow \pi^*$ transition energy for the isoamide-type of nitrogens with a concomitant decrease in their screening. A similar decrease in screening is observed when the $-\text{SCH}_3$ group is introduced.

Similar data from some CNDO/S parameterized calculations on some small nitrogen containing molecules and ions and some heterocycles are presented in Tables IV and V. (39, 40) As shown in

TABLE IV

Some calculated contributions to the paramagnetic component of the nitrogen screening tensor in ppm (39)

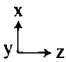
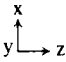
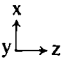
Molecule	Component	Transition	Calculated transition energy (eV)	Contribution to σ^p
$\text{N} \equiv \text{N}$ 	X	$1\sigma \rightarrow 6\pi^*$	31.783	-20.844
		$3\sigma \rightarrow 6\pi^*$	5.854	-498.581
		$4\pi \rightarrow 8\sigma^*$	17.565	-138.702
	Y	This component is identical to the X component		
	Z	This component makes no contribution to σ^p		
$\text{H}-\text{C} \equiv \text{N}$ 	X	$1\sigma \rightarrow 6\pi^*$	27.937	-15.168
		$2\sigma \rightarrow 6\pi^*$	16.388	12.731
		$3\sigma \rightarrow 6\pi^*$	7.145	-383.589
		$5\pi \rightarrow 8\sigma^*$	9.870	-6.738
		$6\pi \rightarrow 9\sigma^*$	15.728	-133.981
	Y	This component is identical to the X component		
$\text{CH}_3-\text{C} \equiv \text{N}$ 	X	$1\sigma \rightarrow 10\pi^*$	30.695	-5.25
		$4\pi \rightarrow 12\sigma^*$	17.06	5.771
		$4\pi \rightarrow 15\sigma^*$	24.808	-7.665
		$6\sigma \rightarrow 9\pi^*$	7.25	-67.595
		$6\sigma \rightarrow 10\pi^*$	7.25	-273.105
	Z	This component makes no contribution to σ^p		

TABLE IV—*cont.*

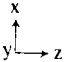
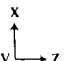
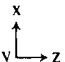
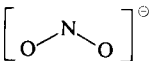
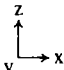
Molecule	Component	Transition	Calculated transition energy (eV)	Contribution to σ^p
CH ₃ C≡N 	X	$7\pi \rightarrow 12\sigma^*$	11.502	-5.193
		$7\pi \rightarrow 15\sigma^*$	15.936	-20.738
		$8\pi \rightarrow 12\sigma^*$	11.502	-22.029
		$8\pi \rightarrow 15\sigma^*$	15.936	-87.972
	Y	This component is identical to the X component		
	Z	This component makes no contribution to σ^p		
CH ₃ NC 	X	$2\sigma \rightarrow 9\pi^*$	25.642	-20.276
		$2\sigma \rightarrow 10\pi^*$	25.642	-5.333
		$3\sigma \rightarrow 9\pi^*$	15.114	-15.473
		$3\sigma \rightarrow 13\pi^*$	20.139	-5.280
		$5\pi \rightarrow 14\sigma^*$	17.857	-12.477
		$5\pi \rightarrow 15\sigma^*$	24.745	-33.165
		$6\sigma \rightarrow 9\pi^*$	6.206	-123.031
		$6\sigma \rightarrow 10\pi^*$	6.206	-32.357
	Y	$7\pi \rightarrow 15\sigma^*$	15.969	-22.445
		$8\pi \rightarrow 14\sigma^*$	11.371	15.771
		$8\pi \rightarrow 15\sigma^*$	15.969	-121.954
		This compound is identical to the X component		
ONO [⊖] 	X	$2\sigma \rightarrow 10\pi^*$	35.674	-63.762
		$5\pi \rightarrow 12\sigma^*$	29.162	-137.855
		$6\sigma \rightarrow 10\pi^*$	10.406	-168.747
	Y	This component is identical to the X component		
	Z	This component makes no contribution to σ^p		
 	X	$1\sigma \rightarrow 10\pi^*$	40.159	-8.723
		$4\sigma \rightarrow 10\pi^*$	10.075	-84.035
		$6\pi \rightarrow 11\sigma^*$	21.138	-61.914
		$8\sigma \rightarrow 10\pi^*$	2.732	-905.774
	Y	$2\sigma \rightarrow 11\sigma^*$	43.676	-16.975
		$3\sigma \rightarrow 12\sigma^*$	29.26	-21.442
		$4\sigma \rightarrow 12\sigma^*$	25.594	-88.645
		$5\sigma \rightarrow 11\sigma^*$	23.958	-23.326
		$7\sigma \rightarrow 11\sigma^*$	16.911	14.985
		$8\sigma \rightarrow 12\sigma^*$	18.342	18.400
		$2\sigma \rightarrow 10\pi^*$	29.318	-53.043
		$5\sigma \rightarrow 10\pi^*$	10.24	-140.027
	Z	$6\pi \rightarrow 12\sigma^*$	23.322	-121.814
		$7\sigma \rightarrow 10\pi^*$	3.69	-111.342

TABLE V

Some calculated contributions to the paramagnetic component of the nitrogen screening tensor for some N-heterocycles in ppm (40)

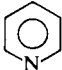
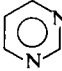
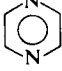
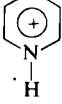
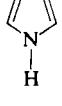
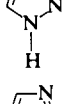
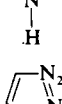
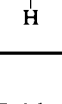
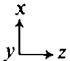
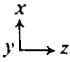
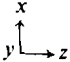
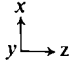
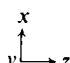
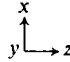
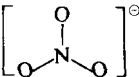
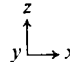
Molecule	Transition					Total
	$\sigma \rightarrow \sigma^*$	$n \rightarrow \sigma^*$	$\sigma \rightarrow \pi^*$	$n \rightarrow \pi^*$	$\pi \rightarrow \sigma^*$	
	-38.22	-26.40	-93.30	-129.75	-90.47	-378.14
	-34.14	-30.23	-75.25	-132.66	-92.28	-364.57
	-25.18	-39.08	-72.18	-174.11	-86.16	-396.71
	-52.51		-97.27		-122.06	-271.86
	-51.30		-80.85		-126.72	-262.38
	N -26.03 NH -49.80	-39.86 -0.75	-50.91 -64.97	-148.23 -24.7	-115.69 -134.31	-380.7 -274.5
	N -28.50 NH -51.51	-36.97 -2.11	-73.12 -79.36	-152.54 -4.02	-101.24 -129.57	-392.45 -266.56
	N ₁ -27.96 N ₂ -30.70 NH -47.41	-34.62 -32.83 -4.21	-46.42 -42.76 -64.76	-183.17 -215.14 -41.91	-117.51 -101.07 -132.23	-409.69 -422.50 -290.52

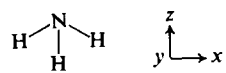
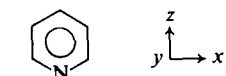
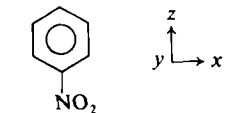
Table IV the largest contributor to σ^p , for the linear species N_2 , HCN, CH_3CN , CH_3NC and NO_2^+ , is the lowest energy $\sigma \rightarrow \pi^*$ transition. However, for CH_3NC and NO_2^+ there are also significant contributions from higher energy $\pi \rightarrow \sigma^*$ transitions.

In the case of the bent ion, NO_2^- , the X component of σ^p is dominated by the lowest energy $\sigma \rightarrow \pi^*$ transition. The other in-plane component,

TABLE VI

Comparison of some experimental ^{14}N screening anisotropies and values calculated from CNDO/S eigenfunctions (39)

Molecule	Axis	Calculated (ppm) ^a				Experimental (ppm)				
		σ_{xx}^p	σ_{yy}^p	σ_{zz}^p	$\Delta\sigma$	σ^b	$\Delta\sigma$	Ref.	σ^b	Ref.
$\text{N}\equiv\text{N}$		-658.13	-658.13	0.0	658.13	-124.0	657 ± 20	(42)	-100 ± 20	(42)
HCN		-525.74	-525.74	0.0	525.74	-30.34	577 ± 20	(52)	-37 ± 20 -30	(52) (57)
$\text{N}-\text{N}^*-\text{O}$		-392.88	-383.95	-21.02	367.4	43.77	512 ± 10	(53)	5	(57)
$\text{N}^*-\text{N}-\text{O}$		-445.56	-173.17	-18.78	440.6	8.28	369 ± 15	(53)	89	(57)
CH_3CN		-494.19	-494.19	-22.53	471.66	-16.47	452 ± 10	(54)	-16 ± 10	(52)
CH_3NC		-384.86	-384.86	18.34	403.20	68.45	360 ± 73	(56)	130 ± 20 85	(56) (58)
		-456.49	-98.76	-456.45	357.73	-16.91	210 ± 5	(55)	115 ± 20	(55)

	-248.71	-248.71	-183.58	65.13	99.51	39 ± 10	(17)	260 ± 20	(17)
	-542.43	-193.87	-395.11	276.4	-49.52	672	(59)		
	-458.88	-112.18	-359.71	297.12	13.10	398	(59)		

^a For those molecules which do not possess a two fold or higher axis of symmetry the tensor is diagonalized by a similarity transformation.

^b These are averaged values for the total nuclear screening as defined by equations (6) and (8).

Z, has large donations from two low energy $\sigma \rightarrow \pi^*$ transitions together with a smaller amount from a higher energy $\pi \rightarrow \sigma^*$ transition. The out-of-plane component is composed of a number of $\sigma \rightarrow \sigma^*$ contributions.

The major contribution to σ^p for the pyridine-type nitrogen atoms included in Table V arises from the $n \rightarrow \pi^*$ transitions while the $\pi \rightarrow \sigma^*$ and $\sigma \rightarrow \pi^*$ transitions also make significant contributions. For the pyrrole-type nitrogen atoms the effective removal of the lone pair leaves the $\pi \rightarrow \sigma^*$ and $\sigma \rightarrow \pi^*$ transitions as the dominant ones. In all cases the higher energy $\sigma \rightarrow \sigma^*$ and $n \rightarrow \sigma^*$ transitions provide only minor contributions.

Relatively few experimental values of the anisotropy, $\Delta\sigma$, of the nitrogen screening tensor have been reported. The available data are compared with the results of some CNDO/S calculations in Table VI.

On account of the approximations inherent in the CNDO/S procedure significant contributions from σ^d to $\Delta\sigma$ are not expected. Consequently only the diagonal components of σ^p are included in the estimates of $\Delta\sigma$ obtained from equations (5) and (7) and presented in Table VI. (39)

In most cases the agreement between the calculated and experimental anisotropies is satisfactory. For N_2O the agreement would be improved if the assignments for the two nitrogen nuclei were reversed.

Table VI also reveals that in general the agreement between the calculated and measured values of the absolute nitrogen screening is reasonable. Nitrate ion and ammonia are notable exceptions to this, solid state interactions and hydrogen-bonding could be, at least, partially, responsible for these discrepancies (Section III). In most cases the calculated values of $\Delta\sigma$ and σ compare favourably with those obtained from *ab initio* calculations. (39)

Comparison of the observed and calculated nitrogen chemical shifts, with respect to nitrate ion, for the species reported in Table VI requires a least squares line with a correlation coefficient of 0.91 and a standard deviation of 50 ppm. (39) The calculated nitrogen chemical shifts are found to be systematically to low frequency of the observed ones. This is a consequence of the calculated value of σ for nitrate being about 100 ppm greater than the experimental result. This difference may reflect interactions involving the nitrate ion in solution and suggests that it is not the best choice of standard for nitrogen chemical shift measurements as discussed in Section III.

Equation (10) is often simplified by replacing the excitation energies by a mean value, ΔE , to give the Average Excitation Energy (AEE) approximation. Since overlap is neglected in the semi-empirical

molecular orbitals used, it follows that,

$$\sum_j^{\text{occ}} C_{j\mu} C_{j\lambda} + \sum_k^{\text{unocc}} C_{k\mu} C_{k\lambda} = \delta_{\mu\lambda} \quad (19)$$

By incorporating equation (19) and the AEE approximation, equation (10) becomes,

$$\sigma_A^p = -\frac{\mu_0}{4\pi} \frac{\hbar^2 e^2}{2m^2} \frac{1}{\Delta E} \langle r^{-3} \rangle_{2p} \sum_B Q_{AB} \quad (20)$$

where the summation over B includes atom A and,

$$\begin{aligned} Q_{AB} = & \frac{4}{3} \delta_{AB} (P_{X_A X_B} + P_{Y_A Y_B} P_{Z_A Z_B}) \\ & - \frac{2}{3} (P_{X_A X_B} P_{Y_A Y_B} + P_{X_A X_B} P_{Z_A Z_B} + P_{Y_A Y_B} P_{Z_A Z_B}) \\ & + \frac{2}{3} (P_{X_A Y_B} P_{X_B Y_A} + P_{X_A Z_B} P_{X_B Z_A} + P_{Y_A Z_B} P_{Y_B Z_A}) \end{aligned} \quad (21)$$

The P 's are defined by equation (4).

Equation (21) represents the imbalance of the populations of the orbitals around nucleus A .

By combining equations (11) and (20), σ_A^p becomes,

$$\sigma_A^p = -\frac{30 \cdot 1885}{\Delta E} Z_{2p}^3 \sum_B Q_{AB} \quad (22)$$

Equation (22) has been used in several calculations of nitrogen screening constants, including those based upon $P-P-P$ π electron data for some azine-N-oxides, (45) π electron calculations together with σ bond polarization estimates for some mono-substituted pyridines (46) and INDO calculations on some simple azines. (47). INDO charge densities have also been reported for some methylanilines. (48) In general this method is successful in accounting for gross chemical shift trends in series of closely related molecules as discussed in Section V. However, its utility is limited by the necessity of choosing a value for ΔE which cannot be decided by *a priori* arguments since it is not directly related to any of the observed electronic transitions in the molecules concerned.

An analysis of the various contributions to σ^p given by equation (20) shows that, for nitrogen nuclei in series of closely related molecules, significant changes occur in both the $\langle r^{-3} \rangle_{2p}$ and $\sum Q_{AB}$ terms in passing along the series. In general changes in the latter term are larger than in the former. Equations (5) and (15) show that both of these terms depend upon the nitrogen charge density. The greatest dependence occurring when the nitrogen has a lone pair of electrons and its sigma bonds are

significantly polarized. This provides a rationale for the reported dependence of the nitrogen chemical shifts on charge density in some 6-membered heterocycles (1d) methylanilines (48) and pentazole. (51)

Use of equation (22) rather than equation (10) in determining σ^p restricts the understanding of the relationship between nuclear screening and various aspects of molecular electronic structure. An example of this is provided by some AEE calculations on the deshielding of the pyridine nitrogen atom with respect to that in the pyridinium ion. It was claimed that the deshielding arises mainly from a low lying $n \rightarrow \pi^*$ transition together with a substantial contribution from a $\sigma \rightarrow \pi^*$ transition. (49, 50) The CNDO/S data reported in Table V show that the relative pyridine deshielding is due to $n \rightarrow \pi^*$ and $n \rightarrow \sigma^*$ transitions only. The $\sigma \rightarrow \sigma^*$, $\sigma \rightarrow \pi^*$ and $\pi \rightarrow \sigma^*$ transitions all produce shielding contributions for pyridine relative to the pyridinium ion.

In general, it appears that calculations of σ^p based upon equation (10) provide a reasonable insight into the chemically interesting factors which determine nitrogen screening data.

III. CALIBRATION OF SPECTRA

There has been considerable confusion as far as the calibration of nitrogen NMR spectra is concerned. This situation has not improved very much since the appearance of a comprehensive discussion on the subject, (1d) possibly it has grown worse. Modern spectroscopic techniques, in both ^{14}N and ^{15}N NMR, allow the determination of the positions of nitrogen resonance signals with a precision of the order of 0.1 ppm, but this does not mean that the accuracy of chemical shift determinations is of the same order. Very often careless use of reference compounds may make a precision of 0.1 ppm in signal position quite meaningless from the point of view of differences in actual screening constants.

First of all, it is necessary to consider the practical limits of accuracy in determining nitrogen chemical shifts. It is well known that an accurate estimate of sample temperature within a NMR probe poses a serious problem which is amplified, particularly in nitrogen NMR spectroscopy where large sample tubes are usually used, by the uncertainty of temperature gradients within the sample. It seems likely that an uncertainty of at least $\pm 2^\circ\text{C}$, and more probably $\pm 4^\circ\text{C}$, is something which can hardly be avoided, even in modern NMR spectrometers. The temperature dependence of nitrogen chemical shifts has been measured for some simple molecules (60, see also ref. 1d, p. 253), and the temperature coefficient found to be about 0.1 ppm per 5°C with the exception of NH_3 (liquid) where it is twice as large. Since the uncertainty

of bulk magnetic susceptibility effects in the technique of external referencing may be easily of the order of a few tenths of a ppm, it seems that ± 0.1 ppm constitute the limits of accuracy for determining nitrogen chemical shifts if bulk susceptibility corrections are applied, and at least ± 0.2 otherwise. It is shown later that the use of internal reference compounds, i.e., those dissolved in the sample, cannot provide a basis for the precise measurement of nitrogen chemical shifts, since no internal standard is inert to medium effects.

Theoretically, any external standard may be used, provided that it is clearly defined, and that precise data are available which make possible the accurate recalculation of nitrogen chemical shifts referred to other standards. Practically, there are limitations concerning the concentration of nitrogen nuclei in the reference compound, the sensitivity of its nitrogen chemical shift to concentration and solvent effects in the case of solutions, effects due to possible impurities, nuclear Overhauser effects on the resonance upon proton decoupling etc.

It seems likely that nitromethane, CH_3NO_2 , as a neat liquid will constitute a good external standard (61) for various reasons. It is a not-too-volatile, non-hygroscopic liquid with a high nitrogen concentration (*ca.* 18 M), surpassed in the latter by only a few compounds such as CH_3CN , CH_3NH_2 and NH_3 , all of which are hygroscopic and reveal a considerable effect on their nitrogen chemical shifts when contaminated by water. The ^{14}N signal of CH_3NO_2 is rather narrow which makes it suitable for ^{14}N NMR spectroscopy, whilst that of $\text{CH}_3^{15}\text{NO}_2$ shows little change in total intensity upon proton decoupling. (62) $\text{CH}_3^{15}\text{NO}_2$ may also be conveniently used in double-resonance determinations of nitrogen chemical shifts from proton spectra. A great deal of data (up to 1972) on nitrogen chemical shifts has already been recalculated to the internal CH_3NO_2 , (1d) and since the accuracy of the early measurements was usually not better than ± 2 ppm, they may be directly compared with those referred to external, neat CH_3NO_2 , either without any or with only minor corrections.

We shall use henceforth the nitrogen signal of *neat nitromethane external standard* as a reference point on the scale of nitrogen chemical shifts. Since chemical shifts expressed on a dimensionless scale represent differences in nuclear screening constants, we shall adopt the so-called *screening-constant scale* (1d) where shifts to (higher fields) *lower frequencies are taken as positive*.* Thus a positive chemical shift corresponds to a positive change in the screening constant.

* Editorial note. Although this is opposite to the frequency scale for chemical shifts it is consistent with the data presented in ref. 1 to which this review makes frequent reference. See also ref. 3 and references therein.

TABLE VII

Precise values of differences in nitrogen screening constants for selected molecules and ions^a in ppm, referred to external neat nitromethane

Compound	Solvent or state	Nitrogen screening constant
CH ₃ NO ₂	neat liquid, 18.42 M	0.0000 (arbitrary)
	0.30 M in DMSO	-2.01 ± 0.12
	0.30 M in H ₂ O	-1.98 ± 0.12
	0.30 M in D ₂ O	-1.94 ± 0.13
	0.30 M in 11.73 HCl _{aq}	-1.95 ± 0.14
	0.30 M in DMF	-0.69 ± 0.13
	0.30 M in MeCN	+0.20 ± 0.13
	0.30 M in Me ₂ CO	+0.77 ± 0.10
	0.30 M in dioxane	+1.82 ± 0.13
	0.30 M in MeOH	+2.01 ± 0.13
	0.30 M in EtOH	+2.70 ± 0.12
	0.30 M in CH ₂ Cl ₂	+3.21 ± 0.13
	0.30 M in CH ₂ Br ₂	+3.41 ± 0.12
	0.30 M in CHCl ₃	+3.79 ± 0.13
	0.30 M in Et ₂ O	+3.91 ± 0.13
	0.30 M in benzene	+4.38 ± 0.11
	0.30 M in CCl ₄	+7.10 ± 0.11
C(NO ₂) ₄	neat liquid, 8.31 M	+46.59 ± 0.09
NO ₃ [⊖]	K [⊕] , 0.30 M in H ₂ O	+3.55 ± 0.12
	Na [⊕] , 0.30 M in H ₂ O	+3.53 ± 0.12
	Na [⊕] , 7.93 M in H ₂ O (satd.)	+3.70 ± 0.12
	NH ₄ [⊕] , 12.30 M in H ₂ O (satd.)	+3.98 ± 0.12
	NH ₄ [⊕] , 5.00 M in 2.00 M HNO ₃	+4.64 ± 0.12
	NH ₄ [⊕] , 8.00 M in 2.00 M HCl	+4.93 ± 0.11
	NH ₄ [⊕] , 5.00 M in 2.00 M HCl	+5.23 ± 0.11
	NH ₄ [⊕] , 4.00 M in 2.00 M HNO ₃	+5.55 ± 0.11
	NH ₄ [⊕] , 4.50 M in 3.00 M HCl	+6.30 ± 0.10
HNO ₃	1.00 M in H ₂ O	+4.43 ± 0.11
	7.00 M in H ₂ O	+12.59 ± 0.12
	10.00 M in H ₂ O	+18.23 ± 0.13
	15.71 M in H ₂ O (70.0% w/w)	+31.31 ± 0.08
NH ₄ [⊕]	Cl [⊖] , 1.00 M in 10.00 M HCl	+349.92 ± 0.13
	Cl [⊖] , 5.00 M in 2.00 M HCl (supersatd.)	+352.49 ± 0.11
	Cl [⊖] , 5.64 M in H ₂ O (satd.)	+352.89 ± 0.17
	NO ₃ [⊖] , 4.50 M in 3.00 M HCl	+357.10 ± 0.12
	NO ₃ [⊖] , 5.00 M in 2.00 M HCl	+358.01 ± 0.13
	NO ₃ [⊖] , 8.00 M in 2.00 M HCl	+358.03 ± 0.14
	NO ₃ [⊖] , 5.00 M in 2.00 M HNO ₃	+358.96 ± 0.17

TABLE VII—*cont.*

Compound	Solvent or state	Nitrogen screening constant
	NO_2^- , 4.00 M in 2.00 M HNO_3	$+359.06 \pm 0.15$
	NO_2^- , 12.30 M in H_2O (satd.)	$+359.55 \pm 0.17$
Me_4N^+	Cl^- , 6.03 M in H_2O (satd.)	$+336.69 \pm 0.09$
	I^- , 0.30 M in H_2O	$+337.31 \pm 0.13$
	Cl^- , 0.30 M in H_2O	$+337.67 \pm 0.11$
Et_4N^+	Cl^- , 4.58 M in H_2O (satd.)	$+315.84 \pm 0.09$
	Cl^- , 0.30 M in H_2O	$+316.29 \pm 0.13$
HCONMe_2	neat liquid, 12.92 M	$+277.00 \pm 0.09$
	0.30 M in H_2O	$+264.58 \pm 0.31$
NH_3	neat liquid, 34.80 M	$+381.93 \pm 0.14$
NMe_3	neat liquid, 9.8 M	$+368.59 \pm 0.10$
MeNH_2	neat liquid, 43.22 M	$+378.73 \pm 0.15$
MeCN	neat liquid, 18.79 M	$+136.40 \pm 0.10$
	0.30 M in CCl_4	$+127.44 \pm 0.28$
	0.30 M in Me_2CO	$+132.99 \pm 0.13$
	0.30 M in H_2O	$+144.94 \pm 0.26$
PhNO_2	neat liquid, 8.31 M	$+9.56 \pm 0.12$
	0.30 M in CCl_4	$+12.18 \pm 0.18$
$(\text{NCO})^-$	K^+ , 0.30 M in H_2O	$+302.60 \pm 0.14$
	K^+ , 6.21 M in H_2O (satd.)	$+302.91 \pm 0.14$
$(\text{NCS})^-$	K^+ , 9.51 M in H_2O (satd.)	$+170.04 \pm 0.11$
	K^+ , 0.30 M in H_2O	$+174.07 \pm 0.17$
$(\text{NNN})^-$	Na^+ , 0.30 M in H_2O	$+131.51 \pm 0.12$ (centr.)
		$+280.60 \pm 0.12$ (term.)
	Na^+ , 5.13 M in H_2O (satd.)	$+132.16 \pm 0.10$ (centr.)
		$+281.69 \pm 0.12$ (term.)
$(\text{CN})^-$	K^+ , 8.5 M in H_2O (satd.)	$+102.48 \pm 0.09$
	K^+ , 0.30 M in H_2O	$+106.11 \pm 0.12$
NO_2^-	Na^+ , 0.30 M in H_2O	-227.60 ± 0.33
	Na^+ , 7.56 M in H_2O (satd.)	-228.89 ± 0.25
Pyridine	neat liquid, 12.30 M	$+62.01 \pm 0.14$

TABLE VII—*cont.*

Compound	Solvent or state	Nitrogen screening constant
	0.30 M in CCl ₄	+58.01 ± 0.37
	0.30 M in Et ₂ O	+59.20 ± 0.31
	0.30 M in Me ₂ CO	+64.01 ± 0.30
	0.50 M in H ₂ O	+84.38 ± 0.59
Pyridinium ion	Cl [⊖] , 0.50 M in 10.0 M HCl	+178.96 ± 0.09

^a Data from ref. 61; ¹⁴N spectra at 4.3345785 MHz (±0.5 Hz), sample temperature 30 ± 2°C; concentric spherical sample containers are used in order to eliminate bulk susceptibility effects on shifts and signal shape; external standards are used, CH₃NO₂ (neat liquid) and, for signals within ±15 ppm of that of neat CH₃NO₂, tetranitromethane (neat liquid); reported shifts represent values obtained from iterative fitting of theoretical and experimental lineshapes using a differential saturation method, ref. 63, reported errors are standard deviations for the fitting of at least 200 data points, and represent 68% confidence limits; for shifts which are recalculated from values referred to C(NO₂)₄, the error of the shift of C(NO₂)₄ relative to CH₃NO₂ is included.

In order to provide a means for the precise recalculation of nitrogen chemical shifts reported since 1972, it is necessary to have accurate values of the differences in the screening constants between neat CH₃NO₂ and the large number of reference compounds which have so far been used. Table VII shows the results of precise ¹⁴N measurements (61) which have been carried out in concentric spherical sample and reference containers in order to eliminate bulk susceptibility effects on the shifts. Since the technique adopted (61, 63) involves the accumulation of a large number of individually calibrated spectra with the subsequent use of a full-lineshape analysis by the differential saturation method, (63) the resulting random errors comprise those from minor temperature variations, phase drifts, frequency instability, sweep non-linearity, etc. so that systematic errors should be insignificant as compared with random errors.

A systematic error which always appears in the calculation of chemical shifts, relative to an arbitrary standard, results from differences in frequencies or magnetic field intensities at which the reference signals appear. Theoretically, a difference in frequency (or field intensity) between two resonance signals should be divided by that of the signal of a bare nucleus in order to give a true difference in the screening constant. If any other frequency is used, e.g. that of an arbitrary standard, the error (in ppm) depends on the screening constant of the standard and the magnitude of the shift. Since the signal of neat

CH_3NO_2 appears almost in the middle of the range of nitrogen chemical shifts of diamagnetic molecules, (1d) and because there are reasons to believe (explained at the end of this section) that the nitrogen resonance of neat CH_3NO_2 appears at about 130–170 ppm to high frequency of that of a bare nitrogen nucleus, the systematic error is less than 0.1 ppm at the limits of ± 500 ppm from CH_3NO_2 which covers the entire range of nitrogen chemical shifts of diamagnetic molecules.

The data in Table VII show that solvent and concentration effects on nitrogen screening constants are quite considerable from the point of view of an accuracy of the order of 0.1 ppm and that no internal reference is really suitable for precise measurements.

Nitromethane itself is characterized by a range of about 9 ppm due to solvent effects on its signal position. In most commonly used solvents the shift is about +2 to +4 ppm (from neat CH_3NO_2), very close to that of the NO_3^- ion in aqueous solutions of alkali metal nitrates, *ca.* +3.5 ppm (Table VII). Thus the unified chemical shift scale (1d) based on the internal standards, CH_3NO_2 for non-aqueous and NO_3^- for aqueous solutions, which has been used for older data, seems to be justified. This is true at least to the level of accuracy of the early experimental methods, in spite of claims to the contrary (64) which are based on measurements on an aqueous solution of CH_3NO_2 and KNO_3 , where the difference may reach 5.5 ppm (Table VII). The data for CH_3NO_2 (Table VII) may be used for approximate recalculations of nitrogen screening constants measured directly from CH_3NO_2 as internal standard.

The question of intermolecular effects on the shift of CH_3NO_2 has also been discussed in a paper (62) reporting ^{15}N measurements for relatively concentrated (*ca.* 5 M) solutions, without bulk susceptibility corrections, and with the use of $\text{Cr}(\text{acac})_3$, 0.03 M, as a T_1 relaxation reagent for eliminating saturation effects in the pulsed Fourier-transform technique. Since there are inconsistencies both in the relative magnitudes of solvent effects on the CH_3NO_2 shift and in the signs of effects, as compared with the data in Table VII, as well as differences of 1–2 ppm for CH_3CN and $\text{HCON}(\text{CH}_3)_2$ (neat liquids) between the data in ref. 62 and Table VII, it seems that apart from bulk susceptibility effects and those due to high concentrations, in the case of nitromethane solutions, the presence of $\text{Cr}(\text{acac})_3$ may affect the nitrogen chemical shifts. This reagent has been shown (65) to induce shifts as large as 1 ppm in ^{13}C spectra at concentrations of 0.05 M.

The NO_3^- ion in aqueous solutions, used in a large number of papers as an external reference, should be treated with caution. There is only a small concentration dependence of its relative nitrogen screening

constant in KNO_3 or NaNO_3 aqueous solutions (+3.5 to +3.7 ppm, Table VII), but the shift is sensitive to pH and shows considerable changes between that for NaNO_3 (or KNO_3) and acidified NH_4NO_3 solutions (Table VII). If the exact composition of a NH_4NO_3 solution is not reported, the uncertainty of the shift of the standard may amount to several ppm, and statements to the effect that "acidified NH_4NO_3 was used as a standard" may seriously affect the significance of the results.

The use of HNO_3 solution as an external standard has led to much confusion. First of all, the shift is extremely sensitive to HNO_3 concentration (Table VII) and even small errors in the latter may lead to a considerable uncertainty in the former. Secondly, in a number of papers (36, 66–68) *ca.* 10 M HNO_3 was reported as an external standard, whilst its shift relative to saturated aqueous $(\text{CH}_3)_4\text{NCl}$ suggests (36) that the actual concentration was somewhere in the vicinity of 2 M (see Table VII). In one instance (69) "external HNO_3 " was reported as a standard, and this leaves a range of uncertainty of about 40 ppm; the only means of recalculating such results to any common scale is to compare the data reported with other results obtained for the same compounds. In another case, (53) the signal of 7 M HNO_3 is quite erroneously assumed to coincide with that of the NO_3^- ion (Table VII).

The $(\text{CH}_3)_4\text{N}^+$ ion, another popular standard, shows a small but significant dependence of its nitrogen chemical shift on the concentration and on the gegenion involved (Table VII). In some papers (34, 36) 12 M aqueous $(\text{CH}_3)_4\text{NCl}$ has been reported as a standard, but since the solubility of the salt in water even at elevated temperatures is *ca.* 6 M, the standard was probably a saturated solution. Its shift relative to neat CH_3NO_2 (36) (+336.7 ppm) is in very good agreement with that for the saturated solution reported in Table VII.

The NH_4^+ ion has also frequently been used as a standard, but the data in Table VII indicate that its nitrogen chemical shift is critically dependent on the gegenion, the concentration and the presence of mineral acids. If the exact composition of a solution containing NH_4^+ is not specified, the standard is almost worthless since the uncertainty about its shift may reach 10 ppm. It is easy to make a mistake such as that probably made in ref. 70 where the reported standard is saturated aqueous NH_4Cl , but this gives a discrepancy of about 9 ppm with other data (see footnote (a) in Table XII), and the standard was probably saturated aqueous NH_4NO_3 where the NH_4^+ resonance is *ca.* 7 ppm to lower frequencies than that in saturated NH_4Cl (Table VII). One should also be cautious with the difference between the chemical shifts of NO_3^-

and NH_4^+ in solutions of ammonium nitrate which is sometimes used for the calibration of nitrogen NMR spectra. In a saturated solution in water, the difference is 355.58 ± 0.20 ppm (Table VII), which is in good agreement with a value of 355.5 ± 0.5 reported elsewhere, (1f, 64, 71) but it is very dependent on medium effects, e.g., in 4.5 M NH_4NO_3 in 3 M HCl it is only 350.8 ± 0.15 ppm (Table VII). The fact that NH_4Cl and NH_4NO_3 may be, and have been, used in various combinations of concentrations and solution components, each of which is characterized by a distinct value of the shift for NH_4^+ , makes the use of such standards not recommendable.

One of the main purposes of the present review is to bring all the nitrogen shift data published since 1972 onto a common screening constant scale. These are collected in Tables VII–XXXI and the methods of recalculation of the shifts, based mostly on the data from Table VII, are given in footnotes. Table VII may also be used for introducing minor corrections to the older data referred to internal CH_3NO_2 as well as for recalculating those referred directly to other standards (1d).

It may be interesting to look for indications of the position of the resonance of a bare nitrogen nucleus which corresponds to the absolute zero on the screening constant scale of nitrogen chemical shifts. There are two simple molecules, N_2 (ref. 1d, p. 173, and references therein) and NH_3 (see Table I), for which the spin-rotational coupling constants have been measured in the gaseous phase. The results have made possible theoretical calculations of the screening constants with less arbitrariness than in the case of conventional *ab-initio* or semi-empirical MO calculations. The calculated values for gaseous N_2 , *ca.* -100 ppm, and for gaseous NH_3 , *ca.* $+270$ ppm, may be compared with the most recent measurement for liquid N_2 , *ca.* $+70$ from CH_3NO_2 (Table XXX), and the data for gaseous NH_3 (Table VIII), *ca.* $+400$ ppm from neat CH_3NO_2 . Thus, the origin of the absolute screening constant scale of nitrogen chemical shifts seems to lie at *ca.* $+170$ ppm from CH_3NO_2 (from the N_2 data) or at $+130$ ppm (from the NH_3 data). The data from N_2 may include large errors because of low accuracy in the measurement of the spin-rotational constant and the lack of nitrogen screening constant data for the gaseous phase. The accuracy in this respect is much better for NH_3 , but there may be errors involved in neglecting vibrational effects, particularly those concerning the conformational inversion of the umbrella-shaped NH_3 molecules. Thus, it seems that the values quoted should be considered as rough estimates and that without obtaining a good set of consistent results for a larger number of simple molecules it is far too early to try to establish an absolute scale of nitrogen screening constants.

IV. EXPERIMENTAL TECHNIQUES

The experimental aspects of nitrogen NMR have already been reviewed (1b) in detail, and only the most recent trends will be discussed here. The advent of pulsed Fourier-transform techniques (72) has resulted in a major breakthrough in the feasibility of obtaining ^{15}N natural-abundance NMR spectra even on large molecules. The use of high magnetic fields, i.e. 4 T and more, combined with that of large-bore sample tubes, up to 25 mm in diameter, has brought benefit to both ^{14}N and ^{15}N NMR spectroscopy from the point of view of sensitivity. The analysis of the entire lineshapes of ^{14}N resonance signals, particularly when coupled with the so-called differential saturation technique, allows one to extricate accurate information about the chemical shifts and relaxation times of ^{14}N nuclei even when they give broad and overlapping resonance signals. In most cases, besides those where there is a severe signal overlap of resonances characterized by almost the same signal width, ^{14}N NMR spectroscopy may now afford chemical shift data with an accuracy not worse than that found for ^{15}N spectra.

A. Pulsed Fourier-transform method (PFT)

The method is well known, (72) and its applications to nitrogen NMR have already been discussed. (1b) However, much more experience has been accumulated since 1972, and its merits as well as its limitations in the field of ^{14}N and ^{15}N NMR are more evident. The PFT technique has made possible, the measurement of natural-abundance ^{15}N spectra due to a large gain in sensitivity in a given time, compared with the continuous-wave (CW) method, for sharp resonance signals which appear within a broad spectral range. The sensitivity of the PFT method has recently been augmented (73) by the use of high magnetic fields, e.g. 4.2 T, 25 mm sample tubes, and the quadrature detection technique where a pulse is applied with a frequency occurring within the spectral range involved. Such a combination of experimental improvements has led to usable ^{15}N natural-abundance spectra (73) for a number of biopolymers, with concentrations of the order of 0.01 M, within 20–40 hours of spectra accumulation. Another example may be found in an investigation of dipeptides (74) where the same technique has been applied to 0.2 M aqueous solutions of a number of dipeptides with a typical accumulation time of 6 hours. The amount of nitrogen chemical shift data from natural-abundance ^{15}N spectra has considerably increased (48, 67, 73–76) since 1972 when their share was almost negligible.

However, most of the ^{15}N natural-abundance data involve nitrogen atoms in various NH groups where the negative nuclear Overhauser

effect (NOE) for ^{15}N nuclei decoupled from protons acts favourably, that is in the direction of an inverted signal with a net gain in total intensity. Usually, because of a very significant decrease in ^{15}N signal intensity due to ^1H - ^{15}N spin-spin splitting, it is necessary to decouple the protons. In this case the negative magnetogyric ratio of ^{15}N , due to the NOE upon proton decoupling, can lead to a decrease in signal intensity.

In the "extreme narrowing" region of correlation times for molecular rotations, i.e. very fast molecular rotations with respect to the resonance frequency, the following applies:

$$(2\pi\nu\tau_c)^2 \ll 1 \quad (23)$$

where ν is the resonance frequency, and τ_c is the correlation time. Under these conditions the NOE may modify the total intensity of a ^{15}N signal by a factor ranging from +1 (no effect) to -3.93 (maximum effect) in proportion to the percentage of ^{15}N - ^1H dipole-dipole contributions to the overall spin-lattice relaxation rate ($1/T_1$). Thus the range between +1 and -1 corresponds to a net loss in the total intensity, and a complete cancelling (or "nulling") of the signal is possible when the dipole-dipole mechanism contributes about 20% to the relaxation rate (77, and the references therein). This may also happen for a fast chemical exchange of ^{15}N between inequivalent sites with different NOE intensity factors, if the weighted average of the latter is zero. The same situation may arise in off-resonance decoupling experiments (77) with ^{15}N , since the NOE is only partially effective, the corresponding intensity factor may attain a value within the ± 1 range.

When the correlation time for molecular reorientation is increased outside the extreme narrowing region, the extreme value of the intensity factor may vary from -3.93, for ^{15}N in the extreme narrowing condition, to +0.88 for very long correlation times. (77) Depending on the resonance frequency, a complete ^{15}N signal nulling may occur at certain values of τ_c , e.g., 6×10^{-9} sec for ^{15}N nuclei resonating at 9.12 MHz. This point has been demonstrated experimentally for a decapeptide, Gramicidin-S. (77)

The NOE may be quenched by the use of properly gated decoupling in the PFT technique, but this enhances signals which are diminished by the NOE at the cost of those which are NOE enhanced. Even then caution is advisable when adjusting the decoupler duty-cycle since a leakage of the NOE, due to misadjustment, may lead to complete signal nulling.

Another factor which hampers routine applications of ^{15}N NMR spectroscopy is concerned with the relatively long spin-lattice relaxation

times, T_1 , of ^{15}N nuclei, especially for nitrogen atoms which are not bonded directly to hydrogen atoms. In the PFT technique, if the interval between the pulses is less than $6 T_1$, significant saturation effects take place and diminish the signal intensity without broadening it. This is a serious problem since increasing the interval reduces the effectiveness of the PFT method relative to the CW method.

There are three general ways of circumventing this difficulty. (72) First, it is possible to add a small amount of a " T_1 reagent", such as $\text{Cr}(\text{acac})_3$, as was done in some ^{15}N measurements (62) in order to shorten T_1 . One should be cautious, however, with the use of such reagents, since it had been shown (65) that $\text{Cr}(\text{acac})_3$ may induce significant shifts of the resonance signals. Another method is to decrease the pulse duration time, t_p , or the "pulse angle", to values less than the flip angle of 90° . The resulting loss in signal may be more than offset by the shorter time required between the pulses. However, the optimization depends on T_1 and T_2^* , and may be performed only for signals with a given value of T_1 , otherwise a compromise must be found. Typical pulse angles used in ^{15}N natural-abundance NMR measurements lie within the range of 20° – 40° . (48, 74–76) The third method (72) for overcoming the saturation effects due to long T_1 times consists of using multiple pulse sequences. These are effective under conditions such that $T_1 \cong T_2 \gg T_2^*$, where T_2^* is the experimental transverse relaxation time corresponding to the actual signal-width. Such methods have not yet been tried in ^{15}N NMR spectroscopy. Multiple pulse sequences in the PFT method may be (72) and have been (73) profitably used for the determination of T_1 relaxation times of ^{15}N nuclei.

Attempts have been made (66, 70) to ascribe changes in the nuclear Overhauser effect, in the proton-decoupled ^{15}N spectra of labelled glycine at various pH values, to proton exchange modulation and to changes in rotational correlation times. Thus, the NOE was suggested as a new source of information about proton exchange rates and molecular rotations. However, it was shown recently (78) that the pH dependence of the NOE resulted from the presence of traces of paramagnetic impurities in the samples of glycine, and a warning was advanced to alert investigators of the NMR properties of ^{15}N -labelled amino acids and peptides to the effect of traces of paramagnetic impurities. A convenient method for the removal of such contaminations has been reported. (78)

The application of the PFT technique to ^{14}N spectra is less effective than for ^{15}N because of the quadrupolar relaxation of ^{14}N nuclei which results in a large range of signal widths, from less than 1 Hz to several kHz, depending on the molecular environment of the ^{14}N nuclei. The

gain in signal intensity in the PFT method, as compared with the CW method, may be expressed (79) in terms of the signal-to-noise (S/N) ratio obtained during the same time of spectra accumulation as:

$$\frac{S/N \text{ (PFT)}}{S/N \text{ (CW)}} = 0.799 \left(\frac{\Delta\nu}{\Delta\nu_{1/2}} \right)^{1/2} G(x) \quad (24)$$

where

$$G(x) = \left\{ \frac{2 \cdot [1 - \exp(-x)]^2}{x \cdot [1 - \exp(-2x)]} \right\}^{1/2} \quad (25)$$

and

$$x = \frac{A}{T_1} \quad (26)$$

In these equations $\Delta\nu$ is the spectral range of frequencies considered, $\Delta\nu_{1/2}$ is the signal half-height width in Hz, T_1 is the spin-lattice relaxation time and A is the acquisition time of the free induction decay. For quadrupolar nuclei in liquids, usually $T_1 = T_2^* = T_Q$, where T_Q is defined by equation (35), so that $T_1 = (\pi\Delta\nu_{1/2})^{-1}$. Equations (24) to (26) indicate that the maximum gain factor is:

$$0.799 \left(\frac{\Delta\nu}{\Delta\nu_{1/2}} \right)^{1/2}$$

since $G(x) \leq 1$, and that it must be different for signals of different widths. Moreover, it is realized only for $G(x) \cong 1$, i.e. for sufficiently short acquisition times (high enough pulse repetition rates) relative to T_1 . Thus, ^{14}N signal optimization in the PFT technique may be performed only for a chosen value of $T_1 = T_Q$, but the best value of A affects the spectral resolution, $R = 1/A$, and leads to broadening which may be significant for other signals in the spectrum, namely those with longer T_Q values. Short acquisition times also give saturation effects in narrow ^{14}N resonance signals. The PFT technique is most profitably used (79) for the measurement of relatively long T_1 values of ^{14}N nuclei.

An interesting method, which employs the PFT technique, has been proposed (80) for extracting ^{15}N satellites from the proton spectra of compounds with ^{15}N at natural-abundance in order to obtain the values of ^{15}N - ^1H coupling constants. The method consists of alternatively generating ^{15}N -decoupled and ^{15}N -undecoupled proton free induction decays which are subsequently subtracted from one another. Thus, at least theoretically, the accumulated free induction decay should give, after a Fourier transformation, only the satellite peaks. This technique

has been successfully tested (81) for a number of amides and named the AISEFT (abundant isotope signal elimination by FT) method.

High resolution spectra ^{15}N in the solid state of $(\text{NH}_4)_2\text{SO}_4$, NH_4NO_3 , and glycine have been reported from measurements based on pulsed decoupling of ^1H nuclei. (55)

B. Differential saturation technique

The main difficulties encountered in the measurement and analysis of ^{14}N NMR spectra are concerned with the considerable range of signal widths and severe signal overlap. However, the information contained in the line-widths makes possible an insight into molecular structure which is quite independent of that obtained from nitrogen chemical shifts. In order to obtain accurate spectral parameters from ^{14}N NMR spectra, such as chemical shifts and relaxation times, one has to consider the entire lineshape of the signals involved. This is because spectral points which are quite far away from the peak centre still carry much information about these parameters. This is even more important in those cases where the ^{14}N signals are overlapping to a considerable degree. Even a full lineshape analysis by an iterative fitting of theoretical curves to experimental data may be unsatisfactory from the point of either convergence or the magnitude of errors in the optimized parameters. However, this may be dealt with by taking advantage of changes in the resonance lineshapes which occur upon increasing the saturation level. Such changes depend on the quadrupolar relaxation times, in the case of ^{14}N nuclei, and are usually quite different for nitrogen atoms at inequivalent sites.

A simple differential saturation method has been proposed (63) in which the differential saturation effects are obtained at the same overall irradiation level due to an audio-frequency modulation of the resonance frequency in the continuous-wave mode of operation. This results in the appearance of sidebands in addition to the centre band of the spectrum. By a judicious selection of the modulation index, the saturation of signals in the sidebands may be made to amount to 10–0.1% of those in the centre band. The lineshape of such a combination of the centre band and the two closest sidebands may be adjusted to that corresponding to the function:

$$\begin{aligned}
 G_i(\nu) = & [1 + 4\pi^2 T_2^2 (\nu_i - \nu)^2 + \gamma^2 B_1^2 T_1 T_2 J_0^2]^{-1} \\
 & - (J_0 - J_2)(2J_0)^{-1} [1 + 4\pi^2 T_2^2 (\nu_i \pm \nu_M - \nu)^2 \\
 & + \gamma^2 B_1^2 T_1 T_2 J_1^2]^{-1}
 \end{aligned} \tag{27}$$

where i denotes the nucleus in question, ν_i is its resonance frequency, ν_M is the modulation frequency, and J_n are Bessel functions, of the first kind, of the modulation index. An iterative fitting of the function:

$$f(\nu) = A + B\nu + C \sum_i G_i(\nu) \quad (28)$$

has been performed where the first two terms describe the background, C is the vertical calibration factor and the summation over i involves all the nuclei represented in the spectrum. This method gives a good convergence even in the case of quite complicated ^{14}N spectra. (63) The same technique has been adopted for obtaining high-precision data on the screening constant differences of a number of compounds used as references in the calibration of nitrogen NMR spectra (Table VII). An important advantage of this method is that it provides accurate estimates of both the shift and the relaxation times of the ^{14}N nuclei.

V. CORRELATION OF RELATIVE NITROGEN SCREENING CONSTANTS WITH MOLECULAR STRUCTURE

Since (1d) there is no intrinsic isotope effect between ^{15}N and ^{14}N , as far as the screening constant is concerned, ^{15}N and ^{14}N chemical shifts may be used interchangeably. A great deal of relative nitrogen screening constant data has accumulated since the last appearance of a detailed discussion (1d) of correlations between them and molecular structure. Apart from specific relationships between nitrogen nuclear screening and the electronic structure within various molecular systems, some general conclusions may be drawn from the experimental data. Solvent effects on nitrogen chemical shifts play quite an important role, as shown in Tables VII and VIII but these are only usually revealed for sufficiently dilute solutions. Most of the older chemical shift data (1d) refer to either neat liquids or concentrated solutions where solute-solute interactions are still large enough to partially obscure solvent effects.

If the molecular environment of a nitrogen atom does not isolate it from direct intermolecular interactions, a range of about 10 ppm seems to be quite normal for solvent effects on the nitrogen chemical shift of a compound dissolved in a range of commonly used solvents. Some of them, like H_2O , result in a shift value at one of the extremes of the range, sometimes as far as 20 ppm from other values, as in the case of pyridine (Table VII). Carbon tetrachloride seems also to give solvent effects which place the corresponding nitrogen chemical shift of the solute at the opposite extreme to that for aqueous solutions. This has been observed (Table VII) for CH_3NO_2 , CH_3CN and pyridine. The data on

TABLE VIII

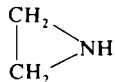
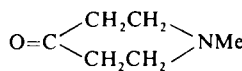
Nitrogen screening constants of some aliphatic amines in ppm, referred to external neat nitromethane

Compound	Solvent or state	Nitrogen screening constant	Notes
NH ₃	gaseous	+399.9 ± 0.2	<i>a, c</i>
	inf. dil. Me ₂ O	+390.1 ± 0.2	<i>a</i>
	inf. dil. Me ₃ H	+387.8 ± 0.2	<i>a</i>
	inf. dil. Me ₂ NH	+387.7 ± 0.2	<i>a</i>
	inf. dil. Et ₂ O	+387.1 ± 0.2	<i>a</i>
	inf. dil. Me ₄ C	+386.7 ± 0.2	<i>a</i>
	inf. dil. MeNH ₂	+385.5 ± 0.2	<i>a</i>
	inf. dil. Et ₃ N	+385.4 ± 0.2	<i>a</i>
	inf. dil. Et ₂ NH	+385.1 ± 0.2	<i>a</i>
	inf. dil. MeOH	+384.4 ± 0.2	<i>a</i>
	inf. dil. EtNH ₂	+384.2 ± 0.2	<i>a</i>
	neat liquid	+381.93 ± 0.14	<i>b</i>
	inf. dil. CCl ₄	+381.9 ± 0.2	<i>a</i>
	inf. dil. EtOH	+381.2 ± 0.2	<i>a</i>
	inf. dil. H ₂ O	+378.4 ± 0.2	<i>a</i>
MeNH ₂	gaseous	+385.4 ± 0.2	<i>c</i>
	neat liquid	+378.73 ± 0.15	<i>b</i>
		+378.0 ± 0.2	<i>c</i>
	0.2 M, cyclohexane	+377.2 ± 0.2	<i>d</i>
	0.2 M, DMF	+378.5 ± 0.2	<i>d</i>
	0.2 M, DMSO	+376.5 ± 0.2	<i>d</i>
	0.2 M, CCl ₄	+376.4 ± 0.2	<i>d</i>
Me ₂ NH	gaseous	+373.8 ± 0.2	<i>c</i>
	neat liquid	+371.2 ± 0.2	<i>c</i>
Me ₃ N	gaseous	+372.8 ± 0.2	<i>c</i>
	inf. dil. Me ₂ O	+368.8 ± 0.2	<i>e</i>
	inf. dil. Me ₄ C	+368.6 ± 0.2	<i>e</i>
	neat liquid	+368.59 ± 0.10	<i>b</i>
	inf. dil. Me ₂ NH	+367.8 ± 0.2	<i>e</i>
	inf. dil. Et ₂ NH	+367.8 ± 0.2	<i>e</i>
	inf. dil. MeNH ₂	+367.7 ± 0.2	<i>e</i>
	inf. dil. EtNH ₂	+367.7 ± 0.2	<i>e</i>
	inf. dil. NH ₃	+367.4 ± 0.2	<i>e</i>
	inf. dil. CCl	+365.5 ± 0.2	<i>e</i>
	inf. dil. EtOH	+363.9 ± 0.2	<i>e</i>
	inf. dil. MeOH	+363.6 ± 0.2	<i>e</i>
	inf. dil. H ₂ O	+361.7 ± 0.2	<i>e</i>
	0.1 M, cyclohexane	+367.9 ± 0.2	<i>d</i>
	0.1 M, CDCl ₃	+364.4 ± 0.2	<i>d</i>

TABLE VIII—*cont.*

Compound	Solvent or state	Nitrogen screening constant	Notes
PrNH ₂	neat liquid	+362.1 ± 0.2	<i>f</i>
BuNH ₂	neat liquid	+358.4 ± 0.2	<i>f</i>
	neat liquid	+359.2 ± 0.2	<i>g</i>
Me(CH ₂) ₄ NH ₂	neat liquid	+359.7 ± 0.2	<i>f</i>
<i>i</i> -BuNH ₂	neat liquid	+363.5 ± 0.2	<i>f</i>
H ₂ NCH ₂ CH ₂ NH ₂	neat liquid	+364.8 ± 0.2	<i>f</i>
H ₂ N(CH ₂) ₃ NH ₂	neat liquid	+360.3 ± 0.2	<i>f</i>
H ₂ N(CH ₂) ₄ NH ₂	neat liquid	+360.0 ± 0.2	<i>f</i>
H ₂ N(CH ₂) ₅ NH ₂	neat liquid	+360.0 ± 0.2	<i>f</i>
H ₂ N(CH ₂) ₆ NH ₂	neat liquid	+359.7 ± 0.2	<i>f</i>
HOCH ₂ CH ₂ NH ₂	neat liquid	+365.7 ± 0.2	<i>f</i>
MeOCH ₂ CH ₂ NH ₂	neat liquid	+367.8 ± 0.2	<i>f</i>
NC-CH ₂ CH ₂ NH ₂	neat liquid	+361.7 ± 0.2 (NH ₂)	<i>f</i>
PhCH ₂ NH ₂	neat liquid	+358.5 ± 0.2	<i>f</i>
PhCH ₂ CH ₂ NH ₂	neat liquid	+360.6 ± 0.2	<i>f</i>
Ph(CH ₂) ₃ NH ₂	neat liquid	+358.9 ± 0.2	<i>f</i>
CH ₂ =CHCH ₂ NH ₂	neat liquid	+361.6 ± 0.2	<i>f</i>
Cyclopropyl-CH ₂ NH ₂	neat liquid	+358.9 ± 0.2	<i>f</i>
<i>i</i> -PrNH ₂	neat liquid	+338.3 ± 0.2	<i>f</i>
EtCH(Me)NH ₂	neat liquid	+341.5 ± 0.2	<i>f</i>
PrCH(Me)NH ₂	neat liquid	+339.2 ± 0.2	<i>f</i>
HOCH ₂ CH(Me)NH ₂	neat liquid	+346.0 ± 0.2	<i>f, g</i>
PhCH(Me)NH ₂	neat liquid	+338.1 ± 0.2	<i>f</i>
Cyclopropylamine	neat liquid	+352.6 ± 0.2	<i>f</i>
Cyclobutylamine	neat liquid	+337.7 ± 0.2	<i>f</i>
Cyclopentylamine	neat liquid	+343.0 ± 0.2	<i>f</i>
Cyclohexylamine	neat liquid	+339.4 ± 0.2	<i>f</i>
<i>trans</i> -1,2-Diaminocyclobutane	neat liquid	+342.0 ± 0.2	<i>f</i>
<i>cis</i> -1,2-Diaminocyclobutane	neat liquid	+355.5 ± 0.2	<i>f</i>
<i>i</i> -BuNH ₂	neat liquid	+323.5 ± 0.2	<i>f</i>
HOCH ₂ C(Me ₃)NH ₂	neat liquid	+332.9 ± 0.2	<i>f</i>
Et ₂ NH	neat liquid	+334.0 ± 0.2	<i>f</i>
		+332.6 ± 0.2	<i>g</i>
MeNHEt	neat liquid	+352.5 ± 0.2	<i>g</i>
MeNHBu	neat liquid	+356.1 ± 0.2	<i>g</i>
Pr ₂ NH	neat liquid	+341.3 ± 0.2	<i>g</i>
Bu ₂ NH	neat liquid	+340.5 ± 0.2	<i>g</i>
<i>i</i> -Bu ₂ NH	neat liquid	+345.4 ± 0.2	<i>g</i>
Dipentylamine	neat liquid	+339.9 ± 0.2	<i>g</i>
Dihexylamine	neat liquid	+339.9 ± 0.2	<i>g</i>
Diheptylamine	neat liquid	+339.8 ± 0.2	<i>g</i>
Diisopentylamine	neat liquid	+340.2 ± 0.2	<i>g</i>
Pyrrolidine	neat liquid	+343.4 ± 0.2	<i>f</i>

TABLE VIII—*cont.*

Compound	Solvent or state	Nitrogen screening constant	Notes
Piperidine	neat liquid	+342.6 ± 0.2	<i>f</i>
		+341.6 ± 0.2	<i>g</i>
Piperazine	satd. in dioxane	+346.3 ± 0.2	<i>f</i>
Morpholine	neat liquid	+349.8 ± 0.2	<i>f</i>
<i>i</i> -Pr ₂ NH	neat liquid	+304.4 ± 0.2	<i>f, g</i>
EtCH(Me)NHCH(Me)Et	neat liquid	+312.6 ± 0.2 (meso)	<i>g</i>
		+313.1 ± 0.2 (DL)	<i>g</i>
BuCH(Me)NHCH(Me)Bu	neat liquid	+311.0 ± 0.2 (meso)	<i>g</i>
		+311.4 ± 0.2 (DL)	<i>g</i>
<i>i</i> -PrNH- <i>t</i> -Bu	neat liquid	+298.0 ± 0.2	<i>g</i>
	neat liquid	+393.3 ± 0.2	<i>f</i>
Bu ₃ N	neat liquid	+341.3 ± 0.2	<i>g</i>
Me ₂ NCH ₂ CH ₂ NMe ₂	neat liquid	+359.6 ± 0.2	<i>f</i>
N-Me-piperidine	neat liquid	+341.3 ± 0.2	<i>g</i>
	neat liquid	+343.7 ± 0.2	<i>g</i>
Nicotine	neat liquid	+327.9 ± 0.2 (NMe)	<i>f</i>

^a Ref. 84, ¹⁵N spectra of labelled compounds, originally referred to external gaseous NH₃, recalculated with NH₃ (neat liquid) shift of +381.93 ppm from neat CH₃NO₂; corrected for liquid volume susceptibilities.

^b Ref. 61, ¹⁴N spectra, neat CH₃NO₂ external reference in concentric spherical sample containers in order to eliminate bulk susceptibility effects; differential saturation technique and full lineshape analysis as in ref. 63, errors quoted are standard deviations for about 200 data points.

^c Ref. 60, ¹⁵N spectra of labelled compounds, originally referred to gaseous NH₃, recalculated as in footnote (a) and extrapolated to 30°C.

^d Ref. 85, proton spectra of ¹⁵N-labelled compounds, ¹⁵N decoupling; recalculated with CH₃NH₂ (neat liquid) shift, +378.73 from neat CH₃NO₂, and (CH₃)₃N (neat liquid) shift, +368.59 from CH₃NO₂, ref. 61 Table VII.

^e Ref. 86, ¹⁵N spectra of ¹⁵N(CH₃)₃ shifts corrected for liquid volume susceptibility, originally referred to gaseous (CH₃)₃N, recalculated with (CH₃)₃N (neat liquid) shift, +368.59 from CH₃NO₂, ref. 61, see also Table VII.

^f Ref. 67, ¹⁵N natural-abundance spectra, concentric cylindrical sample tubes, no correction for bulk susceptibility effects; referred to what is reported as *ca.* 10 M H¹⁵NO₃; from data reported for this standard sample relative to (CH₃)₄N[⊕]Cl[⊖] in subsequent papers (34, 36) its shift is *ca.* +6.1 ppm from neat CH₃NO₂; this corresponds to a HNO₃ concentration of between 1 M and 2 M, as reckoned from data in Table VII; errors quoted are ±0.2 ppm, but comparison of results with those from ref. 36, suggests ±1 ppm as more realistic limits.

^g Ref. 36, ¹⁵N natural-abundance spectra, coaxial cylindrical sample tubes, no correction for bulk susceptibility effects; referred externally to what was reported as *ca.* 12 M (CH₃)₄N[⊕]Cl[⊖]

TABLE IX

Nitrogen screening constants of some arylamines in ppm, referred to external neat nitromethane

Compound	Solvent or state	Nitrogen screening constant	Notes
Aniline	neat liquid	$+325.4 \pm 0.2$	<i>a, c</i>
	12% in C_6H_6	$+326.9 \pm 0.2$	<i>b</i>
	25% in CCl_4	$+325.9 \pm 0.2$	<i>b</i>
2-Me-	neat liquid	$+327.7 \pm 0.2$	<i>c</i>
3-Me-	neat liquid	$+326.3 \pm 0.2$	<i>c</i>
4-Me-	neat liquid	$+328.0 \pm 0.2$	<i>c</i>
2,3-Me ₂ -	neat liquid	$+329.1 \pm 0.2$	<i>c</i>
2,4-Me ₂ -	neat liquid	$+330.3 \pm 0.2$	<i>c</i>
2,5-Me ₂ -	neat liquid	$+328.5 \pm 0.2$	<i>c</i>
2,6-Me ₂ -	neat liquid	$+330.9 \pm 0.2$	<i>c</i>
3,4-Me ₂ -	melt, 55°C	$+329.0 \pm 0.2$	<i>b</i>
	satd., C_6H_6	$+327.0 \pm 0.2$	<i>b</i>
3,5-Me ₂ -	neat liquid	$+327.0 \pm 0.2$	<i>c</i>
2-Cl-	neat liquid	$+326.3 \pm 0.2$	<i>c</i>
3-Cl-	neat liquid	$+324.2 \pm 0.2$	<i>c</i>
2-Br-	neat liquid	$+321.1 \pm 0.2$	<i>c</i>
3-Br-	neat liquid	$+323.4 \pm 0.2$	<i>c</i>
2-MeO-	neat liquid	$+335.9 \pm 0.2$	<i>c</i>
2-Cl-6-Me-	neat liquid	$+328.5 \pm 0.2$	<i>c</i>
2-Br-4-Me-	neat liquid	$+323.6 \pm 0.2$	<i>c</i>

^a Ref. 67, see footnote (f) in Table VIII.

^b Ref. 48, ^{15}N natural-abundance spectra, originally referred to 2.9 M $^{15}NH_4Cl$ in 1 M HCl as external standard in a sealed capillary, recalculated to CH_3NO_2 scale through the aniline (neat liquid) shift in the Table; no corrections for bulk susceptibility effects are made.

^c Ref. 68, ^{15}N natural-abundance spectra, originally referred to "external $H^{15}NO_3$ " which is probably the same standard as in ref. 67, for comments see footnote (f) in Table VIII.

compared with those discussed in our previous review (ref. 1d, p. 174–184). The existence of the β -effect on the shifts of the amino group, which results in a high-frequency shift of the nitrogen resonance signal upon replacing the corresponding H atom with an alkyl group, seems now to be well proven. A regression analysis of the shifts has been

in D_2O , but since the solubility of the latter at ambient temperatures is *ca.* 6 M, this is a more probable value; recalculated to CH_3NO_2 scale with $(CH_3)_3NCl$ (6.03 M) shift, +336.69 ppm, ref. 61, Table VII, which is in a very good agreement with the value reported in ref. 36, assignments of *meso* and DL forms may be reversed; accuracy quoted is ± 0.2 ppm, but comparison with data in Table VII (61) suggests that it is not better than ± 0.6 ppm.

attempted (67, 36) in terms of the α , β , γ and δ effects on the shifts, and the following values are reported (36) after some modifications of earlier (67) considerations:

introduction of an alkyl group into position	relative shift in ppm
α	-7.8
β	-18.6
γ	+2.4
σ	-2.5

However, the results are obtained for neat liquids, and the absolute values below 10 ppm should be treated with some suspicion, because of the possible solvent effects in a situation where each compound is a solvent for itself and there are as many solvents as compounds.

The nitrogen screening constants for the simplest alkyl amines in the gaseous phase, CH_3NH_2 , $(\text{CH}_3)_2\text{NH}$, $(\text{CH}_3)_3\text{N}$ as well as those of some simple alkylammonium ions have been calculated (30) using the valence-bond (VB) formalism and the AEE approximation to yield a reasonable fit with the experimental differences, relative to gaseous NH_3 , by varying the value of the mean excitation energy. A purely empirical approach has also been used (30) to express the shifts (referred to that of NH_4^+) in terms of four parameters:

$\Delta(\text{L})$ —lone pair effect, +42.0 ppm;

$\Delta(\text{Me})$ —Me group effect, +1.0 ppm;

$\Delta(\text{Me-L})$ —effect of interaction between Me and lone pair, -3.5 ppm;

$\Delta(\text{Me-Me})$ —effect of interaction between Me groups, -8.0 ppm.

These values represent the results of a least-squares fit to experimental data. The importance of such calculations lies not in the numerical values themselves, which may carry uncertainties due to solvent effects on the shifts of the alkylammonium ions and NH_4^+ (Table VII), but in an indication of the role of interactions between alkyl groups and between lone electron pairs and alkyl groups in the determination of the shift of the amino group. Thus, a simple regression analysis (36, 67) seems to have little significance with respect to the α -effect.

A regression analysis has also been tried (48, 68) for the nitrogen chemical shifts of a number of substituted anilines (Table IX). The following values of increments (in ppm) to the shifts of neat PhNH_2 are reported:

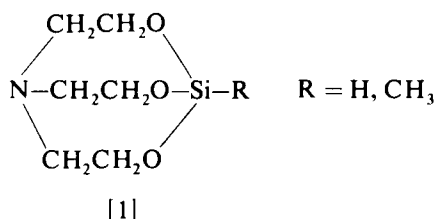
	Me	Cl	Br	OMe
ortho	+2.37	+0.92	-4.22	+10.51
meta	+0.77	-1.17	-1.95	—
para	+2.55	—	—	—

Since these results are based on the data for neat liquids, similar objections may be made as those for the case of alkyl amines. Since the range of the shifts (Table IX) is less than 10 ppm, if we exclude the shift of 2-methoxyaniline, any correlations with either INDO-MO calculated electron densities for isolated molecules (48) or with the ^{13}C and ^{19}F chemical shifts of the corresponding toluenes and fluorobenzenes (68) may be of little significance.

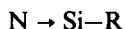
B. Aminosilanes and aminoboranes

A great deal of experimental data on the nitrogen chemical shifts of aminosilanes and aminoboranes have been reported in the review period (Table X). Unfortunately, there are indications (see footnotes d and e in Table X) that the accuracy of a considerable part of the data is not high enough to seriously consider changes in the shifts that are smaller than 10 ppm.

An important question concerning the nitrogen chemical shifts of aminosilanes is whether the spectral data can give indications of the existence of nitrogen-silicon donor-acceptor bonds. (87, 88) In the case of two silatranes [1] a high-frequency shift of about 9 ppm has been



observed (Table X, note b) upon replacing a hydrogen atom with a methyl group which is reminiscent of the well-known β -effect. This has been explained as being due to the existence of a $\text{N} \rightarrow \text{Si}$ transannular bond so that the system



may exhibit the β -effect on the nitrogen chemical shift through the Si atom. (88)

The shifts of $\text{R}_3\text{SiCH}_2\text{NH}_2$ compounds ($\text{R} = \text{Me, OEt}$) fall within the range of $+376 \pm 1$ ppm (87) whilst those for $\text{R}_3\text{SiCH}_2\text{CH}_2\text{NH}_2$ and $\text{R}_3\text{SiCH}_2\text{CH}_2\text{CH}_2\text{NH}_2$ are $+349 \pm 1$ and $+356 \pm 1$, respectively. Those for longer alkylamino side-chains are within the normal range of shifts of $-\text{CH}_2-\text{NH}_2$ groups, $+360 \pm 5$ ppm. This may indicate that some intramolecular interactions of the donor-acceptor type may exist between N and Si in the $\text{R}_3\text{SiCH}_2\text{CH}_2\text{NH}_2$ compounds since the shift,

TABLE X

Nitrogen screening constants of some aminosilanes and aminoboranes in ppm, referred to external neat nitromethane

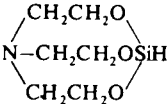
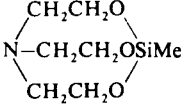
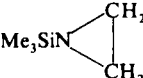
Compound	Solvent or state	Nitrogen screening constant	Notes
$\text{Me}_3\text{SiCH}_2\text{NH}_2$	neat liquid	$+376 \pm 3$	<i>a</i>
$\text{Me}_2\text{Si}(\text{OEt})\text{CH}_2\text{NH}_2$	neat liquid	$+376 \pm 3$	<i>a</i>
$\text{MeSi}(\text{OEt})_2\text{CH}_2\text{NH}_2$	neat liquid	$+378 \pm 3$	<i>a</i>
$(\text{EtO})_3\text{SiCH}_2\text{NH}_2$	neat liquid	$+377 \pm 3$	<i>a</i>
$\text{Me}_3\text{SiCH}_2\text{CH}_2\text{NH}_2$	neat liquid	$+348 \pm 3$	<i>a</i>
$(\text{EtO})_3\text{SiCH}_2\text{CH}_2\text{NH}_2$	neat liquid	$+349 \pm 3$	<i>a</i>
$\text{Me}_3\text{SiCH}_2\text{CH}_2\text{CH}_2\text{NH}_2$	neat liquid	$+355 \pm 3$	<i>a</i>
$\text{Me}_2\text{Si}(\text{OEt})\text{CH}_2\text{CH}_2\text{CH}_2\text{NH}_2$	neat liquid	$+355 \pm 3$	<i>a</i>
$\text{MeSi}(\text{OEt})_2\text{CH}_2\text{CH}_2\text{CH}_2\text{NH}_2$	neat liquid	$+355 \pm 3$	<i>a</i>
$(\text{EtO})_3\text{SiCH}_2\text{CH}_2\text{CH}_2\text{NH}_2$	neat liquid	$+356 \pm 3$	<i>a</i>
$\text{Me}_3\text{SiCH}_2\text{CH}_2\text{CH}_2\text{CH}_2\text{NH}_2$	neat liquid	$+357 \pm 3$	<i>a</i>
	CH_2Cl_2 , 0.8 M	$+358 \pm 4$	<i>b</i>
	CH_2Cl_2 , 0.8 M	$+349 \pm 4$	<i>b</i>
Et_3SiNH_2	neat liquid	$+373 \pm 1$	<i>c</i>
Me_3SiNHMe	neat liquid	$+377 \pm 5$	<i>d</i>
Me_3SiNHEt	neat liquid	$+347 \pm 5$	<i>d</i>
$\text{Me}_3\text{SiNH-}i\text{-Pr}$	neat liquid	$+334 \pm 5$	<i>d</i>
$\text{Me}_3\text{SiNH-}s\text{-Bu}$	neat liquid	$+342 \pm 5$	<i>d</i>
$\text{Me}_3\text{SiNH-}t\text{-Bu}$	neat liquid	$+325 \pm 5$	<i>d</i>
Me_3SiNHPh	neat liquid	$+324 \pm 5$	<i>d</i>
$\text{Me}_3\text{SiNMe}_2$	neat liquid	$+378 \pm 5$	<i>d</i>
$\text{Me}_3\text{SiNEt}_2$	neat liquid	$+347 \pm 5$	<i>d</i>
$\text{Me}_3\text{SiN}(i\text{-Pr})_2$	neat liquid	$+318 \pm 5$	<i>d</i>
	neat liquid	$+368 \pm 5$	<i>d</i>
$\text{Me}_3\text{SiN}(\text{CH}_2)_4$	neat liquid	$+345 \pm 5$	<i>d</i>
$(\text{Me}_3\text{Si})_2\text{NH}$	neat liquid	$+355 \pm 5$; $+352 \pm 2$	<i>d, c</i>
$(\text{Me}_3\text{Si})_2\text{NMe}$	neat liquid	$+374 \pm 5$; $+361 \pm 3$	<i>d, c</i>
$(\text{Me}_3\text{Si})_2\text{NEt}$	neat liquid	$+344 \pm 5$	<i>d</i>
$(\text{Me}_3\text{Si})_2\text{N-}i\text{-Pr}$	neat liquid	$+327 \pm 5$	<i>d</i>
$(\text{Me}_3\text{Si})_2\text{N-}t\text{-Bu}$	neat liquid	$+320 \pm 10$	<i>d</i>
$(\text{Me}_3\text{Si})_2\text{NPh}$	neat liquid	$+291 \pm 10$	<i>d</i>
$(\text{Me}_2\text{ClSi})_2\text{NH}$	neat liquid	$+326 \pm 5$	<i>d</i>

TABLE X—*cont.*

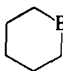
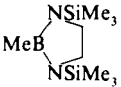
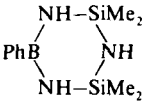
Compound	Solvent or state	Nitrogen screening constant	Notes
$\text{Me}_2\text{ClSiNHHSiMe}_3$	neat liquid	$+348 \pm 5$	<i>d</i>
$\text{MeCl}_2\text{SiNHHSiMe}_3$	neat liquid	$+328 \pm 5$	<i>d</i>
$\text{Cl}_3\text{SiNHHSiMe}_3$	neat liquid	$+322 \pm 5$	<i>d</i>
$(\text{Cl}_3\text{Si})_2\text{NH}$	neat liquid	$+297 \pm 5$	<i>d</i>
$\text{Me}_2\text{ClSiN(Me)SiMe}_3$	neat liquid	$+341 \pm 5$	<i>d</i>
$\text{Cl}_3\text{SiN(Me)SiMe}_3$	neat liquid	$+340 \pm 5$	<i>d</i>
$(\text{Me}_2\text{ClSi})_2\text{NMe}$	neat liquid	$+338 \pm 5$	<i>d</i>
$\text{MeCl}_2\text{SiN(Me)SiMe}_3$	neat liquid	$+337 \pm 5$	<i>d</i>
$\text{MeCl}_2\text{SiN(Me)SiMe}_2\text{Cl}$	neat liquid	$+338 \pm 5$	<i>d</i>
$(\text{Cl}_2\text{MeSi})_2\text{NMe}$	neat liquid	$+318 \pm 5$	<i>d</i>
$(\text{MeO})_2\text{SiNHHSiMe}_3$	neat liquid	$+369 \pm 1$	<i>c</i>
$(\text{MeO})_2\text{SiNHHSi(OMe)}_3$	neat liquid	$+380 \pm 3$	<i>c</i>
$\text{Me}_2\text{Si(NHMe)}_2$	neat liquid	$+367 \pm 5$	<i>d</i>
$(\text{Me}_2\text{SiNH})_3$	neat liquid	$+347 \pm 5$	<i>d</i>
$(\text{Me}_2\text{SiNH})_4$	neat liquid	$+336 \pm 5$	<i>d</i>
$(\text{Me}_2\text{SiNMe})_3$	neat liquid	$+336 \pm 5$	<i>d</i>
$(\text{Me}_3\text{Si})_3\text{N}$	neat liquid	$+348 \pm 5; +345 \pm 2$	<i>d, c</i>
$\text{Me}_2\text{Si(NMe}_2)_2$	neat liquid	$+374 \pm 5$	<i>d</i>
$\text{MeSi(NMe}_2)_3$	neat liquid	$+371 \pm 5$	<i>d</i>
$\text{Si(NMe}_2)_4$	neat liquid	$+370 \pm 5$	<i>d</i>
$\text{Me}_2\text{BNHSiMe}_3$	neat liquid	$+286 \pm 5$	<i>d</i>
$\text{Me}_2\text{BN(Me)SiMe}_3$	neat liquid	$+291 \pm 5$	<i>d</i>
$\text{Me}_2\text{BN(Et)SiMe}_3$	neat liquid	$+264 \pm 5$	<i>d</i>
$\text{Me}_2\text{BN}(i\text{-Pr)SiMe}_3$	neat liquid	$+260 \pm 5$	<i>d</i>
$\text{Me}_2\text{BN}(s\text{-Bu)SiMe}_3$	neat liquid	$+261 \pm 5$	<i>d</i>
$\text{Me}_2\text{BN}(t\text{-Bu)SiMe}_3$	neat liquid	$+261 \pm 5$	<i>d</i>
$\text{Me}_2\text{BN(Ph)SiMe}_3$	neat liquid	$+254 \pm 5$	<i>d</i>
$\text{Me}_2\text{BN(SiMe}_3)_2$	neat liquid	$+285 \pm 5$	<i>d</i>
 B-NHSiMe_3	neat liquid	$+280 \pm 5$	<i>d</i>
$\text{Et}_2\text{BNHSiMe}_3$	neat liquid	$+292 \pm 5$	<i>d</i>
$\text{Ph}_2\text{BNHSiMe}_3$	neat liquid	$+284 \pm 10$	<i>d</i>
$\text{Ph}_2\text{BN(Me)SiMe}_3$	neat liquid	$+294 \pm 10$	<i>d</i>
$\text{MeB(-NMe-SiMe}_3)_2$	neat liquid	$+305 \pm 10$	<i>d</i>
	neat liquid	$+309 \pm 5$	<i>d</i>
	CH_2Cl_2	$+314 \pm 5$	<i>g</i>

TABLE X—*cont.*

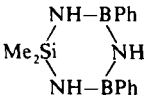
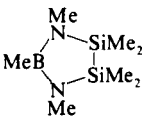
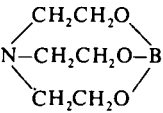
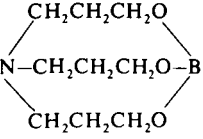
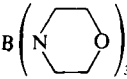
Compound	Solvent or state	Nitrogen screening constant	Notes
	CH ₂ Cl ₂	+296 ± 5	<i>g</i>
	neat liquid	+311 ± 5	<i>d</i>
MeB(Br)—N(SiMe ₃) ₂	neat liquid	+280 ± 5	<i>d</i>
ClB[N(SiMe ₃) ₂] ₂	neat liquid	+326 ± 10	<i>d</i>
B(—NMe—SiMe ₃) ₃	neat liquid	+325 ± 10	<i>d</i>
Al[N(SiMe ₃) ₂] ₃	neat liquid	+314 ± 10	<i>d</i>
(PhBNH) ₃	CH ₂ Cl ₂	+272 ± 5	<i>g</i>
	CH ₂ Cl ₂ , 0.5 M	+328 ± 5	<i>b</i>
	CH ₂ Cl ₂ , 0.5 M	+340 ± 5	<i>b</i>
B(NMe ₂) ₃	neat liquid	+369 ± 5	<i>e</i>
B(NEt ₂) ₃	neat liquid	+348 ± 10	<i>e</i>
B[N(CH ₂) ₄] ₃	CH ₂ Cl ₂	+342 ± 10	<i>e</i>
B[N(CH ₃) ₃] ₃	CH ₂ Cl ₂	+336 ± 10	<i>e</i>
	CH ₂ Cl ₂	+313 ± 10	<i>e</i>
B(NHMe) ₃	neat liquid	+356 ± 5	<i>e</i>
B(NHEt) ₃	neat liquid	+349 ± 5	<i>e</i>
B(NHPr) ₃	neat liquid	+340 ± 10	<i>e</i>
B(NH- <i>i</i> -Pr) ₃	neat liquid	+330 ± 10	<i>e</i>
B(NH- <i>s</i> -Bu) ₃	neat liquid	+330 ± 10	<i>e</i>
B(NH- <i>t</i> -Bu) ₃	neat liquid	+297 ± 10	<i>e</i>
1,8,10,9-Triazaboradecaline	benzene	+335 ± 10	<i>e</i>
HB(NMe ₂) ₂	neat liquid	+343 ± 5	<i>e</i>
MeB(NMe ₂) ₂	neat liquid	+341 ± 5	<i>e</i>
EtB(NMe ₂) ₂	neat liquid	+341 ± 5	<i>e</i>
PrB(NMe ₂) ₂	neat liquid	+344 ± 5	<i>e</i>
BuB(NMe ₂) ₂	neat liquid	+337 ± 10	<i>e</i>

TABLE X—*cont.*





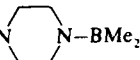
Compound	Solvent or state	Nitrogen screening constant	Notes
PhB(NMe ₂) ₂	benzene	+286 ± 10	<i>e</i>
HB(NEt ₂) ₂	neat liquid	+295 ± 10	<i>e</i>
MeB(NEt ₂) ₂	neat liquid	+300 ± 10	<i>e</i>
EtB(NEt ₂) ₂	neat liquid	+301 ± 10	<i>e</i>
PhB(NEt ₂) ₂	benzene	+289 ± 10	<i>e</i>
MeB(NHMe) ₂	neat liquid	+355 ± 5	<i>e</i>
BuB(NHMe) ₂	neat liquid	+345 ± 5	<i>e</i>
PhB(NHMe) ₂	neat liquid	+318 ± 10	<i>e</i>
MeB(NHEt) ₂	neat liquid	+304 ± 5	<i>e</i>
MeB(NH- <i>i</i> -Pr) ₂	neat liquid	+297 ± 10	<i>e</i>
Me ₂ BNMe ₂	neat liquid	+300 ± 5	<i>e</i>
Et ₂ BNMe ₂	neat liquid	+306 ± 5	<i>e</i>
Bu ₂ BNMe ₂	benzene	+311 ± 10	<i>e</i>
Ph ₂ BNMe ₂	benzene	+261 ± 10	<i>e</i>
Me ₂ BNEt ₂	neat liquid	+263 ± 5	<i>e</i>
Et ₂ BNEt ₂	neat liquid	+266 ± 5	<i>e</i>
Ph ₂ BNEt ₂	benzene	+279 ± 10	<i>e</i>
Me ₂ BNHMe	neat liquid	+286 ± 5	<i>e</i>
Me ₂ BNHEt	neat liquid	+287 ± 5	<i>e</i>
Me ₂ BNH- <i>i</i> -Pr	neat liquid	+263 ± 5	<i>e</i>
Me ₂ BNH- <i>t</i> -Bu	neat liquid	+248 ± 5	<i>e</i>
Me ₂ BNH(cyclohexyl)	neat liquid	+259 ± 5	<i>e</i>
Me ₂ BNHPh	neat liquid	+259 ± 5	<i>e</i>
Me ₂ BNH-C ₆ H ₄ -MeO	neat liquid	+267 ± 5	<i>e</i>
Me ₂ B-N 	neat liquid	+276 ± 5	<i>e</i>
Me ₂ B-N 	neat liquid	+278 ± 5	<i>e</i>
Me ₂ B-N 	neat liquid	+265 ± 5	<i>e</i>
Me ₂ B-N 	neat liquid	+274 ± 5 +344 ± 5	<i>e</i> <i>e</i>
Me ₂ B-N 	neat liquid	+262 ± 5	<i>e</i>
Me ₂ BN(Me)-cyclohexyl	neat liquid	+266 ± 10	<i>e</i>
Me ₂ BN(Me)Ph	neat liquid	+276 ± 5	<i>e</i>
Bu ₂ BNH ₂	neat liquid	+309 ± 5	<i>e</i>
Et ₂ BNH ₂	neat liquid	+299 ± 5	<i>e</i>

TABLE X—*cont.*




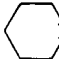
Compound	Solvent or state	Nitrogen screening constant	Notes
B(NHNMe ₂) ₃	CCl ₄	+321 ± 5	<i>e</i>
		+277 ± 5	<i>e</i>
MeB(NHNMe ₂) ₂	benzene	+317 ± 5	<i>e</i>
		+252 ± 5	<i>e</i>
Me ₂ BNHNMe ₂	benzene	+313 ± 5	<i>e</i>
		+221 ± 5	<i>e</i>
(Et ₂ B) ₂ NH	benzene	+254 ± 5	<i>e</i>
(Et ₂ B) ₂ NMe	neat liquid	+257 ± 5	<i>e</i>
(Ph ₂ B) ₂ NH	benzene	+244 ± 10	<i>e</i>
(Ph ₂ B) ₂ NMe	CH ₂ Cl ₂	+214 ± 10	<i>e</i>
ClB(NMe ₂) ₂	neat liquid	+341 ± 5	<i>e</i>
BrB(NMe ₂) ₂	neat liquid	+284 ± 5	<i>e</i>
IB(NMe ₂) ₂	neat liquid	+293 ± 10	<i>e</i>
FB(NEt ₂) ₂	neat liquid	+371 ± 10	<i>e</i>
ClB(NEt ₂) ₂	neat liquid	+308 ± 10	<i>e</i>
BrB(NEt ₂) ₂	neat liquid	+289 ± 10	<i>e</i>
IB(NEt ₂) ₂	neat liquid	+275 ± 10	<i>e</i>
Cl ₂ BNMe ₂	neat liquid	+301 ± 5	<i>e</i>
Br ₂ BNMe ₂	neat liquid	+263 ± 5	<i>e</i>
I ₂ BNMe ₂	neat liquid	+259 ± 5	<i>e</i>
Cl ₂ BNEt ₂	neat liquid	+269 ± 5	<i>e</i>
Br ₂ BNEt ₂	neat liquid	+251 ± 5	<i>e</i>
I ₂ BNEt ₂	neat liquid	+242 ± 5	<i>e</i>
F ₂ BN- <i>i</i> -Pr ₂	neat liquid	+299 ± 5	<i>e</i>
H ₃ N-BH ₃	MeOCH ₂ CH ₂ OMe	+374 ± 5	<i>f</i>
H ₃ N-BMe ₃	neat liquid	+340 ± 5	<i>f</i>
H ₃ N-BEt ₃	neat liquid	+356 ± 5	<i>f</i>
MeH ₂ N-BH ₃	MeOCH ₂ CH ₂ OMe	+371 ± 5	<i>f</i>
MeH ₂ N-BMe ₃	MeOCH ₂ CH ₂ OMe	+339 ± 5	<i>f</i>
MeH ₂ N-BEt ₃	neat liquid	+347 ± 5	<i>f</i>
Me ₂ HN-BH ₃	MeOCH ₂ CH ₂ OMe	+364 ± 5	<i>f</i>
Me ₂ HN-BMe ₃	neat liquid	+348 ± 5	<i>f</i>
Me ₂ HN-BEt ₃	neat liquid	+360 ± 10	<i>f</i>
Me ₃ N-BH ₃	CH ₂ Cl ₂	+344 ± 5	<i>f</i>
Me ₃ N-BMe ₃	CH ₂ Cl ₂	+349 ± 5	<i>f</i>
Me ₃ N-BEt ₃	CHCl ₂ CHCl ₂	+349 ± 10	<i>f</i>
 NH-BH ₃	MeOCH ₂ CH ₂ OMe	+381 ± 5	<i>f</i>
 NH-BMe ₃	neat liquid	+361 ± 5	<i>f</i>
 NH-BEt ₃	neat liquid	+363 ± 5	<i>f</i>

TABLE X—*cont.*

Compound	Solvent or state	Nitrogen screening constant	Notes
 NH-BH ₃	CH ₂ Cl ₂	+336 ± 5	<i>f</i>
Et ₃ N-BH ₃	neat liquid	+339 ± 5	<i>f</i>
EtH ₂ N-BMe ₃	neat liquid	+326 ± 5	<i>f</i>
<i>i</i> -PrH ₂ N-BMe ₃	neat liquid	+298 ± 5	<i>f</i>
<i>t</i> -BuH ₂ N-BMe ₃	neat liquid	+290 ± 5	<i>f</i>

^a Ref. 87, ¹⁴N spectra, referred to external CH₃NO₂.

^b Ref. 88, ¹⁴N spectra, referred to external CH₃NO₂.

^c Ref. 89, ¹⁴N spectra, referred to internal CH₃NO₂; no correction is applied to the data in this Table.

^d Ref. 90, ¹⁴N spectra, originally referred to saturated aqueous NaNO₃, +3.7 ppm from neat CH₃NO₂ (Table VII), as external standard.

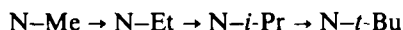
^e Ref. 91, ¹⁴N spectra, as in footnote (d); accuracy is reported as ±2 ppm for signals of width below 300 Hz and ±5 ppm otherwise, however, shifts reported in this work for a number of simple amines show discrepancies with the results of precise ¹⁴N and ¹⁵N measurements (Tables VII and VIII) which make ±5 and ±10 ppm. limits more reasonable; recalculation of shifts to external CH₃NO₂ scale (this does not introduce an error larger than 0.2 ppm) gives for (CH₃)₃N in H₂O, +369 ppm (ref. 91) and +361.7 (Table VII), for neat BuNH₂, +353 ppm (ref. 91) and +359.2 ppm (Table VII), for NH₃ in H₂O, +380 ppm and 378.4 ppm, respectively, for NH₃ in Et₂O, +380 and +387.1 ppm, respectively, for neat Et₂NH, +340 and +334.0 ppm, respectively; this should also apply to results from footnotes (d) and (f).

^f Ref. 92, ¹⁴N spectra, as in footnotes (d) and (e).

^g Ref. 93, ¹⁴N spectra, as in footnotes (d) and (e).

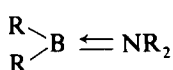
+349 ppm, is almost the same as in the case of methylsilatrane. One should note, however, that the nitrogen chemical shifts of this class of compounds are only slightly to high frequency of those for the corresponding amines, and the differences do not exceed 7 ppm.

The shifts of silylamines of the type R₃SiNR₂ (Table X, notes c and d) show the same β-effect as found in the case of amines, i.e., a high frequency shift along the sequence:

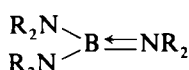


A direct comparison with amines which have a hydrogen atom instead of the SiR₃ moiety, made in ref. 90, does not seem to be of much significance since it neglects hydrogen bonding effects, not to speak of the obvious differences between H and SiR₃. A survey of the data in Tables VIII and X indicates that as far as nitrogen chemical shifts are concerned, the trialkylsilyl group roughly corresponds to the CH₃ group.

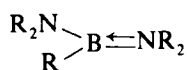
The chemical shifts in the silylaminoboranes, $R_2B-N(R')SiMe_3$ (Table X, note d), are to much higher frequencies than those of the amines. (90) The shifts are rather insensitive to changes in R , but they show the β -effect upon changes in R' . The same effect has been observed (91) for some aminoboranes, $R_2B-NR'_2$ (Table X, note e). The chemical shifts of the aminoboranes have been discussed (91) in terms of the delocalization of the lone electron pairs of the nitrogen atoms in the structural systems [2] to [5].



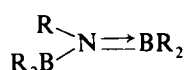
[2]



[3]



[4]



[5]

The nitrogen chemical shifts of the tetracoordinate boron–nitrogen adducts, $R_3B \leftarrow NR'_3$ (Table X, note f), have been measured. (92) If we compare the data for the corresponding amines (Table VIII) with those for the adducts, high-frequency shifts are observed upon the formation

TABLE XI

Nitrogen screening constants of some ammonium ions in ppm, referred to external neat nitromethane

Compound	Solution	Nitrogen screening constant	Notes
$NH_4^+(Cl^-, NO_3^-)$	H_2O , HCl , HNO_3	+359.1 to +349.9	<i>a</i>
$MeNH_3^+(Cl^-)$	5 M in 1 M HCl	+357.4 \pm 0.3	<i>b</i>
$Me_2NH_2^+(Cl^-)$	5 M in 1 M HCl	+355.3 \pm 0.3	<i>b</i>
$Me_3NH^+(Cl^-)$	5 M in 1 M HCl	+348.1 \pm 0.3	<i>b</i>
$Me_4N^+(Cl^-)$	0.30 M in H_2O	+337.67 \pm 0.11	<i>c</i>
	6.03 M in H_2O (satd.)	+336.69 \pm 0.09	<i>c</i>
	satd. in H_2O (?)	+336.7 \pm 0.2	<i>d</i>
$Me_4N^+(I^-)$	0.30 M in H_2O	+337.31 \pm 0.13	<i>c</i>
	ca. 0.3 M in H_2O	+337.8 \pm 0.2	<i>d</i>
$Me_3N^+CH_2COO^-$	0.2 M in H_2O , pH 7.10	+335 \pm 1	<i>e</i>
$Me_3N^+CH_2CH_2OH (Cl^-)$	0.1 M in H_2O , pH 7.1	+333 \pm 1	<i>e</i>
$Et_4N^+(Cl^-)$	0.30 M in H_2O	+316.29 \pm 0.13	<i>c</i>
	4.58 M in H_2O (satd.)	+315.84 \pm 0.09	<i>c</i>

^a See Table VII.

^b Ref. 94, ^{15}N spectra of labelled compounds, originally referred to liquid NH_3 , +381.93 ppm from neat CH_3NO_2 , Table VII; no bulk susceptibility correction.

^c Ref. 61, see also Table VII for comments; ^{14}N spectra, concentric spherical sample containers.

^d Ref. 36, natural-abundance ^{15}N spectra; $(CH_3)_4NCl$ concentration reported as 12 M, probably saturated, i.e., ca. 6 M in water.

^e Ref. 82, ^{14}N spectra, see footnote (b) in Table XII.

of the latter. A rather good linear correlation is found (92) between the ^{14}N and ^{11}B chemical shifts of the adducts as well as between the nitrogen chemical shifts of the adducts and the ^{13}C chemical shifts of the isoelectronic alkanes.

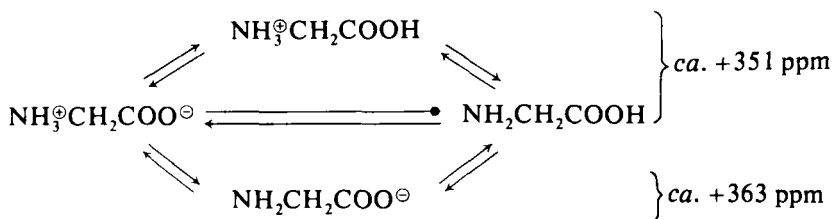
C. Ammonium ions

Relatively little new information on the shifts of ammonium ions has been reported (Table XI) compared with the volume of older data (ref. 1d, pp. 179–184). However, precise measurements of the nitrogen chemical shift of the NH_4^+ ion (Tables VII and XI) indicate that the shift is quite dependent on the gegenion and on medium effects (61, 218) (Section III). There is an evident β -effect on the shift of NR_4^+ when $\text{R} = \text{CH}_3$ is replaced by $\text{R} = \text{C}_2\text{H}_5$ (Table XI). The protonation of an amine usually results in a high frequency shift of the nitrogen resonance, but the magnitude of the effect is variable.

D. Amino acids, peptides and related structures

During the review period, amino acids and their derivatives have been extensively investigated by means of nitrogen NMR spectroscopy. Amino acids contain amino groups which, under appropriate conditions, may be protonated to give the corresponding ammonium ions. Peptides, in addition to possessing terminal amino groups or their derivatives, contain amide-type nitrogen atoms in their peptide links. Distinction between the latter and the former by nitrogen NMR is usually straightforward since the amide-type nitrogen atoms give resonance signals at appreciably higher frequencies, by *ca.* 100 ppm, than those for the amino groups and ammonium ions (Tables XII and XIII).

Amino acids exist in several forms in aqueous solutions, such as those for the simplest amino acid, glycine [6]. The forms present depend upon



[6]

the state of protonation of the amino and carboxyl moieties, thus the corresponding chemical shifts in nitrogen NMR are dependent on the pH of the solution, particularly if more than one form is present in the solution. ^{15}N measurements on aqueous glycine within a pH range of

TABLE XII

Nitrogen screening constants of some amino-acids in ppm (± 0.3) referred to external neat nitromethane

Compound	Solvent	Nitrogen screening constant	Notes
Glycine	H ₂ O, pH 0.5	+352.2	<i>a</i>
	pH 2.8	+351.0	<i>a</i>
	pH 3.7	+350.4	<i>a</i>
	pH 6.0	+350.4	<i>a</i>
	pH 6.3	+350.2	<i>a</i>
	pH 6.6	+350.1	<i>a</i>
	pH 7.25	+352 ($\pm ?$)	<i>b</i>
	pH 13.6	+362.6	<i>a</i>
	H ₂ O, 6 M HCl	+350.4	<i>c</i>
	6 M NaOH	+354.7	<i>c</i>
Alanine	H ₂ O, 6 M HCl	+337.1	<i>c</i>
	H ₂ O	+337.3	<i>c</i>
	H ₂ O, pH 7.42	+338 ($\pm ?$)	<i>b</i>
Valine	H ₂ O, 6 M HCl	+344.0	<i>c</i>
	H ₂ O	+344.1	<i>c</i>
	H ₂ O, pH 7.42	+345 ($\pm ?$)	<i>b</i>
Leucine	H ₂ O, 6 M HCl	+338.7	<i>c</i>
	H ₂ O, pH 7.47	+342 ($\pm ?$)	<i>b</i>
Iso-Leucine	H ₂ O, pH 7.47	+340 ($\pm ?$)	<i>b</i>
Serine	H ₂ O, pH 2.4	+344.0	<i>d</i>
	pH 7.14	+346 ($\pm ?$)	<i>b</i>
Threonine	H ₂ O, pH 7.05	+348 ($\pm ?$)	<i>b</i>
Aspartic acid	H ₂ O, 6 M HCl	+340.3	<i>c</i>
	H ₂ O, pH 7.29	+342 ($\pm ?$)	<i>b</i>
Asparagine	H ₂ O, pH 0.8	+338.1 (CHNH ₃ ⁺)	<i>d</i>
		+268.1 (CONH ₂)	<i>d</i>
	H ₂ O, pH 7.26	+339.7 ($\pm ?$) (CHNH ₂)	<i>b</i>
		+267.9 ($\pm ?$) (CONH ₂)	<i>b</i>
Glutamine	H ₂ O, pH 1.0	+323.5 (CHNH ₃ ⁺)	<i>d</i>
		+251.7 (CONH ₂)	<i>d</i>
	H ₂ O, pH 7.35	+340 ($\pm ?$) (CHNH ₂)	<i>b</i>
		+270 ($\pm ?$) (CONH ₂)	<i>b</i>
Glutamic acid	H ₂ O, 6 M HCl	+338.9	<i>c</i>
	H ₂ O, pH 7.50	+338 ($\pm ?$)	<i>b</i>
Lysine	H ₂ O, pH 2.6	+345.9 (α)	<i>d</i>
		+338.9 (ϵ)	<i>d</i>
	H ₂ O, pH 7.38	+341 ($\pm ?$) (α)	<i>b</i>
		+348 ($\pm ?$) (ϵ)	<i>b</i>

TABLE XII—*cont.*

Compound	Solvent	Nitrogen screening constant	Notes
Hydroxy-lysine	H ₂ O, pH 7.20	+342 (±?) (α)	<i>b</i>
		+354 (±?) (ϵ)	<i>b</i>
Histidine	H ₂ O, pH 7.09	+341 (±?)	<i>b</i>
		+203 (±?) (imido-N3)	<i>b</i>
		+153 (±?) (imido-N1)	<i>b</i>
Arginine	H ₂ O, pH 2.1	+338.7 (α)	<i>d</i>
		+307.4 (ω)	<i>d</i>
		+294.9 (imino- ϵ)	<i>d</i>
	H ₂ O, pH 7.45	+341 (±?) (α)	<i>b</i>
		+318 (±?) (others)	<i>b</i>
Phenylalanine	H ₂ O	+341.0	<i>c</i>
	H ₂ O, pH 7.2	+352 (±?)	<i>b</i>
	pH 9.4	+329 (±?)	<i>b</i>
Tyrosine	H ₂ O, 6 M HCl	+340.5	<i>c</i>
	H ₂ O, pH 10.56	+318 (±?)	<i>b</i>
Tryptophan	H ₂ O, pH 7.15	+349 (±?) (α)	<i>b</i>
		+299 (±?) (NH)	<i>b</i>
Cysteine	H ₂ O, pH 0.0	+338.1	<i>d</i>
	pH 7.32	+341 (±?)	<i>b</i>
Cystine	H ₂ O, pH 10.58	+339 (±?)	<i>b</i>
Cysteic acid	H ₂ O, pH 7.20	+342 (±?)	<i>b</i>
Methionine	H ₂ O, pH 7.10	+341 (±?)	<i>b</i>
Ethionine	H ₂ O, pH 10.80	+347 (±?)	<i>b</i>
Proline	H ₂ O, pH 7.35	+328 (±?)	<i>b</i>
Hydroxy-proline	H ₂ O, pH 7.50	+329 (±?)	<i>b</i>
Ornithine	H ₂ O, 6 M HCl	+338.9 (α)	<i>c</i>
	H ₂ O	+339.1 (α)	<i>c</i>
	H ₂ O, pH 7.15	+345 (±?) (α)	<i>b</i>
		+349 (±?) (δ)	<i>b</i>
α -Aminobutyric acid	H ₂ O, pH 7.2	+342 (±?)	<i>b</i>
α,γ -Diaminobutyric acid	H ₂ O, pH 7.42	+342 (±?) (α)	<i>b</i>
		+349 (±?) (γ)	<i>b</i>
Citrulline	H ₂ O, pH 0.1	+340.9 (α)	<i>d</i>
		+304.0 (ω)	<i>d</i>
		+291.7 (imino- ϵ)	<i>d</i>
Taurine	H ₂ O, pH 7.20	+349 (±?)	<i>b</i>
Penicillamine	H ₂ O, pH 3.83	+342 (±?)	<i>b</i>
3-Nitrotyrosine	H ₂ O pH 10.59	+343 (±?) (NH ₂)	<i>b</i>
Ethylglycinate hydrochloride	H ₂ O, pH 0.5–7.3	+353.1	<i>a</i>

^a Ref. 66, ¹⁵N spectra of labelled glycine; originally referred to what is reported as external 10 M H¹⁵NO₃, +6.1 ppm from neat CH₃NO₂, probably *ca.* 2 M HNO₃; for comments see footnote (f) in Table VIII; similar measurements for glycine are recorded in ref. 70, and referred to what is reported as saturated aqueous ¹⁵NH₄Cl, but recalculation according to Table VII gives a discrepancy of *ca.* 9 ppm with the data from ref. 66, reasonable agreement may be obtained by assuming that saturated aqueous NH₄NO₃, not NH₄Cl, has actually been

0.5 to 13.6 (66, 70), (Table XII), indicate that the shift of the NH_3^+ group is almost the same in the cation and in the zwitterion, *ca.* +351 ppm, whilst the NH_2 group (in alkaline solutions) is characterized by a shift of about +363 ppm. The same has been observed in ^{15}N doubly-labelled glycylglycine, (96) where the corresponding values are about +353 and +364 ppm (Table XIII). The amide nitrogen atom in glycylglycine (96) shows a difference in its nitrogen chemical shift depending on the state of the carboxyl moiety, *ca.* +264 ppm in $\text{RCONHCH}_2\text{COO}^-$, and *ca.* +270 ppm in $\text{RCONHCH}_2\text{COOH}$. Thus, the processes of protonation and deprotonation of NH_2 , NH_3^+ , COO^- and COOH , respectively, are independently visible in the nitrogen NMR spectra of such peptides.

The inertness of the nitrogen chemical shift of the NH_3^+ moiety to the state of the carboxyl group has been shown for a number of amino acids (95) (Table XII, note c). The entire range of occurrence of NH_3^+ and NH_2 signals is about +335 to +365 ppm (Tables XII and XIII). The data on some simple dipeptides (74) indicate that the amino resonance can prove useful as a means of identification of N-terminal residues in the peptides (Table XIII).

The nitrogen atoms which are involved in peptide linkages are characterized by a range of nitrogen chemical shifts from about +250 to 270 ppm (Tables XII and XIII). In simple dipeptides, (74) the shift is dependent on the nature of the C-terminal residue as well as on the nature of the preceding N-terminal residue.

The pH-dependent equilibrium in aqueous solutions of arginine has been interpreted (69) in terms of the observed ^{15}N chemical shifts, shown in [7] to [10]. However, it is not clear why the signal at the lowest frequency, +349 ppm from CH_3NO_2 observed at pH 13.5, should not be assigned to the $-\text{CH}(\text{NH}_2)\text{COO}^-$ moiety rather than to the guanidine residue, and that at +295 ppm to an averaged signal of the $\text{H}_2\text{NC}(=\text{NH})-$ group. The data given in Table XV suggest that the

used (see Table VII), the glycine used in both ref. 66, and ref. 70, is probably contaminated with traces of paramagnetic impurities, as shown in ref. 78.

^b Ref. 82, ^{15}N spectra, superconducting solenoid operating at 7.5 T, pulsed Fourier-transform technique; originally referred to external NO_3^- ion in 4.5 M NH_4NO_3 in 3 M HCl, +6.30 ppm from neat CH_3NO_2 according to Table VII; concentrations in H_2O *ca.* 0.1–0.2 M; errors in chemical shifts not reported, probably from ± 1 to ± 10 ppm depending on signal width and signal overlap.

^c Ref. 95, ^{15}N spectra of labelled amino acids, referred to glycine in H_2O at isoelectric point, +350.1 ppm from neat CH_3NO_2 (this Table).

^d Ref. 69, natural-abundance ^{15}N spectra; assignments based upon decoupling effects; originally referred to "external HNO_3 ", recalculated to neat CH_3NO_2 with the valine shift of +344.0 ppm (this Table); thus, "external HNO_3 " shift should be *ca.* +8.1 ppm from neat CH_3NO_2 which corresponds to *ca.* 4 M HNO_3 , Table VII.

TABLE XIII

Nitrogen screening constants of some peptides in ppm, referred to external neat nitromethane

Compound	Solvent	Screening constants		Notes
		Amine-ammonium nitrogen	Amide nitrogen	
Glycyl-glycine	H ₂ O, 1-0.05 M,			
	pH 12-9.5	+364.5 ± 0.2 (NH ₂)		<i>a</i>
	pH 12-5		+264.4 ± 0.2 (CONHCH ₂ COO [⊖])	<i>a</i>
	pH 7-2.5	+352.8 ± 0.2 (NH ₃ [⊕])		<i>a</i>
	pH 1.5-1		+270.2 ± 0.2 (CONHCH ₂ COOH)	<i>a</i>
	0.2 M, pH 5.8	+353.3 ± 0.2	+264.8 ± 0.2	<i>b</i>
	0.2 M, pH 7.1	+356 (±?)	+268 (±?)	<i>c</i>
	0.2 M, pH 5.6	+339.4 ± 0.2	+264.8 ± 0.2	<i>b</i>
Alanyl-glycine	0.2 M, pH 5.9	+344.6 ± 0.2	+260.2 ± 0.2	<i>b</i>
Valyl-glycine	0.2 M, pH 5.4	+341.2 ± 0.2	+261.5 ± 0.2	<i>b</i>
Leucyl-glycine	0.2 M, pH 5.1	+352.8 ± 0.2	+250.3 ± 0.2	<i>b</i>
Glycyl-alanine	0.2 M, pH 6.2	+339.8 ± 0.2	+250.3 ± 0.2	<i>b</i>
Alanyl-alanine	0.2 M, pH 6.1	+345.0 ± 0.2	+247.0 ± 0.2	<i>b</i>
Valyl-alanine	0.2 M, pH 5.4	+341.1 ± 0.2	+248.4 ± 0.2	<i>b</i>
Leucyl-alanine	0.2 M, pH 5.7	+353.0 ± 0.2	+256.6 ± 0.2	<i>b</i>
Glycyl-valine	0.2 M, pH 5.8	+339.5 ± 0.2	+256.6 ± 0.2	<i>b</i>
Alanyl-valine	0.2 M, pH 5.6	+345.0 ± 0.2	+252.2 ± 0.2	<i>b</i>
Valyl-valine	0.2 M, pH 5.7	+341.2 ± 0.2	+254.4 ± 0.2	<i>b</i>
Leucyl-valine	0.2 M, pH 5.8	+353.3 ± 0.2	+252.5 ± 0.2	<i>b</i>
Glycyl-leucine	0.2 M, pH 5.3	+339.5 ± 0.2	+253.1 ± 0.2	<i>b</i>
Alanyl-leucine	0.2 M, pH 5.1	+345.3 ± 0.2	+249.3 ± 0.2	<i>b</i>
Valyl-leucine	0.2 M, pH 5.0	+341.6 ± 0.2	+250.6 ± 0.2	<i>b</i>
Leucyl-leucine	0.1 M, pH 7.1	+354 (±?)	?	<i>c</i>
Glycyl-tyrosine	0.1 M, pH 7.2	+358 (±?)	?	<i>c</i>
Glycyl-histidine	0.1 M, pH 7.2	+354 (±?)	?	<i>c</i>

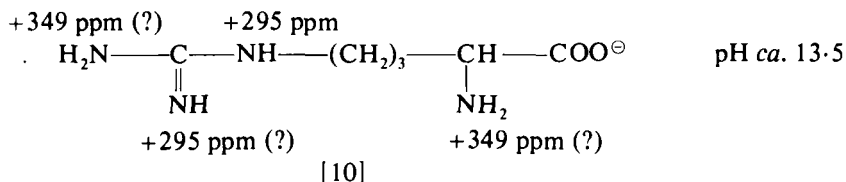
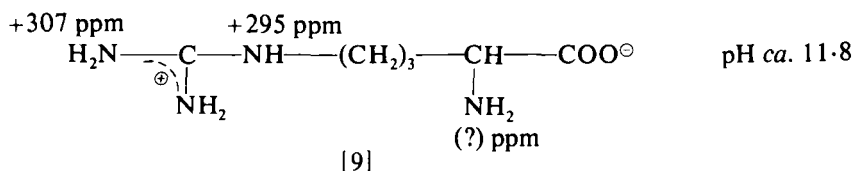
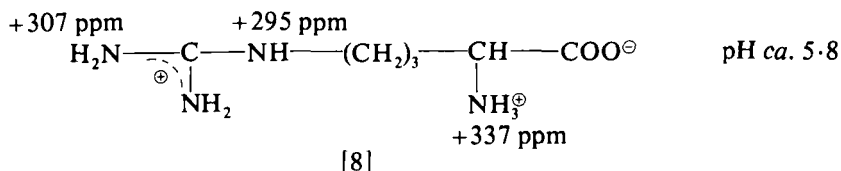
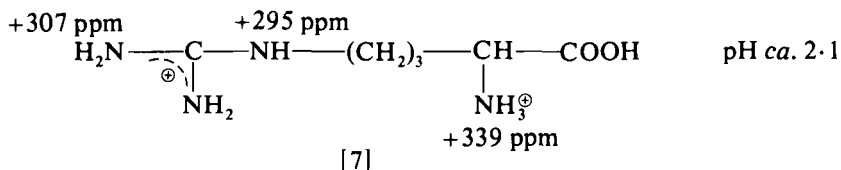
^a Ref. 96, ¹⁵N spectra of doubly labelled glycyl-glycine, originally referred to external 4 M ¹⁵NH₄[⊕] NO₃[⊖] in 2 M HNO₃, +359.06 ppm from neat CH₃NO₂, Table VII; the entire titration curves are reported.

^b Ref. 74, natural-abundance ¹⁵N spectra at 18.23 MHz, originally referred to external 1.0 M D¹⁵NO₃, +4.43 ppm from neat CH₃NO₂, Table VII.

^c Ref. 82, see footnote (b) in Table XII.

=NH signal of the guanidine residue should appear at about +200 ppm from CH₃NO₂.

¹⁵N NMR spectroscopy has started to probe into quite large molecular systems composed of amino acid residues. An investigation of the ¹⁵N spectrum of hemoglobin which is ¹⁵N enriched in the glycydyl residues (97, 220) reveals a doublet, ¹J(N-H) = 94 Hz, at 271.1 ppm



from CH_3NO_2 , and a partially resolved shoulder at +262.5 ppm. These signals are attributed to the NH groups that are hydrogen-bonded to water (+262.5 ppm), and to those that are intramolecularly hydrogen-bonded to peptide carbonyl groups (+271.1 ppm). This is in agreement with the data on dimethylformamide (Table VII) where an appreciable high-frequency shift is observed upon dilution with H_2O (from +277.0 to +264.6 ppm). Recent developments in the technique of ^{15}N NMR have produced the possibility of obtaining natural-abundance ^{15}N spectra for a number of biopolymers (73) such as some enzymes (lysozyme and related molecules), protamines, pepsin, hemoglobin, vitamin B_{12} and transfer ribonucleic acids (tRNA). The spectra contain partially resolved resonances in the amide region, +248 to +270 ppm, the arginine guanidino-NH at +294.7 ppm, the guanidino- NH_2^{\oplus} signal at +307.9 ppm, the NH_3^{\oplus} moieties in the region of +340 to +348 ppm and the NH terminal proline amino groups at +326 ppm. In the case of yeast tRNA, it is possible to assign the observed signals by reference to the corresponding data on monophosphates of guanosine (G), cytidine (C), adenosine (A) and uridine (U): +306.6 ppm (G), +301.3 ppm (A),

+285.4 ppm (C), +232.4 ppm (G, U), +221.7 ppm (U), +170 to +184 ppm (C), +140 to +156 ppm (G, A), where all the shifts have been recalculated to the external neat CH_3NO_2 scale.

Nuclear Overhauser effect enhancements (NOE) in the ^{15}N spectra of such biopolymers give some information about the mobility of various sections of these molecules. NOE-induced signal nulling has been considered in the example of a decapeptide, Gramicidin-S. (77) Anomalies in the NOE for the ^{15}N spectra of glycine at various pH values have been claimed to constitute a means of observation of proton exchange rates and molecular rotations, (66, 70) but this has subsequently been shown to result from traces of paramagnetic impurities in the samples of glycine. (78) Line widths of the ^{14}N resonances of some simple amino acids have been investigated (98) as a function of pH in order to obtain information on the weak complexes formed between amino acids and nucleic acids.

The high-resolution ^{15}N spectrum using natural abundance of ^{15}N in solid glycine, obtained by the pulsed decoupling technique, shows no detectable chemical shift anisotropy. (55)

TABLE XIV

Nitrogen screening constants of some hydrazines in ppm (+0.5), referred to external neat nitromethane

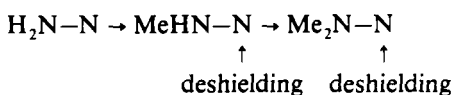
Compound (neat liquid unless stated otherwise)	Nitrogen screening constants			Notes
	NH_2	NHR	NR_2	
H_2NNH_2	+334.8	—	—	<i>a</i>
$\text{H}_2\text{NNH}_2 (\text{H}_2\text{O})$	+330.7	—	—	<i>b</i>
MeNHNH_2	+305.5	+328.0	—	<i>a</i>
Me_2NNH_2	+281.4	—	+322.7	<i>a</i>
MeNHNHMe	—	+306.6	—	<i>a</i>
Me_2NNHMe	—	+285.3	+307.7	<i>a</i>
PhNHNH_2	+319.5	+294.2	—	<i>a</i>
	+320.5	+295.6	—	<i>b</i>
PhNHNHPh (dioxane)	—	+287.6	—	<i>a</i>
Ph_2NNH_2	+293.2	—	not observed	<i>a</i>

^a Ref. 100, ^{15}N natural-abundance spectra, originally referred to "external HNO_3 ", probably +6.1 ppm from neat CH_3NO_2 for comments, see footnote (f) in Table VIII; assignments for methyl-hydrazines are based on assumption of additive effects of CH_3 groups as well as ^{15}N labelling at N-2 of 1,1-dimethylhydrazine; assignments for phenylhydrazines based on decoupling effects and NOE.

^b Ref. 99, ^{15}N natural-abundance spectra, assignments for PhNHNH_2 are reversed in original paper.

E. Hydrazines

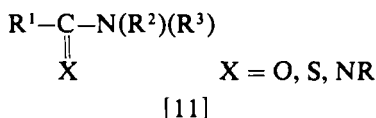
The nitrogen resonance signals of hydrazines occur (99, 100) in a range of about +340 to +280 ppm, as shown in Table XIV. This means that their shifts are, on the average, to higher frequencies than those of amines, but the corresponding ranges of shifts are overlapping (Tables VIII and IX). There seems to be a considerable β -effect (100) transmitted through a nitrogen atom.



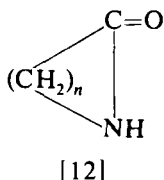
since a regression analysis gives a value of *ca.* -25 ppm per methyl group. There seems to be also an α -effect of about -4 ppm per methyl, but its significance is less certain because the measurements were made on neat liquids, and the intermolecular effects on the shifts may be of the same order of magnitude.

F. Amides, ureas, guanidines and related structures

The compounds considered here are represented by the general structure [11]. Relatively little new data on amides, in comparison with



those furnished in ref. 1d, have been reported. Cyclic amides (lactams) have been shown (76) to have nitrogen chemical shifts which are quite independent of the ring size, [12], where *n* varies from 3 to 8 (Table



XV). However, some important information may be obtained from nitrogen NMR spectra concerning isomeric and tautomeric forms where amide-type structures are involved. It has been shown (101) that nitrogen chemical shifts are far superior to ^{13}C shifts in the determination of the tautomeric equilibria of pyridone, [13a]-hydroxypyridine, [13b], systems. This point is discussed further in Section V K.

TABLE XV

Nitrogen screening constants of some $R^1C(=X)N(R^2)(R^3)$ compounds (amides, ureas, guanidines, and related structures) in ppm, referred to external neat nitromethane

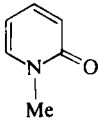
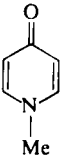
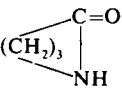
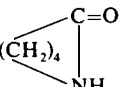
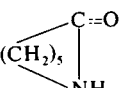
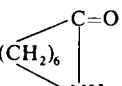
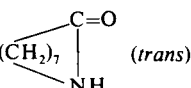
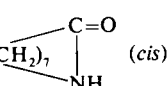
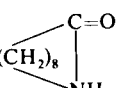
Compound	Solvent or state	Nitrogen screening constant	Notes
NH_2CHO	neat liquid	$+267.7 \pm 0.2$	<i>a</i>
$MeNHCHO$	neat liquid	$+270.2 \pm 0.2$	<i>a</i>
Me_2NCHO	neat liquid	$+277.00 \pm 0.09$	<i>b</i>
		$+276.4 \pm 0.2$	<i>a</i>
	0.30 M in H_2O	$+264.58 \pm 0.31$	<i>b</i>
Bu_2NCHO	neat liquid	$+254.5 \pm 0.2$	<i>a</i>
NH_2COOEt	neat liquid	$+308.2 \pm 0.2$	<i>a</i>
$EtNHCOOEt$	neat liquid	$+294.9 \pm 0.2$	<i>a</i>
NH_2CONH_2	H_2O (?)	$+303.6 \pm 0.2$	<i>a</i>
	H_2O , satd.	$+306.3 \pm 0.7$	<i>c</i>
$Me_2NCONMe_2$	neat liquid	$+317.8 \pm 0.2$	<i>a</i>
		$+320.5 \pm 0.2$	<i>c</i>
	H_2O , satd.	$+316 \pm 2$	<i>c</i>
$MeNHCONHMe$	H_2O , satd.	$+301 \pm 3$	<i>c</i>
$Me_2NC(=NH)OMe$	neat liquid	$+320 \pm 4$ ($=NMe_2$)	<i>c</i>
		$+283.3 \pm 0.4$ ($=NH$)	<i>c</i>
NH_2CSNH_2	H_2O , satd.	$+272.8 \pm 0.4$	<i>c</i>
Me_2NCSMe_2	Me_2CO , satd.	$+301.3 \pm 0.9$	<i>c</i>
$Me_2NC(=NMe)SMe$	neat liquid	$+300 \pm 4$ ($=NMe_2$)	<i>c</i>
		$+121 \pm 1$ ($=NMe$)	<i>c</i>
$NH_2C(=NH)NH_2$	0.2 M in H_2O pH 7.11	$+307$ ($\pm?$)	<i>d</i>
	0.05 M in H_2O (alkaline soln.)	$+188$ ($\pm?$)	<i>d</i>
$Me_2NC(=NH)NMe_2$	neat liquid	$+333 \pm 2$ ($=NMe_2$)	<i>c</i>
		$+207.8 \pm 0.7$ ($=NH$)	<i>c</i>
$Me_2NC(=NMe)NMe_2$	neat liquid	$+334 \pm 2$ ($=NMe_2$)	<i>c</i>
		$+187 \pm 1$ ($=NMe$)	<i>c</i>
	Me_2CO , 1:3 v/v	$+216 \pm 2$	<i>e</i>
	neat liquid	$+215 \pm 3$	<i>e</i>
	$MeOH$, 1:3 v/v	$+214 \pm 1$	<i>e</i>
	Me_2CO , 1:3 v/v	$+248 \pm 2$	<i>e</i>
	$MeOH$, 1:3 v/v	$+240 \pm 3$	<i>e</i>

TABLE XV—*cont.*

Compound	Solvent or state	Nitrogen screening constant	Notes
	CHCl ₃ , 2.0 M	+263.7 ± 0.2	<i>f</i>
	DMSO, 2.0 M	+264.5 ± 0.2	<i>f</i>
	CHCl ₃ , 2.0 M	+264.1 ± 0.2	<i>f</i>
	DMSO, 2.0 M	+265.8 ± 0.2	<i>f</i>
	CHCl ₃ , 2.0 M	+260.8 ± 0.2	<i>f</i>
	DMSO, 2.0 M	+261.8 ± 0.2	<i>f</i>
	CHCl ₃ , 2.0 M	+260.7 ± 0.2	<i>f</i>
	DMSO, 2.0 M	+261.9 ± 0.2	<i>f</i>
	CHCl ₃ , 2.0 M	+260.8 ± 0.2	<i>f</i>
	DMSO, 2.0 M	+260.9 ± 0.2	<i>f</i>
	95% EtOH, 2.0 M	+258.6 ± 0.2	<i>f</i>
	CHCl ₃ , 2.0 M	+257.8 ± 0.2	<i>f</i>
	DMSO, 2.0 M	+258.8 ± 0.2	<i>f</i>
	95% EtOH, 2.0 M	+255.9 ± 0.2	<i>f</i>
	CHCl ₃ , 2.0 M	+259.9 ± 0.2	<i>f</i>
	DMSO, 2.0 M	+260.4 ± 0.2	<i>f</i>
Me(CH ₂) ₇ CONH(CH ₂) ₆ Me	CHCl ₃ , 2.0 M	+260.9 ± 0.2	<i>f</i>
	95% EtOH, 2.0 M	+259.0 ± 0.2	<i>f</i>

^a Ref. 36, natural-abundance ¹⁵N spectra.

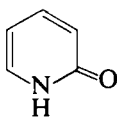
^b Ref. 61, see also Table VII for comments; ¹⁴N spectra, concentric spherical sample containers, full lineshape analysis.

^c Ref. 38, ¹⁴N spectra, originally referred to either internal KNO₃ (for aqueous solutions, +3.5 ppm from neat CH₃NO₂, Table VII) or CH₃NO₂ (recalculated according to Table VII); differential saturation technique and lineshape analysis (63).

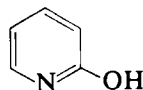
^d Ref. 82, ¹⁴N spectra, see footnote (b) in Table XII.

^e Ref. 101, ¹⁴N spectra, originally referred to internal CH₃NO₂, recalculated according to Table VII.

^f Ref. 76, ¹⁵N natural-abundance spectra, originally referred to 1.0 M HNO₃, +4.4 ppm from neat CH₃NO₂, Table VII.



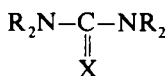
(a)



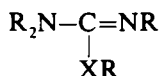
(b)

[13]

The isomeric structures of the amido, [14a], and iso-amido type, [14b], have been investigated by nitrogen NMR using as examples the



(a)

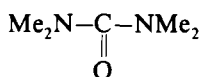


(b)

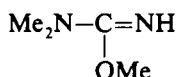
[14]

X = O, S, NR

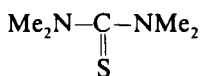
methyl derivatives of urea, thiourea and guanidine. (38) It is found (38) that there is rather little difference in the chemical shifts of the NR_2 moieties between the amido- [15] and isoamido-structures [16] but there



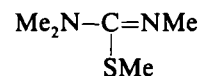
+ 320 ppm



+ 320 ppm + 238 ppm



+ 301 ppm

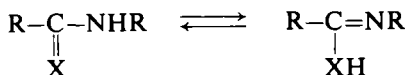


+ 300 ppm + 121 ppm

[15]

[16]

is a large high-frequency shift for the $=\text{NR}$ moiety in the isoamido system of derivatives of urea, and larger still for the thio-derivatives. The shifts for systems where tautomerism is possible due to the presence of mobile hydrogen atoms [17] show that in urea derivatives the



[17]

contribution of the iso-amide structures is insignificant. However, it is significant (up to 30%) in thiourea derivatives. This has been used as an argument to show that the high-frequency nitrogen shifts of thioamides, compared with amides, (1d) result from differences in the position of the

tautomeric equilibrium rather than from appreciable intrinsic differences in the shifts of the amido and thioamido structures.

G. Cyano, cyanato groups and related structures

It has already been shown (ref. 1d, pp. 197–204) that nitrogen chemical shifts clearly differentiate between various structures which contain a CN moiety in a linear system of three atoms:

R—CN	nitriles	+120 to +140 ppm
R—NC	isonitriles	+180 to +220 ppm
R—OCN	cyantes	ca. +200 ppm
R—SCN	thiocyanates	ca. +100 ppm
R—NCO	isocyanates	+330 to +365 ppm
R—NCS	isothiocyanates	+260 to +290 ppm
R—CNO	fulminates (nitrile N-oxides)	+160 to +180 ppm

It is interesting to note that the shifts of the ambidentate ligands NCO^\ominus and NCS^\ominus appear almost mid-way between those for the corresponding

TABLE XVI

Nitrogen screening constants of some cyanides, cyanates, and fulminates in ppm, referred to external neat nitromethane

Compound	Solvent or state	Nitrogen screening constant	Notes
MeCN	neat liquid	$+136.40 \pm 0.10$	<i>a</i>
	CCl_4 , 0.3 M	$+127.44 \pm 0.28$	<i>a</i>
	Me_2CO , 0.3 M	$+132.99 \pm 0.13$	<i>a</i>
	H_2O , 0.3 M	$+144.94 \pm 0.26$	<i>a</i>
$\text{CN}^\ominus (\text{K}^\oplus)$	H_2O , satd.	$+102.48 \pm 0.09$	<i>a</i>
	0.3 M	$+106.11 \pm 0.12$	<i>a</i>
$\text{NCO}^\ominus (\text{K}^\oplus)$	H_2O , satd.	$+302.91 \pm 0.14$	<i>a</i>
	0.3 M	$+302.60 \pm 0.14$	<i>a</i>
$\text{NCS}^\ominus (\text{K}^\oplus)$	H_2O , satd.	$+170.04 \pm 0.11$	<i>a</i>
	0.3 M	$+174.07 \pm 0.17$	<i>a</i>
Ph—OCN	neat liquid	$+211 \pm 3$	<i>b</i>
<i>p</i> -Me—C ₆ H ₄ —OCN	neat liquid	$+213 \pm 3$	<i>b</i>
<i>p</i> -Cl—C ₆ H ₄ —OCN	neat liquid	$+212 \pm 3$ (75°C)	<i>b</i>
<i>p</i> -MeO—C ₆ H ₄ —OCN	neat liquid	$+215 \pm 3$	<i>b</i>
<i>p</i> -NO ₂ —C ₆ H ₄ —OCN	neat liquid	$+189 \pm 5$ (85°C)	<i>b</i>
2,4,6-Trimethylphenyl-CNO	CH_2Cl_2	$+170.4 \pm 0.2$	<i>c</i>

^a Ref. 61, ^{14}N spectra, concentric spherical sample containers, full lineshape analysis by differential saturation technique, see Table VII for comments.

^b Ref. 102, ^{14}N spectra, referred to external CH_3NO_2 .

^c Ref. 34, ^{15}N spectrum of labelled fulminate, originally referred to what is reported as 12 M(CH_3)₄ NCl in H_2O , which probably is saturated (ca. 6 M), +336.7 ppm from CH_3NO_2 , Table VII.

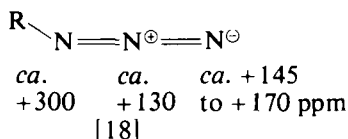
isomeric pairs of N- and O- or S-derivatives. More recent measurements (102) have enlarged the amount of shift data on aryl cyanates, Ar-OCN, where the shift seems to be only slightly affected by *para*-substitution when compared with PhOCN. An exception is the *para*-NO₂ substituent which results in a high-frequency shift of the resonance of the CN group.

The recently measured chemical shift of 2,4,6-trimethylphenyl fulminate (Table XVI) is in good agreement with the previous result (ref. 1d, p. 201). The low-frequency shift upon going from PhCN to PhCNO derivatives is an example of the general trend mentioned at the beginning of this section. It has been claimed (34) that the increased screening is mostly due to a change in the diamagnetic term in the screening constant. However, this seems to result from a misunderstanding of the physical significance of this term when considered within the framework of various theoretical approaches. (29)

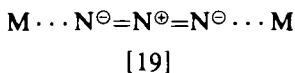
Some precise data (61) are reported in Table XVI on the nitrogen chemical shifts of CH₃CN, CN[⊖], NCO[⊖] and NCS[⊖]. Attention is drawn to the appreciable solvent effects on the shift of CH₃CN, giving a range of 20 ppm.

H. Azides

The azido group may occur in an unsymmetrical covalently bonded system [18], which gives rise to three signals (ref. 1d, p. 197). It may



also act as a ligand with a structure close to that of the azide ion, N₃[⊖]. In which case it may be coordinated either unsymmetrically or symmetrically, e.g. the bridge-like structure [19]. The latter case should be



characterized by only two signals close to those observed for the free azide ion (Table XVII). Recent data on some inorganic azides, (103) shown in Table XVII, seem to suggest that either possibility may be realized. However, caution is advisable when making such conclusions, since the ¹⁴N spectra (103) in those cases where only two signals are observed may contain a third signal which has not been detected because of its width and because of signal overlap.

TABLE XVII

Nitrogen screening constants of some azides in ppm, referred to external neat nitromethane

Compound	Solvent or state	Nitrogen screening constant	Notes
(NNN) [⊖] (Na [⊕])	H ₂ O, 0.30 M	+131.51 ± 0.12 (N-central)	<i>a</i>
		+280.60 ± 0.12 (N-terminal)	<i>a</i>
	5.13 M (satd.)	+132.16 ± 0.10 (N-central)	<i>a</i>
		+281.69 ± 0.12 (N-terminal)	<i>a</i>
PhN ₃	Me ₂ CO, 2 M	+286 ± 2 (PhN)	<i>b</i>
		+134.4 ± 0.8 (N-central)	<i>b</i>
		+144.4 ± 0.9 (N-terminal)	<i>b</i>
<i>p</i> -(NMe ₂)—C ₆ H ₄ —N ₃	Et ₂ O, 2 M	+285 ± 4 (PhN, NMe ₂)	<i>b</i>
		+138.3 ± 0.4 (N-central)	<i>b</i>
		+149 ± 1 (N-terminal)	<i>b</i>
<i>t</i> -BuN ₃	neat liquid	+286 ± 2 (<i>t</i> -BuN)	<i>c</i>
		+134 ± 2 (N-central)	<i>c</i>
		+162 ± 2 (N-terminal)	<i>c</i>
Me ₃ SiN ₃	neat liquid	+320 ± 2 (SiN)	<i>c</i>
		+141 ± 2 (N-central)	<i>c</i>
		+207 ± 2 (N-terminal)	<i>c</i>
Me ₃ GeN ₃	neat liquid	+314 ± 2 (GeN)	<i>c</i>
		+135 ± 2 (N-central)	<i>c</i>
		+209 ± 2 (N-terminal)	<i>c</i>
Me ₃ SnN ₃	Me ₂ CO	+276 ± 2 (SnN, N-terminal)	<i>c</i>
		+137 ± 2 (N-central)	<i>c</i>
Et ₃ SnN ₃	benzene	+287 ± 2 (SnN, N-terminal)	<i>c</i>
		+141 ± 2 (N-central)	<i>c</i>
Me ₃ PbN ₃	Me ₂ CO	+280 ± 2 (PbN, N-terminal)	<i>c</i>
		+142 ± 2 (N-central)	<i>c</i>
Me ₂ BN ₃	toluene	+140 ± 2 (N-central)	<i>c</i>
		+214 ± 2 (N-terminal)	<i>c</i>
Me ₂ AlN ₃	supercooled melt	+144 ± 2 (N-central)	<i>c</i>
Et ₂ TiN ₃	Me ₂ CO	+268 ± 2 (TiN, N-terminal)	<i>c</i>
		+134 ± 2 (N-central)	<i>c</i>
Me ₂ AsN ₃	neat liquid	+252 ± 2 (AsN, N-terminal)	<i>c</i>
		+135 ± 2 (N-terminal)	<i>c</i>
	Me ₂ CO	+256 ± 2 (AsN, N-terminal)	<i>c</i>
2-Ph-4-N ₃ -quinazoline	CF ₃ COOH	+136 ± 2 (N-central)	<i>c</i>
		+250.8 ± 0.2 (C—N)	<i>d</i>
		+128.8 ± 0.2 (N-terminal)	<i>d</i>

^a Ref. 61, ¹⁴N spectra, concentric spherical sample containers, full lineshape analysis by differential saturation technique, see Table VII for details.

^b Ref. 51, ¹⁴N spectra, originally referred to internal CH₃NO₂, recalculated with CH₃NO₂ shifts in (CH₃)₂CO, +0.8 ppm from neat CH₃NO₂, and in Et₂O, +3.9 ppm, Table VII.

^c Ref. 103, ¹⁴N spectra, originally referred to saturated aqueous NaNO₃, +3.5 ppm from neat CH₃NO₂, by sample replacement method.

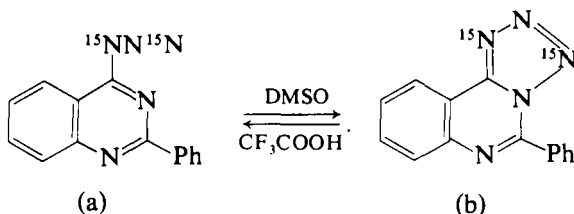
^d Ref. 104, ¹⁵N spectra of compound labelled at N-terminal and C—N atoms.

It should be noted that the most recent nitrogen chemical shift data on PhN_3 (51) give a value of +144 ppm for the terminal N atom, which is quite different from that reported earlier (ref. 1d, p. 199, and references therein), i.e. +194 ppm for a benzene solution.

The chemical shift of the C–N nitrogen atom in R–N_3 exhibits the β -effect, as can be seen from the series [20] to [22].

$\text{Me–N=N}^{\oplus}=\text{N}^{\ominus}$	$\text{Et–N=N}^{\oplus}=\text{N}^{\ominus}$	$t\text{-Bu–N=N}^{\oplus}=\text{N}^{\ominus}$
+320 ppm	+305 ppm	+285 ppm
[20]	[21]	[22]
(ref. 1d)	(ref. 1d)	(Table XVII)

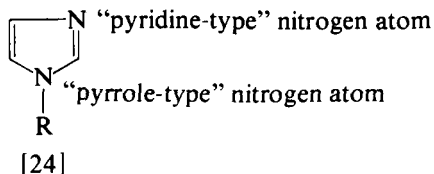
The nitrogen chemical shifts of the ^{15}N -labelled compounds (104) which are involved in the azido-tetrazoloazino valence tautomerism (Table XVII, note d) [23], reveal that in CF_3COOH the azido-form,



[23a], is dominant whilst in DMSO the tetrazolopyrimidine form is favoured [23b].

I. Azoles and their derivatives

Five-membered conjugated heterocycles which contain nitrogen atoms (azoles) have been thoroughly investigated by nitrogen NMR spectroscopy (ref. 1d, pp. 204–218). Some additional data are now available (Table XVIII). There are two types of nitrogen atoms in such heterocyclic structures, e.g. the case of imidazole derivatives [24]. The



“pyrrole-type” is characterized by nitrogen chemical shifts to low frequencies compared with those for the “pyridine-type” nitrogen atoms in the same molecule. However, in general there is some overlap of the corresponding spectral ranges of shifts.

TABLE XVIII

Nitrogen screening constants of some azoles in ppm, referred to external neat nitromethane


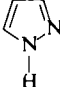
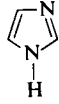
Compound	Solvent or state	Nitrogen screening constant	Notes
Pyrrole 	neat liquid	+231.4 ± 0.4	<i>a</i>
	Me ₂ CO, 0.15 M	+229.6 ± 0.4	<i>a</i>
	Me ₂ CO, <i>ca.</i> 40%	+229 ± 2	<i>b</i>
	DMSO, 0.15 M	+222.3 ± 0.4	<i>a</i>
	CCl ₄ , 0.10 M	+236.4 ± 0.4	<i>a</i>
	H ₂ O, 0.55 M	+224 ± 1	<i>a</i>
N-Me-pyrrole	Me ₂ CO, 0.15 M	+230 ± 1	<i>a</i>
	Me ₂ CO, <i>ca.</i> 40%	+230 ± 1	<i>b</i>
	CCl ₄ , 0.10 M	+234 ± 2	<i>a</i>
2-NO ₂ -pyrrole	Me ₂ CO, <i>ca.</i> 40%	+227 ± 5	<i>b</i>
N-Me-2-NO ₂ -pyrrole	Me ₂ CO, <i>ca.</i> 40%	+228 ± 5	<i>b</i>
2,4-Dinitropyrrole	Me ₂ CO, <i>ca.</i> 40%	+227 ± 5	<i>b</i>
N-Me-2,4-dinitropyrrole	Me ₂ CO, <i>ca.</i> 40%	+225 ± 5	<i>b</i>
2,5-Dinitropyrrole	Me ₂ CO, <i>ca.</i> 40%	+236 ± 5	<i>b</i>
Pyrazole 	CHCl ₃ , 3 M	+133 ± 1	<i>c</i>
	Me ₂ CO, 0.15 M	+129 ± 2	<i>a</i>
	H ₂ O, 0.55 M	+134 ± 1	<i>a</i>
	DMSO, 0.15 M	+176 ± 1 (=NH)	<i>a</i>
N-Me-pyrazole	Me ₂ CO, 0.15 M	+174 ± 2 (=NMe)	<i>a</i>
		+72 ± 2 (=N)	<i>a</i>
	CCl ₄ , 0.10 M	+179 ± 3 (=NMe)	<i>a</i>
		+68 ± 2 (=N)	<i>a</i>
	H ₂ O, 0.55 M	+178 ± 2 (=NMe)	<i>a</i>
		+93 ± 3 (≡N)	<i>a</i>
	CHCl ₃ , 3 M	+180.8 ± 0.3 (=NMe)	<i>c</i>
		+72.6 ± 0.8 (≡N)	<i>c</i>
	CHCl ₃ , 3 M	+134 ± 2	<i>c</i>
	CHCl ₃ , 3 M	+182 ± 1 (=NMe)	<i>c</i>
3-Me-pyrazole = 5-Me-pyrazole	CHCl ₃ , 3 M	+78 ± 3 (≡N)	<i>c</i>
		+183 ± 1 (=NMe)	<i>c</i>
		+71 ± 3 (≡N)	<i>c</i>
1,3-Dimethylpyrazole	CHCl ₃ , 3 M	+162 ± 5 (=NSi)	<i>j</i>
		+59 ± 10 (≡N)	<i>j</i>
N-SiMe ₃ -pyrazole	Me ₂ CO, 0.15 M	+171 ± 1	<i>a</i>
	MeOH, 0.25 M	+177 ± 2	<i>a</i>
	DMSO, 0.15 M	+168 ± 1	<i>a</i>
	<i>ca.</i> 20%	+167 ± 3	<i>b</i>
	H ₂ O, 0.55 M	+176 ± 1	<i>a</i>
	satd.	+177 ± 1	<i>d</i>
Imidazole 	neat liquid	+218.4 ± 0.2 (=NMe)	<i>e</i>
		(+213 ± 3 ??) (=NMe)	<i>a</i>
	Me ₂ CO, 0.15 M	+217 ± 1 (=NMe)	<i>a</i>
		+123 ± 1 (≡N)	<i>a</i>

TABLE XVIII—*cont.*

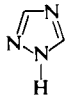
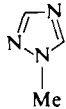
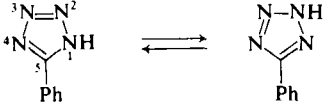
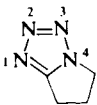
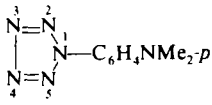
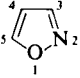
Compound	Solvent or state	Nitrogen screening constant	Notes
	CCl ₄ , 0.10 M	+218 ± 1 (=NMe)	<i>a</i>
		+109 ± 3 (≡N)	<i>a</i>
	H ₂ O, 0.55 M	+210 ± 1 (=NMe)	<i>a</i>
		+134 ± 5 (≡N)	<i>a</i>
4(5)-NO ₂ -imidazole	DMSO, <i>ca.</i> 20%	+202 ± 5	<i>b</i>
N-Me-4-NO ₂ -imidazole	DMSO, <i>ca.</i> 20%	+208 ± 5	<i>b</i>
2-Me-4(5)-NO ₂ -imidazole	DMSO, <i>ca.</i> 20%	+203 ± 5	<i>b</i>
4,5-Dinitroimidazole	Me ₂ CO, <i>ca.</i> 20%	+158 ± 3	<i>b</i>
2-Me-4,5-dinitroimidazole	Me ₂ CO, <i>ca.</i> 20%	+160 ± 3	<i>b</i>
1,2,4-Triazole	Me ₂ CO, 0.15 M	+135 ± 1	<i>a</i>
	DMSO, 0.15 M	+132 ± 3	<i>a</i>
		+174 ± 2 (=NH)	<i>a</i>
	H ₂ O, 0.55 M	+142 ± 3	<i>a</i>
1-Me-1,2,4-triazole	Me ₂ CO, 0.15 M	+152 ± 2 (=NMe)	<i>a</i>
		+119 ± 2 (≡N)	<i>a</i>
		+51 ± 3 (≡N)	<i>a</i>
	CCl ₄ , 0.10 M	+170 ± 2 (=NMe)	<i>a</i>
		+113 ± 2 (≡N)	<i>a</i>
		+42 ± 2 (≡N)	<i>a</i>
	H ₂ O, 0.55 M	+160 ± 4 (=NMe)	<i>a</i>
		+140 ± 2 (≡N)	<i>a</i>
		+46 ± 3 (≡N)	<i>a</i>
5-Phenyltetrazole	DMSO, <i>ca.</i> 3 M	+88.6 ± 0.3 (N1, N4)	<i>f</i>
		+29.8 ± 0.3 (N2, N3)	<i>f</i>
N-SiMe ₃ -imidazole	neat liquid	+168 ± 10	<i>j</i>
1-SiMe ₃ -1,2,4-triazole	neat liquid	+151 ± 10 (≡NSi)	<i>j</i>
		+105 ± 10 (N, N)	<i>j</i>
Trimethylenetetrazole	H ₂ O, satd.	+133 ± 1 (N-4)	<i>d</i>
		+79 ± 3 (N-1)	<i>d</i>
		+29 ± 4 (N-2, N-3)	<i>d</i>
		-11 ± 4 (N-2, N-3)	<i>d</i>
<i>p</i> -N,N-Dimethylaminophenylpentazole	CH ₂ Cl ₂ + MeOH	+73 ± 1 (N-1)	<i>h</i>
			
Isoxazole	neat liquid	-2.9 ± 0.2	<i>e</i>
			

TABLE XVIII—*cont.*

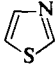
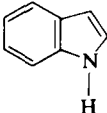
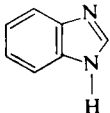
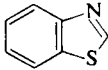
Compound	Solvent or state	Nitrogen screening constant	Notes
3(2,4,6-Trimethylphenyl)-isoxazole	CH ₂ Cl ₂	+0.8 ± 0.2	<i>g</i>
3(2,4,6-Trimethylphenyl)-4,5-dihydroisoxazole	CH ₂ Cl ₂	+10.0 ± 0.2	<i>g</i>
Thiazole 	neat liquid	+57.2 ± 0.2	<i>e</i>
		+56 ± 1	<i>a</i>
	Me ₂ CO, 0.15 M	+55 ± 1	<i>a</i>
	DMSO, 0.15 M	+53 ± 2	<i>a</i>
	H ₂ O, 0.55 M	+62 ± 4	<i>a</i>
Indole 	DMSO, satd.	+247.2 ± 0.3	<i>i</i>
	2.0 M	+245.5 ± 0.3	<i>i</i>
	CdCl ₂ , satd.	+253.6 ± 0.3	<i>i</i>
2-COOH-indole	DMSO, 2.0 M	+244.8 ± 0.3	<i>i</i>
2-Me-indole	DMSO, satd.	+242.9 ± 0.3	<i>i</i>
	2.0 M	+241.5 ± 0.3	<i>i</i>
	CDCl ₃ , satd.	+248.8 ± 0.3	<i>i</i>
3-Me-indole	DMSO, 2.0 M	+259.8 ± 0.3	<i>i</i>
	CDCl ₃ , satd.	+258.6 ± 0.3	<i>i</i>
2,3-Me ₂ -indole	DMSO, 2.0 M	+245.3 ± 0.3	<i>i</i>
2,5-Me ₂ -indole	DMSO, 2.0 M	+242.7 ± 0.3	<i>i</i>
3-CHO-indole	DMSO, satd.	+232.5 ± 0.3	<i>i</i>
	2.0 M	+232.3 ± 0.3	<i>i</i>
3-COMe-indole	DMSO, satd.	+236.6 ± 0.3	<i>i</i>
	2.0 M	+236.1 ± 0.3	<i>i</i>
3-OCOMe-indole	DMSO, satd.	+257.5 ± 0.3	<i>i</i>
3-CH ₂ COOH-indole	DMSO, satd.	+249.5 ± 0.3	<i>i</i>
	2.0 M	+248.7 ± 0.3	<i>i</i>
3-CH ₂ CH ₂ COOH-indole	DMSO, satd.	+251.2 ± 0.3	<i>i</i>
5-F-indole	CDCl ₃ , satd.	+255.2 ± 0.3	<i>i</i>
5-Cl-indole	DMSO, 1.4 M	+244.0 ± 0.3	<i>i</i>
	CDCl ₃ , satd.	+254.2 ± 0.3	<i>i</i>
5-Br-indole	DMSO, 1.3 M	+243.8 ± 0.3	<i>i</i>
5-NO ₂ -indole	DMSO, 1.5 M	+238.6 ± 0.3	<i>i</i>
5-CN-indole	DMSO, satd.	+240.7 ± 0.3	<i>i</i>
	CDCl ₃ , satd.	+247.5 ± 0.3	<i>i</i>
5-COOH-indole	DMSO, satd.	+242.8 ± 0.3	<i>i</i>
	2.0 M	+241.9 ± 0.3	<i>i</i>
5-OH-indole	DMSO, satd.	+249.5 ± 0.3	<i>i</i>
5-OMe-indole	DMSO, satd.	+248.4 ± 0.3	<i>i</i>
	1.0 M	+246.8 ± 0.3	<i>i</i>
	CDCl ₃ , satd.	+254.9 ± 10.3	<i>i</i>
5-Me-indole	DMSO, 0.5 M	+246.3 ± 0.3	<i>i</i>
	CDCl ₃ , satd.	+254.8 ± 0.3	<i>i</i>
5-NH ₂ -indole	DMSO, satd.	+249.4 ± 0.3	<i>i</i>
	1.0 M	+248.6 ± 0.3	<i>i</i>

TABLE XVIII—*cont.*

Compound	Solvent or state	Nitrogen screening constant	Notes
6-Ome-indole	CDCl ₃ , satd.	+253.9 ± 0.3	<i>i</i>
7-Ome-indole	CDCl ₃ , satd.	+257.8 ± 0.3	<i>i</i>
7-Me-indole	DMSO, 1.0 M	+246.1 ± 0.3	<i>i</i>
Benzimidazole 	CDCl ₃ , satd.	+255.8 ± 0.3	<i>i</i>
	Me ₂ CO, 0.15 M	+185 ± 2	<i>a</i>
	DMSO, 0.15 M	+237 ± 4 (=NH)	<i>a</i>
N-Me-benzimidazole	Me ₂ CO, 0.15 M	+134 ± 1 (≡N)	<i>a</i>
		+231 ± 1 (=NMe)	<i>a</i>
	CCl ₄ , 0.10 M	+127 ± 6 (≡N)	<i>a</i>
		+237 ± 6 (=NMe)	<i>a</i>
Benzothiazole 	Me ₂ CO, 0.15 M	+61 ± 1	<i>a</i>

^a Ref. 105, proton spectra, ¹⁴N decoupling, see footnote (b) in Table XXI.

^b Ref. 106, ¹⁴N spectra, referred to external CH₃NO₂.

^c Ref. 107, ¹⁴N spectra, originally referred to internal CH₃NO₂, recalculated with CH₃NO₂ shift in CHCl₃ of +3.79 ppm from neat CH₃NO₂.

^d Ref. 108, ¹⁴N spectra at 6.1 T, originally referred to NO₃[−] in "acidified NH₄NO₃", probably *ca.* +5 ppm from CH₃NO₂, Table VII; shifts reported in this Table are read directly from spectral plots, since numerical values are given only for imidazole.

^e Ref. 36, ¹⁵N natural-abundance spectra.

^f Ref. 109, ¹⁵N spectra of labelled compounds, assignments by selective labelling; originally referred to NO₃[−] ion, probably *ca.* +3.8 ppm from neat CH₃NO₂, Table VII.

^g Ref. 34, ¹⁵N spectra of labelled compounds; originally referred to what is reported as 12 M aqueous (CH₃)₄NCl, probably saturated (*ca.* 6 M), +336.7 ppm from neat CH₃NO₂, ref. 36 and Table VII.

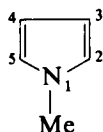
^h Ref. 51, ¹⁴N spectrum, referred to internal CH₃NO₂ in 1:1 CH₂Cl₂ + CH₃OH, recalculated with shifts in Table VII.

ⁱ Ref. 75, ¹⁵N natural-abundance spectra, originally referred to 1.0 M HNO₃, +4.4 ppm from neat CH₃NO₂, Table VII and 5.6 M (CH₃)₄NCl in H₂O, +336.7 ppm from neat CH₃NO₂ (+332.3 ppm from 1.0 M HNO₃).

^j Ref. 92, ¹⁴N spectra, originally referred to satd. aqueous NaNO₃, +3.7 ppm from neat CH₃NO₂, Table VII; for comments, see Table X footnotes (d) and (e).

Approximate additivity rules for the chemical shifts of azoles have been reported (110). For the "pyrrole-type" nitrogen atoms, the shifts may be related to that of N-Me-pyrrole [25]. They are composed of the algebraical summation of the following contributions:

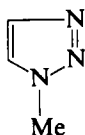
−50 ± 1.5 ppm for each "pyridine-type" nitrogen atom at positions 2 or 5;



[25]

- -30 ± 4 ppm for each "pyridine-type" nitrogen atom at positions 3 or 4;
- -12 ± 2 ppm additionally for each "pyridine-type" nitrogen atom which is adjacent to that already at position 2 or 5;
- $+ 7 \pm 2.5$ ppm additionally for each "pyridine-type" nitrogen atom which is adjacent to that already at position 3 or 4

Thus, for 1-Me-1,2,3-triazole [26] the shift of the N-Me nitrogen atom relative to N-Me-pyrrole should be $-50 - 30 - 12 + 7 = -85 \pm 10$



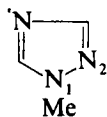
[26]

ppm whilst for neat liquids the shift is found to be -88 ± 2 ppm. (ref. 1d, pp. 208–209). The same system may be used for benzo-derivatives of azoles relative to N-Me-indole. (110)

Similar rules are reported (110) for the "pyridine-type" nitrogen atoms at position 2 (or 5) relative to that in N-Me-pyrazole as well as at position 3 (or 4) relative to that in 1-Me-imidazole. A set of five parameters representing the interactions between nitrogen atoms at various positions has been calculated by a regression analysis:

interaction	shift increment \pm std. deviation
(1, 2)	-48 ± 6 ppm
<u>(2, 3) + (3, 2)</u>	-79 ± 7 ppm
<u>2</u>	
<u>(2, 4) + (4, 2)</u>	$+23 \pm 8$ ppm
<u>2</u>	
(2, 5)	-23 ± 9 ppm
(3, 4)	-51 ± 9 ppm

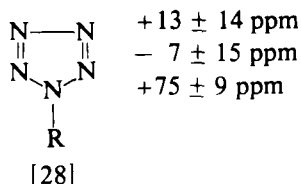
Thus, for 1-Me-1,2,4-triazole [27] the shift for N-2 (as compared with



[27]

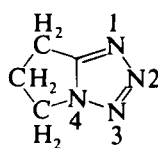
that of N-Me pyrrole) should be $-48 + 23 = -25 \pm 10$ ppm whilst the experimental value (in organic solvents) is -23 ± 6 ppm.

Such additivity rules are used in spectroscopic arguments for the existence of the pentazole ring system in solutions. The rules (110) predict the following values of the nitrogen chemical shifts in pentazole [28]. Since the only proof of the existence of such a ring structure, in



some unstable products of the reaction between *p*-substituted benzenediazonium salts and lithium azide, comes from the isotopic composition of the nitrogen gas evolved from compounds which are obtained from ^{15}N -labelled LiN_3 , an attempt has been made (51) to provide direct spectroscopic evidence for the ring structure. The ^{14}N spectrum of a solution of the supposed *p*-NMe₂-phenyl pentazole in a 1:1 (v/v) CH_3OH and CH_2Cl_2 mixture reveals the presence of a sharp signal at $+70 \pm 1$ ppm (from CH_3NO_2) which diminishes with time, in addition to the spectrum of PhN_3 which is the final product of the decomposition, with N_2 evolution. Since the shift, $+70$ ppm, is almost exactly the same as that predicted by the additivity rules, and since the ^{14}N signals of "pyrrole-type" nitrogen atoms are usually the sharpest in the spectra of azoles, (1d), it seems that this is the first direct evidence for the pentazole ring structure.

The ^{14}N spectrum of trimethylenetetrazole obtained (108) in a high magnetic field, 6.1 T, shows four signals which are given the tentative assignments reported in Table XVIII (note d). However, these assignments may be made more complete by using the additivity rules [29]. Considering the fact that these rules are based on the chemical

nitrogen chemical shifts			
		predicted by additivity rules from ref. 110	found in ref. 108
	N-1	$+92 \pm 12$	$+79$
	N-2	-10 ± 11	-11
	N-3	$+16 \pm 12$	$+29$
	N-4	$+147 \pm 7$	$+133$
[29]			

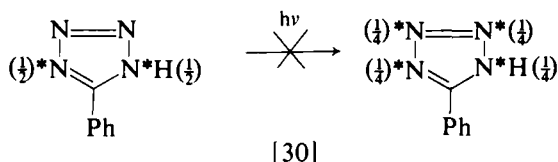
shifts of N-CH₃ derivatives, mostly neat liquids, the agreement is quite satisfactory and certainly good enough for an unambiguous assignment of the observed chemical shifts.

The data in Table XVIII show that there are appreciable solvent

effects on the nitrogen chemical shifts of azoles, and the range of such effects may reach 20 ppm if aqueous solutions are included, or about 10 ppm otherwise.

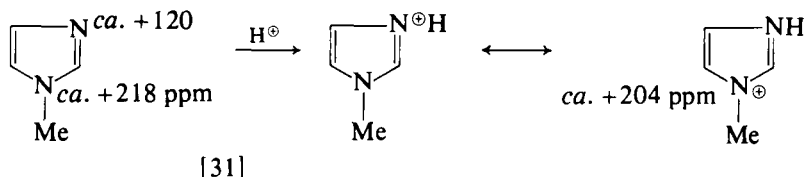
There are rather insignificant effects on the azole chemical shifts following the introduction of substituents in the azole ring system. Nitro derivatives of pyrrole, pyrazole and imidazole (106) give nitrogen resonance signals within the range of solvent effects and experimental errors in the shifts of the parent structures (Table XVIII). A comprehensive study of substituted indoles (75) in DMSO and CDCl_3 (Table XVIII, note i) indicates that the range of nitrogen chemical shifts is about 25 ppm for a large variety of substituents, and that no obvious correlation with the character of the substituent groups is evident. There is no significant change in the shifts when the N-CH_3 group in imidazole is replaced by the $\text{N-Si(CH}_3)_3$ moiety (Table XVIII, notes a and j).

The ^{15}N NMR spectra of fully and selectively labelled 5-phenyltetrazoles (Table XVIII, note f) demonstrate that photochemical ring transposition does not occur in the system [30].



The asterisks and numbers in parentheses denote the sites and distribution of ^{15}N nuclei. (109)

Cations derived from azole structures by protonation of "pyridine-type" nitrogen atoms, e.g. [31], show an appreciable low-frequency shift



of the resonance corresponding to the protonated nitrogen atom. This is in accord with the general rules outlined at the beginning of this section. Stable cations derived from the imidazole structure by N-methylation (Table XIX, note c) provide another example of the existence of the β -effect on chemical shifts [32], [33].

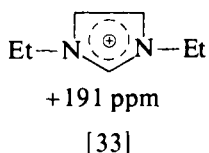
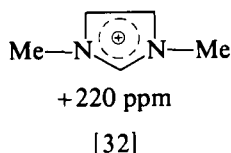


TABLE XIX

Nitrogen screening constants of some ionic species derived from azoles in ppm, referred to external neat nitromethane

Compound and solvent	Nitrogen screening constant	Notes
Cations derived from:		
Pyrrole in HCl/H ₂ O	+191 ± 5	<i>c</i>
Imidazole in H ₂ SO ₄	+207 ± 2 (50°C)	<i>a</i>
	+212 ± 2	<i>b</i>
in CF ₃ COOH	+210 ± 2	<i>b</i>
N-Me-imidazole in CF ₃ COOH	+204 ± 5	<i>b</i>
4(5)-NO ₂ -imidazole in H ₂ SO ₄	+201 ± 5 (50°C)	<i>a</i>
1-Me-1,2,4-triazole in CF ₃ COOH	+206 ± 2 (=NH)	<i>b</i>
	+49 ± 2 (≡N)	<i>b</i>
	+206 ± 2 (=NMe)	<i>b</i>
Thiazole in CF ₃ COOH	+178 ± 2	<i>b</i>
Anions derived from:		
Pyrrole, Li [⊕] salt in tetrahydrofuran	+205 ± 5	<i>a</i>
2-NO ₂ -pyrrole, Na [⊕] salt in H ₂ O	+123 ± 8	<i>a</i>
2,4-Dinitropyrrole, Na [⊕] salt in H ₂ O	+130 ± 20	<i>a</i>
2,5-Dinitropyrrole, Na [⊕] salt in H ₂ O	+128 ± 10	<i>a</i>
Imidazole, K [⊕] salt in H ₂ O	+147 ± 3 (50°C)	<i>a</i>
4(5)-NO ₂ -imidazole, K [⊕] salt in H ₂ O	+129 ± 5 (50°C)	<i>a</i>
2-Me-4-NO ₂ -imidazole, K [⊕] salt, H ₂ O	+129 ± 10 (50°C)	<i>a</i>
Pyrazole, Li [⊕] salt in tetrahydrofuran	+115 ± 10	<i>c</i>
Stable cations derived from azoles:		
N,N'-di-Me-imidazolium iodide (in CH ₂ Cl ₂)	+220 ± 5	<i>c</i>
1,2,3-tri-Me-imidazolium iodide (in H ₂ O)	+203 ± 5	<i>c</i>
N,N'-di-Et-imidazolium bromide (in CH ₂ Cl ₂)	+191 ± 5	<i>c</i>
1-SiMe ₃ -3-Me-imidazolium iodide (in CH ₂ Cl ₂)	+180 ± 10 (=NSi)	<i>c</i>
	+216 ± 10 (≡NMe)	<i>c</i>
N,N'-di-Me-pyrazolium iodide (in H ₂ O)	+174 ± 5	<i>c</i>
N-Me-isothiazolium iodide (in H ₂ O)	+175 ± 5	<i>c</i>

^a Ref. 215, ¹⁴N spectra, referred to external CH₃NO₂.

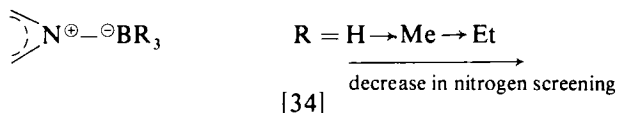
^b Ref. 105, proton spectra, ¹⁴N decoupling, see footnote (b) in Table XXI.

^c Ref. 80, ¹⁴N spectra, originally referred to satd. aqueous NaNO₃, +3.7 ppm from neat CH₃NO₂, Table VII; see footnotes (d) and (e) in Table X.

Anions derived from azole systems (Table XIX) exhibit their nitrogen resonance signals at higher frequencies than those of the parent structures. The effect is enhanced by the presence of electron-withdrawing groups such as NO₂.

If the lone electron pair of a "pyridine-type" nitrogen atom in an azole ring system is coordinated to a BR₃ group in the corresponding borane adduct, an increase in the screening of the nitrogen nucleus involved is observed (Table XXIV), according to the general rules. However, the

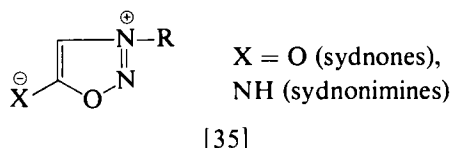
magnitude of the shift depends to a considerable extent on the substituents R in the BR_3 group, since an evident β -effect is found in the series [34].



In the case of some azoloazines (Table XXII) it has been shown that the nitrogen screening is smaller than in the parent azoles and that a good linear relationship exists between the shifts of the parent azoles and the analogous azoloazines. (63)

J. Sydnones, sydnonimines and related structures

Sydnones and sydnonimines are represented by conventional formulae [35]. They are the betaine isomers of the corresponding 5-OH (or



NH)-1,2,3-oxadiazoles. The ^{14}N spectra of sydnones show a sharp signal which is superimposed on a broad resonance (111). The sharp signal at about +100 ppm may be assigned to the $\text{N}^{\oplus}-\text{R}$ moiety (Table XX), since the line-width is typical for such structures and because the spectrum of 3,4-diphenylsydnone-2- ^{15}N indicates (112) that the N-2 shift is +42 ppm.

However, the spectral data for compounds which might be thought of as sydnonimines [36b], obtained by the neutralization of sydnonimine

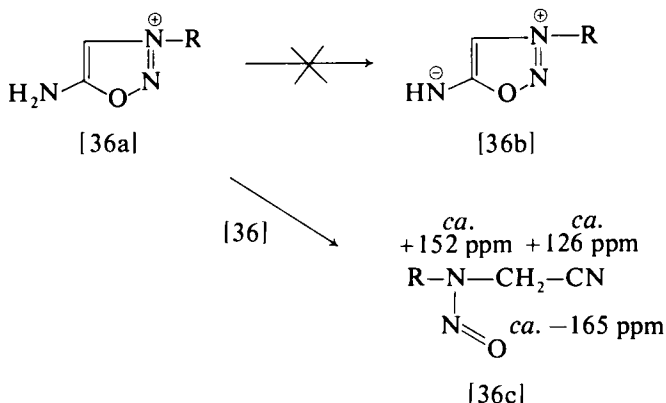


TABLE XX

Nitrogen screening constants of some sydnones, sydnonimines, and related structures in ppm (± 1), referred to external neat nitromethane

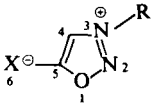
			
Compound	Solvent	Nitrogen screening constant	Notes
Sydnones (X = O)			
<i>R</i>			
Me	Me ₂ CO	+108 (N [⊖] -3)	<i>a</i>
Et	Me ₂ CO	+97 (N [⊖] -3)	<i>a</i>
	neat	+96 (N [⊖] -3)	<i>a</i>
<i>i</i> -Pr	Me ₂ CO	+84 (N [⊖] -3)	<i>a</i>
Pr	Me ₂ CO	+98 (N [⊖] -3)	<i>a</i>
Bu	Me ₂ CO	+98 (N [⊖] -3)	<i>a</i>
	Et ₂ O	+101 (N [⊖] -3)	<i>a</i>
<i>i</i> -Bu	Me ₂ CO	+99 (N [⊖] -3)	<i>a</i>
	neat	+97 (N [⊖] -3)	<i>a</i>
<i>s</i> -Bu	Me ₂ CO	+87 (N [⊖] -3)	<i>a</i>
<i>t</i> -Bu	Me ₂ CO	+79 (N [⊖] -3)	<i>a</i>
cyclohexyl	Me ₂ CO	+86 (N [⊖] -3)	<i>a</i>
Ph-CH ₂	Me ₂ CO	+96 (N [⊖] -3)	<i>a</i>
Ph	Me ₂ CO	+98 (N [⊖] -3)	<i>a</i>
<i>p</i> -Cl-C ₆ H ₄	Me ₂ CO	+100 (N [⊖] -3)	<i>a</i>
<i>p</i> -Br-C ₆ H ₄	Me ₂ CO	+100 (N [⊖] -3)	<i>a</i>
<i>p</i> -NO ₂ -C ₆ H ₄	Me ₂ CO	+102 (N [⊖] -3)	<i>a</i>
3-pyridyl	Me ₂ CO	+103 (N [⊖] -3)	<i>a</i>
Ph-; Br at C-4	Me ₂ CO	+100 (N [⊖] -3)	<i>a</i>
Ph-; NO ₂ at C-4	Me ₂ CO	+101 (N [⊖] -3)	<i>a</i>
Ph-; Ph at C-4	(CD ₃) ₂ CO	+41.8 ± 0.2 (N-2)	<i>b</i>
	20% H ₂ SO ₄ + (CD ₃) ₂ CO	+30.1 ± 0.2 (N-2)	<i>b</i>
	CF ₃ COOH	+27.2 ± 0.2 (N-2)	<i>b</i>
	60% H ₂ SO ₄ + D ₂ O	+11.9 ± 0.2 (N-2)	<i>b</i>
Acetylsydnonimines (X = N-COCH₃)			
<i>R</i>			
Me	Me ₂ CO	+27 ± 5 (N-2)	<i>a</i>
		+109 (N [⊖] -3)	<i>a</i>
		+205 ± 8 (N-6)	<i>a</i>
Et	Me ₂ CO	+97 (N [⊖] -3)	<i>a</i>
	MeOH	+97 (N [⊖] -3)	<i>a</i>
<i>i</i> -Pr	Me ₂ CO	+86 (N [⊖] -3)	<i>a</i>
Pr	Me ₂ CO	+98 (N [⊖] -3)	<i>a</i>
Bu	Me ₂ CO	+98 (N [⊖] -3)	<i>a</i>
Ph	Me ₂ CO	+97 (N [⊖] -3)	<i>a</i>

TABLE XX—cont.

Compound	Solvent	Nitrogen screening constant	Notes
Sydnone hydrochlorides (X = O; +HCl)			
<i>R</i>			
Me	MeOH	+94 ± 5 (N [⊖] -3)	<i>a</i>
Et	MeOH	+88 ± 5 (N [⊖] -3)	<i>a</i>
<i>i</i> -Pr	MeOH	+83 ± 5 (N [⊖] -3)	<i>a</i>
Sydnonimine hydrochlorides (X = NH; +HCl)			
<i>R</i>			
Me	MeOH	+106 ± 2 (N [⊖] -3)	<i>a</i>
Et	MeOH	+95 ± 3 (N [⊖] -3)	<i>a</i>
<i>i</i> -Pr	MeOH	+87 ± 4 (N [⊖] -3)	<i>a</i>
PhCH ₂	MeOH	+94 ± 2 (N [⊖] -3)	<i>a</i>
Ph	MeOH	+96 ± 4 (N [⊖] -3)	<i>a</i>
Acetylsydnonimine hydrochlorides (X = NCOCH ₃ ; +HCl)			
<i>R</i>			
Me	MeOH	+104 ± 5 (N [⊖] -3)	<i>a</i>
Et	MeOH	+92 ± 3 (N [⊖] -3)	<i>a</i>
<i>i</i> -Pr	MeOH	+84 ± 4 (N [⊖] -3)	<i>a</i>

^a Ref. 111, ¹⁴N spectra, referred to external CH₃NO₂.

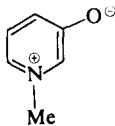
^b Ref. 112, ¹⁵N spectra of compound labelled at N-2; originally referred to ¹⁵NO₃[⊖] ion in NH₄NO₃, probably +4.0 ppm from neat CH₃NO₂, Table VII; Cr(acac)₃ added (0.03 M) to solutions in acetone and acetone + H₂SO₄ in order to quench the NOE.

hydrochlorides [36a], indicate (111) that they are actually N-nitroso-amines with a cyano group at the α-position [36c]. Their nitrogen spectra contain three signals with screening constants which are typical of the N–NO and CN groups. (ref. 1d and Table XXVIII) The proton spectra are also compatible with the open-chain structure. Since the transformation is reversible, it may be concluded that sydnonimines do not exist as such in the sense that the equilibrium with the cyanomethyl-alkyl nitroso-amines is shifted almost completely to the latter structure.

Sydnone and sydnonimine hydrochlorides (Table XX) give nitrogen resonance signals which are typical of the N[⊖]–R group in sydnones, and the proton spectra show singlets due to the proton at C-4. This and the observation of the ¹⁵N–H coupling for sydnonimine hydrochlorides labelled at the exocyclic nitrogen atom (section VI. A) indicate that the additional proton is attached to the exocyclic nitrogen or oxygen atom.

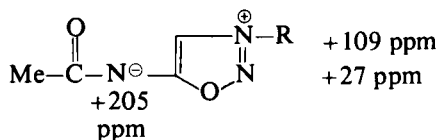
TABLE XXI

Nitrogen screening constants of some azines in ppm, referred to external neat nitromethane

Compound	Solvent or state	Nitrogen screening constant	Notes
Pyridine	neat liquid	$+62.01 \pm 0.14$	<i>a</i>
		$+62 \pm 1$	<i>b</i>
	0.30 M in Me ₂ CO	$+64.01 \pm 0.30$	<i>a</i>
	0.15 M in Me ₂ CO	$(+58 \pm 1 \text{ ??})$	<i>b</i>
	0.30 M in Et ₂ O	$+59.20 \pm 0.31$	<i>a</i>
	0.30 M in CCl ₄	$+58.01 \pm 0.37$	<i>a</i>
	0.50 M in H ₂ O	$+84.38 \pm 0.59$	<i>a</i>
		$(+81 \pm 6)$	<i>b</i>
2-MeO-pyridine	neat liquid	$+109 \pm 3$	<i>c</i>
	Me ₂ CO, 1:3 v/v	$+111 \pm 2$	<i>c</i>
	MeOH, 1:3 v/v	$+119 \pm 2$	<i>c</i>
3-MeO-pyridine	neat liquid	$+60 \pm 3$	<i>c</i>
	Me ₂ CO, 1:3 v/v	$+64 \pm 3$	<i>c</i>
	MeOH, 1:3 v/v	$+67 \pm 4$	<i>c</i>
	MeOH, 1:3 v/v	$+181 \pm 1$	<i>c</i>
(N-Me-3-oxypyridyl-betaine)			
4-MeO-pyridine	neat liquid	$+89 \pm 4$	<i>c</i>
	Me ₂ CO, 1:3 v/v	$+91 \pm 3$	<i>c</i>
	MeOH, 1:3 v/v	$+95 \pm 4$	<i>c</i>
2-OH-pyridine \rightleftharpoons 2-pyridone	Me ₂ CO, 1:3 v/v	$+209 \pm 2$	<i>c</i>
	MeOH, 1:3 v/v	$+212 \pm 2$	<i>c</i>
3-OH-pyridine	Me ₂ CO, 1:3 v/v	$+67 \pm 4$	<i>c</i>
	MeOH, 1:3 v/v	$+71 \pm 4$	<i>c</i>
4-OH-pyridine \rightleftharpoons 4-pyridone	Me ₂ CO, satd.	$+222 \pm 4$	<i>c</i>
	MeOH, 1:3 v/v	$+227 \pm 3$	<i>c</i>
Pyridinium ion (Cl [⊖])	0.5 M in 10 M HCl	$+178.96 \pm 0.09$	<i>a</i>
Quinoline	Me ₂ CO, 0.15 M	$+64 \pm 1$	<i>b</i>
	CCl ₄ , 1:1 v/v	$+64.0 \pm 0.5$	<i>d</i>
	MeOH, 1:1 v/v	$+78.8 \pm 0.5$	<i>d</i>
Quinolinium ion (HSO ₄ [⊖])	H ₂ SO ₄ , 1:3 v/v	$+193.1 \pm 0.5$	<i>d</i>
Pyrazine (1,4-Diazine)	Me ₂ CO, 0.15 M	$+44 \pm 1$	<i>b</i>
Pyrimidine (1,3-Diazine)	Me ₂ CO, 0.15 M	$+84 \pm 1$	<i>b</i>
	H ₂ O, 0.5 M	$+92 \pm 2$	<i>b</i>
	neat liquid	$+85.4 \pm 0.2$	<i>e</i>
1,3,5-Triazine	Me ₂ CO, 0.15 M	$+97 \pm 1$	<i>b</i>
	H ₂ O, 0.5 M	$+104 \pm 10$	<i>b</i>

^a Ref. 61, see also Table VII for comments; ¹⁴N spectra, concentric spherical sample containers, full lineshape analysis.

It is possible, however, to obtain sydnonimine derivatives of the type [37]. Structure [37] has three nitrogen resonance signals in its spectrum.

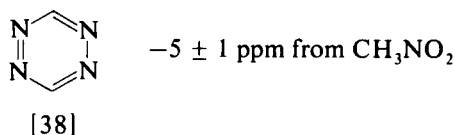


N-acetylsydnonimine [37]

(111) The assignments of which are based on selective ^{15}N -labelling and provide spectroscopic proof of the identity of the molecular structure as [37].

K. Azines and their derivatives

Six-membered conjugated heterocycles which contain nitrogen atoms (azines) have also been extensively examined by nitrogen NMR methods (ref. 1d, pp. 218–219). Additivity rules for their nitrogen chemical shifts, relative to that of pyridine, have been reported (113) in terms of 1,2- (-73 ± 4 ppm), 1,3- ($+22 \pm 3$ ppm), and 1,4-interactions (-20 ± 6 ppm) in the six-membered ring. The observed shift for 1,2,4,5-tetrazine (113) [38], where each nitrogen atom is involved in all three such interactions



with the remaining nitrogen atoms, comes very close to the calculated value of $-73 + 22 - 20 = -71$ ppm from pyridine or about -9 ppm from nitromethane.

The relative nitrogen screening constants of pyridine, pyrazine, pyridazine, pyrimidine, 1,3,5-triazine and 1,2,4,5-tetrazine show a very good linear correlation with theoretical values of the local paramagnetic term calculated by the AEE approximation. (47) A similarly satisfactory

^b Ref. 105, proton spectra, ^{14}N decoupling, originally referred to " NH_4^+ ion", probably that in 4.5 M NH_4NO_3 in 3 M HCl, +357.10 ppm from neat CH_3NO_2 , Table VII, as indicated in previous work, ref. 114; large deviation of pyridine shift for acetone solution from that in Table VII suggests that experimental errors are much larger than reported, particularly for dilute solutions.

^c Ref. 101, ^{14}N spectra, originally referred to internal CH_3NO_2 , recalculated according to Table VII.

^d Ref. 115, ^{15}N spectra of labelled quinoline, originally referred to 5 M NH_4Cl in 2 M HCl, +352.49 ppm from neat CH_3NO_2 , Table VII.

^e Ref. 36 natural-abundance ^{15}N spectra.

TABLE XXII

Nitrogen screening constants of some azoloazines in ppm, referred to external neat nitromethane

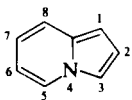
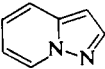
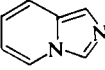
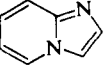
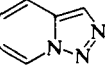
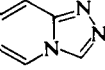
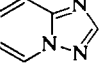
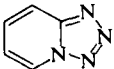
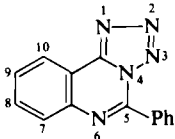
Compound	Solution	Nitrogen screening constant	¹⁴ N resonance half-height width (Hz)	Notes
Indolizine (Pyrrocoline) 	Et ₂ O, satd.	+191.2 ± 0.2	86 ± 2	<i>a</i>
3-Azaindolizine (Pyrazolo[1,5-a]pyridine) 	Et ₂ O, 0.5 M	+79.2 ± 1.7 (N3) +145.4 ± 0.3 (N4)	342 ± 18 89 ± 3	<i>a</i> <i>a</i>
2-Azaindolizine (Imidazo[1,5-a]pyridine) 	Et ₂ O, 0.5 M	+141.6 ± 4.2 (N2) +190.8 ± 0.2 (N4)	917 ± 56 93 ± 2	<i>a</i> <i>a</i>
1-Azaindolizine (Imidazo[1,2-a]pyridine) 	Et ₂ O, 0.5 M	+135.5 ± 1.0 (N1) +181.6 ± 0.2 (N4)	270 ± 10 54 ± 1	<i>a</i> <i>a</i>
2,3-Diazaindolizine (1,2,3-Triazolo[1,5-a]pyridine) 	Et ₂ O, 0.5 M	+44.8 ± 3.2 (N2) -26.7 ± 3.9 (N3) +123.8 ± 0.2 (N4)	702 ± 15 1210 ± 69 156 ± 2	<i>a</i> <i>a</i> <i>a</i>
1,2-Diazaindolizine (1,2,4-Triazolo[4,3-a]pyridine) 	Et ₂ O, 0.5 M	+64.9 ± 4.2 (N1) +122.0 ± 9.0 (N2) +189.4 ± 0.2 (N4)	632 ± 28 1285 ± 149 93 ± 2	<i>a</i> <i>a</i> <i>a</i>
1,3-Diazaindolizine (1,2,4-Triazolo[1,5-a]pyridine) 	Et ₂ O, 0.5 M	+153.9 ± 1.0 (N1) +98.0 ± 2.2 (N3) +144.6 ± 0.3 (N4)	264 ± 10 616 ± 32 104 ± 2	<i>a</i> <i>a</i> <i>a</i>

TABLE XXII—*cont.*

Compound	Solution	Nitrogen screening constant	¹⁴ N resonance half-height width (Hz)	Notes
1,2,3-Triazaindolizine (Tetrazolo[1,5-a]pyridine)	Et ₂ O + Me ₂ CO (1:1), satd.	+65.7 ± 1.2 (N1) +74.4 ± 11.2 (N2) +13.9 ± 2.4 (N3) +133.1 ± 0.2 (N4)	224 ± 9 1275 ± 260 344 ± 31 68 ± 2	<i>a</i> <i>a</i> <i>a</i> <i>a</i>
				
5-Ph-tetrazolo[5,1-c]quinazoline	DMSO	+71.0 ± 0.2 (N1) +30.4 ± 0.2 (N3)	— —	<i>b</i> <i>b</i>
				

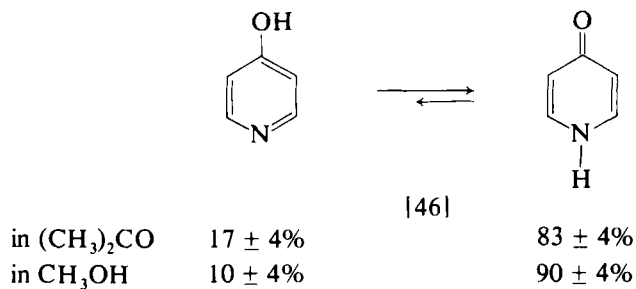
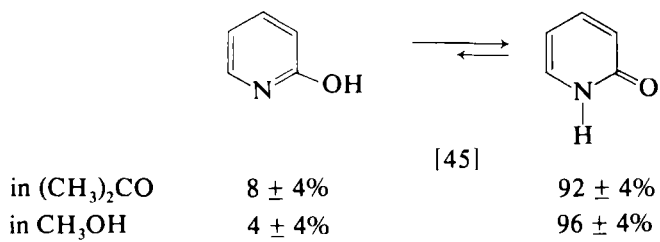
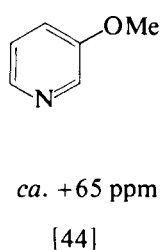
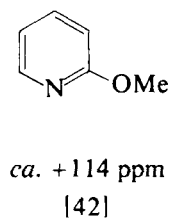
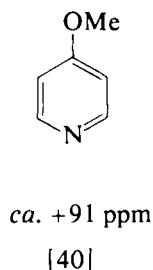
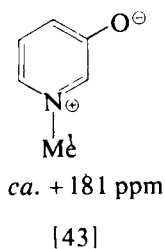
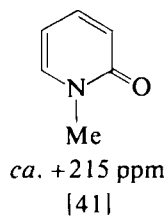
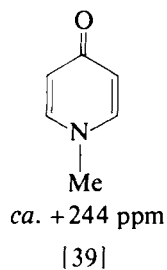
^a Ref. 63, ¹⁴N spectra, originally referred to internal CH₃NO₂, recalculated with CH₃NO₂ shift in Et₂O, +3.9 ppm from neat CH₃NO₂, or that for 1:1 Et₂O + (CH₃)₂CO solvent, +2.3 ppm from neat CH₃NO₂, Table VII; shifts and line-widths (for unsaturated signals) are obtained by complete line-shape analysis using differential saturation method; errors quoted are standard deviations for the fitting of about 200 data points; assignments are based on independent comparisons of experimental values of shifts and line-widths with theoretically calculated ones.

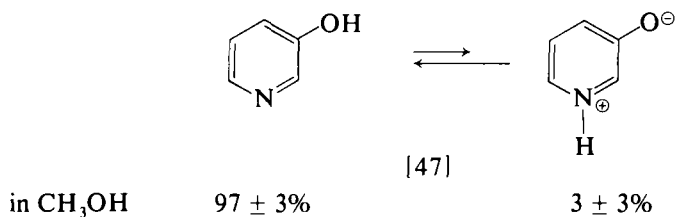
^b Ref. 104, ¹⁵N spectrum of compound labelled at N-1 and N-3, referred to external CH₃NO₂.

agreement has been reported for the azoloazines shown in Table XXII. (63)

It should be noted that the nitrogen chemical shifts of azines are sensitive to medium effects, and that usually the values for aqueous solutions depart from those in organic solvents by 10–20 ppm to lower frequencies (Table XXI).

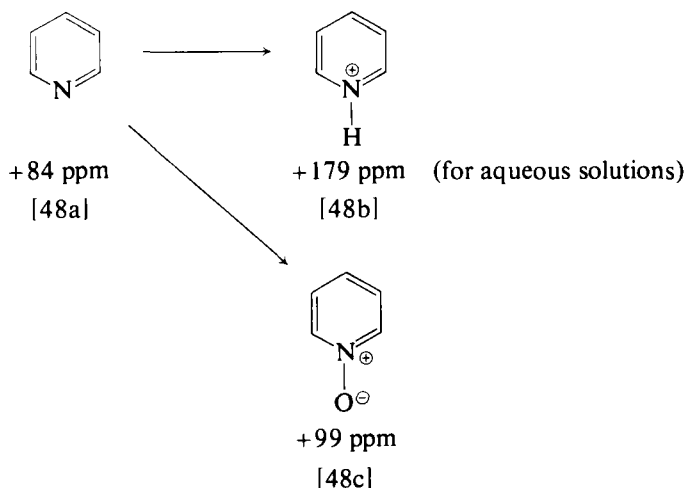
The tautomeric equilibria between hydroxy-pyridines and the corresponding pyridone or betaine forms (Table XXI) have been determined (101) with quite good accuracy from the nitrogen chemical shifts due to the fact that the corresponding N–Me and O–Me derivatives (Tables XV and XXI) [39] to [42], are characterized by such different chemical shifts that the possible errors in assigning these values to the corresponding NH and OH tautomers (probably not larger than 3 ppm) are not critical here. The same applies to the isomeric pair of 3-MeO-pyridine and N–Me-3-oxypyridyl betaine (Table XXI) [43], [44]. The shifts for the N–Me and O–Me derivatives have been used, together with those observed for the NH and OH forms in an equilibrium, to yield the following estimates of the tautomeric equilibria





[45] to [47]. Nitrogen chemical shifts are far superior to those of ^{13}C in the estimation of such equilibria because the ^{13}C shifts in this case are only slightly different for the various tautomeric forms. The differences usually occur within the range of possible solvent and concentration effects, and within that due to the effects of N- or O-methylation on the shifts of model compounds. (101)

Protonation of the nitrogen atoms in azine ring systems results in an appreciable increase in the screening of the nitrogen nucleus, (1d) according to the general trend in the shifts produced upon coordination of the lone electron pair in an unsaturated system. Some accurate data have recently been reported for the pyridinium [48b] and quinolinium



ions (Table XXI). The same direction for the change of the shift is observed when the lone pair at the nitrogen atom [48a] is replaced by a N-oxide bond (Table XXIII), [48c]. However, the magnitude of the displacement is smaller than that for the formation of the corresponding azinium ion. The shifts of azine N-oxides follow a linear relationship with those for the parent azines (45, 116) which may be used for

TABLE XXIII

Nitrogen screening constants of some azine N-oxides in ppm (± 1) if not stated otherwise, referred to external neat nitromethane

Compound	Solvent	Nitrogen screening constant	Notes
Pyridine N-oxide	Me ₂ CO	+86	<i>a</i>
	MeOH	+96	<i>a</i>
	CHCl ₃	+89	<i>a</i>
	H ₂ O	+99	<i>a</i>
2-NH ₂ -pyridine N-oxide	MeOH	+140 \pm 3 (NO)	<i>a</i>
3-NH ₂ -pyridine N-oxide	MeOH	+102 \pm 2 (NO)	<i>a</i>
4-NH ₂ -pyridine N-oxide	MeOH	+139 \pm 10 (NO)	<i>a</i>
2-NMe ₂ -pyridine N-oxide	Me ₂ CO	+106	<i>a</i>
	MeOH	+122 \pm 2	<i>a</i>
3-NMe ₂ -pyridine N-oxide	Me ₂ CO	+85	<i>a</i>
	MeOH	+102 \pm 2	<i>a</i>
4-NMe ₂ -pyridine N-oxide	MeOH	+152 \pm 8	<i>a</i>
	CHCl ₃	+135 \pm 5	<i>a</i>
	CHCl ₃	+158 \pm 10	<i>a</i>
2-OH-pyridine N-oxide	H ₂ O	+162 \pm 10	<i>a</i>
	MeOH	+98 \pm 4	<i>a</i>
3-OH-pyridine N-oxide	H ₂ O	+101 \pm 4	<i>a</i>
	MeOH	+144 \pm 5	<i>a</i>
4-OH-pyridine N-oxide	H ₂ O	+136 \pm 8	<i>a</i>
	Me ₂ CO	+146 \pm 10	<i>a</i>
2-OMe-pyridine N-oxide	Me ₂ CO	+91	<i>a</i>
3-OMe-pyridine N-oxide	Me ₂ CO	+103	<i>a</i>
4-OMe-pyridine N-oxide	MeOH	+107	<i>a</i>
2-CH ₂ OH-pyridine N-oxide	MeOH	+102 \pm 2	<i>a</i>
3-CH ₂ OH-pyridine N-oxide	MeOH	+99 \pm 3	<i>a</i>
4-CH ₂ OH-pyridine N-oxide	Me ₂ CO	+86	<i>a</i>
2-Me-pyridine N-oxide	MeOH	+99 \pm 2	<i>a</i>
	Me ₂ CO	+83	<i>a</i>
3-Me-pyridine N-oxide	MeOH	+97 \pm 2	<i>a</i>
	Me ₂ CO	+88	<i>a</i>
4-Me-pyridine N-oxide	MeOH	+107 \pm 2	<i>a</i>
	Me ₂ CO	+89	<i>a</i>
2-Cl-pyridine N-oxide	Me ₂ CO	+81	<i>a</i>
3-Cl-pyridine N-oxide	Me ₂ CO	+85	<i>a</i>
4-Cl-pyridine N-oxide	Me ₂ CO	+87	<i>a</i>
2-Br-pyridine N-oxide	Me ₂ CO	+80	<i>a</i>
3-Br-pyridine N-oxide	Me ₂ CO	+85	<i>a</i>
4-Br-pyridine N-oxide	MeOH	+89 (NO)	<i>a</i>
2-CN-pyridine N-oxide	MeOH	+92 (NO)	<i>a</i>
3-CN-pyridine N-oxide	H ₂ O	+90 (NO)	<i>a</i>
4-CN-pyridine N-oxide	Me ₂ CO	+104 \pm 2	<i>a</i>
2-COMe-pyridine N-oxide	Me ₂ CO	+88	<i>a</i>
3-COMe-pyridine N-oxide			

TABLE XXIII—*cont.*

Compound	Solvent	Nitrogen screening constant	Notes
4-COMe-pyridine N-oxide	Me ₂ CO	+77	<i>a</i>
2-CHO-pyridine N-oxide	Me ₂ CO	+81	<i>a</i>
3-CHO-pyridine N-oxide	Me ₂ CO	+82	<i>a</i>
4-CHO-pyridine N-oxide	Me ₂ CO	+73	<i>a</i>
2-COOH-pyridine N-oxide	Me ₂ CO	+103	<i>a</i>
	H ₂ O	+106 ± 3	<i>a</i>
3-COOH-pyridine N-oxide	H ₂ O	+82 ± 6	<i>a</i>
4-COOH-pyridine N-oxide	H ₂ O	+79 ± 8	<i>a</i>
2-NO ₂ -pyridine N-oxide	Me ₂ CO	+99 (NO)	<i>a</i>
3-NO ₂ -pyridine N-oxide	Me ₂ CO	+82 (NO)	<i>a</i>
	MeOH	+92 ± 2 (NO)	<i>a</i>
	CHCl ₃	+82 ± 2 (NO)	<i>a</i>
4-NO ₂ -pyridine N-oxide	Me ₂ CO	+71 (NO)	<i>a</i>
	MeOH	+79 (NO)	<i>a</i>
	CHCl ₃	+73 (NO)	<i>a</i>
2-(2-pyridyl)-pyridine N-oxide	H ₂ O	+98 ± 2 (NO)	<i>a</i>
3-(3-pyridyl)-pyridine N-oxide	H ₂ O	+94 ± 2 (NO)	<i>a</i>
4-(4-pyridyl)-pyridine N-oxide	H ₂ O	+98 ± 5 (NO)	<i>a</i>
Quinoline N-oxide	Me ₂ CO	+95	<i>b</i>
	MeOH	+107	<i>b</i>
	CHCl ₃	+99	<i>b</i>
Isoquinoline N-oxide	Me ₂ CO	+90	<i>b</i>
	MeOH	+112 ± 2	<i>b</i>
	CHCl ₃	+97	<i>b</i>
Acridine N-oxide	Me ₂ CO	+110 ± 2	<i>b</i>
Pyridazine N-oxide	Me ₂ CO	+55 (NO)	<i>b</i>
	MeOH	+59 (NO)	<i>b</i>
	CHCl ₃	+57 (NO)	<i>b</i>
Pyrimidine N-oxide	Me ₂ CO	+91 (NO)	<i>b</i>
Pyrazine N-oxide	Me ₂ CO	+68 (NO)	<i>b</i>
	MeOH	+73 (NO)	<i>b</i>
	CHCl ₃	+70 (NO)	<i>b</i>
Phthalazine N-oxide	Me ₂ CO	+67 (NO)	<i>b</i>
	MeOH	+77 (NO)	<i>b</i>
Cinnoline 1-N-oxide	Me ₂ CO	+59 (NO)	<i>b</i>
Cinnoline 2-N-oxide	Me ₂ CO	+53 (NO)	<i>b</i>
Quinazoline 1-N-oxide	Me ₂ CO	+96 (NO) (calcd.)	<i>b</i>
Quinazoline 3-N-oxide	Me ₂ CO	+92 ± 2 (NO)	<i>b</i>
	MeOH	+105 ± 2 (NO)	<i>b</i>
Quinoxazoline N-oxide	Me ₂ CO	+77 (NO)	<i>b</i>
	MeOH	+84 (NO)	<i>b</i>
	CHCl ₃	+80 (NO)	<i>b</i>
Phenazine N-oxide	Me ₂ CO	+90 ± 2 (NO)	<i>b</i>
	H ₂ O	+97 ± 3 (NO)	<i>b</i>
Cinnoline N,N'-dioxide	DMSO	+68 ± 5 (NO, N'O)	<i>b</i>

TABLE XXIII—*cont.*

Compound	Solvent	Nitrogen screening constant	Notes
Quinazoline N,N'-dioxide	DMSO	+90 ± 5 (NO, N'O)	<i>b</i>
Pyrazine N,N'-dioxide	DMSO	+96 ± 5	<i>b</i>
Quinoxaline N,N'-dioxide	H ₂ O	+105 ± 4	<i>b</i>
	DMSO	+103 ± 3	<i>b</i>
Phenazine N,N'-dioxide	(CCl ₃) ₂ CO	+103 ± 5	<i>b</i>
	H ₂ O	+106 ± 5	<i>b</i>

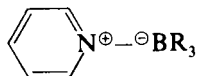
^a Ref. 116, ¹⁴N spectra, originally referred to internal CH₃NO₂, recalculated with solvent shifts for CH₃NO₂ from Table VII.

^b Ref. 45, ¹⁴N spectra, originally referred to internal CH₃NO₂, recalculated with solvent shifts for CH₃NO₂ from Table VII; the screening of quinazoline 1-N-oxide, a compound hereto unknown, is calculated from the additivity rules for the nitrogen screening of azine N-oxides.

predicting the shifts for azines from the data on the corresponding N-oxides and vice versa. There is also a reasonable correlation of the azine N-oxide shifts with the SCF-PPP calculated π -charge densities at the nitrogen atoms. (45)

A regression analysis has been performed (45) on the chemical shifts of some azine-N-oxides in terms of 10 parameters which include interactions between the N–O moiety and the nitrogen atoms at positions 2, 3, and 4 in the six-membered ring. Effects due to additional fused rings in the system and corrections for interactions between “pyridine-type” nitrogen atoms are also included. The additivity rules for the shifts are then used to predict those for a number of azine N-oxides which have been hitherto unknown or not examined by nitrogen NMR spectroscopy. (45)

The borane adducts of azine of the type [49] show a low-frequency



[49]

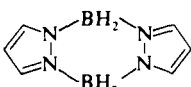
shift of the corresponding nitrogen resonance signal, (92) but its magnitude is dependent on the character of the substituent groups R, since there is a clear β -effect (Table XXIV), similar to that observed for the BR₃ adducts of azoles.

TABLE XXIV

Nitrogen screening constants of some borane adducts of azines and azoles^a in ppm, referred to external neat nitromethane

Compound	Solvent or state	Nitrogen screening constant
N-BH ₃ -pyridine	CH ₂ Cl ₂	+140 ± 5
N-BMe ₃ -pyridine	CH ₂ Cl ₂	+112 ± 5
N-BEt ₃ -pyridine	Et ₂ O	+112 ± 10
N-BBr ₃ -pyridine	toluene	+152 ± 5
N,N'-(BEt ₃) ₂ -pyrazine	CH ₂ Cl ₂	+84 ± 10
N-BH ₃ -2,6-di-Me-pyridine	CH ₂ Cl ₂	+146 ± 5
N-BH ₃ -quinoline	CH ₂ Cl ₂	+139 ± 5
N-BMe ₃ -quinoline	CH ₂ Cl ₂	+94 ± 5
N-BEt ₃ -quinoline	Et ₂ O	+93 ± 5
N-BH ₃ -8-Me-quinoline	CH ₂ Cl ₂	+158 ± 10
N-BH ₃ -isoquinoline	CH ₂ Cl ₂	+154 ± 10
N-BMe ₃ -isoquinoline	CH ₂ Cl ₂	+112 ± 5
N-BEt ₃ -isoquinoline	Et ₂ O	+113 ± 10
N-BH ₃ -3-Me-isoquinoline	CH ₂ Cl ₂	+152 ± 10
N-BEt ₃ -3-me-isoquinoline	CH ₂ Cl ₂	+85 ± 10
3-BH ₃ -imidazole	CH ₂ Cl ₂	+209 ± 10
3-BMe ₃ -imidazole	CH ₂ Cl ₂	+211 ± 5 (NH) +168 ± 10 (NB)
3-BEt ₃ -imidazole	CH ₂ Cl ₂	+194 ± 10 (NH) +148 ± 10 (NB)
1-Me-3-BH ₃ -imidazole	CH ₂ Cl ₂	+218 ± 5 (NMe) +177 ± 5 (NB)
1-Me-3-BMe ₃ -imidazole	CH ₂ Cl ₂	+221 ± 10 (NMe) +153 ± 10 (NB)
1-Me-3-BEt ₃ -imidazole	CH ₂ Cl ₂	+206 ± 10 (NMe) +154 ± 10 (NB)
1-Et-3-BH ₃ -imidazole	CH ₂ Cl ₂	+196 ± 10 (NEt) +180 ± 10 (NB)
1-Et-3-BMe ₃ -imidazole	CH ₂ Cl ₂	+200 ± 5 (NEt) +136 ± 10 (NB)
1-Et-3-BEt ₃ -imidazole	neat liquid	+197 ± 10 (NEt)
1,2-di-Me-3-BH ₃ -imidazole	CH ₂ Cl ₂	+208 ± 10 (NMe) +177 ± 10 (NB)
1,2-di-Me-3-BMe ₃ -imidazole	CH ₂ Cl ₂	+220 ± 10 (NMe) +139 ± 10 (NB)
1,2-di-Me-3-BEt ₃ -imidazole	CH ₂ Cl ₂	+202 ± 10 (NMe) +153 ± 10 (NB)
1-SiMe ₃ -3-BH ₃ -imidazole	CH ₂ Cl ₂	+175 ± 10 (NSi) +205 ± 10 (NB)
1-SiMe ₃ -3-BMe ₃ -imidazole	CH ₂ Cl ₂	+146 ± 10 (NSi) +197 ± 10 (NB)

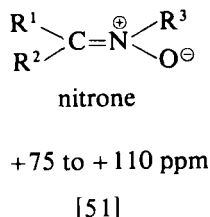
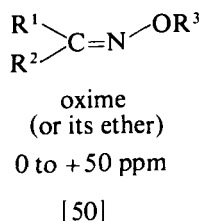
TABLE XXIV—*cont.*

Compound	Solvent or state	Nitrogen screening constant
1-SiMe ₃ -3-BEt ₃ -imidazole	Et ₂ O	+155 ± 10 (NSi) +193 ± 10 (NB)
2-BH ₃ -pyrazole	CH ₂ Cl ₂	+157 ± 10 (NH) +124 ± 10 (NB)
2-BMe ₃ -pyrazole	CH ₂ Cl ₂	+156 ± 10 (NH) +90 ± 10 (NB)
1-Me-2-BH ₃ -pyrazole	tetrahydrofuran	+173 ± 5 (NMe) +145 ± 5 (NB)
1-Me-2-BMe ₃ -pyrazole	neat liquid	+166 ± 10 (NMe) +86 ± 10 (NB)
1-SiMe ₃ -2-BH ₃ -pyrazole	CH ₂ Cl ₂	+139 ± 10
	CH ₂ Cl ₂	+113 ± 5
1-Me-4-BMe ₃ -1,2,4-triazole	CH ₂ Cl ₂	+164 ± 10 (NMe) +72 ± 10 (N) +138 ± 10 (NB)
N-BH ₃ -isothiazole	CH ₂ Cl ₂	+136 ± 5
N-BMe ₃ -isothiazole	neat liquid	+100 ± 5

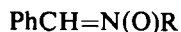
^a Ref. 92. ¹⁴N spectra, originally referred to satd. aqueous NaNO₃, +3.7 ppm from neat CH₃NO₂, Table VII; for comments see Table X, footnotes d and e.

L. Oximes and nitrones

Oximes and nitrones are mutually isomeric structures [50], [51] which are clearly distinguished by means of their nitrogen chemical



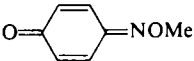
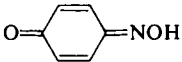


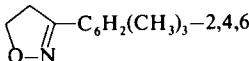
shifts (Table XXV). The usual β -effect is observed for nitrones (Table XXV).



↓
decrease in nitrogen screening

TABLE XXV

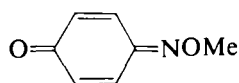
Nitrogen screening constants of some oximes and nitrones in ppm, referred to external neat nitromethane

Compound	Solvent	Nitrogen screening constant	Notes
$\text{Me}_2\text{C}=\text{NOH}$	Et_2O , satd.	$+52 \pm 4$	<i>a</i>
$\text{Me}_2\text{C}=\text{NOMe}$	neat liquid	$+12 \pm 1$	<i>a</i>
	Et_2O , 3 M	$+12 \pm 1$	<i>a</i>
$(\text{Me}_2\text{C}=\text{NHOH})^\oplus\text{Cl}^\ominus$	conc. HCl , satd.	$+107 \pm 7$	<i>a</i>
$\text{MeCH}=\text{NOH}$	Et_2O , satd.	$+31 \pm 2$	<i>a</i>
$\text{MeCH}=\text{NOMe}$	Et_2O , 1 M	0 ± 7	<i>a</i>
$\text{H}_2\text{C}=\text{NOH}$	Et_2O , 1 M	$+2 \pm 5$	<i>a</i>
	Et_2O , 3 M	$+5 \pm 6$	<i>a</i>
	Me_2CO , satd.	-51 ± 13	<i>a</i>
			
			
2,4,6-Trimethylphenyl- $\text{CH}=\text{NOH}$	DMSO	$+5.7 \pm 0.2$	<i>b</i>
	CH_2Cl_2	$+10.0 \pm 0.2$	<i>b</i>
$\text{PhCH}=\text{N(O)Me}$	Me_2CO , satd.	$+104 \pm 1$	<i>a</i>
$\text{PhCH}=\text{N(O)}t\text{-Bu}$	Me_2CO , satd.	$+75 \pm 1$	<i>a</i>
$\text{PhCH}=\text{N(O)Ph}$	Me_2CO , satd.	$+95 \pm 1$	<i>a</i>
$\text{PhCMe}=\text{N(O)Me}$	Me_2CO , satd.	$+109 \pm 1$	<i>a</i>

^a Ref. 117, ^{14}N spectra, originally referred to internal CH_3NO_2 , recalculated with the shifts of CH_3NO_2 in $(\text{CH}_3)_2\text{CO}$ of $+0.8$ ppm, in Et_2O of $+3.9$ ppm, and in conc. HCl of -1.9 ppm from neat CH_3NO_2 , Table VII.

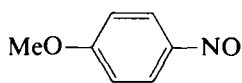
^b Ref. 34, ^{15}N spectra of labelled compounds originally referred to what is reported as 12 M $(\text{CH}_3)_4\text{NCl}$ in H_2O , probably saturated (*ca.* 6 M), $+336.7$ ppm from CH_3NO_2 , Table VII.

Oximes may be involved in tautomeric equilibria with nitroso compounds. The very large difference between the tautomeric forms, from the point of view of nitrogen screening as estimated (117) from the shifts of the corresponding methyl derivatives [52], [53], (Tables XXV and XXVIII), makes nitrogen NMR an attractive means of investigation



+ 5 ppm

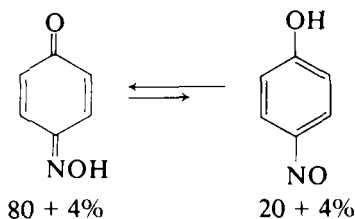
[52]



-428 ppm

[53]

of such equilibria. On the basis of the nitrogen chemical shifts, the following estimate has been obtained (117) for the equilibrium [54]

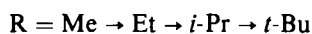
 $80 \pm 4\%$ $20 \pm 4\%$

[54]

involving *p*-benzoquinone mono-oxime and *p*-nitrosophenol in $(\text{CH}_3)_2\text{CO}$.

M. Nitro compounds and nitrates

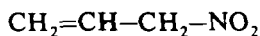
The nitrogen chemical shifts of the NO_2 group in nitroalkanes and conjugated nitro compounds were extensively examined before 1972 (ref. 1d, pp. 233–244). There is a clear β -effect on the chemical shift in nitroalkanes (1d),



↓
decrease in nitrogen screening

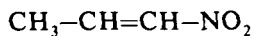
whilst electron-attaching substituents at the $\text{C}-\text{NO}_2$ carbon atom give an opposite effect. The NO_2 group attached to a conjugated ring is characterized by a shift to lower frequencies than that observed for the nitro group in nitroalkanes (1d).

In the review period, additional data became available (118) for nitroalkene systems (Table XXVI, note h). The structures with a double bond system separated from the NO_2 group by at least one saturated carbon atom give NO_2 shifts within the range characteristic of nitroalkanes. However, the presence of a double bond in a position conjugated to the NO_2 system results in an increased screening (Table XXVI) by 10–20 ppm [55], [56].



-6.5 ppm

[55]



+ 2 ppm

[56]

TABLE XXVI

Nitrogen screening constants of some nitro compounds and their derivatives in ppm, referred to external neat nitromethane

Compound	Solvent or state	Nitrogen screening constant	Notes
$\text{NO}_2^- (\text{Na}^+)$	H_2O , 0.30 M	-227.60 ± 0.33	<i>a</i>
	7.56 M (satd.)	-228.89 ± 0.25	<i>a</i>
MeNO_2	neat liquid	0.0000 (arbitrary)	<i>a</i>
	0.3 M, various solvents	-2 to $+7$	<i>d</i>
$(\text{COOMe})_2\text{CHNO}_2$	neat liquid	$+16 \pm 4$	<i>b</i>
$[(\text{COOMe})_2\text{CNO}_2]^\ominus \text{Na}^+$	H_2O	$+31 \pm 5$	<i>b</i>
$(\text{COOMe})_2\text{C}=\text{N}(\text{O})\text{OMe}$	Me_2CO^*	$+70 \pm 5$	<i>b</i>
$(\text{COOMe})_2\text{C}=\text{N}(\text{O})\text{OSiMe}_3$	neat liquid	$+18 \pm 4$	<i>b</i>
$\text{C}(\text{NO})_2$	neat liquid	$+46.59 \pm 0.09$	<i>a</i>
PhNO_2	neat liquid	$+9.56 \pm 0.12$	<i>a</i>
	CCl_4 , 0.30 M	$+12.18 \pm 0.18$	<i>a</i>
<i>o</i> -(SiMe_3)- C_6H_4 - NO_2	CDCl_3	$+5.1 \pm 0.2$	<i>c</i>
<i>m</i> -(SiMe_3)- C_6H_4 - NO_2	CDCl_3	$+9.6 \pm 0.2$	<i>c</i>
<i>p</i> -(SiMe_3)- C_6H_4 - NO_2	CDCl_3	$+9.9 \pm 0.2$	<i>c</i>
2- NO_2 -pyrrole	Me_2CO	$+22.5 \pm 1 (\text{NO}_2)$	<i>d</i>
		$+23.1 \pm 0.5 (\text{NO}_2)$	<i>d, e</i>
its Na^+ salt	H_2O	$+27.5 \pm 1 (\text{NO}_2)$	<i>f</i>
		$+28.3 \pm 0.5 (\text{NO}_2)$	<i>f, g</i>
N-Me-2- NO_2 -pyrrole	Me_2CO	$+22.5 \pm 1 (\text{NO}_2)$	<i>d</i>
3- NO_2 -pyrrole	Me_2CO	$+13.5 \pm 0.5 (\text{NO}_2)$	<i>d, e</i>
its Na^+ salt	H_2O	$+16.3 \pm 0.5 (\text{NO}_2)$	<i>f, g</i>
2,4-Dinitropyrrole	Me_2CO	$+25.7 \pm 0.5 (2\text{-NO}_2)$	<i>d, e</i>
		$+18.3 \pm 0.5 (3\text{-NO}_2)$	<i>d, e</i>
2,5-Dinitropyrrole	Me_2CO	$+25 \pm 1 (\text{NO}_2)$	<i>d</i>
		$+25.5 \pm 0.5 (\text{NO}_2)$	<i>d, e</i>
its Na^+ salt	H_2O	$+14 \pm 1 (\text{NO}_2)$	<i>f</i>
		$+13.7 \pm 0.5 (\text{NO}_2)$	<i>f, g</i>
4(5)- NO_2 -imidazole	DMSO	$+16 \pm 2 (\text{NO}_2)$	<i>d</i>
its Na^+ salt	H_2O	$+14 \pm 2 (50^\circ\text{C}) (\text{NO}_2)$	<i>f</i>
its protonated form	H_2SO_4	$+30 \pm 1 (50^\circ\text{C}) (\text{NO}_2)$	<i>f</i>
N-Me-4- NO_2 -imidazole	DMSO	$+17 \pm 2$	<i>d</i>
2-Me-4(5)- NO_2 -imidazole	DMSO	$+16 \pm 2 (\text{NO}_2)$	<i>d</i>
its K^+ salt	H_2O	$+19 \pm 3 (\text{NO}_2)$	<i>f</i>
4,5-Dinitroimidazole	Me_2CO	$+28 \pm 1 (\text{NO}_2)$	<i>d</i>
	DMSO	$+28 \pm 2 (\text{NO}_2)$	<i>d</i>
its K^+ salt	H_2O	$+17 \pm 2 (\text{NO}_2)$	<i>f</i>
2-Me-4,5-dinitroimidazole	Me_2CO	$+27 \pm 1 (\text{NO}_2)$	<i>d</i>
its K^+ salt	H_2O	$+17 \pm 2 (50^\circ\text{C}) (\text{NO}_2)$	<i>f</i>
$\text{CH}_2=\text{CHCH}_2\text{NO}_2$	neat liquid	-6.5 ± 0.5	<i>h</i>
$\text{MeCH}=\text{CHNO}_2$	DMF	$+2 \pm 2$	<i>h</i>
$\text{MeCH}=\text{C}(\text{Me})\text{NO}_2$	DMF	-2 ± 2	<i>h</i>
$\text{CH}_2=\text{C}(t\text{-Bu})\text{NO}_2$	neat liquid	-2 ± 1	<i>h</i>

TABLE XXVI—*cont.*

Compound	Solvent or state	Nitrogen screening constant	Notes
3-NO ₂ -cyclopentene	DMF	-20 ± 2	<i>h</i>
2-Me-3-NO ₂ -cyclopentene	DMF	-20 ± 1	<i>h</i>
1-NO ₂ -cyclohexene	DMF	+5 ± 2	<i>h</i>
3-NO ₂ -cyclohexene	DMF	-18 ± 1	<i>h</i>
2-Me-3-NO ₂ -cyclohexene	DMF	-17 ± 2	<i>h</i>
1-NO ₂ -cycloheptene	DMF	0 ± 2	<i>h</i>
(CH ₂ =CHCHNO ₂) [⊖] Na [⊕]	20% NaOH	+76 ± 5	<i>h</i>
Na [⊖] salt of 3-nitrocyclohexene	20% NaOH	+84 ± 15	<i>h</i>
Na [⊖] salt of 2-Me-3-nitrocyclohexene	20% NaOH	+84 ± 15	<i>h</i>
EtOC(=O)NHNO ₂	neat liquid	+47 ± 2 (NO ₂)	<i>i</i>
MeN(NO ₂)BEt ₂	CH ₂ Cl ₂	+27 ± 2 (NO ₂)	<i>i</i>
MeN=N(O)OBEt ₂	CH ₂ Cl ₂	+55 ± 2 (NO)	<i>i</i>
MeN(NO ₂)BEt ₂ ·pyridine	pyridine	+21 ± 2 (NO ₂)	<i>i</i>

^a Ref. 61, ¹⁴N spectra, concentric spherical sample containers, full lineshape analysis by differential saturation method, see Table VII for details.

^b Ref. 216, ¹⁴N spectra, originally referred to external neat CH₃NO₂.

^c Ref. 217, ¹⁵N spectra of labelled compounds.

^d Ref. 106, ¹⁴N spectra, originally referred to external CH₃NO₂.

^e Same as in footnote (d), ¹⁵N natural-abundance spectra.

^f Ref. 110, ¹⁴N spectra, originally referred to external CH₃NO₂.

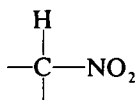
^g Same as in footnote (f), ¹⁵N natural-abundance spectra.

^h Ref. 118, ¹⁴N spectra, originally referred to internal CH₃NO₂, recalculated with CH₃NO₂ shift in DMF of -0.7 ppm from neat CH₃NO₂, Table VII and that for satd. aqueous NaNO₃ of +3.5 ppm.

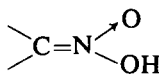
ⁱ Ref. 119, ¹⁴N and ¹⁵N natural-abundance spectra, referred to CH₃NO₂ (¹⁴N) or EtOCONH¹⁵NO₂; shift of the latter is erroneously assumed to be +41 ppm from CH₃NO₂, whilst comparison of ¹⁴N and ¹⁵N shifts reported for the same compound suggests +47 ppm.

Precise data for CH₃NO₂ and C₆H₅NO₂ in dilute solutions, (61) in Tables VII and XXVI, indicate that there are considerable solvent effects on the NO₂ shift. It is interesting that the shift for CH₃NO₂ in H₂O is the same as in concentrated aqueous HCl (Table VII), and that CCl₄ as a solvent gives an extreme low-frequency value for the CH₃NO₂ shift.

Nitroalkanes [57] are isomeric with aci-nitroalkanes [58] and the

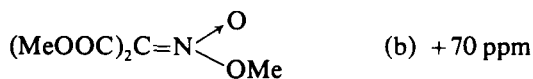


[57]



[58]

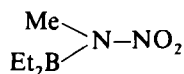
nitrogen chemical shifts for such isomeric pairs seem to be quite different (118) [59a], [59b], as shown in Table XXVI.



[59]

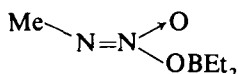
Anions derived from nitro compounds are characterized by a broad range of nitrogen chemical shifts (Table XXVI). There is no significant difference between the shifts of the NO_2 moiety of nitro derivatives of azoles and the corresponding sodium or potassium salts, but anions derived from nitroalkenes show a considerable increase in the nitrogen shielding when compared with the parent compounds.

The NO_2 group in nitramines, R_2NNO_2 , is known (ref. 1d, p. 241) to exhibit its nitrogen resonance at lower frequencies than that of C-nitro compounds. Some further examples (Table XXVI) are available from recent studies (119) on the isomeric systems [60], [61].



+27 ppm (NO_2)

[60]

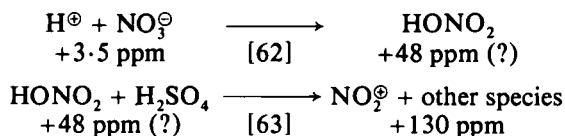


+55 ppm (NO_2)

[61]

Covalent nitrates, $\text{R}-\text{O}-\text{NO}_2$, are characterized by an even larger shift to lower frequencies of the nitrogen resonance (ref. 1d, p. 241). Further examples are given in Table XXVII. The nitrate ion, NO_3^- , gives a resonance signal at about +3.5 ppm in neutral aqueous solutions, almost in the centre of the range of the CH_3NO_2 shifts in various solvents. However, it is sensitive to pH and concentration in acidic solutions (Table VII). The chemical shift of HNO_3 is so concentration dependent that it may serve as a measure of the concentration (Tables VII and XXVII).

The increased screening of nitrogen, from *ca.* +3.5 ppm for very dilute solutions, to *ca.* +48 ppm for 100% HNO_3 , may result from the increasing concentration of the HONO_2 species [62], since the same shift is observed for simple covalent nitrates, CH_3ONO_2 and $\text{C}_2\text{H}_5\text{ONO}_2$ (Table XXVIII). The addition of 100% H_2SO_4 to 100% HNO_3 results in a further increase in screening, up to a value of +130 ppm which is characteristic of the NO_2^+ ion [63] (Table XXX) and may be explained as being due to the increasing concentration of the latter.



This is certainly an oversimplification since the chemical shift for 100% HNO_3 may represent a weighted average of those for the various molecular species present.

Since the nitrate group, NO_3^{\ominus} , has been shown by X-ray crystallography (ref. 71, and references therein) to behave as a unidentate, MONO_2 , bidentate, MO_2NO , bridging bidentate, $\text{MON}(\text{O})\text{OM}$ or bridging terdentate, $\text{MON}(\text{OM})\text{OM}$, ligand, an attempt has been made (71) to obtain information about the type of bonding of the NO_3^{\ominus} group in diamagnetic inorganic nitrates and nitrate-complexes in solution (Table XXVII). Indications of covalent bonding to metal are obtained from the increased screening of the nitrogen nuclei when compared with the NO_3^{\ominus} ion. However, the nitrogen chemical shifts seem to be the same for both the unidentate and bidentate systems of bonding. (71)

N. Nitroso compounds

The nitroso group, NO , is known (ref. 1d, p. 244) to have its nitrogen resonance signal at the high-frequency limit of the range of relative nitrogen screening constants for diamagnetic molecules. More recent data are given in Table XXVIII.

In nitroso-amines, R_2NNO , the shift for the NO group is about -160 ppm, whilst that for the amino moiety is about $+130$ ppm and it shows the usual β -effect upon replacing CH_3 with C_2H_5 (Table XXVIII). The nitrogen signal of the NO group in conjugated nitroso compounds appears at far higher frequencies, -400 to -550 ppm from CH_3NO_2 . It seems that the screening constant is very sensitive to substituent effects, since the difference between *p*-MeO-nitrosobenzene and nitrosobenzene is about 100 ppm. Because the nitrogen screening constant of the NO group is so different from those of other nitrogen-containing structures, nitrogen NMR may easily detect its presence. Tautomeric equilibria between *p*-benzoquinone mono-oxime and *p*-nitrosophenol as well as between various possible tautomers of 2,4-dinitrosoresorcinol (117) offer good examples of potential applications of nitrogen NMR in structural investigations.

O. Azo and diazo compounds

Simple azo compounds, [64], where R can be an alkyl or an aryl substituent, are known (1d, p. 231) to have their nitrogen resonance signals at -130 to -155 ppm from CH_3NO_2 . The recent data (Table

TABLE XXVII

Nitrogen screening constants of some nitrates in ppm, referred to external neat nitromethane

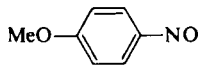
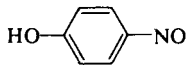
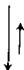
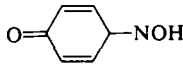
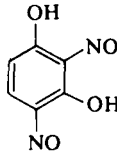
Compound	Solvent or state	Nitrogen screening constant	Notes
$\text{NO}_3^- (\text{K}^+)$	H_2O , 0.30 M	$+3.55 \pm 0.12$	<i>a</i>
$\text{NO}_3^- (\text{Na}^+)$	H_2O , 0.30 M	$+3.53 \pm 0.14$	<i>a</i>
	7.93 M (satd.)	$+3.70 \pm 0.12$	<i>a</i>
$\text{NO}_3^- (\text{NH}_4^+)$	H_2O ; HCl ; HNO_3	$+3.98$ to $+6.30$	<i>a</i>
HNO_3	H_2O , 1.00 M	$+4.43 \pm 0.11$	<i>a</i>
	7.00 M	$+12.59 \pm 0.12$	<i>a</i>
	10.00 M	$+18.23 \pm 0.13$	<i>a</i>
	15.71 M (70.0%)	$+31.31 \pm 0.08$	<i>a</i>
	neat liquid	$+47 \pm 2$	<i>b</i>
O_2NONO_2	neat liquid	$+66 \pm 2$	<i>b</i>
	MeNO_2	$+62 \pm 2$	<i>b</i>
MeC(=O)ONO_2	neat liquid	$+68 \pm 2$	<i>b</i>
MeONO_2	neat liquid	$+40 \pm 2$	<i>b</i>
	CCl_4	$+40 \pm 2$	<i>b</i>
EtONO_2	neat liquid	$+40 \pm 2$	<i>b</i>
	CCl_4	$+41 \pm 2$	<i>b</i>
$\text{Ti}(\text{O}_2\text{NO})_4$	CCl_4 ; MeNO_2 ; HNO_3 (100%)	$+29 \pm 2$	<i>b</i>
$[\text{NO}]^+[\text{Au}(\text{ONO}_2)_4]^-$	MeNO_2	$+29 \pm 2$ (ONO_2)	<i>b</i>
$(\text{CrO}_2)(\text{NO}_3)_2$	neat; CCl_4	$+27 \pm 2$	<i>b</i>
	100% HNO_3	$+29 \pm 2$	<i>b</i>
$\text{Sn}(\text{O}_2\text{NO})_4$	CCl_4 ; MeNO_2	$+28 \pm 2$	<i>b</i>
$\text{Al}(\text{NO}_3)_3 \cdot 2 \text{ MeCN}$	MeCOOEt	$+26 \pm 2$ (NO_3)	<i>b</i>
$[\text{NO}_2]^+[\text{Ga}(\text{NO}_3)_4]^-$	MeNO_2	$+26 \pm 2$ (NO_3)	<i>b</i>
		$+129 \pm 2$ (NO_2) [⊙]	<i>b</i>
$(\text{VO})(\text{NO}_3)_3$	neat; CCl_4 ; MeCN ; 100% HNO_3	$+25 \pm 2$	<i>b</i>
MeHgNO_3	benzene	$+18 \pm 2$	<i>b</i>
$[\text{NH}_4]_2[\text{Ce}(\text{ONO}_2)_6]$	$\text{PO}(\text{OBu})_3$	$+18 \pm 2$	<i>b</i>
	EtOH	$+15 \pm 2$	<i>b</i>
	H_2O	$+12 \pm 2$	<i>b</i>
	MeCN	$+11 \pm 2$	<i>b</i>
	propylene carbonate	$+9 \pm 2$	<i>b</i>
$\text{Co}(\text{O}_2\text{NO})_3$	CCl_4	$+15 \pm 2$	<i>b</i>
	100% HNO_3	$+17 \pm 2$	<i>b</i>
$[\text{Ph}_4\text{As}]_2[\text{Zn}(\text{O}_2\text{NO})_4]$	MeCN	$+13 \pm 2$	<i>b</i>
$\text{Th}(\text{O}_2\text{NO})_4 \cdot 5 \text{ H}_2\text{O}$	H_2O	$+9 \pm 2$	<i>b</i>
$(\text{UO}_2)(\text{NO}_3)_2$	MeOH	$+8 \pm 2$	<i>b</i>
$\text{RuNO}(\text{NO}_3)_3(\text{H}_2\text{O})_2 \cdot x \text{ H}_2\text{O}$	$\text{PO}(\text{OBu})_3$	$+8 \pm 2$ (NO_3)	<i>b</i>
$\text{Cd}(\text{NO}_3)_2 \cdot \text{MeCN}$	MeCN	$+6 \pm 2$	<i>b</i>
$[\text{Ph}_4\text{As}]_2[\text{Cd}(\text{NO}_3)_4]$	MeCN	$+4 \pm 2$	<i>b</i>

^a Ref. 61, ^{14}N spectra, concentric spherical sample containers, full lineshape analysis by differential saturation method, see Table VII for details and comments.

^b Ref. 71, ^{14}N spectra, referred to NO_3^- in saturated aqueous NH_4NO_3 , $+3.98$ ppm from neat CH_3NO_2 ; sample substitution technique is used and no experimental errors are reported (probably not smaller than ± 2 ppm).

TABLE XXVIII

Nitrogen screening constants of some nitroso compounds in ppm, referred to external neat nitromethane

Compound	Solvent or state	Nitrogen screening constant	Notes
Me_2NNO	Me_2CO	$+149 \pm 1$ (N) -157 ± 1 (NO)	<i>a</i> <i>a</i>
Et_2NNO	Me_2CO	$+124 \pm 2$ (N) -160 ± 3 (NO)	<i>a</i> <i>a</i>
$\text{MeN(NO)CH}_2\text{CN}$	Me_2CO	$+152 \pm 4$ (N) $+126 \pm 4$ (CN) -164 ± 4 (NO)	<i>b</i> <i>b</i> <i>b</i>
$\text{EtN(NO)CH}_2\text{CN}$	Me_2CO	-165 ± 4 (NO)	<i>b</i>
	Et_2O , 3 M	-428 ± 10	<i>c</i>
	Me_2CO , satd.	-51 ± 13	<i>c</i>
			
			
Nitrosobenzene	Et_2O , satd.	-536 ± 3	<i>c</i>
	Me_2CO , satd.	-529 ± 4	<i>c</i>
	Me_2CO , satd.	-514 ± 10	<i>c</i>

^a Ref. 111, ¹⁴N spectra, referred to external neat CH_3NO_2 .

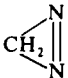

^b Ref. 111, ¹⁴N spectra of ¹⁵N labelled compounds, $\text{CH}_3^{15}\text{N(NO)CH}_2\text{CN}$, $\text{CH}_3\text{N}(^{15}\text{NO})\text{CH}_2\text{CN}$, and $\text{CH}_3\text{N(NO)CH}_2\text{C}^{15}\text{N}$.

^c Ref. 117, ¹⁴N spectra, originally referred to internal CH_3NO_2 , recalculated with CH_3NO_2 shifts in $(\text{CH}_3)_2\text{CO}$ of $+0.8$ ppm, and $(\text{C}_2\text{H}_5)_2\text{O}$ of $+3.9$ ppm from neat CH_3NO_2 , Table VII.

XXIX) show that if R is a carboalkoxy group then the resonance is shifted to about -170 ppm. When R is a dialkylamino group, a considerable increase in screening of the nuclei in the $\text{N}=\text{N}$ moiety is observed when compared with other azo groups [64]. In the case of [64c] the signal of the NR_2 group appears to exhibit the usual β -effect

TABLE XXIX

Nitrogen screening constants of some azo and diazo compounds in ppm, referred to external neat nitromethane

Compound	Solvent or state	Nitrogen screening constant	Notes
	Et ₂ O	+52 ± 6	<i>a</i>
Et ₂ N-N=N-NEt ₂	neat liquid	+303 ± 7 (NEt ₂) +37 ± 5 (N=N)	<i>a</i> <i>a</i>
Me ₂ N-N=N-NMe ₂	neat liquid	+244 ± 5 (NMe ₂) -23 ± 5 (N=N)	<i>a</i> <i>a</i>
EtOOC-N=N-COOEt	Et ₂ O	-158 ± 2	<i>a</i>
	Et ₂ O, 1 : 1 v/v	-168 ± 2	<i>c</i>
<i>n</i> -BuOOC-N=N-CCOBu- <i>n</i>	Et ₂ O, 1 : 1 v/v	-169 ± 2	<i>c</i>
CH ₂ -N [⊕] =N [⊖]	Et ₂ O	+95 ± 2 (terminal) (?) -9 ± 2 (central) (?)	<i>a</i> <i>a</i>
Ph ₂ C=N [⊕] =N [⊖]	CH ₂ Cl ₂	+86 ± 2 (terminal) (?) -55 ± 2 (central) (?)	<i>a</i> <i>a</i>
EtOOCCH=N [⊕] =N [⊖]	?	+115 ± 2 (terminal) (?) +24 ± 7 (central) (?)	<i>a</i> <i>a</i>
	60% H ₂ SO ₄	+140 ± 0.5 (N [⊕]) +23 ± 0.5 (N [⊖])	<i>b</i> <i>b</i>
Ph-N=N-NMe ₂	CDCl ₃	+20.6 ± 0.3 (NPh) -71.4 ± 0.3 (N)	<i>d</i> <i>d</i>
		+225.4 ± 0.3 (NMe ₂)	<i>d</i>
<i>p</i> -MeO-Ph-N=N-NMe ₂	CDCl ₃	-71.4 ± 0.3 (N)	<i>d</i>
		+228.3 ± 0.3 (NMe ₂)	<i>d</i>
<i>p</i> -Cl-Ph-N=N-NMe ₂	CDCl ₃	+25.4 ± 0.3 (NPh) -70.9 ± 0.3 (N)	<i>d</i> <i>d</i>
		+223.8 ± 0.3 (NMe ₂)	<i>d</i>
<i>p</i> -NO ₂ -Ph-N=N-NMe ₂	CDCl ₃	+32.7 ± 0.3 (NPh) -75.3 ± 0.3 (N)	<i>d</i> <i>d</i>
		+214.7 ± 0.3 (NMe ₂)	<i>d</i>

^a Ref. 57, ¹⁴N spectra, originally referred to NH₄[⊕] ion in aqueous saturated NH₄NO₃ as external reference, +359.55 ppm from neat CH₃NO₂, Table VII; signal assignment for =N[⊕]=N[⊖] groups is dubious since reversed assignment is suggested by data from footnote (b).

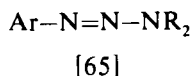
^b Ref. 120, ¹⁵N spectra of singly labelled compounds, at N[⊕] and N[⊖], respectively; originally referred to external KNO₃, +3.5 ppm from neat CH₃NO₂, Table VII.

^c Ref. 121, ¹⁴N spectra, referred to external CH₃NO₂.

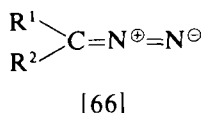
^d Ref. 122, ¹⁵N spectra of labelled compounds, originally referred to "acidified saturated aqueous NH₄Cl", probably *ca.* +352.7 ppm from neat CH₃NO₂, Table VII.

		Shielding in N=N moiety
$R-N=N-R$	(a) $R=Et, Ph$	-130 to -155 ppm
	(b) $R=COOR'$	ca. -170 ppm
	(c) $R=NR'_2$	-20 to +40 ppm
	[64]	

upon replacing the CH_3 group by C_2H_5 . The shift of the NR_2 group is almost the same in unsymmetrical structures such as those of the aryl triazenes (Table XXIX, note d) [65]. The assignments reported in Table XXIX, for the N=N signals of aryl triazenes, (122) are tentative, since the shift at about +25 ppm has been ascribed to the $N-C_6H_5$ nitrogen atom on the basis of larger chemical shift changes upon *para*-substitution.



The diazo, compounds which may be conventionally represented by structure [66], show two resonance signals in their nitrogen spectra



(Table XXIX). The shift of the low-frequency signal, +86 to +140 ppm, seems to be less effected by the nature of the substituents R. This has been used as an argument (57) for its assignment to the terminal (N^\ominus) nitrogen atom. Comparison with the shifts of the azido group, $R-N=N^+=N^\ominus$ have also been made. However, this appears to be misleading, since the measurements for selectively ^{15}N labelled diazo derivatives (120), reported in Table XXIX (note b), show that the reversed assignment should be made, i.e., that the more highly screened nucleus belongs to the central (N^\oplus) nitrogen atom.

The nitrogen spectra clearly differentiate between the isomeric structures of diazomethane [67] and diazine [68]. An attempt has been

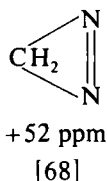
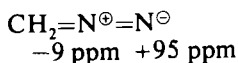


TABLE XXX

Nitrogen screening constants of some small inorganic molecules and ions in ppm, referred to external neat nitromethane

Compound	Solvent or state	Nitrogen screening constant	Notes
N ₂	liquid (77 K)	+70.2 ± 1.5	<i>a</i>
NO ₂ [⊖] [Ga(NO ₃) ₄] [⊖]	MeNO ₂	+129 ± 2 (NO ₂ [⊖])	<i>b</i>
HNO ₃	neat liquid	+44.5 ± 0.5	<i>c</i>
HNO ₃ (100%) + H ₂ SO ₄ (100%)	14.7 mol % H ₂ SO ₄	+47.8 ± 0.5	<i>c</i>
	21.4 mol % H ₂ SO ₄	+49.1 ± 0.5	<i>c</i>
	32.2 mol % H ₂ SO ₄	+52.8 ± 0.5	<i>c</i>
	41.1 mol % H ₂ SO ₄	+61.8 ± 0.5	<i>c</i>
	59.7 mol % H ₂ SO ₄	+74.0 ± 1	<i>c</i>
	65.7 mol % H ₂ SO ₄	+77.7 ± 1	<i>c</i>
	76.9 mol % H ₂ SO ₄	+99.0 ± 1	<i>c</i>
	77.0 mol % H ₂ SO ₄	+101.2 ± 1	<i>c</i>
	83.3 mol % H ₂ SO ₄	+120.7 ± 1	<i>c</i>
	88.1 mol % H ₂ SO ₄	+129.7 ± 1	<i>c</i>
NNO	CCl ₄ (30°C)	+148.0 ± 0.1 (central)	<i>d</i>
		+232.3 ± 0.1 (terminal)	<i>d</i>

See Table VII for some additional data

^a Ref. 126, ¹⁵N natural-abundance spectrum of liquid N₂ at 77 K, originally referred to 5 M NH₄NO₃ in 2 M HNO₃, +358.96 and +4.64 ppm from neat CH₃NO₂ (Table VII, by sample substitution method; possible errors include effects of a large difference in temperatures between sample and standard, and liquid oxygen contamination).

^b Ref. 71, ¹⁴N spectra, referred to NO₃[⊖] ion in saturated aqueous NH₄NO₃, +3.98 ppm from neat CH₃NO₂, Table VII.

^c Ref. 223, ¹⁴N spectra, originally referred to saturated aqueous KNO₃, +3.7 ppm from neat CH₃NO₂, Table VII.

^d Ref. 53, ¹⁵N spectra of doubly labelled NNO, originally referred to *ca.* 7 M HNO₃, +12.6 ppm from neat CH₃NO₂.

made (57) to interpret the observed screening of the nitrogen nuclei in azo-, diazo and related structures in terms of molecular paramagnetic and diamagnetic terms according to Ramsey's definition. However, the limitations of this approach must be taken into account when considering these results.

P. Miscellaneous structures

Reasonably accurate values of the nitrogen screening constants are now available for a number of simple ions and small molecules (Tables VII, XXX and XXXI). The recently measured value for liquid N₂, (126) about +70 ppm from CH₃NO₂, resolves the contradiction about this shift in the older data (ref. 1d, p. 173, and references therein).

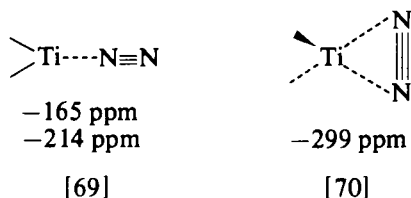
TABLE XXXI

Nitrogen screening constants of some guanidinium, amidinium, imonium and isothiuronium cations^a in ppm, referred to external neat nitromethane

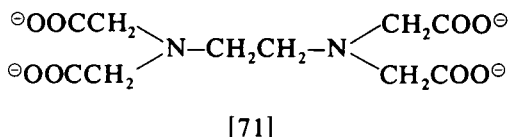
Cation	Nitrogen screening constant
$\text{C}(\text{NH}_2)_3^\oplus$	$+318 \pm 5$
$\text{HC}(\text{NH}_2)_2^\oplus$	$+271 \pm 5$
$\text{CH}_2=\text{NMe}^\oplus$	$+212 \pm 5$
$(\text{Me}_2\text{N})_2\text{CSMe}^\oplus$	$+304 \pm 5$
$(\text{MeHN})_2\text{CSMe}^\oplus$	$+282 \pm 5$
$(\text{H}_2\text{N})_2\text{CSMe}^\oplus$	$+274 \pm 5$

^a Ref. 80, ¹⁴N spectra, originally referred to satd. aqueous NaNO₃, +3.7 ppm from neat CH₃NO₂; see footnotes (d) and (e) in Table X.

The ^{15}N spectrum of a diamagnetic complex of $^{15}\text{N}_2$ with permethyltitanocene (123) at -61°C shows a pair of doublets, which are assigned to the "end-on" complex structure [69], and a singlet, attributed to the "edge-on" structure [70]. The nitrogen chemical shifts (originally referred to what was reported as 11 M $(\text{C}_2\text{H}_5)_4\text{NCl}$ in H_2O , probably a saturated solution, *ca.* 4.6 M, Table VII) are recalculated here on the neat CH_3NO_2 scale.



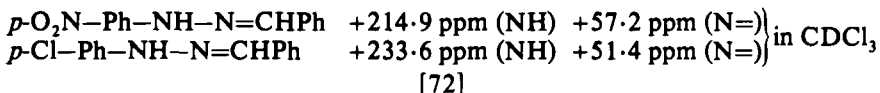
Various anions derived from ethylenediamine-tetraacetic acid (EDTA) have been investigated by ^{15}N NMR spectroscopy. (124) The chemical shifts are referred to the tetra-anion [71], hence they cannot be



compared with those on the nitromethane or any other scale. For a number of EDTA complexes with closed-shell metal ions the range of shifts is +5 to -17 ppm from that of the tetra-anion. This small range of

observed shifts contrasts with the calculated changes in the diamagnetic term which provides a range of 300 ppm. (124) However, this is simply a consequence of the method adopted for calculating this term which has no physical meaning. (29)

Some data are available (125) for some phenylhydrazones [72]. These



data are taken from ^{15}N spectra of labelled compounds, the shifts are recalculated to the CH_3NO_2 scale from the original standard, saturated aqueous NH_4Cl which appears at +352.9 ppm from nitromethane, (Table VII).

Q. Studies on paramagnetic molecules

In a paramagnetic environment large shifts and broadened NMR signals are expected. (2b) The shifts may arise either from the presence of unpaired electron spin density at the nucleus concerned—contact shifts, or from anisotropy in the electronic g tensor—dipolar shifts. (2b)

The line broadening is produced by the rapidly fluctuating local magnetic fields due to the unpaired electrons. Since nitrogen atoms often act as coordination centres in transition metal complexes, nitrogen NMR is a useful tool for investigating the bonding, structure and reactions of such molecules.

Lincoln and West have used ^{14}N NMR to obtain kinetic data on several ligand exchange reactions. Among the systems they have studied are cobalt(II) complexes with acetonitrile, (128) acetonitrile exchange with cobalt(II) complexes of triethylenetetramine, (129) 2,2',2''-tri-aminotriethylamine, (130) 2,2',2''-tri(*N,N*-dimethylamino)triethylamine, (130) 2-hydroxymethyl-2-methylpropane-1,3-diol, (131) 2,2',2''-nitrilotriethanol, (132) and 2,2-di(aminomethyl)propan-1-ol. (132) They have also reported on pyridine exchange in bis(pentane-2,4-dionato)-dipyridine cobalt(II) and nickel(II). (133)

Several kinetic studies have been reported on nickel(II) complexes including acetonitrile exchange (134, 136) with complexes formed by nickel(II) and 2,2',2''-tri-aminotriethylamine, (130) 2,2',2''-tri(*N,N*-dimethylamino)-triethylamine, (130) 2,2-di(hydroxymethyl)-1-propanol, (135) 2,2-di(aminomethyl)-1-propylamine, (135) 2,2-di(aminomethyl)-1-propanol (135) and 2,2',2''-trihydroxytriethylamine. (135)

Contact shifts in the ^{14}N spectra of acetonitrile complexes of copper(II), nickel(II), cobalt(II) and titanium(III) have been investigated. (136) Direct evidence for both positive and negative contributions to the shifts from σ and π ligand spin densities is reported.

Aniline and the fluoroanilines exhibit ^{14}N contact shifts in the presence of (pentane-2,4-dionato) nickel(II). By comparing the shifts with spin densities calculated by the INDO molecular orbital procedure a structure is proposed for the complexes formed in solution. (137) Contact shifts have also been reported from the ^{14}N spectra of some cobalt(II) nitrate complexes. (138) In the case of $[\text{Co}(\text{H}_2\text{O})_5\text{NO}_3]^\oplus$ the chemical shift of the nitrate ligand is reported to be 2360 ± 100 ppm to high frequency of the free nitrate ion. (222)

The importance of contact, rather than dipolar contributions to the shifts induced by lanthanide shift reagents in the NMR spectra of nuclei other than protons has recently been reviewed. (2b) A second order perturbation calculation of the spin density has provided an estimate of the relative contact shifts experienced by nuclei bonded to various lanthanide shift reagents. (139) The theoretical estimates are in agreement with the ^{14}N NMR data on pyridine in the presence of lanthanide ions, showing that the contact interaction is dominant. ^{14}N NMR studies, employing lanthanide shift reagents, have demonstrated their utility in deciding between structures whose ^{14}N chemical shifts are close together. (140)

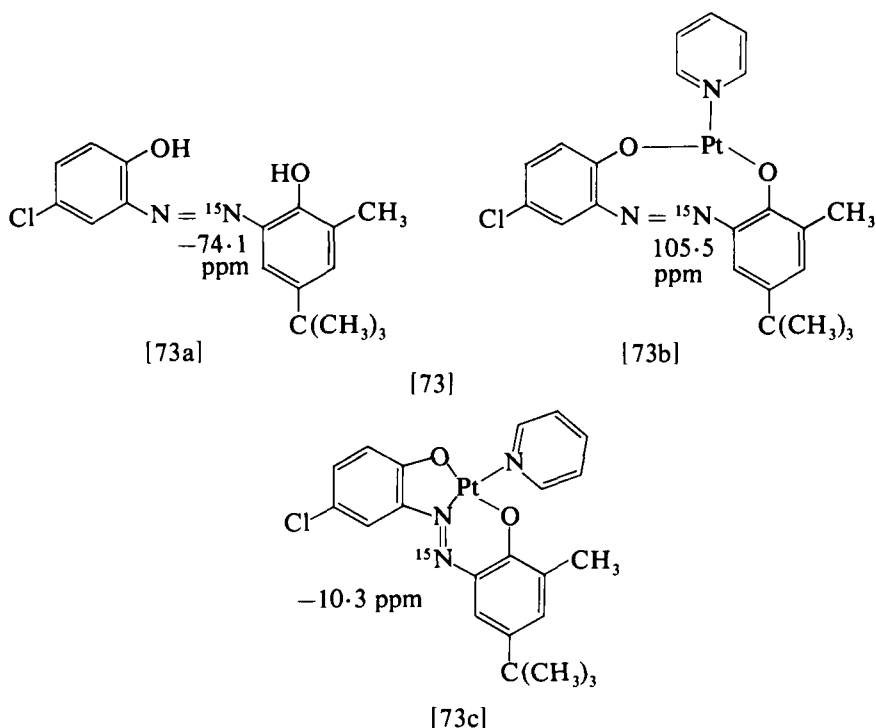
R. Studies on diamagnetic metal complexes

Some ^{15}N NMR investigations have been reported on diamagnetic metal complexes. In one study evidence for the edge on coordination of molecular nitrogen in a titanium complex has been presented. (123, 143)

Some pentammino cobalt(III) complexes display a ^{15}N chemical shift difference for the NH_3 groups *cis* and *trans* to a series of ligands X. (141) The shifts are found to be solvent dependent, in contrast to an earlier report (142) and are related to the Co-N bond strength. It is claimed that the Co-N bond *trans* to X is stronger than in $[\text{Co}(\text{NH}_3)_6]^{3\oplus}$ when X is H_2O , Cl^\ominus or Br^\ominus . The *cis* Co-N bond is also stronger but not as strong as the *trans* bond. When X is NO_2^\ominus the *trans* Co-N bond is still stronger than the *cis* but both are reported to be weaker than in $[\text{Co}(\text{NH}_3)_6]^{2\oplus}$. (141)

In the case of some Pt(II) complexes of some unsymmetrical *o,o'*-dihydroxydiarylazo ligands [73a], ^{15}N parameters are reported to be useful in the solution of subtle structural problems. (125) ^{15}N coordination shifts to lower frequencies of 179.6 and 63.8 ppm respectively are reported for [73b] and [73c].

The smaller coordination shift for the ^{15}N nucleus in [73c] is consistent with its lone pair of electrons remaining free, whereas they are used for the coordination of the ^{15}N atom in [73b]. The possibility of hydrazone structures [72] contributing to the molecule, rather than the azo-forms [73], is excluded on the basis that the hydrazine nitrogen



signal appears at more than 100 ppm to low frequencies of those in the azo structures.*

VI. CORRELATION OF NITROGEN SPIN-SPIN COUPLING CONSTANTS WITH MOLECULAR STRUCTURE

The problems encountered in dealing with the spin-spin coupling constants between ^{14}N or ^{15}N and other nuclei have already been discussed in detail (ref. 1e, pp. 261–317). Here we shall consider more recent observations which include also $^{15}\text{N}-^{15}\text{N}$ coupling. Since there is a simple relationship between the coupling constants of ^{14}N or ^{15}N with other nuclei, equation (29),

$$J(^{14}\text{N}-\text{X}) = -0.7129 J(^{15}\text{N}-\text{X}) \quad (29)$$

and because most of the experimental data come from measurements on ^{15}N -labelled compounds, we have recalculated all observed ^{14}N

* *Note added in proof.* The isotope effect has been reported for N_2O_3 and related structures (225). Values of the order of 0.1–0.3 ppm are claimed. It probably arises from small differences in the average N–N separation, in the vibrational ground state, for molecules with $^{14}\text{N}-^{15}\text{N}$ and $^{15}\text{N}-^{15}\text{N}$ bonds.

couplings to those of ^{15}N nuclei. Sometimes, it is convenient to use the reduced coupling constant, equation (30),

$$K_{ij} = 4\pi^2 J_{ij} / (h\gamma_i\gamma_j) \quad (30)$$

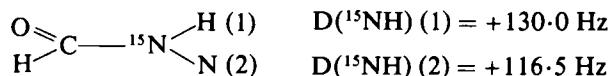
where γ_i is the magnetogyric ratio of nucleus i , and the constant K is given in either cm^{-3} or in NA^2m^{-3} ($1 \text{ NA}^2\text{m}^{-3} = 10 \text{ cm}^{-3}$). The following conversion factors may be used:

$$\begin{aligned} -0.822 J(^{15}\text{N}-\text{H}) \text{ (in Hz)} &= K(^{15}\text{N}-\text{H}) \text{ (in cm}^{-3}\text{)} \\ -3.26 J(^{15}\text{N}-^{13}\text{C}) &= K(^{15}\text{N}-^{13}\text{C}) \\ 8.10 J(^{15}\text{N}-^{15}\text{N}) &= K(^{15}\text{N}-^{15}\text{N}) \end{aligned} \quad (31)$$

A. $^1\text{J}(^{15}\text{N}-\text{H})$

The one-bond coupling constant $^1\text{J}(\text{N}-\text{H})$ has the largest absolute value among N-H coupling constants. It is negative when ^{15}N is involved as shown for example, in the recent measurements on ^{15}N -formamide in a lyotropic nematic phase (144) and in other investigations. (145, 146) It increases in absolute value with an increasing amount of s -character in the bonding orbitals (ref. 1e, p. 269).

The nematic phase studies (144) on ^{15}N -formamide revealed, in addition to the scalar coupling constant J , the values of the dipolar



couplings, $\text{D}(^{15}\text{NH})$. The entire set of dipolar coupling constants, required to explain the observed nematic phase spectrum of formamide, suggests that the molecule is not planar under the experimental conditions employed, and that the average life-time of the non-planar form is greater than 0.1 sec.

A recently developed technique of subtracting ^{15}N -decoupled from ^{15}N -undecoupled proton spectra (81, 221) permits the measurement of larger $^{15}\text{N}-\text{H}$ couplings, mostly $^1\text{J}(\text{N}-\text{H})$, from the very weak ^{15}N satellites observed in proton spectra. A number of $^1\text{J}(\text{N}-\text{H})$ values for amides have been measured by this method (Table XXXII, note b).

The INDOR technique of decoupling ^{14}N from ^1H (150) has been shown to yield two different values of $^1\text{J}(\text{N}-\text{H})$ in formamide, but the experimental errors are much larger than those found in the measurement of $^{15}\text{N}-\text{H}$ couplings.

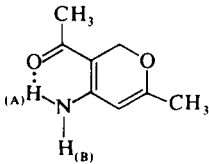
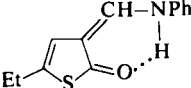
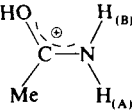
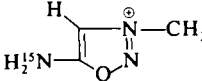
The $^1\text{J}(\text{N}-\text{H})$ values in some dipeptides (95), shown in Table XXXII (note d), are within the range characteristic of amides. The small variation found in the values has been proposed as an indication of *cis-trans* isomerism about the peptide bond.

TABLE XXXII

Some values of $^1J(^{15}\text{N}-\text{H})$ in Hz

Compound	Solvent	$^1J(^{15}\text{N}-\text{H})$	Notes
$\begin{array}{c} \text{O} \\ \parallel \\ \text{H}-\text{C}-^{15}\text{N} \begin{array}{l} \text{H}_{(\text{A})} \\ \text{H}_{(\text{B})} \end{array} \end{array}$	nematic phase	-86.9 ± 0.1 (A)	<i>a</i>
		-91.3 ± 0.1 (B)	<i>a</i>
	none	(-88.3 ± 0.1) (A)	<i>b</i>
		(-90.7 ± 0.1) (B)	<i>b</i>
MeCONHMe	none	(-93.0 ± 0.1)	<i>b</i>
EtCONHMe	none	(-92.9 ± 0.1)	<i>b</i>
<i>i</i> -PrCONHMe	none	(-92.7 ± 0.1)	<i>b</i>
<i>t</i> -BuCONHMe	CCl ₄	(-92.3 ± 0.1)	<i>b</i>
MeCONHCH ₂ COOMe	acetone	(-93.5 ± 0.1)	<i>b</i>
MeCONHCH(Et)COOMe	acetone	(-92.6 ± 0.1)	<i>b</i>
MeCONHCH(<i>i</i> -Pr)COOMe	acetone	(-92.6 ± 0.1)	<i>b</i>
NH ₃ ⁺ CH ₂ CONHCH ₂ COOH	H ₂ O	(-94.1 ± 0.1) (NH ₃ ⁺)	<i>c</i>
N-Ac-DL-Ala- ¹⁵ N	H ₂ O, pH 6	(-93.30 ± 0.05)	<i>d</i>
Valinomycin (L-Val- ¹⁵ N)	CCl ₄	(-93.55 ± 0.05)	<i>d</i>
L-Ala-L-Phe- ¹⁵ N	H ₂ O, pH 2	(-92.15 ± 0.05)	<i>d</i>
L-Ala-L-Ala- ¹⁵ N	H ₂ O, pH 2	(-93.24 ± 0.05)	<i>d</i>
L-Phe-Gly- ¹⁵ N	H ₂ O, pH 2	(-93.15 ± 0.05)	<i>d</i>
L-Val-Gly- ¹⁵ N	H ₂ O, pH 2	(-94.45 ± 0.05)	<i>d</i>
<i>c</i> -L-Ala-L-Ala- ¹⁵ N	H ₂ O, pH 2	(-91.13 ± 0.05)	<i>d</i>
<i>c</i> -L-Val-Gly- ¹⁵ N	H ₂ O, pH 2	(-91.07 ± 0.05)	<i>d</i>
	DMSO	(-90.00 ± 0.05)	<i>d</i>
<i>c</i> -L-Phe-Gly- ¹⁵ N	DMSO	(-90.50 ± 0.05)	<i>d</i>
<i>c</i> -L-Ala-L-Phe- ¹⁵ N	DMSO	(-89.30 ± 0.05)	<i>d</i>
Pyrrole	none	-96.48 ± 0.05	<i>e</i>
(CF ₃) ₂ PNH ₂	none (?)	(-85.6 ± 0.1)	<i>f</i>
(C ₂ F ₅) ₂ PNH ₂	none (?)	(-85.8 ± 0.1)	<i>f</i>
[(CF ₃) ₂ P] ₂ NH	none (?)	(-81.9 ± 0.1)	<i>f</i>
(CH ₃)(CF ₃)PNH ₂	none (?)	(-79.9 ± 0.1)	<i>f</i>
[(CH ₃)(CF ₃)P] ₂ NH	none (?)	$(-77.5, 78.7 \pm 0.1)$	<i>f</i>
F ₂ PNH ₂	none (?)	(-82.7 ± 0.1)	<i>f</i>
F ₃ P(NH ₂) ₂	none (?)	(-87.5 ± 0.1)	<i>f</i>
F ₄ PNH ₂	HCCl ₂ F	(-90.3 ± 0.1)	<i>f</i>
(CF ₃) ₂ AsNH ₂	none (?)	(-73.4 ± 0.1)	<i>f</i>
[CF ₃] ₂ As ₂ NH	none (?)	(-79.0 ± 0.1)	<i>f</i>
(CF ₃)SNH ₂	none (?)	(-80.6 ± 0.1)	<i>f</i>
[(CF ₃)S] ₂ NH	none (?)	(-99.1 ± 0.1)	<i>f</i>
(SiH ₃) ₂ NH	none (?)	(-71.4 ± 0.1)	<i>f</i>
H ₃ B ₃ N ₃ H ₃	?	(-78.0 ± 0.1)	<i>f</i>
(SiMe ₃) ₂ NH	CCl ₄	(-63.1 ± 0.1)	<i>g</i>
Ph ₃ SiNH ₂	CCl ₄	(-71.0 ± 0.1)	<i>g</i>
<i>trans</i> -PhC(Me)=CHNHPh	DMSO	(-90.8 ± 0.1)	<i>h</i>
<i>trans</i> -(<i>p</i> -MeO-Ph)C(Me)=CHNHPh	DMSO	(-91.1 ± 0.1)	<i>h</i>
<i>trans</i> -(<i>p</i> -NO ₂ -Ph)C(Me)=CHNHPh	DMSO	(-91.2 ± 0.1)	<i>h</i>

TABLE XXXII—cont.

Compound	Solvent	$^1J(^{15}\text{N}-\text{H})$	Notes
	DMSO	-91.0 ± 0.1 -92.3 ± 0.1	<i>i</i> (A) <i>i</i> (B)
	dioxan	-93.0 ± 0.1	<i>i</i>
	FSO ₃ H	$(-)96.6 \pm 0.1$ $(-)93.2 \pm 0.1$	<i>j</i> (A) <i>j</i> (B)
	H ₂ SO ₄ , 100%	$(-)96.0 \pm 0.1$ $(-)92.8 \pm 0.1$	<i>j</i> (A) <i>j</i> (B)
	CF ₃ COOH	$(-)96.8 \pm 0.1$	<i>k</i>

^a ¹⁵N label; nematic phase measurements, 7% Na₂SO₄, 36% sodium decyl sulphate, 7% decanol, 50% water, acidified with dilute H₂SO₄; ref. 144.

^b From ¹⁵N satellites in proton spectra of unlabelled cpds. by accumulation of ¹⁵N-decoupled and reversed ¹⁵N-undecoupled spectra; signs not determined; ref. 81.

^c ¹⁵N label; signs not determined; ref. 96.

^d ¹⁵N-labelled amino acids; signs not determined; ref. 95.

^e ¹⁵N-labelled pyrrole, ¹³C satellite analysis in proton spectra; ref. 146.

^f ¹⁵N label; ref. 147.

^g Recalculated from ¹⁴N-¹H couplings observed in ¹H and ¹⁴N spectra; signs not determined; ref. 89.

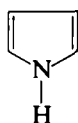
^h ¹⁵N label; ref. 148.

ⁱ ¹⁵N label; ref. 145.

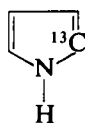
^j ¹⁵N-labelled acetamide; ref. 149.

^k ¹⁵N-labelled sydnimine hydrochloride; ref. 111.

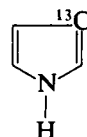
Precise measurements and analysis of the proton spectrum of ¹⁵N-pyrrole, including the ¹³C satellites, indicate that there is no detectable isotope effect by ¹³C on the ¹J(N-H) coupling constant in the molecules [74] to [76]. ¹J(N-H) values for some N-P, N-As and N-Si



[74]



[75]

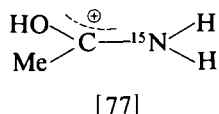


[76]

compounds have been measured (147), and the results are given in Table XXXII (note f). The values of $^1J(\text{N-H})$ have been explained simply in terms of electron density changes in the σ -bond framework without invoking dative $\text{N} \rightarrow \text{P}$ bonding. The absolute value of $^1J(\text{N-H})$ is found to increase in proceeding from XNH_2 to X_2NH compounds. There is a good correlation between the electronegativity of X and the $^1J(\text{N-H})$ value (the absolute value increases with increasing electronegativity of X).

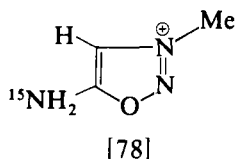
The absolute value of $^1J(^{15}\text{N-H})$ in some enamines (148) was found to be about 91 Hz, (Table XXXII, note g), larger than in aniline (about 83 Hz), and comparable to those for urea, some amides and their vinylogues. This has been explained in terms of an increase in the s-character of the N-H bond in such structures in comparison with aniline.

The question of the site of protonation of amides in strongly acidic media has been thoroughly investigated by means of the proton spectra of ^{15}N -acetamide at various temperatures and acid concentrations. (149) The coupling pattern is consistent with the presence of a large excess of the O-protonated form [77], in anhydrous H_2SO_4 and HSO_3F , in



equilibrium with a very small amount of the N-protonated amide. The $^1J(\text{N-H})$ coupling in the cation is larger than in the unprotonated amide.

The proton spectrum of methylsydnimine hydrochloride [78], ^{15}N -labelled at the exocyclic nitrogen atom, (111) reveals a two-proton



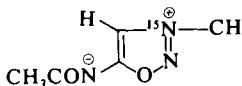
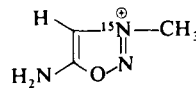
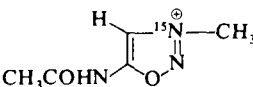
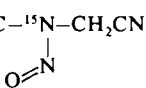
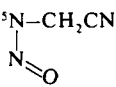
doublet with a typical value of $^1J(\text{N-H})$. This demonstrates that the cation has the structure [78]. The measurement of $^1J(\text{N-H})$ from proton spectra has been used to distinguish between keto and enol isomers. (224)

B. $^2J(^{15}\text{N-H})$

It is known (ref. 1e, p. 292) that the two-bond $^{15}\text{N-C-H}$ coupling is small when the intervening carbon atom is saturated, and the absolute values of $^2J(^{15}\text{N-C-H})$ are seldom higher than about 2 Hz. Some

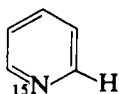
TABLE XXXIII

Some values of $^2J(^{15}\text{N}-\text{H})$ in Hz

Compound	Type of coupling	$2J(^{15}\text{N}-\text{H})$	Notes	
N-Me-4-CN-pyridinium iodide	$\text{N}^{\oplus}-\text{H}(\text{ortho})$	-0.75 ± 0.14	<i>a</i>	
	$\text{N}^{\oplus}-\text{CH}_3$	$(\pm)0.75 \pm 0.14$	<i>a</i>	
N-Me-2-Me-pyridinium iodide	$\text{N}^{\oplus}-\text{CH}_3$	$(\pm)0.57 \pm 0.14$	<i>a</i>	
N-Me-pyridinium iodide	$\text{N}^{\oplus}-\text{H}(\text{ortho})$	-0.71 ± 0.14	<i>a</i>	
	$\text{N}^{\oplus}-\text{CH}_3$	$(\pm)0.29 \pm 0.14$	<i>a</i>	
N-Et-pyridinium bromide	$\text{N}^{\oplus}-\text{H}(\text{ortho})$	-0.57 ± 0.14	<i>a</i>	
N-Me-pyrazinium iodide	$\text{N}^{\oplus}-\text{H}(\text{ortho})$	-0.75 ± 0.14	<i>a</i>	
	$\text{N}^{\oplus}-\text{CH}_3$	$(\pm)0.93 \pm 0.14$	<i>a</i>	
$\text{Me}_3\text{N}^{\oplus}-\text{CH}=\text{CH}_2$ (Br^{\ominus})	$\text{N}^{\oplus}-\text{CH}=\text{}$	$(\pm)2.5 \pm 0.1$	<i>b</i>	
$(\text{Et}_2)(\text{Me})\text{N}^{\oplus}-\text{CH}=\text{CH}_2$ (Br^{\ominus})	$\text{N}^{\oplus}-\text{CH}=\text{}$	$(\pm)2.3 \pm 0.1$	<i>b</i>	
$\text{CD}_3-\text{C}\equiv\text{N}^{\oplus}-\text{Me}$	$\text{N}^{\oplus}-\text{CH}_3$	$(\pm)2.1 \pm 0.1$	<i>c</i>	
Pyrrole	$\text{N}-(\text{C}=\text{))-H$	-4.53 ± 0.05	<i>d</i>	
		-4.55 ± 0.05	<i>e</i>	
		-4.52 ± 0.05	<i>f</i>	
Pyrazole	$\text{N}-(\text{C}=\text{))-H$	-8.94 ± 0.05	<i>f</i>	
	(averaged by tautomerization)			
1,3-Thiazole	$\text{N}-(\text{C}=\text{))-H(2)$	-10.56 ± 0.05	<i>f</i>	
	$\text{N}-(\text{C}=\text{))-H(4)$	-10.6 ± 0.1	<i>f</i>	
Pyridine	$\text{N}-(\text{C}=\text{))-H$	-10.76 ± 0.05	<i>f</i>	
Pyridazine	$\text{N}-(\text{C}=\text{))-H$	-12.04 ± 0.05	<i>f</i>	
$\text{HC}(=\text{O})\text{NH}_2$	$\text{N}-(\text{C}=\text{O))-H$	-14.4 ± 0.1	<i>g</i>	
syn-(2,4,6-Me ₃ -Ph)CH=NOH	$\text{N}-\text{CH}$	$(\pm)2.4 \pm 0.2$	<i>h</i>	
	CDCl_3	$\text{N}^{\oplus}-\text{CH}_3$ $\text{N}^{\oplus}-\text{H}$	$(\pm)2.1 \pm 0.1$ $(\pm)5.5 \pm 0.1$	<i>i</i> <i>i</i>
	CD_3OD CF_3COOH	$\text{N}^{\oplus}-\text{CH}_3$ $\text{N}^{\oplus}-\text{H}$ $\text{N}^{\oplus}-\text{CH}_3$ $\text{N}^{\oplus}-\text{H}$	$(\pm)2.3 \pm 0.1$ $(\pm)4.2 \pm 0.1$ $(\pm)2.5 \pm 0.1$ $(\pm)4.3 \pm 0.1$	<i>i</i> <i>i</i> <i>i</i> <i>i</i>
	CD_3OD CF_3COOH	$\text{N}^{\oplus}-\text{CH}_3$ $\text{N}^{\oplus}-\text{H}$ $\text{N}^{\oplus}-\text{CH}_3$ $\text{N}^{\oplus}-\text{H}$	$(\pm)2.4 \pm 0.1$ $(\pm)4.6 \pm 0.1$ $(\pm)2.3 \pm 0.1$ $(\pm)4.8 \pm 0.1$	<i>i</i> <i>i</i> <i>i</i> <i>i</i>
$\text{H}_3\text{C}-^{15}\text{N}-\text{CH}_2\text{CN}$ 		$\text{N}-\text{CH}_3$ (syn to NO)	$(\pm)1.5 \pm 0.1$	<i>j</i>
		$\text{N}-\text{CH}_3$ (anti to NO)	$(\pm)1.7 \pm 0.1$	<i>j</i>
\updownarrow	CDCl_3	$\text{N}-\text{CH}_2$ (syn to NO)	$(\pm)1.4 \pm 0.1$	<i>j</i>
$\text{H}_3\text{C}-^{15}\text{N}-\text{CH}_2\text{CN}$ 		$\text{N}-\text{CH}_2$ (anti to NO)	$(\pm)1.6 \pm 0.1$	<i>j</i>

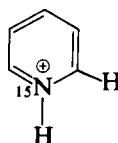
additional examples are given in Table XXXIII for $\text{N}^{\oplus}\text{-CH}_3$ and N-CH_3 groups with typical values of about 2 Hz. The geometrical dependence of the N-C-H coupling in CH_3NH_2 has been predicted from theoretical data. (219)

When the coupling is across a tricoordinate carbon atom involved in a delocalized π -electron system, the absolute value of $^2J(^{15}\text{N-C-H})$ may increase to as much as 16 Hz. (1e) In the review period, the signs of such coupling constants have been determined as negative for formamide, (144) pyrrole, (146, 154, 155) pyrazole, thiazole, pyridine and pyridazine (155) as well as for some azinium ions. (151) The latter afford another example of the decrease in the absolute value of the coupling constant upon protonation of the nitrogen lone pair (Table XXXIII) [79], [80].



$$^2J(\text{N-H}) = -10.8 \text{ Hz}$$

[79]



$$^2J(\text{N-H}) = -0.7 \text{ Hz}$$

[80]

The $^2J(\text{N-H})$ coupling constants for some sydnimine derivatives (Table XXXIII, note i) show that the two-bond coupling is larger across a tricoordinate carbon atom than across the saturated carbon atom of a methyl group. (111)

Theoretical calculations (157) indicate that there should be a strong geometrical dependence of the value of $^2J(\text{N-H})$ in methyleneimine, $\text{H}_2\text{C=NH}$. This is in agreement with the observations made on formaldoxime, $\text{H}_2\text{C=NOH}$.

^a From proton spectra by ^{14}N decoupling, tickling, and simultaneous decoupling of substituent protons; recalculated to ^{15}N ; ref. 151.

^b From proton spectra by ^{14}N decoupling; recalculated to ^{15}N ; ref. 152.

^c As above; ref. 153.

^d ^{15}N -labelled pyrrole; ref. 154.

^e ^{15}N -labelled pyrrole; ref. 146.

^f ^{15}N label; ref. 155 and references therein.

^g ^{15}N -labelled formamide; nematic phase measurements; ref. 144.

^h ^{15}N label; ref. 34.

ⁱ ^{15}N -labelled acetylsydnimine, sydnimine hydrochloride and acetylsydnimine hydrochloride, respectively; ref. 111.

^j ^{15}N -labelled N-methyl, N-cyanomethylnitrosoamine; ref. 156.

TABLE XXXIV

Some values of $^3J(^{15}\text{N}-\text{H})$ in Hz

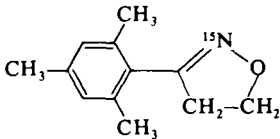
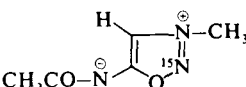
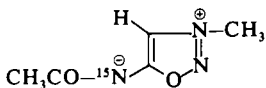
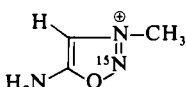
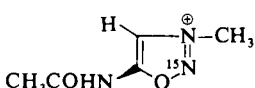
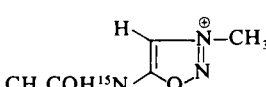
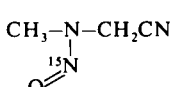
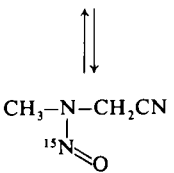
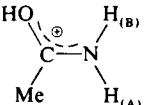
Compound	Type of coupling	$^3J(^{15}\text{N}-\text{H})$	Notes
N-Me-4-CN-pyridinium iodide	$\text{N}^\oplus\text{-H}(\text{meta})$	-2.20 ± 0.2	<i>a</i>
N-Me-2-Me-pyridinium iodide	$\text{N}^\oplus\text{-H}(\text{meta})$	-1.85 ± 0.2	<i>a</i>
N-Me-pyridinium iodide	$\text{N}^\oplus\text{-H}(\text{meta})$	-1.78 ± 0.2	<i>a</i>
N-Et-pyridinium bromide	$\text{N}^\oplus\text{-H}(\text{meta})$	-1.92 ± 0.2	<i>a</i>
	$\text{N}^\oplus\text{-(C)-CH}_3$	$(\pm)1.57 \pm 0.07$	<i>a</i>
N-Me-pyrazinium iodide	$\text{N}^\oplus\text{-H}(\text{meta})$	-1.95 ± 0.2	<i>a</i>
$\text{Me}_3\text{N}^\oplus\text{-CH=CH}_2 (\text{Br}^\ominus)$	$\text{N}^\oplus\text{-(C=C)-H}$		<i>b</i>
	(<i>trans</i>)	$(\pm)4.0 \pm 0.1$	
	(<i>cis</i>)	$(\pm)1.8 \pm 0.1$	<i>b</i>
$(\text{Et}_2)(\text{Me})\text{N}^\oplus\text{-CH=CH}_2 (\text{Br}^\ominus)$	$\text{N}^\oplus\text{-(C=C)-H}$		<i>b</i>
	(<i>trans</i>)	$(\pm)3.7 \pm 0.1$	
	(<i>cis</i>)	$(\pm)1.6 \pm 0.1$	<i>b</i>
Pyrrole	N-(C=C)-H	-5.34 ± 0.05	<i>c</i>
		-5.35 ± 0.05	<i>d</i>
		$(\pm)5.39 \pm 0.05$	<i>e</i>
Pyrazole	N-(C=C)-H	-3.37 ± 0.05	<i>e</i>
	N-(N=C)-H	-4.28 ± 0.05	<i>e</i>
1,3-Thiazole	N-(C=C)-H	-1.97 ± 0.05	<i>e</i>
Pyridine	N-(C=C)-H	-1.53 ± 0.05	<i>e</i>
Pyridazine	N-(C=C)-H	-1.12 ± 0.05	<i>e</i>
	N-(N-C)-H	-3.70 ± 0.05	<i>e</i>
	N=(C-C)-H	$(\pm)2.3 \pm 0.2$	<i>f</i>
2- $^{15}\text{NO}_2$ -pyrrole (and its anion)	$(\text{O}_2)\text{N-(C=C)-H}$	-0.30 ± 0.05	<i>g</i>
	same in anion	$+0.35 \pm 0.05$	<i>g</i>
3- $^{15}\text{NO}_2$ -pyrrole (and its anion)	$(\text{O}_2)\text{N-(C=C)-H}$	$(\pm)0.20 \pm 0.05$	<i>g</i>
	same in anion	$+0.45 \pm 0.05$	<i>g</i>
	$(\text{O}_2)\text{N-(C-C)-H}$	<i>ca. 0</i>	<i>g</i>
	same in anion	<i>ca. 0</i>	<i>g</i>
2,4-di- $^{15}\text{NO}_2$ -pyrrole (and its anion)	2- $(\text{O}_2)\text{N-(C=C)-H}$	-0.40 ± 0.05	<i>g</i>
	same in anion	<i>ca. 0</i>	<i>g</i>
	4- $(\text{O}_2)\text{N-(C=C)-H}$	-0.30 ± 0.05	<i>g</i>
	same in anion	<i>ca. 0</i>	<i>g</i>
	4- $(\text{O}_2)\text{N-(C-C)-H}$	-0.45 ± 0.05	<i>g</i>
	same in anion	<i>ca. 0</i>	<i>g</i>
	N-(N)-CH_3	$(\pm)2.6 \pm 0.1$	<i>i</i>
CDCl_3	N-(N)-CH	<i>ca. 0</i>	<i>i</i>

TABLE XXXIV—*cont.*

Compound	Type of coupling	$^3J(^{15}\text{N}-\text{H})$	Notes
 $\text{CH}_3\text{CO}-^{15}\text{N}$	CDCl_3	$\text{N}-(\text{CO})-\text{CH}_3$ $\text{N}-(\text{C})-\text{CH}$	$(\pm)1.9 \pm 0.1$ <i>ca.</i> 0 <i>i</i> <i>i</i>
 H_2N	CD_3OD CF_3COOH	$\text{N}-(\text{N})-\text{CH}_3$ $\text{N}-(\text{N})-\text{CH}$ $\text{N}-(\text{N})-\text{CH}_3$ $\text{N}-(\text{N})-\text{CH}$	$(\pm)2.9 \pm 0.1$ <i>ca.</i> 0 $(\pm)2.9 \pm 0.1$ <i>ca.</i> 0 <i>i</i> <i>i</i>
 CH_3COHN	CD_3OD CF_3COOH	$\text{N}-(\text{N})-\text{CH}_3$ $\text{N}-(\text{N})-\text{CH}$ $\text{N}-(\text{N})-\text{CH}_3$ $\text{N}-(\text{N})-\text{CH}$	$(\pm)3.1 \pm 0.1$ <i>ca.</i> 0 $(\pm)3.0 \pm 0.1$ <i>ca.</i> 0 <i>i</i> <i>i</i>
 $\text{CH}_3\text{COH}^{15}\text{N}$	CD_3OD CF_3COOH	$\text{N}-(\text{CO})-\text{CH}_3$ $\text{N}-(\text{C})-\text{CH}$ $\text{N}-(\text{CO})-\text{CH}_3$ $\text{N}-(\text{C})-\text{CH}$	$(\pm)1.4 \pm 0.1$ <i>ca.</i> 0 $(\pm)1.6 \pm 0.1$ <i>ca.</i> 0 <i>i</i> <i>i</i>
 $\text{CH}_3-\text{N}-\text{CH}_2\text{CN}$	CDCl_3	$\text{N}-(\text{N})-\text{CH}_3$ (anti to NO) (syn to NO)	$(\pm)1.8 \pm 0.1$ <i>ca.</i> 0 <i>j</i> <i>j</i>
 $\text{CH}_3-\text{N}-\text{CH}_2\text{CN}$	CDCl_3	$\text{N}-(\text{N})-\text{CH}_2$ (anti to NO) (syn to NO)	$(\pm)1.7 \pm 0.1$ <i>ca.</i> 0 <i>j</i> <i>j</i>
$\text{CH}_3-\text{N}(\text{NO})\text{CH}_2\text{C}\equiv^{15}\text{N}$	CDCl_3	$\text{N}\equiv\text{C}-\text{CH}_2$	$(\pm)1.5 \pm 0.1$ <i>j</i>
 HO Me		$\text{N}-(\text{C})-\text{CH}_3$	$(\pm)1.8 \pm 0.1$ (in FSO_3H) $(\pm)2.0 \pm 0.1$ (in 100% H_2SO_4) <i>h</i> <i>h</i>

^a From proton spectra by ^{14}N tickling and simultaneous decoupling of substituent protons; recalculated to ^{15}N ; ref. 151.

^b From proton spectra by ^{14}N decoupling; recalculated to ^{15}N ; ref. 152.

^c ^{15}N -labelled pyrrole; ref. 154.

^d ^{15}N -labelled pyrrole; ref. 146.

^e ^{15}N label; ref 155 and references therein.

^f ^{15}N -labelled compound; ref. 34.

^g ^{15}N -labelled nitro groups, proton spectra, ^{15}N decoupling; ref. 158.

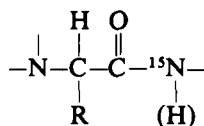
^h ^{15}N -labelled acetamide; ref. 149.

ⁱ ^{15}N -labelled acetylsydnimine, sydnimine hydrochloride and acetylsydnimine hydrochloride, respectively; ref. 111.

^j ^{15}N -labelled N-methyl,N-cyanomethylnitrosamine; ref. 156.

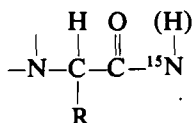
C. ${}^3J({}^{15}\text{N-H})$

The three-bond N-H coupling across at least one saturated carbon atom is usually called the vicinal coupling. Its magnitude depends on the geometry of the system (ref. 1e, p. 297). This is also the case when one of the intervening carbon atoms forms part of a carbonyl group, as suggested by consideration of the couplings in peptide molecules. (95, 159, 160) Equations (32) and (33) have been postulated (159) for the ${}^3J(\text{N-H})$ couplings in *trans*-amide [81] and *cis*-amide systems [82].



[81]

$${}^3J({}^{15}\text{N-H}) = -5.15 \cos^2 \theta + 2.30 \cos \theta + 0.98 \text{ Hz} \quad (32)$$



[82]

$${}^3J({}^{15}\text{N-H}) = -5.34 \cos^2 \theta + 2.15 \cos \theta + 0.87 \text{ Hz} \quad (33)$$

In these equations θ is the N-C-C-H dihedral angle. A similar treatment (160) gives equation (34) which neglects the effects of *cis-trans* amide isomerism.

$${}^3J({}^{15}\text{N-H}) = -4.6 \cos^2 \theta + 3.0 \cos \theta + 0.8 \text{ Hz} \quad (34)$$

A number of ${}^3J(\text{N-H})$ coupling constants have been experimentally determined (95) for some dipeptides (Table XXXV, N-H _{α} couplings), but since the absolute values are rather small, experimental errors tend to obscure the geometrical effects.

${}^3J({}^{15}\text{N-H})$ coupling constants across two saturated carbon atoms have been determined (95) for a number of dipeptides (Table XXXV, N-H _{β} couplings) and their significance in estimating molecular geometry discussed. It was deduced that the absolute values of ${}^3J(\text{N-H})_{\text{trans}}$ and ${}^3J(\text{N-H})_{\text{gauche}}$ are 4.8 ± 0.1 and 1.8 ± 0.1 Hz, respectively.

It is evident from the values given in Table XXXIV that in azine ring systems the three-bond N-C-C-H couplings are much smaller in absolute value than are the two-bond couplings, and that there is little difference between the ${}^3J(\text{N-H})$ values of azines and their protonated cationic forms. The ${}^3J({}^{15}\text{N-H})$ couplings in azine and azole systems

TABLE XXXV

Some absolute values of vicinal $^3J(^{15}\text{N}-\text{H})$ in Hz ± 0.05 Hz for some amino-acids and peptides

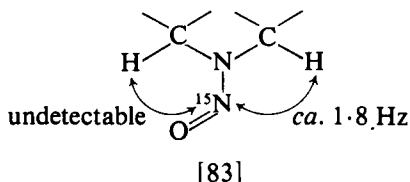
$\begin{array}{c} \text{O} \quad \text{H} \quad \text{H}_\alpha \\ \parallel \quad \quad \\ -\text{C}-\text{C}-\text{N}-\text{C}-\text{C}-^{15}\text{N}- \\ \quad \quad \\ \text{R} \quad \quad \text{O} \end{array}$		
Compound	Solvent	$^3J(^{15}\text{N}-\text{H}_\alpha)$
Valinomycin (L-Val- ^{15}N)	CCl_4	1.20
L-Ala-L-Ala- ^{15}N	D_2O , pH 2	1.20
L-Val-Gly- ^{15}N	D_2O , pH 2	<1
L-Ala-L-Phe- ^{15}N	D_2O , pH 2	<1
c-L-Val-Gly- ^{15}N	D_2O , pH 2	1.02
c-L-Ala-L-Phe- ^{15}N	DMSO	1.85
c-L-Val-Gly- ^{15}N	DMSO	<1
c-L-Phe-Gly- ^{15}N	DMSO	<1

$\begin{array}{c} \text{O} \quad \text{H} \\ \parallel \quad \\ -\text{C}-\text{C}-^{15}\text{N}-\text{C}-\text{C}-\text{H}_\beta \\ \quad \quad \quad \quad \\ \text{H} \quad \quad \text{C}=\text{O} \\ \quad \quad \quad \\ \quad \quad \quad \text{N}- \end{array}$		
Compound	Solvent	$^3J(^{15}\text{N}-\text{H}_\beta)$
Tyr- ^{15}N	D_2O , pH 10	2.75, 2.95
Asp- ^{15}N	D_2O , pH 10	2.80, 3.70
Phe- ^{15}N	D_2O , pH 1	2.20, 2.35
Ala- ^{15}N	D_2O , pH 1	3.10
N-Ac-DL-Ala- ^{15}N	H_2O , pH 6	3.04
L-Ala-L-Ala- ^{15}N	H_2O , pH 2	3.05
L-Ala-L-Phe- ^{15}N	H_2O , pH 2	2.30, 3.40
c-L-Ala-L-Phe- ^{15}N	DMSO	1.90, 3.20

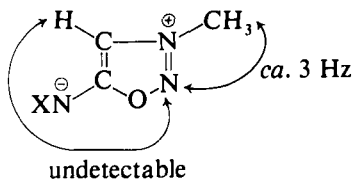
Note: ^{15}N -labelled amino-acids, proton spectra, ref. 95.

have been shown to be negative (Table XXXIV). A small coupling is observed between the $^{15}\text{NO}_2$ group and the nearest ring protons in nitro-derivatives of pyrrole (Table XXXIV, note g).

An apparent geometrical dependence of the $^3J(^{15}\text{N}-\text{N}-\text{C}-\text{H})$ coupling constants of some N-nitrosamine derivatives, [83] (Table XXXIV,



note j), has been reported. It is interesting to note that, formally, the same effects of geometry on $^3J(\text{N-H})$ values are found in sydnonimines [84].



[84]

D. $^4J(^{15}\text{N-H})$

The absolute values of $^{15}\text{N-H}$ coupling constants across four bonds are small but measurable in a number of unsaturated molecules (Table XXXVI). It has been shown that in pyridazine the $^4J(^{15}\text{N-H})$ coupling is negative. (155) The coupling of the nitrogen nucleus, in the NO_2 groups in nitropyrroles, with ring protons is slightly stronger across four bonds than across three bonds (Tables XXXV and XXXVI).

TABLE XXXVI

Some values of $^4J(^{15}\text{N-H})$ in Hz

Compound	Type of coupling	$^4J(^{15}\text{N-H})$	Notes
N-Me-pyridinium iodide	$\text{N}^+-\text{H}(\text{para})$	$(\pm)0.06 \pm 0.03$	a
N-Et-pyridinium bromide	$\text{N}^+-\text{H}(\text{para})$	$(\pm)0.04 \pm 0.03$	a
Pyridine	$\text{N}-(\text{C}=\text{C}-\text{C})-\text{H}$	$(\pm)0.21 \pm 0.05$	b
Pyridazine	$\text{N}-(\text{C}=\text{C}-\text{C})-\text{H}$	-0.367 ± 0.05	b
2- $^{15}\text{NO}_2$ -pyrrole (and its anion)	$(\text{O}_2)\text{N}-(\text{C}-\text{NH}-\text{C})-\text{H}$	-0.85 ± 0.05	c
	same in anion	-0.50 ± 0.05	c
	$(\text{O}_2)\text{N}-(\text{C}=\text{C}-\text{C})-\text{H}$	-0.80 ± 0.05	c
	same in anion	-0.60 ± 0.05	c
3- $^{15}\text{NO}_2$ -pyrrole (and its anion)	$(\text{O}_2)\text{N}-(\text{C}-\text{C}=\text{C})-\text{H}$	$(\pm)0.80 \pm 0.05$	c
	same in anion	-0.70 ± 0.05	c
2,4-di- $^{15}\text{NO}_2$ -pyrrole (and its anion)	2- $(\text{O}_2)\text{N}-(\text{C}-\text{NH}-\text{C})-\text{H}$	-0.95 ± 0.05	c
	same in anion	ca. $(\pm)0.4$	c

^a From proton spectra by ^{14}N tickling and simultaneous decoupling of substituent protons; recalculated to ^{15}N ; ref. 151.

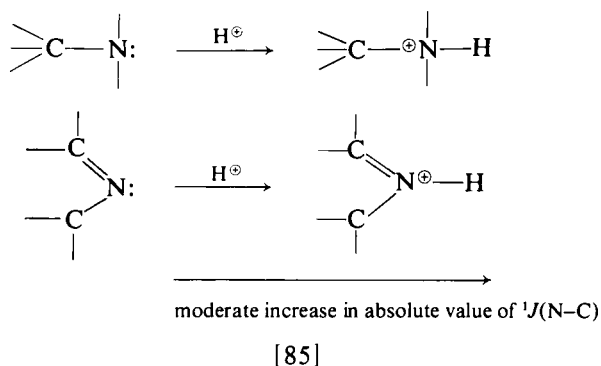
^b ^{15}N labelled compounds; ref. 155 and references therein.

^c ^{15}N -labelled nitro groups, proton spectra, ^{15}N decoupling; ref. 158.

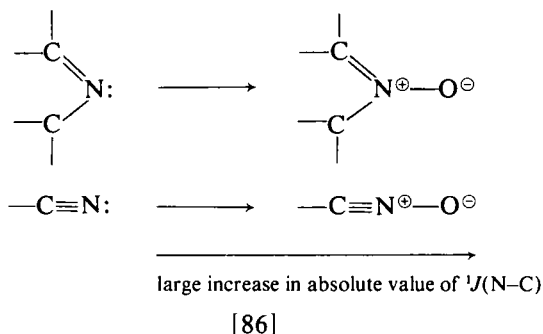
E. $^{15}\text{N}-^{13}\text{C}$ couplings

Nitrogen-carbon spin-spin coupling may provide interesting structural information, mostly from the ^{13}C NMR spectra of ^{15}N -labelled

compounds. (ref. 1e, pp. 286–289) There seems to be rather little encouragement for the interpretation of $^1J(\text{N}-\text{C})$ coupling constants in terms of the *s*-character of the bonding orbitals of carbon and nitrogen (ref. 1e, and references therein). The more recent data, shown in Table XXXVII, are also discouraging from the point of view of such an interpretation. The $^1J(\text{N}-\text{C})$ coupling is larger in arylamines than in alkylamines, but in oximes to is comparable to the latter as well as to that in azine ring systems. The effect of protonation of the lone electron pair in alkyl amines and azines increases the absolute value of $^1J(\text{N}-\text{C})$ [85]. This effect is much more pronounced upon the formation of an N-



oxide bond in an unsaturated system [86]. An extreme value of the one-bond coupling, 77.5 Hz, has been found (34) in the fulminate group, $-\text{CNO}$ (Table XXXVII), which is an N-oxide of the cyano group.



In saturated systems, the $^3J(\text{N}-\text{C})$ values are comparable in absolute magnitude to the $^1J(\text{N}-\text{C})$ couplings. So far there has been no evidence presented of their relative signs. In conjugated ring systems the absolute values of N-C couplings diminish with an increase in the number of intervening bonds.

TABLE XXXVII

Some values of ^{15}N — ^{13}C coupling constants in Hz(absolute values if sign not specified; ± 3 in the last decimal place if not stated otherwise)

Compound	$^1J(^{15}\text{N}-^{13}\text{C})$	$^2J(^{15}\text{N}-^{13}\text{C})$	$^3J(^{15}\text{N}-^{13}\text{C})$	$^4J(^{15}\text{N}-^{13}\text{C})$	$^5J(^{15}\text{N}-^{13}\text{C})$	Notes
Ph—NH ₂ (in acetone)	11.47	−2.68	−1.29	0.27		<i>a</i>
<i>n</i> -Pr—NH ₂ (in CDCl ₃)	3.9	1.2	1.4			<i>b</i>
<i>n</i> -Pr—NH ₃ ⁺ Cl [−] (in CDCl ₃)	4.4	<0.2	1.3			<i>b</i>
Quinuclidine (in CDCl ₃)	2.1	<0.2	2.8			<i>b</i>
Quinuclidine-HCl (in CDCl ₃)	4.8	0.2	6.7			<i>b</i>
HCONH ₂ (neat)	13.9					<i>c</i>
(inf. dil. H ₂ O)	14.8					
NH ₃ ⁺ CH ₂ CO ¹⁵ NHCH ₂ COOH	17.7					<i>d</i>
	(± 0.15)					
NH ₃ ⁺ CH ₂ CO ¹⁵ NHCH ₂ COO [−]	18.9					<i>d</i>
	(± 0.15)					
2,4,6-tri-Me—Ph)CNO	77.5	2.2	1.0	<0.5	0.8	<i>e</i>
(in CH ₂ Cl ₂)	(± 0.5)	(± 0.1)	(± 0.1)		(± 0.1)	
H ₂ C=NOH (in H ₂ O)	2.96					<i>f</i>
MeCH=NOH (E, anti) (H ₂ O)	4.0	9.0				<i>f</i>
MeCH=NOH (Z, syn) (H ₂ O)	2.3	1.8				<i>f</i>
EtCH=NOH (E) (H ₂ O)	2.4	7.3	0			<i>f</i>
EtCH=NOH (Z) (H ₂ O)	1.6	1.4	0			<i>f</i>
EtC(Me)=NOH (E) (CDCl ₃)	3.6	0 (CH ₃)	0			<i>f</i>
		10.5 (CH ₂)				
EtC(Me)=NOH (Z) (CDCl ₃)	3.4	11.1 (CH ₃)	0			<i>f</i>
		1.8 (CH ₂)				
Et ₂ C=NOH (CDCl ₃)	2.7	10.2 (anti)	2.1 (anti)			<i>f</i>
		2.0 (syn)	0 (syn)			
H ₂ C=CHC(Me)=NOH (E)	4.3	1.8 (CH ₃)	6.1			<i>f</i>
(in benzene)		11.6 (CH=)				

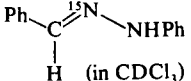
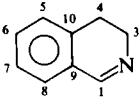
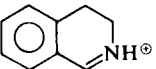
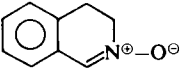
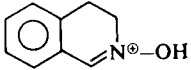
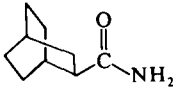
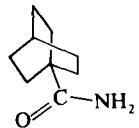
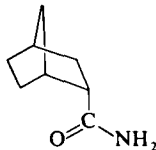
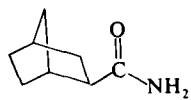
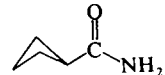
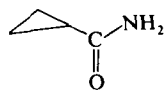
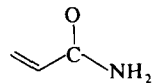
$\text{H}_2\text{C}=\text{CHC}(\text{Me})=\text{NOH}$ (Z) (in benzene)	3.5	11.6 (CH_3) 1.8 ($\text{CH}=\text{}$)	2.4			<i>f</i>
$\text{PhCH}=\text{NOH}$ (E) (CDCl_3)	4.8	7.3	2.8	0	0.8	<i>f</i>
2-Cyclohexenone oxime (Z) (benzene)	4.0	1.8 ($\text{CH}=\text{}$) 2.4 (CH_2)	3.1 ($\text{CH}=\text{}$)	0		<i>f</i>
2-Cyclohexenone oxime (E) (benzene)	5.0	11.0 ($\text{CH}=\text{}$) 1.4 (CH_2)	6.1 ($\text{CH}=\text{}$)	0		<i>f</i>
<i>trans</i> -Cinnamaldehyde oxime (E) (benzene)	5.2	9.1	5.6			<i>f</i>
<i>trans</i> -Cinnamaldehyde oxime (Z) (benzene)	?	?	3.9			<i>f</i>
 (in CDCl_3)	7.2	7.9 (PhC) 5.2 (PhN)	3.4 (PhC) 2.8 (PhN)	1.0 (PhC)		<i>f</i>
	2.9 (C-1)	<i>ca.</i> 2 (C-9)				
	3.4 (C-3)	<1 (C-4)	<1	<1	<1	<i>g</i>
	5.6 (C-1)		1.5 (C-8)			
	5.9 (C-3)	<1	<i>ca.</i> 2 (C-10)	<1	<1	<i>g</i>
	21.5 (C-1)		3.4 (C-8)			
	7.8 (C-3)	<1	2.4 (C-10)	<1	<1	<i>g</i>

TABLE XXXVII—*cont.*

Compound	$^1J(^{15}\text{N}-^{13}\text{C})$	$^2J(^{15}\text{N}-^{13}\text{C})$	$^3J(^{15}\text{N}-^{13}\text{C})$	$^4J(^{15}\text{N}-^{13}\text{C})$	$^5J(^{15}\text{N}-^{13}\text{C})$	Notes
	20.5 (C-1)		3.9 (C-8)			
	6.8 (C-3)	<1	2.4 (C-10)	<1	<1	<i>g</i>
	13.4	7.4				<i>h</i>
	13.4	6.9				<i>h</i>
	14.0	7.8				<i>h</i>
	14.3	8.2				<i>h</i>
	14.5	8.0				<i>h</i>

	15.1	10.3	<i>h</i>
	15.0	9.0	<i>h</i>

^a Ref. 161, ¹³C spectra.

^b Ref. 162, ¹³C spectra.

^c Ref. 163, doubly labelled (¹³C and ¹⁵N) formamide, ¹³C spectra.

^d Ref. 96, ¹³C spectra.

^e Ref. 34, ¹³C spectra.

^f Ref. 164, ¹³C spectra.

^g Ref. 165, ¹³C spectra.

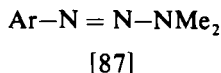
^h Ref. 166, ¹³C spectra.

The ${}^2J(\text{N}-\text{C})$ coupling constants in oximes (164) show a strong dependence upon the geometry of the bonds involved (Table XXXVII).

A theoretical calculation of the ${}^{15}\text{N}-{}^{13}\text{C}$ coupling has been carried out (157) by the sum-over-excited states approach using INDO-MO data. The calculation included the Fermi contact, spin-dipolar, and orbital interactions. For the one-bond coupling, the contact term is shown to be dominant, but there are appreciable contributions from the other terms especially when multiple bonding occurs which explains the lack of a reasonable correlation between ${}^1J(\text{N}-\text{C})$ and the s -electron contribution to the C-N bond. Calculations using the finite perturbation method, together with INDO data, point to a similar conclusion. (212-214)

F. ${}^{15}\text{N}-{}^{15}\text{N}$ couplings

Nitrogen-nitrogen coupling is usually detected in the ${}^{15}\text{N}$ spectra of doubly labelled compounds. Some data on ${}^1J({}^{15}\text{N}-{}^{15}\text{N})$ coupling constants are now available (Table XXXVIII). The coupling is relatively small in the hydrazine, $\text{R}_3\text{N}-\text{NR}_3$, and nitramine, R_2NNO_2 , structures but it is enhanced in hydrazones, $\text{C}=\text{N}-\text{NR}_2$, and in various derivatives with $\text{R}-\text{N}=\text{N}-\text{R}'$. The largest value so far observed is for the nitroso-amino moiety, R_2NNO (Table XXXVIII, note a). There are some indications (167) that the value of ${}^1J(\text{N}-\text{N})$ may be correlated with the s -electron densities on the nitrogen atoms involved. However, it is too early to draw definite conclusions. The rather large coupling in the $\text{N}-\text{Me}_2$ fragment of aryl triazenes [87] (122)



indicates that the $\text{N}-\text{Me}_2$ bond in such structures has appreciable double-bond character.

G. Other couplings

A large coupling has been observed between ${}^{15}\text{N}$ and ${}^{195}\text{Pt}$ in one of two isomeric complexes of some azo-derivatives. (125) The value of 523 Hz found for the ${}^1J({}^{195}\text{Pt}-{}^{15}\text{N})$ coupling indicates direct bonding between platinum and a trigonally-hybridized nitrogen atom since the values of the couplings for tetrahedrally-hybridized nitrogen atoms in ${}^{15}\text{N}$ -dodecylamine complexes of Pt(II) and Pt(IV) are of the order of 220-350 Hz. (127) Further, there are reasons to believe (127) that the absolute value of the coupling should increase with increasing s -character of the Pt-N bond.

TABLE XXXVIII

Some absolute values of $^1J(^{15}\text{N}-^{15}\text{N})$ in Hz

Compound	Solvent	$^1J(^{15}\text{N}-^{15}\text{N})$	Notes
PhNHNH_2	DMSO	6.7 ± 0.6	<i>a</i>
$\text{PhNHN}=\text{CHC}_6\text{H}_4\text{NO}_2$ - <i>p</i>	DMSO	10.7 ± 0.6	<i>a</i>
<i>trans</i> - $\text{PhN}=\text{N}(\text{O})\text{Ph}$	ether	13.7 ± 0.6	<i>a</i>
<i>p</i> -Hydroxyazobenzene	acetone	15.0 ± 0.6	<i>a</i>
$(\text{PhCH}_2)_2\text{NNO}$	DMSO	19.0 ± 0.6	<i>a</i>
Me_2NNO_2	CDCl_3	4.9 ± 0.6	<i>a</i>
$(\text{Me})(2,4,6\text{-trinitro-Ph})\text{NNO}_2$	DMSO	4.9 ± 0.6	<i>a</i>
$(-\text{CH}_2\text{N}(\text{NO}_2)-)_3$	DMSO	8.9 ± 0.6	<i>a</i>
$(-\text{CH}_2\text{N}(\text{NO}_2)-)_4$	DMSO	4.5 ± 0.6	<i>a</i>
$\begin{array}{c} \text{CH}_2-\text{N}-\text{CH}_2 \\ \quad \quad \\ \text{O}_2\text{NN} \quad \text{CH}_2 \quad \text{NNO}_2 \\ \quad \quad \\ \text{CH}_2-\text{N}-\text{CH}_2 \end{array}$	DMSO	8.5 ± 0.6	<i>a</i>
$(\text{C}_5\text{Me}_5)_2\text{TiN}_2$	toluene	7 ± 2	<i>b</i>
<i>p</i> - $\text{R}-\text{C}_6\text{H}_4-\text{N}=\text{N}-\text{NMe}_2$			
$\text{R}-\text{NO}_2, \text{N}=\text{N}-\text{Ph}$	CDCl_3	12.8 ± 0.7	<i>c</i>
$\text{N}-\text{NMe}_2$	CDCl_3	13.4 ± 0.7	<i>c</i>
$\text{R}-\text{Cl}, \text{N}=\text{N}-\text{Ph}$	CDCl_3	12.8 ± 0.7	<i>c</i>
$\text{N}=\text{NMe}_2$	CDCl_3	13.4 ± 0.7	<i>c</i>
$\text{R}-\text{H}, \text{N}=\text{N}-\text{Ph}$	CDCl_3	12.8 ± 0.7	<i>c</i>
$\text{N}-\text{NMe}_2$	CDCl_3	14.0 ± 0.7	<i>c</i>
$\text{R}-\text{OCH}_3, \text{N}=\text{N}-\text{Ph}$	CDCl_3	12.2 ± 0.7	<i>c</i>
$\text{N}-\text{NMe}_2$	CDCl_3	14.0 ± 0.7	<i>c</i>

^a Doubly labelled compounds; ref. 167 and references therein.^b $^{15}\text{N}_2$ complex of permethyltitanocene; ref. 168.^c ^{15}N triply labelled compounds; ref. 122.

VII. RELAXATION PHENOMENA

Since ^{14}N has $I = 1$ its relaxation is usually dominated by quadrupolar interactions. These produce broad lines, both in the ^{14}N NMR spectrum and in the spectra of nuclei spin-spin coupled to nitrogen. (1a, 2a) The ^{15}N nucleus has $I = \frac{1}{2}$, thus in a diamagnetic, chemically stable molecule it is relaxed by one or more of several less efficient mechanisms.

A. ^{14}N Relaxation

Under extreme narrowing conditions the molecular correlation time, τ_c , is related to the nuclear resonance frequency by equation (23). These conditions are usually found in low viscosity solutions and within their

confines the effect of the quadrupole moment of a ^{14}N nucleus on its relaxation time, T_Q , is given by,

$$\frac{1}{T_Q} = \frac{3}{8} \left(1 + \frac{\eta^2}{3} \right) \chi^2 \tau_c \quad (35)$$

where the nuclear quadrupole coupling constant, χ in frequency units, between the quadrupole moment, eQ , and the electric field gradient at the nucleus, eq , is given by

$$\chi = \frac{eqeQ}{h} \quad (36)$$

In equation (35) η describes the deviation of the electric field gradient from axial symmetry.

From equation (36) it is apparent that a resultant field gradient at the ^{14}N nucleus is necessary to produce quadrupolar relaxation. If the nucleus is at the centre of a static tetrahedron of bonded atoms the field gradient should be zero, in which case the ^{14}N relaxation will occur by other processes. This has been demonstrated for solid ND_4Cl in the region of the order-disorder phase transition at 248.9 K. Below 220 K the ^{14}N relaxation is dominated by the dipolar mechanism whereas in the region of the phase transition the quadrupolar interaction is the major one. This arises from the presence of a time dependent field gradient caused by the ammonium ion changing its orientation. (169)

In aqueous solutions the ^{14}N relaxation of symmetrical ammonium salts occurs due to the reorientation of water dipoles. (79) From relaxation studies on the highly strained N,N -dimethyl-aziridinium cation it is reported that the electronic distribution around the nitrogen nucleus is distorted from tetrahedral symmetry. (79)

Equation (35) has been employed in obtaining values of τ_c for the nitrogen nucleus in diethylamine in the presence of several normal alcohols. (170) In this investigation it has been assumed that the electric field gradient at the ^{14}N nucleus is independent of solute and has the same value in solution as in pure solid diethylamine. On the basis of these assumptions it is reported that for water and the lighter alcohols τ_c is dominated by hydrogen bonding. However, chain hindrance controls τ_c when the alcohol chain length is in excess of ten atoms. (170)

Various models have been proposed relating quadrupolar relaxation times to the correlation times of molecular motions. (1c) The more sophisticated the model considered the greater the number of parameters involved and thus the necessity for more independent NMR measurements. These may be obtained from a consideration of both ^{14}N and ^2H relaxation data on a series of closely related molecules. Ordinary and

deuterated methyl-, dimethyl- and trimethyl-amine have been studied. (171) The relaxation times have been interpreted on the basis of a large-step isotropic reorientation model. The results show that in methylamine the internal reorientations of the methyl group are fast compared to the overall molecular rotations, whereas in dimethylamine they are of comparable magnitude and in trimethylamine the overall molecular motions are the faster. (171)

A similar study has been reported on specifically deuterated pyridines in a series of aqueous solutions. (172) A rotational diffusion model is used to interpret the relaxation data. The diffusion constant for reorientation around the C_2 axis of pyridine is found to increase as the viscosity of the solution increases whereas the constant for reorientation about the axis perpendicular to the molecular plane decreases as the amount of water present in the solution increases. These observations are attributed to short range ordering due to hydrogen bond formation. (172) Diffusional reorientation constants have also been reported for a number of monosubstituted pyridines in various solvents. (46)

^{14}N relaxation measurements between 77 K and 276 K, the melting point, have been reported for *N,N*-dimethyl piperazine. (173) The relaxation times are found to be dominated by rotation of the methyl groups between 120 and 200 K. At higher temperatures hindered rotation of the whole molecule controls the ^{14}N relaxation. (173)

In the presence of a strong external electric field, E , the molecular dipoles of a polar fluid acquire a small average orientation parallel to the applied field. When the electric and magnetic fields are parallel the ^{14}N NMR signal of a pure polar liquid is split by ΔV

$$\Delta V = \frac{3}{2}\chi\left\langle\frac{3}{2}\cos^2\theta - \frac{1}{2}\right\rangle_E \quad (37)$$

where θ is the angle between the static magnetic field and the axis of the largest component of the electric field gradient at the ^{14}N nucleus. The average $\langle\frac{3}{2}\cos^2\theta - \frac{1}{2}\rangle_E$ is known as the alignment of the liquid, which becomes zero in the absence of the field, E . If the value of the alignment is available from studies on other nuclei in the same molecule then χ can be obtained from equation (37).

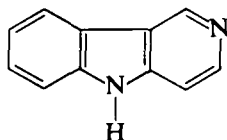
^{14}N NMR measurements in the presence of an applied electric field and discussions of χ and the alignment have been presented for 2,4,6-trifluoronitrobenzene, (174) nitrobenzene, (175) perdeuteronitrobenzene (176) and nitromethane. (175)

A ^{14}N NMR study of order fluctuations in the isotropic phase of liquid crystals has been reported. (209) The experimental data for the isotropic phases of *p*-azoxyanisole and of diethylazoxy benzoate are accounted for in terms of short range order fluctuations of the nematic and of the smectic types respectively.

Solid state ^{14}N NMR measurements have been reported for ND_4Cl , (169) $(\text{CH}_3)_4\text{NMnCl}_3$, (177) $\text{NH}_4\text{Al}(\text{SO}_4)_2 \cdot 12\text{H}_2\text{O}$, (178) KCN , (179) NaCN (179) and $\text{Ba}(\text{NO}_3)_2$. (180) These studies have yielded values for the ^{14}N chemical shifts and quadrupole coupling constants and, where appropriate, the asymmetry parameter η in equation (35). By following the temperature dependence of the ^{14}N relaxation time in the cubic phases of NaCN and KCN the activation energy of the reorientational motion of the cyanide ions is obtained. It is reported at 300 K to be $1.41 \pm 0.02 \text{ kcal mole}^{-1}$ in NaCN and $0.50 \pm 0.25 \text{ kcal mole}^{-1}$ in KCN . (179)

The question of calculating bandshapes for nuclei with $I = \frac{1}{2}$ in liquids containing quadrupolar nuclei has recently been reinvestigated. In his early treatment, Pople (181) assumed that the spin eigenfunctions of the individual molecules belong to a time-independent spin Hamiltonian. The problem is then treated by the arguments used in chemical exchange situations. However, it has been pointed out that the assumption made by Pople concerning the spin eigenfunctions of the individual molecules is incorrect, (182) and that the resulting bandshapes can be in serious error for systems with more than one quadrupolar nucleus. (182) These shortcomings may be removed by means of Redfield's relaxation theory as demonstrated for a group of $I = \frac{1}{2}$ nuclei scalar coupled to relaxing quadrupolar nuclei in any spin system. (183) Results have been presented for the $^2\text{A}^2\text{B}^3\text{X}$ spin system and the $|^2\text{A}^3\text{X}|_2$ system of *cis* N_2F_2 . (183)

Line broadening has been observed in the proton spectrum of some carbolines [88]. (184) It appears that both ^{14}N quadrupolar relaxation



[88]

and chemical exchange contribute to the broadening of the "pyrrole-type" proton, while protons in the "pyridine ring" are most strongly influenced by chemical exchange. (184)

In the period under review both *ab initio* and semi-empirical molecular orbital calculations of the electric field gradients at ^{14}N nuclei have been reported. Pyrazole and imidazole have been the subjects of an *ab initio* approach using double zeta functions. (185) The calculated values of χ and η are in good agreement with experimental results obtained from microwave studies. The agreement is considerably better

than that obtained in earlier calculations using minimal basis sets of gaussian functions. (186)

INDO molecular orbital calculations of χ and η have been reported for some azoloazines (63) and for $\text{Ba}(\text{NO}_3)_2$. (180) The agreement with experimental ^{14}N NMR data is reasonable for the azoloazines.

Crystallographic data on $\text{Ba}(\text{NO}_3)_2$ suggest that the two ^{14}N nuclei are inequivalent. (187) This model has been shown to be incorrect by a ^{14}N NMR study. (180) Further support is afforded by the calculation of χ for the crystallographic model which is not in agreement with the value obtained from ^{14}N NMR data. (180)

The ^{14}N quadrupole coupling constants for pyridine, pyrazine, benzonitrile and a number of small nitrogen-containing molecules have been calculated by the MINDO/3 approach. (206) Bearing in mind that some of the experimental data are taken from solid state measurements the overall agreement between the calculated and experimental results is good. The MINDO/3 results for NH_3 and HCN are in reasonable agreement with *ab initio* data although large differences appear in some of the individual contributions obtained by these two methods. (206)

BEEM- π electron calculations have been performed for twenty pyridines and values reported for χ and η . (188) In general good agreement with the experimental ^{14}N results is obtained. The poorest agreement being for the aminopyridines. (188)

Although not strictly within the compass of the present review some references to ^{14}N quadrupole coupling constants, obtained by microwave and NQR spectroscopy, are included for the sake of completeness. A high resolution microwave study of *N,N*-diazirine has been reported. (189) NQR data are given for 2,3,3-benzothiadiazole, (190) 2,1,3-benzoselenadiazole, (190) 2,5-dimethyl-1,3,4-thiadiazole, (190) 2-imidazolineone, (190) guanine hydrochloride, (190, 208) hexamethyl phosphorous triamide, (190) hexamethyl phosphoric triamide, (190) isoxazole, (191) hydroxyurea, (192) hexamethylenetetramine, (193) nitromethane, (194) nitrobenzene, (194) sodium nitrite, (207) *p*-chloro aniline, (195) some nitrosamines, (196) some oximes, (197) some nitrogen-silicon compounds, (198) some substituted ammonium ions, (199, 200) protonated and deuterated glycine, (210) some guanidine complexes and substituted ureas (208) and some amino acids. (200, 201)

B. ^{15}N Relaxation

In general if a proton is attached to the ^{15}N nucleus then intramolecular dipole-dipole relaxation is the dominant process. (202) If the nitrogen does not have an attached nucleus with $I = \frac{1}{2}$ then the

relaxation usually occurs more slowly by the spin-rotation, chemical shift anisotropy and dipole-dipole mechanisms arising from long range intramolecular and intermolecular interactions.

Scalar spin-spin interactions between nuclei can also contribute to nuclear relaxation. Chemical exchange modulation of the ^{15}N - ^1H scalar interaction in glycine has been reported. (66) However, it has been demonstrated that this is not a viable mechanism for ^{15}N relaxation in glycine and that dipole-dipole interaction together with spin-rotation is responsible. (70) The value of $^1J(\text{N-H})$ in glycine is 73 Hz which is too small to produce significant ^{15}N relaxation when modulated by chemical exchange. (70) More recently these conclusions on glycine have been invalidated by the reported presence of paramagnetic impurities. (78)

In the case of labelled *N*-butyl nitrite it has been claimed that spin-internal rotation is exclusively responsible for ^{15}N relaxation. (43) The rate of relaxation is close to the fastest reported for ^{15}N , even when a proton is directly bonded, and has been attributed to the conformational energetics of the C-nitrite bond. (203)

^{15}N relaxation in nitrobenzene has been studied at 14 and 32 MHz at temperatures between -10 and 60°C . (204) At low frequencies spin rotation interactions dominate and at lower temperatures intermolecular dipole-dipole interactions become important. However, at 32 MHz the predominant relaxation process is due to chemical shift anisotropy. (204)

A similar investigation from -60 to 55°C at 14 and 30 MHz has been reported for pyridine. (205) At low temperatures the major relaxation mechanisms are chemical shift anisotropy and intermolecular dipole-dipole interactions. The spin-rotation interaction becoming more important at higher temperatures. (205)

Liquid nitrogen has been studied between 63.1 and 77.3 K and in the β solid phase at temperatures down to 38 K. (211) The ^{15}N relaxation is found to be dominated by the spin-rotation interaction.

From a comparable investigation on $^{14}\text{N}_2$ it is found that the molecular correlation time exhibits a discontinuity at the triple point implying that the molecules reorient more rapidly in the solid than in the liquid. It is reported that the Hubbard relationship for the rotational diffusion of spherical molecules in a liquid is approached below 85 K for nitrogen in the liquid state and may be applicable in the solid also. (211)

In conclusion, we hope we have provided a reasonably comprehensive coverage of the nitrogen NMR literature appearing between 1972 and the middle of 1976. The volume and spread of this literature reflects the current, widely disseminated interests in nitrogen NMR.

REFERENCES

1. M. Witanowski and G. A. Webb (eds.), "Nitrogen NMR", Plenum Press, London, 1973.
 - (a) G. A. Webb and M. Witanowski, "Theoretical Background to Nitrogen NMR", p. 1.
 - (b) E. W. Randall, "Experimental Aspects of Nitrogen NMR", p. 41.
 - (c) J. M. Lehn and J. P. Kintzinger, "Nitrogen-14 Nuclear Quadrupole Effects", p. 79.
 - (d) M. Witanowski, L. Stefaniak and H. Januszewski, "Nitrogen Chemical Shifts in Organic Compounds", p. 163.
 - (e) T. Axenrod, "Correlations of Nitrogen Coupling Constants with Molecular Structure", p. 261.
 - (f) N. Logan, "Applications of ^{14}N NMR Data in the Study of Inorganic Molecules", p. 319.
2. (a) M. Witanowski and G. A. Webb, "Annual Reports on NMR Spectroscopy", E. F. Mooney (ed.), 1972, **5A**, 395.
(b) G. A. Webb, "Annual Reports on NMR Spectroscopy", E. F. Mooney (ed.), 1975, **6A**, 1.
3. W. T. Raynes, in "Specialist Periodical Report on NMR", Vol. 3, R. K. Harris (ed.), Chemical Society, London, 1974, p. 1.
4. N. F. Ramsey, *Phys. Rev.*, 1950, **77**, 567.
5. N. F. Ramsey, *Phys. Rev.*, 1950, **78**, 699.
6. N. F. Ramsey, *Phys. Rev.*, 1952, **86**, 243.
7. G. A. Webb in "NMR of nuclei other than protons", T. Axenrod and G. A. Webb (eds.), John Wiley, New York, 1974, p. 57.
8. R. Ditchfield and P. D. Ellis, in "Topics in ^{13}C NMR Spectroscopy", Vol. 1, G. C. Levy (ed.), John Wiley, New York, 1974, p. 1.
9. K. A. K. Ebraheem and G. A. Webb, in "Progress in NMR Spectroscopy", J. W. Emsley, J. Feeney and L. H. Sutcliffe (eds.), 1977, in the press.
10. R. B. Mallion, in "Specialist Periodical Report on NMR", Vol. 4, R. K. Harris (ed.), Chemical Society, London, 1975, p. 1.
11. R. Ditchfield, D. P. Miller and J. A. Pople, *J. Chem. Phys.*, 1971, **54**, 4186.
12. R. M. Stevens, R. M. Pitzer and W. N. Lipscomb, *J. Chem. Phys.*, 1963, **38**, 550.
13. G. P. Arrighini, M. Maestro and R. Moccia, *Chem. Phys. Letters*, 1970, **7**, 351.
14. B. R. Appleman, T. Tokuhiko, G. Fraenkel and C. W. Kern, *J. Chem. Phys.*, 1974, **60**, 2574.
15. T. K. Ha and C. T. O'Konski, *Intl. J. Quant. Chem.*, 1973, **7**, 609.
16. T. D. Gierke and W. H. Flygare, *J. Amer. Chem. Soc.*, 1972, **94**, 7277.
17. S. G. Kukolich and S. C. Wofsky, *J. Chem. Phys.*, 1970, **52**, 5477.
18. J. A. Pople, *Discuss. Faraday Soc.*, 1962, **34**, 7.
19. J. A. Pople, *Mol. Phys.*, 1964, **7**, 301.
20. A. Saika and C. P. Slichter, *J. Chem. Phys.*, 1954, **22**, 26.
21. R. Ditchfield, *Mol. Phys.*, 1974, **27**, 789.
22. J. A. Pople, *J. Chem. Phys.*, 1962, **37**, 53.
23. J. A. Pople, *J. Chem. Phys.*, 1960, **37**, 60.
24. J. A. Pople and D. L. Beveridge, "Approximate Molecular Orbital Theory", McGraw-Hill, New York, 1970.
25. J. C. Slater, *Phys. Rev.*, 1938, **36**, 57.
26. G. Burns, *J. Chem. Phys.*, 1966, **41**, 1521.
27. H. M. McConnell, *J. Chem. Phys.*, 1957, **27**, 226.
28. P. D. Ellis, G. E. Maciel and J. W. McIver, *J. Amer. Chem. Soc.*, 1972, **94**, 4069.
29. K. A. K. Ebraheem, G. A. Webb and M. Witanowski, *Org. Magn. Resonance*, 1976, **8**, 317.

30. W. M. Litchman, *J. Magn. Resonance*, 1973, **12**, 182.
31. R. Grinter and J. Mason, *J. Chem. Soc.*, 1970, **A**, 2196.
32. W. B. Moniz and C. F. Poranski, *J. Magn. Resonance*, 1973, **11**, 62.
33. F. O. Ellison, *J. Chem. Phys.*, 1964, **41**, 2018.
34. M. Christl, J. P. Warren, B. L. Hawkins and J. D. Roberts, *J. Amer. Chem. Soc.*, 1973, **95**, 4392.
35. R. Hagen, J. P. Warren, D. H. Hunter and J. D. Roberts, *J. Amer. Chem. Soc.*, 1973, **95**, 5712.
36. J. P. Warren and J. D. Roberts, *J. Phys. Chem.*, 1974, **78**, 2507.
37. K. F. Chew, W. Derbyshire and N. Logan, *J.C.S. Faraday Trans.*, 2, 1973, **68**, 594.
38. M. Witanowski, L. Stefaniak, S. Szymański and G. A. Webb, *Tetrahedron*, 1976, **32**, 2127.
39. K. A. K. Ebraheem and G. A. Webb, *Org. Magn. Resonance*, in the press.
40. K. A. K. Ebraheem, G. A. Webb and M. Witanowski. Submitted to *Org. Magn. Resonance*.
41. M. R. Baker and N. F. Ramsey, *Phys. Rev.*, 1964, **133A**, 1533.
42. S. I. Chan, M. R. Baker and N. F. Ramsey, *Phys. Rev.*, 1966, **136A**, 1224.
43. J. E. Kent and E. L. W. Wagner, *J. Chem. Phys.*, 1966, **44**, 3530.
44. C. H. Bradley, G. E. Hawkes, E. W. Randall and J. D. Roberts, *J. Amer. Chem. Soc.*, 1975, **97**, 1958.
45. L. Stefaniak, *Spect. Acta*, 1976, **32A**, 345.
46. M. Witanowski, L. Stefaniak, H. Januszewski, T. Saluvere and G. A. Webb, *Adv. in Mol. Relax. Processes*, 1973, **5**, 169.
47. M. Witanowski, L. Stefaniak, H. Januszewski and G. A. Webb, *J. Magn. Resonance*, 1974, **16**, 69.
48. G. Adler and R. L. Lichter, *J. Org. Chem.*, 1974, **39**, 3547.
49. J. W. Emsley, *J. Chem. Soc.*, 1968, **A**, 1387.
50. V. M. S. Gil and J. N. Murrell, *Trans. Faraday Soc.*, 1964, **60**, 248.
51. M. Witanowski, L. Stefaniak, H. Januszewski, K. Bahadur and G. A. Webb, *J. Cryst. Mol. Struct.*, 1975, **5**, 137.
52. B. R. Appleman and B. P. Dailey in "Advances in Magnetic Resonance", Vol. 7, J. S. Waugh (ed.), Academic Press, New York, 1974, p. 231.
53. P. K. Bhattacharyya and B. P. Dailey, *J. Chem. Phys.*, 1973, **59**, 5820.
54. J. D. Kennedy and W. McFarlane, *Mol. Phys.*, 1975, **29**, 593.
55. M. G. Gibby, R. G. Griffin, A. Pines and J. S. Waugh, *Chem. Phys. Letters*, 1972, **17**, 80.
56. C. S. Yannoni, *J. Chem. Phys.*, 1970, **52**, 2005.
57. J. Mason and J. G. Vinter, *J.C.S. Dalton*, 1975, 2522.
58. S. S. Dharmatti, K. J. Sundra Rao and R. Vijayaraghavan, *Nuovo Cim.*, 1959, **11**, 656.
59. H. W. Spiers, *Ber. Bunsen-Gesell. Für Phys. Chem.*, 1975, **79**, 1009.
60. M. Alei, A. E. Florin, W. M. Litchman and J. F. O'Brien *Phys. Chem.*, 1971, **75**, 932.
61. M. Witanowski, L. Stefaniak, S. Szymański and H. Januszewski, submitted to *J. Magn. Resonance*.
62. R. L. Lichter, *J. Magn. Resonance*, 1975, **18**, 367.
63. M. Witanowski, L. Stefaniak, S. Szymański, Z. Grabowski and G. A. Webb, *J. Magn. Resonance*, 1976, **21**, 185.
64. M. A. Healy and A. Morris, *Spect. Acta*, 1975, **31A**, 1695.
65. G. C. Levy, U. Edlund and J. G. Hexen, *J. Magn. Resonance*, 1975, **19**, 259.
66. R. A. Cooper, R. L. Lichter and J. D. Roberts, *J. Amer. Chem. Soc.*, 1973, **95**, 3724.
67. R. L. Lichter and J. D. Roberts, *J. Amer. Chem. Soc.*, 1972, **94**, 2495.
68. R. L. Lichter and J. D. Roberts, *Org. Magn. Resonance*, 1974, **6**, 636.
69. T. Suzuki, T. Yamaguchi and M. Imanari, *Tetrahedron Letters*, 1974, 1809.
70. T. K. Leipter and J. H. Noggle, *J. Amer. Chem. Soc.*, 1975, **97**, 269.

71. K. F. Chew, M. A. Healy, M. J. Khalil, N. Logan and W. Derbyshire, *J.C.S. Dalton* 1975, 1315.
72. T. C. Farrar and E. D. Becker, "Pulse and Fourier Transform NMR, Introduction to Theory and Methods", Academic Press, New York, 1971.
73. D. Gust, R. B. Moon and J. D. Roberts, *Proc. Natl. Acad. Sci., USA*, 1975, **72**, 4696.
74. T. B. Posner, V. Markowski, P. Loftus and J. D. Roberts, *J.C.S., Chem. Comm.*, 1975, 769.
75. E. Rosenberg, K. L. Williamson and J. D. Roberts, *Org. Magn. Resonance*, 1976, **8**, 117.
76. K. L. Williamson and J. D. Roberts, *J. Amer. Chem. Soc.*, 1976, **98**, 5082.
77. G. E. Hawkes, W. M. Litchman and E. W. Randall, *J. Magn. Resonance*, 1975, **19**, 255.
78. C. S. Irving and A. Lapidot, *J. Amer. Chem. Soc.*, 1975, **97**, 5945.
79. J. P. Kintzinger and J. M. Lehn, *Helv. Chim. Acta*, 1975, **58**, 905.
80. H. Nöth and B. Wrackmeyer, *Chem. Ber.*, 1974, **107**, 3089.
81. J. P. Marchal and D. Canet, *J. Amer. Chem. Soc.*, 1975, **97**, 6581.
82. R. E. Richards and N. A. Thomas, *J.C.S. Perkin II*, 1974, 368.
83. M. Witanowski, *Pure and Applied Chemistry*, 1974, **37**, 225.
84. W. M. Litchman, M. Alei and A. E. Florin, *J. Amer. Chem. Soc.*, 1969, **91**, 6574.
85. L. Paolillo and E. D. Becker, *J. Magn. Resonance*, 1970, **2**, 168.
86. M. Alei, A. E. Florin and W. M. Litchman, *J. Amer. Chem. Soc.*, 1970, **92**, 4828.
87. J. Schraml, N. Duc-Chuý, V. Chvalovsky, M. Mägi and E. Lippmaa, *Org. Magn. Resonance*, 1975, **7**, 379.
88. M. Witanowski, L. Stefaniak, H. Januszewski, M. G. Voronkov and S. N. Tandura, *Bull. Acad. Polon. Sci., Sér. sci. chim.*, 1976, **24**, 281.
89. K. A. Andrianov, W. F. Andronov, W. A. Drozdov, D. Y. Zhinkin, A. P. Kreshkov and M. M. Morgunova, *Dokl. Akad. Nauk SSSR*, 1972, **202**, 583.
90. H. Nöth, W. Tinhof and B. Wrackmeyer, *Chem. Ber.*, 1974, **107**, 518.
91. W. Beck, W. Becker, H. Nöth and B. Wrackmeyer, *Chem. Ber.*, 1972, **105**, 2883.
92. H. Nöth and B. Wrackmeyer, *Chem. Ber.*, 1974, **107**, 3070.
93. H. Nöth, W. Tinhof and T. Taeger, *Chem. Ber.*, 1974, **107**, 3113.
94. M. Alei, A. E. Florin and W. M. Litchman, *J. Phys. Chem.*, 1971, **75**, 1758.
95. J. A. Sogn, W. A. Gibbons and E. W. Randall, *Biochemistry*, 1973, **12**, 2100.
96. C. S. Irving and A. Lapidot, *J.C.S., Chem. Comm.*, 1976, 43.
97. A. Lapidot, C. S. Irving and Z. Malik, *J. Amer. Chem. Soc.*, 1976, **98**, 632.
98. E. A. Cohen, A. M. Shiller, S. I. Chan and S. L. Manatt, *Org. Mag. Resonance*, 1975, **7**, 605.
99. J. M. Briggs, L. F. Farnell and E. W. Randall, *J.C.S., Chem. Comm.*, 1971, 680.
100. R. L. Lichter and J. D. Roberts, *J. Amer. Chem. Soc.*, 1972, **94**, 4904.
101. L. Stefaniak, *Tetrahedron*, 1976, **32**, 1065.
102. R. Radeaglia, W. Storek, G. Engelhardt, F. Ritschl, E. Lippmaa, T. Pehk, M. Mägi and D. Martin, *Org. Magn. Resonance*, 1973, **5**, 419.
103. J. Müller, *J. Organometallic Chem.*, 1973, **51**, 119.
104. C. Thétaz, F. W. Wehrli and C. Wentrup, *Helv. Chim. Acta*, 1976, **59**, 259.
105. H. Saito, Y. Tanaka and S. Nagata, *J. Amer. Chem. Soc.*, 1973, **95**, 324.
106. E. Lippmaa, M. Mägi, S. S. Novikov, L. I. Khmel'nitskii, A. S. Prikhodko, O. V. Lebedev and L. V. Epishina, *Org. Magn. Resonance*, 1972, **4**, 153.
107. M. Witanowski, L. Stefaniak, H. Januszewski and J. Elguero, *J. Chim. Phys.*, 1973, 697.
108. E. B. Baker and A. I. Popov, *J. Phys. Chem.*, 1972, **76**, 2403.
109. P. Scheiner and W. M. Litchman, *J.C.S., Chem. Comm.*, 1972, 781.
110. M. Witanowski, L. Stefaniak, H. Januszewski and G. A. Webb, *Bull. Acad. Polon. Sci., Sér. sci. chim.*, 1973, **21**, 71.
111. L. Stefaniak, *Tetrahedron*, in press.

112. B. J. Buglass, *J.C.S., Chem. Comm.*, 1974, 313.
113. M. Witkowski, L. Stefaniak, H. Januszewski, Z. Grabowski and G. A. Webb, *Bull. Acad. Polon. Sci., Sér. sci. chim.*, 1972, **20**, 917.
114. H. Saito and K. Nekuda, *J. Amer. Chem. Soc.*, 1971, **93**, 1072.
115. P. S. Pregosin, E. W. Randall and A. I. White, *J.C.S. Perkin II*, 1972, 1.
116. L. Stefaniak and A. Grabowska, *Bull. Acad. Polon. Sci., Sér. sci. chim.*, 1974, **22**, 267.
117. M. Witkowski, L. Stefaniak, H. Januszewski, S. Szymański and G. A. Webb, *Tetrahedron*, 1973, **29**, 2833.
118. M. Witkowski, L. Stefaniak, H. Januszewski and H. Piotrowska, *Bull. Acad. Polon. Sci., Sér. sci. chim.*, 1975, **23**, 333.
119. S. L. Joffe, L. M. Leonteva, A. L. Blumenfeld, O. P. Shitov and V. A. Tertiakovskii, *Izv. Akad. Nauk. SSSR, Ser. Khim.*, 1974, **7**, 1659.
120. H. Böttcher, E. Lippmaa and T. A. Saluvere, *Z. Chem.*, 1972, **12**, 385.
121. L. Stefaniak, unpublished results.
122. T. Axenrod, P. Mangiaracina and P. S. Pregosin, *Helv. Chim. Acta*, 1976, **59**, 1655.
123. J. E. Bercaw, E. Rosenberg and J. D. Roberts, *J. Amer. Chem. Soc.*, 1974, **96**, 612.
124. R. Hagen, J. P. Warren, D. H. Hunter and J. D. Roberts, *J. Amer. Chem. Soc.*, 1973, **95**, 5712.
125. P. S. Pregosin and E. Steiner, *Helv. Chim. Acta*, 1976, **59**, 376.
126. C. H. Bradley, G. E. Hawkes, E. W. Randall and J. D. Roberts, *J. Amer. Chem. Soc.*, 1975, **97**, 1958.
127. P. S. Pregosin, H. Omura and L. M. Venanzi, *J. Amer. Chem. Soc.*, 1973, **95**, 2047.
128. R. J. West and S. F. Lincoln, *Inorg. Chem.*, 1972, **11**, 1688.
129. S. F. Lincoln and R. J. West, *Aust. J. Chem.*, 1972, **25**, 469.
130. R. J. West and S. F. Lincoln, *Inorg. Chem.*, 1973, **12**, 494.
131. S. F. Lincoln and R. J. West, *Aust. J. Chem.*, 1974, **27**, 97.
132. S. F. Lincoln, *Aust. J. Chem.*, 1974, **27**, 899.
133. S. F. Lincoln, *J.C.S., Dalton*, 1973, 1896.
134. S. F. Lincoln and R. J. West, *Aust. J. Chem.*, 1973, **26**, 255.
135. S. F. Lincoln and R. J. West, *J. Amer. Chem. Soc.*, 1974, **96**, 400.
136. V. K. Kapur and B. B. Wayland, *J. Phys. Chem.*, 1973, **77**, 634.
137. C. Chachaty, A. Forchioni and J. Virlet, *Canad. J. Chem.*, 1975, **53**, 648.
138. A. P. Gulya, B. A. Sherbakov and A. B. Ablov, *Doklady Akad. Nauk. SSSR*, 1973, **209**, 854.
139. R. M. Golding and M. P. Halton, *Aust. J. Chem.*, 1972, **25**, 2577.
140. M. Witkowski, L. Stefaniak, H. Januszewski and G. A. Webb, *J. Cryst. Mol. Struct.*, 1973, **5**, 141.
141. Y. Nakashima, M. Muto, I. Takagi and K. Kawano, *Chem. Letters*, 1975, 1075.
142. B. M. Fung, S. C. Wei, T. H. Martin and I. Y. Wei, *Inorg. Chem.*, 1973, **12**, 1203.
143. J. E. Bercaw, *J. Amer. Chem. Soc.*, 1974, **96**, 5087.
144. L. W. Reeves, J. M. Riveros, R. A. Spragg and J. A. Vavin, *Mol. Phys.*, 1973, **25**, 9.
145. V. V. Negrebtiskii, V. S. Bogdanov and A. V. Kessenikh, *Z. Strukt. Khim.*, 1971, **12**, 716.
146. J. M. Briggs, E. Rahkamaa and E. W. Randall, *J. Magn. Resonance*, 1973, **12**, 40.
147. A. H. Cowley and J. R. Schweiger, *J. Amer. Chem. Soc.*, 1973, **95**, 4179.
148. H. Ahlbrecht and G. Papke, *Tetrahedron Letters*, 1972, **43**, 4443.
149. M. Liler, *J.C.S. Perkin II*, 1972, 816.
150. V. Barboiu, *Mol. Phys.*, 1974, **28**, 707.
151. C. E. McFarlane and W. McFarlane, *Org. Magn. Resonance*, 1972, **4**, 161.
152. M. Ueyama-Ohtsuru and K. Tori, *Org. Magn. Resonance*, 1972, **4**, 913.
153. L. A. Lee and J. W. Wheeler, *J. Org. Chem.*, 1972, **37**, 497.

154. J. M. Briggs, E. Rahkamaa and E. W. Randall, *J. Magn. Resonance*, 1973, **11**, 416.
155. J. P. Jacobsen, O. Snerling, E. J. Pedersen, J. T. Nielsen and K. Schaumburg, *J. Magn. Resonance*, 1973, **10**, 130.
156. L. Stefaniak and M. Witanowski, *Bull. Acad. Polon. Sci., Sér. sci. chim.*, in press.
157. S. Nagata, T. Yamybe, K. Hirao and K. Fukui, *J. Phys. Chem.*, 1975, **79**, 1863.
158. V. V. Negrebetskii, A. V. Kessenikh, S. S. Novikov, L. Khmel'nitskii, A. S. Prikhodko and O. V. Lebedev, *Lzv. Akad. Nauk SSSR, Ser. Khim.*, 1971, 2613B.
159. M. Barfield and H. L. Gearhart, *Mol. Phys.*, 1974, **27**, 889.
160. V. F. Bystrov, Y. D. Gavrilov and V. N. Solkan, *J. Magn. Resonance*, 1975, **19**, 123.
161. M. Hansen and H. J. Jakobsen, *Acta Chem. Scand.*, 1972, **26**, 2150.
162. S. Berger and J. D. Roberts, *J. Amer. Chem. Soc.*, 1974, **96**, 6757.
163. J. F. Hinton, K. H. Ladner and W. E. Stewart, *J. Magn. Resonance*, 1973, **12**, 90.
164. R. L. Lichter, D. E. Dorman and R. Wasylshen, *J. Amer. Chem. Soc.*, 1974, **96**, 930.
165. M. Christl, *Org. Magn. Resonance*, 1975, **7**, 349.
166. R. L. Lichter, C. G. Fehder, P. H. Patton and J. Combes, *J.C.S., Chem. Comm.*, 1974, 114.
167. S. Bulusu, J. R. Autera and T. Axenrod, *J.C.S., Chem. Comm.*, 1973, 602.
168. J. P. Kintzinger and J. M. Lehn, *Mol. Phys.*, 1974, **27**, 491.
169. D. F. Cooke and K. R. Jeffrey, *J. Magn. Resonance*, 1975, **18**, 455.
170. T. J. Rowland, *J. Chem. Phys.*, 1975, **63**, 608.
171. A. Loewenstein and R. Waiman, *Mol. Phys.*, 1973, **25**, 49.
172. J. P. Kintzinger, *Mol. Phys.*, 1975, **30**, 673.
173. A. Tzalmona and A. Kaplan, *J. Chem. Phys.*, 1974, **61**, 1912.
174. J. Biemond, B. J. M. Neijzen and C. Maclean, *Chem. Phys.*, 1973, **1**, 335.
175. J. Biemond, S. Van Der Goot and C. Maclean, *Chem. Phys. Letters*, 1975, **32**, 390.
176. J. Biemond and C. Maclean, *Mol. Phys.*, 1973, **26**, 409.
177. A. Baviera, G. Bonera and F. Borsa, *Phys. Letters*, 1975, **51A**, 463.
178. W. C. Bailey and H. S. Story, *J. Chem. Phys.*, 1974, **60**, 1952.
179. D. E. O'Reilly, E. M. Petersen, C. E. Scheie and P. K. Kadaha, *J. Chem. Phys.*, 1973, **58**, 3018.
180. N. Weiden and A. Weiss, 18th Ampere Congress Proceedings, 1974, 257.
181. J. A. Pople, *Mol. Phys.*, 1958, **1**, 168.
182. N. C. Pyper, *Mol. Phys.*, 1971, **21**, 977.
183. R. K. Harris and N. C. Pyper, *Mol. Phys.*, 1975, **29**, 206.
184. F. Balkan and M. L. Heffernan, *Aust. J. Chem.*, 1973, **26**, 1523.
185. T. K. Ha, *Chem. Phys. Letters*, 1976, **37**, 315.
186. E. Kochanski, J. M. Lehn and B. Levy, *Theoret. Chim. Acta*, 1971, **22**, 11.
187. R. Birnstock, *Z. Krist.*, 1967, **124**, 310.
188. L. Krause and M. A. Whitehead, *Mol. Phys.*, 1973, **26**, 503.
189. J. M. Pochan and W. H. Flygare, *J. Phys. Chem.*, 1972, **76**, 2249.
190. L. Krause and M. A. Whitehead, *Mol. Phys.*, 1973, **25**, 99.
191. E. G. Sauer and T. Oja, *J. Chem. Phys.*, 1973, **58**, 2650.
192. E. G. Sauer and P. J. Bray, *J. Chem. Phys.*, 1973, **58**, 2662.
193. A. Colligiari, R. Ambrosetti and F. Salvetti, *J. Chem. Phys.*, 1974, **60**, 1871.
194. S. N. Subbarao, E. G. Sauer and P. J. Bray, *Phys. Letters*, 1973, **42A**, 161.
195. S. Vega, *J. Chem. Phys.*, 1975, **63**, 3769.
196. E. G. Sauer and T. Oja, *J. Chem. Phys.*, 1973, **58**, 2710.
197. E. G. Sauer and P. J. Bray, *J. Chem. Phys.*, 1973, **58**, 21.
198. E. Schempp and M. Chao, *J. Phys. Chem.*, 1976, **80**, 193.
199. R. A. Marino and T. Oja, *J. Chem. Phys.*, 1972, **56**, 5453.

200. D. T. Edmonds, M. J. Hunt and A. L. Mackay, *J. Magn. Resonance*, 1973, **9**, 66.
201. D. T. Edmonds and C. P. Summers, *J. Magn. Resonance*, 1973, **12**, 134.
202. O. D. Giannini, I. M. Armitage, H. Rearson, D. M. Grant and J. D. Roberts, *J. Amer. Chem. Soc.*, 1975, **97**, 3416.
203. J. B. Lambert and D. A. Netzel, *J. Magn. Resonance*, 1975, **20**, 575.
204. D. Schweitzer and H. W. Spiess, *J. Magn. Resonance*, 1974, **16**, 243.
205. D. Schweitzer and H. W. Spiess, *J. Magn. Resonance*, 1974, **15**, 529.
206. M. J. S. Dewar, H. W. Kollmar and S. H. Sock, *J. Amer. Chem. Soc.*, 1975, **97**, 5590.
207. G. Petersen and P. J. Bray, *J. Chem. Phys.*, 1976, **64**, 522.
208. Ling-Hsiang Chen and H. W. Dodgen, *J. Magn. Resonance*, 1976, **22**, 139.
209. R. Y. Dong, E. Tomchuk, J. J. Visintainer, and E. Bock, *Mol. Cryst. Liq. Cryst.*, 1976, **33**, 101.
210. D. T. Edmonds and C. P. Summers, *Chem. Phys. Letters*, 1976, **41**, 482.
211. L. M. Ishol, T. A. Scott and M. Goldblatt, *J. Magn. Resonance*, 1976, **23**, 313.
212. J. M. Schulman and T. Venanzi, *J. Amer. Chem. Soc.*, 1976, **98**, 4701.
213. J. M. Schulman and T. Venanzi, *J. Amer. Chem. Soc.*, 1976, **98**, 6739.
214. Tun Khin and G. A. Webb. Submitted to *Org. Magn. Resonance*.
215. E. Lippmaa, M. Mägi, S. S. Novikov, L. I. Khmelnitskii, A. S. Prikhodko, O. V. Lebedev and L. V. Epishina, *Org. Magn. Resonance*, 1972, **4**, 197.
216. E. Lippmaa, M. Mägi, M. Kashutina, S. Joffe and V. Tartakovskii, *Izv. Akad. Nauk SSSR, Ser. Khim.*, 1972, 188.
217. Y. Limouzin, J. C. Maire, J. D. Roberts and J. Warren, unpublished results, private communication by J. C. Maire.
218. J. M. Briggs and E. W. Randall, *Mol. Phys.*, 1973, **26**, 699.
219. R. M. Aminova and Y. Y. Samitov, *Zh. Strukt. Chim.*, 1974, **15**, 607.
220. A. Lapidot, C. S. Irving and Z. Malik in "Proceedings of the first international Conference on Stable Isotopes in Chemistry, Biology and Medicine", P. D. Klein and S. V. Peterson (eds.), National Technical Information Center, Springfield, 1973, p. 127.
221. D. Canet, J. P. Marchal and J. P. Sarteaux, *Compt. Rend., Series B*, 1974, **279**, 71.
222. V. V. Matveev, Y. G. Gladkii, G. I. Skubnevskaya and Y. N. Molin, *Z. Strukt. Khim.*, 1974, **15**, 931.
223. F. Seel, V. Hartmann and W. Gombler, *Z. Naturforschung*, 1972, **27b**, 325.
224. C. H. Yoder, R. C. Barth, W. M. Richter and F. A. Snavely, *J. Org. Chem.*, 1972, **37**, 4121.
225. H. Schultheiss and E. Fluck, *Z. Naturforschung*, 1977, **32b**, 257.

Spin-Spin Coupling Between Carbon-13 and the First Row Nuclei

RODERICK E. WASYLISHEN

*Department of Chemistry, University of Winnipeg,
Winnipeg, Manitoba, Canada R3B 2E9*

I. Introduction	246
II. Theoretical background	246
III. C-X coupling constants where X is Li, Be or B	248
A. X = Li	248
B. X = Be	248
C. X = B	248
IV. C-C coupling constants	249
A. $^1J(\text{C}-\text{C})$	250
1. Hydrocarbons	250
2. Carboxylic acid derivatives	253
3. Amino acids and other molecules of biological interest	254
4. Miscellaneous $^1J(\text{C}-\text{C})$ values	255
B. $^2J(\text{C}-\text{C})$ in various fragments	256
C. $^3J(\text{C}-\text{C})$	258
1. Saturated fragments	258
2. Unsaturated fragments	262
D. $^nJ(\text{C}-\text{C})$, $n \geq 4$	262
V. N-C coupling constants	262
A. $^1J(\text{N}-\text{C})$	262
1. Amine derivatives	267
2. Amides	273
3. Nitro-compounds	272
4. Oximes and imines	272
5. Nitriles and isonitriles	273
6. Unsaturated heterocyclic derivatives	273
B. $^2J(\text{N}-\text{C})$	273
C. $^3J(\text{N}-\text{C})$	277
1. Saturated fragments	277
2. Unsaturated fragments	279
D. $^nJ(\text{N}-\text{C})$, $n \geq 4$	279
VI. O-C Coupling constants	280
VII. F-C Coupling constants	280
A. Introduction	280
B. Recent literature in which $^nJ(\text{F}-\text{C})$ values are reported	280
VIII. Periodic Trends and Conclusions	286
Acknowledgements	287
References	287

I. INTRODUCTION

The combination of fast Fourier transform techniques with the pulsed excitation of NMR signals has facilitated the measurement of $^{13}\text{C}-\text{X}$ spin-spin coupling constants, ${}^nJ(\text{C}-\text{X})$; where n is the formal number of bonds intervening between the ^{13}C and X nuclei. Accordingly, a significant number of ${}^nJ(\text{C}-\text{X})$, X being a first row element (Li to F), are being reported each year. This review summarizes the work published on these coupling constants from early 1974 to mid-1976. Only coupling constants measured in the isotropic fluid phase are discussed.

In tables which list ${}^nJ(\text{C}-\text{X})$ values, little effort has been made to include the error in the coupling constant as estimated by the original authors. One should consult the original literature for the experimental details. Although an attempt has been made to mention all of the relevant papers published during this time, some work may have been unintentionally missed.

Stothers (1) summarizes the pre-1972 data on $^{13}\text{C}-\text{X}$ coupling constants. C-C; N-C; and P-C coupling constants are reviewed by Llinans, Vincent and Peiffer (2) in 1973. Since 1972, coupling constants have been reviewed annually by Grinter in "Specialist Periodical Reports on NMR". (3)

Some of the theoretical approaches to the calculation of ${}^nJ(\text{C}-\text{X})$ are outlined as a preliminary to the discussion of the experimental data.

II. THEORETICAL BACKGROUND

The nuclear spin-spin coupling constant, ${}^nJ(\text{A}-\text{B})$ is a measure of the energy of interaction between the magnetic moments of nuclei A and B. The interaction is transmitted by a magnetic polarization of the electrons in the molecule and J is therefore an intrinsic second-order property of the molecule, depending in a subtle manner on the details of the electron distribution. It is often convenient to define a reduced spin-spin coupling constant, ${}^nK(\text{A}-\text{B})$, independent of the magnetic moments of A and B

$${}^nK(\text{A}-\text{B}) = \frac{{}^nJ(\text{A}-\text{B})}{\gamma_{\text{A}} \gamma_{\text{B}}} \frac{2\pi}{\hbar} \quad (1)$$

(4) where γ_{A} and γ_{B} are the magnetogyric ratios of A and B, respectively. The energy of interaction, E_{int} , between the nuclear magnetic moments is then

$$E_{\text{int}} = \mu_{\text{A}} \mu_{\text{B}} {}^nK(\text{A}-\text{B}) \quad (2)$$

where μ_A and μ_B are the positive Z components of the magnetic moments of A and B, respectively. The magnetic moment (Z component) of a particular nucleus is given by

$$\mu = \gamma I \hbar \quad (3)$$

where I is the nuclear spin quantum number.

E_{int} arises from three types of interactions between electron and nuclear spins. (5) Thus, ${}^nJ(\text{A-B})$ can be written as a sum of three contributions,

$${}^nJ(\text{A-B}) = {}^nJ(\text{A-B})_o + {}^nJ(\text{A-B})_D + {}^nJ(\text{A-B})_c \quad (4)$$

The terms in equation (4) are generally referred to as the orbital-dipolar interaction (o) between the orbital magnetic fields of the electrons and the nuclear spin dipole, the spin-dipolar interaction (D) between the spin magnetic moments of the electrons and nucleus and the Fermi contact interaction (c) between the electron and nuclear spins, respectively. Discussion of the mathematical forms of each of these three terms appears elsewhere. (3-9)

The Fermi contact contribution to a coupling constant, ${}^nJ(\text{A-B})$, is proportional to the product of the s -electron densities at the coupled nuclei, $s_A^2(\text{O})s_B^2(\text{O})$. (11-17) Both the orbital and dipolar contributions are proportional to the product of the one-centre integrals $\langle r^{-3} \rangle_A$ and $\langle r^{-3} \rangle_B$, where $\langle r^{-3} \rangle_A$ and $\langle r^{-3} \rangle_B$ are the expectation values of r^{-3} for valence shell p orbitals on atoms A and B respectively. (14-17) Thus one can write the total coupling constant

$${}^nJ(\text{A-B}) = a_{AB} {}^nJ'_c + b_{AB} ({}^nJ'_o + {}^nJ'_D) \quad (5)$$

where ${}^nJ'_c$, ${}^nJ'_o$ and ${}^nJ'_D$ are respectively, the contact, orbital, and dipolar contributions, omitting the integral products given by

$$a_{AB} = s_A^2(\text{O})s_B^2(\text{O}) \quad \text{and} \\ b_{AB} = \langle r^{-3} \rangle_A \langle r^{-3} \rangle_B$$

One of the most successful methods of calculating nuclear spin coupling constants involves application of SCF perturbation theory and use of the INDO molecular orbital (MO) approximations. (8-17) In most theoretical studies a_{AB} and b_{AB} are taken as empirical parameters, adjusted to give best agreement between theory and experiment. Values of the individual integrals calculated from Slater exponents (14) are given in Table I.

As the number of electrons in the p orbitals increases, the magnitude of ${}^nJ'_o$ and ${}^nJ'_D$ generally increases. (8, 15-19) Thus, in going from X = Li to F, the orbital and spin dipolar contributions to ${}^nJ(\text{C-X})$ are expected to become more important. Also, for ${}^1J(\text{C-C})$ and ${}^1J(\text{N-C})$ it

TABLE I

**s-Electron densities and $\langle r^{-3} \rangle$ values
from Slater orbitals (14)**

Nucleus	$s^2(O)$	$\langle r^{-3} \rangle$
H	0.550	—
B	1.523	0.732
C	3.012	1.430
N	5.246	2.472
O	8.376	3.925
F	12.554	5.859

appears that the orbital and dipolar mechanisms are generally more important when the coupled nuclei are connected by multiple bonds. (16, 17, 20) This result was predicted in an earlier MO theory by Pople and Santry. (4)

Several reviews dealing with the theory and calculation of nuclear spin-spin coupling constants have appeared. (3, 7-9).

III. C-X COUPLING CONSTANTS WHERE X IS Li, Be OR B

A. X = Li

Both ^6Li and ^7Li possess magnetic moments and electric quadrupole moments. Carbon-13 coupling to the most abundant isotope, ^7Li (92.58%, $I = 3/2$), has been observed only in the methyllithium tetramer. (21) In $(\text{LiCH}_3)_4$, $^1J(\text{C}-^7\text{Li}) = +15$ Hz, much larger than the value of 0.77 Hz calculated by Cowley and White. (22)

In methyllithium, INDO calculations assuming only the Fermi contact mechanism predict $^1J(\text{C}-^7\text{Li}) \simeq 25.6$ Hz. (23)

B. X = Be

^9Be has a spin of $3/2$ and a natural abundance of 100%. Apparently, no $^nJ(\text{C}-\text{Be})$ values have been reported.

C. X = B

The naturally occurring isotopes of boron, ^{10}B (19.58%) and ^{11}B (80.42%) have spin quantum numbers of 3 and $3/2$, respectively. Experimental $^nJ(\text{C}-^{11}\text{B})$ values and those calculated using an INDO-MO method, assuming only the Fermi contact mechanism, are given in Table II. (24-27) It is apparent that the calculations account for the major patterns of substituent effects on $^1J(\text{C}-\text{B})$ and that, if the orbital and dipolar mechanisms are important for these coupling constants,

TABLE II

Observed and calculated $^1J(^{13}\text{C}-^{11}\text{B})$ values in Hz (24-27)

Compound	Observed	Calculated	$P^2_{s(\text{C})s(\text{B})}$ ^a
1-CH(CH ₃) ₂ B ₅ H ₈	75.0 ± 0.5	71.6	0.0974
1-CH ₃ B ₅ H ₈	72.7 ± 0.2	72.6	0.1050
1-CH ₃ CH ₂ B ₅ H ₈	72.1 ± 0.5	72.8	0.1017
B(C ₂ H ₅) ₃	<65	65.8	0.1166
1,1-(CH ₃) ₂ B ₂ H ₄	61.3	51.0	0.0952
BH ₃ CN [⊖]	53.0	51.7	0.1143
B(C ₂ H ₅) ₃	<52	44.8	0.0788
Na [⊕] B(C ₆ H ₅) ₄ [⊖]	49.4 ± 1.0 ^b	—	—
(<i>n</i> -Bu) ₄ N [⊕] B(C ₆ H ₅) ₄ [⊖]	48.8 ± 1.0 ^c	—	—
B(CH ₃) ₃	46.7	42.1	0.0964
(CH ₃) ₃ B·N(CH ₃) ₃	35 ± 2 ^d	—	—
BH ₃ CO	30.2 ± 0.4	29.3	0.1027
LiB(CH ₃) ₄	22 ± 2 ^d	—	—

^a See text.^b For Na[⊕]B(C₆H₅)₄[⊖]: $^2J(\text{C}-\text{B}) = 1.5 \pm 0.05$ Hz, $^3J(\text{C}-\text{B}) = 2.7 \pm 0.05$ Hz, $^4J(\text{C}-\text{B}) = 0.5 \pm 0.1$ Hz. (25)^c For (*n*-Bu)₄N[⊕]B(C₆H₅)₄[⊖]: $^2J(\text{C}-\text{B}) = 1.4 \pm 0.05$ Hz, $^3J(\text{C}-\text{B}) = 2.8 \pm 0.05$ Hz, $^4J(\text{C}-\text{B}) = 0.6 \pm 0.1$ Hz. (25)^d Data from ref. 27.

their contributions are constant. The calculations of Hall *et al.* (26) indicate that no correlation exists between the calculated square of the $2s_{\text{C}}$ and $2s_{\text{B}}$ bond order, $P^2(2s_{\text{C}})$ ($2s_{\text{B}}$), and $^1J(\text{C}-^{11}\text{B})$. In an earlier publication (27) it had been suggested that

$$\%s_{\text{B}}, \%s_{\text{C}} = 9.0 \ ^1J(\text{C}-^{11}\text{B}) + 380 \quad (6)$$

where $\%s_{\text{B}}$ and $\%s_{\text{C}}$ are the percent *s* characters at the boron and carbon nuclei, respectively. The INDO calculations lend no support to a relationship of this type.

IV. C-C COUPLING CONSTANTS

Although it is possible to measure one-bond ^{13}C - ^{13}C coupling constants in unenriched samples (^{13}C natural abundance is 1.108%), (28, 29) such measurements are not routine on most spectrometers. Most of the reported data on C-C coupling in the past two years have been obtained from ^{13}C labelled compounds.

Carbon-carbon coupling constants have been reviewed by Maciel, (29) and by Marshall and co-workers. (30) Maciel presents a good account of substituent effects on $^1J(\text{C}-\text{C})$ while the other review deals with long-range C-C coupling constants.

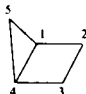
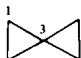
The application of C–C coupling constants in biosynthetic studies has been discussed in a number of papers (31–34) and will not be reviewed here.

A. $^1J(\text{C}–\text{C})$ values

1. Hydrocarbons

Early work indicated that $^1J(\text{C}–\text{C})$ is related to the apparent hybridization of the bonded carbon atoms. (35) Some of the early results

TABLE III
Some early $^1J(^{13}\text{C}–^{13}\text{C})$ spin–spin coupling data in Hz

	Coupled nuclei	$^1J(\text{C}–\text{C})$	Reference
	$\text{C}_4–\text{C}_5$	16.0	(35)
	$\text{C}_1–\text{C}_3$	20.2	(35)
ethane		34.6	(36, 37)
toluene	$\text{C}_1–\text{CH}_3$	44.2	(38, 39)
benzene		57.0	(28)
ethylene		67.6	(36, 37)
allene		98.7	(35)
acetylene		171.5	(36, 37)

are summarized in Table III. The dependence of $^1J(\text{C}–\text{C})$ on the apparent hybridization of the two carbon atoms was interpreted using semi-empirical equations such as

$$^1J(\text{C}–\text{C}) \simeq 0.0575 \%s_A \%s_B \quad (7)$$

Such expressions are based on the dominance of the Fermi contact mechanism. (38) Negative values of $^1J(\text{C}–\text{C})$ are not possible on the basis of equation (7).

In 1971, Maciel *et al.* (40) reported $^1J(\text{C}–\text{C})$ values calculated using the finite perturbation technique (FPT) in conjunction with molecular orbital theory at the INDO level of approximation. The calculations were carried out on more than 75 molecules and only the Fermi contact contribution was evaluated. Molecules with strained rings were not considered. Reasonable agreement with experiment was realized and it was observed that computed $^1J(\text{C}–\text{C})$ values were approximately related to $P_{s(\text{C})_A}^2 s(\text{C})_B$. In addition, it was found that computed $^1J(\text{C}–\text{C})$ and

$P_{s(\text{C})_A s(\text{C})_B}^2$ values were roughly equally successful in accounting for variations in $^1J(\text{C}-\text{C})$. These results suggest the dominance of the Fermi contact term.

Blizzard and Santry (16, 17) also examined C-C coupling constants using the INDO-FPT method. They included the orbital and spin dipolar terms as well as the contact term. Of the 15 molecules considered none were cyclic hydrocarbons. The contact term was found to be the most important, followed by the orbital and spin dipolar terms. The authors reported that the contact term completely dominates in the case of C-C single bonds, while the other terms become important when the two carbons are joined by multiple bonds.

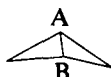
More recently Newton, Schulman and Manus (41) considered the relationship between experimental $^1J(\text{C}-\text{C})$ values in 12 different hydrocarbons and the product of the percent *s* character in the two bonding carbon atomic hybrids obtained from localization of INDO molecular orbitals (see Fig. 1). They found that

$$^1J(\text{C}_A-\text{C}_B) = 0.0621 \%s_A \%s_B - 10.2 \text{ Hz} \quad (8)$$

It is interesting to note the negative intercept in the plot of Fig. 1. On the basis of equation (8) negative values for $^1J(\text{C}-\text{C})$ in benzvalene [1] and



[1]



[2]

bicyclobutane [2] are predicted. In a later publication Schulman and Newton (42) used the method of Blizzard and Santry (15, 17) to calculate and compare the relative importance of the three coupling mechanisms in a number of acyclic and cyclic hydrocarbons. The noncontact terms make a large relative contribution to $^1J(\text{C}-\text{C})$ for three-membered rings. In the case of benzvalene and bicyclobutane all three terms are negative.

A negative intercept in the plot of $^1J(\text{C}-\text{C})$ against %*s* character has been recognized by Weigert and Roberts. (28) The predictions made in the latter papers have been borne out by experiment. Pomerantz, Fink and Gray (43, 44) determined a value of -5.4 ± 0.5 Hz for the bridgehead-bridgehead ^{13}C - ^{13}C coupling in the bicyclobutane derivative [3]. Further calculations on bicyclobutane and 1-methylbicyclo[1.1.0]butane by Schulman and Venani, (45) examine the influence of geometry and methyl substitution on calculated $^1J(\text{C}-\text{C})$ values in these

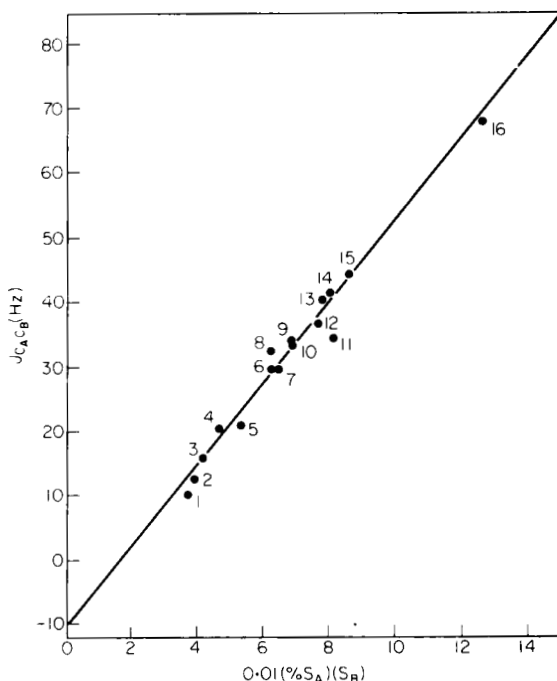
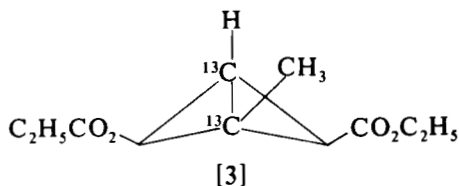
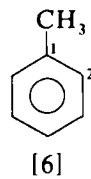
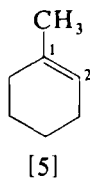
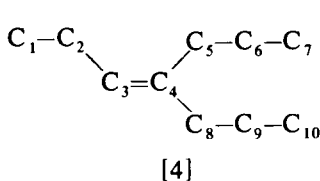


FIG. 1. Some observed nuclear spin-spin coupling constants between singly bonded carbons in 12 hydrocarbons plotted against the product of the per cent s characters in the two bonding carbon atomic hybrids obtained from localization of INDO molecular orbitals. The bonds indicated by number on the figure are for: (1) cyclopropane, (2) quadricyclene, C_1-C_2 , (3) bicyclo[2.1.0]pentane, C_4-C_5 , (4) spiro[3.3]heptane, C_1-C_2 , (5) bicyclo[1.1.0]butane C_1-C_2 , (6) cyclobutane, (7) norbornene, C_3-C_4 , (8) norbornane, C_1-C_7 , (9) norbornane, C_1-C_2 , (10) neopentane, (11) ethane, (12) bicyclo[2.1.0]pentane, C_1-C_2 , (13) norbornene, C_1-C_7 , (14) quadricyclene, C_1-C_7 , (15) toluene, C_1-C_7 , (16) methylacetylene, C_2-C_3 .



strained molecules. It is interesting that the central bond in bicyclobutane has an unusual hybridization: sp^{18} (INDO) and sp^{24} (*ab initio*).

$^1J(C-C)$ values have been measured in 4- ^{13}C -4-propyl-3-heptene [4], 1- ^{13}C -1-methyl-cyclohexene [5] and 1- ^{13}C -toluene [6]. (46) In [4], $^1J(C_3-C_4)$ is 73.1 Hz while $^1J(C_4-C_5)$ and $^1J(C_4-C_8)$ are 41.6 and 43.0 Hz

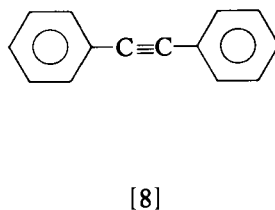
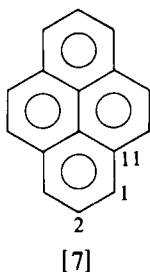


respectively. In [5], $^1J(\text{C}_1-\text{C}_2)$ is 73.6 Hz, while $^1J(\text{C}_1-\text{C}_6)$ and $^1J(\text{C}_1-\text{C}_7)$ are 40.1 and 44.8 Hz. In toluene [6] $^1J(\text{C}_1-\text{C}_2)$ is 57.3 Hz, which is very similar to the value of 57.0 Hz observed in benzene and other monosubstituted benzenes. (28) The observed values for $^1J(\text{C}_3-\text{C}_4)$ and $^1J(\text{C}_1-\text{C}_2)$ in [4] and [5] are approximately 6 Hz larger than the value of 67.2 Hz in ethylene. Similar increases occur in propene and isobutene, and it has been suggested that the value of $^1J(\text{C}-\text{C})$ in ethylene derivatives depends on the number of carbon-substituents at the double bond. (29, 47, 48)

For butadiene $^1J(\text{C}_1-\text{C}_2)$ is 68.8 Hz while $^1J(\text{C}_2-\text{C}_3)$ is 57.3 Hz. (48)

$^1J(\text{C}_1-\text{C}_7)$ in toluene is 44.2 Hz, similar to the values observed for $^1J(\text{C}_4-\text{C}_8)$ and $^1J(\text{C}_1-\text{C}_7)$ in [4] and [5].

In pyrene [7] $^1J(\text{C}_1-\text{C}_2)$ is 57 Hz While $^1J(\text{C}_1-\text{C}_{11})$ is 58.9 Hz. (49) In naphthalene $^1J(\text{C}_1-\text{C}_2)$ is 60.3 Hz. (49) In diphenylacetylene [8],



$^1J(\text{C}-\text{C})$ is 185.0 Hz across the acetylenic bond. (50) This appears to be the largest value reported so far for $^1J(\text{C}-\text{C})$.

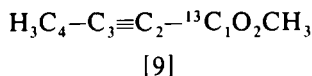
2. Carboxylic acid derivatives

Experimental $^1J(\text{C}-\text{C})$ values are available for some ^{13}C -carboxyl aliphatic carboxylic acids. (51) $^1J(\text{C}_0-\text{C})$ varies between 54.4 and 59.2 Hz. The authors conclude that factors other than ring strain are important in giving rise to this variation in $^1J(\text{C}_0-\text{C})$. $^1J(\text{C}_0-\text{C})$ values in the $\text{C}=\text{C}-\text{C}-\text{CO}_2\text{H}$ fragment (52) also fall within the range of values given above.

In aromatic carboxylic acid derivatives $^1J(\text{C}_0-\text{C})$ is approximately 16 Hz greater than in aliphatic derivatives. For example, in benzoic acid

and pyrene-1-carboxylic- ^{13}C -acid, $^1J(\text{C}_0-\text{C}_1)$ is 71.87 Hz (52) and 72.1 Hz, (53) respectively. In sodium benzoate $^1J(\text{C}_0-\text{C}_1)$ decreases to 65.90 Hz. (54) In the methyl ester of benzoic acid and in ethyl pyrene-1-carboxylate- ^{13}C , $^1J(\text{C}-\text{C})$ is 74.79 Hz (54) and 75.76 Hz, (53) respectively. Similar changes take place in acetic acid derivatives. The $^1J(\text{C}_0-\text{C})$ values in sodium acetate, acetic acid, and ethyl acetate are 51.6 Hz, 56.7 Hz and 58.8 Hz respectively. (55)

Linde and Jakobsen (56) have measured a value of 127.5 Hz for $^1J(\text{C}_1-\text{C}_2)$ in [9] and nicely demonstrated the utilization of selective



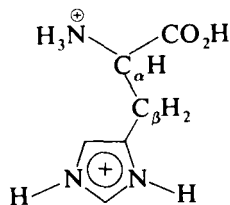
population transfer (SPT) in the measurement of the relative signs of long-range coupling constants to C_1 using the mono- ^{13}C -labelled compound.

3. Amino acids and other molecules of biological interest

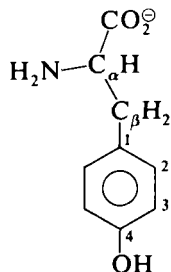
The pH-dependencies of one-bond C-C coupling constants in a number of amino acids have been reported by Tran-Dinh *et al.* (57, 58) Each carbon in the amino acids was uniformly enriched to 85%. The values of $^1J(\text{C}_0-\text{C}_\alpha)$ are similar to those observed in aliphatic carboxylic acids. In the zwitterion, $^1J(\text{C}_0-\text{C}_\alpha)$ values lie between 53.4 and 54.1 Hz; upon protonation of the carboxyl group this coupling constant increases by about 6 Hz.

The coupling constants $^1J(\text{C}_\alpha-\text{C}_\beta)$ are very similar and generally lie between 33 and 37 Hz. Only $^1J(\text{C}_0-\text{C}_\alpha)$ varies appreciably as a function of pH and reflects the ionization of the carboxyl group.

In histidine [10], at pH 0.8 $^1J(\text{C}_\beta-\text{C}_5)$ is 51.0 Hz and $^1J(\text{C}_4-\text{C}_5)$ is



[10]



[11]

74.5 Hz. (54) In tyrosine [11], at pH 11.3 $^1J(\text{C}_\beta-\text{C}_1)$ is 33.7 Hz (note that this value is considerably smaller than the one in toluene and may

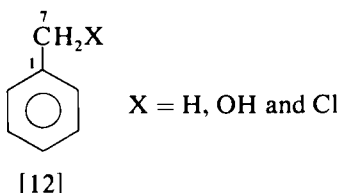
be incorrect), $^1J(\text{C}_1-\text{C}_2)$ is 57.5, $^1J(\text{C}_2-\text{C}_3)$ is 58.0, and $^1J(\text{C}_3-\text{C}_4)$ is 60.5 Hz. (58)

Sogn, Graig and Gibbons (59) have also reported $^1J(\text{C}-\text{C})$ values in a number of amino acids. The measurements were carried out in 6 N HCl.

For the proline residue in Gly-Pro-Gly and L-Glu-His-Pro-NH₂, $^1J(\text{C}_\alpha-\text{C}_\beta)$ in the *trans* isomers is about 1.4 Hz greater than the corresponding value in the *cis* isomer. (60)

4. Miscellaneous $^1J(\text{C}-\text{C})$ values

In benzyl derivatives [12], substituent effects on $^1J(\text{C}_1-\text{C}_7)$ appear to be small. (54) The presence of the OH and Cl groups in [12] leads to an

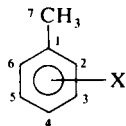


increase of 3.5 and 3.6 Hz, respectively compared to the value in toluene. The increases in the corresponding substituted ethanes, relative to ethane, are 3.1 and 1.5 Hz, respectively. (61, 29)

Marshall and Ihrig (62) have also examined the influence of ring substituents on carbon-carbon coupling constants in a number of *o*- and *p*-substituted toluenes ($^{13}\text{CH}_3$). The results are presented in Table IV

TABLE IV

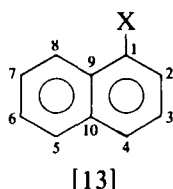
$^nJ(\text{C}-\text{C})$ values in some *ortho* and *para* substituted toluenes in Hz (62)



Substituent X	$^1J(\text{C}_1-\text{C}_7)$	$^2J(\text{C}_2-\text{C}_7)$	$^3J(\text{C}_3-\text{C}_7)$	$^4J(\text{C}_4-\text{C}_7)$	$^3J(\text{C}_5-\text{C}_4)$	$^2J(\text{C}_6-\text{C}_7)$
H	44.19	3.10	3.84	0.86	3.84	3.10
2-NO ₂	43.55	~1.0	1.53	0.50	3.60	2.20
2-NH ₂	45.00	~1.0	1.64	0.62	3.87	2.47
2-I	46.85	<0.5	2.42	0.66	3.55	3.48
2-CN	43.82	~0.8	2.40	0.73	3.87	2.83
4-NO ₂	43.45	3.46	3.87	—	3.87	3.46
4-NH ₂	45.91	3.17	4.19	<0.56	4.19	3.17

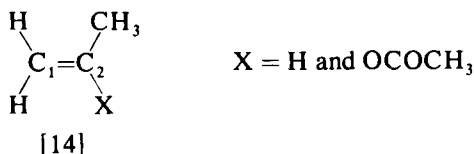
which shows that the range of observed $^1J(C_1-C_7)$ values is less than 3.5 Hz.

In naphthalene [13], $^1J(C_1-C_2)$ is 60.3 Hz. (49) Replacement of the



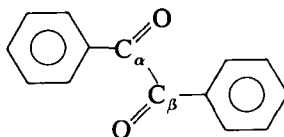
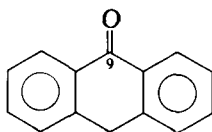
- X
- (a) H
 - (b) OH
 - (c) OCOCH₃

proton by an OH group at C₁ results in an increase of at least 8.5 Hz (49, 63) for $^1J(C_1-C_2)$. In 1-acetoxynaphthalene [13c] this coupling is 74.0 Hz. (63), an increase of 14 Hz relative to naphthalene. In [14],



$^1J(C_1-C_2)$ similarly increases from 70.0 (X = H) to 84.2 Hz (X = OCOCH₃). (29, 47) It is interesting to note that $^1J(C_1-C_9)$ in [13b] and [13c] are equal, within experimental error, but that $^1J(C_1-C_2)$ is 4.0 Hz greater in [13c] than in [13b].

In 9-¹³C-9-methoxyanthracene $^1J(C_9-C_{12})$ and $^1J(C_9-C_{13})$ are 69.89 Hz. (64) Unfortunately, $^1J(C-C)$ values are not available for anthracene. In 9-¹³C-anthrone [15], $^1J(C-C)$ is 54.9 Hz, (64) almost identical



to the value (54.5 Hz) reported for $^1J(C_\alpha-C_\beta)$ in benzil- α,β -¹³C₂ [16]. (50) The value of $^1J(C-C)$ in acetone is 40.6 Hz. (28)

B. $^2J(C-C)$ in various fragments

Geminal C-C coupling constant data are available for a variety of compounds but, unfortunately, signs of this coupling constant have only been determined in very few instances. (29) Also, calculations of the

relative importance of the various couplings mechanisms are sparse. In this section an attempt is made to discuss the $^2J(\text{C}-\text{C})$ values measured in a number of different fragments. Such an approach has proven useful in the interpretation of $^2J(\text{C}-\text{H})$ values. (65)

1. The $\text{C}_3-\text{C}_2-\text{C}_1-\text{X}$ fragment

$^2J(\text{C}-\text{C})$ in this fragment is generally small. For example, in a number of 1-substituted butanes $^2J(\text{C}_1-\text{C}_3)$ is generally less than 1 Hz. (30) It appears that substituents have only a small effect on this coupling constant.

In 2-methyl-2-butanol, $^2J(\text{C}_1-\text{C}_3)$ is 2.4 Hz. (66) If substituent effects on $^2J(\text{C}-\text{C})$ and $^2J(\text{C}-\text{H})$ in saturated fragments are similar then one would predict a positive value for the coupling observed in 2-methyl-2-butanol. (67)

2. The $\begin{array}{c} \text{C}^* \\ | \\ \text{C}-\text{C}^* \\ | \\ \text{R} \end{array} = \text{X}$ fragment

In two different alkene derivatives ($\text{X} = \text{C}$) Marshall and Miller (46) found $^2J(\text{C}-\text{C})$ to be 2.0, 2.0 and 2.3 Hz. In a number of carboxylic acids ($\text{X} = \text{O}$, $\text{R} = \text{OH}$), $^2J(\text{C}-\text{C})$ is less than 2 Hz. (51)

3. The $\begin{array}{c} \text{C}^* \\ | \\ \text{C}-\text{C}^* \end{array} \equiv \text{X}$ fragment

For $\text{X} = \text{N}$, $^2J(\text{C}-\text{C})$ is approximately 33 Hz. (68) The sign of this coupling constant is not known.

4. The $\begin{array}{c} \text{C}^* \\ | \\ \text{C}-\text{C}^* \end{array} = \text{C}$ fragment

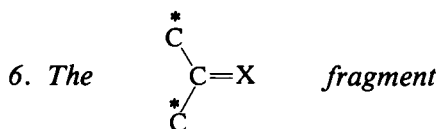
In 1-methylcyclohexene and 4-propyl-3-heptene, $^2J(\text{C}-\text{C})$ is less than 1 Hz in this fragment. (46)

In histidine $^2J(\text{C}_\beta-\text{C}_4)$ is 5.9 Hz. (58) The values observed in toluene derivatives vary between 0.0 and 3.5 Hz. In a number of benzyl derivatives studied by Marshall and co-workers, (54) $^2J(\text{C}-\text{C})$ varies between 3.1 and 3.7 Hz. (62)

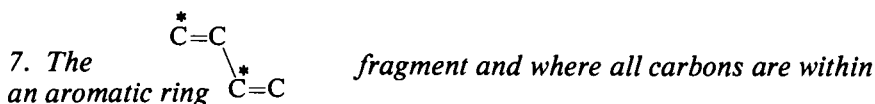
5. The $\text{C}^*-\text{C}^* \equiv \text{C}$ fragment

In compound [9], $^2J(\text{C}_1-\text{C}_3)$ is +20.3 Hz. (56, 69) Similarly, a positive value of 13.1 Hz has been found for $^2J(\text{C}-\text{C})$ in diphenylacetyl-

ene. (50) The value of 11.8 Hz observed for ${}^2J(\text{C}-\text{C})$ in propyne (28) must also be positive.



In acetone, ${}^2J(\text{C}-\text{C})$ is +16.1 Hz (70) and can be compared with the large positive values of ${}^2J(\text{H}-\text{H})$ in formaldehyde (71, 72) and of ${}^2J(\text{C}-\text{H})$ in acetaldehyde. (67, 73) In benzil this coupling is also large and positive, +14.0 Hz. However, in benzildihydrazone, ${}^2J(\text{C}-\text{C})$ is only +4.9 Hz. (50)



In butadiene, (48) naphthalene, (49) and pyrene (49, 53) the measured ${}^2J(\text{C}-\text{C})$ values are less than 2.5 Hz. In the few substituted naphthalenes (49, 63) and pyrenes, (49, 53) which have been studied, ${}^2J(\text{C}-\text{C})$ does not exceed 3 Hz.

8. Miscellaneous ${}^2J(\text{C}-\text{C})$ values

In dimethylmercury (74) ${}^2J(\text{C}-\text{C})$ is +22.4 Hz.

Negative values have been reported for a bicyclo[1.1.0]butane derivative [3], (44) methyl tetrolate [9], (56) and methylchloroformate. (75) In the latter two compounds the coupled nuclei are separated by an oxygen atom.

C. ${}^3J(\text{C}-\text{C})$

1. Saturated fragments

In the saturated XCCH fragments ${}^3J(\text{X}-\text{H})$ coupling constants depend critically on the XCCH dihedral angle (i.e. the dihedral angle measured from the plane in which the two bonds containing the coupled nuclei are eclipsed). The dihedral angle dependence of ${}^3J(\text{X}-\text{H})$ results primarily from interaction of vicinal hybrid orbitals directed towards X and H. (6, 66, 76-78) Generally this angular dependence of ${}^3J(\text{X}-\text{H})$ is adequately described by a "Karplus like" equation of the form

$${}^3J(\text{X}-\text{H}) = A \cos^2 \phi + B \cos \phi + C \quad (9)$$

where A , B , and C are empirical constants and ϕ is the XCCH dihedral angle. (The interested reader should consult the following papers for lists of relevant references. (3, 51, 66, 79)) ${}^3J(\text{X}-\text{H})$ values are generally a

maximum at $\phi = 180^\circ$, a minimum near $\phi = 90^\circ$ and intermediate at $\phi = 0^\circ$. That is, B is negative, $|A| > |B|$, and $C \approx 0$.

In 1973, Marshall and Miller (51) showed that, in a series of carboxylic acids, $^3J(\text{C}-\text{C})$ in the $^{13}\text{C}-\text{C}-\text{C}-^{13}\text{C}-\text{OOH}$ fragment is roughly dependent on the $^{13}\text{C}-\text{C}-\text{C}-^{13}\text{C}$ dihedral angle. For dihedral angles near 0° , 60° and 180° , the observed values of $^3J(\text{C}-\text{C})$ are approximately 2.4, 0 and 5 Hz, respectively. However, near $\phi \approx 180^\circ$ the experimental data show considerable scatter.

TABLE V

Some calculated vicinal $^{13}\text{C}-^{13}\text{C}$ coupling constants in Hz for butane, 2-butanol, and butanoic acid at 30° intervals of the dihedral angle ϕ (80)

Dihedral angle ϕ deg	$^3J(\text{C}-\text{C})$		
	Butane	2-butanol ^a	Butanoic acid ^b
0	5.79	5.34	1.76
30	3.96	3.79	0.90
60	1.94	1.97	— ^c
90	0.56	0.50	0.13
120	1.45	1.10	— ^c
150	3.34	2.77	4.24
180	4.27	3.82	5.87

^a The orientation of the OH is *trans* to the C_2-H bond. A plot of $^3J(\text{C}-\text{C})$ vs. ϕ is not symmetrical about $\phi = 180^\circ$. (80)

^b For butanoic acid it would not be easy to obtain coupling constants for all values of the dihedral angle in Table V because certain conformations are of very high energy due to strong steric interactions between the C_4 methyl group and the carboxyl group. The carboxyl group was oriented in such a way that the carbonyl eclipses the C_3 carbon atom. Thus, coupling in butanoic acid depends on the variation of *two* dihedral angles.

^c Calculated values for these conformations were considered unreliable because of the very high energies associated with steric interactions between the C_4 methyl group and the carboxyl.

Doddrell *et al.* (80, 66) have examined the angular dependence of $^3J(\text{C}-\text{C})$ in a number of aliphatic and alicyclic alcohols. In contrast to the carboxylic acids, $^3J(\text{C}-\text{C})$ is observed to be a maximum, ~ 5.4 Hz, for a dihedral angle near 0° . For the *trans* arrangement, $\phi = 180^\circ$, $^3J(\text{C}-\text{C})$ is ~ 3.2 Hz. At dihedral angles of 90° and 270° , $^3J(\text{C}-\text{C})$ is less than 0.4 Hz. Observed $^3J(\text{C}-\text{C})$ values for the alcohols and carboxylic acids (66, 80, 52) have been compared with values calculated (INDO-FPT) for the model compounds butane, 2-butanol, and butanoic acid. The calculated coupling constants are given in Table V. (80) Also, experimental and calculated $^3J(\text{C}-\text{C})$ values for the carboxylic acids are shown in Fig. 2. The calculations, which assumed only the Fermi contact

mechanism, are in good agreement with experiment. The authors (52) find that, in contrast to vicinal coupling constants involving protons, the simple form of equation (9) does not provide an adequate quantitative representation of the observed $^3J(\text{C}-\text{C})$ values. It has been suggested that deviations from equation (9) may result from the importance of direct (electron-mediated) coupling, which depends on both proximity

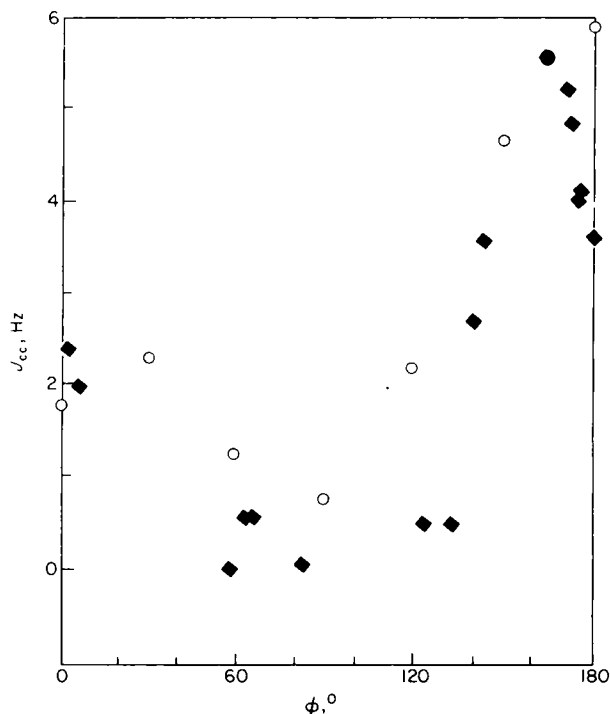


FIG. 2. Some observed $^3J(\text{C}-\text{C})$ values (◆) for aliphatic and alicyclic carboxylic acids compared with theoretical $^3J(\text{C}-\text{C})$ values (○) for butanoic acid, plotted against the dihedral angle ϕ .

and bond orientation effects. (81) These interactions are expected to be most important at small values of the dihedral angle.

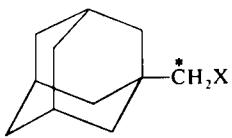
Vicinal C-C coupling constants in aromatic and dihydro aromatic carboxylic acids have recently been reported by Marshall and co-workers. (52) π -Electron coupling paths modify the form of the angular dependence observed for $^3J(\text{C}-\text{C})$ in aliphatic systems. As found previously for other vicinal couplings (e.g. H-H; C-H, and N-H), the π -electron paths are most important at dihedral angles of 90° where the σ - π exchange interaction is most effective. (82, 83) Thus, at dihedral

angles where spin information is transmitted most efficiently by the π -electron paths, the σ contribution is less important and vice versa. The net result is that, in the ^{13}C -C-C- ^{13}C fragment, $^3J(\text{C}-\text{C})$ values are expected to be of little value in conformational analysis. (52)

Substituent effects on $^3J(\text{C}-\text{C})$ values in a series of 1-substituted butyl compounds and in a series of 11-substituted 1-methyladamantane compounds have recently been reported by Barfield *et al.* (84) The experimental results are shown in Table VI. In the adamantane derivatives $^3J(\text{C}-\text{C})$ values are 1.2 Hz to 1.4 Hz less than the vicinal

TABLE VI

Some observed values of vicinal C-C coupling constants in a series of $^{13}\text{C}_1$ -labelled, C_1 -substituted butanes and in a series of $^{13}\text{C}_{11}$ -labelled, C_{11} -substituted 1-methyladamantanes in Hz (84)

Substituent X	$\text{CH}_3\text{CH}_2\text{CH}_2^*\text{CH}_2\text{X}$	
	$^3J(\text{C}-\text{C})$	$^3J(\text{C}-\text{C})$
H	—	3.2
OH	4.6	3.3
CN	4.7	3.4
F	4.3	—
Cl	4.8	3.4
Br	5.2	—
I	4.9	3.7

coupling constants for the substituted butanes (see Table VI). This result was unexpected since in the adamantane derivatives the coupled nuclei have $\phi \simeq 180^\circ$, while in the butanes the gauche conformations ($\phi = 60^\circ$) are also expected to be important. The observed experimental trends in Table VI are reproduced by INDO-FPT calculations. The apparent anomalies are explained by an impinging multiple rear lobe effect which causes a reduction in $^3J(\text{C}-\text{C})_{\text{trans}}$ for the adamantane derivatives.

In amino acids $^3J(\text{C}_\alpha-\text{C}_\gamma)$ varies between 1.5 and 3.5 Hz. (57, 58) For the proline residue in the tripeptide hormone thyrotropin-releasing factor (TRF, LGlu-His-Pro-NH₂) Haar *et al.* (60) report that $^3J(\text{C}_\alpha-\text{C}_\gamma) \leq 0.5$ and $^3J(\text{C}_\alpha-\text{C}_\beta) = 3.9$ Hz. Using the angular dependence of $^3J(\text{C}-\text{C})$ predicted by Barfield *et al.*, (66, 52) Haar and co-workers (60) conclude that the proline residue in TRF is preferentially in the *endo* conformation in contrast to proline itself.

2. Unsaturated fragments

Three-bond C—C coupling constants are available for butadiene, (48) some naphthalene, (49, 63) anthracene, (64) and pyrene (49, 53) derivatives. Factors other than dihedral angle must be important for determining $^3J(\text{C—C})$ in these systems. For example, in pyrene- $^{13}\text{C}_1$, $^3J(\text{C}_1\text{—C}_9)_{\text{trans}}$ and $^3J(\text{C}_1\text{—C}_{15})_{\text{trans}}$ are 5.82 and 3.05 Hz respectively. (49, 53) A similar trend is apparent in 9-methylanthracene- $^{13}\text{C}_9$, (64) where $^3J(\text{C}_9\text{—C}_7)_{\text{trans}}$ is 5.95 Hz while $^3J(\text{C}_9\text{—C}_5)_{\text{trans}}$ is 3.13 Hz.

$^2J(\text{C—C})$ and $^3J(\text{C—C})$ values in the naphthalene (63) and anthracene (64) derivatives have been plotted against the sum of the π -bond orders. Reasonable correlations are obtained if one assumes that $^2J(\text{C—C})$ is negative in these systems.

Vicinal as well as one- and two-bond C—C coupling constants have been measured in some barbituric acid derivatives. (85)

D. $^nJ(\text{C—C})$, $n \geq 4$

Long-range carbon—carbon coupling constants have been reported in a few studies. (49–54, 62–64) These coupling constants are generally less than 1 Hz. More data, including the signs, are required.

V. N—C COUPLING CONSTANTS

Almost all $J(\text{N—C})$ values have been obtained from the ^{13}C NMR spectra of ^{15}N -enriched compounds (^{15}N natural abundance is only 0.365%). (86–88) The ^{15}N nucleus has a spin of 1/2 and a negative gyromagnetic ratio hence $J(^{15}\text{N—C})$ values are opposite in sign to $K(\text{N—C})$.

$$K(\text{N—C}) = -3.268 \times 10^{20} J(^{15}\text{N—C})$$

where $K(\text{N—C})$ is in cm^{-3} and $J(^{15}\text{N—C})$ is in Hz. (89) The more abundant ^{14}N nucleus (99.635% natural abundance) has a spin of 1 and a positive gyromagnetic ratio. Except in cases where the electric field gradient at this nucleus is small, because of the high symmetry of the bonding arrangement, the quadrupolar relaxation mechanism is very effective. (90) Under these conditions the ^{14}N nucleus is effectively decoupled and $^{14}\text{N—C}$ coupling constants cannot be observed directly from ^{13}C NMR spectra.

All values reported here are of $^{15}\text{N—}^{13}\text{C}$ coupling constants. Brackets will be used to indicate that the sign of the coupling constant is not known with certainty.

TABLE VII

Some observed $J(^{15}\text{N}-^{13}\text{C})$ values in Hz

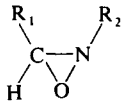
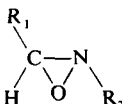
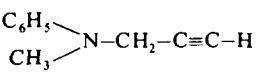
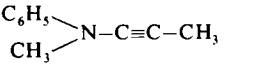
Compounds	$J(^{15}\text{N}-^{13}\text{C})$	Reference
<i>Amines</i>		
 $\text{N}-\text{C}_{\text{ring}}$ $\text{R}_1 = 4\text{-nitrophenyl}$ $\text{R}_2 = \text{isopropyl}$	+4.9	91
	-3.1	91
methylamine (neat)	-4.5	93
1-propylamine	(-)3.9	94
1-propylamine . HCl	(-)4.4	94
quinuclidine	(-)2.1	94
quinuclidine . HCl	(-)4.8	94
$\text{NH}_2\text{CH}_2\text{COO}^\ominus$	(-)4.8	95
$^\ominus\text{NH}_3\text{CH}_2\text{COO}^\ominus$	(-)6.2	95
$\text{NH}_2\text{CH}(\text{CH}_3)\text{COO}^\ominus$	(-)4.4	95
$^\ominus\text{NH}_3\text{CH}(\text{CH}_3)\text{COO}^\ominus$	(-)5.6	95
aniline (neat)	-10.9	96
in CCl_4	-11.1	96
in CDCl_3	-10.9	96
in acetone- d_6	-11.45	97, 98
in $\text{DMSO}-\text{d}_6$	-12.1	96
anilinium ion	(-)8.9	96
4-methylaniline	(-)10.5	96
2-methylaniline	(-)10.5	96
4-nitroaniline (acetone- d_6)	(-)14.9	96
in $\text{DMSO}-\text{d}_6$	(-)15.0	96
4-nitroanilinium ion	(-)9.2	96
2-aminobenzoic acid (pD \approx 12)	(-)10.7	96
N-methylaniline $\text{N}-\text{C}_1$	(-)13.0	99
$\text{N}-\text{CH}_3$	(-)10.3	99
 $\text{N}-\text{C}_1$ $\text{N}-\text{CH}_3$ $\text{N}-\text{CH}_2^-$	(-)12.5 (-)9.6 (-)9.65	99 99 99
 $\text{N}-\text{C}_1$ $\text{N}-\text{CH}_3$ $\text{N}-\text{C}\equiv$	(-)16.2 (-)12.2 (-)36.2	99 99 99
<i>Amides</i>		
Formamide (neat)	(-)13.9	100
in H_2O	(-)14.8	100

TABLE VII—*cont.*

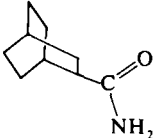
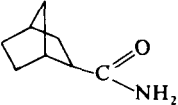
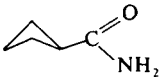
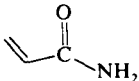
Compounds		$J(^{15}\text{N}-\text{C})$	Reference
	in DMSO- d_6	(-)-13.4	101
	in DMSO- d_6	(-)-14.3	101
	in DMSO- d_6	(-)-14.5	101
	in DMSO- d_6	(-)-15.0	101
Acetanilide in CDCl_3	N-C ₁	(-) 14.3	96
	N-CO	(-) 14.3 \pm 1	96
in acetone- d_6	N-C ₁	(-) 14.7	96
	N-CO	(-) 13.8 \pm 1	96
<i>Nitro compounds</i>			
CH_3NO_2		-10.5	88, 102
nitrobenzene		-14.57	103
<i>Oximes and imines</i>			
formaldoxime	in H_2O	(\pm)2.96	104
acetaldoxime (E)	in H_2O	(\pm)4.0	104
acetaldoxime (Z)	in H_2O	(\pm)2.3	104
propionaldoxime (E)	in H_2O	(\pm)2.4	104
propionaldoxime (Z)	in H_2O	(\pm)1.6	104
2-cyclohexenone (E)	in C_6D_6	(\pm)5.0	104
2-cyclohexenone (Z)	in C_6D_6	(\pm)4.0	104
benzaldoxime (E)	in CDCl_3	(\pm)4.8	104
mesitaldoxime (E)	in DMSO	(\pm)2.8	104
acetophenone oxime (E)	in CDCl_3	(\pm)3.9	105
acetone- d_6	in acetone- d_6	(\pm)2.4	105
$\begin{array}{c} \text{R}_1 \\ \diagdown \\ \text{C}=\text{N}-\text{R}_2 \\ \diagup \\ \text{H} \end{array}$ (E)		-5.0	89
$\text{R}_1 = 9\text{-anthryl}$			
$\text{R}_2 = \text{tert-butyl}$			
$\begin{array}{c} \text{R}_1 \\ \diagdown \\ \text{C}=\text{N}-\text{R}_2 \\ \diagup \\ \text{H} \end{array}$ (Z)		-5.0	89
$\text{R}_1 = 9\text{-anthryl}$			
$\text{R}_2 = \text{tert-butyl}$			

TABLE VII—*cont.*


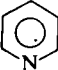
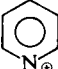
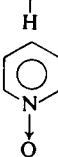
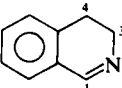
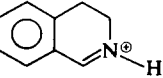
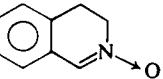
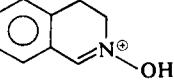
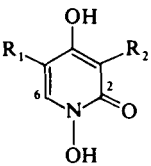
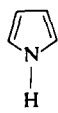
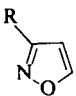
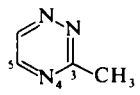
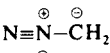
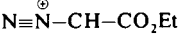
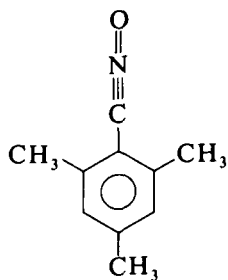
Compounds		¹ J (¹³ N—C)	Reference
<i>Nitriles and isonitriles</i>			
CH ₃ C≡N		−17.5	106, 107
CH ₃ CH ₂ C≡N		(−)16.4	107
(CH ₃) ₂ CHC≡N		(−)15.4	107
(CH ₃) ₃ CC≡N		(−)15.0	107
	N≡C	C—N	
CH ₃ N≡C	−8.88	−9.8	108, 109
CH ₃ CH ₂ N≡C	(−)7.4	(−)9.1	110, 111
(CH ₃) ₂ CH N≡C	(−)6.7	(−)7.8	111
(CH ₃) ₃ C—N≡C	(−)5.2	(−)7.0	110, 111
H ₂ C=C—N≡C	(−)7	(−)16.4	111
H ₂ C=C=CH—N≡C	(−)6.6	(−)20.0	111
 —N≡C	(−)7.3	(−)18.5	111
<i>Unsaturated heterocyclic derivatives</i>			
		+0.62	95, 98
		−11.85	95, 98, 104
		−15.23	98
	N—C ₁	(±)2.9	112
	N—C ₃	(±)3.4	112
	N—C ₁	(−)15.6	112
	N—C ₃	(−)5.9	112
	N—C ₁	(−)21.5	112
	N—C ₃	(−)7.8	112
	N—C ₁	(−)20.5	112
	N—C ₃	(−)6.8	112

TABLE VII—*cont.*

Compounds		$^1J(^{15}\text{N}-\text{C})$	Reference
	N-C ₂	(-)11.0	113
	N-C ₆	(-)15.0	113
R ₁ = <i>p</i> -hydroxyphenyl R ₂ = 4,6-dimethyl- <i>trans-trans</i> -octa-2,4-dienoyl			
		-12.98	98
		(±)4.0	92
R = mesityl			
	N ₄ -C ₃	(±)3.6	114
	N ₄ -C ₅	(±)1.0	114
<i>Miscellaneous</i>			
		(-)24.0	115
		(-)21.2	115

A. $^1J(\text{N}-\text{C})$

Reported values of $^1J(\text{N}-\text{C})$ range from +4.9 Hz in an oxaziridine derivative (91) to (-) 77.5 Hz in 2,4,6-trimethylbenzonitrile-N-oxide



[17]. (92) However, with the exception of [17], $|^1J(\text{N}-\text{C})|$ is generally less than 35 Hz. $^1J(\text{N}-\text{C})$ values in a number of compounds are given in Table VII.

The first interpretation of nitrogen-carbon coupling constants was presented by Binsch *et al.* (116) in 1964. For several compounds, they found that $^1J(\text{N}-\text{C})$ appears to be related to the product of the percent *s*-characters of the directly bound nitrogen and carbon atoms. Implying the dominance of the Fermi contact mechanism and an average energy approximation, these workers suggested that (negative sign inserted here)

$$\%s_{\text{N}} \%s_{\text{C}} = -80 \, ^1J(^{15}\text{N}-^{13}\text{C}) \quad (10)$$

Later studies have shown that equation (10) is inadequate and that the assumptions made in formulating this equation are in general unjustified. Of course, lack of agreement between observed $^1J(\text{N}-\text{C})$ and values predicted on the basis of equation (10) does not necessarily imply that the spin dipolar and orbital contributions are significant.

In 1970, Maciel *et al.* (40) carried out semi-empirical INDO-FPT-

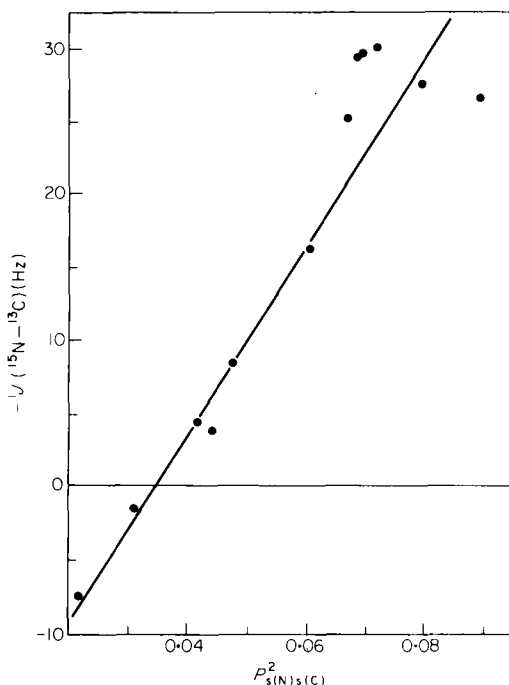


FIG. 3. Plot of calculated $^1J(\text{N}-\text{C})$ values against $P^2_{s(\text{N})s(\text{C})}$ values for some amine derivatives. Three points fall at $^1J(\text{N}-\text{C}) \approx -16.3$ Hz and $P^2_{s(\text{N})s(\text{C})} 0.061$.

TABLE VIII

Some calculated values for " $J(\text{N}-\text{C})$ in Hz" compared with observed data

Molecule	Coupled nuclei	$J(\text{N}-\text{C})_c$	$J(\text{N}-\text{C})_o$	$J(\text{N}-\text{C})_D$	$J(\text{N}-\text{C})_{\text{total}}$	$J(\text{N}-\text{C})_c^h$	$J(\text{N}-\text{C})_{\text{observed}}^c$
Acetonitrile	$\text{N}\equiv\text{C}-$	2.8	-10.7	-17.3	-25.2	6.2 (40)	-17.5
	$\text{N}-\text{C}$	3.1	0.3	0.1	3.5	—	3.0
Methyl isocyanide	$-\text{N}\equiv\text{C}$	18.4	-8.1	-13.9	-3.6	—	-9.1
	$\text{N}-\text{C}$	-11.9	0.2	-0.1	-11.8	—	-10.7
Methylamine	$\text{N}-\text{C}$	-2.7	0.2	-0.1	-2.6	-3.7 (96)	-4.5
Pyrrole	$\text{N}-\text{C}_1$	-14.8	0.9	0.0	-13.9	-30.0 (96)	-13.0
	$\text{N}-\text{C}_2$	-0.6	-0.1	-0.1	-0.8	-1.0 (98)	-3.9
Pyridine	$\text{N}-\text{C}_1$	-0.7	1.6	-0.3	0.6	-1.5 (104) ^e	0.6
	$\text{N}-\text{C}_2$	2.9	-0.1	0.3	3.1	6.0 (104) ^e	2.5
	$\text{N}-\text{C}_3$	-3.2	-0.1	-0.4	-3.7	-6.6 (104) ^e	-3.9
Pyridinium ion	$\text{N}-\text{C}_1$	-13.5	1.2	-0.2	-12.5	-27.5 (96)	-11.9
	$\text{N}-\text{C}_2$	3.6	0.0	0.1	3.7	7.4 (104)	2.0
	$\text{N}-\text{C}_3$	-4.3	-0.1	-0.3	-4.4	-8.7 (104)	-5.3

Aniline	N-C ₁	-8.0	0.4	-0.1	-7.7	-16.3 (96)	-11.4
	N-C ₂	-0.1	0.0	-0.2	-0.3	-0.5 (96)	-2.7
	N-C ₃	-1.6	0.0	0.0	-1.6	-0.8 (96)	-1.3
	N-C ₄	-0.7	0.0	-0.1	-0.8	-1.7 (98)	0.3
Aziridine	N-C	3.7	0.4	0.0	4.1	7.6 (96)	-
Formamide	N-C	-11.4	0.7	0.0	-10.7	-26.4 (96)	-
Formaldoxime	N-C	0.5	1.9	-0.9	1.5	-	2.9 ^b
Nitromethane	N-C	-17.8	0.2	-0.1	-17.7	-	-10.5
Nitrobenzene	N-C ₁ ^d	-29.53	-	-	-29.25	-	-14.57
	N-C ₂ ^d	3.65	-	-	3.35	-	-1.67
	N-C ₃ ^d	-5.09	-	-	-5.20	-	-2.32
	N-C ₄ ^d	1.20	-	-	1.29	-	±0.60
Benzonitrile oxide	N≡C	-34.4	-23.0	-17.8	-75.2	-73.5 (96)	~-77.5

^a All values are from ref. 20 unless otherwise indicated. Triple bond values are calculated assuming $a = 13.10$ and $b = 20.85 \text{ a}_0^{-3}$. (see note added in proof, ref. 20).

^b $J(\text{N}-\text{C})_c$ values calculated using the s orbital densities at the nucleus given on p. 154 of ref. 13.

^c See Table VII for references to experimental data.

^d See ref. 103.

^e Similar values are given in ref. 117.

MO calculations on a small number of molecules for which experimental data were available at that time. Only the Fermi contact contribution was considered and although agreement with experiment is rather poor, it is interesting that no correlation between calculated $^1J(\text{N}-\text{C})$ values and $P_{s(\text{N})s(\text{C})}^2$ was found. This result is in contrast to the calculated results obtained for carbon-carbon coupling constants. More recent INDO-FPT calculations on a series of amine derivatives indicate that the Fermi contact contribution to $^1J(\text{N}-\text{C})$ is related to $P_{s(\text{N})s(\text{C})}^2$ in this class of structurally similar compounds. (96) The results of these calculations are illustrated in Fig. 3.

Recent INDO-FPT calculations predict that, for the $\text{N}\equiv\text{C}$ bond, the orbital and spin-dipolar contributions to $J(\text{N}-\text{C})$ become significant. (20) The results of these calculations by Schulman and Venanzi (20) are

TABLE IX

Some results of INDO calculations for $^1J(\text{N}\equiv\text{C})$ in acetonitrile

Contact	Orbital	Dipolar	Total	Method
1.8	-0.2	-1.9	-0.3	<i>a</i>
5.01	-1.02	-5.04	-1.05	<i>b</i>
2.8	-10.7	-17.3	-25.2	<i>c</i>
6.2	—	—	6.2	<i>d</i>

^a Ref. 118. Sum-over-state perturbation method. The values of the one-centre integrals, $s_i^2(\text{O})$ and $\langle r^{-3} \rangle_i$, are quoted from those summarized by Morton. (120)

^b Ref. 119. Sum-over-state perturbation method. $s_i^2(\text{O})$ values from Pople and co-workers. (13) $\langle r^{-3} \rangle_{\text{C}} = 1.430$ a.u. and $\langle r^{-3} \rangle_{\text{N}} = 2.472$ a.u.

^c Ref. 20. Finite-perturbation theory. $a = 13.10$ and $b = 20.85$.

^d Ref. 40. Finite-perturbation theory.

given in Table VIII. With the exception of $\text{N}\equiv\text{C}$ bonds, the orbital contribution to $J(\text{N}-\text{C})$ is 2.1 Hz or less, while the spin-dipolar contribution is always predicted to be less than ± 1.0 Hz. In compounds such as pyridine and formaldoxime, where the Fermi contact contribution is small, the orbital and dipolar contributions are predicted to dominate. For comparison, INDO-FPT calculations assuming only the Fermi contact mechanism are also included in Table VIII.

Two groups of workers (110, 118, 119) have carried out sum-over-state INDO calculations, which also indicate that the orbital and spin-dipolar contributions are significant across the $\text{C}\equiv\text{N}$ triple bond. Calculated results for $^1J(\text{N}-\text{C})$ in acetonitrile are summarized in Table IX. Although there is lack of agreement in the total $^1J(\text{N}-\text{C})$ calculated, the Fermi contact contribution is consistently positive while the other two mechanisms give rise to negative contributions.

As mentioned earlier, one of the problems in the calculation of

$J(\text{C-X})$ is the choice of values for the atomic integrals, $s_i^2(\text{O})$ and $\langle r_i^{-3} \rangle$. Pople *et al.*, (11–13) Blizzard and Santry, (15–17) and Schulman *et al.* (20, 42) use a least squares fitting procedure, which is reasonable if sufficient experimental data exist.

Schulman and Venanzi (20) have evaluated $a \equiv s_{\text{C}}^2(\text{O}) s_{\text{N}}^2(\text{O})$ and $b \equiv \langle r^{-3} \rangle_{\text{C}} \langle r^{-3} \rangle_{\text{N}}$. For other than triple bonds they find that a is 13.79 a.u. and b is 1.77 a.u., while for triple bonds a is 13.10 a.u. and b is 20.85 a.u. In the opinion of the reviewer the large difference calculated for b in these two cases is not reasonable. Furthermore, if one assumes a value of 2.5 a.u. or 2.88 a.u. for $\langle r^{-3} \rangle_{\text{C}}$, as obtained earlier by Schulman and Newton (42) and by Blizzard and Santry (16, 17) from their studies of C–C coupling constants, then one obtains $\langle r^{-3} \rangle_{\text{N}} \leq 0.71$ a.u. when the N atom is singly bonded to carbon. The conclusion that $\langle r^{-3} \rangle_{\text{N}}$ is less than one-half $\langle r^{-3} \rangle_{\text{C}}$ also seems unreasonable (see Table I). One must ask how much agreement should be expected between observed $J(\text{C-X})$ values and those obtained from semi-empirical MO calculations at the INDO level of approximation, and to what extent the disagreement between theory and experiment is due to inadequacy of the wave functions.

Finally, in using the INDO-FPT method to obtain “ a ” and “ b ” by a least squares procedure, as in ref. 20, it would seem most reasonable to omit two-bond coupling constants in the fit. It is known that, although the INDO calculations are generally successful in predicting the correct trends for $^2J(\text{A-B})$, the absolute values are generally in poor agreement with experiment. (121)

Despite the problems mentioned above, the $^1J(\text{N-C})$ values calculated by Schulman and Venanzi are the best available at this time. Clearly, more experimental data, with signs, are required before the Pople *et al.* (10–13) and Blizzard-Santry (15–17) approach can be more thoroughly tested.

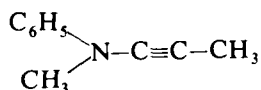
Early experimental work on $^1J(\text{N-C})$ has been summarized by Randall, (86) Lichter, (87) and Axenrod. (88) In the discussion that follows, empirical trends, observed for $^1J(\text{N-C})$ in different classes of nitrogen compounds, are presented.

1. Amine derivatives

Values of $^1J(\text{N-C})$ for the amine derivatives in Table VII vary between +4.9 Hz, in the strained oxaziridine ring, and (–) 36.2 Hz when the nitrogen is connected to the acetylenic carbon in ^{15}N -methylphenylpropynylamine. (99) The positive value of $^1J(\text{N-C})$ is in qualitative agreement with the value of 1.53 Hz calculated for oxaziridine using INDO-FPT (Fermi contact term only). (96) The negative $^1K(\text{N-C})$ value for the strained oxaziridine ring and the

qualitative increase in ${}^1K(\text{N}-\text{C})$, as the N-C bond order increases, is analogous to the trends observed for ${}^1J(\text{C}-\text{C})$.

Bottin-Strzalko *et al.* (99) have found that equation (10) does not give consistent values of s_{N} when applied to the three ${}^1J(\text{N}-\text{C})$ values in N-methylphenylpropylamine [18]. It would be of interest to carry out an INDO calculation for this molecule and compare the calculated $p_{s(\text{N})s(\text{C})}^2$ values with the observed ${}^1J(\text{N}-\text{C})$ values. Reasonable agreement between these observed and calculated values has been found previously for a number of amines. (96)



[18]

Nitrogen protonation results in an increase in ${}^1K(\text{N}-\text{C})$ for aliphatic amines (94) and a decrease in ${}^1K(\text{N}-\text{C})$ for aniline. (96) These observations are in accord with the calculations presented in ref. 96.

For the amine derivatives in Table VII it is probable that the Fermi contact mechanism dominates in almost all cases.

2. Amides

The reported ${}^1J(\text{N}-\text{C})$ values in amides vary over a relatively narrow range. The magnitude of ${}^1J(\text{N}-\text{C})$ in formamide-water solutions increases as the mole fraction of water increases. (100) This increase in ${}^1J(\text{N}-\text{C})$ has been attributed to an increase in the C-N double bond character as the solvent polarity increases. Similar arguments may explain the observed increase in ${}^1K(\text{N}-\text{C})$ observed for aniline in polar solvents. (96) The sign of ${}^1J(\text{N}-\text{C})$ for this class of compounds must be negative.

3. Nitro-compounds

The values of ${}^1J(\text{N}-\text{C})$ in nitromethane and nitrobenzene are -10.5 Hz and -14.6 Hz, respectively. (102, 103) Calculations by Schulman and Venanzi (20) and by Ernst *et al.* (103) suggest that orbital and spin-dipolar contributions to these couplings are negligible.

4. Oximes and imines

The absolute value of ${}^1J(\text{N}-\text{C})$ in oximes and imine derivatives is generally less than 5 Hz. MO calculations (20, 104) successfully indicate that the Fermi contact contribution to ${}^1J(\text{N}-\text{C})$ in these compounds is small. This result appears to be quite general for molecules which contain nitrogen lone pairs with considerably s-character. (20) Pyridine

is a classic example, the observed value of $^1J(\text{N}-\text{C})$ being only $+0.6$ Hz.

For the oximes the absolute value of $^1J(\text{N}-\text{C})$ in the E isomer is larger than the corresponding value in the Z isomer. (91) Assuming a positive value for $^1J(\text{N}-\text{C})$ in acetaldoxime, Schulman and Venanzi (20) suggest that the lone-pair in the Z isomer has more *p*-character than in the E isomer. As the *p*-character of the nitrogen lone-pair increases, $^1J(\text{N}-\text{C})$ becomes more negative. A similar argument may be used to account for the more positive value of $^1J(\text{N}-\text{C})$ in the Z isomer of the oxaridine derivative given in Table VII.

5. Nitriles and isonitriles

Values of $^1J(\text{C}-\text{N})$ across the triple bond in nitriles and isonitriles are negative. (106, 109) In both acetonitrile and methylisocyanide the Fermi contact contribution to $^1J(\text{N}-\text{C})$ is predicted to be positive and, for the methylisocyanide, quite large. The orbital and spin-dipolar mechanisms are predicted to make a negative contribution; thus it appears that the latter two mechanisms are important for coupling across triple bonds.

For the isonitriles, $^1J(\text{N}-\text{C})$ across the single bond is negative; (109) the absolute value appears to increase as the *s*-character of the C-N single bond increases. The Fermi contact contribution is expected to dominate this latter coupling.

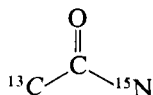
6. Unsaturated heterocyclic derivatives

If the nitrogen has a lone-pair with considerable *s*-character, and hence resembles the nitrogen atom in oximes or imines, $|^1J(\text{N}-\text{C})|$ is generally less than 4 Hz. The Fermi contact contribution to these coupling constants is predicted to be small. (20, 104) (See ref. 20 for a reasonable "explanation".)

Where one has a "pyrrole-type" nitrogen $|^1J(\text{N}-\text{C})| > 10$ Hz. Relatively large absolute values of $^1J(\text{N}-\text{C})$ are also observed in unsaturated N-oxides, and in protonated pyridine and quinoline derivatives. (122)

B. $^2J(\text{N}-\text{C})$

Some observed and calculated $^2J(\text{N}-\text{C})$ values are given in Table X. Values of $^2J(\text{N}-\text{C})$ in the fragment [19] of amides vary between $(-)$ 6.5 Hz in propionamide (87) and $(-)$ 10.3 Hz in cyclopropylmethanamide.



[19]

TABLE X

Some representative observed and calculated $^2J(\text{N}-\text{C})$ values

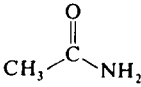
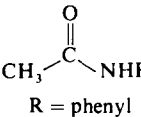
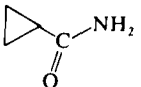
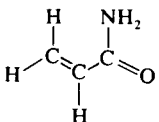
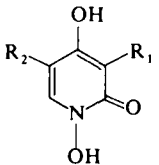
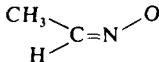
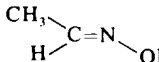
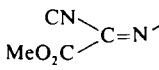
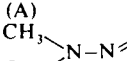
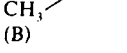
Compound	$^2J(^{15}\text{N}-\text{C})_{\text{observed}}$	$^2J(^{15}\text{N}-\text{C})_{\text{calculated}}$	Reference
	(-)9.5	—	87
 R = phenyl	(-)9.0	-3.48 ^a	87
	(-)10.3	—	101
	(-)9.0	—	101
	N-C ₃ (-)9.2	—	113
	(±)1.8	1.76 ^b	104
	(-)9.0	-3.11 ^b	104
E-acetophenone oxime	N-C ₁	(-)9.3	105
	N-C _{Methyl}	(±)1.0	105
	N-CN	(±)2.2	122
	N-CO ₂ Me	(-)10.6	122
(A) 	N-CH ₃ (A)	(-)7.5 Hz	95
(B) 	N-CH ₃ (B)	(±)1.4 Hz	95

TABLE X—*cont.*

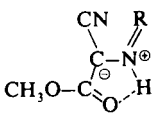
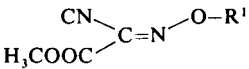
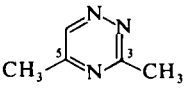
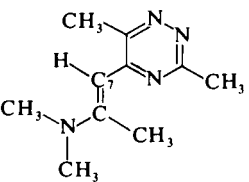
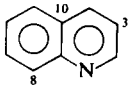
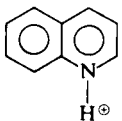
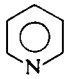
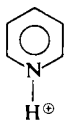
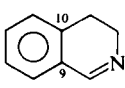
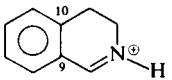

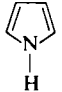
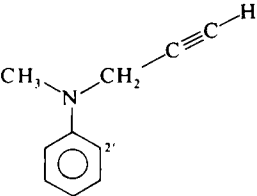
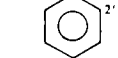
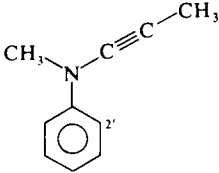
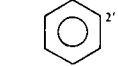
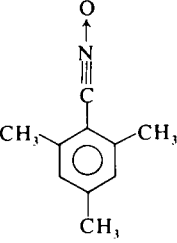
Compound		$^2J(^{15}\text{N}-\text{C})_{\text{observed}}$	$^2J(^{15}\text{N}-\text{C})_{\text{calculated}}$	Reference
	N-CN	(\pm)2.0	—	122
	N-CO ₂ Me	(\pm)3.3	—	122
	N-CN	(\pm)1.0	—	122
	N-CO ₂ Me	(-)10.5	—	122
	N-(3-CH ₃)	(-)9.2	—	114
	N-(5-CH ₃)	(-)8.9	—	114
	N-(3-CH ₃)	(-)10.3	—	114
	N-C ₇	(-)5.5	—	114
	N-C ₃	(+)2.7	8.64 ^b	123
	N-C ₁₀	(+)2.1	6.32 ^b	123
	N-C ₈	(-)9.3	-2.58 ^b	123
	N-C ₃	(+)1	7.37 ^b	123
	N-C ₁₀	(+)1	5.46 ^b	123
	N-C ₈	(+)1	4.42	123
		+2.53	3.1 ^c	98
		+2.01	3.7 ^c	98
	N-C ₉	~(\pm)2	—	112
	N-C ₁₀	<1	—	112
	N-C ₉	<1	—	112
	N-C ₁₀	~(\pm)2	—	112

TABLE X—*cont.*

Compound	$^2J(^{15}\text{N}-\text{C})_{\text{observed}}$	$^2J(^{15}\text{N}-\text{C})_{\text{calculated}}$	Reference
	+1.43	5.8 ^c	98
	-3.92	-0.8 ^c	98(a)
aniline	-2.68	-0.3 ^c , -0.5 ^d	98
anilinium ion	(-)1.5	+2.5 ^d	96
N-methylaniline	(-)2.5	—	99
	(±)0.9	—	99
 N-C _{2'}	-2.1	—	99
	±5.5	—	99
 N-C _{2'}	-2.3	—	99
1-propylamine	±1.2	—	94
1-propylamine·HCl	<0.2	—	94
nitrobenzene	-1.67	+3.3 ^c	103
CH ₃ CN	+3.0	3.5 ^c	106
	(±)2.2	—	92

^a Ref. 23. ^b Ref. 104. ^c Ref. 20. ^d Ref. 96. ^e Ref. 103.

(101) $^2K(\text{N}-\text{C})$ is probably positive, analogous to the relatively large positive values of $^2J(\text{C}-\text{C})$ observed in acetone and other ketones. The calculated value of $^2J(\text{N}-\text{C})$ for acetanilide is -3.5 Hz, approximately 5.5 Hz too positive.

The dependence of $^2J(\text{N}-\text{C})$ on lone-pair orientation is illustrated for several of the molecules in Table X. For example, in the oximes and triazines the absolute value of $^2J(\text{N}-\text{C})$ is greatly enhanced when the nitrogen lone-pair lies *cis* to the carbon. The INDO-FPT calculations and experimental data on $^2J(\text{N}-\text{H})$ and $^2J(\text{P}-\text{C})$ strongly suggest that a proximate lone-pair makes a positive contribution to the reduced coupling constant. (124–126) For example, the value *calculated* for $^2J(^{15}\text{N}-\text{C}_3)$ in quinoline is $+8.64$ Hz. The coupling to C_8 , which is proximate to the nitrogen lone-pair, is calculated as -2.58 Hz (a difference of 11.22 Hz). That is, although the calculated values are too positive, $^2J(\text{N}-\text{C}_8)$ is about 11 Hz more negative than $^2J(\text{N}-\text{C}_3)$, in good agreement with experiment. Notice that in protonated quinoline, the observed values of $^2J(\text{N}-\text{C}_8)$ and $^2J(\text{N}-\text{C}_3)$ are approximately 11 Hz|. The INDO calculations predict these values to differ by less than 3 Hz.

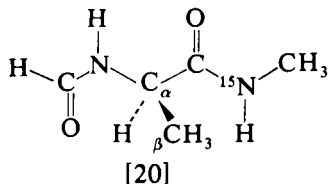
$^2J(\text{N}-\text{C})$ values have not been observed in a study of the amino acids glycine and alanine. (95)

C. $^3J(\text{N}-\text{C})$

Observed values of some vicinal $^{15}\text{N}-^{13}\text{C}$ coupling constants are given in Table XI. MO calculations generally predict the sign of this coupling to be negative in both saturated and unsaturated fragments. (20, 23, 96, 98, 103, 104, 127)

1. Saturated fragments

INDO-FPT calculations of the Fermi contact contribution to $^3J(\text{N}-\text{C})$ in the peptide fragment [20], by Solkan and Bystrov, (127) find that



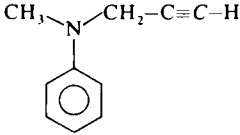
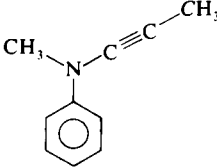
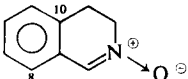
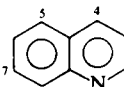
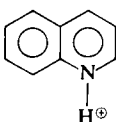
the dependence of $^3J(^{15}\text{N}-\text{C}^1-\text{C}_\alpha-\text{C}_\beta)$ on the $^{15}\text{N}-\text{C}^1-\text{C}_\alpha-\text{C}_\beta$ dihedral angle, ϕ , is described in an approximate manner by equation (11).

$$^3J(^{15}\text{N}-\text{C}_\beta) = -2.6 \cos^2 \phi - 0.6 \cos \phi \quad (11)$$

Equation (11) predicts $^3J(\text{N}-\text{C}_\beta)$ to be -3.2 , 0.0 and -2.0 Hz for dihedral angles of 0° , 90° and 180° , respectively.

TABLE XI

Some observed and calculated values of $3J(^{15}\text{N}-\text{C})$

	$^3J(\text{N}-\text{C})_{\text{observed}}$	$^3J(\text{N}-\text{C})_{\text{calculated}}$	Reference
1-propylamine	(-)1.4	—	94
1-propylamine-HCl	(-)1.3	—	94
quinuclidine	(-)2.8	—	94
quinuclidine-HCl	(-)6.7	—	94
	± 0.8	—	99
	< 0.5	—	99
aniline	-1.29	$-0.8^a, -1.6^b$	98
anilinium	(-)2.1	-3.3^a	96
nitrobenzene	-2.32	-5.20^c	103
pyridine-N-oxide	-5.17	-5.2^b	98
	$\text{N}-\text{C}_8$ $\text{N}-\text{C}_{10}$	$(-)3.4$ $(-)2.4$	112
pyridine	-3.85	$-6.60^d, -3.7^b$	98
pyridinium ion	-5.30	$-8.72^d, -4.4^b$	98
	$\text{N}-\text{C}_4$ $\text{N}-\text{C}_5$ $\text{N}-\text{C}_7$	$(-)3.5$ ~ 0 $(-)3.9$	123 123 123
	$\text{N}-\text{C}_4$ $\text{N}-\text{C}_5$ $\text{N}-\text{C}_7$	$(-)4.6$ ~ 0 $(-)2.7$	123 123 123

^a Ref. 96. ^b Ref. 20. ^c Ref. 103. ^d Ref. 104.

The absolute value of $|^3J(\text{N}-\text{C})|_{\text{cis}}$ is predicted to be greater than $|^3J(\text{N}-\text{C})|_{\text{trans}}$.

Di Blasi and Kopple (128) were unable to resolve vicinal ^{15}N - ^{13}C coupling constants in peptide models having $^{15}\text{N}-\text{C}-\text{C}_\alpha-\text{C}_\beta$ dihedral

angles constrained to approximately 110° and 160° . They estimated $^3J(\text{N}-\text{C}) < 1$ Hz for these dihedral angles. For $\phi = 160^\circ$, equation (11) predicts a value of ~ -1.7 Hz.

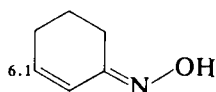
In a number of saturated amides, Lichter *et al.* (101) also failed to observe any vicinal ^{15}N -C coupling constants.

However, $^3J(\text{N}-\text{C})$ values are observed for 1-propylamine, quinuclidine and their hydrochlorides. (94) In saturated amines it is unlikely that it will be possible to describe calculated $^3J(\text{N}-\text{C})$ values in terms of simple "Karplus-type" equations. Other factors, such as the orientation of the nitrogen lone-pair (important for $^3J(\text{N}-\text{H})$), will undoubtedly be important. (124)

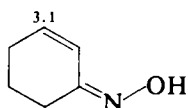
Recent $^3J(\text{P}-\text{C})$ data indicate that this coupling may not depend on the dihedral angle in a simple "Karplus" manner. (129)

2. Unsaturated fragments

In oximes $^3J(\text{N}-\text{C})$ depends on the orientation of the nitrogen lone-pair. (104) For example, in [21] and [22] the coupled nuclei are *trans* to

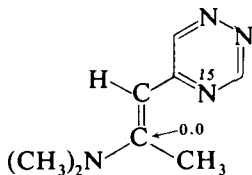


[21]

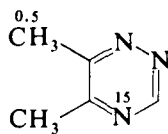


[22]

each other but the $^3J(\text{N}-\text{C})$ values differ by a factor of two. In the 1,2,4-triazine derivatives [23] and [24], $^3J(\text{N}-\text{C})$ is small. (114) The coupled



[23]



[24]

N and C nuclei in [22] and [24] have the same relative orientation. However, the very different values observed for $^3J(\text{N}-\text{C})$ suggest that factors other than lone-pair orientation are important in these systems.

D. $^nJ(\text{N}-\text{C}), n \geq 4$

These are generally less than 1 Hz. An exception is the value of ± 3.9 Hz observed for the proximate CH_3 and ^{15}N in the 1,2,4-triazine derivative [23]. (114)

VI. O-C COUPLING CONSTANTS

The ^{17}O nucleus (natural abundance 0.037%) has spin 5/2, and a negative gyromagnetic ratio. The only reported ^{17}O -C coupling constant is the one estimated for acetone- ^{17}O , where $^1J(^{17}\text{O}-\text{C}) \simeq 22$ Hz. INDO-FPT calculations predict $^1J(^{17}\text{O}-\text{C}) = +17.7$ Hz ($^1K(\text{O}-\text{C}) = -43.2 \times 10^{20} \text{ cm}^{-3}$). (23)

VII. F-C COUPLING CONSTANTS

A. Introduction

These coupling constants are generally quite large and relatively easy to measure. A good discussion of $^nJ(\text{F}-\text{C})$ is given by Stothers. (1) The present account will be less comprehensive than that given for $^nJ(\text{C}-\text{C})$ and $^nJ(\text{N}-\text{C})$.

Most values of $^1J(\text{F}-\text{C})$ fall between -158 Hz, observed for methylfluoride, and -369 Hz observed for FCHO. (130) Calculations by Blizzard and Santry (16, 17) predict substantial orbital and spin-dipolar contributions to $^1J(\text{F}-\text{C})$.

$^2J(\text{F}-\text{C})$ is generally positive and can be as large as 100 Hz. (131) The only negative value reported is for ethylfluoride, (132) but it is not clear if and how the sign was determined. The value reported in *n*-hexylfluoride is $+19.9$ Hz. (133) Table XII lists values where the signs have been determined.

The value of $^3J(\text{F}-\text{C})$ is generally less than 20 Hz in magnitude. Unfortunately, signs have been reported for only a few $^3J(\text{F}-\text{C})$ values.

B. Recent literature in which $^nJ(\text{F}-\text{C})$ values are reported

Sojka and co-workers (141) report $^1J(\text{F}-\text{C})$ for a number of substituted trifluoromethanes.

$^nJ(\text{F}-\text{C})$ values in a number of glycosyl fluorides are given by Bock and Pedersen. (142) The absolute value of $^1J(\text{F}-\text{C})$ values in the α -pyranosyl fluorides (fluorine atom axial [25]) are generally 10 Hz larger than the values in the corresponding β -pyranosyl fluorides (fluorine atom equatorial [26]). For example, for $\text{R}_1 = \text{R}_2 = \text{R}_3 = \text{H}$, $^1J(\text{F}-\text{C})_\alpha$ is

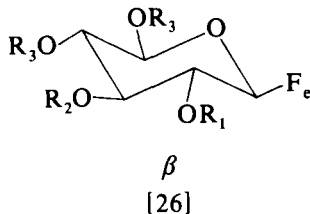
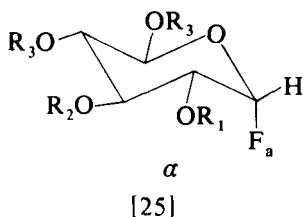
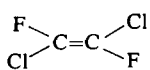
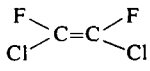
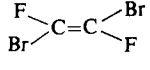
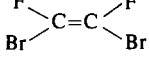
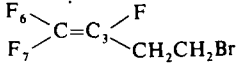
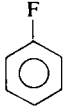
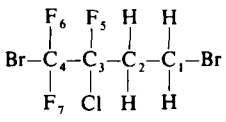
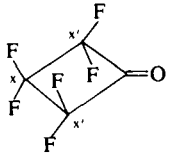


TABLE XII

Some examples of observed $^2J(\text{F}-\text{C})$ data

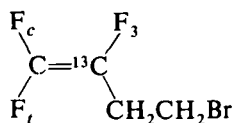
Compound	$^2J(\text{F}-\text{C})$	Reference
FCOCOF	103.2	131
	54.5	134
	37.0	134
	102.5	135
	35.8	135
	F_6-C_3 17 F_7-C_3 53	136 136
	21.0	133
$\text{Cl}_2\text{CFCCl}_2\text{F}$	34.9	137
	F_5-C_2 21 $\text{F}_{6,7}-\text{C}_3$ 30 F_5-C_4 35	138
$\text{CF}_3\text{CH}_2\text{CH}_2\text{CF}_3$	30.9	139
<i>n</i> -hexylfluoride	19.9	133
	$\text{F}-\text{C}_x$ 24.7 $\text{F}-\text{C}_{x'}$ 24.7	140 140

-222.2 Hz and $^1J(\text{F}-\text{C})_\beta$ is -211.3 Hz. Analogous results are obtained for $^1J(\text{C}_1-\text{H})$ values. (143) The $^2J(\text{F}-\text{C}_2)$ values in the α - and β -pyranosyl fluorides are approximately $+25$ Hz and $+35$ to $+40$ Hz when the substituent at C_2 is equatorial and axial, respectively. The

$^3J(\text{F}-\text{C}_3)$ values in the β -pyranosyl fluorides are 4–10 Hz, while in the α -derivatives they are 0–6 Hz. In the latter the fluorine and C_3 atoms have a *gauche* orientation, while in the former they are *trans* oriented. On the basis of the results obtained for other three-bond coupling constants in saturated systems, one would expect $^3J(\text{F}-\text{C})$ to depend on dihedral angle. However, keeping in mind the results discussed for $^3J(\text{C}-\text{C})$ and $^3J(\text{N}-\text{C})$, and the results discussed by Stothers, (1) it is unlikely that one will be able to describe this dependence by a simple “Karplus” equation.

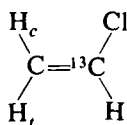
$^nJ(\text{F}-\text{C})$ values have been reported for some nucleoside derivatives where the sugar moiety is fluorinated. (144)

For 1-bromo-3,3,4-trifluorobutene-4 [27], Hinton and Jaques (136)



[27]

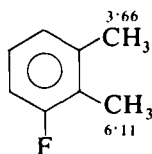
observe $^2J(\text{F}_c-\text{C})$ to be +17 Hz while $^2J(\text{F}_t-\text{C})$ is +53 Hz. It is interesting to compare these results with those obtained for $^2J(\text{C}-\text{H})$ in vinyl chloride [28]. In this case, $^2J(\text{C}-\text{H}_c)$ is -7.9 Hz while $^2J(\text{C}-\text{H}_t)$ is



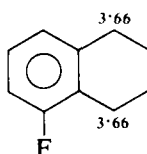
[28]

+7.5 Hz. (145, 146) Thus in both [27] and [28], $^2J(\text{C}-\text{X}_t) > ^2J(\text{C}-\text{X}_c)$ where X is *trans* or *cis* to an electronegative substituent which is bonded to ^{13}C (i.e. F_3 in [27] and Cl in [28]).

Adcock *et al.* (147) report $^nJ(\text{F}-\text{C})$ values in several fluorobenzocycloalkenes. The value of $^3J(\text{F}-\text{C})$, involving the aliphatic carbon, is strongly dependent on the fused ring size. Some results for $^3J(\text{F}-\text{C})$ and $^4J(\text{F}-\text{C})$ in these compounds are illustrated in [29], [30],

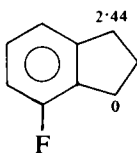


[29]

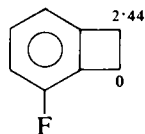


[30]

[31], and [32]. The latter two compounds are examples where $^4J(\text{F}-\text{C})$ along the planar zig-zag path is greater than $^3J(\text{F}-\text{C})_{\text{cis}}$.



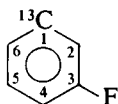
[31]



[32]

Substituent effects on $^nJ(\text{F}-\text{C})$ values in fluorobenzenes have been discussed by a number of authors. (133, 148–153) The coupling constants in fluorobenzene are reported to be $^1J(\text{F}-\text{C}) = -245.2$ Hz, $^2J(\text{F}-\text{C}) = +21.0$ Hz, $^3J(\text{F}-\text{C}) = +7.8$ Hz and $^4J(\text{F}-\text{C}) = +3.2$ Hz. (133, 148, 150)

Wray and Lincoln (151) have carried out a complete analysis of the ^{19}F , ^{13}C and ^1H NMR spectra of 1,3,5-trifluorobenzene. They report $^1J(\text{F}-\text{C})$ as -248.63 Hz, $^2J(\text{F}-\text{C})$ as $+25.91$ Hz, $^3J(\text{F}-\text{C})$ as -15.39 Hz and $^4J(\text{F}-\text{C})$ as $+4.34$ Hz. More recent experiments (154) indicate that the sign of $^3J(\text{F}-\text{C})$ is positive, as expected on the basis of an alternating substituent effect. (82, 146) For example, in [33] an



[33]

electronegative substituent at C_1 should lead to an increase in $^3J(\text{F}-\text{C}_1)$ relative to the value in fluorobenzene, while an electronegative substituent at C_2 should result in a decrease in $^3J(\text{F}-\text{C}_1)$. (82) In 1,3-difluorobenzene, $^3J(\text{F}-\text{C}_3) \simeq 12.1$ Hz (146) while in 1,2-difluorobenzene $^3J(\text{F}_1-\text{C}_3)$ is 0.53 Hz. (152)

This latter result was obtained by Ernst and co-workers (152) and illustrates the necessity for complete analyses of both the ^{13}C and ^{13}C -satellite spectra. $^3J(\text{F}_1-\text{C}_3)$ was estimated as -3.0 Hz in an earlier study. (146)

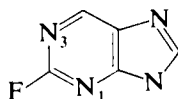
Fluorine-carbon coupling constants, measured for 2-, 3-, and 4-fluoropyridine and pyridinium ions, (155) have been compared with values calculated assuming only the Fermi contact mechanism. Many of the experimental trends are paralleled by those for $^nJ(\text{C}-\text{H})$ values observed in pyridine and fluorobenzene. The INDO calculations qualitatively reproduce the experimental trends.

In 2-fluoropyridine, $^1J(\text{F}-\text{C})$ is -236.3 Hz, more positive than the $^1J(\text{F}-\text{C})$ values of -255.1 and -261.8 Hz observed in 3- and 4-fluoropyridine, respectively. Protonation induces an increase in the absolute value of $^1J(\text{F}-\text{C})$ in 2- and 4-fluoropyridine, while that of 3-fluoropyridine is unaffected.

$^2J(\text{F}-\text{C})$ values show considerable variation. For example, in 2-fluoropyridine $^2J(\text{F}_2-\text{C}_3)$ is 37.6 Hz while in 3-fluoropyridine $^2J(\text{F}_3-\text{C}_2)$ is 22.6 Hz. A similar trend is observed in pyridine (156) where $^2J(\text{C}_2-\text{H}_3)$ is ~ 5.4 Hz less than $^2J(\text{C}_3-\text{H}_2)$. On protonation $^2J(\text{F}_2-\text{C}_3)$ decreases by 13.2 Hz while $^2J(\text{F}_3-\text{C}_2)$ increases by 12.1 Hz.

In 2-fluoropyridine, $^3J(\text{F}_2-\text{C}_6)$ is 14.9 Hz compared to a value of 7.5 Hz for $^3J(\text{F}_2-\text{C}_4)$. Similarly $^3J(\text{C}_2-\text{H}_6)$ is much larger than other $^3J(\text{C}-\text{H})$ values in pyridine. (156)

In 2-fluoropurine [34], (157) where the C_2 carbon is adjacent to two



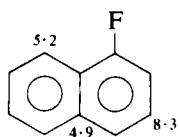
[34]

“pyridine-type” nitrogens, $^1J(\text{F}-\text{C})$ is -207.5 Hz, approximately 30 Hz more positive than the value obtained in 2-fluoropyridine. The values of the $^3J(\text{F}-\text{C})$ across N_1 and N_3 are 15.9 and 17.1 Hz, respectively, and are the largest $^3J(\text{F}-\text{C})$ values reported in “aromatic systems”.

The $^nJ(\text{F}-\text{C})$ values in 1-fluoro and in 2-fluoro-naphthalene have been measured by Ernst (158) and by Doddrell *et al.* (153). Although their values for 1-fluoronaphthalene agree, there are a number of discrepancies concerning the assignment of the various carbon resonances in 2-fluoronaphthalene.

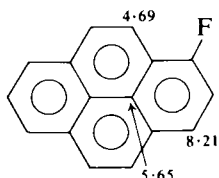
Doddrell *et al.* (153) have reported an extensive study of $^nJ(\text{F}-\text{C})$ values for a large number of fluorinated and trifluorinated aromatic compounds. Included are data on *ortho*-, *meta*- and *para*-fluorostyrene, fluoro- and trifluoromethyl-substituted naphthalenes, 2- and 3-fluoro-substituted pyridine, and on a number of fluoroquinolines. Observations on the fluoronaphthalenes, pyridines and quinolines are compared with calculations using the INDO procedure (Fermi contact contribution only). The authors point out that the neglect of the orbital and spin-dipolar mechanisms is only part of the reason for the rather poor agreement found between observed and calculated geminal and long-range $J(\text{F}-\text{C})$ values. A valence-bond formulation has been applied to the rationalization of values of $^2J(\text{F}-\text{C})$ and $^3J(\text{F}-\text{C})$. It is possible to relate $^2J(\text{F}-\text{C})$ and $^3J(\text{F}-\text{C})$ to various F-H coupling constants under

conditions of perfect pairing. For 1-fluoronaphthalene [35] the authors suggest that a combination of conformation, substituent and bond order



[35]

must be responsible for the three different values observed for $^3J(\text{F}-\text{C})$. The $^3J(\text{F}-\text{C})$ values in 1-fluoronaphthalene can be compared with the values in 1-fluoropyrene [36]. (159)

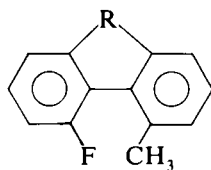


[36]

In 2-trifluoromethylnaphthalene, $^3J(\text{F}-\text{C}_1)$ is 4.5 Hz, and $^3J(\text{F}-\text{C}_3)$ is 3.2 Hz. (153) INDO calculated π -bond orders of 0.765 and 0.516 for C_1-C_2 and C_2-C_3 , respectively, suggest that this difference is at least partly responsible for the difference in the observed $^3J(\text{F}-\text{C})$ values.

In trifluoromethyl benzene, $^3J(\text{F}-\text{C})$ is 3.9 Hz, $^4J(\text{F}-\text{C})$ is 0 Hz, and $^5J(\text{F}-\text{C})$ is 1.3 Hz. Doddrell *et al.* have suggested a cancellation of σ and π contributions, leading to the small value for $^4J(\text{F}-\text{C})$.

$^5J(\text{F}-\text{C})$ values between the proximate carbon and fluorine nuclei in five different 4-methyl-5-fluorophenanthrenes derivatives [37] are almost



[37]

exactly twice the magnitude of the corresponding $^6J(\text{F}-\text{CH}_3)$ values. (160) Jerome and Servis have suggested that this observation implies that fluorine-methyl hydrogen coupling may result from interactions centred on the fluorine and methyl carbon atoms rather than on the fluorine and hydrogen nuclei. This suggestion is substantiated to some extent by recent INDO-MO calculations. (161)

VIII. PERIODIC TRENDS AND CONCLUSIONS

Calculated values (Fermi contact contribution only) of $^1K(C-X)$ in a number of aliphatic methyl-X compounds are given in Table XIII. (23) As X increases in atomic number from 3 (Li) to 9 (F), $^1K(C-X)$ increases, reaching a maximum for $X = CH_3$, and then rapidly decreases and becomes negative for $X = OH$ and $X = F$. The experimental results discussed in this review qualitatively verify these predictions.

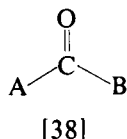
TABLE XIII

Some calculated values of $^1J(C-X)$ and $^1K(C-X)$

Compound	X	$^1J(C-X) \text{ Hz}$	$^1K(C-X) \text{ cm}^{-3} \times 10^{-22}$
CH_3Li	Li	25.6	0.218
$(CH_3)_2Be$	Be	-16.5	0.388
$(CH_3)BH_2$	B	51.1	0.528
CH_3CH_3	C	41.4	0.546
$CH_3^{15}NH_2$	N	-4.6	0.150
CH_3OH	O	21.4	-0.522
CH_3F	F	-237.3	-0.835

As one moves down Group IV, $^1K(X-C)$ increases. (162) Both positive and negative $^1K(P-C)$ values are known for trivalent phosphorus compounds. (1, 3) Observed values of $^1K(Se-C)$ and $^1K(Te-C)$ are negative (163, 164) and therefore it is likely that $^1K(O-C)$ values will also be negative, as predicted by the INDO calculations.

Many of the two- and three-bond C-X coupling constants discussed here display trends analogous to the corresponding $J(X-H)$ values. For example, the $^2K(A-B)$ values in [38] generally appear to be large and positive.



Almost all measured $^3K(C-X)$ values are positive. In saturated fragments, this coupling also appears to depend on the dihedral angle. However, as X increases in atomic number the angular dependence of $^3K(C-X)$ becomes more difficult to predict. It appears that subtle changes in conformation and electronic structure can result in marked changes in $^3K(C-X)$ where $X \neq H$.

Clearly, more calculations and experimental data with signs are required before the potential of $^nJ(\text{C-X})$ values as a probe of the details of molecular structure is fully realized.

Acknowledgements

I would like to acknowledge the helpful comments of Professor Ted Schaefer and Dr. George Tomlinson. I wish to express my gratitude to a numbers of authors for supplying me with preprints of their work prior to publication. I am indebted to Mrs. Urmilla Deonauth for her careful typing of the manuscript. The assistance of Mr. John Bukata and Mr. Walter Niemczura is also appreciated.

Note added in proof

Some references to recent papers in which C-C, N-C and F-C coupling constants are discussed are (165-170), (171-176) and (177) respectively.

REFERENCES

1. J. B. Stothers, "Carbon-13 Nuclear Magnetic Resonance Spectroscopy", Academic Press, New York, 1972, Chapter 10.
2. J.-R. Llinas, E.-J. Vincent and G. Peiffer, *Bull. Soc. Chim. France*, 1973, 3209.
3. R. Grinter, in "Specialist Periodical Reports, Nuclear Magnetic Resonance", R. K. Harris (ed.), The Chemical Society, London, 1972-1976, Vol. 1-5.
4. J. A. Pople and D. P. Santry, *Mol. Phys.*, 1964, **8**, 1.
5. N. F. Ramsey, *Phys. Rev.*, 1953, **91**, 303.
6. M. Barfield and D. M. Grant, in "Advances in Magnetic Resonance", J. S. Waugh (ed.), Academic Press, New York, 1965, Vol. 1, p. 149.
7. J. N. Murrell, in "Progress in NMR Spectroscopy", J. W. Emsley, J. Feeney and L. H. Sutcliffe (eds.), Pergamon Press, Oxford, 1971, Vol. 6, p. 1.
8. P. D. Ellis and R. Ditchfield, in "Topics in Carbon-13 NMR Spectroscopy", G. C. Levy (ed.), Wiley-Interscience, New York, 1976, Vol. 2, p. 433.
9. J. Kowalewski, in "Progress in NMR Spectroscopy", J. W. Emsley, J. Feeney and L. H. Sutcliffe (eds.), Pergamon Press, Oxford, to be published.
10. J. A. Pople, D. L. Beveridge and P. A. Dobosh, *J. Chem. Phys.*, 1967, **47**, 2026.
11. J. A. Pople, J. W. McIver, Jr. and N. S. Ostlund, *Chem. Phys. Letters*, 1967, **1**, 465.
12. J. A. Pople, J. W. McIver, Jr. and N. S. Ostlund, *J. Chem. Phys.*, 1968, **49**, 2960, 2965.
13. J. A. Pople and D. L. Beveridge, "Approximate Molecular Orbital Theory", McGraw-Hill, New York, 1970.
14. A. D. C. Towl and K. Schaumburg, *Mol. Phys.*, 1971, **22**, 49.
15. A. C. Blizzard and D. P. Santry, *Chem. Commun.*, 1970, 1085.
16. A. C. Blizzard and D. P. Santry, *J. Chem. Phys.*, 1971, **55**, 950.
17. A. C. Blizzard and D. P. Santry, *J. Chem. Phys.*, 1973, **58**, 4714.
18. C. J. Jameson and H. S. Gutowsky, *J. Chem. Phys.*, 1969, **51**, 2790.
19. W. McFarlane, *Quart. Rev.*, 1969, **23**, 187.
20. J. M. Schulman and T. Venanzi, *J. Amer. Chem. Soc.*, 1976, **98**, 4701.

21. W. McFarlane and D. S. Rycroft, *J. Organometal. Chem.*, 1974, **64**, 303.
22. A. H. Cowley and W. D. White, *J. Amer. Chem. Soc.*, 1969, **91**, 34.
23. R. Wasylishen, unpublished results.
24. P. D. Ellis, J. D. Odom, D. W. Lowman and A. D. Cardin, *J. Amer. Chem. Soc.*, 1971, **93**, 6704.
25. J. D. Odom, L. W. Hall and P. D. Ellis, *Org. Magn. Resonance*, 1974, **6**, 360.
26. L. W. Hall, D. W. Lowman, P. D. Ellis and J. D. Odom, *Inorg. Chem.* 1975, **14**, 580.
27. V. V. Negrebetskii, V. S. Bogdanov, A. V. Kessenikh, P. V. Petrovskii, N. Y. Bubnov and B. M. Mikhailov, *Zh. Obshch. Khim.*, 1974, **44**, 1882.
28. F. T. Weigert and J. D. Roberts, *J. Amer. Chem. Soc.*, 1972, **94**, 6021.
29. G. E. Maciel, in "Nuclear Magnetic Resonance Spectroscopy of Nuclei Other Than Protons" T. Axenrod and G. A. Webb (eds.) Wiley-Interscience, New York, 1974, p. 187.
30. J. L. Marshall, D. E. Miiller, S. A. Conn, R. Seiwel and A. M. Ihrig, *Acc. Chem. Res.*, 1974, **7**, 333.
31. H. Seto and M. Tanabe, *Tetrahedron Lett.*, 1974, 651.
32. A. G. McInnes, D. G. Smith, J. A. Walter, L. C. Vining and J. L. C. Weight, *J.C.S. Chem. Comm.*, 1975, 66.
33. J. Polonsky, G. Lukacs, N. Cagnoli-Bellavita and P. Ceccherelli, *Tetrahedron Lett.*, 1974, 481.
34. R. E. London, V. H. Kollman and N. A. Matwiyoff, *J. Amer. Chem. Soc.*, 1975, **97**, 3565.
35. R. D. Bertrand, D. M. Grant, E. L. Allred, J. C. Hinshaw and A. B. Strong, *J. Amer. Chem. Soc.*, 1972, **94**, 997.
36. R. M. Lynden-Bell and N. Sheppard, *Proc. Roy. Soc. London Ser. A*, 1962, **269**, 385.
37. D. M. Graham and C. E. Holloway, *Can. J. Chem.*, 1963, **41**, 2114.
38. K. Frie and H. J. Bernstein, *J. Chem. Phys.*, 1963, **38**, 1216.
39. J. L. Marshall, A. M. Ihrig and D. E. Miiller, *J. Mol. Spectrosc.*, 1972, **43**, 323.
40. G. E. Maciel, J. W. McIver, Jr., N. S. Ostlund and J. A. Pople, *J. Amer. Chem. Soc.*, 1970, **92**, 11.
41. M. D. Newton, J. M. Schulman and M. M. Manus, *J. Amer. Chem. Soc.*, 1974, **96**, 17.
42. J. M. Schulman and M. D. Newton, *J. Amer. Soc.*, 1974, **96**, 6295.
43. M. Pomerantz and R. Fink, *J.C.S. Chem. Common.*, 1975, 430.
44. M. Pomerantz, R. Fink and G. A. Gray, *J. Amer. Chem. Soc.*, 1976, **98**, 291.
45. J. M. Schulman and T. J. Venanzi, *Tetrahedron Lett.*, 1976, 1461.
46. J. L. Marshall and D. E. Miiller, *Org. Magn. Resonance*, 1974, **6**, 395.
47. V. J. Bartuska and G. E. Maciel, *J. Magn. Resonance*, 1972, **7**, 36.
48. G. Becher, W. Luttker and G. Schrumpf, *Angew. Chem., Int. Ed., Engl.*, 1973, **12**, 339.
49. P. E. Hansen, O. K. Poulsen and A. Berg, *Org. Magn. Resonance*, 1975, **7**, 475.
50. P. E. Hansen, O. K. Poulsen and A. Berg, *Org. Magn. Resonance.*, 1975, **7**, 405.
51. J. L. Marshall and D. E. Miiller, *J. Amer. Chem. Soc.*, 1973, **95**, 8305.
52. J. L. Marshall, L. G. Faehl, A. M. Ihrig and M. Barfield, *J. Amer. Chem. Soc.*, 1976, **98**, 3406.
53. P. E. Hansen, O. K. Poulsen and A. Berg, *Org. Magn. Resonance.*, 1975, **7**, 23.
54. A. M. Ihrig and J. L. Marshall, *J. Amer. Chem. Soc.*, 1972, **94**, 1756.
55. G. A. Grey, P. D. Ellis, P. D. Traficante and G. E. Maciel, *J. Magn. Resonance*, 1969, **1**, 41.
56. S. A. Linde and H. J. Jakobsen, *J. Amer. Chem. Soc.*, 1976, **98**, 1041.
57. S. Tran-Dihn, S. Fermandjian, E. Sala, R. Mermet-Bouvier, M. Cohen and P. Fromageot, *J. Amer. Chem. Soc.*, 1974, **96**, 1484.
58. S. Tran-Dinh, S. Fermandjian, E. Sala, R. Mermet-Bouvier and P. Fromageot, *J. Amer. Chem. Soc.*, 1975, **97**, 1267.

59. J. A. Sogn, L. C. Craig and W. A. Gibbons, *J. Amer. Chem. Soc.*, 1974, **96**, 4694.
60. W. Haar, S. Femandjian, J. Vicar, K. Blaha and P. Fromageot, *Proc. Nat. Acad. Sci. U.S.A.*, 1975, **72**, 4948.
61. V. J. Bartuska and G. E. Maciel, *J. Magn. Resonance*, 1971, **5**, 211.
62. J. L. Marshall and A. M. Ihrig, *Org. Magn. Resonance*, 1973, **5**, 235.
63. S. Berger and K.-P. Zeller, *J.C.S. Chem. Comm.*, 1975, 423.
64. J. L. Marshall, A. M. Ihrig and D. E. Müller, *J. Magn. Resonance*, 1974, **16**, 439.
65. C. J. Jameson and M. C. Damasco, *Mol. Phys.*, 1970, **18**, 491.
66. M. Barfield, I. Burfitt and D. Doddrell, *J. Amer. Chem. Soc.*, 1975, **97**, 2631.
67. D. F. Ewing, in "Annual Reports on NMR Spectroscopy", E. F. Mooney (ed.), Academic Press, New York, 1975, **6A**, 389.
68. G. A. Gray, G. E. Maciel and P. D. Ellis, *J. Magn. Resonance*, 1969, **1**, 407.
69. J. L. Marshall, D. E. Müller, H. C. Dorn and G. E. Maciel, *J. Amer. Chem. Soc.*, 1975, **97**, 460.
70. H. Dreeskamp, K. Hilderbrand and G. Pfisterer, *Mol. Phys.*, 1969, **17**, 429.
71. J. A. Pople and A. A. Bothner-by, *J. Chem. Phys.*, 1965, **42**, 1339.
72. B. L. Shapiro, R. M. Kopchik and S. J. Ebersole, *J. Chem. Phys.*, 1963, **39**, 3154.
73. E. Sackmann and H. Dreeskamp, *Spectrochim. Acta*, 1965, **21**, 2005.
74. C. Schumann, H. Dreeskamp and K. Hildenbrand, *J. Magn. Resonance*, 1975, **18**, 97.
75. D. Ziessow, *J. Chem. Phys.*, 1971, **55**, 984.
76. M. Karplus, *J. Chem. Phys.*, 1959, **30**, 11.
77. M. Karplus, *J. Amer. Chem. Soc.*, 1963, **85**, 2870.
78. M. Barfield and M. Karplus, *J. Amer. Chem. Soc.*, 1969, **91**, 1.
79. R. Wasylishen and T. Schaefer, *Can. J. Chem.*, 1972, **50**, 2710.
80. D. Doddrell, I. Burfitt, J. B. Grutzner and M. Barfield, *J. Amer. Chem. Soc.*, 1974, **96**, 1241.
81. R. Wasylishen and M. Barfield, *J. Amer. Chem. Soc.*, 1975, **97**, 4545.
82. R. Wasylishen and T. Schaefer, *Can. J. Chem.*, 1973, **51**, 961.
83. R. Wasylishen and T. Schaefer, *Can. J. Chem.*, 1972, **50**, 2989.
84. M. Barfield, S. A. Conn, J. L. Marshall and D. E. Müller, *J. Amer. Chem. Soc.*, 1976, **98**, 6253.
85. R. C. Long, Jr. and J. H. Goldstein, *J. Magn. Resonance*, 1974, **16**, 228.
86. E. W. Randall and D. G. Gilles, in "Progress in nuclear magnetic resonance spectroscopy", J. W. Emsley, J. Feeney and L. H. Sutcliffe (eds.), Pergamon Press, Oxford, 1971, Vol. 6, p. 119.
87. R. L. Lichter, in "Determination of organic structures by physical method", F. C. Nachod and J. J. Zuckerman (eds.), Academic Press, New York, 1972, Vol. 4, p. 195.
88. T. Axenrod, in "Nitrogen NMR", G. A. Webb and M. Witanowski (ed.), Plenum Publishing Co., New York, 1973, p. 261.
89. H. J. C. Yeh, H. Ziffer, D. M. Jerina and D. R. Boyd, *J. Amer. Chem. Soc.*, 1973, **95**, 2741.
90. J. M. Lehn and J. P. Kintzinger, in "Nitrogen NMR", G. A. Webb and M. Witanowski (eds.), Plenum Publishing Co., New York, 1973, p. 79.
91. W. B. Jennings, D. R. Boyd, C. G. Watson, E. D. Becker, R. B. Bradley and D. M. Jerina, *J. Amer. Chem. Soc.*, 1972, **94**, 8501.
92. M. Christl, J. P. Warren, B. L. Hawkins and J. D. Roberts, *J. Amer. Chem. Soc.*, 1973, **95**, 4392.
93. L. Paolillo and E. D. Becker, *J. Magn. Resonance*, 1970, **3**, 200.
94. S. Berger and J. D. Roberts, *J. Amer. Soc.*, 1974, **96**, 6757.
95. R. L. Lichter and J. D. Roberts, *J. Amer. Chem. Soc.*, 1971, **93**, 5218.
96. R. E. Wasylishen, *Can. J. Chem.*, 1976, **54**, 833.

97. M. Hansen and H. J. Jakobsen, *Acta. Chem. Scand.*, 1972, **26**, 2151.
98. (a) T. Bundgaard, H. J. Jakobsen and E. J. Rahkamaa, *J. Magn. Resonance*, 1975, **19**, 345.
(b) T. Bundgaard and H. J. Jakobsen, *Tetrahedron Lett.*, 1976, 1621.
99. T. Brottin-Strzalko, M. J. Pouet and M. P. Simonnin, *Org. Magn. Resonance*, 1976, **8**, 120.
100. J. F. Hinton, K. H. Ladner and W. E. Stewart, *J. Magn. Resonance*, 1973, **12**, 90.
101. R. L. Lichter, C. G. Fehder, P. H. Patton, J. Coombes and D. E. Dorman, *J.C.S. Chem. Comm.*, 1974, p. 114.
102. E. D. Becker, private communication.
103. L. Ernst, E. Lustig and V. Wray, *J. Magn. Resonance*, 1976, **22**, 459.
104. R. L. Lichter, D. E. Dorman and R. Wasylishen, *J. Amer. Chem. Soc.*, 1974, **96**, 930.
105. G. W. Buchanan and B. A. Dawson, *Can. J. Chem.*, 1976, **54**, 790.
106. W. McFarlane, *Mol. Phys.*, 1966, **10**, 603.
107. G. A. Gray, Ph.D. Dissertation, University of Calif., Davis, 1967.
108. N. J. Koole, D. Knol and M. J. A. De Bie, *J. Magn. Resonance*, 1976, **21**, 499.
109. W. McFarlane, *J. Chem. Soc., (A)*, 1967, 1660.
110. I. Morishima, A. Mizuno, T. Yonezawa and K. Goto, *Chem. Comm.*, 1970, 1321.
111. R. W. Stephany, M. J. A. De Bie and W. Drenth, *Org. Magn. Resonance*, 1974, **6**, 45.
112. M. Christl, *Org. Magn. Resonance*, 1975, **7**, 349.
113. A. G. McInnes, D. G. Smith, C.-K. Wat, L. C. Vining and J. L. C. Wright, *J.C.S. Chem. Comm.*, 1974, 201.
114. S. Braun, *Org. Magn. Resonance*, 1976, **8**, 273.
115. T. A. Albright and W. J. Freeman, *Org. Magn. Resonance*, 1976, **9**, 75.
116. G. Binsch, J. B. Lambert, B. W. Roberts and J. D. Roberts, *J. Amer. Chem. Soc.*, 1964, **86**, 5564.
117. V. Galasso, *Org. Magn. Resonance*, 1974, **6**, 5.
118. H. Nakatsuji, I. Morishima, H. Kato and T. Yonezawa, *Bull. Chem. Soc. Japan*, 1971, **44**, 2010.
119. S. Nagata, T. Yamabe, K. Hirao and K. Fukui, *J. Phys. Chem.*, 1975, **79**, 1863.
120. J. R. Morton, *Chem. Revs.*, 1964, **64**, 453.
121. M. Barfield, V. J. Hruby and J.-P. Merald, *J. Amer. Chem. Soc.*, 1976, **98**, 1308.
122. H. Fritz, D. Clerin and J.-P. Fleury, *Org. Magn. Resonance*, 1976, **8**, 269.
123. P. S. Pregosin, E. W. Randall and A. I. White, *J.C.S. Perkin II*, 1972, 1.
124. R. Wasylishen, in "Nuclear Magnetic Resonance Spectroscopy of Nuclei Other Than Protons", T. Axenrod and G. A. Webb (eds.), Wiley Interscience, New York, 1974, p. 105.
125. G. A. Gray and S. E. Cramer, *J. Org. Chem.*, 1972, **37**, 3470.
126. S. Srensen, R. S. Hansen and H. J. Jakobsen, *J. Amer. Chem. Soc.*, 1972, **94**, 5900.
127. V. N. Solkan and V. F. Bystrov, *Izvest. Akad. Nauk S.S.S.R. Ser. Khim.*, 1974, 102. (English translation: *Bull. Acad. Sci.: U.S.S.R. Div. of Chem. Sci.*, 1976, **23**, 95).
128. R. DiBlasi and K. D. Kopple, *J.C.S. Chem. Comm.*, 1975, 33.
129. G. W. Buchanan and C. Benezra, *Can. J. Chem.*, 1976, **54**, 231.
130. N. Muller and D. T. Carr, *J. Phys. Chem.*, 1963, **67**, 112.
131. J. Bacon and R. J. Gillespie, *J. Chem. Phys.*, 1963, **38**, 781.
132. H. Jensen and K. Schaumborg, *Mol. Phys.*, 1971, **22**, 1041.
133. F. J. Weigert and J. D. Roberts, *J. Amer. Chem. Soc.*, 1971, **93**, 2361.
134. R. Kaiser and A. Saika, *Mol. Phys.*, 1968, **15**, 221.
135. J. Reuben and A. Demiel, *J. Chem. Phys.*, 1966, **44**, 2216.
136. J. F. Hinton and L. W. Jaques, *J. Magn. Resonance*, 1973, **11**, 229.
137. G. V. D. Tiers, *J. Phys. Chem.*, 1963, **67**, 928.
138. J. F. Hinton and L. W. Jaques, *J. Magn. Resonance*, 1975, **17**, 95.

139. R. J. Abraham and P. Loftus, *J.C.S. Perkin II*, 1975, 535.
140. R. G. Green, L. H. Sutcliffe, B. Taylor and S. M. Walker, *Spectrochim. Acta*, 1974, **30A**, 703.
141. R. A. DeMarco, W. B. Fox, W. B. Moniz and S. A. Sojka, *J. Magn. Resonance*, 1975, **18**, 522.
142. K. Bock and C. Pedersen, *Acta Chem. Scand.*, 1975, **B29**, 000.
143. K. Bock and C. Pedersen, *J.C.S. Perkin II*, 1974, 293.
144. F. Nouaille, A.-M. Sepulchre, G. Lukacs, A. Kornprobst and S. D. Gero, *Bull. Soc. Chim. France*, 1974, 143.
145. K. M. Crecely, R. W. Crecely and J. H. Goldstein, *J. Mol. Spectrosc.*, 1971, **37**, 252.
146. F. J. Weigert and J. D. Roberts, *J. Phys. Chem.*, 1969, **73**, 449.
147. W. Adcock, B. D. Gupta, T. C. Khor, D. Doddrell and W. Kitching, *J. Org. Chem.*, 1976, **41**, 751.
148. G. Miyajima, and H. Akiyama, *Org. Magn. Resonance*, 1972, **4**, 811.
149. R. D. Singh and S. N. Singh, *J. Magn. Resonance*, 1974, **16**, 110.
150. V. A. Chertkov and N. M. Sergeyev, *J. Magn. Resonance*, 1976, **21**, 159.
151. V. Wray and D. N. Lincoln, *J. Magn. Resonance*, 1975, **18**, 374.
152. L. Ernst, D. N. Lincoln and V. Wray, *J. Magn. Resonance*, 1976, **21**, 115.
153. D. Doddrell, M. Barfield, W. Adcock, M. Aurangzeb and D. Jordan, *J.C.S. Perkin II*, 1976, 402.
154. L. Ernst, private communication.
155. R. L. Lichter and R. E. Wasylishen, *J. Amer. Chem. Soc.*, 1975, **97**, 1808.
156. M. Hansen and H. J. Jakobsen, *J. Mag. Resonance*, 1973, **10**, 74.
157. M. C. Thorpe, W. C. Coburn, Jr. and J. A. Montgomery, *J. Magn. Resonance*, 1974, **15**, 98.
158. L. Ernst, *Z. Naturforsch.*, 1975, **30B**, 788.
159. A. Berg, P. E. Hansen and H. J. Jakobsen, *Acta Chem. Scand.*, 1972, **26**, 2159.
160. F. R. Jerome and K. L. Servis, *J. Amer. Chem. Soc.*, 1972, **94**, 5896.
161. R. E. Wasylishen and M. Barfield, *J. Amer. Chem. Soc.*, 1975, **97**, 4545.
162. D. K. Dalling and H. S. Gutowsky, *J. Chem. Phys.*, 1971, **55**, 4959.
163. H. Dreeskamp and G. Pfister, *Mol. Phys.*, 1968, **14**, 295.
164. W. McFarlane, *Mol. Phys.*, 1967, **12**, 243.
165. P. E. Hansen, O. K. Poulsen and A. Berg, *Org. Magn. Resonance*, 1976, **8**, 632.
166. P. Lazzeretti, F. Taddei and R. Zanasi, *J. Amer. Chem. Soc.*, 1976, **98**, 7989.
167. T. E. Walker, R. E. London, T. W. Whaley, R. Barker and N. A. Matwiyoff, *J. Amer. Chem. Soc.*, 1976, **98**, 5807.
168. S. Berger and K.-P. Zeller, *Chem. Comm.*, 1976, 649.
169. E. Leete, *J. Amer. Chem. Soc.*, 1977, **99**, 648.
170. G. Popják, J. Edmond, F. A. L. Anet and N. R. Easton, Jr., *J. Amer. Chem. Soc.*, 1977, **99**, 931.
171. J. M. Schulman and T. Venanzi, *J. Amer. Chem. Soc.*, 1976, **98**, 6739.
172. F. R. Kreissl, E. W. Meineke, E. O. Fischer and J. D. Roberts, *J. Organometal. Chem.*, 1976, **108**, C29.
173. S. Berger and H. Kaletsch, *Org. Magn. Resonance*, 1976, **8**, 438.
174. A. Severge, F. Jüttner, E. Breitmaier and G. Jung, *Biochim. Biophys. Acta*, 1976, **437**, 289.
175. D. F. Wiemer, D. I. C. Scopes and N. J. Leonard, *J. Org. Chem.*, 1976, **41**, 3051.
176. G. W. Buchanan and B. A. Dawson, *Can. J. Chem.*, 1977, **55**, 1437.
177. R. J. Spear, D. A. Forsyth and G. A. Olah, *J. Amer. Chem. Soc.*, 1976, **98**, 2493.

SUBJECT INDEX

The numbers in **bold** indicate the pages on which the topic is discussed in detail.

A

Ab initio calculations of nitrogen chemical shifts, **119**
 Absolute nitrogen screening, calculation of, 134
 Absolute screening constant scale for nitrogen, 143
 Absolute screening of nitrogen molecule, 128, 143
 Absolute screening of nitromethane, 128
 Acetic acid, $^1J(\text{C}-\text{C})$ in, 254
 Aci-nitroalkanes, nitrogen chemical shifts of, 205
 Additivity rules for nitrogen chemical shifts of azoles, 182, 184
 AISEFT technique in nitrogen NMR, 148
 Aliphatic amines, nitrogen screening constants of, 151
 Aliphatic carboxylic acids, $^1J(\text{C}-\text{C})$ in, 253
 Alkynylrhodium complexes, ^{19}F data on, 55
 π -allyl complexes of iron, ^{19}F data on, 23
 Amides, nitrogen screening constants of, **171**
 Amidinium ions, nitrogen screening constants of, 212
 Amines, nitrogen screening constants of, **150**
 Amino acids, nitrogen screening constants of, **164**
 Amino acids, pH dependence of nitrogen chemical shifts, 164, 167
 Aminoboranes, nitrogen screening constants of, **156**
 Aminosilanes, nitrogen screening constants of, **156**
 Ammonia, nitrogen chemical shift of, 119, 143
 Ammonia, temperature coefficient for nitrogen chemical shift of, 136
 Ammonium ion as an external reference in nitrogen NMR, 142
 Anisotropy of nitrogen screening tensor, 132
 Anisotropy of nuclear screening tensor, 122

Aromatic carboxylic acids, $^1J(\text{C}-\text{C})$ in, 254
 Arylamines, nitrogen screening constants of, 154
 Average excitation energy approximation, 134
 Azides, nitrogen screening constants of, **176**
 Azine-*N*-oxides, calculation of nitrogen chemical shift of, 135
 Azine *N*-oxides, nitrogen screening constants of, 196
 Azines, calculation of nitrogen chemical shifts of, 135
 Azines, nitrogen screening constants of, **191**
 Azo compounds, nitrogen screening constants of, **206**
 Azoles, nitrogen screening constants of, **178**
 Azoloazines, nitrogen screening constants of, 192

B

Benzoic acid, $^1J(\text{C}-\text{C})$ in, 254
 Benzvalene, $^1J(\text{C}-\text{C})$ in, 251
 Bicyclobutane, $^1J(\text{C}-\text{C})$ in, 251
 Bicyclobutane derivative, $^1J(\text{C}-\text{C})$ in, 251
 Biopolymers, nitrogen NMR data on, 144
 Borane adducts of azines, nitrogen screening constants of, 199
 Borane adducts of azoles, nitrogen screening constants of, 199
 Butadiene, $^1J(\text{C}-\text{C})$ in, 253

C

Calibration of nitrogen spectra, **136**
 Carbon-beryllium coupling constants, **248**
 Carbon-boron coupling constants, **248**
 Carbon-carbon coupling constants, **249**
 Carbon-lithium coupling constants, **248**
 Cobalt (II) complexes, nitrogen NMR kinetic data on, 213
 Cobalt (III) complexes, nitrogen NMR of, 214

- Contact contribution to spin-spin coupling, 247
- Contact shifts, ^{19}F data on, 110
- Contact shifts in nitrogen NMR, 213
- Contributions to the paramagnetic component of the nitrogen screening tensor of some *N*-heterocycles, 131
- Contributions to the paramagnetic component of the nitrogen screening tensor of some small molecules and ions, 129
- Contributions to the paramagnetic component of the nitrogen screening tensor of urea and analogues, 129
- Copper(II) complexes, nitrogen NMR of, 213
- Cyanates, nitrogen screening constants of, 175
- Cyanides, nitrogen screening constants of, 175
- Cyclopentadienylcobalt complexes, ^{19}F data on, 48
- Cyclopentadienyl iron complexes, ^{19}F data on, 37

D

- Diamagnetic contribution to nitrogen screening tensor, calculation of, 124
- Diamagnetic metal complexes, nitrogen NMR of, 214
- Diazo compounds, nitrogen screening constants of, 206
- Differential saturation technique in nitrogen NMR, 140, 144, 148
- Dihydrofuran complexes, 5, 13
- Dipeptides, nitrogen NMR data on, 144
- Diphenylacetylene, $^1J(\text{C}-\text{C})$ in, 253
- Dipolar contribution to spin-spin coupling, 247
- Dipolar shifts in nitrogen NMR, 213
- Dithiophosphine complexes with nickel and palladium, ^{19}F data on, 99

E

- EDTA complexes, nitrogen chemical shifts of, 212
- β -Effect in nitrogen NMR, 150, 155, 156, 162, 187, 198, 202
- Electric field gradient at ^{14}N nuclei, calculation of, 236
- Ethylacetate, $^1J(\text{C}-\text{C})$ in, 254

- Ethylpyrene-1-carboxylate- $^{13}\text{C}_1$ $^1J(\text{C}-\text{C})$ in, 254
- Experimental techniques in nitrogen NMR, 144
- External electric field, effect of on ^{14}N relaxation, 235
- External standards for nitrogen spectra, 137

F

- ^{19}F chemical shifts of some complexes, of
 - chromium, 7
 - iron, 18
 - manganese, 11
 - molybdenum, 7
 - osmium, 18
 - rhenium, 11
 - ruthenium, 18
- ^{19}F chemical shifts of some fluoroacyliridium compounds, 57
- ^{19}F chemical shifts of some iron complexes of fluorinated sulphines, 45
- ^{19}F chemical shifts of some tetrafluoroethylene complexes of iridium, 57
- ^{19}F , chemical shift standards, 2
- ^{19}F NMR parameters of some chromium complexes, 6, 10
- ^{19}F NMR parameters of some cyclopentadienylperfluoroethyl cobalt complexes, 48
- ^{19}F NMR parameters of some fluoroalkylcobalt and rhodium complexes, 46
- ^{19}F NMR parameters of some fluoro-olefin complexes, 58
- ^{19}F NMR parameters of some iron complexes of fluorinated phosphines, 40
- ^{19}F NMR parameters of some manganese complexes, 10
- ^{19}F NMR parameters of some molybdenum complexes, 6, 10
- ^{19}F NMR parameters of some olefin complexes of iron and ruthenium, 31
- ^{19}F NMR parameters of some platinum(II) complexes, 70
- ^{19}F NMR parameters of some platinum(IV) complexes, 83, 85, 92
- ^{19}F NMR parameters of some (polyfluorocycloheptadiene) iron tricarboxyl compounds, 34
- Finite perturbation calculation of $^1J(\text{C}-\text{C})$, 251

- Fluorinated arsine complexes, ^{19}F data on, 9, 15
- Fluoro-acetylene complexes of manganese, ^{19}F data on, 11
- Fluoroacyliridium complexes, ^{19}F data on, 57
- Fluoroalkyl derivatives, 2
- of chromium, 3
 - of cobalt, 45
 - of copper, 100
 - of gold, 100
 - of groups IIIb–Vb, 2
 - of iridium, 45
 - of iron, 18
 - of manganese, 11
 - of molybdenum, 3
 - of nickel, 69
 - of osmium, 18
 - of palladium, 69
 - of platinum, 69
 - of rhenium, 11
 - of rhodium, 45
 - of ruthenium, 18
 - of silver, 100
 - of tungsten, 3
- Fluoroaromatic derivatives of transition metals, 102
- Fluoroaryl transition metal complexes, ^{19}F data on, 104
- Fluorobenzyl cobalt complexes, ^{19}F data on, 102
- Fluorocarbon complexes, ^{19}F data on, 7
- Fluoroheteroaromatic derivatives of transition metals, 102
- Fluoro-olefin complexes, ^{19}F data on, 58
- Fluoro-olefin complexes of iron, ^{19}F data on, 31
- Fluoro-olefin complexes of manganese, ^{19}F data on, 11
- Fluorophenyl cobalt complexes, ^{19}F data on, 102
- Formamide, dipolar couplings in, 216
- Fulminates nitrogen screening constants of, 175
- G**
- Glycine, nitrogen NMR data on, 146
- Gramicidin-S, nitrogen NMR data on, 145, 170
- Guanidines, nitrogen screening constants of, 171
- Guanidinium ions nitrogen screening constants of, 212
- H**
- N*-heterocycles, calculation of the nitrogen chemical shifts of, 131
- Hexafluoroacetone complexes of gold, ^{19}F data on, 100
- Hexafluoroacetone complexes of iron, ^{19}F data on, 38
- Hexafluoroacetone complex of platinum, ^{19}F data on, 78
- Hexafluoroacetone complexes of rhodium, ^{19}F data on, 68
- Hexafluorobicyclo[2,2,0]hexa-2,5-diene complexes, ^{19}F data on, 74
- Hexafluorobutadiene complex with iron, ^{19}F data on, 21
- Hexafluorobuta-1,3-diene platinum complexes, ^{19}F data on, 86
- Hexafluorobut-2-yne complexes of ruthenium, ^{19}F data on, 33
- Hexafluoropropene complexes of iron, ^{19}F data on, 20, 26, 29
- Heptafluoro-*n*-propyl iron complexes, ^{19}F data on, 18
- Hydrazines, nitrogen screening constants of, 171
- Hydrogen cyanide, nitrogen chemical shift of, 121
- Hydroxy pyridines, study of tautomeric equilibria, 193
- I**
- Imonium ions, nitrogen screening constants of, 212
- Internal standards for nitrogen spectra, 137
- Ions derived from azoles, nitrogen screening constants of, 186
- Isocyanates, nitrogen screening constants of, 175
- Isocyanides, nitrogen screening constants of, 175
- Isothiocyanates, nitrogen screening constants of, 175
- Isothiouronium ions, nitrogen screening constants of, 212

J

- $J(^{15}\text{N}-^{13}\text{C})$, **226**
 $^1J(\text{C}-\text{C})$ in acetic acid, 254
 $^1J(\text{C}-\text{C})$ in acetone, 256
 $^1J(\text{C}-\text{C})$ in acetoxynaphthalene, 256
 $^1J(\text{C}-\text{C})$ in aliphatic carboxylic acids, 253
 $^1J(\text{C}-\text{C})$ in 9- ^{13}C -anthrone, 256
 $^1J(\text{C}-\text{C})$ in aromatic carboxylic acids, 254
 $^1J(\text{C}-\text{C})$ in benzil- α - β - $^{13}\text{C}_2$, 256
 $^1J(\text{C}-\text{C})$ in benzoic acid, 254
 $^1J(\text{C}-\text{C})$ in benzvalene, 251
 $^1J(\text{C}-\text{C})$ in benzyl derivatives, 255
 $^1J(\text{C}-\text{C})$ in bicyclobutane, 251
 $^1J(\text{C}-\text{C})$ in a bicyclobutane derivative, 251
 $^1J(\text{C}-\text{C})$ in butadiene, 253
 $^1J(\text{C}-\text{C})$ in diphenylacetylene, 253
 $^1J(\text{C}-\text{C})$, dipolar contribution to, 248
 $^1J(\text{C}-\text{C})$ in ethyl acetate, 254
 $^1J(\text{C}-\text{C})$ in ethylpyrene-1-carboxylate- ^{13}C , 254
 $^1J(\text{C}-\text{C})$, finite perturbation calculation of, 251
 $^1J(\text{C}-\text{C})$ in histidine, 254
 $^1J(\text{C}-\text{C})$ in 9- ^{13}C -9-methoxy-anthracene, 256
 $^1J(\text{C}-\text{C})$ in 1-methylbicyclo[1.1.0]butane, 251
 $^1J(\text{C}-\text{C})$ in 1- ^{13}C -1-methyl cyclohexene, 252
 $^1J(\text{C}-\text{C})$ in naphthalene, 253, 256
 $^1J(\text{C}-\text{C})$, orbital contribution to, 248
 $^1J(\text{C}-\text{C})$ in proline residues, 254
 $^1J(\text{C}-\text{C})$ in 4- ^{13}C -4-propyl-3-heptene, 252
 $^1J(\text{C}-\text{C})$ in pyrene, 253
 $^1J(\text{C}-\text{C})$ in pyrene-1-carboxylic- ^{13}C acid, 254
 $^1J(\text{C}-\text{C})$, relation to S character of bond, 251
 $^1J(\text{C}-\text{C})$ in sodium acetate, 254
 $^1J(\text{C}-\text{C})$ in sodium benzoate, 254
 $^1J(\text{C}-\text{C})$ in some amino acids, **254**
 $^1J(\text{C}-\text{C})$ in some biological molecules, **254**
 $^1J(\text{C}-\text{C})$ in some carboxylic acids, **253**
 $^1J(\text{C}-\text{C})$ in some hydrocarbons, 251
 $^1J(\text{C}-\text{C})$ in some substituted toluenes, 255
 $^1J(\text{C}-\text{C})$ in 1- ^{13}C -toluene, 252
 $^1J(\text{C}-\text{C})$ in tyrosine, 254
 $^1J(\text{C}-\text{C})$ values, **250**
 $^1J(\text{F}-\text{C})$ in fluorobenzene, 283
 $^1J(\text{F}-\text{C})$ in 2-fluoropurine, 284
 $^1J(\text{F}-\text{C})$ in fluoropyridines, 284
 $^1J(\text{F}-\text{C})$ in some pyranosyl fluorides, 280
 $^1J(\text{F}-\text{C})$ in some trifluoromethanes, 280
 $^1J(^{15}\text{N}-\text{C})$ in acetonitrile, 270
 $^1J(^{15}\text{N}-\text{C})$ in aliphatic amines, 272
 $^1J(^{15}\text{N}-\text{C})$ in aniline, 272
 $^1J(^{15}\text{N}-\text{C})$, dipolar contribution to, 248
 $^1J(^{15}\text{N}-\text{C})$ in *N*-methylphenylpropylamine, 272
 $^1J(^{15}\text{N}-\text{C})$, orbital contribution to, 248
 $^1J(^{15}\text{N}-\text{C})$, in some alkylamines, 227
 in some amides, **263**, 272
 in some amines, **263**
 in some amine derivatives, **271**
 in some arylamines, 227
 in some azines, 277
 in some imines, **264**, 272
 in some isonitriles, **265**, 273
 $^1J(^{15}\text{N}-\text{C})$, in some nitriles, **265**, 273
 in some nitro compounds, **264**, 272
 in some oximes, 227, **264**, 272
 in some unsaturated heterocyclic derivatives, **265**, 273
 $^1J(^{15}\text{N}-\text{H})$, **216**
 $^1J(^{15}\text{N}-\text{H})$, in some dipeptides, 216
 in some enamines, 219
 in methylsydnimine hydrochloride, 219
 $^1J(^{15}\text{N}-^{15}\text{N})$, **232**
 $^1J(\text{O}-\text{C})$ in acetone, 280
 $^1J(\text{P}-\text{F})$, in a chromium complex, 103
 in some iron complexes, 42
 in some rhodium complexes, 45
 in a tungsten complex, 6
 $^1J(^{195}\text{Pt}-^{15}\text{N})$, in some platinum(II) complexes of azo-derivatives, 232
 $^1J(\text{Pt}-\text{Pt})$ in a dimeric platinum(II) complex, 78
 $^2J(\text{C}-\text{C})$ in acetaldehyde, 258
 $^2J(\text{C}-\text{C})$ in acetone, 258
 $^2J(\text{C}-\text{C})$ in benzil, 258
 $^2J(\text{C}-\text{C})$ in benzildihydrazone, 258
 $^2J(\text{C}-\text{C})$ in a bicyclo[1.1.0]butane derivative, 258
 $^2J(\text{C}-\text{C})$ in butadiene, 258
 $^2J(\text{C}-\text{C})$ in dimethylmercury, 258
 $^2J(\text{C}-\text{C})$ in diphenylacetylene, 257
 $^2J(\text{C}-\text{C})$ in formaldehyde, 258
 $^2J(\text{C}-\text{C})$ in 2-methyl-2-butanol, 257
 $^2J(\text{C}-\text{C})$ in methylchloroformate, 258
 $^2J(\text{C}-\text{C})$ in 1-methylcyclohexene, 257
 $^2J(\text{C}-\text{C})$ in methyltetrolate, 258
 $^2J(\text{C}-\text{C})$ in naphthalene, 258
 $^2J(\text{C}-\text{C})$ in 4-propyl-3-heptone, 257
 $^2J(\text{C}-\text{C})$ in propyne, 258
 $^2J(\text{C}-\text{C})$ in pyrene, 258
 $^2J(\text{C}-\text{C})$ in some carboxylic acids, 257
 $^2J(\text{C}-\text{C})$ in various fragments, **256**

- $^2J(\text{F}-\text{C})$ in 1-bromo-3,3,4-trifluorobutene-4, 282
- $^2J(\text{F}-\text{C})$ in ethylfluoride, 280
- $^2J(\text{F}-\text{C})$ in fluorobenzene, 283
- $^2J(\text{F}-\text{C})$ in fluoropyridines, 284
- $^2J(\text{F}-\text{C})$ in *n*-hexylfluoride, 280
- $^2J(\text{F}-\text{C})$ in some pyranosylfluorides, 281
- $^2J(\text{F}-\text{C})$ in various molecules, **281**
- $^2J(\text{F}-\text{F})$, in some chromium complexes, 7, 8
- in some cobalt complexes, 48
- in some iridium complexes, 62
- in some iron complexes, 23, 24, 25, 26, 27, 30
- in some molybdenum complexes, 7, 8
- in some platinum complexes, 74, 82
- $^2J(^{15}\text{N}-\text{C})$, in some oximes, 232
- in various molecules, **273**
- $^2J(^{15}\text{N}-\text{H})$, **219**
- $^2J(^{15}\text{N}-\text{H})$, in methyleneimine, 221
- in some sydnonimines, 221
- $^2J(^{15}\text{N}-\text{H})$ values, signs of, 221
- $^2J(\text{P}-\text{F})$, in some iron complexes, 39, 40
- in some molybdenum complexes, 6
- in some nickel complexes, 95, 96
- in a tungsten complex, 6
- $^2J(\text{P}-\text{P})$, in some molybdenum complexes, 6
- $^2J(\text{Pt}-\text{F})$ in some platinum(II) complexes, 70, 77
- in some platinum(IV) complexes, 72, 73, 82
- $^2J(\text{Rh}-\text{F})$, in some rhodium complexes, 45
- $^3J(\text{Ag}-\text{F})$ in some silver complexes, 101
- $^3J(\text{C}-\text{C})$ in butadiene, 262
- $^3J(\text{C}-\text{C})$ in butane, 259
- $^3J(\text{C}-\text{C})$ in butanoic acid, 259
- $^3J(\text{C}-\text{C})$ in 2-butanol, 259
- $^3J(\text{C}-\text{C})$ in some alcohols, 259
- $^3J(\text{C}-\text{C})$ in some amino acids, 261
- $^3J(\text{C}-\text{C})$ in some anthracene derivatives, 262
- $^3J(\text{C}-\text{C})$ in some aromatic carboxylic acids, 260
- $^3J(\text{C}-\text{C})$ in some barbituric acid derivatives, 262
- $^3J(\text{C}-\text{C})$ in some carboxylic acids, 259
- $^3J(\text{C}-\text{C})$ in some naphthalene derivatives, 262
- $^3J(\text{C}-\text{C})$ in some pyrene derivatives, 262
- $^3J(\text{C}-\text{C})$ in some saturated fragments, **258**
- $^3J(\text{C}-\text{C})$ in some I-substituted butyl compounds, 261
- $^3J(\text{C}-\text{C})$ in some II-substituted 1-methyladamantanes, 261
- $^3J(\text{C}-\text{C})$ in some unsaturated fragments, **262**
- $^3J(\text{F}-\text{C})$ in 1,2-difluorobenzene, 283
- $^3J(\text{F}-\text{C})$ in 1,3-difluorobenzene, 283
- $^3J(\text{F}-\text{C})$ in fluorobenzene, 283
- $^3J(\text{F}-\text{C})$ in 1-fluoronaphthalene, 285
- $^3J(\text{F}-\text{C})$ in 1-fluoropyrene, 285
- $^3J(\text{F}-\text{C})$ in some fluorobenzocycloalkenes, 282
- $^3J(\text{F}-\text{C})$ in some pyranosylfluorides, 282
- $^3J(\text{F}-\text{C})$ in trifluoromethylbenzene, 285
- $^3J(\text{F}-\text{C})$ in 2-trifluoromethylnaphthalene, 285
- $^3J(\text{F}-\text{F})$, in some chromium complexes, 7, 8
- in some cobalt complexes, 51
- in some gold complexes, 100
- in some iron complexes, 23, 24, 25, 26, 27, 28, 29
- in some molybdenum complexes, 7, 8
- in some platinum(IV) complexes, 82, 86
- in some silver complexes, 101
- $^3J(\text{F}-\text{H})$, in some chromium complexes, 7, 8
- in some cobalt complexes, 63
- in some gold complexes, 100
- in some iron complexes, 23, 24, 25, 26, 27, 28, 29
- in some molybdenum complexes, 7, 8
- in some nickel complexes, 95
- $^3J(^{15}\text{N}-\text{C})$ in some peptides, 277
- $^3J(^{15}\text{N}-\text{C})$ in 1-propylamine, 279
- $^3J(^{15}\text{N}-\text{C})$ in quinuclidine, 279
- $^3J(^{15}\text{N}-\text{C})$ in some oximes, 279
- $^3J(^{15}\text{N}-\text{C})$ in some saturated fragments, **277**
- $^3J(^{15}\text{N}-\text{C})$ in some triazines, 279
- $^3J(^{15}\text{N}-\text{C})$ in some unsaturated fragments, **279**
- $^3J(^{15}\text{N}-\text{C})$ in various molecules, **277**
- $^3J(^{15}\text{N}-\text{H})$, **224**
- $^3J(^{15}\text{N}-\text{H})$, in some amino-acids, 225
- in some azines, 224
- in some azoles, 224
- in some *N*-nitrosamines, 225
- in some peptides, 225
- in some pyrroles, 225
- in some sydnonimines, 226
- $^3J(\text{P}-\text{F})$, in some cobalt complexes, 48, 49, 51
- in some gold complexes, 100
- in some iron complexes, 19, 26
- in some nickel complexes, 76, 94
- $^3J(\text{Pt}-\text{F})$, in some platinum complexes, 95, 99
- in some platinum(II) complexes, 77, 78
- in some platinum(IV) complexes, 73, 74, 75, 82, 83, 88, 90, 91

- $^4J(\text{F}-\text{C})$ in fluorobenzene, 283
 $^4J(\text{F}-\text{C})$ in some fluorobenzocycloalkenes, 282
 $^4J(\text{F}-\text{C})$ in trifluoromethylbenzene, 285
 $^4J(\text{F}-\text{F})$, in some cobalt complexes, 67
 in some iridium complexes, 62
 in some iron complexes, 28
 in some platinum complexes, 80
 in some platinum(IV) complexes, 86
 in some rhodium complexes, 68, 69
 in some silver complexes, 101
 $^4J(\text{F}-\text{H})$, in some gold complexes, 100
 in some iron complexes, 23, 24, 25
 $^4J(^{15}\text{N}-\text{C})$ in a triazine, 279
 $^4J(^{15}\text{N}-\text{H})$, **226**
 $^4J(^{15}\text{N}-\text{H})$, in pyridazine, 226
 in some nitropyrroles, 226
 $^4J(\text{P}-\text{F})$, in some iridium complexes, 54, 55, 66
 in some iron complexes, 39, 40
 in some molybdenum complexes, 6
 in some palladium complexes, 97
 in some platinum complexes, 78
 in some platinum(IV) complexes, 83
 $^4J(\text{Pt}-\text{F})$, in some platinum complexes, 79
 in some platinum(II) complexes, 78
 in some platinum(IV) complexes, 87, 80
 $^5J(\text{F}-\text{C})$ in some 4-methyl-5-fluorophenanthrenes, 285
 $^5J(\text{F}-\text{C})$ in trifluoromethylbenzene, 285
 $^5J(\text{F}-\text{F})$, in some iridium complexes, 54, 55
 in some palladium complexes, 88, 89, 90
 in some platinum(IV) complexes, 86, 87, 88, 89
 in some silver complexes, 101
 $^5J(\text{P}-\text{F})$, in some iridium complexes, 66
 in some palladium complexes, 88
 in some platinum(IV) complexes, 87
 in some rhodium complexes, 65
 $^5J(\text{Pt}-\text{F})$ in some platinum(IV) complexes, 91

L

- Lactams, nitrogen screening constants of, 171
 Lanthanide shift reagents, 2
 in nitrogen NMR, 214
 Liquid nitrogen, N relaxation in, 238
 Long range C-C coupling constants, 262
 Long range N-C coupling constants, 279

M

- Methylanilines, calculation of nitrogen chemical shifts of, 135
 1-Methylbicyclo[1.1.0]butane, calculated
 $^1J(\text{C}-\text{C})$ in, 251
 2-Methyl-2-butanol, $^2J(\text{C}-\text{C})$ in, 257
 1- ^{13}C -1-methylcyclohexene, $^1J(\text{C}-\text{C})$ in, 252
 Molecular nitrogen complex with permethyl-titanocene, nitrogen chemical shift of, 212
 Mono-substituted pyridines, calculation of nitrogen chemical shift of, 135

N

- ^{14}N relaxation, **233**
 ^{15}N relaxation, **237**
 ^{15}N relaxation by spin-internal rotation, 238
 Naphthalene, $^1J(\text{C}-\text{C})$ in, 253
 Natural abundance ^{15}N NMR, 144
 Nickel(II) complexes, nitrogen NMR kinetic data on, 213
 Nitrate ion as an external reference in nitrogen NMR, 141
 Nitrates, nitrogen screening constants of, **202**
 Nitric acid as an external reference in nitrogen NMR, 142
 Nitroalkanes, nitrogen chemical shifts of, 204
 Nitroalkenes, nitrogen chemical shifts of, 202
 Nitro compounds, nitrogen screening constants of, **202**
 Nitrogen chemical shifts *ab initio* calculations of, **119**
 Nitrogen chemical shift of ammonia, calculation of, 119
 Nitrogen chemical shift of hydrogen cyanide, 121
 Nitrogen chemical shifts, of urea and some analogues, 127
 Nitrogen chemical shifts screening constant scale for, 137
 Nitrogen chemical shifts, semi-empirical calculations of, **122**
 Nitrogen chemical shifts temperature dependence of, 136
 Nitrogen molecule, absolute screening of, 128, 143
 Nitrogen NMR experimental aspects of, **144**
 Nitrogen quadrupole coupling constants, calculation of, 237
 determination of, 237

- Nitrogen relaxation phenomena, **233**
Nitrogen screening constants, correlation of, with molecular structure, **149**
Nitrogen screening constants, of amides, **171**
 of amidinium ions, **212**
 of amines, **150**
 of amino acids, **164**
 of aminoboranes, **156**
 of aminosilanes, **156**
 of ammonium ions, **164**
 of azides, **176**
 of azines, **191**
 of azine *N*-oxides, **196**
 of azo compounds, **206**
 of azoles, **178**
 of azoloazines, **192**
 of borane adducts of azines, **199**
 of borane adducts of azoles, **199**
 of cyanates, **175**
 of cyanides, **175**
 of diazo compounds, **206**
 of EDTA complexes, **212**
 of fulminates, **175**
 of guanidines, **171**
 of guanidinium ions, **212**
 of hydrazines, **171**
 of imonium ions **212**
 of ions derived from azoles, **186**
 of isocyanates, **175**
 of isocyanides, **175**
 of isothiocyanates, **175**
 of isothiuronium ions, **212**
 of lactones, **171**
 of nitrates, **202**
 of nitro compounds, **202**
 of nitrones, **200**
 of nitroso compounds, **206**
 of oximes, **200**
 of peptides, **164**
 of phenylhydrazones, **213**
 of small inorganic molecules, **211**
 of sydnones, **187**
 of sydnonimines, **187**
 of thiocyanates, **175**
 of ureas, **171**
Nitrogen screening constants, theory of, **118**
Nitrogen screening tensor, anisotropy of, **132**
Nitrogen screening tensor, calculation of diamagnetic contribution to, **124**
Nitrogen spectra, calibration of, **136**
Nitrogen spin-spin coupling constants, correlation of with molecular structure, **215**
Nitromethane, absolute screening of, **128**
Nitromethane as an external standard in nitrogen NMR, **137**
Nitrones, nitrogen screening constants of, **200**
Nitroso compounds, nitrogen screening constants of, **206**
Nuclear overhauser effect for ^{15}N nuclei, **144**, **170**
Nuclear screening tensor, anisotropy of, **122**
- O**
- Orbital contribution to spin-spin coupling, **247**
Order-disorder transition in ND_4Cl , **234**
Oximes, nitrogen screening constants of, **200**
- P**
- Paramagnetic molecules, nitrogen NMR of, **213**
Pentazole ring system, nitrogen NMR evidence for, **184**
Peptides, nitrogen screening constants of, **164**
Perfluoroalkyl complexes of silver, ^{19}F data on, **101**
 π -Perfluoroallylcobalt complex, ^{19}F data on, **51**
Perfluorobut-2-yne complexes, ^{19}F data on, **87**
Perfluorobut-2-yne complex of iridium, ^{19}F data on, **54**
Perfluorobut-2-yne complex of palladium, ^{19}F data on, **90**
Perfluorobut-2-yne complexes of ruthenium, ^{19}F data on, **36**
Perfluoroisopropyl complexes of iridium, ^{19}F data on, **50**
Perfluoropinacol complexes with nickel, ^{19}F data on, **98**
Phenylhydrazones, nitrogen screening constants of, **213**
Platinum(II) complexes, nitrogen NMR of, **214**
Polyfluorocyclohepta-1,3-diene iron tricarbonyl complexes, ^{19}F data on, **34**
Precise differences in nitrogen, screening constants, **138**
 $4\text{-}^{13}\text{C}$ -4-propyl-3-heptene, $^1J(\text{C}-\text{C})$ in, **252**

Protonation of azines, effect on nitrogen screening of, 195
Pulsed Fourier-transform nitrogen NMR, **144**
Pyrene $^1J(\text{C}-\text{C})$ in, 253
Pyrene-1-carboxylic- ^{13}C acid, $^1J(\text{C}-\text{C})$ in, 254
Pyridine, contributions to nitrogen chemical shift of, 136
Pyridinium ion, contributions to nitrogen chemical shift of, 136

Q

Quadrupolar relaxation models, 234

R

Reduced spin-spin coupling constant, 246
Relaxation reagents, use of in nitrogen NMR, 141, 146

S

Screening constant scale for nitrogen, 137
Selective population transfer, 254
Silver heptafluorobutyrate, use of as shift reagent, 3
Small inorganic molecules and ions, nitrogen screening constants of, 211
Small nitrogen containing molecules and ions calculation of the nitrogen chemical shifts of, 129
Sodium acetate, $^1J(\text{C}-\text{C})$ in, 254
Sodium benzoate, $^1J(\text{C}-\text{C})$ in, 254
Solid state ^{14}N NMR measurements, 236
Solvent effects on nitrogen chemical shifts, 149
Some calculated values of N-C coupling constants, **268**
Substituted ammonium ions nitrogen screening constants of, **164**
Sydnones, nitrogen screening constants of, **187**
Sydnonimines, nitrogen screening constants of, **187**

T

Temperature dependence of nitrogen chemical shifts, 136
Temperature dependence of the ^{19}F parameters of some cobalt complexes, 48
Temperature gradients, effects on nitrogen chemical shifts of, 136

Tetrafluoroethyl complexes of platinum, ^{19}F data on, 72
Tetrafluoroethylene complexes of iridium, ^{19}F data on, **57**
Tetrafluoroethylene complexes of iron, ^{19}F data on, 20
Tetrafluoroethylene complex with platinum, ^{19}F data on, 77, 92
Tetrahydrofuran complexes, 5, 13
Tetramethyl ammonium ion as an external reference in nitrogen NMR, 142
Thiocyanates, nitrogen screening constants of, **175**
Titanium(III) complexes, nitrogen NMR of, 213
1- ^{13}C -Toluene, $^1J(\text{C}-\text{C})$ in, 252
Trifluoroacetate complexes of ruthenium and osmium, ^{19}F data on, 45
Trifluoroethylene complexes with iron, ^{19}F data on, 22
Trifluoroiodomethane complexes, ^{19}F data on, 100
Trifluoromethylbenzene complexes, ^{19}F data on, 64
Trifluoromethylphosphorus complexes of molybdenum and chromium, ^{19}F data on, 6
Trifluoromethyl-platinum(II) complexes, ^{19}F data on, **70**
3,3,3-trifluoropropyne, ^{19}F data on, 87
Trifluorovinylplatinum complexes, ^{19}F data on, 82

U

Urea and some analogues, nitrogen chemical shifts of, 127
contributions to the paramagnetic component of the nitrogen screening tensor of, 129
Ureas, nitrogen screening constants of, **171**

V

Vanadium(III) complexes, isotropic shifts of, 3
Variable temperature studies of some chromium, molybdenum and tungsten complexes, 9
bis(vinylfluoride) rhodium complex, ^{19}F data on, 59